Fri. Jun 4, 2021

[J] Oral | P (Space and Planetary Sciences)：P-PS Planetary Sciences

10:45 AM - 12:15 PM JST | 1:45 AM - 3:15 AM UTC | Ch.03 Zoom Room 03

[P-PS05] Lunar science and exploration

convener:N Masaki Nishino(Japan Aerospace Exploration Agency, Institute of Space and Astronautical Science), Masahiro KAYAMA(Department of General Systems Studies, Graduate School of Arts and Sciences, The University of Tokyo), Hiroshi Nagaoka(Institute of Physical and Chemical Research), Yusuke Nakauchi(Japan Aerospace Exploration Agency), Chairperson:Hiroshi Nagaoka(Institute of Physical and Chemical Research), Masaki N Nishino(Japan Aerospace Exploration Agency, Institute of Space and Astronautical Science)

10:45 AM - 11:00 AM JST | 1:45 AM - 2:00 AM UTC

[PPS05-01] Numerical simulation of lunar seismic wave: Updated scattering structure around Apollo12 landing site from coda fitting approach

★Invited Papers

*Keisuke Onodera[1,2,3], Taichi Kawamura[2], Satoshi Tanaka[1,3], Yoshiaki Ishihara[4], Takuto Maeda[5] (1.The Graduate University for Advanced Studies, 2.IPGP/Université de Paris, 3.ISAS/JAXA, 4.JAXA Space Exploration Center, 5.Hirosaki University)

11:00 AM - 11:15 AM JST | 2:00 AM - 2:15 AM UTC

[PPS05-02] Effects of magma-generation and transport of heat and heat producing elements by migrating magma on the thermal history of the Moon.

*Kenyo U[1], Hiroki Hasumi[1], Masaki Ogawa[1] (1.The University of Tokyo)

11:15 AM - 11:30 AM JST | 2:15 AM - 2:30 AM UTC

[PPS05-03] Mass wasting process on lunar crater walls inferred from boulder falls

*Ayame Ikeda[1], Hiroyuki Kumagai[1], Tomokatsu Morota[2] (1.Graduate School of Environmental Studies, Nagoya University, 2.Department of Earth and Planetary Science, The University of Tokyo)

11:30 AM - 11:45 AM JST | 2:30 AM - 2:45 AM UTC

[PPS05-04] Recent boulder falls within the Finsen crater, an assessment of ongoing geological activities

*Trishit Ruj[1], Goro Komatsu[2], Kenji Kawai[1], Hanaya Okuda[3], Zhiyong Xiao[4], Deepak Dhingra[5] (1.Department of Earth and Planetary Science, School of Science, The University of Tokyo, 2.International Research School of Planetary Sciences, Università G. d'Annunzio, Viale Pindaro 42, 65127, Pescara, Italy, 3.Department of Ocean Floor Geoscience, Atmosphere and Ocean Research Institute, University of Tokyo, Kashiwanoha 5-1-5, Kashiwa, Chiba 277-8564, Japan, 4.Planetary Environmental and Astrobiological Research Laboratory, School of Atmospheric Sciences, Sun Yat-sen University, Zhuhai, China, 5.Department of Earth Sciences, Indian Institute of Technology Kanpur, Kanpur, UP 208016, India)

11:45 AM - 12:00 PM JST | 2:45 AM - 3:00 AM UTC

[PPS05-05] Lunar Surface Mapping by SLAM Technology on Bionic Legged Rover

*LIANG CHEN[1], Takehiko Arai[1], Makiko Ohtake[2] (1.Ashikaga University, 2.University of Aizu)

12:00 PM - 12:15 PM JST | 3:00 AM - 3:15 AM UTC

[PPS05-06] Deciphering the planetary water flux from the water record expected at lunar pole

*Ko Hashizume[1], Chihiro Yamanaka[2], Masahiro KAYAMA[3], Makiko Ohtake[4] (1.Ibaraki University, 2.Osaka University, 3.The University of Tokyo, 4.The University of Aizu)

[J] Oral | P (Space and Planetary Sciences)：P-PS Planetary Sciences

1:45 PM - 3:15 PM JST | 4:45 AM - 6:15 AM UTC | Ch.03 Zoom Room 03

[P-PS05] Lunar science and exploration

convener:N Masaki Nishino(Japan Aerospace Exploration Agency, Institute of Space and Astronautical Science), Masahiro KAYAMA(Department of General Systems Studies, Graduate School of Arts and Sciences, The University of Tokyo), Hiroshi Nagaoka(Institute of Physical and Chemical Research), Yusuke Nakauchi(Japan Aerospace Exploration Agency), Chairperson:Yusuke Nakauchi(Japan Aerospace Exploration Agency), Masahiro KAYAMA(Department of General Systems Studies, Graduate School of Arts and Sciences, The University of Tokyo)

1:45 PM - 2:00 PM JST | 4:45 AM - 5:00 AM UTC

[PPS05-07] Scientific approaches to promotion of the lunar polar exploration

*Masahiro KAYAMA[1], Makiko Ohtake[2], Ko Hashizume[3], Kazuto Saiki[4], Chihiro Yamanaka[4], Reiko Nomura[5], Makoto Hareyama[6], Yoshifumi Saito[5], Teruaki Enoto[7], Hideaki Miyamoto[1], Tomokatsu Morota[1], Yuzuru Karouji[5], Yoshiaki Ishihara[5], Hiroyasu Mizuno[5], Takeshi Hoshino[5], Dai ASOH[5] (1.The University of Tokyo, 2.University of Aizu, 3.Ibaraki University, 4.Osaka University, 5.JAXA, 6.St. Marianna University, 7.RIKEN)

2:00 PM - 2:15 PM JST | 5:00 AM - 5:15 AM UTC

[PPS05-08] **Latest Status on Japanese Lunar Polar Exploration Mission**

*DAI ASOH[1], Takeshi HOSHINO[1], Yuzuru KAROUJI[1], Hiroka INOUE[1], Makiko OHTAKE[2] (1.Japan Aerospace Exploration Agency, 2.University of Aizu)

2:15 PM - 2:30 PM JST | 5:15 AM - 5:30 AM UTC

[PPS05-09] Light source investigation of the volatile spectral signals observed at the lunar polar regions

*Makiko Ohtake[1], Yusuke Nakauchi[2], Satoshi Tanaka[2], Keisuke Onodera[3], Hiroshi Nagaoka[2] (1.University of Aizu, 2.Japan Aerospace Exploration Agency, 3.The Graduate University for Advanced Studies (SOKENDAI))

2:30 PM - 2:45 PM JST | 5:30 AM - 5:45 AM UTC

[PPS05-10] Auto-Focus system of Multi-Band Camera (Engineering Model) on SLIM

*Yusuke Nakauchi[1], Hiroyuki Sato[1], Hiroshi Nagaoka[1], Kazuto Saiki[2], Makiko Ohtake[3], Hiroaki Shiraishi[1], Chikatoshi Honda[3], Yoshiaki Ishihara[1] (1.Japan Aerospace Exploration Agency, 2.Osaka University, 3.The University of Aizu)

2:45 PM - 3:00 PM JST | 5:45 AM - 6:00 AM UTC

[PPS05-11] Current mission scenario of UZUME (Unprecedented Zipangu Underworld of the Moon Exploration)

*Junichi Haruyama[1] (1.Japan Aerospace Exploration Agency)

3:00 PM - 3:15 PM JST | 6:00 AM - 6:15 AM UTC

[PPS05-12] Numerical Simulations on Surface Charging Properties of Lunar Surface Cavities

*Nakazono Jin[1], Yohei Miyake[2], Hideyuki Usui[3] (1.Kobe University , 2.Education Center on Computational Science and Engineering, Kobe University, 3.Graduate school of system informatics Kobe University)

[J] Oral | P (Space and Planetary Sciences)：P-PS Planetary Sciences

9:00 AM - 10:30 AM JST | 12:00 AM - 1:30 AM UTC | Ch.04 Zoom Room 04

[P-PS06] Planetary Sciences

convener:Yusuke Nakauchi(Japan Aerospace Exploration Agency), Hiroshi Kikuchi(Japan Aerospace Exploration Agency), Chairperson:Keisuke Sugiura(Tokyo Institute of Technology, Earth Life Science Institute), Makito Kobayashi(Department of Earth and Planetary Science, School of Science, University of Tokyo)

9:00 AM - 9:15 AM JST | 12:00 AM - 12:15 AM UTC

[PPS06-13] Global climate and river transport simulations of early Mars during the late Noachian and the early Hesperian

*Arihiro Kamada[1], Takeshi Kuroda[1], Yasumasa Kasaba[1], Naoki Terada[1], Hiromu Nakagawa[1] (1.Graduate School of Science, Tohoku University)

9:15 AM - 9:30 AM JST | 12:15 AM - 12:30 AM UTC

[PPS06-14] Water-ice content estimation on the Martian subsurface based on the permittivity

*Makito Kobayashi[1], Hideaki Miyamoto[2] (1.Department of Earth and Planetary Science, School of Science, University of Tokyo, 2.Department of Systems Innovation, School of Engineering, University of Tokyo)

9:30 AM - 9:45 AM JST | 12:30 AM - 12:45 AM UTC

[PPS06-15] Shock remanent magnetization intensity and stability structures of single-domain titanomagnetite-bearing basalt sample

*Masahiko Sato[1], Kosuke Kurosawa[2], Shota Kato[1], Masashi Ushioda[3], Sunao Hasegawa[4] (1.The University of Tokyo, 2.Planetary Exploration Research Center, Chiba Institute of Technology, 3.Shikoku Research Institute Inc., 4.Japan Aerospace Exploration Agency)

9:45 AM - 10:00 AM JST | 12:45 AM - 1:00 AM UTC

[PPS06-16] Numerical Study of the Formation Scenario of Mesosiderite Meteorites Through a Giant Impact Onto a Differentiated Asteroid

*Keisuke Sugiura[1], Makiko K. Haba[2], Hidenori Genda[1] (1.Tokyo Institute of Technology, Earth Life Science Institute, 2.Tokyo Institute of Technology, Department of Earth and Planetary Sciences)

10:00 AM - 10:15 AM JST | 1:00 AM - 1:15 AM UTC

[PPS06-17] High velocity impact experiments on porous ice aggregates simulating cometary nuclei: Estimation of energy partition from projectile kinetic energy to post shock heat

*Haruka Sasai[1], Minami Yasui[1], Masahiko Arakawa[1], Kei Shirai[1] (1.Kobe University)

10:15 AM - 10:30 AM JST | 1:15 AM - 1:30 AM UTC

[PPS06-18] Effect of porosity on restitution coefficient and sticking properties of snowball simulating Saturn's rings

*Yukari Toyoda[1], Masahiko Arakawa[1], Minami Yasui[1] (1.Graduate School of Science, Kobe University)

[J] Oral | P (Space and Planetary Sciences)：P-PS Planetary Sciences

3:30 PM - 5:00 PM JST | 6:30 AM - 8:00 AM UTC | Ch.04 Zoom Room 04

[P-PS07] Formation and evolution of planetary materials in the Solar System

convener:Megumi Matsumoto(Graduate School of Science, Tohoku University), Shin Ozawa(Department of Earth Science, Graduate School of Science, Tohoku University), Yuki Hibiya(Submarine Resources Research Center, Japan Agency for Marine-Earth Science and Technology), Noriyuki Kawasaki(Department of Earth and Planetary Sciences, Graduate School of Science, Hokkaido University), Chairperson:Megumi Matsumoto(Graduate School of Science, Tohoku University), Shin Ozawa(Department of Earth Science, Graduate School of Science, Tohoku University)

3:30 PM - 3:45 PM JST | 6:30 AM - 6:45 AM UTC

[PPS07-01] Detection of hexamethylenetetramine in carbonaceous meteorites and its role for chemical evolution

*Yasuhiro Oba[1], Yoshinori Takano[2], Hiroshi Naraoka[3], Yoshihiro Furukawa[4], Shogo Tachibana[5,6], Daniel P Glavin[7], Jason P Dworkin[7] (1.Institute of Low Temperature Science, Hokkaido University, 2.JAMSTEC, 3.Kyushu University, 4.Tohoku University, 5.University of Tokyo, 6.ISAS/JAXA, 7.NASA Goddard Space Flight Center)

3:45 PM - 4:00 PM JST | 6:45 AM - 7:00 AM UTC

[PPS07-02] Isotopic constraint on the origin of organic matter in carbonaceous chondrites

*Yoshihiro Furukawa[1], Yoshinari Iwasa[1], Yoshito Chikaraishi[2] (1.Graduate School of Science, Tohoku University, 2.Institute of Low Temperature Science)

4:00 PM - 4:30 PM JST | 7:00 AM - 7:30 AM UTC

[PPS07-03] **What kinds of the meteorite are CM chondrites?**

★Invited Papers

*Makoto Kimura[1] (1.National Institute of Polar Research)

4:30 PM - 4:45 PM JST | 7:30 AM - 7:45 AM UTC

[PPS07-04] The first fall-observed and recovered meteorite in Japan: Narashino meteorite

*Atsushi Takenouchi[1], Shigekazu Yoneda[2], Akira Yamaguchi[1], Ryuji Okazaki[3], Naoki Takahashi[4], Naoki Shirai[5], Yasunori Fujiwara, Ryuho Kataoka[1] (1.National Institute of Polar Research, 2.National Museum of Nature and Scienece, 3.Kyushu University, 4.Natural History Museum and Institute, Chiba, 5.Tokyo Metropolitan University)

4:45 PM - 5:00 PM JST | 7:45 AM - 8:00 AM UTC

[PPS07-05] High spatial resolution three-color CT imaging of CM and CI meteorites and their heated samples for a rehearsal analysis of Ryugu

*Junya Matsuno[1], Akira Tsuchiyama[1], Megumi Matsumoto[2], Yuri Fujioka[2], Tomoki Nakamura[2], Kentaro Uesugi[3], Akihisa Takeuchi[3], Masahiro Yasutake[3], Tsukasa Nakano[4], Naoto Nakano[6], Rubino Stefano[5], Shota Okumura[6], Akira Miyake[6] (1.Ritsumeikan University, 2.Tohoku University, 3.JASRI/SPring-8, 4.AIST, 5.Institut d'Astrophysique Spatiale, 6.Kyoto University)

[J] Oral | P (Space and Planetary Sciences)：P-EM Solar-Terrestrial Sciences, Space Electromagnetism & Space Environment

9:00 AM - 10:30 AM JST | 12:00 AM - 1:30 AM UTC | Ch.06 Zoom Room 06

[P-EM15] Space Plasma Physics: Theory and Simulation

convener:Takanobu Amano(Department of Earth and Planetary Science, University of Tokyo), Yohei Miyake(Education Center on Computational Science and Engineering, Kobe University), Takayuki Umeda(Institute for Space-Earth Environmental Research, Nagoya University), Tadas Nakamura(Fukui Prefectural University), Chairperson:Takanobu Amano(Department of Earth and Planetary Science, University of Tokyo), Masanori Iwamoto(Faculty of Engineering Sciences, Kyushu University)

9:00 AM - 9:15 AM JST | 12:00 AM - 12:15 AM UTC

[PEM15-01] Observation of non-gyrotropy of electrons caused by wave-particle interaction with intense whistler mode waves in mirror mode structures in the magnetosheath

*Naritoshi Kitamura[1], Masahiro Kitahara[2], Scott A Boardsen[3,4], Takanobu Amano[1], Daniel J Gershman[3], Yoshiharu Omura[5], Satoko Nakamura[2], Masafumi Shoji[2], Yuto Katoh[6], Hirotsugu Kojima[5], Yoshizumi Miyoshi[2], Yoshifumi Saito[7], Masafumi Hirahara[2], Shoichiro Yokota[8], Barbara L Giles[3], William R Paterson[3], Craig J Pollock[9], Olivier Le Contel[10], Christopher T Russell[11], Narges Ahmadi[12], Per-Arne Lindqvist[13], Robert E Ergun[12], James L Burch[14] (1.Department of Earth and Planetary Science, Graduate School of Science, The University of Tokyo, 2.Institute for Space-Earth Environmental Research, Nagoya University, 3.NASA Goddard Space Flight Center, 4.Goddard Planetary Heliophysics Institute, University of Maryland, 5.Research Institute for Sustainable Humanosphere, Kyoto University, 6.Department of Geophysics, Graduate School of Science, Tohoku University, 7.Institute of Space and Astronautical Science, Japan Aerospace Exploration Agency, 8.Department of Earth and Space Science, Graduate School of Science, Osaka University, 9.Denali Scientific, 10.Laboratoire de Physique des Plasmas, CNRS/Ecole Polytechnique/Sorbonne Université/Université Paris-Sud/Observatoire de Paris, 11.Department of Earth, Planetary, and Space Science, University of California, Los Angeles, 12.Laboratory for Atmospheric and Space Physics, University of Colorado, Boulder, 13.Royal Institute of Technology, 14.Southwest Research Institute)

9:15 AM - 9:30 AM JST | 12:15 AM - 12:30 AM UTC

[PEM15-02] **Simulation for wave-particle interactions of triggered emissions in a uniform magnetic field**

*Yuya Fujiwara[1], Takeshi Nogi[1], Yoshiharu Omura[1] (1.Research Institute for Sustainable Humanosphere, Kyoto University)

9:30 AM - 9:45 AM JST | 12:30 AM - 12:45 AM UTC

[PEM15-03] Synchrotron Maser Emission from Relativistic Shocks

*Masanori Iwamoto[1], Takanobu Amano[2], Yosuke Matsumoto[3], Shuichi Matsukiyo[1], Masahiro Hoshino[2] (1. Faculty of Engineering Sciences, Kyushu University, 2.Department of Earth and Planetary Science, University of Tokyo, 3.Graduate School of Science, Chiba University)

9:45 AM - 10:00 AM JST | 12:45 AM - 1:00 AM UTC

[PEM15-04] Synchrotron maser instability in an electron-ion plasma

*Shuichi Matsukiyo[1], Yodai Esaki[2], Masanori Iwamoto[1] (1.Faculty of Engineering Sciences, Kyushu University, 2.Interdisciplinary Graduate School of Engineering Sciences, Kyushu University)

10:00 AM - 10:15 AM JST | 1:00 AM - 1:15 AM UTC

[PEM15-05] Trajectory analysis of energetic electrons in quasi-perpendicular shock structure

*Fumiko Otsuka[1], Shuichi Matsukiyo[1], Mitsuo Oka[2] (1.Earth System Science and Technology, 2.UC Berkeley)

10:15 AM - 10:30 AM JST | 1:15 AM - 1:30 AM UTC

[PEM15-06] Simulation of temperature anisotropy instability by a fluid model with non-local closure

*Taiki Jikei[1], Takanobu Amano[1] (1.The University of Tokyo)

[J] Oral | P (Space and Planetary Sciences)：P-EM Solar-Terrestrial Sciences, Space Electromagnetism & Space Environment

10:45 AM - 12:15 PM JST | 1:45 AM - 3:15 AM UTC | Ch.06 Zoom Room 06

[P-EM15] Space Plasma Physics: Theory and Simulation

convener:Takanobu Amano(Department of Earth and Planetary Science, University of Tokyo), Yohei Miyake(Education Center on Computational Science and Engineering, Kobe University), Takayuki Umeda(Institute for Space-Earth Environmental Research, Nagoya University), Tadas Nakamura(Fukui Prefectural University), Chairperson:Shogo Isayama(Interdisciplinary Graduate School of Engineering Sciences, Kyushu University), Seiji Zenitani(Kobe University)

10:45 AM - 11:00 AM JST | 1:45 AM - 2:00 AM UTC

[PEM15-07] Neutral depletion and the density limit of the helicon plasma

*Shogo Isayama[1], Shunjiro Shinohara[2], Tohru Hada[1], Shih Hung Chen[3] (1.Interdisciplinary Graduate School of Engineering Sciences, Kyushu University, 2.Institute of Engineering, Tokyo University of Agriculture and Technology, 3.Department of Physics, National Central University)

11:00 AM - 11:15 AM JST | 2:00 AM - 2:15 AM UTC

[PEM15-08] Development of a magnetospheric global MHD simulation model for GEO-X mission

*Yosuke Matsumoto[1], Yoshizumi Miyoshi[2] (1.Graduate School of Science, Chiba University, 2.Institute for Space–Earth Environmental Research)

11:15 AM - 11:30 AM JST | 2:15 AM - 2:30 AM UTC

[PEM15-09] Full multiple Buneman-Boris solvers in nonrelativistic particle-in-cell simulation

*Seiji Zenitani[1], Tsunehiko N Kato[2] (1.Kobe University, 2.National Astronomical Observatory of Japan)

11:30 AM - 11:45 AM JST | 2:30 AM - 2:45 AM UTC

[PEM15-10] 2-D PIC simulations of surface charging processes on the nightside of Phobos

*Masaki Tanabe[1], Naoki Terada[1], Yohei Miyake[2], Hideyuki Usui[3] (1.Tohoku University planetary atomosphere, 2.Education Center on Computational Science and Engineering, Kobe University, 3.Graduate School of System Informatics, Kobe University)

11:45 AM - 12:00 PM JST | 2:45 AM - 3:00 AM UTC

[PEM15-11] Study on Electric Field Sensor Impedance in Magnetized Plasma by PIC Simulation.

*Ibuki Fukasawa[1], Hirotsugu Kojima[1], Yohei Miyake[2], Hideyuki Usui[3], Satoshi Kurita[1] (1.Research institute for sustainable humanosphere, Kyoto University, 2.Education Center on Computational Science and Engineering, Kobe University, 3.Graduate school of system informatics, Kobe University)

12:00 PM - 12:15 PM JST | 3:00 AM - 3:15 AM UTC

[PEM15-12] Spin-modulated components in Electric Field Detector (EFD) of Plasma Wave Experiment (PWE) aboard the Arase satellite

*Satoko Nakamura[1], Yoshizumi Miyoshi[1], Yasumasa Kasaba[2], Tomoko Nakagawa[3], Tomoaki Hori[1], Shoya Matsuda[4], Masafumi Shoji[1], Atsushi Kumamoto[7], Fuminori Tsuchiya[2], Ayako Matsuoka[5], Yoshiya Kasahara[6] (1.Institute for Space-Earth Environmental Research, Nagoya University, 2.Planetary Plasma and Atmospheric Research Center, Tohoku University, 3.Information and Communication Engineering, Tohoku Institute of Technology, 4.Institute of Space and Astronautical Science/Japan Aerospace Exploration Agency, 5.Data Analysis Center for Geomagnetism and Space Magnetism, Graduate School of Science, Kyoto University, 6.Information Media Center, Kanazawa University, 7.Department of Geophysics, Graduate School of Science, Tohoku University)

[J] Oral | P (Space and Planetary Sciences)：P-CG Complex & General

10:45 AM - 12:15 PM JST | 1:45 AM - 3:15 AM UTC | Ch.04 Zoom Room 04

[P-CG19] Origin and evolution of materials in space

convener:Aki Takigawa(Department of Earth and Planetary Science, The University of Tokyo), Hitoshi Miura(Graduate School of Science, Department of Information and Basic Science, Nagoya City University), Takafumi Ootsubo(National Astronomical Observatory of Japan, National Institutes of Natural Sciences), Hideko Nomura(Division of Science, National Astronomical Observatory of Japan), Chairperson:Sota ARAKAWA(National Astronomical Observatory of Japan), Daiki Yamamoto(Institute of Space and Astronautical Science, Japan Aerospace eXploration Agency)

10:45 AM - 11:00 AM JST | 1:45 AM - 2:00 AM UTC

[PCG19-01] Nucleation efficiency of dust approaching from microgravity experiments

★Invited Papers

*Yuki Kimura[1] (1.Institute of Low Temperature Science, Hokkaido University)

11:00 AM - 11:15 AM JST | 2:00 AM - 2:15 AM UTC

[PCG19-02] **Investigation of mid-infrared long-term variability of dusty AGB stars by using multi-epoch scan data of AKARI and WISE**

*Kengo Tachibana[1], Takashi Miyata[1], Takafumi Kamizuka[1], Ryou Ohsawa[1], Satoshi Takita[1], Akiharu Nakagawa[2], Yoshifusa Ita[3], Mizuho Uchiyama[4] (1.The University of Tokyo, 2.Kagoshima University, 3.Tohoku University, 4.ISAS/JAXA)

11:15 AM - 11:30 AM JST | 2:15 AM - 2:30 AM UTC

[PCG19-03] The birth environment and current location of the Solar system in the Galactic disc, using Milky-Way simulations and radioactive isotopes

*Yusuke Fujimoto[1] (1.Earth and Planets Laboratory, Carnegie Institution for Science)

11:30 AM - 11:45 AM JST | 2:30 AM - 2:45 AM UTC

[PCG19-04] Mutual Relation among the Circummultiple Structure, the Circumstellar Disk, and the Outflow: the Young Multiple IRAS 16293-2422 Source A Case

*Yoko Oya[1] (1.The University of Tokyo)

11:45 AM - 12:00 PM JST | 2:45 AM - 3:00 AM UTC

[PCG19-05] Investigating the impact of X-rays on the molecular abundances of envelopes and disks around low-mass protostars with ngVLA

*Shota Notsu[1], Nami Sakai[1], Hideko Nomura[2], Ewine F. van Dishoeck[3], Catherine Walsh[4], Arthur D. Bosman[5] (1.Star and Planet Formation Laboratory, RIKEN Cluster for Pioneering Research, 2.Division of Science, National Astronomical Observatory of Japan, 3.Leiden Observatory, Faculty of Science, Leiden University, 4.School of Physics and Astronomy, University of Leeds, 5.Department of Astronomy, University of Michigan)

12:00 PM - 12:15 PM JST | 3:00 AM - 3:15 AM UTC

[PCG19-06] Hot Salty Disks around Massive Protostars: A New Connection from Star-Formation Observation to Meteoritics?

★Invited Papers

*Kei Tanaka[1,2] (1.University of Colorado Boulder, 2.National Astronomical Observatory of Japan)

[J] Oral | P (Space and Planetary Sciences)：P-CG Complex & General

1:45 PM - 3:15 PM JST | 4:45 AM - 6:15 AM UTC | Ch.04 Zoom Room 04

[P-CG19] Origin and evolution of materials in space

convener:Aki Takigawa(Department of Earth and Planetary Science, The University of Tokyo), Hitoshi Miura(Graduate School of Science, Department of Information and Basic Science, Nagoya City University), Takafumi Ootsubo(National Astronomical Observatory of Japan, National Institutes of Natural Sciences), Hideko Nomura(Division of Science, National Astronomical Observatory of Japan), Chairperson:Yoko Oya(The University of Tokyo), Shota Notsu(Star and Planet Formation Laboratory, RIKEN Cluster for Pioneering Research)

1:45 PM - 2:00 PM JST | 4:45 AM - 5:00 AM UTC

[PCG19-07] Measurability of CO isotopologue ratio in PPDs with ALMA

*Tomohiro Yoshida[1], Hideko Nomura[2], Kenji Furuya[2], Takashi Tsukagoshi[2] (1.Faculty of Science, Kyoto University, 2.Division of Science, National Astronomical Observatory of Japan)

2:00 PM - 2:15 PM JST | 5:00 AM - 5:15 AM UTC

[PCG19-08] Oxygen isotope exchange kinetics between amorphous silicate dust and CO gas: Implication for oxygen isotope evolution in the early Solar System

*Daiki Yamamoto[1,2], Shogo Tachibana[1,2], Noriyuki Kawasaki[3], Michiru Kamibayashi[2], Hisayoshi Yurimoto[3] (1.Institute of Space and Astronautical Science, Japan Aerospace eXploration Agency , 2.UTokyo Organization for Planetary Space Science, The University of Tokyo, 3.Department of Natural History Sciences, Hokkaido University)

2:15 PM - 2:30 PM JST | 5:15 AM - 5:30 AM UTC

[PCG19-09] On the crystallinity of silicate dust in evolving protoplanetary disks due to magnetically driven disk winds

*Sota ARAKAWA[1], Yuji Matsumoto[2], Mitsuhiko Honda[3] (1.National Astronomical Observatory of Japan, 2.Institute of Astronomy and Astrophysics, Academia Sinica, 3.Okayama University of Science)

2:30 PM - 2:45 PM JST | 5:30 AM - 5:45 AM UTC

[PCG19-10] **Crystallization of amorphous Mg-Fe silicate dust: Implications for thermal processes in the early Solar System**

*Ryosuke Sakurai[1], Kodai Kobayashi[2], Daiki Yamamoto[3], Aki Takigawa[1], Shogo Tachibana[3,4] (1.Department of Earth and Planetary Science, UTokyo, 2.Department of Natural History Sciences, Hokkaido Univ., 3.Department of Solar System Sciences, ISAS, JAXA, 4.UTokyo Organization for Planetary and Space Science (UTOPS))

2:45 PM - 3:00 PM JST | 5:45 AM - 6:00 AM UTC

[PCG19-11] A novel laboratory approach to studying photochemistry of liquid organic interfaces

★Invited Papers

*Tetsuya Hama[1], Naoki Numadate[1] (1.Komaba Institute for Science, The University of Tokyo)

3:00 PM - 3:15 PM JST | 6:00 AM - 6:15 AM UTC

[PCG19-12] Assessing the potential of biogenic gases as exoplanet biosignatures

★Invited Papers

*Yuka Fujii[1], Yu Komatsu[2], Alexis Gilbert[3], Sebastian Danielache[4], Mayuko Nakagawa[3] (1.National Astronomical Observatory of Japan, 2.Astrobiology Center, 3.Tokyo Institute of Technology, 4.Sophia University)

[J] Oral | A (Atmospheric and Hydrospheric Sciences)：A-AS Atmospheric Sciences, Meteorology & Atmospheric Environment

9:00 AM - 10:30 AM JST | 12:00 AM - 1:30 AM UTC | Ch.07 Zoom Room 07

[A-AS07] Weather, Climate, and Environmental Science Studies using High-Performance Computing

convener:Hisashi Yashiro(National Institute for Environmental Studies), Takuya Kawabata(Meteorological Research Institute), Tomoki Miyakawa(Atmosphere and Ocean Research Institute, The University of Tokyo), Koji Terasaki(RIKEN Center for Computational Science), Chairperson:Hisashi Yashiro(National Institute for Environmental Studies)

9:00 AM - 9:15 AM JST | 12:00 AM - 12:15 AM UTC

[AAS07-01] Atmospheric large eddy simulation with DALES on Fugaku

★Invited Papers

*Fredrik Jansson[1], Martin Janssens[1,2], Jisk Attema[3], Johanna Grönqvist, Franziska Glassmeier[1], Yousuke Sato[4], Masaki Satoh[5], Pier Siebesma[1] (1.Delft University of Technology, 2.Wageningen University & Research, 3.Netherlands eScience Center, 4.Faculty of Science, Hokkaido University, 5.Atmosphere and Ocean Research Institute, The University of Tokyo)

9:15 AM - 9:30 AM JST | 12:15 AM - 12:30 AM UTC

[AAS07-02] Big Data Assimilation: Real-time Demonstration Experiment of 30-second-update Forecasting in Tokyo in August 2020

*Takemasa Miyoshi[1], Takumi Honda[1], Arata Amemiya[1], Shigenori Otsuka[1], Yasumitsu Maejima[1], James David Taylor[1], Hirofumi Tomita[1], Seiya Nishizawa[1], Kenta Sueki[1], Tsuyoshi Yamaura[1], Yutaka Ishikawa[1], Shinsuke Satoh[2], Tomoo Ushio[3], Kana Koike[4], Erika Hoshi[4], Kengo Nakajima[5] (1.RIKEN, 2.NICT, 3.Osaka University, 4.MTI Ltd., 5.University of Tokyo)

9:30 AM - 9:45 AM JST | 12:30 AM - 12:45 AM UTC

[AAS07-03] 1000-member 18-km-mesh SCALE-LETKF experiment with conventional observations in summer 2020

*Arata Amemiya[1], Takemasa Miyoshi[1] (1.RIKEN Center for Computational Science)

9:45 AM - 10:00 AM JST | 12:45 AM - 1:00 AM UTC

[AAS07-04] Progress in Tropical Weather and Climate Prediction with Global Storm-Resolving Models

★Invited Papers

*Falko Judt[1] (1.National Center for Atmospheric Research)

10:00 AM - 10:15 AM JST | 1:00 AM - 1:15 AM UTC

[AAS07-05] **A 1000-member 14-km mesh global ensemble experiment to target typhoon FAXAI (2019)**

*Yohei Yamada[1], Masuo Nakano[1], Tomoki Miyakawa[2], Chihiro Kodama[1], Ying-Wen Chen[2], Hisashi Yashiro[3], Tomoe Nasuno[1], Masaki Satoh[2] (1.Japan Agency for Marine-Earth Science and Technology, 2.Atmosphere and Ocean Research Institute, The University of Tokyo, 3.National Institute for Environmental Studies)

10:15 AM - 10:30 AM JST | 1:15 AM - 1:30 AM UTC

[AAS07-06] A 1024-Member Data Assimilation and Forecast Experiment with NICAM-LETKF Using Fugaku: A Heavy Rainfall Event in Kyushu in July 2020

*Koji Terasaki[1], Takemasa Miyoshi[1] (1.RIKEN Center for Computational Science)

[J] Oral | A (Atmospheric and Hydrospheric Sciences)：A-AS Atmospheric Sciences, Meteorology & Atmospheric Environment

10:45 AM - 12:15 PM JST | 1:45 AM - 3:15 AM UTC | Ch.07 Zoom Room 07

[A-AS07] Weather, Climate, and Environmental Science Studies using High-Performance Computing

convener:Hisashi Yashiro(National Institute for Environmental Studies), Takuya Kawabata(Meteorological Research Institute), Tomoki Miyakawa(Atmosphere and Ocean Research Institute, The University of Tokyo), Koji Terasaki(RIKEN Center for Computational Science), Chairperson:Takuya Kawabata(Meteorological Research Institute)

10:45 AM - 11:00 AM JST | 1:45 AM - 2:00 AM UTC

[AAS07-07] Early results of the evaluation of the JRA-3Q reanalysis

★Invited Papers

*Yayoi Harada[1], Shinya Kobayashi[2], Yuki Kosaka[2], Jotaro Chiba[2], Takayuki Tokuhiro[2] (1.Meteorological Research Institute / Japan Meteorological Agency, 2.Office of Earth System Modeling / Numerical Prediction Division / Japan Meteorological Agency)

11:00 AM - 11:15 AM JST | 2:00 AM - 2:15 AM UTC

[AAS07-08] Quality assessment of the third Japanese Reanalysis for Three Quarters of a Century (JRA-3Q) during a pre-satellite era

*Hiroaki Naoe[1], Shinya Kobayashi[2], Yuki Kosaka[2], Jotaro Chiba[2], Takayuki Tokuhiro[2], Yayoi Harada[1] (1.Meteorological Research Institute / Japan Meteorological Agency, 2.Office of Earth System Modeling / Numerical Prediction Division / Japan Meteorological Agency)

11:15 AM - 11:30 AM JST | 2:15 AM - 2:30 AM UTC

[AAS07-09] Emulating rainfall-runoff-inundation model with deep convolutional neural network

*Masahiro Momoi[1], Shunji Kotsuki[2], Ryota Kikuchi[3], Satoshi Watanabe[4], Masafumi Yamada[5], Shiori Abe[6], Akira Watanuki[7] (1.DoerResearch Inc., 2.Center for Environmental Remote Sensing, Chiba University, 3.Office of Society Academia Collaboration for Innovation, Kyoto University, 4.School of Engineering, The university of Tokyo, 5.Disaster Prevention Research Institute, Kyoto University, 6.Mitsui Consultants Co., Ltd., 7.Civil Engineering & Eco-Technology Consultants Co.,Ltd.)

11:30 AM - 11:45 AM JST | 2:30 AM - 2:45 AM UTC

[AAS07-10] Microphysics dependency on the reproducibility of the MJO in the DYAMOND winter phase experiment on NICAM

★Invited Papers

*Tamaki Suematsu[1], Yohei Yamada[2], Chihiro Kodama[2], Tomoki Miyakawa[1], Hiroaki Miura[3], Masaki Satoh[1] (1.Atmosphere and Ocean Research Institute, The University of Tokyo, 2.Japan Agency for Marine-Earth Science and Technology, 3.Graduate School of Science, The University of Tokyo)

11:45 AM - 12:00 PM JST | 2:45 AM - 3:00 AM UTC

[AAS07-11] Global large ensemble simulations with a cloud-resolving atmosphere and eddy-resolving ocean model

*Ryusuke Masunaga[1], Tomoki Miyakawa[1] (1.Atmosphere and Ocean Research Institute, The University of Tokyo)

12:00 PM - 12:15 PM JST | 3:00 AM - 3:15 AM UTC

[AAS07-12] Comparison of stable water isotopes between the cloud-microphysical processes simulated by isotope-incorporated NICAM

*Masahiro TANOUE[1], Yuki Takano[2], Kei Yoshimura[3], Hisashi Yashiro[1] (1.National Institute for Environmental Studies, 2.Atmosphere and Ocean Research Institute, The University of Tokyo, 3.Institute of Industrial Science, the University of Tokyo)

[J] Oral | A (Atmospheric and Hydrospheric Sciences)：A-OS Ocean Sciences & Ocean Environment

9:00 AM - 10:30 AM JST | 12:00 AM - 1:30 AM UTC | Ch.09 Zoom Room 09

[A-OS15] Ocean circulation and material cycle in coastal seas

convener:Naoki Furuichi(Fisheries Technology Institute, Japan Fisheries Research and Education Agency), Akihiko Morimoto(Ehime University), Kazuhiko Ichimi(Faculty of Agriculture, Kagawa University), Daisuke Takahashi(Tokai University), Chairperson:Naoki Furuichi(Fisheries Technology Institute, Japan Fisheries Research and Education Agency), Akihiko Morimoto(Ehime University), Tomaso Esposti Ongaro(Istituto Nazionale di Geofisica e Vulcanologia, Italy), Sakshi Ramesh Shiradhonkar (Department of Environment Systems, University of Tokyo)

9:00 AM - 9:15 AM JST | 12:00 AM - 12:15 AM UTC

[AOS15-01] Intrusion of lower water into a coastal bay driven by a tropical storm

*Hajime Nishigaki[1], Kiyoshi Tanaka[2], Chul-hoon Hong[3] (1.Faculty of Science and Technology, Oita University, 2.Atmosphere and Ocean Research Institute, The University of Tokyo, 3.Division of Marine Production System Management, Pukyong National University)

9:15 AM - 9:30 AM JST | 12:15 AM - 12:30 AM UTC

[AOS15-02] Estimating the transport and settlement distribution of abalone larvae in the Otsuchi bay using high-resolution particle tracking model

*Yoshimasa Matsumura[1], Takashi T Sakamoto[1], Yuki Minegishi[1], Jun Hayakawa[1], Kosei Komatsu[1], Kiyoshi Tanaka[1], Koji Hamasaki[1], Tomohiko Kawamura[1] (1.Atmosphere and Ocean Research Institute, University of Tokyo)

9:30 AM - 9:45 AM JST | 12:30 AM - 12:45 AM UTC

[AOS15-03] Study on 3D oceanic transport of coral larvae in reef areas on the northwest coast of Okinawa Main Island

*Kimika Takeyasu[1], Yusuke Uchiyama[1], Xu Zhang[1], Kosei Matsushita[1], Satoshi Mitarai[2] (1.Graduate School of Engineering, Kove University, 2.Okinawa Institute of Science and Technology Graduate University)

9:45 AM - 10:00 AM JST | 12:45 AM - 1:00 AM UTC

[AOS15-04] Numerical study on wave breaking and refection processes on steep bottom slope

*Tsuyoshi Kaneko[1], Yoshihiro Ohmura[2], Naoki Furuichi[2], Shinya Saeki[1] (1.Aratani Civil Engineering Consultants CO.,LTD., 2.Japan Fisheries Research and Education Agency)

10:00 AM - 10:15 AM JST | 1:00 AM - 1:15 AM UTC

[AOS15-05] Operation and observations of the Autonomous Ocean Vehicle (AOV) around Japan coasts

*Kohei Ino[1], Shinji Sugiyama[1], Takahiro Kon[1], Rika Nozawa[1], Chikara TSUCHIYA[1] (1.Hydrographic and Oceanographic Department, Japan Coast Guard)

10:15 AM - 10:30 AM JST | 1:15 AM - 1:30 AM UTC

[AOS15-06] Influence of observational missing on harmonic constants analyzed by the least squares method

*Chikara TSUCHIYA[1], Kohei INO[1], Takahiro KON[1], Rika NOZAWA[1], Shinji SUGIYAMA[1] (1.Hydrographic and Oceanographic Department, Japan Coast Guard)

[J] Oral | A (Atmospheric and Hydrospheric Sciences)：A-OS Ocean Sciences & Ocean Environment

10:45 AM - 12:05 PM JST | 1:45 AM - 3:05 AM UTC | Ch.09 Zoom Room 09

[A-OS15] Ocean circulation and material cycle in coastal seas

convener:Naoki Furuichi(Fisheries Technology Institute, Japan Fisheries Research and Education Agency), Akihiko Morimoto(Ehime University), Kazuhiko Ichimi(Faculty of Agriculture, Kagawa University), Daisuke Takahashi(Tokai University), Chairperson:Naoki Furuichi(Fisheries Technology Institute, Japan Fisheries Research and Education Agency), Akihiko Morimoto(Ehime University), Tomaso Esposti Ongaro(Istituto Nazionale di Geofisica e Vulcanologia, Italy), Sakshi Ramesh Shiradhonkar (Department of Environment Systems, University of Tokyo)

10:45 AM - 11:00 AM JST | 1:45 AM - 2:00 AM UTC

[AOS15-07] Observation of a river front using drones

*Kentaro Takami[1], Shinichiro Kida[2], Atsuhiko Isobe[2] (1.Kyushu University Interdisciplinary Graduate School of Engineering Sciences, 2.Research Institute for Applied Mechanics, Kyushu University)

11:00 AM - 11:15 AM JST | 2:00 AM - 2:15 AM UTC

[AOS15-08] Behavior of suspended particulate matter and Bottom boundary layer processes off Fukushima Prefecture

*Naoki Furuichi[1], Hideki Kaeriyama[2], Koichi Sugimatsu[1] (1.Fisheries Technology Institute, Japan Fisheries Research and Education Agency , 2.Fisheries Research Institute, Japan Fisheries Research and Education Agency)

11:15 AM - 11:30 AM JST | 2:15 AM - 2:30 AM UTC

[AOS15-09] Long-term trends of oxygen concentration in the waters in bank and shelves of the southern Japan Sea

*Tsuneo Ono[1] (1.Fisheries Research and Education Agency)

11:30 AM - 11:45 AM JST | 2:30 AM - 2:45 AM UTC

[AOS15-10] Interannual variations of nutrient concentrations and the mechanisms of nutrient supply in the western Seto Inland Sea

*Sohei Ogawa[1], Naoki Yoshie[1], Hidezirou Ohnishi[1] (1.Center for Marine Environmental Studies, Ehime University)

11:45 AM - 12:00 PM JST | 2:45 AM - 3:00 AM UTC

[AOS15-11] Standing stock and species composition of planktonic copepods occurred in Harima Nada in the eastern Seto Inland Sea, Japan

*Hamazaki Yuya[1], Hitomi Yamaguchi[1], Kuninao Tada[1], Kazuhiko Ichimi[1] (1.Graduate school of Agriculture Kagawa University)

12:00 PM - 12:05 PM JST | 3:00 AM - 3:05 AM UTC

[AOS15-12] Discussion

[J] Oral | A (Atmospheric and Hydrospheric Sciences)：A-OS Ocean Sciences & Ocean Environment

3:30 PM - 5:00 PM JST | 6:30 AM - 8:00 AM UTC | Ch.11 Zoom Room 11

[A-OS17] Chemical and Biological Oceanography

convener:Kazuhiro Misumi(Environmental Science Research Laboratory, Central Research Institute of Electric Power Industry), Sayaka Yasunaka(Japan Agency for Marine-Earth Science and Technology), Chairperson:Kazuhiro Misumi(Environmental Science Research Laboratory, Central Research Institute of Electric Power Industry), Sayaka Yasunaka(Japan Agency for Marine-Earth Science and Technology)

3:30 PM - 3:45 PM JST | 6:30 AM - 6:45 AM UTC

[AOS17-01] A new SI traceable silicon standard solution for certification of nutrients CRM and measurement of silicate in seawater, part two

*Michio Aoyama[1,2], Chikako Cheong[3], Tsutomu Miura[3], Takeshi Fujii[4], Hitoshi Mitsuda[4], Tomomi Sone[5], Hiroshi Uchida[1], Akihiko Murata[1] (1.Research Institute of Global Change, The Japan Agency for Marine-Earth Science and Technology , 2.Center for Research in Isotopes and Environmental Dynamic, Faculty of Life and Environmental Sciences, University of Tsukuba, 3.National Metrology Institute of Japan (NMIJ), National Institute of Advanced Industrial Science and Technology (AIST), 4.Laboratory for Instrumentation and Analysis, KANSO CO., LTD., 5.MARINE WORKS JAPAN LTD.)

3:45 PM - 4:00 PM JST | 6:45 AM - 7:00 AM UTC

[AOS17-02] Spatio-temporal variability of subsurface Chl-a maximum in the world ocean

*Sayaka Yasunaka[1], Tsuneo Ono[2], Kosei Sasaoka[1], Kanako Sato[1] (1.Japan Agency for Marine-Earth Science and Technology, 2.Japan Fisheries Research and Education Agency)

4:00 PM - 4:15 PM JST | 7:00 AM - 7:15 AM UTC

[AOS17-03] **Improvements of ocean biogeochemical simulation of the North Pacific Ocean due to an enhanced horizontal resolution of an ocean model**

*Hiroyuki Tsujino[1], Toyama Katsuya[1], Hideyuki Nakano[1], Shiro Nishikawa[2], Toru Sugiyama[2], Haruka Nishikawa[2], Yoichi Ishikawa[2] (1.Japan Meteorological Agency / Meteorological Research Institute, 2.Japan Agency for Marine-Earth Science and Technology)

4:15 PM - 4:30 PM JST | 7:15 AM - 7:30 AM UTC

[AOS17-04] A modeling study on distribution of dissolved Zinc in the North Pacific

*Kiminori Sugino[1], Akira Oka[1] (1.Atmosphere and Ocean Research Institute, The University of Tokyo)

4:30 PM - 4:45 PM JST | 7:30 AM - 7:45 AM UTC

[AOS17-05] Geographical variation of Sr/Ca in skipjack tuna (*Katsuwonus peamis*) collected from Northwestern Pacific Ocean

*Shohgo Kawashima[1], Takaaki Itai[1] (1.The University of Tokyo)

4:45 PM - 5:00 PM JST | 7:45 AM - 8:00 AM UTC

[AOS17-06] Discussion about marine chemistry and biology

*Kazuhiro Misumi[1] (1.Environmental Science Research Laboratory, Central Research Institute of Electric Power Industry)

[J] Oral | A (Atmospheric and Hydrospheric Sciences)：A-CG Complex & General

9:00 AM - 10:30 AM JST | 12:00 AM - 1:30 AM UTC | Ch.11 Zoom Room 11

[A-CG39] Science in the Arctic Region

convener:Tetsu Nakamura(Faculty of Environmental Earth Science, Hokkaido University), Jun Ono(Japan Agency for Marine-Earth and Science and Technology), Rigen Shimada(Japan Aerospace Exploration Agency), Tomoki Morozumi(Research Faculty of Agriculture, Hokkaido University), Chairperson:Tetsu Nakamura(Faculty of Environmental Earth Science, Hokkaido University), Jun Ono(Japan Agency for Marine-Earth and Science and Technology), Tomoki Morozumi(Research Faculty of Agriculture, Hokkaido University), Rigen Shimada(Japan Aerospace Exploration Agency)

9:00 AM - 9:15 AM JST | 12:00 AM - 12:15 AM UTC

[ACG39-01] Rapid Arctic warming enhances Eurasian heat wave and East Asian heavy rainfall

*Tetsu Nakamura[1], Tomonori Sato[1] (1.Faculty of Environmental Earth Science, Hokkaido University)

9:15 AM - 9:30 AM JST | 12:15 AM - 12:30 AM UTC

[ACG39-02] Seasonal and long-term variations in the top of the atmosphere shortwave radiation over the Arctic

*Michinari Amma[1], Tadahiro Hayasaka[1] (1.Graduate School of Science, Tohoku University)

9:30 AM - 9:45 AM JST | 12:30 AM - 12:45 AM UTC

[ACG39-03] **Machine learning prediction of wildfire over the Republic of Sakha, Russia**

*Teppei J Yasunari[1,2,3], Ichigaku Takigawa[4,5], Kyu-Myong Kim[6], Akira Takeshima[7] (1.Arctic Research Center, Hokkaido University, 2.Global Station for Arctic Research, GI-CoRE, Hokkaido University, Sapporo, Japan, 3.Center for Natural Hazards Research, Hokkaido University, 4.RIKEN Center for Advanced Intelligence Project, 5.Institute for Chemical Reaction Design and Discovery (WPI-ICReDD), Hokkaido University, 6.NASA Goddard Space Flight Center, 7.Department of Civil Engineering, The University of Tokyo)

9:45 AM - 10:00 AM JST | 12:45 AM - 1:00 AM UTC

[ACG39-04] Recent Fire Trends in the Arctic Region under Climate Change

*Hiroshi Hayasaka[1] (1.Arctic Research Center, Hokkaido University)

10:00 AM - 10:15 AM JST | 1:00 AM - 1:15 AM UTC

[ACG39-05] Thaw subsidence and frost heave after 2018-20 wildfires around Batagay detected by InSAR and field observation

*Kazuki Yanagiya[1], Masato Furuya[2], Go Iwahana[3,4], Petr Danilov[5] (1.Graduate School of Science, Hokkiado University, 2.Department of Earth and Planetary Sciences, Hokkaido University, 3.International Arctic Research Center, University of Alaska Fairbanks, 4.Arctic Research Center, Hokkaido University, 5.Institute of Northern Applied Ecology North-Eastern Federal University in Yakutsk)

10:15 AM - 10:30 AM JST | 1:15 AM - 1:30 AM UTC

[ACG39-06] Detection of surface displacement caused by permafrost in Lena river delta using Sentinel-1 InSAR

*Ryuji Yamaguchi[1] (1.Department of Natural History Sciences, Graduate School of Science, Hokkaido University)

[J] Oral | A (Atmospheric and Hydrospheric Sciences)：A-CG Complex & General

10:45 AM - 12:15 PM JST | 1:45 AM - 3:15 AM UTC | Ch.11 Zoom Room 11

[A-CG39] Science in the Arctic Region

convener:Tetsu Nakamura(Faculty of Environmental Earth Science, Hokkaido University), Jun Ono(Japan Agency for Marine-Earth and Science and Technology), Rigen Shimada(Japan Aerospace Exploration Agency), Tomoki Morozumi(Research Faculty of Agriculture, Hokkaido University), Chairperson:Tetsu Nakamura(Faculty of Environmental Earth Science, Hokkaido University), Jun Ono(Japan Agency for Marine-Earth and Science and Technology), Tomoki Morozumi(Research Faculty of Agriculture, Hokkaido University), Rigen Shimada(Japan Aerospace Exploration Agency)

10:45 AM - 11:00 AM JST | 1:45 AM - 2:00 AM UTC

[ACG39-07] Research progresses of PAWCs (Pan-Arctic Water-Carbon Cycles) focusing on water-carbon cycles in northern Eurasia

★Invited Papers

*Tetsuya Hiyama[1], Hotaek Park[2], Tomonori Sato[3], Hiroki Mizuochi[4], Akihiko Ito[5], Kazuhito Ichii[6], Yoshihiro Iijima[7] (1.Institute for Space-Earth Environmental Research, Nagoya University, 2.Japan Agency for Marine-Earth Science and Technology, 3.Graduate School of Environmental Science, Hokkaido University, 4.Geological Survey of Japan, National Institute of Advanced Industrial Science and Technology, 5.Center for Global Environmental Research, National Institute for Environmental Studies, 6.Center for Environmental Remote Sensing, Chiba University, 7.Graduate School of Bioresources, Mie University)

11:00 AM - 11:15 AM JST | 2:00 AM - 2:15 AM UTC

[ACG39-08] PMIP4/CMIP6 last interglacial simulations using three different versions of MIROC: importance of vegetation

*Ryouta O'ishi[1], Wing-Le Chan[1], Ayako Abe-Ouchi[1,2,3], Sam Sherriff-Tadano[1], Rumi Ohgaito[3], Masakazu Yoshimori[1] (1.Atmosphere and Ocean Research Institute, the Universitoy of Tokyo, 2.National Institute of Polar Research, 3.Japan Agency for Marine–Earth Science and Technology)

11:15 AM - 11:30 AM JST | 2:15 AM - 2:30 AM UTC

[ACG39-09] Future projection of greenhouse gas emissions due to permafrost degradation with a global land surface model

*Tokuta Yokohata[1], Kazuyuki Saito[2], Go Iwahana[3], Katsumasa Tanaka[1,4] (1.National Institute for Environmental Studies, 2.Japan Agency for Marine-Earth Science and Technology, 3.University of Alaska, Fairbanks, 4.Laboratoire des Sciences du Climat et de l'Environnement (LSCE), Commissariat à l'énergie atomique et aux énergies alternatives (CEA))

11:30 AM - 11:45 AM JST | 2:30 AM - 2:45 AM UTC

[ACG39-10] Record high Pacific Arctic seawater temperatures and delayed sea ice advance in response to episodic atmospheric blocking

*Tsubasa Kodaira[1], Takuji Waseda[1], Takehiko Nose[1], Jun Inoue[2] (1.The University of Tokyo, 2.NIPR)

11:45 AM - 12:00 PM JST | 2:45 AM - 3:00 AM UTC

[ACG39-11] Laboratory experiments of ice floe formation under wave motions

*Yasushi Fujiwara[1], Tomotaka Katsuno[1], Takuji Waseda[1], Takehiko Nose[1], Tsubasa Kodaira[1] (1.Graduate School of Frontier Sciences, the University of Tokyo)

12:00 PM - 12:15 PM JST | 3:00 AM - 3:15 AM UTC

[ACG39-12] Experimental research on wave attenuation in the Marginal Ice Zone

*Tomotaka Katsuno[1], Yasushi Fujiwara[1], Takuji Waseda[1], Takehiko Nose[1], Tsubasa Kodaira[1] (1.Graduate School of Frontier Sciences, University of Tokyo)

[J] Oral | A (Atmospheric and Hydrospheric Sciences)：A-CG Complex & General

1:45 PM - 3:15 PM JST | 4:45 AM - 6:15 AM UTC | Ch.11 Zoom Room 11

[A-CG39] Science in the Arctic Region

convener:Tetsu Nakamura(Faculty of Environmental Earth Science, Hokkaido University), Jun Ono(Japan Agency for Marine-Earth and Science and Technology), Rigen Shimada(Japan Aerospace Exploration Agency), Tomoki Morozumi(Research Faculty of Agriculture, Hokkaido University), Chairperson:Tetsu Nakamura(Faculty of Environmental Earth Science, Hokkaido University), Jun Ono(Japan Agency for Marine-Earth and Science and Technology), Tomoki Morozumi(Research Faculty of Agriculture, Hokkaido University), Rigen Shimada(Japan Aerospace Exploration Agency)

1:45 PM - 2:00 PM JST | 4:45 AM - 5:00 AM UTC

[ACG39-13] Impacts of Riverine Carbon and Nutrient Delivery on Arctic Ocean Acidification

*Yuanxin Zhang[1], Michiyo Yamamoto-Kawai[1], Eiji Watanabe[2] (1.Tokyo University of Marine Science and Technology, 2.Japan Agency for Marine-Earth Science and Technology)

2:00 PM - 2:15 PM JST | 5:00 AM - 5:15 AM UTC

[ACG39-14] Spreading of aragonite undersaturated water in the Canada Basin of the Arctic Ocean

*Haruka Tsujimoto[1], Michiyo Yamamoto-Kawai[1], Yuanxin Zhang[1] (1.Tokyo University of Marine Science and Technology)

2:15 PM - 2:30 PM JST | 5:15 AM - 5:30 AM UTC

[ACG39-15] Glacier and whale monitoring with an Ocean-Bottom Seismometer at the calving front

*Evgeny A. Podolskiy[1], Yoshio Murai[2], Naoya Kanna[3], Shin Sugiyama[4] (1.Arctic Research Center, Hokkaido University, 2.Institute of Seismology and Volcanology, Faculty of Science, Hokkaido University, 3.Atmosphere and Ocean Research Institute, University of Tokyo, 4.Institute of Low Temperature Science, Hokkaido University)

2:30 PM - 2:45 PM JST | 5:30 AM - 5:45 AM UTC

[ACG39-16] Cloud radiative effect on the 2019 major surface melt area expansion over the Greenland ice sheet

*Masashi Niwano[1,2], Akihiro Hashimoto[1], Teruo Aoki[2,1], Satoshi Hirose [3], Rigen Shimada[4], Motoshi Nishimura[2], Masahiro Hori[5] (1.Meteorological Research Institute, 2.National Institute of Polar Research, 3.New Chitose Aviation Weather Station, Japan Meteorological Agency, 4.Earth Observation Research Center, Japan Aerospace Exploration Agency, 5.School of Sustainable Design, University of Toyama)

2:45 PM - 3:00 PM JST | 5:45 AM - 6:00 AM UTC

[ACG39-17] Mass loss of the Greenland ice sheet until the year 3000 simulated with the model SICOPOLIS

*Ralf Greve[1,2], Christopher Chambers[1], Reinhard Calov[3] (1.Institute of Low Temperature Science, Hokkaido University, Sapporo, Japan, 2.Arctic Research Center, Hokkaido University, Sapporo, Japan, 3.Potsdam Institute for Climate Impact Research, Member of the Leibniz Association, Potsdam, Germany)

3:00 PM - 3:15 PM JST | 6:00 AM - 6:15 AM UTC

[ACG39-18] **Supraglacial lakes evolution on Tracy and Heilprin Glaciers, northwestern Greenland**

*YEFAN WANG[1,2], Shin Sugiyama[1] (1.Institute of Low Temperature Science, Hokkaido University, 2.Graduate School of Environmental Science, Hokkaido University)

[J] Oral | H (Human Geosciences)：H-GG Geography

3:30 PM - 5:00 PM JST | 6:30 AM - 8:00 AM UTC | Ch.16 Zoom Room 16

[H-GG01] Use and management of natural resources and environment: Dialogues between earth and social sciences

convener:Gen Ueda(Graduate School of Social Sciences, Hitotsubashi University), Yoshinori OTSUKI(Institute of Geography, Graduate School of Science, Tohoku University), Takahisa Furuichi(Forest and Forest Products Research Institute), Toru Sasaki(Miyagi University of Education), Chairperson:Gen Ueda(Graduate School of Social Sciences, Hitotsubashi University), Yoshinori OTSUKI(Institute of Geography, Graduate School of Science, Tohoku University), Toru Sasaki(Miyagi University of Education)

3:30 PM - 3:45 PM JST | 6:30 AM - 6:45 AM UTC

[HGG01-01] Disaster Adaptive Strategy in a Flood-Prone area in Sri Lanka: A Case Study of Response and Recovery of Hard Rain and Flood Disaster

*Tsuchida Ryo[1] (1.Graduate School of Advanced Integrated Studies in Human Survivability, Kyoto University)

3:45 PM - 4:00 PM JST | 6:45 AM - 7:00 AM UTC

[HGG01-02] Is it possible to achieve economic development and environmental improvement?

*Toru Sasaki[1] (1.Miyagi University of Education)

4:00 PM - 4:15 PM JST | 7:00 AM - 7:15 AM UTC

[HGG01-03] Changes in "Tajima Cattle System" in Ojiro, Kami Town, Hyogo Prefecture: How to Continue to Nurture "Unique Cattle Here?"

*DAICHI KOHMOTO[1] (1.Nara University of Education)

4:15 PM - 4:30 PM JST | 7:15 AM - 7:30 AM UTC

[HGG01-04] Human and Physical Aspects in Geography: Research Issues on Natural Resources and Environment

*Gen Ueda[1], Yoshinori OTSUKI[2], Takahisa Furuichi[3] (1.Graduate School of Social Sciences, Hitotsubashi University, 2.Graduate School of Science, Tohoku University, 3.Forest and Forest Products Research Institute)

4:30 PM - 4:45 PM JST | 7:30 AM - 7:45 AM UTC

[HGG01-05] **Geographical implications of disturbed forest and degraded landscape from historical and present perspectives in Japan**

*Takahisa Furuichi[1,2,3], Hiromu Daimaru[1], Wataru Murakami[1], Takashi Okamoto[1], Toru Sasaki[3], Gen Ueda[4] (1.Forest and Forest Products Research Institute, 2.University of the Sunshine Coast, 3.Miyagi University of Education, 4.Graduate School of Social Sciences, Hitotsubashi University)

4:45 PM - 5:00 PM JST | 7:45 AM - 8:00 AM UTC

[HGG01-06] Biomagnetic monitoring investigations of the spatial distribution of atmospheric fine magnetic particles:
case study of the Toyama-shi area, Japan

*Hiroki Shibata[1], Kazuo Kawasaki[1], Keiji Horikawa[1] (1.University of Toyama)

[J] Oral | H (Human Geosciences)：H-GM Geomorphology

9:00 AM - 10:30 AM JST | 12:00 AM - 1:30 AM UTC | Ch.14 Zoom Room 14

[H-GM03] Geomorphology

convener:Tsuyoshi Hattanji(Faculty of Life and Environmental Sciences, University of Tsukuba), Masayuki Seto(Fukushima Future Center for Regional Revitalization, Fukushima University), Chairperson:Tsuyoshi Hattanji(Faculty of Life and Environmental Sciences, University of Tsukuba)

9:00 AM - 9:15 AM JST | 12:00 AM - 12:15 AM UTC

[HGM03-01] Uplift-induced drainage divide migration and channel reorganization:Laboratory model experiment

*Akimasa Sakashita[1], Noritaka Endo[1] (1.Kanazawa university)

9:15 AM - 9:30 AM JST | 12:15 AM - 12:30 AM UTC

[HGM03-02] Adjustment timescales of channel width and hillslope angle to accelerated uplift: Insights into a basin-scale steady state

*Naoya Takahashi[1], J Bruce H Shyu[2], Yuki Matsushi[3], Ryoga Ohta[4], Shinji Toda[5] (1.Department of Earth Science, Graduate school of Science, Tohoku University, 2.Department of Geosciences, National Taiwan University, 3.Disaster Prevention Research Institute, Kyoto University, 4.Graduate school of Science, Kyoto University, 5.International Research Institute of Disaster Science, Tohoku University)

9:30 AM - 9:45 AM JST | 12:30 AM - 12:45 AM UTC

[HGM03-03] **Development of “steady-state” landforms in geomorphic experiments and the concept of “threshold hillslope”**

*Shunji Ouchi

9:45 AM - 10:00 AM JST | 12:45 AM - 1:00 AM UTC

[HGM03-04] Causes of concentrated revetment damage in the Hatto River in eastern Tottori Prefecture during the heavy rains in western Japan in July 2018

*Yoshinori Kodama[1], Taishi Sugimoto (1.Faculty of Agriculture, Tottori Univ.)

10:00 AM - 10:15 AM JST | 1:00 AM - 1:15 AM UTC

[HGM03-05] Initiation factors of an incised meandering river in steep mountainous terrain: a case study of the Higashigouchi River with high-angle bedding plane

*Takuma Watakabe[1], Hikaru Osawa[2], Noriyuki Arai[3], Issei Doi[3], Yosuke Yamakawa[2] (1.Kansai Research Center, Forestry and Forest Products Research Institute, 2.Mountain Science Center, Univ. of Tsukuba, 3. Disaster Prevention Research Institute, Kyoto University)

10:15 AM - 10:30 AM JST | 1:15 AM - 1:30 AM UTC

[HGM03-06] Generation of Terrain Classification Data for Ground Vulnerability Assessment Using 30m DEM by Digital Terrain Analysis

*Junko Iwahashi[1], Dai Yamazaki[2], Takayuki Nakano[1], Ryo Endo[1] (1.GSI of Japan, 2.Institute of Industrial Science, The University of Tokyo)

[J] Oral | H (Human Geosciences)：H-GM Geomorphology

10:45 AM - 12:15 PM JST | 1:45 AM - 3:15 AM UTC | Ch.14 Zoom Room 14

[H-GM03] Geomorphology

convener:Tsuyoshi Hattanji(Faculty of Life and Environmental Sciences, University of Tsukuba), Masayuki Seto(Fukushima Future Center for Regional Revitalization, Fukushima University), Chairperson:Masayuki Seto(Fukushima Future Center for Regional Revitalization, Fukushima University)

10:45 AM - 11:00 AM JST | 1:45 AM - 2:00 AM UTC

[HGM03-07] Analysis of step-structure affecting Cs and sediment transport at hillslope scale

*Seigo Fujiwara[1], Yuichi Onda[2], Yoshifumi Wakiyama[3], Toshiaki Anzai[4], Hiroaki Kato[2] (1.Master Program in Geosciences, Degree Programs in Life and Earth Sciences, University of Tsukuba, 2.Center for Research in Isotopes and Environmental Dynamics, University of Tsukuba, 3.Institute of Environmental Radioactivity, Fukushima University, 4.School of Life and Environmental Sciences, University of Tsukuba)

11:00 AM - 11:15 AM JST | 2:00 AM - 2:15 AM UTC

[HGM03-08] Lithological Controls on Mechanisms of Shallow Landslides Triggered by an Extreme Rainfall Event:

Comparative Survey on Hillslopes underlain by Granite and Granodiorite in the Northern Abukuma Mountains

*Arihito Kondo[1], Yuki Matsushi[2], Yoshinori OTSUKI[1] (1.Institute of Geography, Graduate School of Science, Tohoku University, 2.Disaster Prevention Research Institute, Kyoto University)

11:15 AM - 11:30 AM JST | 2:15 AM - 2:30 AM UTC

[HGM03-09] Reconstructing the transition of hillslope denudation in granite watersheds using cosmogenic nuclides: quantifying the anthropogenic impacts on soil coverage in the Tanakami Mountains, central Japan

*Ryoga Ohta[1,2], Yuki Matsushi[3], Hiroyuki Matsuzaki[4] (1.Graduate School of Science, Kyoto university, 2.JSPS Research Fellow DC, 3.Disaster Prevention Research Institute, Kyoto University, 4.Micro Analysis Laboratory, Tandem Accelerator, The University of Tokyo)

11:30 AM - 11:45 AM JST | 2:30 AM - 2:45 AM UTC

[HGM03-10] Distribution of infilling rates in hollows estimated from radiocarbon dates and high-resolution DEMs -A case study of granitic mountain slopes in Hiroshima City, Hiroshima Prefecture-

*Wataru Koga[1], Tsuyoshi Hattanji[2], Takahisa Furuichi[3], Shoji Doshida[4], Yasushi Tanaka[5] (1.University of Tsukuba graduate school of Life and Environmental Science, 2.University of Tsukuba department of Life and Environmental Science, 3.Forestry and Forest Products Research Institute, 4.National Research Institute of Fire and Disaster, 5.Komazawa University Faculty of Letters)

11:45 AM - 12:00 PM JST | 2:45 AM - 3:00 AM UTC

[HGM03-11] Paleoenvironment in Lake Olgoy, Mongolia based on the anaylses of sediment from the paleoshoreline

*Yuma Shibuya[1] (1.KANAZAWA UNIVERSITY)

12:00 PM - 12:15 PM JST | 3:00 AM - 3:15 AM UTC

[HGM03-12] 3D geomorphological analysis method for sea cliff: A case study of Miocene sedimentary rocks in Yonaguni Island

*Hayate Kimura[1], Toshihiko Ichihara[2], Hironobu Kan[1] (1.Graduate School of Integrated Sciences for Global Society, Kyushu University, 2.Sedimentary Environments Research)

[J] Oral | H (Human Geosciences)：H-SC Social Earth Sciences & Civil/Urban System Sciences

9:00 AM - 10:30 AM JST | 12:00 AM - 1:30 AM UTC | Ch.15 Zoom Room 15

[H-SC05] CCUS (Carbon Dioxide Capture, Utilization, and Storage) for Climate Mitigation

convener:Masao Sorai(Institute for Geo-Resources and Environment, National Institute of Advanced Industrial Science and Technology), Ziqiu Xue(Research Institute of Innovative Tech for the Earth), Masaatsu Aichi(Graduate School of Frontier Sciences, University of Tokyo), Yoshihiro Konno(The University of Tokyo), Chairperson:Masao Sorai(Institute for Geo-Resources and Environment, National Institute of Advanced Industrial Science and Technology)

9:00 AM - 9:15 AM JST | 12:00 AM - 12:15 AM UTC

[HSC05-01] Progresses of Nano-Scale Study on CO2 Utilization and Storage

*Yunfeng Liang[1] (1.The University of Tokyo)

9:15 AM - 9:30 AM JST | 12:15 AM - 12:30 AM UTC

[HSC05-02] Molecular Dynamics Study on Coal Matrix Swelling Characteristics by CO2, N2, and CO2–N2 Mixture

*Jinrong Cao[1], Yunfeng Liang[1], Yoshihiro Masuda[1], Ziqiu Xue[2], Toshifumi Matsuoka[3] (1.Department of Systems Innovation, The University of Tokyo, 2.Research Institute of Innovative Technology for the Earth, 3.Emeritus Professor, Kyoto University)

9:30 AM - 9:45 AM JST | 12:30 AM - 12:45 AM UTC

[HSC05-03] Wettability of CO_2/Water/Mineral Systems: Comparison of Water-wet and CO_2-wet systems by thermodynamics and molecular dynamics

*Masashige Shiga[1,2], Masaatsu Aichi[1], Masao Sorai[2] (1.The University of Tokyo, 2.AIST)

9:45 AM - 10:00 AM JST | 12:45 AM - 1:00 AM UTC

[HSC05-04] Coupled chemical osmosis and rock deformation: Numerical investigations and their comparison with experimental results

*Shogo Hirota[1], Tomochika Tokunaga[1], Ziqiu Xue[2], Takayuki Miyoshi[2,3], Hyuck Park[2] (1.Department of Environmental Systems, Graduate School of Frontier Science, the University of Tokyo, 2.Research Institute of Innovative Technology for the Earth, 3.Geological Carbon Dioxide Storage Technology Research Association)

10:00 AM - 10:15 AM JST | 1:00 AM - 1:15 AM UTC

[HSC05-05] Evaluation of Caprock Sealing Performance in Saline Aquifer Storage

*Yuuki Shigeoka[1], Haruki Nishiyama[1], Hiroshi Kinoto[1], Yukiko Shoji[2], Takaomi Tobase[2] (1.J-POWER Business Survice Corporation, 2.Electric Power Development Co.)

10:15 AM - 10:30 AM JST | 1:15 AM - 1:30 AM UTC

[HSC05-06] Recent advances in value of information analysis and application to geological CO_2 storage

*Takashi Goda[1], Kozo Sato[1], Takahiro Nakajima[2,3] (1.School of Engineering, The University of Tokyo, 2.Geological Carbon Dioxide Storage Technology Research Association, 3.Research Institute of Innovative Technology for the Earth)

[J] Oral | H (Human Geosciences)：H-SC Social Earth Sciences & Civil/Urban System Sciences

10:45 AM - 12:15 PM JST | 1:45 AM - 3:15 AM UTC | Ch.15 Zoom Room 15

[H-SC05] CCUS (Carbon Dioxide Capture, Utilization, and Storage) for Climate Mitigation

convener:Masao Sorai(Institute for Geo-Resources and Environment, National Institute of Advanced Industrial Science and Technology), Ziqiu Xue(Research Institute of Innovative Tech for the Earth), Masaatsu Aichi(Graduate School of Frontier Sciences, University of Tokyo), Yoshihiro Konno(The University of Tokyo), Chairperson:Masaatsu Aichi(Graduate School of Frontier Sciences, University of Tokyo)

10:45 AM - 11:00 AM JST | 1:45 AM - 2:00 AM UTC

[HSC05-07] Downhole Deformation Monitoring with High-Spatial-Resolution Distributed Strain Measurement in Optical Fiber during Water Injection Test

*Rasha Amer[1,2], Ziqiu Xue[1,2], Tsutomu Hashimoto[1,2], Takeya Nagata[1,2] (1.Geological Carbon Dioxide Storage Technology Research Association, 2.Research Institute of Innovative Tech for the Earth)

11:00 AM - 11:15 AM JST | 2:00 AM - 2:15 AM UTC

[HSC05-08] Advantages of Helically Wound optic-fiber Cables on VSP records

*Takayuki Miyoshi[1], Takahiro Nakajima[1], Ziqiu Xue[1] (1.Geological Carbon Dioxide Storage Technology Research Association / Research Institute of Innovative Technology for the Earth)

11:15 AM - 11:30 AM JST | 2:15 AM - 2:30 AM UTC

[HSC05-09] Numerical Simulation of Geophysical Changes based upon CO_2 Geological Storage and Leakage

*Yuki Kano[1,2], Tsuneo Ishido[1,2] (1.Geological Carbon Dioxide Storage Technology Research Association, 2.National Institute of Advanced Industrial Science and Technology)

11:30 AM - 11:45 AM JST | 2:30 AM - 2:45 AM UTC

[HSC05-10] Numerical simulation of electromagnetic exploration for CO_2 monitoring in horizontal multi-layered earth

*Haruhito Takuma[1], Takumi Ueda[1], Takahiro Nakajima[2,3] (1.Waseda University, 2.Geological Carbon Dioxide Storage Technology Research Association, 3.Research Institute of Innovative Technology for the Earth)

11:45 AM - 12:00 PM JST | 2:45 AM - 3:00 AM UTC

[HSC05-11] Observation of self-potential changes around a metal casing due to the injection of low pH solution in laboratory experiments

*Takuya Horikawa[1,2], Masao Sorai[1,2] (1.Geological Carbon Dioxide Storage Technology Research Association, 2.CO2 Geological Storage Research Group, GREEN, GSJ, AIST)

12:00 PM - 12:15 PM JST | 3:00 AM - 3:15 AM UTC

[HSC05-12] **Developing a science-based, quantitative approach for distinguishing CO2 injection-induced earthquakes from natural earthquakes**

*Takeshi Tsuji[1], Chanmaly Chhun[1], Tatsunori Ikeda[1], James Mori[2] (1.Department of Earth Resources Engineering, Kyushu University, 2.Kyoto University)

[J] Oral | H (Human Geosciences)：H-SC Social Earth Sciences & Civil/Urban System Sciences

1:45 PM - 3:15 PM JST | 4:45 AM - 6:15 AM UTC | Ch.15 Zoom Room 15

[H-SC05] CCUS (Carbon Dioxide Capture, Utilization, and Storage) for Climate Mitigation

convener:Masao Sorai(Institute for Geo-Resources and Environment, National Institute of Advanced Industrial Science and Technology), Ziqiu Xue(Research Institute of Innovative Tech for the Earth), Masaatsu Aichi(Graduate School of Frontier Sciences, University of Tokyo), Yoshihiro Konno(The University of Tokyo), Chairperson:Yoshihiro Konno(The University of Tokyo)

1:45 PM - 2:00 PM JST | 4:45 AM - 5:00 AM UTC

[HSC05-13] Development of a biological impact database on marine organisms

*Jiro Suekuni[1], Keisuke Uchimoto[1], Yuji Watanabe[1], Ziqiu Xue[1] (1.Research Institute of Innovative Technology for the Earth)

2:00 PM - 2:15 PM JST | 5:00 AM - 5:15 AM UTC

[HSC05-14] Numerical estimation of leakage suppression using CO_2 hydrate on the oceanic field scale

Takuya Wako[1], Yosuke Sawano[1], *Toru Sato[1] (1.University of Tokyo)

2:15 PM - 2:30 PM JST | 5:15 AM - 5:30 AM UTC

[HSC05-15] Numerical simulation of seafloor ground deformation during CO_2 underground storage using gas hydrate

*Sayuri Kimoto[1], Kento Uehira[1] (1.Kyoto University)

2:30 PM - 2:45 PM JST | 5:30 AM - 5:45 AM UTC

[HSC05-16] **Experimental Study on Formation Behavior of CO2 Hydrate in a Flow Field Assuming Carbon Dioxide Storage in Subseabed**

*Yuichi Magara[1], Taku Nishimura[1], Yoshihiro Konno[1], Yusuke Jin[2], Takaomi Tobase[3] (1.Graduate School of Frontier Science, the University of Tokyo , 2.National Institute of Advanced Industrial Science and Technology, 3.Electric Power Development Co.,Ltd.)

2:45 PM - 3:00 PM JST | 5:45 AM - 6:00 AM UTC

[HSC05-17] Cost analysis of CO_2 transportation in CCS deployed in Japan

*Hirotaka Isogai[1], Corey Adam Myers[2], Takao Nakagaki[2], Takeshi Myoi[3], Junichi Shimizu[3] (1.Department of Modern Mechanical Engineering, Waseda University , 2.Faculty of Waseda University, 3.Geological Carbon Dioxide Storage Technology Research Association / Research Institute of Innovative Technology for the Earth)

3:00 PM - 3:15 PM JST | 6:00 AM - 6:15 AM UTC

[HSC05-18] Consideration about public consensus building of CCS

*Takaomi Tobase[1] (1.Electric Power Development Co., Ltd.)

[J] Oral | H (Human Geosciences)：H-DS Disaster geosciences

9:00 AM - 10:30 AM JST | 12:00 AM - 1:30 AM UTC | Ch.17 Zoom Room 17

[H-DS09] Tsunami and tsunami forecast

convener:Hiroaki Tsushima(Meteorological Research Institute, Japan Meteorological Agency), Chairperson:Hiroaki Tsushima(Meteorological Research Institute, Japan Meteorological Agency)

9:00 AM - 9:15 AM JST | 12:00 AM - 12:15 AM UTC

[HDS09-01] Rapid magnitude estimation using long-period components of seismic waves

*Takahito Nishimiya[1], Akio Katsumata[2] (1.Meteorological Research Institute, Japan Meteorological Agency, 2.University of Toyama)

9:15 AM - 9:30 AM JST | 12:15 AM - 12:30 AM UTC

[HDS09-02] Validation of Tsunami Run-up Simulation Using Observed Tsunami Heights in the Sendai Plain after the 2011 Tohoku Tsunami

*Yoshinori Shigihara[1], Yuuki Eguchi[1], Tsuyoshi Tada[1] (1.Department of Civil and environmental Engineering, National Dedense Academy)

9:30 AM - 9:45 AM JST | 12:30 AM - 12:45 AM UTC

[HDS09-03] Numerical simulations for the 2006 and 2007 Kuril tsunamis

*Keiji Akai[1], Toshitaka Baba[2] (1.Graduate School of Engineering, Tokushima University, 2.Graduate School of Science and Technology, Tokushima University)

9:45 AM - 10:00 AM JST | 12:45 AM - 1:00 AM UTC

[HDS09-04] Causes and Solutions of Computational Instability in Tsunami Calculations by Finite Difference Method for Nonlinear Long Wave Equations

*Masaaki MINAMI[1] (1.Meteorological Research Institute)

10:00 AM - 10:15 AM JST | 1:00 AM - 1:15 AM UTC

[HDS09-05] Tsunami waveform analysis of 1929 Grand banks landslide tsunami

*Tatsuya Nakagaki[1], Yuichiro Tanioka[2] (1.Graduate school of Science, Hokkaido University, 2.Hokkaido University)

10:15 AM - 10:30 AM JST | 1:15 AM - 1:30 AM UTC

[HDS09-06] Development of automatic tsunami-detection method based on continuous analysis of offshore tsunami waveforms

*Hiroaki Tsushima[1], Naotaka YAMAMOTO CHIKASADA[2] (1.Meteorological Research Institute, Japan Meteorological Agency, 2.National Research Institute for Earth Science and Disaster Resilience)

[J] Oral | H (Human Geosciences)：H-CG Complex & General

3:30 PM - 5:00 PM JST | 6:30 AM - 8:00 AM UTC | Ch.15 Zoom Room 15

[H-CG25] Human social activities and earth and planetary sciences

convener:Kazuo Amano(Center for Spatial Information Science, The University of Tokyo), Takashi Oguchi(Center for Spatial Information Science, The University of Tokyo), Kayoko Yamamoto(University of Elctro-Communications), Masaki Ito(Institute of Industrial Science, the University of Tokyo), Chairperson:Kayoko Yamamoto(University of Elctro-Communications), Kazuo Amano(Center for Spatial Information Science, The University of Tokyo)

3:30 PM - 3:45 PM JST | 6:30 AM - 6:45 AM UTC

[HCG25-01] Significance of international webinars on Earth and Planetary Science: Cases of Geography and Geomorphology

*Takashi Oguchi[1] (1.Center for Spatial Information Science, The University of Tokyo)

3:45 PM - 4:00 PM JST | 6:45 AM - 7:00 AM UTC

[HCG25-02] Utilization of Digital Infrastructure Concerning Disaster Countermeasures in Japan

*Kayoko Yamamoto[1] (1.University of Elctro-Communications)

4:00 PM - 4:15 PM JST | 7:00 AM - 7:15 AM UTC

[HCG25-03] An Environmental Learning Support System Incorporating the Life Cycle Concept

*Kayoko Yamamoto[1], Akira Shirato[1] (1.University of Elctro-Communications)

4:15 PM - 4:30 PM JST | 7:15 AM - 7:30 AM UTC

[HCG25-04] Information exchange for earth science major graduates of a university by using Zoom

*Kazuo Amano[1,2], Satoshi Kanaguri[2] (1.Center for Spatial Information Science, The University of Tokyo , 2.Amano Geological Laboratory Japan)

4:30 PM - 4:45 PM JST | 7:30 AM - 7:45 AM UTC

[HCG25-05] How the Relationship between Society and Researchers Changes after the COVID-19 Disaster considering Rapid Spread of Online Technology

*Masaki Ito[1] (1.Institute of Industrial Science, the University of Tokyo)

4:45 PM - 5:00 PM JST | 7:45 AM - 8:00 AM UTC

[HCG25-06] Discussion

[J] Oral | S (Solid Earth Sciences)：S-GD Geodesy

9:00 AM - 10:30 AM JST | 12:00 AM - 1:30 AM UTC | Ch.22 Zoom Room 22

[S-GD01] Geodesy and Global Geodetic Observing System

convener:Koji Matsuo(Geospatial Information Authority of Japan), Yusuke Yokota(Institute of Industrial Science, The University of Tokyo), Toshimichi Otsubo(Hitotsubashi University), Chairperson:Koji Matsuo(Geospatial Information Authority of Japan), Akihisa Hattori(The Graduate University for Advanced Studies)

9:00 AM - 9:15 AM JST | 12:00 AM - 12:15 AM UTC

[SGD01-01] The Airborne Gravity Survey for Development of a New Precise Gravimetric Geoid Model in Japan

*Masahiro Nakashima[1], Kento Iio[1], Yasuhiro Iitsuka[1], Shinobu Kurihara[1], Kumikazu Ochi[1], Shuichi Omori[1], Tokuro Kodama[1], Masato Kuroyanagi[1], Masami Handa[1], Koji Matsuo[1] (1.Geospatial Information Authority of Japan)

9:15 AM - 9:30 AM JST | 12:15 AM - 12:30 AM UTC

[SGD01-02] Accuracy evaluation of airborne gravity data by the three-dimensional least-squares collocation method

*Koji Matsuo[1] (1.Geospatial Information Authority of Japan)

9:30 AM - 9:45 AM JST | 12:30 AM - 12:45 AM UTC

[SGD01-03] Introduction of Absolute Quantum Gravimeter (AQG)

*Masato KUROYANAGI[1], Masami HANDA[1], Tokuro KODAMA[1], Shinobu KURIHARA[1], Kumikazu OCHI[1], Hiroaki YAMAMOTO[1], Shuichi OMORI[1], Kento IIO[1], Masahiro NAKASHIMA[1], Yasuhiro IITSUKA[1] (1.Geospatial Information Authority of Japan)

9:45 AM - 10:00 AM JST | 12:45 AM - 1:00 AM UTC

[SGD01-04] GRACE/GRACE-FO Observed Mass Change Patterns of Antarctica Extracted by ICA Method

*SHI TIANYAN[1], Yoichi Fukuda[1], Koichiro Doi[1], Jun'ichi Okuno[1] (1.Department of Polar Science, Gradualate University for Advanced studies School of Multidisciplinary Sciences)

10:00 AM - 10:15 AM JST | 1:00 AM - 1:15 AM UTC

[SGD01-05] Gravity observations at Jang Bogo Station, Antarctica, and the scale factor calibrations of different type relative gravimeters

*Yoichi Fukuda[1], Jun'ichi Okuno[1], Koichiro Doi[1], Choon-ki Lee[2] (1.National Institute of Polar Research, 2.Korea Polar Research Institute)

10:15 AM - 10:30 AM JST | 1:15 AM - 1:30 AM UTC

[SGD01-06] Parallel observation with superconducting gravimeters TT70 #011 and iGrav #028 at Matsushiro, Japan (2016–2018)

*Yuichi Imanishi[1], Hiroshi Ikeda[2] (1.Earthquake Research Institute, The University of Tokyo, 2.KEK)

[J] Oral | S (Solid Earth Sciences)：S-GD Geodesy

10:45 AM - 12:15 PM JST | 1:45 AM - 3:15 AM UTC | Ch.22 Zoom Room 22

[S-GD01] Geodesy and Global Geodetic Observing System

convener:Koji Matsuo(Geospatial Information Authority of Japan), Yusuke Yokota(Institute of Industrial Science, The University of Tokyo), Toshimichi Otsubo(Hitotsubashi University), Chairperson:Masahiro Nakashima(Geospatial Information Authority of Japan), Yuji ITOH(Earthquake Research Institute, The University of Tokyo)

10:45 AM - 11:00 AM JST | 1:45 AM - 2:00 AM UTC

[SGD01-07] Absolute Gravity Measurements at Teshikaga in 2019 and 2020

*Yuichi Imanishi[1], Ryuichi Nishiyama[1], Kazunari Nawa[2] (1.Earthquake Research Institute, The University of Tokyo, 2.AIST)

11:00 AM - 11:15 AM JST | 2:00 AM - 2:15 AM UTC

[SGD01-08] Reading value dependence of scale factors for LaCoste & Romberg relative gravimeters

*TAMAKI WAKABAYASHI[1], Takahito Kazama[1], Yoichi Fukuda[2], Yuki Abe[3], Shin Yoshikawa[4], Takahiro Ohkura[4], Yuichi Imanishi[5], Ryuichi Nishiyama[5], Keigo Yamamoto[6] (1.Graduate School of Science, Kyoto University, 2.National Institute of Polar Research, 3.Hot Springs Research Institute of Kanagawa Prefecture, 4.Aso Volcanological Laboratory, Kyoto University, 5.Earthquake Research Institute, The University of Tokyo, 6.Disaster Prevention Research Institute, Kyoto University)

11:15 AM - 11:30 AM JST | 2:15 AM - 2:30 AM UTC

[SGD01-09] Vertical Movements of GEONET sites in Niigata region (Part 2)

*Seiichi Shimada[1], Yuka Ito[1], Masaatsu Aichi[1], Takemu Seki[2], Tomochika Tokunaga[1] (1.Graduate School of Frontier Sciences, The University of Tokyo, 2.Department of Systems Innovation, Faculty of Engineering, The University of Tokyo)

11:30 AM - 11:45 AM JST | 2:30 AM - 2:45 AM UTC

[SGD01-10] An Apparent Reduction of Crustal Activity before the Great East Japan Earthquake

*Yasushi Harada[1], Yuka Murai[1] (1.School of Marine Science and Technology, Tokai University)

11:45 AM - 12:00 PM JST | 2:45 AM - 3:00 AM UTC

[SGD01-11] Early afterslip of the 2011 Tohoku-Oki sequence estimated by the GNSS carrier phase to fault slip approach

*Yusuke Tanaka[1], Yusaku Ohta[1], SHINICHI MIYAZAKI[2] (1.Tohoku University, 2.Kyoto University)

12:00 PM - 12:15 PM JST | 3:00 AM - 3:15 AM UTC

[SGD01-12] **Crustal subsidence as the elastic response to the SWJ heavy rain in 2020**

*Kosuke Heki[1], Syachrul Arief[2] (1.Department of Earth and Planetary Sciences, Faculty of Science, Hokkaido University, 2.Indonesia Geospatial Information Agency)

[J] Oral | S (Solid Earth Sciences)：S-GD Geodesy

1:45 PM - 3:15 PM JST | 4:45 AM - 6:15 AM UTC | Ch.22 Zoom Room 22

[S-GD01] Geodesy and Global Geodetic Observing System

convener:Koji Matsuo(Geospatial Information Authority of Japan), Yusuke Yokota(Institute of Industrial Science, The University of Tokyo), Toshimichi Otsubo(Hitotsubashi University), Chairperson:Yuichi Aoyama(National Institute of Polar Research), Shun-ichi Watanabe(Hydrographic and Oceanographic Department, Japan Coast Guard)

1:45 PM - 2:00 PM JST | 4:45 AM - 5:00 AM UTC

[SGD01-13] An Update of Daily Coordinate Product Estimated by the New Analysis Strategy of GEONET

*Naofumi Takamatsu[1], Hiroki Muramatsu[1], Chiaki Kato[1], Keitaro Ohno[1], Satoshi Abe[1], Tomoaki Furuya[1], Yohei Hiyama[1] (1.GSI of Japan)

2:00 PM - 2:15 PM JST | 5:00 AM - 5:15 AM UTC

[SGD01-14] Development of coordinate calculation strategy for GEONET station using multi GNSS PPP aiming future management scheme of the national coordinate

*Hiroyuki Nakagawa[1], Satoshi ABE[1], MURAMATSU Hiroki[1], Naofumi Takamatsu[1] (1.The Geospatial Information Authority of Japan)

2:15 PM - 2:30 PM JST | 5:15 AM - 5:30 AM UTC

[SGD01-15] On the performance of sidereal filter for 30-sec kinematic GPS to mitigate multipath errors

*Yuji ITOH[1], Yosuke Aoki[1] (1.Earthquake Research Institute, The University of Tokyo)

2:30 PM - 2:45 PM JST | 5:30 AM - 5:45 AM UTC

[SGD01-16] Development and assessment of the low-cost multi frequencies GNSS receiver and logger system

*Yusaku Ohta[1] (1.Research Center for Prediction of Earthquakes and Volcanic Eruptions, Graduate School of Science, Tohoku University)

2:45 PM - 3:00 PM JST | 5:45 AM - 6:00 AM UTC

[SGD01-17] Optimization of water vapor analysis using ship-borne GNSS measurement

*Yoshinori Shoji[1] (1.The Second Laboratory of Observation and Data Assimilation Research Department, Meteorological Research Institute)

3:00 PM - 3:15 PM JST | 6:00 AM - 6:15 AM UTC

[SGD01-18] Developmental status of Omni-SLR for small-size, low-cost SLR system

*Toshimichi Otsubo[1], Hiroshi Araki[2], Yusuke Yokota[3], Koichiro Doi[4], Hiroo Kunimori[5], Mihoko Kobayashi[1], Ryo Tsukagoshi[1], Masato Tomomatsu[1], Takehiro Matsumoto[6] (1.Hitotsubashi University, 2.National Astronomical Observatory of Japan, 3.University of Tokyo, 4.National Institute of Polar Research, 5.National Institute of Information and Communications Technology, 6.Japan Aerospace Exploration Agency)

[J] Oral | S (Solid Earth Sciences)：S-GD Geodesy

3:30 PM - 5:00 PM JST | 6:30 AM - 8:00 AM UTC | Ch.22 Zoom Room 22

[S-GD01] Geodesy and Global Geodetic Observing System

convener:Koji Matsuo(Geospatial Information Authority of Japan), Yusuke Yokota(Institute of Industrial Science, The University of Tokyo), Toshimichi Otsubo(Hitotsubashi University), Chairperson:Yuto Nakamura(Hydrographic and Oceanographic Department, Japan Coast Guard), Hiroshi Takiguchi(Japan Aerospace Exploration Agency)

3:30 PM - 3:45 PM JST | 6:30 AM - 6:45 AM UTC

[SGD01-19] The Global Geodetic Observing System (GGOS) – infrastructure underpinning Earth science -

*Basara Miyahara[1], Laura Sánchez[2], Martin Sehnal[3] (1.GSI of Japan, 2.DGFI, Technical University of Munich, 3.BEV, Austrian Federal Office of Metrology and Surveying)

3:45 PM - 4:00 PM JST | 6:45 AM - 7:00 AM UTC

[SGD01-20] GGOS Japan: 2019-2021 Topics

*Toshimichi Otsubo[1], Basara Miyahara[2], Shinobu Kurihara[2], Yusuke Yokota[3], Yu Takagi[2], Shun-ichi Watanabe[4], Hiroshi Takiguchi[5], Yuichi Aoyama[6], Koji Matsuo[2] (1.Hitotsubashi University, 2.Geospatial Information Authority of Japan, 3.University of Tokyo, 4.Hydrographic and Oceanographic Department, Japan Coast Guard, 5.Japan Aerospace Exploration Agency, 6.National Institute of Polar Research)

4:00 PM - 4:15 PM JST | 7:00 AM - 7:15 AM UTC

[SGD01-21] Activity of GGOS working group on DOIs for geodetic data sets from 2019 to 2021

*Yusuke Yokota[1], Toshimichi Otsubo[2], Basara Miyahara[3] (1.Institute of Industrial Science, The University of Tokyo, 2.Hitotsubashi University, 3.Geospatial Information Authority of Japan)

4:15 PM - 4:30 PM JST | 7:15 AM - 7:30 AM UTC

[SGD01-22] SLR/GNSS observations and co-location survey at the Shimosato Hydrographic Observatory

*Yuto Nakamura[1], Shun-ichi Watanabe[1], Noritsune Seo[2], Yusuke Yokota[3], Akira Suzuki[4], Haruka Ueshiba[4] (1.Hydrographic and Oceanographic Department, Japan Coast Guard, 2.Shimosato Hydrographic Observatory, 5th Regional Coast Guard Headquarters, 3.Institute of Industrial Science, University of Tokyo, 4.Geospatial Information Authority of Japan)

4:30 PM - 4:45 PM JST | 7:30 AM - 7:45 AM UTC

[SGD01-23] Current status of Ishioka VLBI station

*Haruka Ueshiba[1], Yu Takagi[1], Tomokazu Nakakuki[1], Saho Matsumoto[1], Kyonosuke Hayashi[1], Toru Yutsudo[1], Katsuhiro Mori[1], Tomokazu Kobayashi[1] (1.Geospatial Information Authority of Japan)

4:45 PM - 5:00 PM JST | 7:45 AM - 8:00 AM UTC

[SGD01-24] Development of Wideband Receiver for Nobel Ground-based Microwave Radiometer -field experiments of the new 16-58 GHz wide-band receiver-

*Ryuichi Ichikawa[1], Hideki Ujihara[1], Shinsuke Satoh[1], Yusaku Ohta[2], Basara Miyahara[3], Hiroshi Munekane[3], Taketo Nagasaki[4], Osamu Tajima[5], Kentaro Araki[6], Takuya Tajiri[6], Hiroshi Takiguchi[7], Takeshi Matsushima[8], Nobuo Matsushima[9], Tatsuya Momotani[10], Kenji Utsunomiya[10] (1.National Institute of Information and Communications Technology, 2.Tohoku University, 3.Geospatial Information Authority of Japan, 4.RIKEN, 5.Kyoto University, 6.Meteorological Research Institute, 7.Japan Aerospace eXploration Agency, 8.Kyushu University, 9.National Institute of Advanced Industrial Science and Technology, 10.Japan Weather Association)

[J] Oral | S (Solid Earth Sciences)：S-SS Seismology

9:00 AM - 10:30 AM JST | 12:00 AM - 1:30 AM UTC | Ch.20 Zoom Room 20

[S-SS08] Fault Rheology and Earthquake Physics

convener:Shunya Kaneki(Disaster Prevention Research Institute, Kyoto University), Makiko Ohtani(Earthquake Research Institute, the University of Tokyo), Keishi Okazaki(Japan Agency for Marine-Earth Science and Technology), Keisuke Yoshida(Tohoku University), Chairperson:Keishi Okazaki(Japan Agency for Marine-Earth Science and Technology), Shunya Kaneki(Disaster Prevention Research Institute, Kyoto University)

9:00 AM - 9:15 AM JST | 12:00 AM - 12:15 AM UTC

[SSS08-07] **New Split-Hopkinson pressure bar installed at Tohoku University to investigate pulverization during fault rupture.**

*Eranga Gayanath Jayawickrama[1], Takuma Sekiguchi[1], Jun Muto[1], Hiroyuki Nagahama[1], Hyung-Seop Shin[2] (1.Tohoku University Department of Earth Science, 2.Andong National University Department of Mechanical Design Engineering)

9:15 AM - 9:30 AM JST | 12:15 AM - 12:30 AM UTC

[SSS08-08] The role of fault zone heterogeneity in producing weak faults and promoting unstable slip

★Invited Papers

*John D Bedford[1,2], Daniel R Faulkner[2], Nadia Lapusta[3] (1.JAMSTEC, 2.Univ. of Liverpool, 3.Caltech)

9:30 AM - 9:45 AM JST | 12:30 AM - 12:45 AM UTC

[SSS08-09] Mechanical amorphization of synthetic fault gouges during rotary-shear friction experiments

*Shunya Kaneki[1], Kiyokazu Oohashi[2], Tetsuro Hirono[3], Hiroyuki Noda[1] (1.Disaster Prevention Research Institute, Kyoto University, 2.Graduate School of Sciences and Technology for Innovation, Yamaguchi University, 3.Graduate School of Science, Osaka University)

9:45 AM - 10:00 AM JST | 12:45 AM - 1:00 AM UTC

[SSS08-10] Friction experiments on volcanic glass-clay mixtures toward understanding the slip behavior of sediments near trench-arc system

*Hanaya Okuda[1,2], Takehiro Hirose[3], Asuka Yamaguchi[1,2] (1.Department of Ocean Floor Geoscience, Atmosphere and Ocean Research Institute, University of Tokyo, 2.Department of Earth and Planetary Science, Graduate School of Science, University of Tokyo, 3.Kochi Institute for Core Sample Research, Japan Agency for Marine-Earth Science and Technology)

10:00 AM - 10:15 AM JST | 1:00 AM - 1:15 AM UTC

[SSS08-11] Frictional properties of greenstone: Effects of the seamount subduction on earthquake generation

*Michiyo Sawai[1], Yuuto Yamauchi[1], Yasutaka Hayasaka[2], Kyuichi Kanagawa[1] (1.Chiba University, 2.Hiroshima University)

10:15 AM - 10:30 AM JST | 1:15 AM - 1:30 AM UTC

[SSS08-12] Rotary shear experiment for understanding frictional behavior of sandstone

*Hiromichi Yano[1], Takeshi Miyamoto[1], Tetsuro Hirono[1] (1.Department of earth and space science, Graduate School of Science, Osaka University)

[J] Oral | S (Solid Earth Sciences)：S-SS Seismology

10:45 AM - 12:00 PM JST | 1:45 AM - 3:00 AM UTC | Ch.20 Zoom Room 20

[S-SS08] Fault Rheology and Earthquake Physics

convener:Shunya Kaneki(Disaster Prevention Research Institute, Kyoto University), Makiko Ohtani(Earthquake Research Institute, the University of Tokyo), Keishi Okazaki(Japan Agency for Marine-Earth Science and Technology), Keisuke Yoshida(Tohoku University), Chairperson:Shunya Kaneki(Disaster Prevention Research Institute, Kyoto University), Keishi Okazaki(Japan Agency for Marine-Earth Science and Technology)

10:45 AM - 11:00 AM JST | 1:45 AM - 2:00 AM UTC

[SSS08-13] Experimental evaluation of thermal maturation of carbonaceous materials under hydrous condition: As a proxy of frictional heating in a fault during an earthquake

*Keita Iwagaki[1], Tetsuro Hirono[1] (1.Department of Earth and Space Science, Graduate School of Science, Osaka University)

11:00 AM - 11:15 AM JST | 2:00 AM - 2:15 AM UTC

[SSS08-14] Overpressured subduction plate boundary caused by mantle-derived fluids: Evidence from noble gas isotope analysis on veins in subduction mélange

★Invited Papers

*Naoki Nishiyama[1], Hirochika Sumino[2], Kohtaro Ujiie[1] (1.University of Tsukuba, 2.The University of Tokyo)

11:15 AM - 11:30 AM JST | 2:15 AM - 2:30 AM UTC

[SSS08-15] Slip trace along an ancient plate boundary fault in the Shimanto accretionary, Hidakagawa Formation, Miyama Unit, Kii Peninsula, Japan: Organic geochemical and elemental approaches

*Ayana Shimamoto[1], Tetsuro Hirono[1], Tsuyoshi Ishikawa[2], Takeaki Ogawa[1] (1.Department of earth and space science, Graduate School of Science, Osaka University, 2.Kochi Institute for Core Sample Research, JAMSTEC)

11:30 AM - 11:45 AM JST | 2:30 AM - 2:45 AM UTC

[SSS08-16] Development of crystallographic preferred orientation during normal faulting in the Pleistocene Ryukyu Limestone

*Kaoru Inoue[1], Kohtaro Ujiie[2], Takayoshi Nagaya[3] (1.Graduate School of Life and Environmental Sciences, University of Tsukuba, 2.Faculty of Life and Environmental Sciences, University of Tsuku, 3.Graduate School of Science, The University of Tokyo)

11:45 AM - 12:00 PM JST | 2:45 AM - 3:00 AM UTC

[SSS08-17] Frictional experiments and numerical simulations for understanding the developing process of composite planar fabrics in faults

*Takeshi Miyamoto[1], Tetsuro Hirono[1], Akari Fuke[1], Satoshi Yukawa[1] (1.Graduate School of Science, Osaka University)

[J] Oral | S (Solid Earth Sciences)：S-SS Seismology

1:45 PM - 3:00 PM JST | 4:45 AM - 6:00 AM UTC | Ch.20 Zoom Room 20

[S-SS08] Fault Rheology and Earthquake Physics

convener:Shunya Kaneki(Disaster Prevention Research Institute, Kyoto University), Makiko Ohtani(Earthquake Research Institute, the University of Tokyo), Keishi Okazaki(Japan Agency for Marine-Earth Science and Technology), Keisuke Yoshida(Tohoku University), Chairperson:Keisuke Yoshida(Tohoku University), Makiko Ohtani(Earthquake Research Institute, the University of Tokyo)

1:45 PM - 2:00 PM JST | 4:45 AM - 5:00 AM UTC

[SSS08-18] Analysis of the source process of the 2016 Off Fukushima, Japan, crustal earthquake using land and seafloor observation data

★Invited Papers

*Hisahiko Kubo[1], Tatsuya Kubota[1], Wataru Suzuki[1], Takeshi Nakamura[2] (1.National Research Institute for Earth Science and Disaster Resilience, 2.Central Research Institute of Electric Power Industry)

2:00 PM - 2:15 PM JST | 5:00 AM - 5:15 AM UTC

[SSS08-19] **Determination of source parameters of the 2011 Tohoku-Oki earthquake from three-component pre-P gravity signals recorded by dense arrays in Japan**

*Nobuki Kame[1], Masaya Kimura[1], Shingo Watada[1], Akito Araya[1], Takashi Kunugi[2], Rongjiang Wang[3] (1.Earthquake Research Institute, the University of Tokyo, 2.National Research Institute for Earth Science and Disaster Resilience, 3.Helmholtz Centre Potsdam, GFZ German Research Centre for Geosciences)

2:15 PM - 2:30 PM JST | 5:15 AM - 5:30 AM UTC

[SSS08-20] Relative fluid pressure distribution around the 2000 Western Tottori Earthquake (M7.3) inferred from focal mechanism data of the aftershock

*Satoshi Matsumoto[1], Yoshihisa Iio[2], Shin'ichi Sakai[3], Aitaro Kato[4] (1.Institute of Seismology and Volcanology, Faculty of Sciences, Kyushu University, 2.Disaster Prevention Research Institute, Kyoto University, 3.The University of Tokyo III/GSII, 4.Earthquake Research Institute, University of Tokyo)

2:30 PM - 2:45 PM JST | 5:30 AM - 5:45 AM UTC

[SSS08-21] Intraslab repeating earthquakes beneath Japan; Implications for fluid-related embrittlement

*Junichi Nakajima[1], Akira Hasegawa[2] (1.Department of Earth and Planetary Sciences, Tokyo Institute of Technology, 2.Graduate School of Science, Tohoku University)

2:45 PM - 3:00 PM JST | 5:45 AM - 6:00 AM UTC

[SSS08-22] Intraplate repeating earthquakes in the Fukushima-Ibaraki border region following the 2011 Tohoku-Oki earthquake

*Rina Ikeda[1], Keisuke Yoshida[1], Ryo Takahashi[2], Toru Matsuzawa[1], Akira Hasegawa[1] (1.Tohoku University, 2.Japan Meteorological Agency)

[J] Oral | S (Solid Earth Sciences)：S-SS Seismology

3:30 PM - 4:45 PM JST | 6:30 AM - 7:45 AM UTC | Ch.20 Zoom Room 20

[S-SS08] Fault Rheology and Earthquake Physics

convener:Shunya Kaneki(Disaster Prevention Research Institute, Kyoto University), Makiko Ohtani(Earthquake Research Institute, the University of Tokyo), Keishi Okazaki(Japan Agency for Marine-Earth Science and Technology), Keisuke Yoshida(Tohoku University), Chairperson:Keisuke Yoshida(Tohoku University), Yusuke Mukuhira(Institute of Fluid Science, Tohoku University)

3:30 PM - 3:45 PM JST | 6:30 AM - 6:45 AM UTC

[SSS08-23] Urgent observation of seafloor crustal movement and installation of seafloor seismographs in preparation for future earthquakes off the east coast of Aomori Prefecture

*Takane Hori[1], Takeshi Iinuma[1], Fumiaki Tomita[1], Motoyuki Kido[2], Chie Honsho[3], Ryosuke Azuma[3], Chi-Hsien Tang[3], Yusaku Ohta[3], Ryoko Nakata[3], Ryota Hino[3], Masanao Shinohara[4], Shuichi Kodaira[1] (1.Research Institute for Marine Geodynamics, Japan Agency for Marine-Earth Science and Technology, 2.International Research Institute of Disaster Science, 3.Graduate School of Science, Tohoku University, 4.Earthquake Research Institute, The University of Tokyo)

3:45 PM - 4:00 PM JST | 6:45 AM - 7:00 AM UTC

[SSS08-24] Hotspots of Hypocenters Illuminated by a Newly-Developed Cross-Correlation-Based Hypocenter and Centroid Relocation Method

*Ta-Wei Chang[1], Satoshi Ide[1] (1.The University of Tokyo)

4:00 PM - 4:15 PM JST | 7:00 AM - 7:15 AM UTC

[SSS08-25] **Microseismic Cloud Growth Process Mainly Controlled by *In-Situ* Stress During Hydraulic Stimulation**

*Yusuke Mukuhira[1], Meihua Yang[5,1], Kyosuke Okamoto[4], Takuya ISHIBASHI[4], Yusuke Kumano[2], Hirokazu Moriya[3], Hiroshi Asanuma[4], Kangnan Yan[5,1], Justin Rubinstein[6], Yinhui Zuo[5], Markus O Häring[7] (1.Institute of Fluid Science, Tohoku University, 2.JAPEX Co., Ltd., 3.School of engineering, Tohoku University, 4.Fukushima Renewable Energy Institute, National Institute of Advanced Industrial Science and Technology, 5.State Key Laboratory of Oil and Gas Geology and Exploitation, Chengdu University of Technology, 6.United States Geological Survey, 7.Häring GeoProject)

4:15 PM - 4:30 PM JST | 7:15 AM - 7:30 AM UTC

[SSS08-26] **Moment tensor analysis for numerous AEs induced by hydraulic fracturing in laboratory**

Rui Tanaka[1], *Makoto Naoi[1], Youqing Chen[1], Kazune Yamamoto[1], Keiichi Imakita[1], Naofumi Tsutsumi[1], Akihiro Shimoda[1], Daiki Hiramatsu[1], Hironori Kawakata[2], Tsuyoshi Ishida[1], Eiichi Fukuyama[1], Hiroyuki Tanaka[3], Yutaro Arima[3], Shigehiro Kitamura[3], Daisuke Hyodo[3] (1.Kyoto University, 2.Ritsumeikan University, 3.JOGMEC)

4:30 PM - 4:45 PM JST | 7:30 AM - 7:45 AM UTC

[SSS08-27] AE events observed during loading velocity step change in large-scale gouge friction experiments

*Shun Watanabe[1], Eiichi Fukuyama[1,2], Futoshi Yamashita[2], Akihiro Shimoda[1] (1.kyoto university, 2.National Research Institute for Earth Science and Disaster Prevention)

[J] Oral | S (Solid Earth Sciences)：S-SS Seismology

9:00 AM - 10:30 AM JST | 12:00 AM - 1:30 AM UTC | Ch.21 Zoom Room 21

[S-SS10] Active faults and paleoseismology

convener:Mamoru Koarai(Earth Science course, College of Science, Ibaraki University), Yoshiki Shirahama(Advanced Industrial Science and Technology, Geological Survey of Japan, Research Institute of Earthquake and Volcano Geology, Active Fault Research Group), Yoshiki Sato(Advanced Industrial Science and Technology, Geological Survey of Japan), Masayuki Yoshimi(Geological Survey of Japan, AIST), Chairperson:Mamoru Koarai(Earth Science course, College of Science, Ibaraki University), Yoshiki Shirahama(Advanced Industrial Science and Technology, Geological Survey of Japan, Research Institute of Earthquake and Volcano Geology, Active Fault Research Group)

9:00 AM - 9:15 AM JST | 12:00 AM - 12:15 AM UTC

[SSS10-01] Introduction

9:15 AM - 9:30 AM JST | 12:15 AM - 12:30 AM UTC

[SSS10-02] Simultaneous rupturing of the Tanna fault and its branch faults in the Kita-Izu fault zone

*Ryuhei Oda[1], Daisuke Ishimura[1], Takehiko Suzuki[1] (1.Tokyo Metropolitan University)

9:30 AM - 9:45 AM JST | 12:30 AM - 12:45 AM UTC

[SSS10-03] Microtremor Array Observation across Active Faults in Ogasawara Iwo-To Island

*Takumi Murakoshi[1], Takayuki Kouno[2] (1.National Defense Academy, 2.Japan Air Self-Defense Force)

9:45 AM - 10:00 AM JST | 12:45 AM - 1:00 AM UTC

[SSS10-04] Rerationship between earthquake disaster and basement depth due to active faults in Iiyma City, Nagano Prefecture

*Mamoru Koarai[1], Keiichi Takami[1], Naoki Hashikami[1], Takayuki Nakano[2], Shigeki Senna[3] (1.Earth Science course, College of Science, Ibaraki University, 2.Geospatial Information Authority of Japan, 3.National Research Institute of Earth Science and Disaster Resilience)

10:00 AM - 10:15 AM JST | 1:00 AM - 1:15 AM UTC

[SSS10-05] Probing shallow region structure of Atotsugawa fault fracture zone with cosmic-ray muon detector

*Katsuya Yamazaki[1], Akimichi Taketa[2], Daisuke Ikeda[3], Kentaro Omura[4] (1.College of Engineering, Chubu University, 2.Earthquake Research Institute, the University of Tokyo, 3.Faculty of Engineering, Kanagawa University, 4.National Research Institute for Earth Science and Disaster Resilience)

10:15 AM - 10:30 AM JST | 1:15 AM - 1:30 AM UTC

[SSS10-06] The Quaternary fault outcrop of the Inagoe fault, Furukawa fault zone, in northern part of Gifu Prefecture, central Japan

*Tomonori Tamura[1], Kiyokazu Oohashi[1], Nagisa Maruo[1] (1.Graduate school of Sciences and Technology for Innovation, Yamaguchi University)

[J] Oral | S (Solid Earth Sciences)：S-SS Seismology

10:45 AM - 12:15 PM JST | 1:45 AM - 3:15 AM UTC | Ch.21 Zoom Room 21

[S-SS10] Active faults and paleoseismology

convener:Mamoru Koarai(Earth Science course, College of Science, Ibaraki University), Yoshiki Shirahama(Advanced Industrial Science and Technology, Geological Survey of Japan, Research Institute of Earthquake and Volcano Geology, Active Fault Research Group), Yoshiki Sato(Advanced Industrial Science and Technology, Geological Survey of Japan), Masayuki Yoshimi(Geological Survey of Japan, AIST), Chairperson:Yoshiki Sato(Advanced Industrial Science and Technology, Geological Survey of Japan), Masayuki Yoshimi(Geological Survey of Japan, AIST)

10:45 AM - 11:00 AM JST | 1:45 AM - 2:00 AM UTC

[SSS10-07] Paleoseismic activity and slip rate of the Obitoke and Tenri faults in the Nara basin

★Invited Papers

*Hiroyuki Tsutsumi[1], Nobuhiko Sugito[2], Haruo Kimura[3], Shozo Kawashima[1], Toranosuke Morishima[1], Kaoru Taniguchi[4], Masashi Omata[4] (1.Department of Environmental Systems Science, Faculty of Science and Engineering, Doshisha University, 2.Faculty of Sustainability Studies, Hosei University, 3.Central Research Institute of Electric Power Industry, 4.Pasco Co.)

11:00 AM - 11:15 AM JST | 2:00 AM - 2:15 AM UTC

[SSS10-08] Distribution of amount of displacement along the Eastern Margin Fault System of Nara basin, Kinki District, Central Japan

*Taku Komatsubara[1] (1.Institute of Geology and Geoinformation, Advanced Industrial Science and Technology)

11:15 AM - 11:30 AM JST | 2:15 AM - 2:30 AM UTC

[SSS10-09] The Oldest Report of a Tsunami in Mexico in 1537 Based on Japanese Literature Is Erroneous

*Yutaka Hayashi[1] (1.Meteorological Research Institute, Japan Meteorological Agency)

11:30 AM - 11:45 AM JST | 2:30 AM - 2:45 AM UTC

[SSS10-10] Discovery of active faults on the coasts of Gulf of Suez and its significance

*Takashi Nakata[1], Steven G. Wesnousky[2], Hideaki Goto[1] (1.Hiroshima University, 2.University of Nevada, Reno)

11:45 AM - 12:15 PM JST | 2:45 AM - 3:15 AM UTC

[SSS10-11] Discussion

[J] Oral | S (Solid Earth Sciences)：S-GL Geology

1:45 PM - 3:15 PM JST | 4:45 AM - 6:15 AM UTC | Ch.23 Zoom Room 23

[S-GL22] Geochronology and Isotope Geology

convener:Takahiro Tagami(Graduate School of Science, Kyoto University), Yuji Sano(Division of Ocean and Earth Systems, Atmosphere and Ocean Research Institute, University of Tokyo), Chairperson:Takahiro Tagami(Graduate School of Science, Kyoto University), Yuji Sano(Center for Advanced Marine Core Research, Kochi University)

1:45 PM - 2:15 PM JST | 4:45 AM - 5:15 AM UTC

[SGL22-01] Inter-method comparison study between $^{40}Ar/^{39}Ar$ and unspiked K-Ar method for some young volcanic rocks

★Invited Papers

*Seiko Yamasaki[1], Daniel P. Miggins[2], Anthony A.P. Koppers[2] (1.Geological Survey of Japan, Advanced Industrial Science and Technology, 2.Oregon State University)

2:15 PM - 2:30 PM JST | 5:15 AM - 5:30 AM UTC

[SGL22-02] Sub-millimeter scale helium measurement for MORB glass

*Hidenori Kumagai[1], Keiko Sato[2,1,3], Ieyoshi Shimizu[1] (1.Japan Agency for Marine-Earth Science and Technology, 2.National Institute of Technology, Fukushima College, 3.Okayama, Univ. of Science)

2:30 PM - 2:45 PM JST | 5:30 AM - 5:45 AM UTC

[SGL22-03] Asteroid shower on the Earth-Moon system 0.8 billion years ago

*Kentaro Terada[1], Tomokatsu Morota[2], Mami Kato[3] (1.Department of Earth and Space Science, Graduate School of Science, Osaka University, 2.Graduate School of Science, The University of Tokyo, 3.MEISEI ELECTRIC CO., LTD)

2:45 PM - 3:15 PM JST | 5:45 AM - 6:15 AM UTC

[SGL22-04] Deciphering the earliest Earth history from nitrogen, a highly-siderophile-highly-volatile element

★Invited Papers

*Ko Hashizume[1], Osamu Ohtaka[2] (1.Faculty of Science, Ibaraki University, 2.Graduate School of Science, Osaka University)

[J] Oral | S (Solid Earth Sciences)：S-VC Volcanology

10:45 AM - 12:15 PM JST | 1:45 AM - 3:15 AM UTC | Ch.25 Zoom Room 25

[S-VC28] Active Volcanism

convener:Yuta Maeda(Nagoya University), Takahiro Miwa(National research institute for earth science and disaster prevention), Takeshi Matsushima(Institute of Seismology and Volcanology, Faculty of Science, Kyushu University), Chairperson:Kohei Hotta(University of Toyama), Hiroshi Munekane(Geospatial Information Aurhotiry of Japan)

10:45 AM - 11:00 AM JST | 1:45 AM - 2:00 AM UTC

[SVC28-01] Reappraisal of the deformation model for Mt. Kusatsu-shirane and Mt. Asama

*Hiroshi Munekane[1] (1.Geospatial Information Aurhotiry of Japan)

11:00 AM - 11:15 AM JST | 2:00 AM - 2:15 AM UTC

[SVC28-02] Volcano monitoring based on InSAR Time-series Analysis

*Satoshi Miura[1], Morishita Yu[2], Yusaku Ohta[1], Tomotsugu Demachi[1], Micaela Colavita[1] (1.Graduate School of Science, Tohoku University, 2.Geospatial Information Authority of Japan)

11:15 AM - 11:30 AM JST | 2:15 AM - 2:30 AM UTC

[SVC28-03] **Evolution of Volcanic Deformation at Domuyo and Laguna del Maule, Southern Andes, Revealed by InSAR Time-series Analyses**

*Micaela Colavita[1], Satoshi Miura[1], Yu Morishita[2] (1.Graduate School of Science, Tohoku University , 2.Geospatial Information Authority of Japan)

11:30 AM - 11:45 AM JST | 2:30 AM - 2:45 AM UTC

[SVC28-04] Evaluation of volcanic activity using "Non-eruptive ground deformation"

*Masato Iguchi[1] (1.Sakurajima Volcano Research Center, Disaster Prevention Research Institute, Kyoto University)

11:45 AM - 12:00 PM JST | 2:45 AM - 3:00 AM UTC

[SVC28-05] The deformation source revealed from leveling surveys in Jigokudani valley, Tateyama volcano, Japan

*Kohei Hotta[1], Shigekazu Kusumoto[2], Hidenori Takahashi[1], Yuichi S. Hayakawa[3] (1.University of Toyama, 2.Kyoto University, 3.Hokkaido University)

12:00 PM - 12:15 PM JST | 3:00 AM - 3:15 AM UTC

[SVC28-06] Crustal structure around Kikai submarine caldera deduced from gravity anomaly

*Tomoko Hanyu[1], Satoshi Shimizu[1], Hiroto Yamaguchi[2], Yuiko Morita, Nobukazu Seama[2,1] (1.Kobe Ocean-Bottom Exploration Center, 2.Department of Planetology, Graduate School of Science, Kobe University)

[J] Oral | S (Solid Earth Sciences)：S-VC Volcanology

1:45 PM - 3:15 PM JST | 4:45 AM - 6:15 AM UTC | Ch.25 Zoom Room 25

[S-VC28] Active Volcanism

convener:Yuta Maeda(Nagoya University), Takahiro Miwa(National research institute for earth science and disaster prevention), Takeshi Matsushima(Institute of Seismology and Volcanology, Faculty of Science, Kyushu University), Chairperson:Takao Ohminato(Earthquake Research Institute, Tokyo University), Yuta Maeda(Nagoya University)

1:45 PM - 2:00 PM JST | 4:45 AM - 5:00 AM UTC

[SVC28-07] Seismic structural imaging of shallow fluid supply beneath Mt. Ontake

*Yuta Maeda[1], Toshiki Watanabe[1] (1.Nagoya University)

2:00 PM - 2:15 PM JST | 5:00 AM - 5:15 AM UTC

[SVC28-08] Temporal variations in seismic scattering anomalies estimated by inversion of envelope widths of volcano-tectonic earthquakes at Taal volcano, Philippines.

*Miki Hamamoto [1], Hiroyuki Kumagai[1], Rudy Lacson[2] (1.Graduate School of Environmental Studies, Nagoya University, 2.PHIVOLCS (Philippine Institute of Volcanology and Seismology))

2:15 PM - 2:30 PM JST | 5:15 AM - 5:30 AM UTC

[SVC28-09] Attenuation characteristics of Hachijojima Island from twofold spectral ratio method using dense seismic observation

*Utako Watanabe[1], Hiroyuki Azuma[1], Yoshiya Oda[1] (1.Tokyo Metropolitan university)

2:30 PM - 2:45 PM JST | 5:30 AM - 5:45 AM UTC

[SVC28-10] Automatic Detection of First Arrival Time of Seismic Waves with the Fine-tuning: Applying to Observed Datas in Hachijojima

*Hikaru Kunimasa[1], HIROYUKI AZUMA[1], Yoshiya Oda[1] (1.Tokyo Metropolitan University)

2:45 PM - 3:00 PM JST | 5:45 AM - 6:00 AM UTC

[SVC28-11] Moment Tensors of Ring-Faulting at Active Volcanoes: Insights into Vertical-CLVD Earthquakes at the Sierra Negra Caldera, Galápagos Islands

*Osamu Sandanbata[1,2], Hiroo Kanamori[3], Luis Rivera[4], Zhongwen Zhan[3], Shingo Watada[2], Kenji Satake[2] (1.National Research Institute for Earth Science and Disaster Resilience, Ibaraki, Japan, 2.Earthquake Research Institute, the University of Tokyo, Tokyo, Japan, 3.California Institute of Technology, Pasadena, CA, USA, 4.Université de Strasbourg, CNRS, ITES UMR 7063, Strasbourg F-67084, France)

3:00 PM - 3:15 PM JST | 6:00 AM - 6:15 AM UTC

[SVC28-12] The 2019-2020 Nishinoshima activity inferred from seismic and infrasound observations in the island

*Takao Ohminato[1], Atsushi Watanabe[1] (1.Earthquake Research Institute, Tokyo University)

[J] Oral | S (Solid Earth Sciences)：S-VC Volcanology

3:30 PM - 5:00 PM JST | 6:30 AM - 8:00 AM UTC | Ch.25 Zoom Room 25

[S-VC28] Active Volcanism

convener:Yuta Maeda(Nagoya University), Takahiro Miwa(National research institute for earth science and disaster prevention), Takeshi Matsushima(Institute of Seismology and Volcanology, Faculty of Science, Kyushu University), Chairperson:Mie Ichihara(Earthquake Research Institute, University of Tokyo), Haruhisa Nakamichi(Sakurajima Volcano Research Center, Disaster Prevention Research Institute, Kyoto University)

3:30 PM - 3:45 PM JST | 6:30 AM - 6:45 AM UTC

[SVC28-13] Dike inflation process below Sakurajima volcano during the earthquake swarm of 15 August 2015

*Haruhisa Nakamichi[1] (1.Sakurajima Volcano Research Center, Disaster Prevention Research Institute, Kyoto University)

3:45 PM - 4:00 PM JST | 6:45 AM - 7:00 AM UTC

[SVC28-14] A preliminary report of a pilot experiment for the sustainable repeating seismic experiment in Aira Caldera, Japan.

*Tomoki Tsutsui[1], Takeshi Tameguri[1], Daisuke Miki[1], Masato Iguchi[1], Masanao Shinohara[2] (1.DPRI, Kyoto University, 2.ERI, University of Tokyo)

4:00 PM - 4:15 PM JST | 7:00 AM - 7:15 AM UTC

[SVC28-15] Temporal variation of b value of volcanic earthquakes associated with the 2008-2011 Shinmoe-dake eruption

*Jun Oikawa[1], Yasuhisa Tajima[2] (1.Earthquake Research Institute, University of Tokyo, 2.Nippon Koei)

4:15 PM - 4:30 PM JST | 7:15 AM - 7:30 AM UTC

[SVC28-16] Long-term base level variations of seismic power at Shinmoedake, revealing fluid migration prior to the 2011 and 2018 eruptions

*Mie Ichihara[1], Takao Ohminato[1], Minoru Takeo[1] (1.Earthquake Research Institute, University of Tokyo)

4:30 PM - 4:45 PM JST | 7:30 AM - 7:45 AM UTC

[SVC28-17] Waveform inversion of the ultra-long-period seismic event associated with a ground tilt motion during the eruption of Mt.Kusatsu-Shirane, Japan, on January 23, 2018

*Ryohei Takahashi[1], Yuta Maeda[1], Toshiki Watanabe[1] (1.Graduate School of Environmental Studies, Nagoya University)

4:45 PM - 5:00 PM JST | 7:45 AM - 8:00 AM UTC

[SVC28-18] Resistivity structure of Mt. Motoshirane, Japan, inferred from an audio-frequency magnetotelluric survey

*Honda Asami[1], Wataru Kanda[1], Takao Koyama[2], Shinichi Takakura[3], Yasuo Matsunaga[1], Tatsuji Nishizawa[1], Satoshi Ikezawa[2] (1.School of Science, Tokyo Institute of Technology, 2.Earthquake Research Institute, the University of Tokyo, 3.National Institute of Advanced Industrial Science and Technology (AIST))

[J] Oral | S (Solid Earth Sciences)：S-TT Technology & Techniques

9:00 AM - 10:00 AM JST | 12:00 AM - 1:00 AM UTC | Ch.18 Zoom Room 18

[S-TT35] Seismic monitoring and processing system

convener:Wataru Suzuki(National Research Institute for Earth Science and Disaster Resilience), Chairperson:Tsunehisa KIMURA(Schlumberger)

9:00 AM - 9:15 AM JST | 12:00 AM - 12:15 AM UTC

[STT35-01] Technological innovation of accelerometers with applications to seismometers

*Peiliang Xu[1] (1.Disaster Prevention Research Institute, Kyoto University)

9:15 AM - 9:30 AM JST | 12:15 AM - 12:30 AM UTC

[STT35-02] Concept of fail-safe seismograph with improved reliability

*Shinji SATO[1] (1.Railway Technical Research Institute)

9:30 AM - 9:45 AM JST | 12:30 AM - 12:45 AM UTC

[STT35-03] Extending the Range of Fiber-optic DAS Systems For Seismicity Monitoring

*Martin Horst Karrenbach[1], Victor Yartsev[1], Steve Cole[1], Richard Hooper[1] (1.OptaSense)

9:45 AM - 10:00 AM JST | 12:45 AM - 1:00 AM UTC

[STT35-04] Rapid Progress of Seismic Monitoring System using Optical Fiber and DAS Technology

*Tsunehisa KIMURA[1] (1.Schlumberger)

[J] Oral | S (Solid Earth Sciences)：S-CG Complex & General

10:45 AM - 12:15 PM JST | 1:45 AM - 3:15 AM UTC | Ch.23 Zoom Room 23

[S-CG47] Evolution and movement of the crustal surface and application of geo- and thermochronology

convener:Noriko Hasebe(Institute of Nature and Environmental Technology, Kanazawa University), Shigeru Sueoka(Japan Atomic Energy Agency), Hiroyuki Tsutsumi(Department of Environmental Systems Science, Faculty of Science and Engineering, Doshisha University), Takahiro Tagami(Graduate School of Science, Kyoto University), Chairperson:Shigeru Sueoka(Japan Atomic Energy Agency)

10:45 AM - 11:15 AM JST | 1:45 AM - 2:15 AM UTC

[SCG47-01] Studies of tectonic geomorphology at the northeastern edge of the Tibetan plateau by the dating method with *in situ* terrestrial cosmogenic nuclides

★Invited Papers

*Yoshiki Shirahama[1] (1.Advanced Industrial Science and Technology, Geological Survey of Japan, Research Institute of Earthquake and Volcano Geology, Active Fault Research Group)

11:15 AM - 11:45 AM JST | 2:15 AM - 2:45 AM UTC

[SCG47-02] Denudation process of high-grade metamorphic nappe in eastern Nepal constrained by thermochronological inverse analysis

★Invited Papers

*Nakajima Toru[1], Tetsuo Kawakami[1], Hideki Iwano[2], Tohru Danhara[2], Harutaka Sakai (1.Division of Earth and Planetary Sciences, Graduate School of Science, Kyoto University, 2.Kyoto Fission-Track Co., Ltd.)

11:45 AM - 12:00 PM JST | 2:45 AM - 3:00 AM UTC

[SCG47-03] Toward the reconstruction of the uplift style of a volcanic arc: Insights from apatite fission-track thermochronometry of granitoids in the northern part of the Ou Backbone Range

*Shoma Fukuda[1], Shigeru Sueoka[1], Yuya Kajita[2], Saya Kagami[1], Tatsunori Yokoyama[1], Takahiro Tagami[2] (1.Japan Atomic Energy Agency, 2.Kyoto University)

12:00 PM - 12:15 PM JST | 3:00 AM - 3:15 AM UTC

[SCG47-04] Constraining thermal/denudation histories in the last 0.1 Myr using OSL thermochronometry applied to samples from deep boreholes -A case study in Rokko Mountains-

*Manabu Ogata[1], Georgina E King[2], Frédéric Herman[2], Shigeru Sueoka[1], Ryuji Yamada[3], Kentaro Omura[3] (1.Tono Geoscience Center, Japan Atomic Energy Agency, 2.Institute of Earth Surface Dynamics, University of Lausanne, 3.National Research Institute for Earth Science and Disaster Prevention)

[J] Oral | S (Solid Earth Sciences)：S-CG Complex & General

9:00 AM - 10:30 AM JST | 12:00 AM - 1:30 AM UTC | Ch.25 Zoom Room 25

[S-CG48] Volcanic roots

convener:Naofumi Aso(Tokyo Institute of Technology), Tsuyoshi Iizuka(University of Tokyo), Yohei Yukutake(Earthquake Research Institute, University of Tokyo), Chairperson:Naofumi Aso(Tokyo Institute of Technology), Tsuyoshi Iizuka(University of Tokyo), Yohei Yukutake(Earthquake Research Institute, University of Tokyo)

9:00 AM - 9:15 AM JST | 12:00 AM - 12:15 AM UTC

[SCG48-01] Transcrustal magmatic mushes - implications for igneous differentiation and the heights of volcano edifices

★Invited Papers

*Jon Blundy[1] (1.University of Oxford)

9:15 AM - 9:30 AM JST | 12:15 AM - 12:30 AM UTC

[SCG48-02] Imaging the fossils of magma supplying system: Electrical resistivity structure of the Mt. Okue batholith

*Ayumu Okubo[1], Koki Aizawa[2], Takeshi Matsushima[2], Agnis Triahadini[1], Yuto Yamamoto[1], Haruto Tanabe[1], Mitsuru Utsugi[3], Ken'ichi Yamazaki[4], Ryokei Yoshimura[4], Shintaro Komatsu[4], Kana Araue[4], Ayako Namigishi[4], Yoshiko Teguri[5], Kaori Tsukamoto[5], Dan Muramatsu[1], Yuto Hayashida, Kosuke Takeishi[5], Miki Ogata[1], Haruna Watanabe[1], Kana Fujimori[1], Naoto Harada[1] (1.Department of Earth and Planetary Sciences, Graduate School of Science, Kyushu University , 2.Institute of Seismology and Volcanology, Faculty of Sciences, Kyushu University, 3.Aso Volcanological Laboratory, Institute for Geothermal Sciences, Graduate School of Science, Kyoto University, 4.Disaster Prevention Research Institute, Kyoto University, 5.JMA)

9:30 AM - 9:45 AM JST | 12:30 AM - 12:45 AM UTC

[SCG48-03] A three-dimensional electrical resistivity model beneath Azumayama Volcano, NE Japan

*Masahiro Ichiki[1], Toshiki Kaida[1], Takashi NAKAYAMA[1], Satoshi Miura[1], Mare Yamamoto[1], Yuichi Morita[2], Makoto Uyeshima[2] (1.Graduate School of Science, Tohoku University, 2.Earthquake Research Institute, The University of Tokyo)

9:45 AM - 10:00 AM JST | 12:45 AM - 1:00 AM UTC

[SCG48-04] Periodic activity of deep low-frequency earthquakes in Meakandake, Nikko and Yakedake

*Ryo Kurihara[1], Kazushige Obara[1] (1.Earthquake Research Institute, The University of Tokyo)

10:00 AM - 10:15 AM JST | 1:00 AM - 1:15 AM UTC

[SCG48-05] The diversity of focal mechanisms of volcanic deep low frequency earthquakes in Northeast Japan caused by spatiotemporal stress pattern

*Genki Oikawa[1], Naofumi Aso[1], Junichi Nakajima[1] (1.Tokyo Institute of Technology)

10:15 AM - 10:30 AM JST | 1:15 AM - 1:30 AM UTC

[SCG48-06] Low-frequency earthquakes in close vicinity of repeating earthquakes in the brittle upper crust of Hakodate, Hokkaido, northern Japan

★Invited Papers

*Keisuke Yoshida[1], Akira Hasegawa[1,2], Shinako Noguchi[2], Keiji Kasahara[2] (1.Tohoku University, 2.Association for the development of earthquake prediction)

[J] Oral | S (Solid Earth Sciences)：S-CG Complex & General

1:45 PM - 3:15 PM JST | 4:45 AM - 6:15 AM UTC | Ch.21 Zoom Room 21

[S-CG49] Structure, evolution and deformation of island arcs associated with subduction processes

convener:Masahiro Ishikawa(Graduate School of Environment and Information Sciences Yokohama National University), Masanao Shinohara(Earthquake Research Institute, University of Tokyo), Makoto MATSUBARA(National Research Institute for Earth Science and Disaster Resilience), Tatsuya Ishiyama(Earthquake Research Institute, University of Tokyo), Chairperson:Masahiro Ishikawa(Graduate School of Environment and Information Sciences Yokohama National University), Makoto MATSUBARA(National Research Institute for Earth Science and Disaster Resilience)

1:45 PM - 2:00 PM JST | 4:45 AM - 5:00 AM UTC

[SCG49-01] Cutoff depth and coseismic slip zone for the large earthquake along the Sea of Japan

*Makoto MATSUBARA[1], Tomoko Elizabeth Yano[1] (1.National Research Institute for Earth Science and Disaster Resilience)

2:00 PM - 2:15 PM JST | 5:00 AM - 5:15 AM UTC

[SCG49-02] Stress loading on offshore faults in the Sea of Japan due to the interplate processes along the northwest and southwest Japan arcs

*Akinori Hashima[1], Hiroshi Sato[1], Tatsuya Ishiyama[1], Andrew M. Freed[2], Thorsten W. Becker[3] (1.Earthquake Research Institute, The University of Tokyo, 2.Purdue University, 3.The University of Texas at Austin)

2:15 PM - 2:30 PM JST | 5:15 AM - 5:30 AM UTC

[SCG49-03] Crustal structure characteristics of the Japan Sea revealed by active source seismic survey

*Tetsuo No[1], Takeshi Sato[2], Shuichi Kodaira[1], Hiroshi Sato[3] (1.JAMSTEC, 2.Sapporo Regional Headquarters, JMA, 3.ERI, University of Tokyo)

2:30 PM - 2:45 PM JST | 5:30 AM - 5:45 AM UTC

[SCG49-04] Seismic structure from the forearc region off Miyagi to the central part of Northern Honshu arc, Japan, revealed by onshore-offshore seismic experiment

*Eiji Kurashimo[1], Hiroshi Sato[1], Takaya Iwasaki[2], Takashi Iidaka[1], Tatsuya Ishiyama[1], Masanao Shinohara[1], Hirokazu Ishige[3], Hidehiko Shimizu[3], Shinji Kawasaki[3], Susumu Abe[3], Naoshi Hirata[4] (1.Earthquake Research Institute, the University of Tokyo, 2.Association for the Development of Earthquake Prediction, 3.JGI, Inc., 4.National Research Institute for Earth Science and Disaster Resilience)

2:45 PM - 3:00 PM JST | 5:45 AM - 6:00 AM UTC

[SCG49-05] The upper crustal structure across the central part of the NE Japan Arc revealed from the 2019 onshore seismic refraction/wide-angle reflection profiling

*Takaya Iwasaki[1], Hiroshi Sato[2], Eiji Kurashimo[2], Hirokazu Ishige[3], Hidehiko Shimizu[3], Tatsuya Ishiyama[2], Takashi Iidaka[2], Masanao Shinohara[2], Shinji Kawasaki[3], Susumu Abe[3], Naoshi Hirata[4] (1.Association for the Development of Earthquake Prediction, 2.ERI, the University of Tokyo, Tokyo 113-0032, Japan, 3.JGI, Inc., 4.National Research Institute for Earth Science and Disaster Resilience)

3:00 PM - 3:15 PM JST | 6:00 AM - 6:15 AM UTC

[SCG49-06] **Crust and Mantle Structure of the Tohoku Region from the Viewpoint of Seismic Anisotropy**

★Invited Papers

*Motoko Ishise[1] (1.Earthquake Reseach Institute, University of Tokyo)

[J] Oral | S (Solid Earth Sciences)：S-CG Complex & General

3:30 PM - 5:00 PM JST | 6:30 AM - 8:00 AM UTC | Ch.21 Zoom Room 21

[S-CG49] Structure, evolution and deformation of island arcs associated with subduction processes

convener:Masahiro Ishikawa(Graduate School of Environment and Information Sciences Yokohama National University), Masanao Shinohara(Earthquake Research Institute, University of Tokyo), Makoto MATSUBARA(National Research Institute for Earth Science and Disaster Resilience), Tatsuya Ishiyama(Earthquake Research Institute, University of Tokyo), Chairperson:Masanao Shinohara(Earthquake Research Institute, University of Tokyo), Tatsuya Ishiyama(Earthquake Research Institute, University of Tokyo)

3:30 PM - 3:45 PM JST | 6:30 AM - 6:45 AM UTC

[SCG49-07] 3-D Crustal Shear Wave Velocity Model Derived from the Adjoint Tomography in the Central Japan

*Kota Mukumoto[1], Takeshi Tsuji[1] (1.Kyushu University)

3:45 PM - 4:00 PM JST | 6:45 AM - 7:00 AM UTC

[SCG49-08] Structure and deformation in the overlying plates of Japanese arcs

★Invited Papers

*Hiroshi Sato[1,2] (1.Earthquake Prediction Research Center, Earthquake Research Institute, The University of Tokyo, 2.Center for Integrated Research and Education of Natural Hazards, Shizuoka University)

4:00 PM - 4:15 PM JST | 7:00 AM - 7:15 AM UTC

[SCG49-09] Magmatic evolution of Cretaceous north Kyushu batholiths and its role in creation of crustal structure

*Masaaki Owada[1], Keisuke Eshima[1], Atsushi Kamei[2] (1.Graduate School of Science and Engineering for Innovation, Yamaguchi University, 2.Interdisciplinary Faculty of Science and Engineering, Shimane University)

4:15 PM - 4:30 PM JST | 7:15 AM - 7:30 AM UTC

[SCG49-10] The fate of the Philippine Sea slab in central Japan

*Kazuki Miyazaki[1], Junichi Nakajima[1], Nobuaki Suenaga[2], Shoichi Yoshioka[2,3] (1.Department of Earth and Planetary Sciences, Tokyo Institute of Technology, 2.Research Center for Urban Safety and Security, Kobe University, 3.Faculty of Science, Graduate School of Science, Kobe University)

4:30 PM - 4:45 PM JST | 7:30 AM - 7:45 AM UTC

[SCG49-11] Contrasting volcano spacing along SW Japan arc caused by difference in age of subducting lithosphere

★Invited Papers

*Takumi Matsumoto[1], Yoshiyuki Tatsumi[2,3], Nobuaki Suenaga[4], Shoichi Yoshioka[4,5], Katsuya Kaneko[5,3] (1.National Research Institute for Earth Science and Disaster Resilience, 2.Research Alliance for Human and Ocean Coevolution, Kobe University, 3.Kobe Ocean-Bottom Exploration Center, Kobe University, 4.Research Center for Urban Safety and Security, Kobe University, 5.Faculty of Science, Graduate School of Science, Kobe University)

4:45 PM - 5:00 PM JST | 7:45 AM - 8:00 AM UTC

[SCG49-12] The thermal structure of the Honshu arc crust deduced from seismic tomography

*Masahiro Ishikawa[1] (1.Graduate School of Environment and Information Sciences Yokohama National University)

[J] Oral | B (Biogeosciences) : B-CG Complex & General

9:00 AM - 10:30 AM JST | 12:00 AM - 1:30 AM UTC | Ch.26 Zoom Room 26

[B-CG04] Decoding the history of Earth: From Hadean to the present

convener:Tsuyoshi Komiya(Department of Earth Science & Astronomy Graduate School of Arts and Sciences The University of Tokyo), Yasuhiro Kato(Department of Systems Innovation, Graduate School of Engineering, University of Tokyo), Katsuhiko Suzuki(Submarine Resources Research Center, Japan Agency for Marine-Earth Science and Technology), Kentaro Nakamura(Department of Systems Innovation, School of Engineering, University of Tokyo), Chairperson:Yoshida Satoshi(Department of Earth and Planetary Science, Graduate School of Science, The University of Tokyo), Tsuyoshi Komiya(Department of Earth Science & Astronomy Graduate School of Arts and Sciences The University of Tokyo)

9:00 AM - 9:15 AM JST | 12:00 AM - 12:15 AM UTC

[BCG04-01] Progress of the end-Permian oceanic anoxia in the pelagic Panthalassa

*Satoshi Takahashi[1], Rie Hori[2], Satoshi Yamakita[3], Yoshiaki Aita[4], Atsushi Takemura[5], Minoru Ikehara[6], Yujin Xiong[7], Simon W. Poulton[7], Paul B. Wignall[7], TAKAAKI ITAI[1], Hamish J. Campbell[8], Bernard K. Spörli[9] (1.Department of Earth and Planetary Science, University of Tokyo, 2.Department of Earth Sciences, Graduate School ofScience and Engineering, Ehime University , 3.Department of Earth Sciences, Faculty of Culture, Miyazaki University, 4.Department ofGeology, Faculty ofAgriculture, Utsunomiya University, 5.Geosciences Institute, Hyogo University ofTeacher Education, 6.Center for Advanced Marine Core Research, Kochi University, 7.School of Earth and Environment, University of Leeds, 8.GNS Science, 9.School of Environment, The University of Auckland)

9:15 AM - 9:30 AM JST | 12:15 AM - 12:30 AM UTC

[BCG04-02] Discovery of the Miocene ocean impact event

*Tatsuo Nozaki[1,2,3,4], Junichiro Ohta[2,4], Takaaki Noguchi[5], Honami Sato[6], Akira Ishikawa[7,1], Yutaro Takaya[8,1,4], Jun-Ichi Kimura[9], Qing Chang[9], Kazuhiko Shimada[10], Jun-ichiro Ishibashi[10], Kazutaka Yasukawa[2,4], Katsunori Kimoto[11], Koichi Iijima[1], Yasuhiro Kato[2,4,1] (1.JAMSTEC/SRRC, 2.Univ. of Tokyo, 3.Kobe Univ., 4.Chiba Tech, 5.Kyushu Univ., 6.Univ. of Padova, 7.Tokyo Tech, 8.Waseda Univ., 9.JAMSTEC/VERC, 10.Kyushu Univ, 11.JAMSTEC/ESS)

9:30 AM - 9:45 AM JST | 12:30 AM - 12:45 AM UTC

[BCG04-03] Geochemistry of the Kawame ferromanganese deposit in the Hayachine Belt: Implications for the oceanic environment in the Late Devonian

*Yusuke Kuwahara[1], Koichiro Fujinaga[2,3], Tatsuo Nozaki[4,3,5,2], Junichiro Ohta[3,2], Kazutaka Yasukawa[3,1,2], Kentaro Nakamura[1], Yasuhiro Kato[3,1,2,4] (1.Department of Systems Innovation, School of Engineering, The University of Tokyo, 2.Ocean Resources Research Center for Next Generation, Chiba Institute of Technology, 3.Frontier Research Center for Energy and Resources, School of Engineering, The University of Tokyo, 4.Research and Development Center for Submarine Resources, Japan Agency for Marine-Earth Science and Technology, 5.Department of Planetology, Graduate School of Science, Kobe University)

9:45 AM - 10:00 AM JST | 12:45 AM - 1:00 AM UTC

[BCG04-04] Paleovegetation changes reconstructed by terrestrial plant biomarker analyses in the sediments deposited across the Cenomanian/Turonian boundary in the Great Valley Sequence, northern California, USA

*Masashi A. Ikeda[1], Ken Sawada[2], Reishi Takashima[3], Hiroshi Nishi[4] (1.Graduate School of Science, Hokkaido University, 2.Department of Earth and Planetary Sciences, Faculty of Science, Hokkaido University, 3.The Center for Academic Resources and Archives, The Tohoku University Museum, Tohoku University, 4.Institute of Dinosaur Research, Fukui Prefectural University)

10:00 AM - 10:15 AM JST | 1:00 AM - 1:15 AM UTC

[BCG04-05] Constraint on the Location of the Australasian Tektite Event based on the Thickness Distribution and Gravel Composition of the Ejecta Deposits across the Eastern Indochina

*Toshihiro Tada[1], Ryuji Tada[1,3,2], Paul A Carling[4], Wickanet Songtham[5], Praphas Chansom[5], Thuyên Lê Xuân[6], Toshihiro Kogure[2], Chang Yu[2], Eiichi Tajika[2] (1.Institute for Geo-Cosmology, Chiba Institute of Technology, 2.Department of Earth and Planetary Science, School of Science, The University of Tokyo, 3.Research Center for Earth System Science, Yunnan University, 4.School of Geography and Environmental Sciences, University of Southampton, 5.Northeastern Research Institute of Petrified Wood & Mineral Resources, Nakhon Ratchasima Rajabhat University, 6.Ho Chi Minh City University of Science)

10:15 AM - 10:30 AM JST | 1:15 AM - 1:30 AM UTC

[BCG04-06] **Paleoproterozoic magmatic flare-up of the Ubendian Belt, SW Tanzania: A crustal growth history events before the amalgamation of the Central African Shield**

*Ariuntsetseg Ganbat[1], Tatsuki Tsujimori[1,2], Nelson Boniface[4], Daniel Pastor-Galan[1,2,3], Shogo Aoki[5,6], Kazumasa Aoki[6] (1.Graduate School of Science, Tohoku University, 2.Center for Northeast Asian Studies, Tohoku University, 3.Frontier Research Institute for Interdisciplinary Sciences, Tohoku University, 4.Department of Geology, University of Dar es Salaam, 5.Graduate School of International Resource Sciences, Akita University, 6.Center for Fundamental Education, Okayama University of Science)

[J] Oral | B (Biogeosciences)：B-CG Complex & General

10:45 AM - 12:15 PM JST | 1:45 AM - 3:15 AM UTC | Ch.26 Zoom Room 26

[B-CG04] Decoding the history of Earth: From Hadean to the present

convener:Tsuyoshi Komiya(Department of Earth Science & Astronomy Graduate School of Arts and Sciences The University of Tokyo), Yasuhiro Kato(Department of Systems Innovation, Graduate School of Engineering, University of Tokyo), Katsuhiko Suzuki(Submarine Resources Research Center, Japan Agency for Marine-Earth Science and Technology), Kentaro Nakamura(Department of Systems Innovation, School of Engineering, University of Tokyo), Chairperson:Toshihiro Tada(Chiba Institute for Technology, Institute for Geo-Cosmology), Tsuyoshi Komiya(Department of Earth Science & Astronomy Graduate School of Arts and Sciences The University of Tokyo)

10:45 AM - 11:00 AM JST | 1:45 AM - 2:00 AM UTC

[BCG04-07] Reconstruct BIF bearing volcano-sedimentary sequence of Neoproterozoic, El-Dabbah Formation, Central Eastern Desert, Egypt

*Shoichi Kiyokawa[1], TAISHI SUZUKI[1], Kenji Horie[2], Mami Takehara[2], Maher Dawoud[3] (1.Department of Earth and Planetary Sciences Faculty of sciences, Kyuushu University, 2.National Institute of Polar Research, 3. Menoufiya University)

11:00 AM - 11:15 AM JST | 2:00 AM - 2:15 AM UTC

[BCG04-08] Occurrence and geochemistry of the Eoarchean carbonate rocks: Deciphering the co-evolution of life and bioessential element contents in the seawater through geologic time

★Invited Papers

*Satoshi Yoshida[1], Yusuke Sawaki[1], Tsuyoshi Komiya[1] (1.Department of Earth Science & Astronomy, Graduate School of Arts and Sciences, The University of Tokyo)

11:15 AM - 11:30 AM JST | 2:15 AM - 2:30 AM UTC

[BCG04-09] Nanoscale analysis of trace elements in the Gunflint microfossils using a NanoSIMS: implication for the elemental cycle in the Paleoproterozoic biosphere

*Akizumi Ishida[1], Kouhei Sasaki[1], Takeshi Kakegawa[1], Naoto Takahata[2], Yuji Sano[2] (1.Department of Earth Science, Graduate school of Science, Tohoku University, 2.Atmosphere and Ocean Research Institute, the University of Tokyo)

11:30 AM - 11:45 AM JST | 2:30 AM - 2:45 AM UTC

[BCG04-10] Nitrogen isotope compositions of ca. 2.0 Ga Zaonega Formation in Russia: their constraints on Paleoproterozoic oceanic environments and microbial activities

★Invited Papers

*Kouhei Sasaki[1], Akizumi Ishida[1], Ko Hashizume[2], Takeshi Kakegawa[1] (1.Tohoku University, 2.Ibaraki University)

11:45 AM - 12:00 PM JST | 2:45 AM - 3:00 AM UTC

[BCG04-11] Upper Limit of the Activity of Anaerobic Microbial Ecosystem in the Early Earth

*Yasuto Watanabe[1], Eiichi Tajika[1], Kazumi Ozaki[2], Peng K Hong[3] (1.The University of Tokyo, 2.Toho University, 3.Chiba Institute of Technology)

12:00 PM - 12:15 PM JST | 3:00 AM - 3:15 AM UTC

[BCG04-12] The micro-scale speciation analyses of sulfur in the Ediacaran limestones: Implications for diagenetic mobilization of sulfur species

★Invited Papers

*Fumihiro Matsuura[1,2], Ryoichi Nakada[3], Yusuke Sawaki[4], Yuichiro Ueno[2,5,6], Masafumi Saitoh[7], Iori Kajitani[1], Tomohiro Usui[1,2] (1.Institute of Space and Astronautical Science, JAXA, 2.Earth-Life Science Institute, Tokyo Tech, 3.Kochi Institute for Core Sample Research, JAMSTEC, 4.Department of Earth Science and Astronomy Graduate School of Arts and Sciences, The University of Tokyo, 5.Institute for Extra-cutting-edge Science and Technology Avant-garde Research (X-star), JAMSTEC, 6.Department of Earth and Planetary Sciences, School of Science, Tokyo Tech, 7.Institut des sciences de la Terre, University of Lausanne)

[J] Oral | M (Multidisciplinary and Interdisciplinary)：M-IS Intersection

9:00 AM - 10:30 AM JST | 12:00 AM - 1:30 AM UTC | Ch.16 Zoom Room 16

[M-IS11] Biogeochemistry

convener:Keisuke Koba(Center for Ecological Research, Kyoto University), Hideaki Shibata(Field Science Center fot Northern Biosphere, Hokkaido University), Naohiko Ohkouchi(Japan Agency for Marine-Earth Science and Technology), Youhei Yamashita(Faculty of Environmental Earth Science, Hokkaido University), Chairperson:Keisuke Koba(Center for Ecological Research, Kyoto University), Yoshiyuki Inagaki(Forestry and Forest Products Research Institute)

9:00 AM - 9:15 AM JST | 12:00 AM - 12:15 AM UTC

[MIS11-01] Source of dissolved black carbon in streams

*Youhei Yamashita[1,2], Daiki Kojima[2], Natsumi Yoshida[2], Hideaki Shibata[3,2] (1.Faculty of Environmental Earth Science, Hokkaido University, 2.Graduate School of Environmental Science, Hokkaido University, 3.Field Science Center for Northern Biosphere, Hokkaido University)

9:15 AM - 9:30 AM JST | 12:15 AM - 12:30 AM UTC

[MIS11-02] Biodegradation kinetics of different molecular-size classes of freshwater dissolved organic matter

*Yasuhiko T. Yamaguchi[1], Koichi Shimotori[2], Akio Imai[2], Yusuke Okazaki[3], Tomoyuki Ohara[1], Miho Nakamura[1], Shoichi Hichiri[1], Takahiro Okamoto[1], Kazuhide Hayakawa[1] (1.Lake Biwa Environmental Research Institute, 2.NIES Lake Biwa Branch Office, National Institute for Environmental Studies, 3.Institute for Chemical Research, Kyoto University)

9:30 AM - 9:45 AM JST | 12:30 AM - 12:45 AM UTC

[MIS11-03] Responses of phytoplankton biomass to river-borne nutrient flux in the coastal waters of Suruga Bay

*Tomoya Iwata[1], Yuri Amada[1], Akifumi Kitabatake[1], Nao Yonehara[1], Mizuho Shikata[1], Hiroshi Kobayashi[1], Mitsuhiro Toratani[3], Akira Tsukagoshi[2], Kenji Kato[2] (1.Faculty of Life and Environmental Sciences, University of Yamanashi, 2.Faculty of Science, Shizuoka University, 3.School of Engineering, Tokai University)

9:45 AM - 10:00 AM JST | 12:45 AM - 1:00 AM UTC

[MIS11-04] Investigation on the sources of arsenic and the formation process of arsenic-rich peat in groundwater level in Asia

*Thinh Van NGUYEN[1], Kuwahara Yoshihiro[1], Masaru Matsumoto[2], Thanh Dinh Xuan[3], Nguyen Dinh Nguyen[3], Myo Zaw[4] (1.Department of Environmental changes, Faculty of Social and Cultural Studies, Kyushu University, Fukuoka, 819-0395, Japan, 2.Institute of Tropical Agriculture, Kyushu University, Fukuoka, 819-0395, Japan, 3.Faculty of Geology, Hanoi University of Science, Vietnam National University, 334 Nguyen Trai, Thanh Xuan, Hanoi, Vietnam., 4.Graduate School of Integrated Sciences for Global Society, Kyushu University, Fukuoka, 819-0395, Japan)

10:00 AM - 10:15 AM JST | 1:00 AM - 1:15 AM UTC

[MIS11-05] Why is Rawanbuki large?

*Masaaki Chiwa[1], Yasuhiro Utsumi[1], Naoaki Tashiro[1], Yuko Yasuda[1,4], Ken'ichi Shinoduka[1,3], Ru Yang[1], Nao Nagano[1], Shusuke Murata[1], Takuma Nakamura[1], Kohei Yamauchi[1], Yuji Kabemura[1], Tatsuro Ando[2], Hiroshi Sawamura[2] (1.Kyushu University Forest, 2.Ashoro Museum of Paleontology, 3.Fukuoka Institute of Technology, 4.Forest Research and Management Organization)

10:15 AM - 10:30 AM JST | 1:15 AM - 1:30 AM UTC

[MIS11-06] Comparison of litter decomposition rates and dissolved organic carbon fluxes in soils across global climatic gradient

*Kazumichi Fujii[1], Chie Hayakawa[2], Yoshiyuki Inagaki[1], Shinya Funakawa[3], Kosaki Kosaki[4] (1.Forestry and Forest Products Research Institute, 2.Utsunomiya University, 3.Kyoto University, 4.Aichi University)

[J] Oral | M (Multidisciplinary and Interdisciplinary)：M-IS Intersection

10:45 AM - 12:15 PM JST | 1:45 AM - 3:15 AM UTC | Ch.16 Zoom Room 16

[M-IS11] Biogeochemistry

convener:Keisuke Koba(Center for Ecological Research, Kyoto University), Hideaki Shibata(Field Science Center fot Northern Biosphere, Hokkaido University), Naohiko Ohkouchi(Japan Agency for Marine-Earth Science and Technology), Youhei Yamashita(Faculty of Environmental Earth Science, Hokkaido University), Chairperson:Keisuke Koba(Center for Ecological Research, Kyoto University), Hideaki Shibata(Field Science Center fot Northern Biosphere, Hokkaido University)

10:45 AM - 11:00 AM JST | 1:45 AM - 2:00 AM UTC

[MIS11-07] Effects of understory vegetation removal on soil nitrogen availability and ectomycorrhizal community composition in a northern forest

*Karibu Fukuzawa[1], Takeshi Taniguchi[2], Masataka Nakayama[3] (1.Field Science Center for Northern Biosphere, Hokkaido University, 2.Arid Land Research Center, Tottori University, 3.Graduate School of Agriculture, Kyoto University)

11:00 AM - 11:15 AM JST | 2:00 AM - 2:15 AM UTC

[MIS11-08] Source identification of nitrate increased in forest streams during rainfall events

*Weitian Ding[1], Urumu Tsunogai[1], Fumiko Nakagawa[1], Hiroyuki Sase[2], Masayuki Morohashi[2], Hiroki Yotsuyanagi[2] (1.Graduate School of Environmental Studies, Nagoya University, 2.Asia Center for Air Pollution Research)

11:15 AM - 11:30 AM JST | 2:15 AM - 2:30 AM UTC

[MIS11-09] Chloride cycling in forested watersheds in the Shimanto River Basin

*Yoshiyuki Inagaki[1], Hisao Sakai[1], Atsushi Torii[1], Yoshiki Shinomiya[1], Kazumichi Fujii[1] (1.Forestry and Forest Products Research Institute)

11:30 AM - 11:45 AM JST | 2:30 AM - 2:45 AM UTC

[MIS11-10] To close the nitrogen budgets at a rice paddy

*Kentaro Hayashi[1] (1.Institute for Agro-Environmental Sciences, NARO)

11:45 AM - 12:00 PM JST | 2:45 AM - 3:00 AM UTC

[MIS11-11] Evaluation of global riverine N_2 and N_2O emissions using biogeochemical model

*Kazuya Nishina[1], Akihiko Ito[1] (1.NIES National Institute of Environmental Studies)

12:00 PM - 12:15 PM JST | 3:00 AM - 3:15 AM UTC

[MIS11-12] Footprint analysis on nutrient runoff from farmland in regions of Japan

*Azusa Oita[1], Yoshiya Touge[2], Taku Ishiro[3], Kaori Matsuoka[1], Yusuke Takata[1], Kentaro Hayashi[1] (1.National Agriculture and Food Research Organization, 2.Tohoku University, 3.Yokohama National University)

[J] Oral | M (Multidisciplinary and Interdisciplinary)：M-IS Intersection

1:45 PM - 3:15 PM JST | 4:45 AM - 6:15 AM UTC | Ch.26 Zoom Room 26

[M-IS16] Paleoclimatology and paleoceanography

convener:Yusuke Okazaki(Department of Earth and Planetary Sciences, Graduate School of Science, Kyushu University), Hitoshi Hasegawa(Faculty of Science and Technology, Kochi University), Atsuko Yamazaki(Faculty of Science, Kyushu University), Akitomo Yamamoto(Japan Agency for Marine-Earth Science and TechnologyAtmosphere and Ocean Research Institute), Chairperson:Atsuko Yamazaki(Faculty of Science, Kyushu University)

1:45 PM - 2:07 PM JST | 4:45 AM - 5:07 AM UTC

[MIS16-01] Recent progress of the microscale isotopic analytical technique of carbonate (MICAL) and the applications to the high resolution environmental analysis

★Invited Papers

*Toyoho Ishimura[1] (1.Graduate School of Human and Environmental Studies, Kyoto University)

2:07 PM - 2:30 PM JST | 5:07 AM - 5:30 AM UTC

[MIS16-02] Coral Sclerochronology: High-temporal resolution windows for Palaeoclimatology, Palaeocenography, and Palaeoecology

★Invited Papers

*Tsuyoshi Watanabe[1] (1.Hokkaido University /KIKAI Institute for coral reefs sciences)

2:30 PM - 2:45 PM JST | 5:30 AM - 5:45 AM UTC

[MIS16-03] **Hydroclimate seasonality during mid- to late Holocene transition: Evidence of East Asian Monsoon dynamics from fossil corals**

*Kevin Lariosa Garas[1,3,4], Tsuyoshi Watanabe[1,3], Atsuko Yamazaki[2,3], Tarou Komagoe[3] (1.Hokkaido University, 2.Kyushu University, 3.Kikai Institute for Coral Reef Sciences, 4.Mines and Geosciences Bureau-Philippines)

2:45 PM - 3:00 PM JST | 5:45 AM - 6:00 AM UTC

[MIS16-04] Reconstruction of Past Hawaiian Sea Surface Temperature (SST) Using Modern Coral Skeletal Sr/Ca ratio: Decadal Response to Trade Winds

*Ryohei Uchiyama[1], Tsuyoshi Watanabe[1,2], Taro Nojiri[3], Takaaki TK Watanabe[1,4], Samuel Kahng[5], Atsuko Yamazaki[1,2,6] (1.Graduate School of Science, Hokkaido University, 2.KIKAI Institute for Coral Reef Sciences, 3.Faculty of Science, Hokkaido University, 4.Universität zu Kiel, 5.University of Hawaii at Manoa, 6.Faculty of Science, Kyushu University)

3:00 PM - 3:15 PM JST | 6:00 AM - 6:15 AM UTC

[MIS16-05] High-spatiotemporal-resolution hindcast simulation for reproducing coral reef environments in Sekisei Lagoon, Okinawa, Japan

*Takashi Nakamura[1], Takafumi Sakuma[1] (1.School of Environment and Society, Tokyo Institute of Technology)

[J] Oral | M (Multidisciplinary and Interdisciplinary)：M-IS Intersection

3:30 PM - 5:00 PM JST | 6:30 AM - 8:00 AM UTC | Ch.26 Zoom Room 26

[M-IS16] Paleoclimatology and paleoceanography

convener:Yusuke Okazaki(Department of Earth and Planetary Sciences, Graduate School of Science, Kyushu University), Hitoshi Hasegawa(Faculty of Science and Technology, Kochi University), Atsuko Yamazaki(Faculty of Science, Kyushu University), Akitomo Yamamoto(Japan Agency for Marine-Earth Science and TechnologyAtmosphere and Ocean Research Institute), Chairperson:Yusuke Okazaki(Department of Earth and Planetary Sciences, Graduate School of Science, Kyushu University)

3:30 PM - 3:52 PM JST | 6:30 AM - 6:52 AM UTC

[MIS16-06] Today's drought extremes, little ice age wet extremes, and quiet 3 centuries in between: observations from Guatemalan varves, 1413±4 to 2015±0 CE

★Invited Papers

*Ikuko Kitaba[1], GPB15 Project Members (1.Ritsumeikan University)

3:52 PM - 4:07 PM JST | 6:52 AM - 7:07 AM UTC

[MIS16-07] Recognition of annual lamination and high-resolurion stable isotopic records of cascade-type tufa.

*Akira Murata[1], Hirokazu Kato[1], Akihiro Kano[1] (1.The University of Tokyo)

4:07 PM - 4:22 PM JST | 7:07 AM - 7:22 AM UTC

[MIS16-08] Effects of environmental changes on planktic foraminiferal shells assessed by the investigation of micro-X-ray CT.

*Shunichi Kinoshita[1], Quan Wang[2], Azumi Kuroyanagi[3], Masafumi MURAYAMA[4], Yurika Ujiie[5], Hodaka Kawahata[2] (1.Department of Geology and Paleontology National Museum of Nature and Science, 2.Atmosphere Ocean Research Institute, the University of Tokyo, 3.Tohoku University Museum, The Center for Academic Resources and Archives, Tohoku University, 4.Faculty of Agriculture and Marine Science, Kochi University, 5.Center for Advanced Marine Core Research, Kochi University)

4:22 PM - 4:37 PM JST | 7:22 AM - 7:37 AM UTC

[MIS16-09] Paleoenvironmental reconstruction of the North Pacific Subtropical Mode Water at the Last Glacial Maximum based on carbon- and oxygen-isotope composition of fossil brachiopod *Basiliola lucida*

*Haruna Sugazawa[1], Hideko Takayanagi[1], Yusuke Yokoyama[2], Takuya Itaki[3], Toshihiro Miyajima[2], Yasufumi Iryu[1] (1.Institute of Geology and Paleontology, Graduate School of Science, Tohoku University, 2.Atmosphere and Ocean Research Institute, The University of Tokyo , 3.Advanced Industrial Science and Technology)

4:37 PM - 5:00 PM JST | 7:37 AM - 8:00 AM UTC

[MIS16-10] Evaluation of proxy system models for stable water isotopes and introduction of their application to paleoclimate studies

★Invited Papers

*Okazaki Atsushi[1], Kei Yoshimura[2] (1.The Pennsylvania State University, 2.The University of Tokyo)

[J] Oral | M (Multidisciplinary and Interdisciplinary) : M-IS Intersection

10:45 AM - 12:15 PM JST | 1:45 AM - 3:15 AM UTC | Ch.19 Zoom Room 19

[M-IS18] Drilling Earth Science

convener:Junichiro Kuroda(Department of Ocean Floor Geoscience, Atmosphere and Ocean Research Institute, the University of Tokyo), Katsuyoshi Michibayashi(Department of Earth and Planetary Sciences, Nagoya University), Osamu Fujiwara(Geological Survey of Japan, National Institute of Advanced Industrial Science and Technology), Kohtaro Ujiie(Faculty of Life and Environmental Sciences, University of Tsukuba), Chairperson:Junichiro Kuroda(Department of Ocean Floor Geoscience, Atmosphere and Ocean Research Institute, the University of Tokyo), Kazutaka Yasukawa(Frontier Research Center for Energy and Resources, School of Engineering, The University of Tokyo)

10:45 AM - 11:00 AM JST | 1:45 AM - 2:00 AM UTC

[MIS18-01] **Age determination of pelagic clay using Monte Carlo simulation constrained by ichthyolith biostratigraphy and bulk cobalt concentrations**

*Kazuhide Mimura[1], Kentaro Nakamura[1], Kazutaka Yasukawa[1,2], Junichiro Ohta[1,2], Koichiro Fujinaga[2,1], Yoichi Usui[3], Yasuhiro Kato[1,2] (1.Department of Systems Innovation, School of Engineering, the University of Tokyo, 2.Ocean Resources Research Center for Next Generation, Chiba Institute of Technology, 3.Japan Agency for Marine-Earth Science and Technology)

11:00 AM - 11:15 AM JST | 2:00 AM - 2:15 AM UTC

[MIS18-02] **Preliminary report of IODP Expedition 378: South Pacific Paleogene Climate**

*Kazutaka Yasukawa[1,2], Erika Tanaka[1], Deborah J Thomas[3], Ursula Röhl[4], Laurel Childress[3], IODP Expedition 378 Science Party[5] (1.School of Engineering, The University of Tokyo, 2.ORCeNG, Chiba Institute of Technology, 3.Texas A&M University, 4.MARUM, University of Bremen, 5.List of scientific participants (http://iodp.tamu.edu/scienceops/precruise/southpacific/participants.html))

11:15 AM - 11:30 AM JST | 2:15 AM - 2:30 AM UTC

[MIS18-03] IODP proposal for re-drilling in the East China Sea to understand the millennial-scale variability of the Asian monsoon during the Quaternary

★Invited Papers

*Yoshimi Kubota[1], Ken Ikehara[2], Kenji Matsuzaki[3], Saki Ishino[2], Ayanori Misawa[2], Makoto Otsubo[2], Masataka Kinoshita[4], Katsura Kameo[3], Chiori Tamura[3], Ryuta Arai[5], Tomohiro Toki[6], Yuki Mitsutome[6], Zhirong Cai[7], Keiko Takehara[8], Kato Koudai[8], Daisuke Kuwano[9], Koshiro Matsuo[10], Keita Suzuki[11], Misaki Horiuchi[11], Yohei Katayama[12], Satoshi Okumura[13], Ryuji Tada[14], Tomohisa Irino[15], Kohsaku Arai[2], Takahiko Inoue[2], Takuya Sagawa[16], Minoru Ikehara[8], Yusuke Okazaki[10], Keiji Horikawa[17] (1.National Museum of Nature and Science, 2.National Institute of Advanced Industrial Science and Technology, 3.Atmosphere and Ocean Research Institute, The university of Tokyo, 4.Earthquake Research Institute, University of Tokyo, 5.Japan Agency for Marine-Earth Science and Technology, 6.University of the Ryukyus, 7.Kyoto University, 8.Kochi University, 9.China University, 10.Kyusyu University, 11.Nippon Marine Enterprises, Ltd., 12.Marine Works Japan, Ltd., 13.MOL Marine Co., Ltd., 14.Hokkaido University, 15.Graduate School of Science, The Univeristy of Tokyo, 16.Kanazawa University, 17.Toyama University)

11:30 AM - 11:45 AM JST | 2:30 AM - 2:45 AM UTC

[MIS18-04] **SCORE proposal off Shikoku, SW Japan: Reconstruction of the Kuroshio state for super interglacials during the Brunhes chron**

*Minoru Ikehara[1], Hiroshi Nishi[2], Tabito Matsu'ura, Kyoko Hagino[1], Takuya Itaki[3], Kyung Eun Lee[4], Yuan-Pin Chang[5], Jianjun Zou[6] (1.Center for Advanced Marine Core Research, Kochi University, 2.Fukui Prefectural University, 3.AIST, 4.Korea Maritime and Ocean University, 5.National Sun Yat-sen University, 6.First Institute of Oceanography)

11:45 AM - 12:00 PM JST | 2:45 AM - 3:00 AM UTC

[MIS18-05] **Organic geochemical characteristic and its significance of Jurassic-Cretaceous terrestrial sediments recovered by IODP deep sea drilling**

*Shutaro Fukushima[1], Takashi Hasegawa[1] (1.Kanazawa University)

12:00 PM - 12:15 PM JST | 3:00 AM - 3:15 AM UTC

[MIS18-06] Carbon isotope stratigraphy of C40-alkenone and its significance: Cretaceous OAE2 horizon, IODP Site U1516

*Takashi Hasegawa[1], Akiko S. Goto[1,2] (1.Faculty of Geoscience and Engineering, Institute of Science and Engineering, Kanazawa University, 2.Center of Ecological Research, Kyoto University)

[J] Oral | M (Multidisciplinary and Interdisciplinary)：M-IS Intersection

1:45 PM - 3:15 PM JST | 4:45 AM - 6:15 AM UTC | Ch.19 Zoom Room 19

[M-IS18] Drilling Earth Science

convener:Junichiro Kuroda(Department of Ocean Floor Geoscience, Atmosphere and Ocean Research Institute, the University of Tokyo), Katsuyoshi Michibayashi(Department of Earth and Planetary Sciences, Nagoya University), Osamu Fujiwara(Geological Survey of Japan, National Institute of Advanced Industrial Science and Technology), Kohtaro Ujiie(Faculty of Life and Environmental Sciences, University of Tsukuba), Chairperson:Yuki Morono(Kochi Institute for Core Sample Research, Japan Agency for Marine-Earth Science and Technology), Junichiro Kuroda(Department of Ocean Floor Geoscience, Atmosphere and Ocean Research Institute, the University of Tokyo)

1:45 PM - 2:00 PM JST | 4:45 AM - 5:00 AM UTC

[MIS18-07] Chronostratigraphic big data assimilation to characterize the Late Cenozoic warming episodes

*Masao IWAI[1], Yuji YAMAMOTO[1], Hiroshi ASAHI[1], Yurika Ujiie[1], Minoru Ikehara[1], Eiichi TOKUYAMA[1] (1.Center for Advanced Marine Core Research, Kochi University)

2:00 PM - 2:15 PM JST | 5:00 AM - 5:15 AM UTC

[MIS18-08] Magnetostratigraphy of IODP Site U1524A from the Ross Sea, Antarctica

*Xiangyu Zhao[1], Saiko Sugisaki[2], Tim van Peer[3], Yusuke Suganuma[1,4], Laura De Santis[5], Robert McKay[6], Denise Kulhanek[7] (1.National Institute of Polar Research, 2.National Institute of Advanced Industrial Science and Technology, Japan, 3.National Oceanography Centre Southampton, University of Southampton, UK, 4.Department of Polar Science, SOKENDAI (The Graduate University for Advanced Studies), Japan , 5.Instituto Nazionale di Oceanografia e di Geofisica Sperimentale, Italy, 6.Antarctic Research Centre, Victoria University of Wellington, Wellington, New Zealand, 7.International Ocean Discovery Program, Texas A&M University, College Station, TX, USA)

2:15 PM - 2:30 PM JST | 5:15 AM - 5:30 AM UTC

[MIS18-09] Discovery of living microbes from the ancient subseafloor sediment up to 101.5 million years old: How is it possible for microbes to survive for such a geological timescale?

★Invited Papers

*Yuki Morono[1] (1.Kochi Institute for Core Sample Research, Japan Agency for Marine-Earth Science and Technology)

2:30 PM - 2:45 PM JST | 5:30 AM - 5:45 AM UTC

[MIS18-10] A signature of heat along a micro-fault in Hikurangi margin, New Zealand: IODP Expedition 375, Site U1518

*Yoshitaka Hashimoto[1], Tomoki Masaoka[1], Hirohito Fujiwara[1] (1.Kochi University)

2:45 PM - 3:00 PM JST | 5:45 AM - 6:00 AM UTC

[MIS18-11] Drilling and monitoring in Hyuga-Nada: Unveiling effects of ridge subduction on slow earthquakes

★Invited Papers

*Rie Nakata[1], Masataka Kinoshita[1], Yoshitaka Hashimoto[2], Yohei Hamada[3] (1.Earthquake Research Institute, University of Tokyo, 2.Kochi University, 3.JAMSTEC)

3:00 PM - 3:15 PM JST | 6:00 AM - 6:15 AM UTC

[MIS18-12] ICDP DSeis project: an overview of the 2020 research activity

★Invited Papers

*Hiroshi Ogasawara[1], Team ICDP DSeis (1.Faculty of Science and Engineering, Ritsumeikan University)

[J] Oral | M (Multidisciplinary and Interdisciplinary) : M-IS Intersection

3:30 PM - 5:00 PM JST | 6:30 AM - 8:00 AM UTC | Ch.19 Zoom Room 19

[M-IS18] Drilling Earth Science

convener:Junichiro Kuroda(Department of Ocean Floor Geoscience, Atmosphere and Ocean Research Institute, the University of Tokyo), Katsuyoshi Michibayashi(Department of Earth and Planetary Sciences, Nagoya University), Osamu Fujiwara(Geological Survey of Japan, National Institute of Advanced Industrial Science and Technology), Kohtaro Ujiie(Faculty of Life and Environmental Sciences, University of Tsukuba), Chairperson:Osamu Fujiwara(Geological Survey of Japan, National Institute of Advanced Industrial Science and Technology), Tomoaki Morishita(School of Geoscience and Civil Engineering, College of Science and Technology, Kanazawa University), Kohtaro Ujiie(Faculty of Life and Environmental Sciences, University of Tsukuba)

3:30 PM - 3:45 PM JST | 6:30 AM - 6:45 AM UTC

[MIS18-13] Drilling of Kikai caldera volcano for elucidation of magma plumbing system and flow-deposition processes of large ignimbrite

★Invited Papers

*Katsuya Kaneko[1], Takeshi Hanyu[1], Reina NAKAOKA[3], Koji Kiyosugi[3], Nobukazu Seama[1], Tetsuo Matsuno[3], Yojiro Yamamoto[2], Tomoko Hanyu[3] (1.Department of Planetology, Graduate School of Science, Kobe University, 2.Japan Agency for Marine-Earth Science and Technology, 3.Kobe Ocean-Bottom Exploration Center, Kobe University)

3:45 PM - 4:00 PM JST | 6:45 AM - 7:00 AM UTC

[MIS18-14] Mado Megamullion: a potential new target for IODP drilling to understand backarc basin lithosphere

*Yasuhiko Ohara[1,2,3], Masakazu Fujii[4], Norikatsu Akizawa[5], Valentin Basch[6], Yumiko Harigane[7], Ken-ichi Hirauchi[8], Osamu Ishizuka[7], Shiki Machida[9], Katsuyoshi Michibayashi[3], Kyoko Okino[5], Alessio Sanfilippo[6], Camilla Sani[6], Sen Atlanta[10], Jonathan E Snow[11], Kenichiro Tani[12], Hiroyuki Yamashita[13] (1.Hydrographic and Oceanographic Department of Japan, 2.Japan Agency for Marine-Earth Science and Technology , 3.Nagoya University, 4.National Insitute of Polar Reseach, 5.Atmosphere and Ocean Research Institute, University of Tokyo, 6.University of Pavia, 7.Geological Survey of Japan, AIST, 8.Shizuoka University, 9.Chiba Institute of Technology, 10.University of Houston, 11.Louisiana State University, 12.National Science Museum, 13.Kanagawa Prefectural Museum of Natural Histroy)

4:00 PM - 4:15 PM JST | 7:00 AM - 7:15 AM UTC

[MIS18-15] Understanding of Oceanic Plate Hydration by drillings into plate bending-induced normal fault in incoming plate at off-Tohoku and the Horoman Peridotite complex

★Invited Papers

*Tomoaki Morishita[1] (1.School of Geoscience and Civil Engineering, College of Science and Technology, Kanazawa University)

4:15 PM - 4:30 PM JST | 7:15 AM - 7:30 AM UTC

[MIS18-16] Introduction to 'New Caledonia Ophiolite Land-to-Sea Drilling Project'

Marguerite Godard[1], Julien Collot[2], Juerg Matter[3], Rupert Sutherland[4], Christian Betzler[5], Vasileios Chatzaras[6], Gaël Erauso[7], François Fournier[7], Frieder Klein[8], Othmar Müntener[9], Martin Patriat[10], Roy Price[11], Shino Suzuki[12], *Yasuhiro Yamada[13] (1.Université de Montpellier, CNRS, France, 2.Geological Survey of New Caledonia, France, 3.University of Southampton, UK, 4.Victoria University of Wellington, NZ, 5.University Hamburg, Germany, 6.The University of Sydney, Australia, 7.Aix-Marseille Université, France, 8.Woods Hole Oceanographic Insitution, USA, 9.University of Lausanne, Switzerland, 10.Ifremer, France, 11.Stony Brook University, USA, 12.Japan Aerospace Exploration Agency, Japan, 13.Japan Agency for Marine-Earth Science and Technology)

4:30 PM - 4:45 PM JST | 7:30 AM - 7:45 AM UTC

[MIS18-17] In-situ stress at the basement under Osaka plain -estimation of stress values by DCDA method in deep seismic obsevation wells-

*Kentaro Omura[1], Akio Funato[2], Takatoshi Ito[3] (1.National Research Institute for Earth Science and Disaster Resilience, 2.Fukada Geological Institute, 3.Institute of Fluid Science, Tohoku University)

4:45 PM - 5:00 PM JST | 7:45 AM - 8:00 AM UTC

[MIS18-18] Tidally-modulated temperature observed at a drillsite in the Noho hydrothermal field in the mid-Okinawa Trough

*Masataka Kinoshita[1], Kazuya Kitada[2], Tatsuo Nozaki[2], Yuka Masaki[3], Lena Maeda[2], Hidenori Kumagai[2] (1.Earthquake Research Institute, University of Tokyo, 2.Japan Agency for Marine-Earth Science and Technology, 3.Cosmos Shoji Co., Ltd.)

[J] Oral | M (Multidisciplinary and Interdisciplinary)：M-IS Intersection

9:00 AM - 10:30 AM JST | 12:00 AM - 1:30 AM UTC | Ch.13 Zoom Room 13

[M-IS23] Mountain Science

convener:Keisuke Suzuki(Research Center for Mountain Environment, Shinshu University), Yoshihiko Kariya(Department of Environmental Geography, Senshu University), Akihiko SASAKI(Department of Geography and Environmental Studies, Kokushikan University), Chiyuki Narama(Niigata University, Program of Field Research in the Environmental Sciences), Chairperson:Kenshiro Arie(Niigata University)

9:00 AM - 9:15 AM JST | 12:00 AM - 12:15 AM UTC

[MIS23-01] Stratigraphy and ages of cores recovered from three linear depressions on the landslide bodies of deep-seated gravitational deformation slopes in the Kamikochi Valley, northern Japanese Alps

*Yoshihiko Kariya[1], Sadao Takaoka[1] (1.Department of Environmental Geography, Senshu University)

9:15 AM - 9:30 AM JST | 12:15 AM - 12:30 AM UTC

[MIS23-02] Comparison between Himalayan river sands and deep-sea Benga Fan sands using heavy mineral assemblage

*Kohki Yoshida[1], Subhadeep Kumar[2], Tomoyuki Hakiai[1], Asako Masuda[1], Lalit Kumar Rai[3] (1.Department of Geology, Faculty of Science, Shinshu University, 2.Department of Geology, Presidency University, 3.Interdisciplinary Graduate School of Science and Technology, Shinshu University)

9:30 AM - 9:45 AM JST | 12:30 AM - 12:45 AM UTC

[MIS23-03] The Characteristic Water Level Changes Mechanism of Kinugasanoike Pond on the Northern Japanese Alps

*Akihiko SASAKI[1], Motoshi Nishimura[2], Keisuke Suzuki[3,4] (1.Department of Geography and Environmental Studies, Kokushikan University, 2.National Institute of Polar Research, 3.Shinshu University, 4.Omachi Alpine Museum)

9:45 AM - 10:00 AM JST | 12:45 AM - 1:00 AM UTC

[MIS23-04] Large-scale flood in North India on 7 February 2021.

*Chiyuki Narama[1], Naho Yamada[2] (1.Niigata University, Program of Field Research in the Environmental Sciences, 2.Graduate School of Science and Technology, Niigata University)

10:00 AM - 10:15 AM JST | 1:00 AM - 1:15 AM UTC

[MIS23-05] Rapid drainage of Lago Greve, a large proglacial lake in Patagonia, observed by satellite in 2020

*Shuntaro Hata[1,2], Shin Sugiyama[2], Kosuke Heki[3] (1.Division of Earth System Science, Graduate School of Environmental Science, Hokkaido University, 2.Institute of Low Temperature Science, Hokkaido University, 3.Department of Earth and Planetary Sciences, Hokkaido University)

10:15 AM - 10:30 AM JST | 1:15 AM - 1:30 AM UTC

[MIS23-06] Mass balance characteristics of three recognized glaciers in the Northern Japanese Alps

★Invited Papers

*Takanobu Sawagaki[1], Satoru Yamaguchi[2], Kotaro FUKUI[3] (1.Faculty of Social Sciences, Hosei University, 2.Snow and ice Research center,, National Research Institute for Earth Science and Disaster prevention, 3.Tateyama Caldera Sabo Museum)

[J] Oral | M (Multidisciplinary and Interdisciplinary)：M-IS Intersection

10:45 AM - 12:15 PM JST | 1:45 AM - 3:15 AM UTC | Ch.13 Zoom Room 13

[M-IS23] Mountain Science

convener:Keisuke Suzuki(Research Center for Mountain Environment, Shinshu University), Yoshihiko Kariya(Department of Environmental Geography, Senshu University), Akihiko SASAKI(Department of Geography and Environmental Studies, Kokushikan University), Chiyuki Narama(Niigata University, Program of Field Research in the Environmental Sciences), Chairperson:Motoshi NISHIMURA(Arctic Environmental Research Center, National Institute of Polar Research)

10:45 AM - 11:00 AM JST | 1:45 AM - 2:00 AM UTC

[MIS23-07] Snow depth distribution in the Kamikochi-Azusa River basin in the Northern Japan Alps

*Keisuke Suzuki[1], Akihiko Sasaki[2] (1.Research Center for Mountain Environment, Shinshu University, 2.Kokushikan University)

11:00 AM - 11:15 AM JST | 2:00 AM - 2:15 AM UTC

[MIS23-08] Snow depth distribution of Mt. Norikura in the Northern Japan Alps

Rui Tanaka[1], Motoshi Nishimura[2], Akihiko Sasaki[3], *Keisuke Suzuki[4] (1.Shinshu University, 2.National Institute of Polar Research, 3.Kokushikan University, 4.Research Center for Mountain Environment, Shinshu University)

11:15 AM - 11:30 AM JST | 2:15 AM - 2:30 AM UTC

[MIS23-09] Cold air pool formed in Kamikochi, Northern Japan Alps

Sari Koyama[1], Motoshi Nishimura[2], Akihiko Sasaki[3], *Keisuke Suzuki[4] (1.Shinshu University, 2.National Institute of Polar Research, 3.Kokushikan University, 4.Research Center for Mountain Environment, Shinshu University)

11:30 AM - 11:50 AM JST | 2:30 AM - 2:50 AM UTC

[MIS23-10] Long-term Measurements of Atmospheric Aerosol, Cloud and Snow at Mt. Tateyama

★Invited Papers

*Kazuma Aoki[1] (1.University of Toyama)

11:50 AM - 12:10 PM JST | 2:50 AM - 3:10 AM UTC

[MIS23-11] Future projections in snow cover over high mountainous areas in central Japan simulated by non-hydrostatic regional climate model

★Invited Papers

*Hiroaki Kawase[1], Takeshi Yamazaki[2], Shiori Sugimoto[3], Akihiko Murata[1], Masaya Nosaka[1], Hidetaka Sasaki[1] (1.Meteorological Research Institute, Japan Meteorological Agency, 2.Tohoku University, 3.Japan Agency for Marine-Earth Science and Technology)

12:10 PM - 12:15 PM JST | 3:10 AM - 3:15 AM UTC

[MIS23-12] Discussion

[J] Oral | M (Multidisciplinary and Interdisciplinary)：M-IS Intersection

1:45 PM - 3:15 PM JST | 4:45 AM - 6:15 AM UTC | Ch.13 Zoom Room 13

[M-IS23] Mountain Science

convener:Keisuke Suzuki(Research Center for Mountain Environment, Shinshu University), Yoshihiko Kariya(Department of Environmental Geography, Senshu University), Akihiko SASAKI(Department of Geography and Environmental Studies, Kokushikan University), Chiyuki Narama(Niigata University, Program of Field Research in the Environmental Sciences), Chairperson:Asaka Konno(Tokoha University)

1:45 PM - 2:00 PM JST | 4:45 AM - 5:00 AM UTC

[MIS23-13] An automated method for drawing land cover maps from time-lapse photographs of alpine landscapes

*Ryotaro Okamoto[1], Hiroyuki Oguma[2], Reiko Ide[2] (1.University of Tsukuba, 2.National Institute for Environmental Studies)

2:00 PM - 2:20 PM JST | 5:00 AM - 5:20 AM UTC

[MIS23-14] The role of mountains in the creation of biodiversity

★Invited Papers

*Tomoya Suzuki[1], Koji Tojo[1,2] (1.Faculty of Science, Shinshu University, 2.Institute of Mountain Science, Shinshu University)

2:20 PM - 2:35 PM JST | 5:20 AM - 5:35 AM UTC

[MIS23-15] Comparison of hypotheses about formation of the pseudo-alpine zone in accordance with topo-climatological survey

*Shiho Maniwa[1], Atsushi Ikeda[1] (1.University of Tsukuba)

2:35 PM - 2:55 PM JST | 5:35 AM - 5:55 AM UTC

[MIS23-16] Expanding process of *Abies mariesii* woodland from pollen records since the early Holocene at the Komatsubara peat bogs, Mt. Naeba, central Japan

★Invited Papers

*Akihiro Yoshida[1], Arata Momohara[2], Yuichiro Kudo[3], Yasuhiro Taniguchi[4] (1.Kagoshima Univ., 2.Chiba Univ., 3.Gakushuin Women's College, 4.Kokugakuin Univ.)

2:55 PM - 3:15 PM JST | 5:55 AM - 6:15 AM UTC

[MIS23-17] The formation of mountain landscape in the headwaters area of the Yodo river : A case study of Large Old-growth Japanese Horse-chestnut Forest

★Invited Papers

*Koki Teshirogi[1] (1.Setsunan University)

[J] Oral | M (Multidisciplinary and Interdisciplinary)：M-GI General Geosciences, Information Geosciences & Simulations

9:00 AM - 10:30 AM JST | 12:00 AM - 1:30 AM UTC | Ch.03 Zoom Room 03

[M-GI35] Computational sciences on the universe, galaxies, stars, planets, and their environments

convener:Yoshi-Yuki Hayashi(Department of Planetology/CPS, Graduate School of Science, Kobe University), Junichiro Makino(Kobe University), Kanya Kusano(Institute for Space-Earth Environmental Research, Nagoya University), Shigeru Ida(Earth-Life Science Institute, Tokyo Institute of Technology), Chairperson:Junichiro Makino(Kobe University), Yoshi-Yuki Hayashi(Department of Planetology/CPS, Graduate School of Science, Kobe University), Kanya Kusano(Institute for Space-Earth Environmental Research, Nagoya University), Eiichiro Kokubo(Division of Science, National Astronomical Observatory of Japan), Takayuki Saitoh(Kobe university)

9:00 AM - 9:15 AM JST | 12:00 AM - 12:15 AM UTC

[MGI35-01] Development of a non-hydrostatic global model of the Venus atmosphere: A simplified Venus simulation

*Hiroki Kashimura[1], Hisashi Yashiro[2], Seiya Nishizawa[3], Hirofumi Tomita[3], Masahiro Takagi[4], Norihiko Sugimoto[5], Kazunori Ogohara[4], Takeshi Kuroda[6], Kensuke Nakajima[7], Masaki Ishiwatari[8], Yoshiyuki O. Takahashi[1], Yoshi-Yuki Hayashi[1] (1.Department of Planetology, Graduate School of Science, Kobe University, 2.Center for Global Environmental Research, National Institute for Environmental Studies, 3.RIKEN Center for Computational Science, 4.Faculty of Science, Kyoto Sangyo University, 5.Department of Physics, Keio University, 6.Department of Geophysics Tohoku University, 7.Department of Earth and Planetary Sciences, Flculty of Sciences, Kyushu University, 8.Department of Cosmosciences, Graduate school of Science, Hokkaido University)

9:15 AM - 9:30 AM JST | 12:15 AM - 12:30 AM UTC

[MGI35-02] MHD simulations of solar flares associated with sunspot formation and evolution

*Takafumi Kaneko[1], Hideyuki Hotta[2], Kanya Kusano[1] (1.Institute for Space-Earth Environmental Research, Nagoya University, 2.Chiba University)

9:30 AM - 9:45 AM JST | 12:30 AM - 12:45 AM UTC

[MGI35-03] A large-eddy simulation of atmospheric boundary layer turbulence using the discontinuous Galerkin method

*Yuta Kawai[1], Hirofumi Tomita[1] (1.RIKEN Center for Computational Science)

9:45 AM - 10:00 AM JST | 12:45 AM - 1:00 AM UTC

[MGI35-04] Semi-analytic modeling of galaxies and AGN in the Fugaku era

*Taira Oogi[1], Hikari Shirakata[2], Masahiro Nagashima[3], Takahiro Nishimichi[4], Toshihiro Kawaguchi[5], Takashi Okamoto[6], Tomoaki Ishiyama[1], Motohiro Enoki[7] (1.Chiba University, 2.Tadano Ltd., 3.Bunkyo University, 4.Yukawa Institute for Theoretical Physics, Kyoto University, 5.Onomichi City University, 6.Hokkaido University, 7.Tokyo Keizai University)

10:00 AM - 10:15 AM JST | 1:00 AM - 1:15 AM UTC

[MGI35-05] Numerical study of the origin of merging binary black holes

*Ataru Tanikawa[1], Michiko S. Fujii[1], Jun Kumamoto[1], Long Wang[1], Alessandro Alberto Trani[1] (1.The University of Tokyo)

10:15 AM - 10:30 AM JST | 1:15 AM - 1:30 AM UTC

[MGI35-06] Discussion

[J] Oral | M (Multidisciplinary and Interdisciplinary)：M-GI General Geosciences, Information Geosciences & Simulations

10:45 AM - 12:15 PM JST | 1:45 AM - 3:15 AM UTC | Ch.18 Zoom Room 18

[M-GI35] Computational sciences on the universe, galaxies, stars, planets, and their environments

convener:Yoshi-Yuki Hayashi(Department of Planetology/CPS, Graduate School of Science, Kobe University), Junichiro Makino(Kobe University), Kanya Kusano(Institute for Space-Earth Environmental Research, Nagoya University), Shigeru Ida(Earth-Life Science Institute, Tokyo Institute of Technology), Chairperson:Yoshi-Yuki Hayashi(Department of Planetology/CPS, Graduate School of Science, Kobe University), Kanya Kusano(Institute for Space-Earth Environmental Research, Nagoya University), Junichiro Makino(Kobe University), Eiichiro Kokubo(Division of Science, National Astronomical Observatory of Japan), Takayuki Saitoh(Kobe university)

10:45 AM - 11:00 AM JST | 1:45 AM - 2:00 AM UTC

[MGI35-07] Acceleration program for Fugaku output generation: Unified view from cosmology to planets

*Junichiro Makino[1] (1.Kobe University)

11:00 AM - 11:15 AM JST | 2:00 AM - 2:15 AM UTC

[MGI35-08] Discussion

11:15 AM - 11:30 AM JST | 2:15 AM - 2:30 AM UTC

[MGI35-09] High-resolution magnetohydrodynamic simulations of two-temperature jet propagation using code CANS+

*Takumi Ohmura[1], Mami Machida[2], Yosuke Matsumoto[3], Ken Ohsuga[4], Ryoji Matsumoto[3] (1.Kyushu University, 2.National Astronomical Observatory of Japan, 3.Chiba University, 4.University of Tsukuba)

11:30 AM - 11:45 AM JST | 2:30 AM - 2:45 AM UTC

[MGI35-10] Core-Collpase Supernova Simulations by Boltzmann-Hydro Code

*Wakana Iwakami[1], Hirotada Okawa[1], Hiroki Nagakura[2], Akira Harada[3], Ryuichiro Akaho[1], Shun Furusawa[6], Hideo Matsufuru[5], Kosuke Sumiyoshi[4], Shoichi Yamada[1] (1.Waseda University, 2.Princeton University, 3.University of Tokyo, 4.Numazu College of Technology, 5.High Energy Accelerator Research Organization, 6.Tokyo University of Science)

11:45 AM - 12:00 PM JST | 2:45 AM - 3:00 AM UTC

[MGI35-11] Development of N-body Simulation Code for Planetary System Formation: GPLUM

*Yota Ishigaki[1,2], Eiichiro Kokubo[3], Junichiro Makino[4], Masaki Fujimoto[2] (1.University of Tokyo, 2.Institute of Space and Astronautical Science, Japan Aerospace Exploration Agency, 3.National Astronomical Observatory of Japan, 4.Kobe University)

12:00 PM - 12:15 PM JST | 3:00 AM - 3:15 AM UTC

[MGI35-12] Rocky Planetesimal Accretion under a Realistic Accretion Condition

*Takashi Shibata[1], Eiichiro Kokubo[1,2], Junichiro Makino[3], Yota Ishigaki[2] (1.National Astronomical Observatory of Japan, 2.The University of Tokyo, 3.Kobe University)

[J] Oral | M (Multidisciplinary and Interdisciplinary)：M-SD Space Development & Earth Observation from Space

9:00 AM - 10:30 AM JST | 12:00 AM - 1:30 AM UTC | Ch.08 Zoom Room 08

[M-SD40] Future Missions of Satellite Earth Observation

convener:Yoshiaki HONDA(Center for Environmental Remote Sensing, Chiba University), Yukari Takayabu(Atmosphere and Ocean Research Institute, the University of Tokyo), Shinichi Sobue(Japan Aerospace Exploration Agency), Kosuke Yamamoto(Japan Aerospace Exploration Agency), Chairperson:Yoshiaki HONDA(Center for Environmental Remote Sensing, Chiba University), Nobuhiro Takahashi(Institute for Space-Earth Environmental Research, Nagoya University), Kosuke Yamamoto(Japan Aerospace Exploration Agency)

9:00 AM - 9:15 AM JST | 12:00 AM - 12:15 AM UTC

[MSD40-01] Introduction

9:15 AM - 9:30 AM JST | 12:15 AM - 12:30 AM UTC

[MSD40-02] Consideration status of the sensors of Himawari follow-on satellite

*Kotaro BESSHO[1], Hiromi OWADA[1], Takuya Sakashita[1], Mikito Yamamoto[1] (1.Japan Meteorological Agency)

9:30 AM - 9:45 AM JST | 12:30 AM - 12:45 AM UTC

[MSD40-03] Lightning Observation from Geo-Stationary Orbit

*Tomoo Ushio[1], LightningGroup MInt (1.Osaka University)

9:45 AM - 10:00 AM JST | 12:45 AM - 1:00 AM UTC

[MSD40-04] Experimental platform for design and advance evaluation of frequent satellite observations to innovate weather, ocean and land surface predictions

*Takemasa Miyoshi[1], Koji Terasaki[1], Shunji Kotsuki[2,1], Shigenori Otsuka[1], Takumi Honda[1], Kohei Takatama[1], Atsushi Okazaki[3,1] (1.RIKEN, 2.Chiba University, 3.Pennsylvania State University)

10:00 AM - 10:15 AM JST | 1:00 AM - 1:15 AM UTC

[MSD40-05] Geostationary Optical Earth Observation Satellite (3)

*Kazuo Oki[1,2], Toshiyoshi Kimura[3], Tadahito Mizutani[3], Masuo Takahashi[3], Takeo Tadono[3] (1.The Univ. of Tokyo, 2.KUAS, 3.JAXA)

10:15 AM - 10:30 AM JST | 1:15 AM - 1:30 AM UTC

[MSD40-06] Geostationary Satellite Ocean Color Mission

*Joji Ishizaka[1], Mitsuhiro Toratani[2], Toru Hirawake[3], Takafumi Hirata[4], Hiroshi Kobayashi[5], Yuji Sakuno[6], Hiroshi Higa[7] (1.Institute for Space-Earth Environmental Research, Nagoya University, 2.Faculty of Engineering, Tokai University, 3.Fisheries Sciences, Hokkaido University, 4.Arctic Research Center, Hokkaido University, 5.Graduate Faculty of Interdisciplinary Research, University of Yamanashi, 6.Graduate School of Engineering, Hiroshima University, 7.Graduate School of Urban Innovation, Yokohama National University)

[J] Oral | M (Multidisciplinary and Interdisciplinary)：M-SD Space Development & Earth Observation from Space

10:45 AM - 12:15 PM JST | 1:45 AM - 3:15 AM UTC | Ch.08 Zoom Room 08

[M-SD40] Future Missions of Satellite Earth Observation

convener:Yoshiaki HONDA(Center for Environmental Remote Sensing, Chiba University), Yukari Takayabu(Atmosphere and Ocean Research Institute, the University of Tokyo), Shinichi Sobue(Japan Aerospace Exploration Agency), Kosuke Yamamoto(Japan Aerospace Exploration Agency), Chairperson:Yoshiaki HONDA(Center for Environmental Remote Sensing, Chiba University), Nobuhiro Takahashi(Institute for Space-Earth Environmental Research, Nagoya University), Kosuke Yamamoto(Japan Aerospace Exploration Agency)

10:45 AM - 11:00 AM JST | 1:45 AM - 2:00 AM UTC

[MSD40-07] Role of Japan on polarization observations from space

*Makiko Nakata[1], Itaru Sano[1], Sonoyo Mukai[2] (1.Kindai University, 2.The Kyoto College of Graduate Studies for Informatics)

11:00 AM - 11:15 AM JST | 2:00 AM - 2:15 AM UTC

[MSD40-08] Comprehensive atmospheric composition measurements and emissions estimations from geostationary orbit over Asia: Rationalizing decarbonization and air pollution mitigation strategies

*Yugo Kanaya[1], YASUKO KASAI[2], Hiroshi Tanimoto[3], Naoko Saitoh[4], Nawo Eguchi[5], Tomohiro Sato[2], Tamaki Fujinawa[3], Prabir Patra[1], Takashi Sekiya[1], Masayuki Takigawa[1], Satellite committee JpSAC (1.JAMSTEC, 2.NICT, 3.NIES, 4.Chiba Univ., 5.Kyushu Univ.)

11:15 AM - 11:30 AM JST | 2:15 AM - 2:30 AM UTC

[MSD40-09] **Multi-footprint Observation Lidar and Imager (MOLI) mission for performing highly precise estimation of elevation, forest height & biomass, and also for providing results of clouds & aerosols measurement**

*Kazuhiro Asai[1], Yasumasa - Hirata[2], Gen - Takao[2], Yoshiaki - Honda[3], Koji - Kajiwara[3], Yoshio - Awaya[4], Junichi - Susaki[5], Takahiro - Endo[6], Nobuo - Sugimoto[7], Tomoaki - Nishizawa[7], Kohei - Mizutani[10], Shoken - Ishii[8], Toshiyoshi - Kimura[9], Tadashi - Imai[9], Yoshito - Sawada[9], Masato - Hayashi[9], Daisuke - Sakaizawa[9], Rei - Mitsuhashi[9], Trung Tat Nguyen[9] (1.Tohoku Institute of Technology, 2.Forestry and Forest Products Research Institute, 3.Chiba University, 4.Gifu University, 5.Kyoto University, 6.The Remote Sensing Technology Center of Japan, 7.National Institute for Environmental Research, 8.Tokyo Metropolitan University, 9.Japan Aerospace Exploration Agency, 10.National Institute of Information and Communications Technology)

11:30 AM - 11:45 AM JST | 2:30 AM - 2:45 AM UTC

[MSD40-10] Cloud-Precipitation observation mission by active sensors (2)

*Nobuhiro Takahashi[1], Kinji Furukawa[2], Yukari Takayabu[3] (1.Institute for Space-Earth Environmental Research, Nagoya University, 2.JAXA, 3.The Atmosphere and Ocean Research Institute (AORI) , the University of Tokyo)

11:45 AM - 12:00 PM JST | 2:45 AM - 3:00 AM UTC

[MSD40-11] Discussion

*Kosuke Yamamoto[1] (1.Japan Aerospace Exploration Agency)

12:00 PM - 12:15 PM JST | 3:00 AM - 3:15 AM UTC

[MSD40-12] Discussion

[J] Oral | M (Multidisciplinary and Interdisciplinary) : M-ZZ Others

3:30 PM - 5:00 PM JST | 6:30 AM - 8:00 AM UTC | Ch.13 Zoom Room 13

[M-ZZ47] Renewable energy and earth science

convener:Hideaki Ohtake(National Institute of Advanced Industrial Science and Technology), Daisuke Nohara(Central Research Institute of Electric Power Industry), Teruhisa Shimada(Graduate School of Science and Technology, Hirosaki University), Fumichika Uno(Nihon University, College of Humanities and Sciences), Chairperson:Teruhisa Shimada(Graduate School of Science and Technology, Hirosaki University)

3:30 PM - 3:32 PM JST | 6:30 AM - 6:32 AM UTC

[MZZ47-01] Introduction

3:32 PM - 3:47 PM JST | 6:32 AM - 6:47 AM UTC

[MZZ47-02] Assessment of small hydropower generation potential in Shiribeshi subprefecture, Hokkaido

Mikiya Kato[2], *Masahiko Fujii[1,2] (1.Faculty of Environmental Earth Science, 2.Graduate School of Environmental Science, Hokkaido University)

3:47 PM - 4:02 PM JST | 6:47 AM - 7:02 AM UTC

[MZZ47-03] Assessment of snow and ice cryogenic energy potential in Hokkaido: a case study in Niseko Town

*Hehuan DUAN[1], Masahiko FUJII[1,2] (1.Graduate School of Environmental Science, Hokkaido University, 2.Faculty of Environmental Earth Science, Hokkaido University)

4:02 PM - 4:17 PM JST | 7:02 AM - 7:17 AM UTC

[MZZ47-04] Examination of the statistical forecast method of sunshine duration in Hokkaido

*Takao Sunamura[1], Hisashi Kato[1], Fumichika Uno[1] (1.Nihon University, College of Humanities and Sciences)

4:17 PM - 4:32 PM JST | 7:17 AM - 7:32 AM UTC

[MZZ47-05] Probabilistic Photovoltaic Power Prediction Based on Ensemble Weather Forecasting

*Daisuke Nohara[1], Yuki Kanno[1] (1.Central Research Institute of Electric Power Industry)

4:32 PM - 4:47 PM JST | 7:32 AM - 7:47 AM UTC

[MZZ47-06] Consideration of the use of the meso-ensemble prediction system under high penetration of renewable energy in future

*Hideaki Ohtake[1,3], Takashi Oozeki[1], Takahiro Takamatsu[1], Yuya Takane[1], Yusuke Mori[4], Shinji Wakao[4], Fumichika Uno[5], Masahiro Kazumori[2], Toshiyuki Nakaegawa[3] (1.National Institute of Advanced Industrial Science and Technology, 2.Japan Meteorological Agency, 3.Meteorological Research Institute, 4.Waseda University, 5.Nihon University)

4:47 PM - 5:00 PM JST | 7:47 AM - 8:00 AM UTC

[MZZ47-07] Discussion

[J] Oral | EVENT : EVENT

12:20 PM - 1:40 PM JST | 3:20 AM - 4:40 AM UTC | Ch.01 Zoom Room 01

[EV-16] Lunchtime Special Lecture

12:20 PM - 1:00 PM JST | 3:20 AM - 4:00 AM UTC

[E-11-19] Progress and Prospects of Global Flood Risk Research

---

1:00 PM - 1:40 PM JST | 4:00 AM - 4:40 AM UTC

[E-11-20] For whom do we do GLOF research in the Himalaya?

[J] Oral | EVENT : EVENT

11:30 AM - 12:15 PM JST | 2:30 AM - 3:15 AM UTC | Ch.17 Zoom Room 17

[EV-18] Exhibitors' Seminar

11:30 AM - 12:15 PM JST | 2:30 AM - 3:15 AM UTC

[E-11-18] Quantitative EDS Explained - How to achieve great results

[J] Oral | EVENT：EVENT

1:45 PM - 3:15 PM JST | 4:45 AM - 6:15 AM UTC | Ch.17 Zoom Room 17

[EV-19] Exhibitors' Pop-Up

1:45 PM - 3:15 PM JST | 4:45 AM - 6:15 AM UTC

[E-11-21] Exhibitors' Pop-Up

[J] Oral | EVENT：EVENT

9:45 AM - 10:30 AM JST | 12:45 AM - 1:30 AM UTC | Ch.19 Zoom Room 19

[EV-20] Exhibitors' Seminar

9:45 AM - 10:30 AM JST | 12:45 AM - 1:30 AM UTC

[E-11-17] Graduate School Programs on Earth Science and Geophysics at Tohoku University

[J] Oral | EVENT：EVENT

9:00 AM - 9:45 AM JST | 12:00 AM - 12:45 AM UTC | Ch.24 Zoom Room 24

[EV-21] Exhibitors' Seminar

9:00 AM - 9:45 AM JST | 12:00 AM - 12:45 AM UTC

[E-11-16] The Challenges of Scientific Drilling Sample Return: (1) IODP Exp. 386 - The Challenging Piston Coring from the Deepest Water Depth Ever / (2) The Science of Mantle Drilling Revisited

[J] Oral | P (Space and Planetary Sciences)：P-PS Planetary Sciences

Fri. Jun 4, 2021 10:45 AM - 12:15 PM JST | Fri. Jun 4, 2021 1:45 AM - 3:15 AM UTC | Ch.03 Zoom Room 03

[P-PS05] Lunar science and exploration

convener:N Masaki Nishino(Japan Aerospace Exploration Agency, Institute of Space and Astronautical Science), Masahiro KAYAMA(Department of General Systems Studies, Graduate School of Arts and Sciences, The University of Tokyo), Hiroshi Nagaoka(Institute of Physical and Chemical Research), Yusuke Nakauchi(Japan Aerospace Exploration Agency), Chairperson:Hiroshi Nagaoka(Institute of Physical and Chemical Research), Masaki N Nishino(Japan Aerospace Exploration Agency, Institute of Space and Astronautical Science)

Scientific data sets acquired by Japanese lunar mission SELENE (Kaguya) have become the standard of the lunar sciences. Other missions such as Chandrayaan-1, LRO, GRAIL, LCROSS, LADEE, Artemis, and Chang'e series as well as ground observations are also providing new knowledges of the Moon. Apollo/Luna samples and lunar meteorite analyses are also being advanced. In concurrence with these studies, some countries including Japan are planning near-future lunar missions. In this session, we will discuss scientific results based on newly acquired lunar data, strategies for future missions, lunar sample analyses, and theoretical and experimental studies of lunar sciences.

10:45 AM - 11:00 AM JST | 1:45 AM - 2:00 AM UTC

[PPS05-01] Numerical simulation of lunar seismic wave: Updated scattering structure around Apollo12 landing site from coda fitting approach

★Invited Papers

*Keisuke Onodera[1,2,3], Taichi Kawamura[2], Satoshi Tanaka[1,3], Yoshiaki Ishihara[4], Takuto Maeda[5] (1.The Graduate University for Advanced Studies, 2.IPGP/Université de Paris, 3.ISAS/JAXA, 4.JAXA Space Exploration Center, 5.Hirosaki University)

11:00 AM - 11:15 AM JST | 2:00 AM - 2:15 AM UTC

[PPS05-02] Effects of magma-generation and transport of heat and heat producing elements by migrating magma on the thermal history of the Moon.

*Kenyo U[1], Hiroki Hasumi[1], Masaki Ogawa[1] (1.The University of Tokyo)

11:15 AM - 11:30 AM JST | 2:15 AM - 2:30 AM UTC

[PPS05-03] Mass wasting process on lunar crater walls inferred from boulder falls

*Ayame Ikeda[1], Hiroyuki Kumagai[1], Tomokatsu Morota[2] (1.Graduate School of Environmental Studies, Nagoya University, 2.Department of Earth and Planetary Science, The University of Tokyo)

11:30 AM - 11:45 AM JST | 2:30 AM - 2:45 AM UTC

[PPS05-04] Recent boulder falls within the Finsen crater, an assessment of ongoing geological activities

*Trishit Ruj[1], Goro Komatsu[2], Kenji Kawai[1], Hanaya Okuda[3], Zhiyong Xiao[4], Deepak Dhingra[5] (1.Department of Earth and Planetary Science, School of Science, The University of Tokyo, 2.International Research School of Planetary Sciences, Università G. d'Annunzio, Viale Pindaro 42, 65127, Pescara, Italy, 3.Department of Ocean Floor Geoscience, Atmosphere and Ocean Research Institute, University of Tokyo, Kashiwanoha 5-1-5, Kashiwa, Chiba 277-8564, Japan, 4.Planetary Environmental and Astrobiological Research Laboratory, School of Atmospheric Sciences, Sun Yat-sen University, Zhuhai, China, 5.Department of Earth Sciences, Indian Institute of Technology Kanpur, Kanpur, UP 208016, India)

11:45 AM - 12:00 PM JST | 2:45 AM - 3:00 AM UTC

[PPS05-05] Lunar Surface Mapping by SLAM Technology on Bionic Legged Rover

*LIANG CHEN[1], Takehiko Arai[1], Makiko Ohtake[2] (1.Ashikaga University, 2.University of Aizu)

12:00 PM - 12:15 PM JST | 3:00 AM - 3:15 AM UTC

[PPS05-06] Deciphering the planetary water flux from the water record expected at lunar pole

*Ko Hashizume[1], Chihiro Yamanaka[2], Masahiro KAYAMA[3], Makiko Ohtake[4] (1.Ibaraki University, 2.Osaka University, 3.The University of Tokyo, 4.The University of Aizu)

Numerical simulation of lunar seismic wave: Updated scattering structure around Apollo12 landing site from coda fitting approach

*Keisuke Onodera[1,2,3], Taichi Kawamura[2], Satoshi Tanaka[1,3], Yoshiaki Ishihara[4], Takuto Maeda[5]

1. The Graduate University for Advanced Studies, 2. IPGP/Université de Paris, 3. ISAS/JAXA, 4. JAXA Space Exploration Center, 5. Hirosaki University

The Apollo lunar seismic observation opened a way to investigate the internal structure of the Moon. Using the Apollo seismic data, previous studies (e.g. [1] and references therein) tried to constrain 1D velocity structure mainly through a classical travel time analysis. Generally, in travel time analysis, the determination of seismic phase arrival (e.g. P, S) is a key to a precise estimation of the inner structure. However, while seismic phases can be read with a precision of 0.1 s for earthquakes, it becomes worse by about 1-3 orders in the case of the Moon due to an intense scattering of regolith and/or megaregolith. Since the arrival reading differs from researcher to researcher, the resulting structures fall within a large error, which implies that the lunar internal structure is still uncertain. As the internal structure gives a crucial information for constraining the origin and evolution of the Moon, this problem is placed as one of the most significant issues in lunar science.

In this study, we propose a novel way to constrain the internal structure. The previous studies or classical seismology determines it based on a point information within time-series (to be clear P, S arrival). On the other hand, we attempt to constrain it by conducting numerical simulations under different parameter settings (like P-wave, S-wave model, scattering model) and by fitting the shape of the observed seismic data by Apollo. Although this kind of approach is not a major way in seismology, we found it possible to constrain not only 1D velocity structure but also internal heterogeneity with this method since a seismic wave envelope actually depends on both internal scattering properties and seismic wave velocity profile.

In the presentation, we will show results of the velocity and scattering structure around Apollo12 landing site estimated by modeling Apollo artificial impacts. After that, we will discuss how our results can contribute to future lunar or other planetary seismic explorations.

Reference

[1] Garcia et al., Lunar seismology: An update on interior structure models, Space Sci. Rev., 215 :50, 2019, https://doi.org/10.1007/s11214-019-0613-y.

Keywords: Moon, Moonquake, Scattering, Apollo, Planetary seismology

©2021. Japan Geoscience Union. All Right Reserved.

Effects of magma-generation and transport of heat and heat producing elements by migrating magma on the thermal history of the Moon.

*Kenyo U[1], Hiroki Hasumi[1], Masaki Ogawa[1]

1. The University of Tokyo

Previous geological and geophysical observations of the Moon indicate its radial expansion in its early history and radial contraction in the later history. The most optimal models that explain this history commonly start from a low initial temperature in the deep mantle. However, this cold origin model is at odds with the giant-impact hypothesis. In order to resolve this difficulty, we numerically calculated the thermal history of the spherically symmetric mantle of the Moon, taking account of thermal diffusion, magma-generation, decay of heat-producing elements (HPEs), and the transport of HPEs by migration of the generated magma.

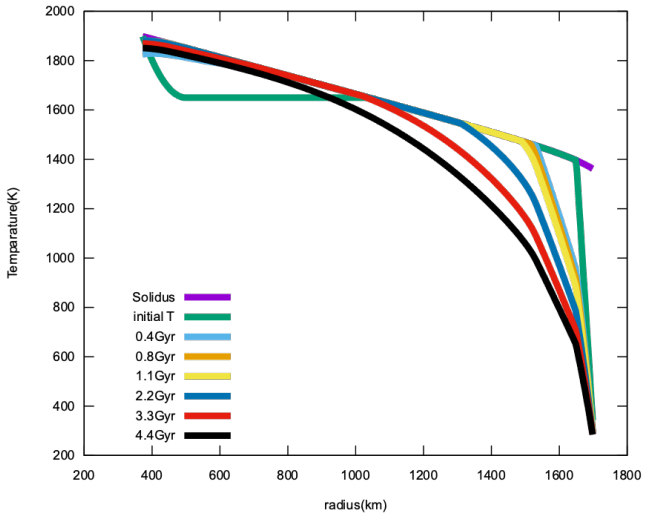
The initial temperature in the deep mantle is high enough to make the temperature in the shallow mantle equal to the solidus temperature. We considered the various amount of the melt-content in the shallow mantle. The temperature is fixed at 270K on the surface boundary, while the core is modeled as a heat bath of uniform temperature. The initial temperature on the CMB is about 1900 K. To take account of the blanket effect of the lunar crust and regolith layer, the thermal conductivity in the crust is about half that of the mantle. We also assume that the mantle is depleted in HPEs relative to the crust by a factor of 8 or 16, as suggested from studies of the Th concentration in the putative primary magmas of mare basalts.

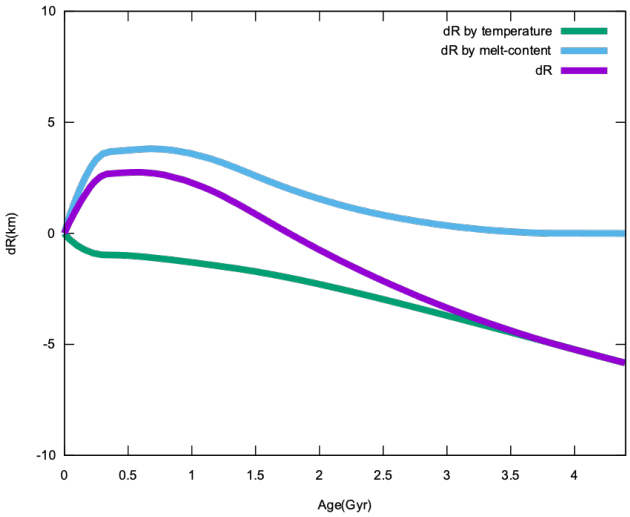
The calculated temperature first increases and then remains equal to the solidus for billions of years due to the contribution from the latent heat of melting, and then decreases due to decay of HPEs. The melt-content increases at first and then gradually diminishes; magma migrates upward and accumulates at the top of the partially molten region. The globally averaged temperature first decreases due to conductive cooling at the base of the mantle, then rises due to internal heating, and after that, gradually decreases owing to the cooling from the surface boundary. The radius first increases mostly by melting and then decreases due to cooling and solidification of the magma in the models that initial melt-content is 0 in the entire mantle.

The calculated temperature distribution at 4.4 Gyr is consistent with the thermal structure inferred from magnetotelluric observation of the Moon.The calculated history of radial change is consistent with that inferred from observations of the lunar gravity field and lobate scarps. Realistic modeling of generation and migration of magma as well as HPE-transport by migrating magma are crucial for understanding the thermal history of the Moon.

Keywords: The Moon, Thermal history, Magma migration, Radial expansion/contraction, Numerical analysis

©2021. Japan Geoscience Union. All Right Reserved.





©2021. Japan Geoscience Union. All Right Reserved.

Mass wasting process on lunar crater walls inferred from boulder falls

*Ayame Ikeda[1], Hiroyuki Kumagai[1], Tomokatsu Morota[2]

1. Graduate School of Environmental Studies, Nagoya University, 2. Department of Earth and Planetary Science, The University of Tokyo

Mass wasting is important to understand topographic degradation processes and present geologic activity on the lunar surface. Moonquakes and/or ground shaking due to impacts may trigger mass movement, but its mechanism remains unknown. Recently, lunar orbiters such as Kaguya and Lunar Reconnaissance Orbiter (LRO) explored the lunar surface, and they found boulder falls and lobate scarps, which are distributed in the lunar surface. Kumar et al. (2016, 2019) indicated that shallow moonquakes might have triggered boulder falls, but they did not consider another effect such as ground shaking due to impacts. In this study, we quantitatively evaluated the effects of both moonquakes and impacts to investigate the cause of boulder falls at the following two sites: Site 1 in a southern part of the Schrödinger basin and Site 2 near the Lorentz basin. Previous hypocenter determinations using waveform data from the Apollo seismic network suggest that a shallow moonquake occurred near Site 2 in 1975 (Nakamura et al., 1979). We investigated boulder falls in craters located within an epicentral distance of about 200 km from the moonquake. The craters with boulder falls on their walls were distributed independent of the epicentral distance, indicating that the shallow moonquake cannot explain the distribution of the boulder falls. We investigated the following surface features at the two sites using image and topography data obtained by LRO and Kaguya: (1) the distributions of boulder falls, small craters, and optical maturity parameter (OMAT), (2) the relationship between slope angles and densities of small craters, and (3) the relationship between acceleration of ground shaking induced by impacts and starting points of boulder falls. We estimated the ages of the crater walls at Sites 1 and 2 to be about 3.5 and 10 Ma, which are younger than the ages of the craters. Steep slope areas have small densities of small craters and high OMAT values or immature surfaces. These areas correspond to boulder sources, where many boulders are exposed. We found the correlation between starting points of boulder falls and acceleration of ground shaking induced by impacts inferred from the spatial distribution of small craters at Site 1. This result strongly suggests that the boulder falls were induced by ground shakings due to impacts. Based on these results we propose mass wasting processes depending on the slope angle to explain the distributions of boulder falls at Sites 1 and 2 as follows. In steep slope areas, regolith falls down the slopes by lunar gravity, and thus the regolith layer is thin. When meteorites hit steep areas, they fracture megaregolith or bedrocks beneath regolith layers and generate boulders, in which clear traces or small craters are not left. When meteorites hit gentle slope areas, where thick regolith layers exist, craters and boulder falls are clearly left. Thus, we propose that the lunar topographic degradation is controlled by such heterogeneities in regolith thickness and surface strength depending on the slope angle, which may not be described by a simple diffusion process.

Keywords: Moon, mass wasting, boulder falls

©2021. Japan Geoscience Union. All Right Reserved.

Recent boulder falls within the Finsen crater, an assessment of ongoing geological activities

*Trishit Ruj[1], Goro Komatsu[2], Kenji Kawai[1], Hanaya Okuda[3], Zhiyong Xiao[4], Deepak Dhingra[5]

1. Department of Earth and Planetary Science, School of Science, The University of Tokyo, 2. International Research School of Planetary Sciences, Università G. d'Annunzio, Viale Pindaro 42, 65127, Pescara, Italy, 3. Department of Ocean Floor Geoscience, Atmosphere and Ocean Research Institute, University of Tokyo, Kashiwanoha 5-1-5, Kashiwa, Chiba 277-8564, Japan, 4. Planetary Environmental and Astrobiological Research Laboratory, School of Atmospheric Sciences, Sun Yat-sen University, Zhuhai, China, 5. Department of Earth Sciences, Indian Institute of Technology Kanpur, Kanpur, UP 208016, India

To better understand the necessary triggers for the origin of the lunar boulder tracks, we report over 400 tracks. The tracks were identified on the southern inner wall and the central peak region of the Finsen crater, located within the South Pole-Aitken basin on the lunar far side. We assessed two main possibilities of triggers, 1) ground shaking excited by the recent impact crater formation events, and 2) moonquakes generated from recent fault reactivation associated with the lobate scarps identified inside and in the vicinity of Finsen. Our assessments revealed that the impact-induced seismicity could have generated the moonquake with the maximum moment magnitude of 3.67. We also estimated that the moonquakes excited by the movements along the lobate scarps had an estimated upper limit of moment magnitude between 7.85 and 7.90, i.e., for the basaltic and noritic basement respectively. The geological mapping and the spatial distribution of the boulder tracks indicate a higher concentration around the vicinity of the lobate scarps. Considering the location of the Finsen crater positioned over the structural discontinuity along the boundary of the central and mid rings of the South Pole-Aitken basin and higher moment magnitude generated from the fault movements, we propose that the region is seismotectonically active, and reactivation of pre-existing faults possibly triggered/triggers the necessary ground motion for the boulders to initiate their movements.

Keywords: Moon, TECTONICS, BOULDER FALL, SOUTH POLE AITKEN BASIN

©2021. Japan Geoscience Union. All Right Reserved.

Lunar Surface Mapping by SLAM Technology on Bionic Legged Rover

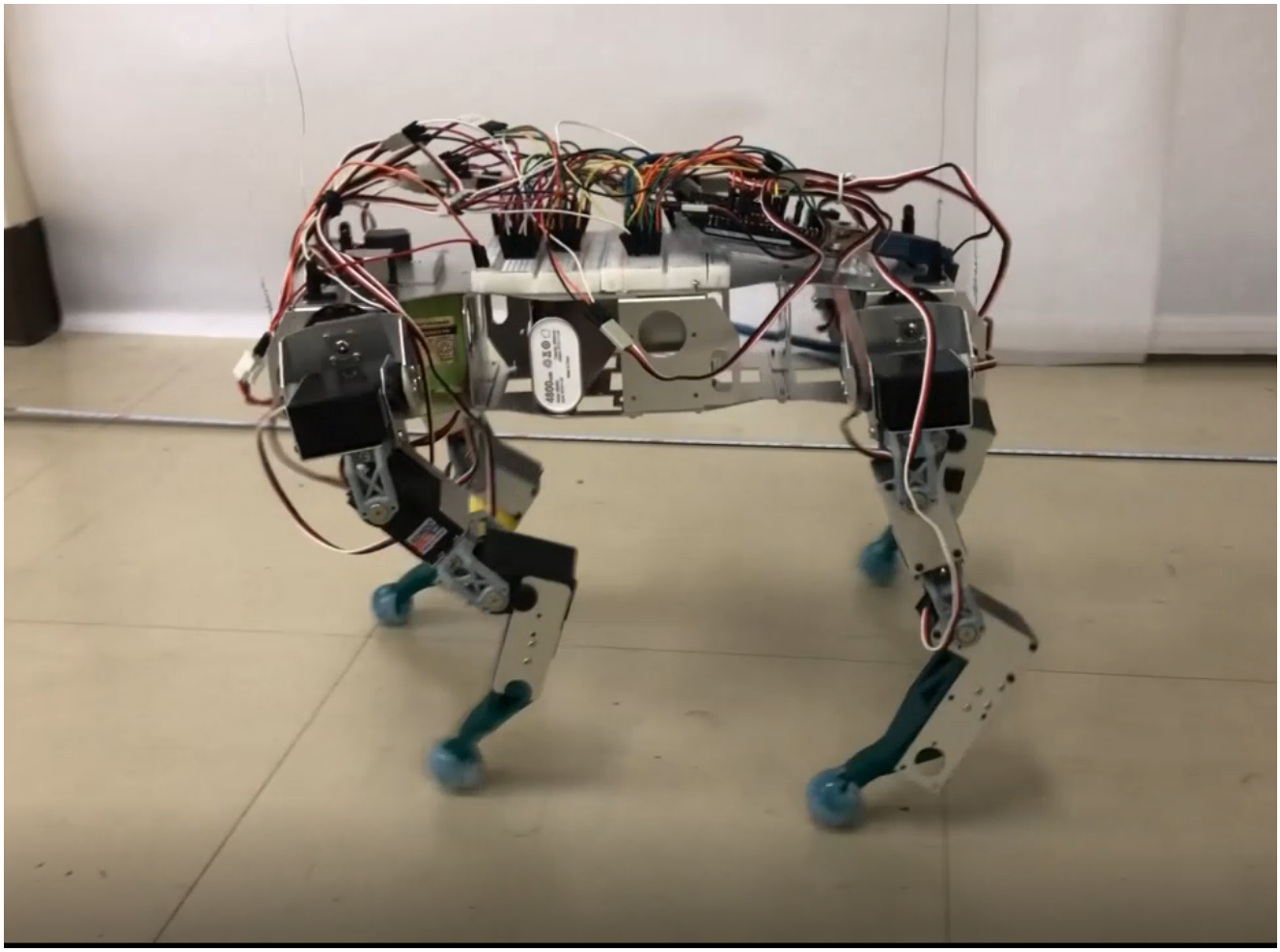
*LIANG CHEN[1], Takehiko Arai[1], Makiko Ohtake[2]

1. Ashikaga University, 2. University of Aizu

Since Apollo's lunar exploration, it is believed that the moon's permanent shadow contains ancient water ice and dust ice poured from comets (Arnold, 1979). LIDAR, a laser altimeter onboard the lunar orbiter SELENE, found out the existence of permanent shadows in the polar regions of the Moon (Noda et al., 2009). The visible and infrared spectroscopic imager M3 onboard the Indian lunar probe Chandrayaan-1 provided data suggesting the existence of water ice (Pieters et al., 2009). Therefore, polar exploration is an important target for the next lunar exploration. We have been developing a bionic rover for lunar exploration. The rover has a bionic mechanism with intelligence, which is more stable moving for complex rocks on the lunar surface than a wheel mechanism. The rover has individual motors for every single joint compared with other legged robots. Hence it has higher flexibility. We have also been developing self-positioning and self-maneuver software that drives the rover autonomously and safely under extreme conditions, even in complex areas on the lunar surface. In this study, we apply a SLAM algorithm for lunar surface mapping. We develop the algorithm of self-position estimation and map construction by the rover itself. The algorithm efficiently discovers target material to investigate by utilizing the lunar surface's topographic and spectroscopic observational data obtained by instruments onboard the rover. The algorithm can project the scientific observation data on the generated map to realize autonomous maneuver without GPS or pre-existing map for efficient lunar polar exploration by integrating these data.

Keywords: Lunar Polar, SLAM, Rover

©2021. Japan Geoscience Union. All Right Reserved.



©2021. Japan Geoscience Union. All Right Reserved.

Deciphering the planetary water flux from the water record expected at lunar pole

*Ko Hashizume[1], Chihiro Yamanaka[2], Masahiro KAYAMA[3], Makiko Ohtake[4]

1. Ibaraki University, 2. Osaka University, 3. The University of Tokyo, 4. The University of Aizu

By the coming Japanese exploration program for the polar region of Moon, water trapped in the regolith will be evaluated as novel space resources. The planned evaluation includes deuterium/hydrogen isotope analyses, to help estimation of the trapping mechanisms of water in the polar regolith. As well as this practical purpose, the isotope analyses also bear fundamental scientific importance, as will be introduced in this talk.

Keywords: Moon, Polar region, Water, Isotopes

©2021. Japan Geoscience Union. All Right Reserved.

[J] Oral | P (Space and Planetary Sciences)：P-PS Planetary Sciences

Fri. Jun 4, 2021 1:45 PM - 3:15 PM JST | Fri. Jun 4, 2021 4:45 AM - 6:15 AM UTC | Ch.03 Zoom Room 03

[P-PS05] Lunar science and exploration

convener:N Masaki Nishino(Japan Aerospace Exploration Agency, Institute of Space and Astronautical Science), Masahiro KAYAMA(Department of General Systems Studies, Graduate School of Arts and Sciences, The University of Tokyo), Hiroshi Nagaoka(Institute of Physical and Chemical Research), Yusuke Nakauchi(Japan Aerospace Exploration Agency), Chairperson:Yusuke Nakauchi(Japan Aerospace Exploration Agency), Masahiro KAYAMA(Department of General Systems Studies, Graduate School of Arts and Sciences, The University of Tokyo)

Scientific data sets acquired by Japanese lunar mission SELENE (Kaguya) have become the standard of the lunar sciences. Other missions such as Chandrayaan-1, LRO, GRAIL, LCROSS, LADEE, Artemis, and Chang'e series as well as ground observations are also providing new knowledges of the Moon. Apollo/Luna samples and lunar meteorite analyses are also being advanced. In concurrence with these studies, some countries including Japan are planning near-future lunar missions. In this session, we will discuss scientific results based on newly acquired lunar data, strategies for future missions, lunar sample analyses, and theoretical and experimental studies of lunar sciences.

1:45 PM - 2:00 PM JST | 4:45 AM - 5:00 AM UTC

[PPS05-07] Scientific approaches to promotion of the lunar polar exploration

*Masahiro KAYAMA[1], Makiko Ohtake[2], Ko Hashizume[3], Kazuto Saiki[4], Chihiro Yamanaka[4], Reiko Nomura[5], Makoto Hareyama[6], Yoshifumi Saito[5], Teruaki Enoto[7], Hideaki Miyamoto[1], Tomokatsu Morota[1], Yuzuru Karouji[5], Yoshiaki Ishihara[5], Hiroyasu Mizuno[5], Takeshi Hoshino[5], Dai ASOH[5] (1.The University of Tokyo, 2.University of Aizu, 3.Ibaraki University, 4.Osaka University, 5.JAXA, 6.St. Marianna University, 7.RIKEN)

2:00 PM - 2:15 PM JST | 5:00 AM - 5:15 AM UTC

[PPS05-08] **Latest Status on Japanese Lunar Polar Exploration Mission**

*DAI ASOH[1], Takeshi HOSHINO[1], Yuzuru KAROUJI[1], Hiroka INOUE[1], Makiko OHTAKE[2] (1.Japan Aerospace Exploration Agency, 2.University of Aizu)

2:15 PM - 2:30 PM JST | 5:15 AM - 5:30 AM UTC

[PPS05-09] Light source investigation of the volatile spectral signals observed at the lunar polar regions

*Makiko Ohtake[1], Yusuke Nakauchi[2], Satoshi Tanaka[2], Keisuke Onodera[3], Hiroshi Nagaoka[2] (1.University of Aizu, 2.Japan Aerospace Exploration Agency, 3.The Graduate University for Advanced Studies (SOKENDAI))

2:30 PM - 2:45 PM JST | 5:30 AM - 5:45 AM UTC

[PPS05-10] Auto-Focus system of Multi-Band Camera (Engineering Model) on SLIM

*Yusuke Nakauchi[1], Hiroyuki Sato[1], Hiroshi Nagaoka[1], Kazuto Saiki[2], Makiko Ohtake[3], Hiroaki Shiraishi[1], Chikatoshi Honda[3], Yoshiaki Ishihara[1] (1.Japan Aerospace Exploration Agency, 2.Osaka University, 3.The University of Aizu)

2:45 PM - 3:00 PM JST | 5:45 AM - 6:00 AM UTC

[PPS05-11] Current mission scenario of UZUME (Unprecedented Zipangu Underworld of the Moon Exploration)

*Junichi Haruyama[1] (1.Japan Aerospace Exploration Agency)

3:00 PM - 3:15 PM JST | 6:00 AM - 6:15 AM UTC

[PPS05-12] Numerical Simulations on Surface Charging Properties of Lunar Surface Cavities

*Nakazono Jin[1], Yohei Miyake[2], Hideyuki Usui[3] (1.Kobe University , 2.Education Center on Computational Science and Engineering, Kobe University, 3.Graduate school of system informatics Kobe University)

Scientific approaches to promotion of the lunar polar exploration

*Masahiro KAYAMA[1], Makiko Ohtake[2], Ko Hashizume[3], Kazuto Saiki[4], Chihiro Yamanaka[4], Reiko Nomura[5], Makoto Hareyama[6], Yoshifumi Saito[5], Teruaki Enoto[7], Hideaki Miyamoto[1], Tomokatsu Morota[1], Yuzuru Karouji[5], Yoshiaki Ishihara[5], Hiroyasu Mizuno[5], Takeshi Hoshino[5], Dai ASOH[5]

1. The University of Tokyo, 2. University of Aizu, 3. Ibaraki University, 4. Osaka University, 5. JAXA, 6. St. Marianna University, 7. RIKEN

The lunar polar exploration (LUPEX, a tentative name), planned by JAXA in collaboration with ISRO, is the robotic landing mission for water resource on a pole of the Moon. In the LUPEX mission scheduled to launch after 2023, the lander will touch down on the lunar polar region, the rover will deploy to travel on the surface, and various types of the attached instruments will measure the lunar materials to search for the water resource and to assess its quantity (the water content), quality (chemical composition of ice, whether it contains only H_2O or other species such as CO_2, CH_4, and H_2S), and usability (vertical and horizontal water distribution to check the accessibility). Lunar water is one of the most important resource in space because it is available for drinking water, breathing oxygen, hydrogen fuel, and building materials for lunar base, and is, therefore, absolutely essential for future manned space activity. Therefore, the attached instruments specialized in water analysis and some of them capable of collection of geological data on the Moon e.g., infrared spectroscopy named Advanced Lunar Imaging Spectrometer (ALIS), lunar thermogravimetric analyzer (LTGA), and aquatic detector using optical resonance (ADORE), were selected. There are, however, still less scientific data obtained from lunar samples or the simulant by experiments and simulations which reproduce ultra- to extreme high vacuum (10^{-7} to 10^{-10} Pa) and a very low temperature environment (<70 K to 390 K) of the lunar pole, in spite of dependence of the volatile properties (absorption, dehydration, and sublimation) on temperature and vacuum. Here, we introduce and review necessity of scientific approaches of collection of the basic data and establishment of the analytical method from the laboratory reproduction experiments and simulations to promote the LUPEX mission.

Lunar water is thought to be derivied from the following origins; solar wind, carbonaceous chondrite/comet collision, and degassing of magmatic eruption. Solar wind-originated hydrogen is implanted into the lunar surface materials and then a part of it changes into structural water via formation of the regolith agglutinate. Carbonaceous chondrite and comet collisions provide structural and hydrated water-bearing minerals such as serpentine and saponite into the Moon. They also theoretically cause formation of evaporate layer of their volatile constituents, supplying various gas (for example, H_2O, CO_2, and CH_4) with the lunar surface. Volatiles of H, C, Cl, F, S and their molecular species are likely to be released by degassing of magmatic eruption from the lunar interior into the surface. Thus, these processes supply various types of volatiles with the Moon, especially the poles under the very low-temperature environment that facilitate migration and deposit of volatiles. Therefore, the attached instruments with the rover of LUPEX should allow in-situ analyses of volatile with wide variety of atomic and molecular species and each of the contents with adequate accuracy and reliability, based on the basic data and the analytical method from the reproduction experiments. In the presentation, we will mention the scientific approaches of the laboratory reproduction experiment for the sake of this achievement, e.g., IR, Thermogravimetric analysis and Thermal Desorption Spectroscopy measurements of the lunar samples and the simulant with various types of structural, hydrate, and adsorbed volatiles to reveal characteristics of volatile signals from the instruments and to clarify absorption, dehydration, and sublimation temperature under the reproduction environment of ultra- to extreme high vacuum and a very low

©2021. Japan Geoscience Union. All Right Reserved.

temperature. The results achieved can be also useful for calibration curve of volatile signals from the instruments, selection of standard materials for water analysis and assessment of the attached instrument performance (spatial resolution, detection limit, and temperature rate and limit).

Keywords: Moon, Water, Mission, Lunar polar region, Water resource

©2021. Japan Geoscience Union. All Right Reserved.

Latest Status on Japanese Lunar Polar Exploration Mission

*DAI ASOH[1], Takeshi HOSHINO[1], Yuzuru KAROUJI[1], Hiroka INOUE[1], Makiko OHTAKE[2]

1. Japan Aerospace Exploration Agency, 2. University of Aizu

Japanese lunar exploration missions:
JAXA aims to conduct sustainable lunar exploration activities in the next 50 years, such as operation of lunar base with international partners and private sectors. To realize this goal, we will conduct technology demonstration step-by-step. In October 2020, Japan, the United States, and six partner nations have agreed to develop practical principles to guide space exploration cooperation and signed the Artemis Agreement. The Japanese government had decided to officially join this international space exploration, and to proceed on coordination in the several areas including sharing of data acquired from our lunar exploration missions and technologies for lunar landing site selection.
Regarding lunar surface robotic missions, JAXA is developing Smart Lander for Investigating the Moon (SLIM), which aims to demonstrate the high-precision landing technology. Following this SLIM mission, Lunar Polar Exploration mission (LUPEX) is aimed at investigating the water ice resources in the lunar polar region. This is a collaborative mission with Indian Space Research Organisation (ISRO).

Objectives of the lunar polar exploration:
There is strong interest in using water ice (if present) as an in-situ resources. Specifically, using water ice as a propellant will significantly affect future exploration scenarios and activities because the propellant generated from the water can be used for ascent from the lunar surface. We need to find out, by direct measurement on the lunar surface, the presence of water ice, it’ s quantity, quality (pure water or contain other phases), and usability (how deep do we need to drill or how much energy is required to get water) in order to assess if we can use it as resources. Obtaining data to understand the principle of the water distribution and concentration is necessary to estimate the quantity and quality of water across the Moon.

Spacecraft configuration:
The spacecraft system is based on direct communication with the Earth. The target mass of the spacecraft (incl. payload and propellant) is about 6ton and the payload mass is about 350kg. After the spacecraft reaches the Moon, it is inserted into a circular orbit having a 100km altitude via a few orbital changes. During powered-descent phase, the position of the lander is estimated by landmark navigation using shadows created by the terrain. After landing, the rover is deployed on the lunar surface using ramps. The rover then prospects water ice with its observation instruments.

Status on the mission:
We passed one of the gate reviews, System Requirement Review (SRR). ISRO/JAXA have almost completed the conceptual design (i.e. Phase-A study) under the Implementation Arrangement (IA) for the LUPEX mission, in which JAXA provides a launch vehicle and a rover while ISRO provides a lander. JAXA is going to select manufactures for the mission instruments to be loaded on the rover and will choose a prime contractor for the rover development in this year. A next gate review, System Definition Review (SDR) will be held by the end of this year.

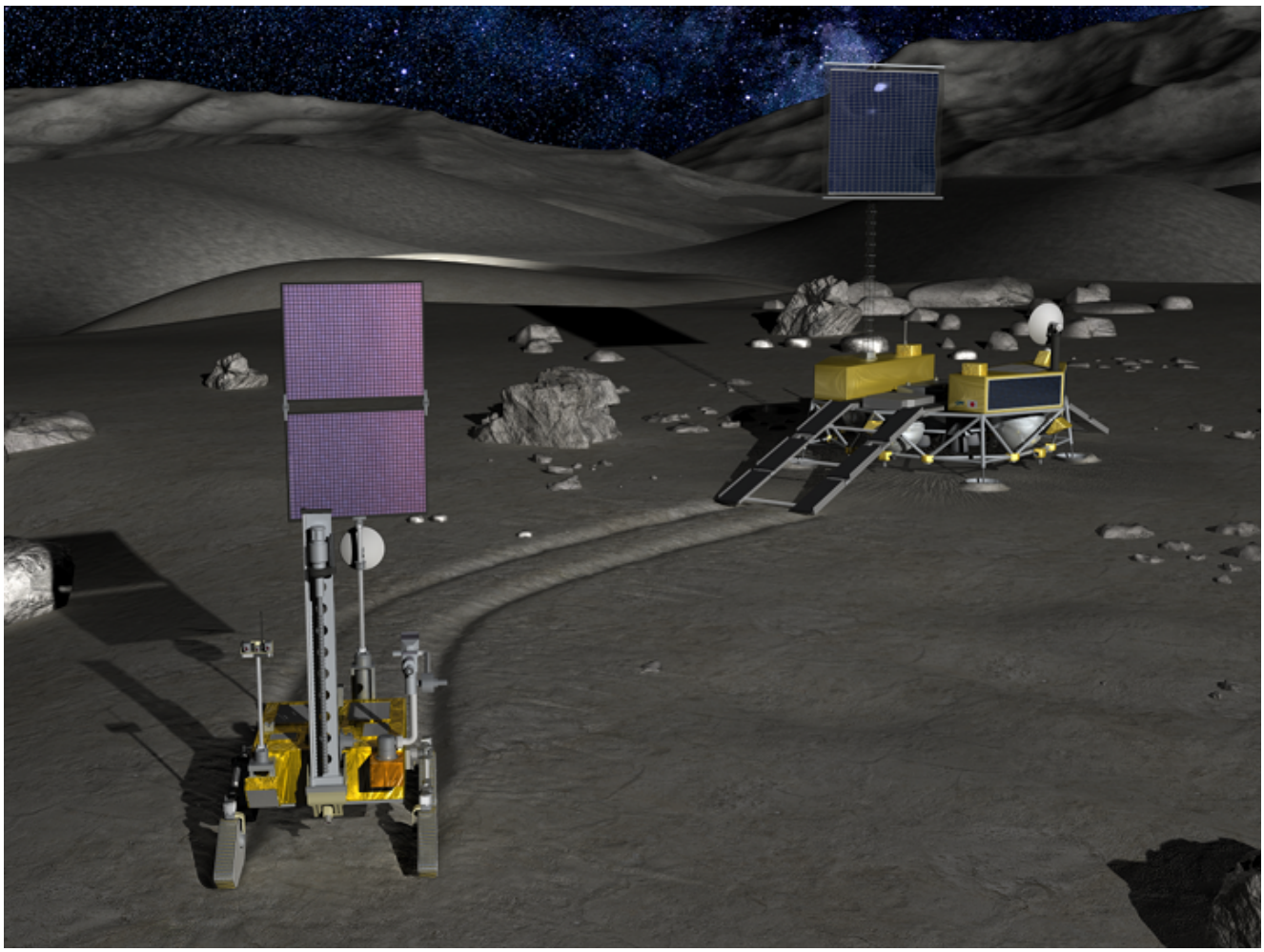
Study on Post-landing Operational Flow:
Depending on the location of the landing site and the sunlight conditions, it is possible to accomplish the mission by rearranging the operation sequences and postponing the planned observation until next

©2021. Japan Geoscience Union. All Right Reserved.

sunlight period. Because of the necessity to locate the landing site quickly after landing, a quick position determination function for the rover system shall be included in the ground system requirements.

Preparation Status of Output Data Creation Team:
LUPEX Pre-project is preparing for the Output Data Creation Team (ODCT) which will be responsible for output data. As a part of the ODCT preparation activities since last summer, the LUPEX Pre-project Team has been interviewing the instrument leads and other members. We are discussing the information on how to process the data obtained from each instrument, combine the derived information and create the products, as well as the observation timing and observation requirements for the operational study.

Keywords: lunar polar exploration, lunar water ice, resource availability



©2021. Japan Geoscience Union. All Right Reserved.

Light source investigation of the volatile spectral signals observed at the lunar polar regions

*Makiko Ohtake[1], Yusuke Nakauchi[2], Satoshi Tanaka[2], Keisuke Onodera[3], Hiroshi Nagaoka[2]

1. University of Aizu, 2. Japan Aerospace Exploration Agency, 3. The Graduate University for Advanced Studies (SOKENDAI)

Recently, the water condensation at the lunar polar region has been suggested by remote sensing observation. However, their distribution, amount, and origin are not clear because of the limitation on the available data. To solve these problems, we have been investigating spectral signatures of the water and other volatile components observed at the lunar polar regions by analyzing Spectral Profiler data onboard SELENE (Kaguya) and reported clear evidence of water ice and other volatile components both on the north and south polar regions.

In this study, we investigate the identified spectral signals at the polar region (> ±80˚ in latitude) to estimate origin of the observed volatile components by checking timing, location, and observational geometry of the volatile signals. The results revealed that the identified signals were detected at the sites experiencing the night (i.e., not directly illuminated) and also these sites are not illuminated by the reflected light from surroundings during the observation. And because of the apparent lack of the light source, we further checked possibility of artificial origin for the identified volatile signals such as stray light or noise of the instrument and calibration error. In addition to the artificial origin, possibility of originated from natural light sources other than those coming from the lunar surface, like earthshine and zodiacal light, were checked. But all of these checks resulted in negative. Therefore, we interpret that the identified signals are real, and they are likely originated from the dust and volatile mixture lofted in space and reflecting the solar light. The signals are localized and continues up to several days in maximum and they are much brighter than the previously observed impact flash. And their observed timings did not coincide with major meteoroid streams in most of the cases. These evidences suggest that not all of the volatile signal were the impact events.

Keywords: Moon, polar regions, volatile component

©2021. Japan Geoscience Union. All Right Reserved.

Auto-Focus system of Multi-Band Camera (Engineering Model) on SLIM

*Yusuke Nakauchi[1], Hiroyuki Sato[1], Hiroshi Nagaoka[1], Kazuto Saiki[2], Makiko Ohtake[3], Hiroaki Shiraishi[1], Chikatoshi Honda[3], Yoshiaki Ishihara[1]

1. Japan Aerospace Exploration Agency, 2. Osaka University, 3. The University of Aizu

Smart Lander for Investigating Moon (SLIM) project will demonstrate a “pin-point” landing within a radius of 100 m on the lunar surface. It will be launched in FY2022. The SLIM aims “SHIOLI” crater (13.3º S, 25.2º E) to derive the detailed mineralogy of the olivine-rich exposures to investigate the composition of the lunar mantle or deep crustal material, and understand their origin. The Multi Band Camera (MBC) is the scientific instrument on board SLIM lander to obtain Mg# (= molar Mg / (Mg + Fe)) of lunar mantle materials. The MBC is composed of a Vis-InGaAs imaging sensor, a filter-wheel with 10 band-pass filters, a movable mirror for panning and tilting, and an autofocus system.

The MBC observes the boulders and regolith distributed around the lander. Since various distances to the objects are expected from a few meters to infinity, the MBC is equipped with an auto-focus (AF) system. The MBC uses the jpeg compression technique. An image with maximum sharpness taken in a best focus position will have the largest image file size after JPEG compression. Using this characteristic, the AF algorithm is designed to automatically find the focus lens position that maximizes the image file size after jpeg compression. Our AF system has been tested using the Engineering Model of MBC (MBC-EM). The imaging target is a picture of lunar surface obtained by previous spacecrafts and basaltic rocks from Hawaii. Our results suggest that the amount of initial movement is important parameter. In the presentation, we will show the results of AF system, and MBC operation plan.

Keywords: Moon, SLIM, Spectroscopy, AutoFocus

©2021. Japan Geoscience Union. All Right Reserved.

Current mission scenario of UZUME (Unprecedented Zipangu Underworld of the Moon Exploration)

*Junichi Haruyama[1]

1. Japan Aerospace Exploration Agency

UZUME (Unprecedented Zipangu Underworld of the Moon Exploration) is a mission that an explorer descends into a vertical hole opening on a lunar underground cavern to understand 1) volcanic activity (lava flow covering) peculiar to gravitational celestial bodies, magnetic field generation in ancient times, meteorite impact history (regolith formation), and formation process of vertical holes themselves. Furthermore, it clarifies the difference in the environment (temperature, radiation, magnetic field) at the bottom of the vertical hole to obtain information that contributes to the understanding of the manifestation and sustainability of life, and 2) the environment of the lunar underground caverns to acquire preliminary information for future exploration and lunar base construction. In this presentation, we will introduce a mission scenario that is currently envisioned and discuss how the scientific objectives will be achieved.

Keywords: Moon, hole, cave, UZUME, exploration, Mars

©2021. Japan Geoscience Union. All Right Reserved.

Numerical Simulations on Surface Charging Properties of Lunar Surface Cavities

*Nakazono Jin[1], Yohei Miyake[2], Hideyuki Usui[3]

1. Kobe University , 2. Education Center on Computational Science and Engineering, Kobe University, 3. Graduate school of system informatics Kobe University

Since the Moon has no atmosphere and no intrinsic magnetic field, solar wind plasma falls directly on the lunar surface and forms an electrostatic environment near the lunar surface. The formation of the electrostatic environment is known to be strongly dependent on the topology and sunlight conditions of the lunar surface. The Moon has a wide range of topographic features, from craters and boulders to surface rocks and regolith layers. In recent years, unique topographic features such as vertical holes have been also identified. The investigation of the unique surface charging characteristics caused by these irregularities and their dependence on spatial scales is very important to quantitatively understand the lunar surface environment, which will be a critical issue in future lunar explorations. In this study, we compare the plasma and electrical environments of lunar holes and hollows with different sizes and shapes using particle simulations to reveal the charging characteristics of lunar surfaces with complex shapes.
We set up a lunar surface with a cavity in the simulation space, and simulated the solar wind plasma flow, and the sunlight illumination and its associated photoelectron emission from the surface. The simulation results show that the surface charging within the cavity can be understood in terms of separate contributions of the solar wind plasma and the photoelectron currents. The solar wind electrons collide with the cavity wall at relatively shallow positions due to their greater thermal motions than ions. Therefore, the proportion of solar wind electrons that approach the bottom of the cavity is small, and the deepest part of the cavity surface will be charged positively. This effect will be moderated as the cavity aperture becomes greater, because it leads to the larger number of solar wind electrons approaching the bottom of the cavity. The photoelectron current basically contributes to the positive charging at the photoelectron release point, which is the well known behavior. On the cavity wall, however, the emitted and recollected photoelectrons behave as they transport negative charge to the deeper part of the cavity, which moderate the positive potential at the bottom of the cavity formed by the solar wind ions.

Keywords: the Moon, plasma, surface charging, hole and cavities, particle simulation

©2021. Japan Geoscience Union. All Right Reserved.

[J] Oral | P (Space and Planetary Sciences)：P-PS Planetary Sciences

Fri. Jun 4, 2021 9:00 AM - 10:30 AM JST | Fri. Jun 4, 2021 12:00 AM - 1:30 AM UTC | Ch.04 Zoom Room 04

[P-PS06] Planetary Sciences

convener:Yusuke Nakauchi(Japan Aerospace Exploration Agency), Hiroshi Kikuchi(Japan Aerospace Exploration Agency), Chairperson:Keisuke Sugiura(Tokyo Institute of Technology, Earth Life Science Institute), Makito Kobayashi(Department of Earth and Planetary Science, School of Science, University of Tokyo)

We call for general interest papers for Planetary Sciences. Planetary Sciences consist o f a variety of studies on the past, present, and future of our solar system and exoplanetary systems, Discussions based on various backgrounds are encouraged.

9:00 AM - 9:15 AM JST | 12:00 AM - 12:15 AM UTC

[PPS06-13] Global climate and river transport simulations of early Mars during the late Noachian and the early Hesperian

*Arihiro Kamada[1], Takeshi Kuroda[1], Yasumasa Kasaba[1], Naoki Terada[1], Hiromu Nakagawa[1] (1.Graduate School of Science, Tohoku University)

9:15 AM - 9:30 AM JST | 12:15 AM - 12:30 AM UTC

[PPS06-14] Water-ice content estimation on the Martian subsurface based on the permittivity

*Makito Kobayashi[1], Hideaki Miyamoto[2] (1.Department of Earth and Planetary Science, School of Science, University of Tokyo, 2.Department of Systems Innovation, School of Engineering, University of Tokyo)

9:30 AM - 9:45 AM JST | 12:30 AM - 12:45 AM UTC

[PPS06-15] Shock remanent magnetization intensity and stability structures of single-domain titanomagnetite-bearing basalt sample

*Masahiko Sato[1], Kosuke Kurosawa[2], Shota Kato[1], Masashi Ushioda[3], Sunao Hasegawa[4] (1.The University of Tokyo, 2.Planetary Exploration Research Center, Chiba Institute of Technology, 3.Shikoku Research Institute Inc., 4.Japan Aerospace Exploration Agency)

9:45 AM - 10:00 AM JST | 12:45 AM - 1:00 AM UTC

[PPS06-16] Numerical Study of the Formation Scenario of Mesosiderite Meteorites Through a Giant Impact Onto a Differentiated Asteroid

*Keisuke Sugiura[1], Makiko K. Haba[2], Hidenori Genda[1] (1.Tokyo Institute of Technology, Earth Life Science Institute, 2.Tokyo Institute of Technology, Department of Earth and Planetary Sciences)

10:00 AM - 10:15 AM JST | 1:00 AM - 1:15 AM UTC

[PPS06-17] High velocity impact experiments on porous ice aggregates simulating cometary nuclei: Estimation of energy partition from projectile kinetic energy to post shock heat

*Haruka Sasai[1], Minami Yasui[1], Masahiko Arakawa[1], Kei Shirai[1] (1.Kobe University)

10:15 AM - 10:30 AM JST | 1:15 AM - 1:30 AM UTC

[PPS06-18] Effect of porosity on restitution coefficient and sticking properties of snowball simulating Saturn’s rings

*Yukari Toyoda[1], Masahiko Arakawa[1], Minami Yasui[1] (1.Graduate School of Science, Kobe University)

Global climate and river transport simulations of early Mars during the late Noachian and the early Hesperian

*Arihiro Kamada[1], Takeshi Kuroda[1], Yasumasa Kasaba[1], Naoki Terada[1], Hiromu Nakagawa[1]

1. Graduate School of Science, Tohoku University

Over the past decades, a number of geological observations of early Mars have suggested the existence of ancient surface river channales during the late Noachian and early Hesperian (3.85-3.6 Ga). The combination of large amounts of liquid water and stable, prolonged fluvial activity is necessary to explain these river systems, suggesting that early Mars must have experienced a long period of stable surface liquid water and a climate sufficiently warm and wet for precipitation to occur. We investigated the late Noachian and the early Hesperian climate using a 3-dimensional paleo-Mars global climate model (PMGCM), assuming a $CO_2/H_2O/H_2$ mixing atmosphere under the “Faint Young Sun” condition. The ancient Martian topography before the formation of the Tharsis bulge was assumed. The cases of surface pressures of 0.5, 1, 1.5 and 2 bar, with H_2 concentrations of 0%, 1%, 3% and 6%, and obliquities of 20˚, 40˚, and 60˚ were investigated. We updated the global river model of Kamada et al. (2020) to a pan-planet river model named CRIS (Catchment-based RIver Simulator), which calculates precipitation infiltration, global river discharge, and the transport of bedload and suspended load sediments for a variety of sediment particle sizes coupled with the PMGCM. We found that an early Martian atmosphere with H_2 concentration of above 3% and Ps of above 1.5 bar could have produced a hospitable surface environment that could support the stable existence of liquid water over long periods. The annual precipitation increased with surface pressure, and the distributions of the precipitation peaks under obliquities of above 40˚ were consistent with the locations in which the majority of the valley networks are currently observed. Moreover, CRIS predicted that surface river systems are limited at high latitudes at obliquity of 20˚, but river activity is enhanced even at low and mid-latitudes as a result of increased summer precipitation at obliquity above 40˚, which is close to the most probable obliquity value of 41.8˚ (Laskar et al., 2004). Our simulation results show that early Mars had a warm and wet environment with precipitation-fed mature river systems incising the VNs that have been recently observed.

Keywords: Mars, valley network, Global climate model

©2021. Japan Geoscience Union. All Right Reserved.

Water-ice content estimation on the Martian subsurface based on the permittivity

*Makito Kobayashi[1], Hideaki Miyamoto[2]

1. Department of Earth and Planetary Science, School of Science, University of Tokyo, 2. Department of Systems Innovation, School of Engineering, University of Tokyo

The ancient Martian surface has retained a large amount of water, which formed large-scale aqueous-related structures, interacted with the rocks and atmosphere, and attributed to the evolution of surface conditions (e.g., Baker, 1992; Carr, 2006; Head and Carr, 2010; Ehlmann and Edwards, 2014). During late-Hesperian to Amazonian, the surface water has dramatically vanished associated with capture into polar region and subsurface (e.g., Holt et al., 2010; Dundas et al., 2018), as well as thermal and nonthermal atmospheric loss (e.g., Jakosky, 2021), and chemical weathering of the regolith (e.g., Ehlmann et al., 2009). However, the amount of vanished water is ambiguous, which is clues to understand the evolution of the Martian environment. Some water could exist on the subsurface at even present, which has been detected by the radar sounders such as MARSIS and SHARAD (e.g., Plaut et al., 2007; Usui et al., 2015; Orosei et al., 2018, 2020). Radar sounders utilize the electrical properties, especially permittivity, to visualize the subsurface structures and make it possible to estimate the amount of water on the subsurface. As the permittivity depends on various parameters such as temperature, density, chemical composition, and so on, it is difficult to estimate the accurate value of the subsurface materials. Indeed, the detection of water-ice is based on the consistency of the topography, that is, the basal topography can be duplicated assuming the permittivity value of water-ice when utilizing the radargram. However, the value also can be explained by the combination of air, water-ice, and dust materials. Then, we calculate the possible composition of air, water-ice, and rocks using the laboratory experimental data under the Martian environment. For the calculation, we use the value of the Martian simulant measured at the HF band, which is utilized for the radar sounders, and the mixing equation (Looyenga, 1965), which is appliable to the low-temperature materials (Hickson et al., 2020), and the possible subsurface vertical structure (e.g., Clifford et al., 2010). As a result, some model that has different the ration of water-ice/dust can explain the permittivity value estimated by radar data. For instance, the ratio of dust and water-ice on the subsurface of the Medusae Fossae Formation may have no change vertically, which indicates that the estimated amount of water-ice might be about 50 % or less. With consideration of subsurface structures in detail, our method is the potential to estimate the amount of water-ice on the Martian subsurface to apply to the radar data globally.

Keywords: relative permittivity, Mars, water-ice, radar sounders

©2021. Japan Geoscience Union. All Right Reserved.

Shock remanent magnetization intensity and stability structures of single-domain titanomagnetite-bearing basalt sample

*Masahiko Sato[1], Kosuke Kurosawa[2], Shota Kato[1], Masashi Ushioda[3], Sunao Hasegawa[4]

1. The University of Tokyo, 2. Planetary Exploration Research Center, Chiba Institute of Technology, 3. Shikoku Research Institute Inc., 4. Japan Aerospace Exploration Agency

Shock remanent magnetization (SRM) is acquired as a result of the shock wave propagation in a magnetic field. Knowledge of a three-dimensional distribution of the SRM intensity is crucial for interpreting the spatial change in magnetic anomalies observed over the crater and reconstructing the paleo-planetary field based on the anomaly data. However, the intensity distribution is an unexplained phenomena concerning SRM properties owing to the lack of subsample magnetization measurements for the experimental SRM-imparted samples. To investigate the SRM intensity and stability structures using a magnetically well-characterized basalt sample bearing fine-grained single-domain titanomagnetite, we conducted the newly designed SRM acquisition experiments and remanence measurements for cube-shaped subsamples cut from the SRM-imparted samples. The pressure and temperature changes during the shock wave propagation were estimated from the impact simulations. Three distinctive aspects of SRM properties are recognized at different pressure ranges: (1) the SRM intensity is almost constant below 0.1 GPa, (2) the SRM intensity linearly increases with increasing pressure up to 1.1 GPa, and (3) the SRM intensity is almost constant, while the SRM stability increases with increasing pressure above 1.9 GPa. Regarding the SRM acquisition mechanisms, the pressure effect was likely dominant below 1.1 GPa, while multiple factors can be considered in the high-pressure range. The systematic changes in the SRM intensity and stability suggest that the crustal rocks containing the single-domain titanomagnetite had an SRM intensity structure at the time of impact, and this structure changed subsequently.

Keywords: Shock remanent magnetization, Single-domain titanomagnetite, Magnetic anomaly, Impact cratering

©2021. Japan Geoscience Union. All Right Reserved.

Numerical Study of the Formation Scenario of Mesosiderite Meteorites Through a Giant Impact Onto a Differentiated Asteroid

*Keisuke Sugiura[1], Makiko K. Haba[2], Hidenori Genda[1]

1. Tokyo Institute of Technology, Earth Life Science Institute, 2. Tokyo Institute of Technology, Department of Earth and Planetary Sciences

Mesosiderites are a kind of stony iron meteorites and contain similar amount of silicates and Fe-Ni metals. Chemical composition and other features of mesosiderites show that those silicates and Fe-Ni metals are, respectively, originated from a crust and a molten metal core of a differentiated asteroid (e.g., Mittlefehldt et al. 1979; Hassanzadeh et al. 1990). The metal components were molten when they mixed with silicates (e.g., Floran 1978). On the other hand, mesosiderites hardly contain olivine, which is main composition of mantle (e.g., Prinz et al. 1980). Measurements of cooling rate of mesosiderite metals show that mesosiderites experienced slow cooling at some depth in asteroids larger than several hundred kilometers (e.g., Haack et al. 1996). Thus, we expect that mesosiderites are formed through the following process: a molten core of a 100 km-sized differentiated asteroid is excavated through an impact of another asteroid and then excavated core mixes with surface crust of the differentiated asteroid. The parent body of mesosiderites should be about 500 km in diameter because its core was molten at the time of metal-crust mixing event (4.5 billion years ago: Haba et al. 2019). Moreover, the mesosiderites' parent body is probably the asteroid Vesta because the O and Cr isotope composition of mesosiderites almost coincides with those of HED meteorites (e.g., Greenwood et al. 2006) and infrared spectra of HED meteorites are similar to those of Vesta (e.g., McCord et al. 1970).

Although excavation and reaccumulation process of a core of a differentiated asteroid through a giant impact are roughly investigated through low-resolution simulations (Scott et al. 2001), there is no work investigating whether a giant impact is possible to produce materials mainly containing crust and metal. In this study, we simulate giant impacts onto a Vesta-like asteroid using the Smoothed Particle Hydrodynamics (SPH) method and investigate detailed distribution of materials on the surface of the impact outcome. Based on the magma ocean model of Vesta (Mandler&Elkins-Tanton 2013), we set the body's radius, core's radius, mantle thickness, and crust thickness to 270 km, 110 km, 120 km, and 40km, respectively. We use an impactor with 0.1 times the target mass. We vary the impact angle from 10 degrees to 50 degrees and the impact velocity from 2 km/s to 5 km/s.
We find that destructive impacts with the mass of the impact outcome becoming half of the original body can excavate the metal core and mix them with the surface crust. Although mantle materials are exposed on about half of the surface of the impact outcome, there are some surface locations mainly containing crust and metal materials. It is possible to produce mesosiderites on such locations. We also find that less destructive impacts hardly excavate the metal core, and more destructive impacts mainly strip the surface crust so that such impacts are difficult to produce materials composed of crust and metal core.

Keywords: stony iron meteorites, mesosiderites, differentiated asteroid, giant impact, numerical simulation, SPH method

©2021. Japan Geoscience Union. All Right Reserved.

High velocity impact experiments on porous ice aggregates simulating cometary nuclei: Estimation of energy partition from projectile kinetic energy to post shock heat

*Haruka Sasai[1], Minami Yasui[1], Masahiko Arakawa[1], Kei Shirai[1]

1. Kobe University

Introduction: Recent spacecraft explorations and ground-based observations have revealed that cometary nuclei have very low density, such as they are highly porous icy bodies (e.g., the bulk porosity of 67P/CG is estimated to be 72-74%) (Pätzold et al., 2016). When a small body collides on such porous icy bodies at high velocities, the high-velocity collision deposits a large amount of heat around the crater cavity due to the strong dissipation of the impact energy associated with the rapid attenuation of shock pressure (Kraus et al., 2010). This deposited energy is called post-shock heat and it is one of the most important heat sources on porous icy bodies. The post shock heating would form a temporal water pond below the impact crater, and aqueous alteration and organic chemical reactions might be promoted in the water pool. Particularly, the formation environment of organic matters on cometary nuclei has not been well known yet, and the chemical reaction in a temporal water pond on comets caused by the impact heating is expected to be one of the possible formation environments. There are several numerical simulations related to the post-shock heat and molten ice mass around the impact craters on icy planetesimals (e.g., Kraus et al., 2011), but laboratory experiments have not been studied yet. In this study, we conducted high-velocity impact experiments on porous icy aggregates simulating icy planetesimals and measured post-shock temperatures directly around the impact crater. Then, we examined the effect of target porosity on the post-shock heating.

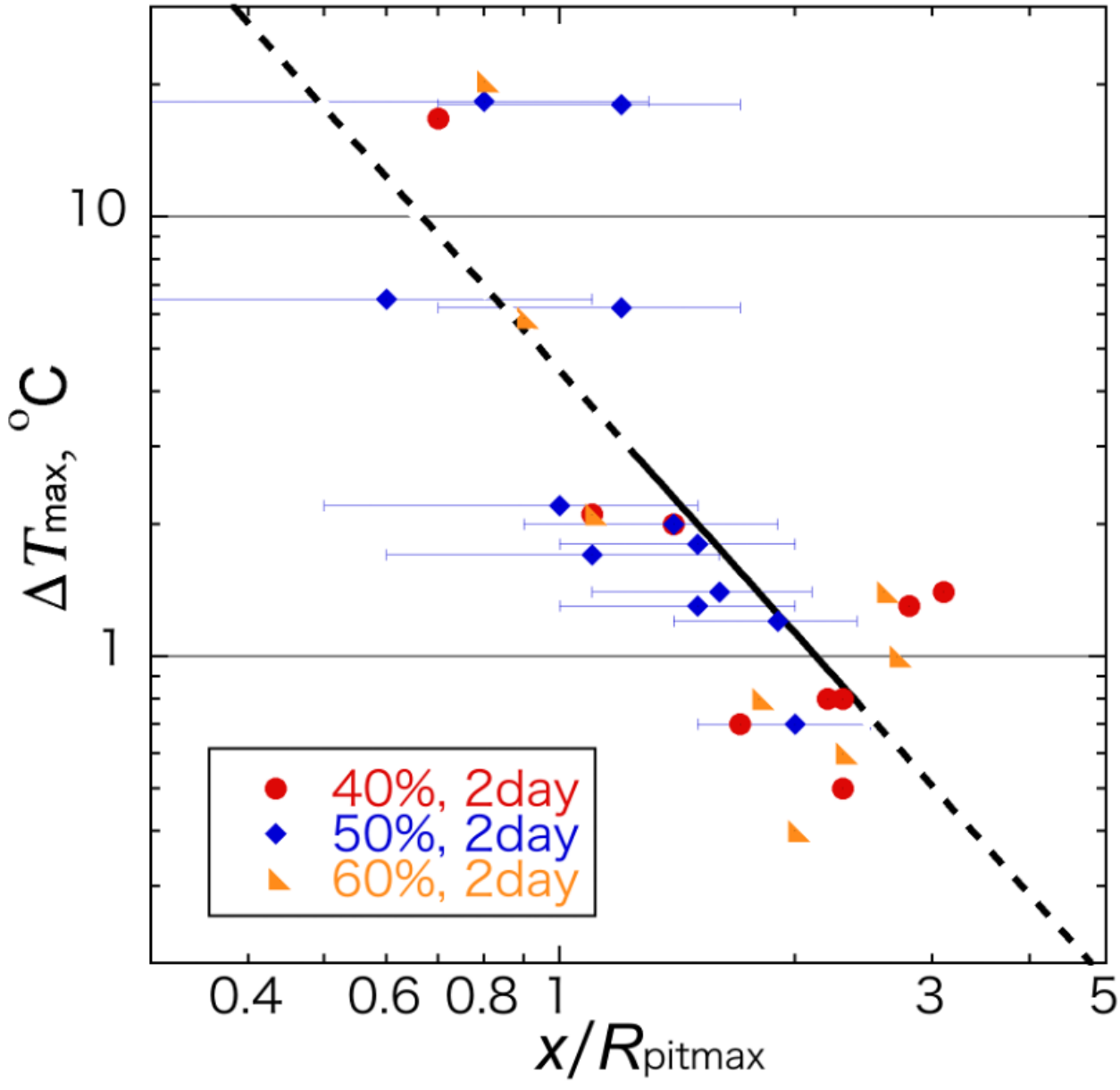
Methods: We prepared cylindrical porous ice targets with the porosity of 40, 50, and 60% by compacting ice grains (< 710 mm). They were sintered in a freezer (-20ºC). 3–5 thermocouples were embedded in the target at different distances from the impact point to measure the temperature. We conducted impact experiments by using a two-stage light gas gun at Kobe Univ. installed in a cold room at -15˚C. The aluminum sphere with the diameter of 2 mm was used as a projectile. The impact velocity was 4.2 km/s for 40% and 60% targets and 3.0–5.8 km/s for 50% targets. We observed cratering processes by using a high-speed camera. The temperatures measured by thermocouples were recorded by a data logger for 5 minutes after the impact. After the impact, we measured the molten ice mass by sieving large ice grains (> 710 mm).

Results & Discussion: The crater diameter increased with increase of the target porosity. The π-scaling law for the crater radius in strength regime was applied to our results (Housen & Holsapple, 2011) and normalized crater size π_R was found to be smaller than that of non-porous ice. The temperature rise decreased exponentially with the increase of the distance from the center of crater cavity, and the temperatures near the crater wall rose up beyond 0 ºC. This means that the ice grains near the crater wall were molten. We used the maximum temperature rise ΔT_{max} of each thermocouple to represent the temperature distribution changing with the distance from the crater center. Furthermore, ΔT_{max} depended on the target porosity and impact velocity; particularly, it was higher as the target porosity is higher at the same distance from the center of crater cavity. However, this systematic change of ΔT_{max} were well scaled by using normalized distance, x/R_{pitmax} (the x is the distance from the center of the crater cavity and, the R_{pitmax} is the maximum radius of the crater cavity), and the relationship was obtained to be

©2021. Japan Geoscience Union. All Right Reserved.

$\Delta T_{max}=4.7(x/R_{pitmax})^{-2.6}$ at x >1.2.
The ΔT_{max} distribution should be reproduced by using simple heat conduction model. We assumed that the post shock heat deposited at a thin layer on the final crater wall conducted outside the crater. The post shock heat was obtained as the energy conversion efficiency depended on the target porosities: It was 0.09 for 40% target, 0.32 for 50% target, and 0.51 for 60% target, respectively.

Keywords: comet, crater, post shock heat, impact melt, porous icy body



©2021. Japan Geoscience Union. All Right Reserved.

Effect of porosity on restitution coefficient and sticking properties of snowball simulating Saturn’ s rings

*Yukari Toyoda[1], Masahiko Arakawa[1], Minami Yasui[1]

1. Graduate School of Science, Kobe University

Saturn's rings have a width of tens of thousands of kilometers and a thickness of hundreds of meters, and they are composed of water ice particles with a diameter of mm to meters. The average relative impact velocity among ring particles is estimated to be < several cm/s, so at such low velocities, sticking of ice particles may occur by surface adhesion force. Numerical simulations indicated that the restitution coefficient must be about 0.6 to maintain a thin annular ring. Therefore, it is necessary to investigate the collisional outcomes of ice particles during low velocity collision such as fracture, rebound and sticking. Although previous laboratory experiments were conducted by using non-porous or frosted ice particles, ring particles are predicted by Cassini's observations to be highly porous ice particles such as ice aggregates. Then, this observation is inconsistent with non-porous ice. Therefore, it is necessary to examine whether the ice aggregates can maintain the thin annular rings of Saturn.

The purpose of this study is to clarify the velocity dependence of restitution coefficient of porous ice and the threshold velocity for sticking of porous ice, we then try to estimate the internal structure of ring particles suitable for maintaining thin annular Saturn rings. Therefore, low-velocity impact experiments were performed between a porous ice ball and a porous ice plate, and we investigated the porosity dependence of the relationship between the impact velocity and the restitution coefficient and the threshold velocity for sticking.

The restitution coefficient was measured by letting a ball fall freely on a plate. Porous ice spheres (the radius of 1.5cm, the porosity of 47%, 53% and 60%) were made by compacting ice particles (the average size of 20μm) into spherical molds. A porous ice plate was used for the target plate which was made in the same way as porous ice spheres (the radius of 1.5 cm, the thickness of 2 cm, the porosity of 43% to 62%). The restitution coefficient was determined by measuring the time interval among collisions using a laser displacement meter. The impact velocity was changed from 2.33 to 76.4 cm / s.

The restitution coefficient of the porous ice ball continued to decrease with the increase of the impact velocity. The restitution coefficient decreased as the porosity increased at high impact velocities, but the porosity dependence was not recognized at low impact velocities of < 10cm/s. This velocity dependence of the restitution coefficient can be expressed by the empirical equation, $e = e_0 * v_i^{-b}$, where e is the restitution coefficient and v_i is the impact velocity, and e_0, b was 0.47, 0.17 at the porosity of 47%, 0.59, 0.36 at 53%, and 0.36, 0.27 at 60%, respectively. But, the low velocity data was obtained in the second and subsequent collisions, suggesting that these multiple collisions might cause a change in the surface state.

We find that mixed region where both rebound and sticking occur was observed as the impact velocity decreased. At lower velocities, the rebound was no longer observed. The threshold velocities for mixing region were 10.3 cm/s at the porosity of 47%, 12.9 cm/s at 53%, and 9.68 cm/s at 60%, respectively. And the threshold velocities for sticking were 3.53 cm/s at the porosity of 47%, 1.27 cm/s at 53%, and 9.22 cm/s at 60%, respectively.

©2021. Japan Geoscience Union. All Right Reserved.

From these results, we infer that rebound does not occur at low impact velocities of < 1cm/s. However, the circumstance temperature of Saturn is about 100 K, which is lower than the temperature at which the experiment was conducted. Then, threshold velocity for sticking considered to be lower. Therefore, by extrapolating the empirical equation obtained in this study assuming that the equation is independent of temperature, it was found that the impact velocity corresponding to the restitution coefficient of 0.6 was 0.24 cm/s at the porosity of 47%, 0.95 cm/s at 53%, and 0.15 cm/s at 60%, respectively.
This velocity range was almost consistent with those of ring particles estimated from the numerical simulation (less than 0.3 to 0.5 cm/s).

Keywords: Saturn's ring, restitution coefficient, sticking

©2021. Japan Geoscience Union. All Right Reserved.

[J] Oral | P (Space and Planetary Sciences)：P-PS Planetary Sciences

Fri. Jun 4, 2021 3:30 PM - 5:00 PM JST | Fri. Jun 4, 2021 6:30 AM - 8:00 AM UTC | Ch.04 Zoom Room 04

[P-PS07] Formation and evolution of planetary materials in the Solar System

convener:Megumi Matsumoto(Graduate School of Science, Tohoku University), Shin Ozawa(Department of Earth Science, Graduate School of Science, Tohoku University), Yuki Hibiya(Submarine Resources Research Center, Japan Agency for Marine-Earth Science and Technology), Noriyuki Kawasaki(Department of Earth and Planetary Sciences, Graduate School of Science, Hokkaido University), Chairperson:Megumi Matsumoto(Graduate School of Science, Tohoku University), Shin Ozawa(Department of Earth Science, Graduate School of Science, Tohoku University)

In this session, we will discuss the material evolution in the Solar System based on extraterrestrial sample analyses and experimental works. We will overlook recent knowledge from primitive materials such as chondrites, interplanetary dust particles, and returned samples by space missions. Research works on meteorite parent body processes such as aqueous alteration, thermal metamorphism, shock metamorphism, volcanic activity, and core-mantle-crust differentiation will also be discussed. The topics of this session include experimental studies which, together with meteorite studies, help us to understand the material formation/evolution in the Solar System as well as processes on meteorite parent bodies. Presentations on new innovative analytical and theoretical techniques in various research fields (chemistry, theoretical calculation, physical property) are highly welcome to improve future studies of the Solar System evolution. This session is J (Japanese) session but English talks are also welcomed.

3:30 PM - 3:45 PM JST | 6:30 AM - 6:45 AM UTC

[PPS07-01] Detection of hexamethylenetetramine in carbonaceous meteorites and its role for chemical evolution

*Yasuhiro Oba[1], Yoshinori Takano[2], Hiroshi Naraoka[3], Yoshihiro Furukawa[4], Shogo Tachibana[5,6], Daniel P Glavin[7], Jason P Dworkin[7] (1.Institute of Low Temperature Science, Hokkaido University, 2.JAMSTEC, 3.Kyushu University, 4.Tohoku University, 5.University of Tokyo, 6.ISAS/JAXA, 7.NASA Goddard Space Flight Center)

3:45 PM - 4:00 PM JST | 6:45 AM - 7:00 AM UTC

[PPS07-02] Isotopic constraint on the origin of organic matter in carbonaceous chondrites

*Yoshihiro Furukawa[1], Yoshinari Iwasa[1], Yoshito Chikaraishi[2] (1.Graduate School of Science, Tohoku University, 2.Institute of Low Temperature Science)

4:00 PM - 4:30 PM JST | 7:00 AM - 7:30 AM UTC

[PPS07-03] **What kinds of the meteorite are CM chondrites?**

★Invited Papers

*Makoto Kimura[1] (1.National Institute of Polar Research)

4:30 PM - 4:45 PM JST | 7:30 AM - 7:45 AM UTC

[PPS07-04] The first fall-observed and recovered meteorite in Japan: Narashino meteorite

*Atsushi Takenouchi[1], Shigekazu Yoneda[2], Akira Yamaguchi[1], Ryuji Okazaki[3], Naoki Takahashi[4], Naoki Shirai[5], Yasunori Fujiwara, Ryuho Kataoka[1] (1.National Institute of Polar Research, 2.National Museum of Nature and Scienece, 3.Kyushu University, 4.Natural History Museum and Institute, Chiba, 5.Tokyo Metropolitan University)

4:45 PM - 5:00 PM JST | 7:45 AM - 8:00 AM UTC

[PPS07-05] High spatial resolution three-color CT imaging of CM and CI meteorites and their heated samples for a rehearsal analysis of Ryugu

*Junya Matsuno[1], Akira Tsuchiyama[1], Megumi Matsumoto[2], Yuri Fujioka[2], Tomoki Nakamura[2], Kentaro Uesugi[3], Akihisa Takeuchi[3], Masahiro Yasutake[3], Tsukasa Nakano[4], Naoto Nakano[6], Rubino Stefano[5],

Shota Okumura[6], Akira Miyake[6] (1.Ritsumeikan University, 2.Tohoku University, 3.JASRI/SPring-8, 4.AIST, 5.Institut d'Astrophysique Spatiale, 6.Kyoto University)

Detection of hexamethylenetetramine in carbonaceous meteorites and its role for chemical evolution

*Yasuhiro Oba[1], Yoshinori Takano[2], Hiroshi Naraoka[3], Yoshihiro Furukawa[4], Shogo Tachibana[5,6], Daniel P Glavin[7], Jason P Dworkin[7]

1. Institute of Low Temperature Science, Hokkaido University, 2. JAMSTEC, 3. Kyushu University, 4. Tohoku University, 5. University of Tokyo, 6. ISAS/JAXA, 7. NASA Goddard Space Flight Center

Hexamethylenetetramine (HMT, $C_6H_{12}N_4$), an organic molecule with a characteristic cage-like structure, is the most abundant product in the photolysis of interstellar ice analogues containing water, methanol, ammonia, etc, under astrophysically relevant conditions. However, despite such properties, HMT has never been detected in any extraterrestrial environments/materials so far. We have for the first time detected HMT in three carbonaceous meteorites (Murchison, Tagish Lake, and Murray) whose concentrations are equivalent to other meteoritic organic molecules such as amino acids. Since HMT can yield formaldehyde and ammonia, which are necessary for the formation of various meteoritic organic molecules such as amino acids and sugars, upon (hydro)thermal degradations on meteorite parent bodies, it should play a vital role for chemical evolution in the solar system. In addition, the detected HMT would have formed by photochemical reactions in the interstellar medium, suggesting that its formation predated the formation of the solar system.

[Ref.] Oba, Y., Takano, Y., Naraoka, H., Furukawa, Y., Glavin, D.P., Dworkin, J.P. and Tachibana, S. (2020) Extraterrestrial hexamethylenetetramine in meteorites-a precursor of prebiotic chemistry in the inner solar system.
Nature Communications, 11, Article number: 6243. doi: 10.1038/s41467-020-20038-x.

Keywords: HMT, carbonaceous meteorites, chemical evolution

©2021. Japan Geoscience Union. All Right Reserved.

Isotopic constraint on the origin of organic matter in carbonaceous chondrites

*Yoshihiro Furukawa[1], Yoshinari Iwasa[1], Yoshito Chikaraishi[2]

1. Graduate School of Science, Tohoku University, 2. Institute of Low Temperature Science

Many solvent-soluble organic matters (SOM) in carbonaceous chondrites such as sugars, amino acids, amines, and aldehydes are enriched in ^{13}C. The reason for the ^{13}C enrichment has not been clear but discussed as some contributions from precursor materials formed in the cold outer solar system. Several reactions/processes have been proposed for the origin of meteorite amino acids, including their formation by the photochemical reaction in a molecular cloud, Fischer–Tropsch type reaction in the solar nebula, Strecker reaction, and Formose-type reaction in the meteorite parent bodies. Formose-type reaction is also discussed as a potential synthetic reaction of solvent insoluble organic matter (IOM) that is the primary carbon host in meteorites and has carbon isotope characteristic depleted in ^{12}C. We hypothesized that kinetic isotope fractionation during the Formose-type reaction might form the large carbon isotope difference between SOM and IOM and conducted experiments to investigate this fractionation. The product amino acids and sugars have significantly enriched in ^{13}C compared with the product IOM analogue. The extents of enrichment are comparable to that have been found in several carbonaceous chondrites. This result proved an isotopic constraint on the formation reactions/processes of organic matter found in carbonaceous chondrites.

©2021. Japan Geoscience Union. All Right Reserved.

What kinds of the meteorite are CM chondrites?

*Makoto Kimura[1]

1. National Institute of Polar Research

CM chondrites are the most abundant group of carbonaceous chondrites and are likely to be related to samples returned by the Hayabusa2 and OSIRIS-REx missions. They are characterized by abundant water and organic materials. However, they show a wide variation of petrological and oxygen isotopic features. CMs experienced varying degrees of aqueous alteration and partly secondary heating. Here I review the variation and formation conditions of these CMs.

CM chondrites have been commonly classified into subtypes 2.7-2.0 after the criteria, such as the alteration features and metal abundance, proposed by Rubin [1]. Kimura et al. [2] recently reported two CMs, Asuka (A) 12169 and A 12236, that experienced very low degrees of aqueous alteration and heating. Chondrules and refractory inclusions show no evidence for alteration, and the matrices hardly contain phyllosilicates. Kimura et al. [2] newly proposed the subtypes 3.0-2.8 of CMs. A 12169 and 12236 are classified into subtypes 3.0 and 2.9, respectively. These chondrites are the most primitive CM chondrites so far reported. This conclusion is supported by recent discoveries, such as abundant organic materials [3] and presolar grains [4,5], the predominant occurrence of amorphous materials in the matrix [6], and primitive features of chondrules in these CMs [7].

Because of the secondary alteration, the primitive features of CMs were not yet enough clarified. However, the discovery of CM3.0 gives a significant hint for the formation conditions of CMs. Although the bulk oxygen isotopic compositions of CMs were reported to be different from those of CO chondrites, the oxygen isotopic compositions of CM3.0-2.9 are overlapped to COs. The precursor material to CMs appears to have been isotopically nearly identical to that of the COs. However, the characteristic features of CMs had primarily been different from those of CO3.0, not only in petrologic features but the bulk chemical compositions. Therefore, CMs and COs are probably not both derived from a single parent body.

The precursor materials of CMs later experienced the aqueous alteration in the parent body by the decay of ^{26}Al [e.g., 8]. The subtypes reflect the degree of such alteration. Some CMs were later subjected to secondary heating to decompose phyllosilicates. Many CMs are breccias and contain various kinds of clasts in them. These clasts are important to give constraints for the evolution and internal structure of the CM parent body [9]. CMs show the complicated formation processes, including alteration, heating, and brecciation. In addition to these CMs, many anomalous CMs or related chondrites have been reported [e.g., 10]. Their oxygen isotopic compositions, bulk chemical compositions, or mineralogical features distinguish them from other CMs. However, the genetic relationships between anomalous and other CMs are open questions.

References

[1] Rubin 2015 MAPS 50, 1595-1612. [2] Kimura et al. 2020 Polar Science 26 100565. [3] Glavin et al. 2020 MAPS 55,1979-2006. [4] Nittler L. R. et al. 2020 MAPS in press. [5] Xu et al. 2020 11th Symposium on Polar Science, OAo05.pdf. [6] Noguchi et al. 2020 51st LPSC, 1666.pdf. [7] Fukuda et al. 2020 11th

©2021. Japan Geoscience Union. All Right Reserved.

Symposium on Polar Science, OAo06.pdf. [8] Fujiya et al. 2012 Nat.Comms. 3,627. [9] Kerraouch et al. 2019 Geochemistry 79, 125518. [10] Brearley 1995 GCA 59, 2291-2317.

Keywords: Meteorite, Carbonaceous chondrite, CM chondrite

©2021. Japan Geoscience Union. All Right Reserved.

The first fall-observed and recovered meteorite in Japan: Narashino meteorite

*Atsushi Takenouchi[1], Shigekazu Yoneda[2], Akira Yamaguchi[1], Ryuji Okazaki[3], Naoki Takahashi[4], Naoki Shirai[5], Yasunori Fujiwara, Ryuho Kataoka[1]

1. National Institute of Polar Research, 2. National Museum of Nature and Scienece, 3. Kyushu University, 4. Natural History Museum and Institute, Chiba, 5. Tokyo Metropolitan University

At 2:32 am JST on July 2, 2020, a fireball was observed over the Kanto region, Japan. Several amateur astronomers recorded the fireball by automated meteor-observation cameras belonging to the SonotaCo low-light video camera network [1] and calculated its trajectory and a strewn field [2-4]. The recovered meteorite is named “Narashino” to be the 53rd meteorites found in Japan and the first one whose trajectory is well-investigated. Here, we report a recovering history and a petrological description of the Narashino meteorite.

Until today, fragments are recovered from three locations in the northern part of the predicted strewn field. A first fragment (63 g) was found on a floor of a corridor in an apartment. Two days later, another 70 g fragment was found in the garden of the same apartment. On the basis of their shapes, they were originally one mass (No. 1) and were crushed when it hit on the wall of the apartment. Later, several small fragments are collected on the top of the apartments, and the total weight of the mass No. 1 becomes more than 156 g. On July 22, the second mass (No. 2) was found in Funabashi city about 1 km northeast of the No. 1 site. The mass broke a roofing tile of an apartment and spread into 2 large (95 g and 73 g) and 11 small fragments. The total weight of mass No. 2 is more than 194 g. The last one (No. 3) was found on October 25, about three months later after the last recovery, at the top of a supermarket located further 1 km north than the second location. The third one is small, weighing 14.67 g, and maybe a piece of a larger unrecovered mass. Gamma rays emitted from cosmogenic radionuclides (52Mn, 48V, 54Mn, 22Na, and 26Al) were measured by the pure Ge detector at the National Museum of Nature and Science, confirming that all of these fragments are recently fallen meteorites. The total weight of the Narashino meteorite so far is about 365 g, which is smaller than the expected mass based on the fireball observation.

A half surface of two large fragments of mass No. 1 is covered by the fusion crust. The first fragment of mass No. 1 is extremely fresh, but the second one looks slightly weathered by rain. The mass No. 2 is also half-covered by fusion crust. The weathering of the mass No. 2 surface is severer than the mass No.1 due to the longer exposure to the weather (20 days), and the same is true for No. 3. However, the weathering reaches just on the surface or in small cracks, thus the interiors of mass No.1 and 2 looks fresh (No. 3 is not investigated except for gamma rays).

For petrological analysis, polished thick and thin sections were made from the mass No. 1 and No. 2 at the National Institute of Polar Research. We observed the sections by FE-SEM and analyzed chemical compositions of constituent minerals by electron microprobe. Narashino meteorite is mainly composed of ferromagnesian silicate (olivine+pyroxene, 63.9 vol.%), albite (10.1 %), Fe-Ni metal (8.7 %), sulfides (3.6 %) and accessory minerals such as chromite (0.53 %) and phosphate (0.47 %). One of the characteristic features of Narashino is its high porosity (12.7 vol%). Olivine compositional ranges are Fa17.0-18.1 (mean=Fa17.7, N=27) for No.1 and Fa16.9-18.0 (mean Fa17.6, N=25) for No.2. Compositional ranges of low-Ca pyroxene are Fs15.4-16.5 (mean=Fs15.8, N=13) and Fs15.5-16.2 (mean=Fs15.8, N=19),

©2021. Japan Geoscience Union. All Right Reserved.

respectively. The size of albite is >50 μm. The above observation indicates that Narashino is H5 chondrite. Since no shock feature was observed, the shock stage of Narashino is S1. Noble gas analysis performed at Kyushu University using fragments of No. 1 and No. 2 yielded the K-Ar gas retention age of about 4.5 Ga, assuming the K content of 780 ppm.

This work is supported by Project to Build an International Collaborative Research Network for Pre-modern Japanese Texts (NIJL-NW project), “Hoshi-ishi 4D project”. In the project, we are continuing to seek a 200-year-old meteorite based on the literature survey. Narashino meteorite fall is similar to the event written in the literature.

Reference

[1] Central Bureau for Astronomical Telegrams, CBET No.4810, July 2020, 12.

[2] Astronomical Circular No.939, Nippon Meteor Society, Oct. 2020, 19-22.

[3] The Heavens, No.1149, Oriental Astronomical Association, Feb. 2021, 64-67.

[4] Astronomical Circular No.938, Nippon Meteor Society, Sep. 2020, 19-22.

Keywords: Narashino meteorite, meteor observation, Ordinary chondrite

©2021. Japan Geoscience Union. All Right Reserved.

High spatial resolution three-color CT imaging of CM and CI meteorites and their heated samples for a rehearsal analysis of Ryugu

*Junya Matsuno[1], Akira Tsuchiyama[1], Megumi Matsumoto[2], Yuri Fujioka[2], Tomoki Nakamura[2], Kentaro Uesugi[3], Akihisa Takeuchi[3], Masahiro Yasutake[3], Tsukasa Nakano[4], Naoto Nakano[6], Rubino Stefano[5], Shota Okumura[6], Akira Miyake[6]

1. Ritsumeikan University, 2. Tohoku University, 3. JASRI/SPring-8, 4. AIST, 5. Institut d'Astrophysique Spatiale, 6. Kyoto University

JAXA's spacecraft "Hayabusa2" returned to Earth last December, and curation of samples collected from the asteroid "Ryugu" is ongoing. Based on the analysis of reflectance spectra and other data, Ryugu is thought to be composed of weakly heated CM and/or CI meteorite-like materials [1]. Since the microstructure of such materials is complex on the sub-micron scale, three-dimensional observations with high spatial resolutions are useful to understand the formation process of the Ryugu samples. Our group is planning to perform XCT analysis of the Ryugu samples at SPring-8 BL47XU, and are preparing for the analysis.

As the rehearsal of the sample analysis, we conducted nano-XCT observations (~70 nm/pixel) of CM and CI meteorites and their heated samples using monochromatic X-rays. The samples were fixed to the top of a Ti needle by FIB or to a carbon fiber using resin. Images of X-ray absorption coefficient (LAC) were obtained at energies of 7.00 and 7.35 keV, which are in between the K-edge of energy of Fe. Images of X-ray refractive index decrement (RID) were also obtained by a one-dimensional scanning X-ray microscope at 8.00 keV [2]. By registration of the three kinds of images, a three-dimensional image as quasi-color image in which each pixel has three variables (LAC of 7.00 keV, LAC of 7.35 keV, and RID of 8.00 keV) was obtained. The 7.00 keV images were segmented using the Chan-Vase method to quantitatively measure particle shapes and porosities.

A comparison of the unheated Murchison meteorite and the sample heated to 400 ˚C for X hours shows that part of the TCI (tochilinite-cronstedtite intergrowth) is magnetized. Furthermore, at 600 ˚C X hours, the matrix and TCI reacted. In the Murray meteorite, the TCI of the sample heated at 600 ˚C for 1 hour retained its shape, but some of it reacted with the matrix.

A comparison of an unheated CI meteorite (the Orgueil meteorite) with its heated sample at 500 ˚C for 50 hours showed that a lip-shaped structure (~5 μm long) of Fe-rich serpentine that was universally observed in the unheated sample was slightly shrunken and detached from the matrix in the heated sample although there were not serious textual changes in its matrix and magnetite. This lip-shaped structure may be a good indicator to constrain the heating conditions for weak thermal metamorphism of CI meteorites[h1] .

[1] Kitazato et al., Science 364, 272–275 (2019)

[2] Takeuchi et al., J. Synchrotron Radiat. 20, 793–800 (2013).

Keywords: Hayabusa 2, Ryugu, nano XCT

©2021. Japan Geoscience Union. All Right Reserved.

[J] Oral | P (Space and Planetary Sciences)：P-EM Solar-Terrestrial Sciences, Space Electromagnetism & Space Environment

Fri. Jun 4, 2021 9:00 AM - 10:30 AM JST | Fri. Jun 4, 2021 12:00 AM - 1:30 AM UTC | Ch.06 Zoom Room 06

[P-EM15] Space Plasma Physics: Theory and Simulation

convener:Takanobu Amano(Department of Earth and Planetary Science, University of Tokyo), Yohei Miyake(Education Center on Computational Science and Engineering, Kobe University), Takayuki Umeda(Institute for Space-Earth Environmental Research, Nagoya University), Tadas Nakamura(Fukui Prefectural University), Chairperson:Takanobu Amano(Department of Earth and Planetary Science, University of Tokyo), Masanori Iwamoto(Faculty of Engineering Sciences, Kyushu University)

This session focuses on studies of space plasma physics via theoretical and numerical approaches. Papers on a wide variety of topics from natural phenomena to artificial plasma environment as well as theoretical and computational methodologies are welcome.

9:00 AM - 9:15 AM JST | 12:00 AM - 12:15 AM UTC

[PEM15-01] Observation of non-gyrotropy of electrons caused by wave-particle interaction with intense whistler mode waves in mirror mode structures in the magnetosheath

*Naritoshi Kitamura[1], Masahiro Kitahara[2], Scott A Boardsen[3,4], Takanobu Amano[1], Daniel J Gershman[3], Yoshiharu Omura[5], Satoko Nakamura[2], Masafumi Shoji[2], Yuto Katoh[6], Hirotsugu Kojima[5], Yoshizumi Miyoshi[2], Yoshifumi Saito[7], Masafumi Hirahara[2], Shoichiro Yokota[8], Barbara L Giles[3], William R Paterson[3], Craig J Pollock[9], Olivier Le Contel[10], Christopher T Russell[11], Narges Ahmadi[12], Per-Arne Lindqvist[13], Robert E Ergun[12], James L Burch[14] (1.Department of Earth and Planetary Science, Graduate School of Science, The University of Tokyo, 2.Institute for Space-Earth Environmental Research, Nagoya University, 3.NASA Goddard Space Flight Center, 4.Goddard Planetary Heliophysics Institute, University of Maryland, 5.Research Institute for Sustainable Humanosphere, Kyoto University, 6.Department of Geophysics, Graduate School of Science, Tohoku University, 7.Institute of Space and Astronautical Science, Japan Aerospace Exploration Agency, 8.Department of Earth and Space Science, Graduate School of Science, Osaka University, 9.Denali Scientific, 10.Laboratoire de Physique des Plasmas, CNRS/Ecole Polytechnique/Sorbonne Université/Université Paris-Sud/Observatoire de Paris, 11.Department of Earth, Planetary, and Space Science, University of California, Los Angeles, 12.Laboratory for Atmospheric and Space Physics, University of Colorado, Boulder, 13.Royal Institute of Technology, 14.Southwest Research Institute)

9:15 AM - 9:30 AM JST | 12:15 AM - 12:30 AM UTC

[PEM15-02] Simulation for wave-particle interactions of triggered emissions in a uniform magnetic field

*Yuya Fujiwara[1], Takeshi Nogi[1], Yoshiharu Omura[1] (1.Research Institute for Sustainable Humanosphere, Kyoto University)

9:30 AM - 9:45 AM JST | 12:30 AM - 12:45 AM UTC

[PEM15-03] Synchrotron Maser Emission from Relativistic Shocks

*Masanori Iwamoto[1], Takanobu Amano[2], Yosuke Matsumoto[3], Shuichi Matsukiyo[1], Masahiro Hoshino[2] (1. Faculty of Engineering Sciences, Kyushu University, 2.Department of Earth and Planetary Science, University of Tokyo, 3.Graduate School of Science, Chiba University)

9:45 AM - 10:00 AM JST | 12:45 AM - 1:00 AM UTC

[PEM15-04] Synchrotron maser instability in an electron-ion plasma

*Shuichi Matsukiyo[1], Yodai Esaki[2], Masanori Iwamoto[1] (1.Faculty of Engineering Sciences, Kyushu University, 2.Interdisciplinary Graduate School of Engineering Sciences, Kyushu University)

10:00 AM - 10:15 AM JST | 1:00 AM - 1:15 AM UTC

[PEM15-05] Trajectory analysis of energetic electrons in quasi-perpendicular shock structure

*Fumiko Otsuka[1], Shuichi Matsukiyo[1], Mitsuo Oka[2] (1.Earth System Science and Technology, 2.UC Berkeley)

10:15 AM - 10:30 AM JST | 1:15 AM - 1:30 AM UTC

[PEM15-06] Simulation of temperature anisotropy instability by a fluid model with non-local closure

*Taiki Jikei[1], Takanobu Amano[1] (1.The University of Tokyo)

Observation of non-gyrotropy of electrons caused by wave-particle interaction with intense whistler mode waves in mirror mode structures in the magnetosheath

*Naritoshi Kitamura[1], Masahiro Kitahara[2], Scott A Boardsen[3,4], Takanobu Amano[1], Daniel J Gershman[3], Yoshiharu Omura[5], Satoko Nakamura[2], Masafumi Shoji[2], Yuto Katoh[6], Hirotsugu Kojima[5], Yoshizumi Miyoshi[2], Yoshifumi Saito[7], Masafumi Hirahara[2], Shoichiro Yokota[8], Barbara L Giles[3], William R Paterson[3], Craig J Pollock[9], Olivier Le Contel[10], Christopher T Russell[11], Narges Ahmadi[12], Per-Arne Lindqvist[13], Robert E Ergun[12], James L Burch[14]

1. Department of Earth and Planetary Science, Graduate School of Science, The University of Tokyo, 2. Institute for Space-Earth Environmental Research, Nagoya University, 3. NASA Goddard Space Flight Center, 4. Goddard Planetary Heliophysics Institute, University of Maryland, 5. Research Institute for Sustainable Humanosphere, Kyoto University, 6. Department of Geophysics, Graduate School of Science, Tohoku University, 7. Institute of Space and Astronautical Science, Japan Aerospace Exploration Agency, 8. Department of Earth and Space Science, Graduate School of Science, Osaka University, 9. Denali Scientific, 10. Laboratoire de Physique des Plasmas, CNRS/Ecole Polytechnique/Sorbonne Université/Université Paris-Sud/Observatoire de Paris, 11. Department of Earth, Planetary, and Space Science, University of California, Los Angeles, 12. Laboratory for Atmospheric and Space Physics, University of Colorado, Boulder, 13. Royal Institute of Technology, 14. Southwest Research Institute

In the magnetosheath region, magnetic mirror structures often appear due to mirror instability. In many magnetic mirror traps in such mirror structures, whistler mode waves called Lion roars are emitted from the vicinity of the minima of the magnetic field intensity along field lines. The waves propagate in the direction of parallel and antiparallel to magnetic field lines. This situation is similar to the magnetic equator in the inner magnetosphere. Here we report the non-gyrotropy of electrons caused by the non-resonant wave-particle interaction around the source region of the whistler mode waves using the data obtained by the Magnetospheric Multiscale (MMS) spacecraft. The burst mode electromagnetic field data obtained by the search-coil magnetometer and the electric field double probes with the sampling rate of 8192 Hz are used for the analysis of whistler mode waves. The background magnetic field is derived from fast survey mode (16 samples/s) magnetometer data. The electron data (6 eV-30 keV) used in this study is from the Fast Plasma Investigation Dual Electron Spectrometer (FPI-DES). However, the temporal resolution of the burst mode FPI-DES data, which is 30 ms, is not sufficient to resolve fluctuations associated with the whistler mode waves with a frequency of about 100 Hz (= period of about 10 ms). Thus, the data are disassembled to the measurement time of each energy and deflection instrument step. The integration time of each step is 196 micro-seconds, which is only about one fiftieth of the period of waves with a frequency of 100 Hz. Using this disassembled dataset, we investigate the existence of non-gyrotropy and the phase relationship with the electromagnetic fields of the whistler mode wave for various energy and pitch angle bins. In some of energy bins, we discovered non-gyrotropy, which was likely caused by non-resonant interaction, at pitch angles much closer to 90° than the cyclotron resonance condition for electrons moving in the opposite direction to the wave propagation direction. Since the magnetic field amplitude of the whistler mode wave reaches several percent of the background magnetic field intensity, even electrons far from the cyclotron resonance velocity oscillate with a non-negligible extent, mainly in the pitch angle direction in the phase space during the passage of one cycle of the wave seen by the electron. Because the electrons have a butterfly distribution, which is thought to be caused by the growth of the mirror traps, the gradient of the phase space density along the diffusion curve along which the electrons oscillate increases at pitch angles closer to 90° than the peak of the butterfly distribution. This relatively large gradient of the phase space density makes it possible to

©2021. Japan Geoscience Union. All Right Reserved.

cause non-gyrotropy observable at the pitch angles.

Keywords: Whistler mode wave, Wave-particle interaction, MMS spacecraft

©2021. Japan Geoscience Union. All Right Reserved.

Simulation for wave-particle interactions of triggered emissions in a uniform magnetic field

*Yuya Fujiwara[1], Takeshi Nogi[1], Yoshiharu Omura[1]

1. Research Institute for Sustainable Humanosphere, Kyoto University

One-dimensional electromagnetic particle simulations were performed for the study of nonlinear process of the whistler-mode triggered emissions in a uniform magnetic field. We put cold and hot electrons initialized by bi-Maxwellian and subtracted bi-Maxwellian distributions, respectively. Driving two orthogonally aligned antennas by right-handed polarized external currents oscillating with frequencies below the electron cyclotron frequency, we generate whistler-mode triggering waves in the simulation system. We report the characteristics of the triggered emissions in terms of the duration and frequency of the triggering wave. In the cases with rising-tone emissions, we analyze dynamics of resonant electrons in the velocity phase space based on the nonlinear wave growth theory. We find that the formation of an electron hole generates rising-tone emissions after the termination of the triggering waves. In the present study, we discuss the initial process of the formation of an electron hole and hill during triggering waves, which causes frequency variations from the constant triggering frequency.

Keywords: whistler-mode wave, triggered emission, PIC simulation

©2021. Japan Geoscience Union. All Right Reserved.

Synchrotron Maser Emission from Relativistic Shocks

*Masanori Iwamoto[1], Takanobu Amano[2], Yosuke Matsumoto[3], Shuichi Matsukiyo[1], Masahiro Hoshino[2]

1. Faculty of Engineering Sciences, Kyushu University, 2. Department of Earth and Planetary Science, University of Tokyo, 3. Graduate School of Science, Chiba University

The origin of fast radio bursts (FRBs; Lorimer et al. 2007) is one of the unsolved problems in astrophysics. Since the high intensity and short duration of FRBs suggest extraordinarily high brightness temperature, the standard emission mechanisms such as synchrotron radiation and thermal bremsstrahlung cannot explain the origin of FRBs. Therefore, FRBs are believed to be coherent emission in the sense that electrons coherently move and radiate electromagnetic waves like emission from a single macro particle.

In relativistic shocks, it is well known that coherent electromagnetic waves are excited by synchrotron maser instability (SMI) in the shock transition (Hoshino & Arons 1991). SMI has been widely studied in space physics and is well known as emission mechanism of auroral kilometric radiation and Jovian decametric radiation. Recently, the SMI is used for the model of FRBs (e.g., Lyubarsky 2014; Beloborodov 2017; Plotnikov & Sironi 2019; Metzger et al. 2019) and attracts much of attention in astrophysics. In this study, by performing particle-in-cell (PIC) simulation of relativistic shocks, we will demonstrate that large-amplitude electromagnetic waves are indeed excited by the SMI. Especially for relatively high magnetization, the wave amplitude is significantly amplified and exceeds that in pair plasmas due to a positive feedback process associated with ion-electron coupling. Based on the simulation results, we will discuss the applicability of the SMI for FRBs in this talk.

Keywords: shock waves, plasma instabilities, high energy astrophysical phenomena

©2021. Japan Geoscience Union. All Right Reserved.

Synchrotron maser instability in an electron-ion plasma

*Shuichi Matsukiyo[1], Yodai Esaki[2], Masanori Iwamoto[1]

1. Faculty of Engineering Sciences, Kyushu University, 2. Interdisciplinary Graduate School of Engineering Sciences, Kyushu University

Synchrotron maser instability driven by relativistic ring distribution of electrons and ions is investigated. The linear analysis reveals that the electron and ion instabilities have characteristic frequencies and wavenumbers proportional to the mass of electrons and ions, respectively, as pointed out in a previous study. The generated waves have both electromagnetic and electrostatic features. The latter feature becomes remarkable when wave phase velocity is below the speed of light. PIC simulation further reveals that the electron instability seldom affects the ion instability due to the large difference of inertial. The ion instability destabilizes larger amplitude waves. In the simulation strong transverse electric field with zero wavenumber is generated. This electric field efficiently accelerates some electrons which are pre-accelerated in the early stage of the simulation due to the electron instability. These electrons finally have the energy comparable to the maximum ion energy. Furthermore, the accelerated electrons excite secondary electron instability. Some parameter dependenses will also be discussed.

Keywords: synchrotron maser instability, particle acceleration, PIC simulation

©2021. Japan Geoscience Union. All Right Reserved.

Trajectory analysis of energetic electrons in quasi-perpendicular shock structure

*Fumiko Otsuka[1], Shuichi Matsukiyo[1], Mitsuo Oka[2]

1. Earth System Science and Technology, 2. UC Berkeley

Electrons are accelerated to very high, non-thermal energies at Earth's quasi-perpendicular bow shock. The shock front reflects some of the incoming solar wind particles, resulting in its characteristic internal structure, i.e., foot and overshoot in the magnetic field on the upstream and downstream sides, respectively, separated by the shock ramp. In this study, we performed PIC simulations to study how electrons are accelerated in such a complex, internal structure of quasi-perpendicular shocks. We used an ion-to-electron mass ratio, 625, that is one order of magnitude larger than that of previous PIC simulations of quasi-perpendicular shocks. The shock parameters are as follows. The Alfven Mach number is 7, upstream plasma beta is 0.3, the shock angles are 70 and 80 degrees.

We have found three types of accelerated electrons: trappings by the thin structures of magnetic trough and electrostatic potential in the shock transition region, a single reflection at the intense overshoot magnetic field, and multiple reflections between the first and second overshoots in the downstream region. To further explore each acceleration mechanism, we investigate which electric field component contributes to the energy gain in each type of the electrons. We also analyze the electromagnetic and electrostatic fields in the shock transition region. The result will be applied to MMS observations.

Keywords: quasi-perpendicular shock, electron acceleration, earth's bow shock

©2021. Japan Geoscience Union. All Right Reserved.

Simulation of temperature anisotropy instability by a fluid model with non-local closure

*Taiki Jikei[1], Takanobu Amano[1]

1. The University of Tokyo

Physical descriptions of collisionless plasmas are given by either fluid models or kinetic models. Fluid models, the most popular one being magnetohydrodynamics (MHD), require relatively less computational resources, so they are suited for multi-dimensional macroscopic simulations. Kinetic models that solve the time evolution of distribution function in six-dimensional phase space are not only too resource-heavy but also make it difficult to understand macroscopic phenomena because of the infinite degree of freedom in velocity space. The common problem with most fluid models is that it does not take into account wave-particle interaction. Although wave-particle interaction is considered a microscopic phenomenon, it often affects the macroscopic dynamics of plasmas in the nonlinear phase through, for example, the relaxation of temperature anisotropy via kinetic instability.
There is a method called Landau closure, which approximates the highest order moment of the Vlasov equation (often the heat flux tensor) by a linear combination of lower-order moments (number density, fluid velocity, and pressure tensor) in the Fourier space. The original Landau closure gives an approximated plasma response for the Landau resonance. We have recently proposed an extension of the non-local closure, which takes into account cyclotron resonance as well. Our model can reproduce not only the cyclotron damping of transverse electromagnetic waves in warm collisionless plasmas but also temperature anisotropy instabilities.
In this study, we compare ion temperature anisotropy instabilities described by a fluid model with local closure (such as MHD with double adiabatic closure), a fluid model with non-local closure, and full kinetic models. Non-local closure that takes into account the cyclotron resonance effect is essential to reproduce electromagnetic cyclotron (EMIC) instability, in which the left-handed polarized wave becomes unstable under the condition that perpendicular pressure is higher than parallel pressure. In parallel firehose instability, on the other hand, the right-handed polarized mode becomes unstable when parallel pressure exceeds the perpendicular pressure. This instability can be described by conventional fluid models such as the Chew-Goldberger-Low (CGL) model. However, it is known that the cyclotron resonance has a critical impact on moderate beta plasmas. We find our non-local closure model can predict a qualitatively correct linear growth rate for both EMIC and firehose instabilities and reproduces the quasilinear isotropization. The isotropization is described by the correlation between off-diagonal pressure and transverse magnetic field. We will discuss possible improvements to the linear growth rate for better qualitative agreement with a fully kinetic model.

Keywords: Plasma simulation, Temperature anisotropy instability

©2021. Japan Geoscience Union. All Right Reserved.

[J] Oral | P (Space and Planetary Sciences)：P-EM Solar-Terrestrial Sciences, Space Electromagnetism & Space Environment

Fri. Jun 4, 2021 10:45 AM - 12:15 PM JST | Fri. Jun 4, 2021 1:45 AM - 3:15 AM UTC | Ch.06 Zoom Room 06

[P-EM15] Space Plasma Physics: Theory and Simulation

convener:Takanobu Amano(Department of Earth and Planetary Science, University of Tokyo), Yohei Miyake(Education Center on Computational Science and Engineering, Kobe University), Takayuki Umeda(Institute for Space-Earth Environmental Research, Nagoya University), Tadas Nakamura(Fukui Prefectural University), Chairperson:Shogo Isayama(Interdisciplinary Graduate School of Engineering Sciences, Kyushu University), Seiji Zenitani(Kobe University)

This session focuses on studies of space plasma physics via theoretical and numerical approaches. Papers on a wide variety of topics from natural phenomena to artificial plasma environment as well as theoretical and computational methodologies are welcome.

10:45 AM - 11:00 AM JST | 1:45 AM - 2:00 AM UTC

[PEM15-07] Neutral depletion and the density limit of the helicon plasma

*Shogo Isayama[1], Shunjiro Shinohara[2], Tohru Hada[1], Shih Hung Chen[3] (1.Interdisciplinary Graduate School of Engineering Sciences, Kyushu University, 2.Institute of Engineering, Tokyo University of Agriculture and Technology, 3.Department of Physics, National Central University)

11:00 AM - 11:15 AM JST | 2:00 AM - 2:15 AM UTC

[PEM15-08] Development of a magnetospheric global MHD simulation model for GEO-X mission

*Yosuke Matsumoto[1], Yoshizumi Miyoshi[2] (1.Graduate School of Science, Chiba University, 2.Institute for Space–Earth Environmental Research)

11:15 AM - 11:30 AM JST | 2:15 AM - 2:30 AM UTC

[PEM15-09] Full multiple Buneman-Boris solvers in nonrelativistic particle-in-cell simulation

*Seiji Zenitani[1], Tsunehiko N Kato[2] (1.Kobe University, 2.National Astronomical Observatory of Japan)

11:30 AM - 11:45 AM JST | 2:30 AM - 2:45 AM UTC

[PEM15-10] 2-D PIC simulations of surface charging processes on the nightside of Phobos

*Masaki Tanabe[1], Naoki Terada[1], Yohei Miyake[2], Hideyuki Usui[3] (1.Tohoku University planetary atomosphere, 2.Education Center on Computational Science and Engineering, Kobe University, 3.Graduate School of System Informatics, Kobe University)

11:45 AM - 12:00 PM JST | 2:45 AM - 3:00 AM UTC

[PEM15-11] Study on Electric Field Sensor Impedance in Magnetized Plasma by PIC Simulation.

*Ibuki Fukasawa[1], Hirotsugu Kojima[1], Yohei Miyake[2], Hideyuki Usui[3], Satoshi Kurita[1] (1.Research institute for sustainable humanosphere, Kyoto University, 2.Education Center on Computational Science and Engineering, Kobe University, 3.Graduate school of system informatics, Kobe University)

12:00 PM - 12:15 PM JST | 3:00 AM - 3:15 AM UTC

[PEM15-12] Spin-modulated components in Electric Field Detector (EFD) of Plasma Wave Experiment (PWE) aboard the Arase satellite

*Satoko Nakamura[1], Yoshizumi Miyoshi[1], Yasumasa Kasaba[2], Tomoko Nakagawa[3], Tomoaki Hori[1], Shoya Matsuda[4], Masafumi Shoji[1], Atsushi Kumamoto[7], Fuminori Tsuchiya[2], Ayako Matsuoka[5], Yoshiya Kasahara[6] (1.Institute for Space-Earth Environmental Research, Nagoya University, 2.Planetary Plasma and Atmospheric Research Center, Tohoku University, 3.Information and Communication Engineering, Tohoku Institute of Technology, 4.Institute of Space and Astronautical Science/Japan Aerospace Exploration Agency, 5.Data Analysis Center for Geomagnetism and Space Magnetism, Graduate School of

Science, Kyoto University, 6.Information Media Center, Kanazawa University, 7.Department of Geophysics, Graduate School of Science, Tohoku University)

Neutral depletion and the density limit of the helicon plasma

*Shogo Isayama[1], Shunjiro Shinohara[2], Tohru Hada[1], Shih Hung Chen[3]

1. Interdisciplinary Graduate School of Engineering Sciences, Kyushu University, 2. Institute of Engineering, Tokyo University of Agriculture and Technology, 3. Department of Physics, National Central University

Neutral depletion is a process in which neutral density decreases due to processes of ionization, neutral heating, and the drag (collision) by ions. In laboratory plasma sources, some experimental [1] and theoretical studies [2] suggest that the neutral depletion plays an important role in determining the plasma transport and the maximum plasma density. The neutral depletion caused by the collision with ions, is known to occur when the plasma pressure is comparable to the neutral gas pressure. If this is the case, the neutrals will naturally be cleared away from the region of high plasma pressure so that the net force balance is maintained. The plasma density consequently saturates to some density limit as the input power is increased. However, the relationship between the neutral depletion and the density limit is not well understood. Physical understanding of this saturation process is important to overcome the density limit of plasma sources.
In our study, we have constructed the self-consistent fluid model to investigate the time evolution of the helicon discharge with the neutral dynamics [3, 4]. In our simulation, the plasma density of ~10^{19} m^{-3} is generated, and the neutrals are depleted to ~10^{20} m^{-3} under a typical set of experimental parameters. When the input power is increased, the plasma density temporarily grows to ~10^{20} m^{-3}, but the neutrals are seriously depleted to ~10^{18} m^{-3}. In this situation, the electron temperature considerably increases since the power absorption (Joule heating) via Coulomb collision still occurs while the loss of energy by the ionization of neutrals becomes very small. As a result, the plasma density decreases to ~10^{19} m^{-3} due to the increase of outflow flux which is created by the strong pressure gradient. In this presentation, we discuss the effect of the neutral depletion and the density limit of the helicon plasma.

[1] S. Shinohara, D. Kuwahara, K. Yano and A. Fruchtman, Phys. Plasmas, **23** 122108 (2016).
[2] A. Fruchtman, J. Phys. D: Appl. Phys. **50**, 473002 (2017) (review paper).
[3] S. Isayama, S. Shinohara, T. Hada and S. H. Chen, Phys. Plasmas, **26** 023517 (2019).
[4] S. Isayama, S. Shinohara, T. Hada and S. H. Chen, Phys. Plasmas, **26** 053504 (2019).

Keywords: Helicon plasma, Neutral depletion, Density limit

©2021. Japan Geoscience Union. All Right Reserved.

Development of a magnetospheric global MHD simulation model for GEO-X mission

*Yosuke Matsumoto[1], Yoshizumi Miyoshi[2]

1. Graduate School of Science, Chiba University, 2. Institute for Space–Earth Environmental Research

In-situ observations by space crafts have revealed plasma dynamics in the terrestrial magnetosphere in response to the solar wind variations. They have provided ample opportunities to understand plasma kinetics in space and astrophysical phenomena where energy release and dissipation by the magnetic reconnection, collision-less shocks, and turbulence are of great interest. After many decades of the in-situ measurement era, GEO-X (Geospace x-ray imager) mission has been proposed by introducing the x-ray imaging technologies in astrophysics to visualize intermediate to global structures of the magnetosphere. The GEO-X project measures charge exchange emissions between oxygen ions in the solar wind and hydrogen atoms from the Earth's atmosphere (geocorona). The x-ray emission strength is strongly dependent on the solar wind oxygen ion distribution around the magnetosphere. Therefore it is crucial to model the global ion density distribution under various solar wind conditions to design the project and understand observational data.

We have developed a global MHD simulation model of the magnetosphere by using the public MHD code CANS+ (Matsumoto+19) as a successor to the GEMSIS-GM model (Matsumoto+10). CANS+ is a shock-capturing, high-resolution MHD code. It has been applied to accretion disks around the black hole (Igarashi+20) and astrophysical jet propagations (Ohmura+20;21). The code is hybrid-parallelized and effectively runs on massively parallel supercomputer systems. We adopted this code to develop the magnetospheric model. For this purpose, we modified the base equation by subtracting the potential field (dipole magnetic field) component from the magnetic field (Miyoshi+10). To maintain the magnetic field's solenoidal property, we introduced the projection method (Brackbill & Barnes80) in addition to the hyperbolic divergence cleaning method (Dedner+02) to manage substantial divergence errors around the inner boundary located at five Earth radii. In this talk, we report the current status of the development and the model's detailed algorithms.

Keywords: Global MHD simulation of the magnetosphere, Geocorona, GEO-X mission

©2021. Japan Geoscience Union. All Right Reserved.

Full multiple Buneman-Boris solvers in nonrelativistic particle-in-cell simulation

*Seiji Zenitani[1], Tsunehiko N Kato[2]

1. Kobe University, 2. National Astronomical Observatory of Japan

We propose a family of numerical solvers for the nonrelativistic Newton–Lorentz equation in particle-in-cell (PIC) simulations. In our recent contribution (Zenitani & Kato 2018), we have subsycled the Lorentz-force part of the two-step Boris solver. In this contribution, we propose to subcycle the entire acceleration part of the two-step Boris solver. We derive a single-step formula for arbitrary subcycle number n. The new solver provides a second-order accuracy, but provides n**2 times smaller error than the conventional two-step solver in the velocity space. We will evaluate key properties of the new solver such as the force-free property and the computational cost.

Keywords: Particle-in-Cell (PIC) simulation, Numerical scheme, Buneman-Boris method

©2021. Japan Geoscience Union. All Right Reserved.

2-D PIC simulations of surface charging processes on the nightside of Phobos

*Masaki Tanabe[1], Naoki Terada[1], Yohei Miyake[2], Hideyuki Usui[3]

1. Tohoku University planetary atomosphere, 2. Education Center on Computational Science and Engineering, Kobe University, 3. Graduate School of System Informatics, Kobe University

The solar wind, the stream of electrically charged particles that the Sun blows out into space, generates a complex plasma environment around an airless small-body and its surface charging. The nightside charging process is not well understood because of the wake formation and other kinetic plasma processes. It is considered that the wake formation process is basically explained by ambipolar diffusion. Previous studies investigated the nightside potential of the Martian moon Phobos using an analytical model based on a self-similar solution [Farrell et al., 2018]. They suggested that the potential of electric charges reaches about -200 V or more on the nightside of Phobos, which is potentially large enough to affect sensitive equipment. However, their analytic model cannot apply for the deep nightside region because of the lack of reproducing kinetic effects, such as ion acceleration and gyro motion. For this limitation, midnight surface potential has not been clarified.

To estimate the midnight surface charging, we utilize self-consistent 2-D particle-in-cell(PIC) simulations that can solve the plasma environment, including kinetic effects. For efficient calculations, we assume scaled-down parameters that are not the real-size radius of Phobos. First, we compare PIC results to two analytic models, the ambipolar diffusion model and the current balance model. A comparison between the self-similar model and PIC results indicates a large gap within several Debye lengths (λD) from the nightside surface. Although the current balance model shows almost the same tendency as PIC results, there are physical limitations that arisen from the simple assumption. This indicates that the current balance model can apply to the surface only with solar zenith angles of $< 98^{\circ}$.

Next, in order to evaluate the effect of scaled-down assumption, we calculate the surface potential for four cases of different body sizes (r = 50, 100, 150, and 200 λD). Based on the previous implication about the ion deflection into the wake region [Nakagawa, 2013], we performed a scaling analysis and revealed the general surface charging process at the nightside of the body. Charging processes are explained by three steps. The first step is the polar sheath formation. In the polar region, ions and electrons continuously impact and the surface gets charged by maintaining the current balance. This process generates an ion sheath near the surface. In the sheath region, stronger electric fields are generated under the assumption in a larger radius case. The second step is ion acceleration by this strong electric field. This step explains the process of ion penetration into the deep wake region. The final step is electron access into the deep nightside region. At the nightside surface near the void, more electrons can hit the surface together with deflected ions. This process leads to strong negative charging at the nightside in the larger radius case.

Our PIC simulations contribute to an understanding of the plasma environment on the nightside of Phobos. These implications can be useful for the Japanese future mission, Mars Moon eXploration (MMX).

Keywords: Phobos, Surface charging, particle-in-cell simulation

©2021. Japan Geoscience Union. All Right Reserved.

Study on Electric Field Sensor Impedance in Magnetized Plasma by PIC Simulation.

*Ibuki Fukasawa[1], Hirotsugu Kojima[1], Yohei Miyake[2], Hideyuki Usui[3], Satoshi Kurita[1]

1. Research institute for sustainable humanosphere, Kyoto University, 2. Education Center on Computational Science and Engineering, Kobe University, 3. Graduate school of system informatics, Kobe University

A dipole antenna has been commonly used as electric-field sensors to observe plasma waves in space plasma. To calibrate electric field measurements, we have been using the assumption that wavelengths are much longer than antenna lengths. However, in the next generation of satellite projects, it is possible that the wavelength is comparable to antenna length and it significantly affects the interpretation of the observation results. Better understanding of electric field sensor responses to short-wavelength plasma waves is required for evaluating intensities and phases of targeted electrostatic waves.

In this research, we simulated the antenna impedances of electric field sensors in magnetized plasmas over electromagnetic waves with short wavelengths. We conducted Particle-In-Cell(PIC) simulations with electric field sensors as inner boundaries. The results were evaluated considering the linear dispersion relations in magnetized plasmas.

According to the calculation results, when the wave number of the antenna resonance is large enough, it is estimated that the resonances are seen at the frequencies of the electron cyclotron harmonics, which are frequently observed in the magnetized plasmas. The results show in some situations that at near the UHR frequency, one or two peaks of the antenna impedance was observed. When the wave number is small enough, the resonances frequencies are shifted to slightly high. The simulation results suggest that the frequencies at where the resonances were seen are determined by the relationship between the length of the antenna and the dispersion relation of the surrounding plasma.

In the present paper, we discuss the characteristics of electric field sensors in plasmas over plasma waves with short wavelengths that are comparable with lengths of electric field sensors.

Keywords: antenna impedance, Particle in Cell, magnetized plasma

©2021. Japan Geoscience Union. All Right Reserved.

Spin-modulated components in Electric Field Detector (EFD) of Plasma Wave Experiment (PWE) aboard the Arase satellite

*Satoko Nakamura[1], Yoshizumi Miyoshi[1], Yasumasa Kasaba[2], Tomoko Nakagawa[3], Tomoaki Hori[1], Shoya Matsuda[4], Masafumi Shoji[1], Atsushi Kumamoto[7], Fuminori Tsuchiya[2], Ayako Matsuoka[5], Yoshiya Kasahara[6]

1. Institute for Space-Earth Environmental Research, Nagoya University, 2. Planetary Plasma and Atmospheric Research Center, Tohoku University, 3. Information and Communication Engineering, Tohoku Institute of Technology, 4. Institute of Space and Astronautical Science/Japan Aerospace Exploration Agency, 5. Data Analysis Center for Geomagnetism and Space Magnetism, Graduate School of Science, Kyoto University, 6. Information Media Center, Kanazawa University, 7. Department of Geophysics, Graduate School of Science, Tohoku University

The 8-Hz potential data measured by the electric field detector (EFD) on board the Arase satellite show spin-modulated distortions from sinusoidal signals due to spin motions. We analyze the influence of these distortions in measurements of DC field in the Earth's magnetosphere. The Arase satellite orbits the altitudes from the perigee of 460 km to the apogee of 32,000 with the inclination of 31˚. Statistical data analysis shows asymmetries and pulsations of the probe potential surrounding the spacecraft to the spin axis.
The distortions cause miscalculations of DC- or low frequency electric fields in both the amplitudes and directions.

Keywords: Arase satellite, Electric field

©2021. Japan Geoscience Union. All Right Reserved.

[J] Oral | P (Space and Planetary Sciences)：P-CG Complex & General

Fri. Jun 4, 2021 10:45 AM - 12:15 PM JST | Fri. Jun 4, 2021 1:45 AM - 3:15 AM UTC | Ch.04 Zoom Room 04

[P-CG19] Origin and evolution of materials in space

convener:Aki Takigawa(Department of Earth and Planetary Science, The University of Tokyo), Hitoshi Miura(Graduate School of Science, Department of Information and Basic Science, Nagoya City University), Takafumi Ootsubo(National Astronomical Observatory of Japan, National Institutes of Natural Sciences), Hideko Nomura(Division of Science, National Astronomical Observatory of Japan), Chairperson:Sota ARAKAWA(National Astronomical Observatory of Japan), Daiki Yamamoto(Institute of Space and Astronautical Science, Japan Aerospace eXploration Agency)

Recent progress of astronomical observations, laboratory experiments, solar-system exploration, and theoretical work have enabled us to attempt to understand the origin and evolution of materials (dust and gas) in space. It is thus important to link further planetary material science and astronomy for a comprehensive understanding of dust and gas in space and their role in the evolution of galaxies, stars, and planetary systems. Infrared observations with future large satellites/telescopes, such as TMT, are suitable for the study of gas and dust, and are expected to bring a new frontier of gas/dust study. In this session, based on the latest results on astronomical observations (ALMA, etc.), experiments, and theoretical studies on materials in space, we discuss the next steps in science for materials in space to maximize the outcome of the observations with the future satellites/telescopes.

10:45 AM - 11:00 AM JST | 1:45 AM - 2:00 AM UTC

[PCG19-01] Nucleation efficiency of dust approaching from microgravity experiments

★Invited Papers

*Yuki Kimura[1] (1.Institute of Low Temperature Science, Hokkaido University)

11:00 AM - 11:15 AM JST | 2:00 AM - 2:15 AM UTC

[PCG19-02] **Investigation of mid-infrared long-term variability of dusty AGB stars by using multi-epoch scan data of AKARI and WISE**

*Kengo Tachibana[1], Takashi Miyata[1], Takafumi Kamizuka[1], Ryou Ohsawa[1], Satoshi Takita[1], Akiharu Nakagawa[2], Yoshifusa Ita[3], Mizuho Uchiyama[4] (1.The University of Tokyo, 2.Kagoshima University, 3.Tohoku University, 4.ISAS/JAXA)

11:15 AM - 11:30 AM JST | 2:15 AM - 2:30 AM UTC

[PCG19-03] The birth environment and current location of the Solar system in the Galactic disc, using Milky-Way simulations and radioactive isotopes

*Yusuke Fujimoto[1] (1.Earth and Planets Laboratory, Carnegie Institution for Science)

11:30 AM - 11:45 AM JST | 2:30 AM - 2:45 AM UTC

[PCG19-04] Mutual Relation among the Circummultiple Structure, the Circumstellar Disk, and the Outflow: the Young Multiple IRAS 16293-2422 Source A Case

*Yoko Oya[1] (1.The University of Tokyo)

11:45 AM - 12:00 PM JST | 2:45 AM - 3:00 AM UTC

[PCG19-05] Investigating the impact of X-rays on the molecular abundances of envelopes and disks around low-mass protostars with ngVLA

*Shota Notsu[1], Nami Sakai[1], Hideko Nomura[2], Ewine F. van Dishoeck[3], Catherine Walsh[4], Arthur D. Bosman[5] (1.Star and Planet Formation Laboratory, RIKEN Cluster for Pioneering Research, 2.Division of Science, National Astronomical Observatory of Japan, 3.Leiden Observatory, Faculty of Science, Leiden University, 4.School of Physics and Astronomy, University of Leeds, 5.Department of Astronomy, University of Michigan)

12:00 PM - 12:15 PM JST | 3:00 AM - 3:15 AM UTC

[PCG19-06] Hot Salty Disks around Massive Protostars: A New Connection from Star-Formation Observation to Meteoritics?

★Invited Papers

*Kei Tanaka[1,2] (1.University of Colorado Boulder, 2.National Astronomical Observatory of Japan)

Nucleation efficiency of dust approaching from microgravity experiments

*Yuki Kimura[1]

1. Institute of Low Temperature Science, Hokkaido University

The aim of this study is understanding the formation process of dust particles via homogeneous nucleation in the gas outflow from an evolved star. We have proceeded an international project named DUST (Determining Unknown yet Significant Traits) and investigated three important properties (the surface free energy, sticking probability, and infrared spectrum) of nanoparticles as dust analogues by experimentally reproducing the nucleation processes of cosmic dust in a microgravity environment. To obtain the three properties, the generated dust analogues in a microgravity environment must be analyzed in the laboratory. At the microgravity level of an aircraft (0.01 –0.1 G), the convection caused by the difference in density cannot be suppressed sufficiently and, therefore, the physical constants cannot be determined precisely. Because of these reasons, we use overseas rockets, which can provide a high-quality microgravity environment of ~10^{-4} G and can recover the produced samples.
The international project was started in 2017 with a cooperation of JAXA/ISAS. First experiment was conducted by launching MASER 14, a sounding rocket of the Swedish Space Corporation, from Esrange Space Center in June 24, 2019 with the supports by German Aerospace Center and Prof. J. Blum of Technische Universität Braunschweig. In addition, the sounding rockets Black Brant IX 343 and 365 were launched from the White Sands Missile Range in October 2019 and September 2020, respectively, and performed microgravity experiments in collaboration with Dr. J. A. Nuth III of NASA/GSFC. Including non-recovery sounding rocket experiment in Japan, we have conducted five flights and a total of 20 nucleation experiments under microgravity environment with strong supports of Prof. Y. Inatomi, JAXA/ISAS. Seven kinds of materials were used so far: iron, tungsten oxide, alumina, silica, magnesium silicate, iron silicate, and titanium carbide.
Originally designed two different kinds of experimental devices (interferometer and IR spectrometer) were mounted on the rocket. The nucleation chamber (about 500 cc) with an evaporation material was prepared in each device. After reaching microgravity, the evaporation source was heated to generate high-temperature gas. The gas cooled down and nucleation occurred homogeneously to form dust analogues. These processes were observed in-situ.
In these experiments, several results have been obtained that differ from the commonly accepted theory. For example, homogeneous nucleation from the gas phase requires much larger supersaturation than expected. One of the major hindrances for nucleation was found to be dimer formation. For example, the nucleation of iron occurred only when the size of critical nucleus was smaller than dimer. The sticking probability was very small, only about 0.002% for iron [1]. It was also found that the final stable crystal was not nucleated directly from the gas phase, but via a liquid phase. In case of large supersaturation, the nucleation temperature is lower. Then, it seems that the solid phase is directly nucleated. However, in fact, a two-step nucleation process is widely observed: droplets nucleate at first, and crystals nucleate in the supercooled droplets. This two-step nucleation easily explained by considering the depression of melting point of a nanoparticle. We reported that this two-step nucleation process is important for understanding the formation process of alumina dust [2]. In addition, the same nucleation process has been observed in various materials in ground-based experiments. Here, in addition to these results, we will present the latest findings concerning nucleation efficiency of titanium carbide, silica and silicate dust based on the nucleation experiments, which are currently being analyzed.
[1] Y. Kimura, et al., *Science Advances*, 3 (2017) e1601992.

©2021. Japan Geoscience Union. All Right Reserved.

[2] S. Ishizuka, Y. Kimura et al., *Nature Communications*, 9 (2018) 3820.

Keywords: nucleation, dust, microgravity, nanoparticle

©2021. Japan Geoscience Union. All Right Reserved.

Investigation of mid-infrared long-term variability of dusty AGB stars by using multi-epoch scan data of AKARI and WISE

*Kengo Tachibana[1], Takashi Miyata[1], Takafumi Kamizuka[1], Ryou Ohsawa[1], Satoshi Takita[1], Akiharu Nakagawa[2], Yoshifusa Ita[3], Mizuho Uchiyama[4]

1. The University of Tokyo, 2. Kagoshima University, 3. Tohoku University, 4. ISAS/JAXA

“How has the Universe evolved to today’s material-rich form?” This is one of the fundamental questions in modern astronomy. Dust is a key component of the life cycle of heavy elements in the Universe, but its origin is not well understood yet. Recent studies indicate that asymptotic giant branch (AGB) stars are one of the main suppliers of dust. Those stars show very strong pulsations of the photosphere, and the stellar pulsation is thought to control formation of dust. However the details have not been revealed yet. Especially observational studies of dusty AGB stars are insufficient so far, because they are relatively faint in optical wavelengths due to the heavy circumstellar dust extinction. Infrared observations of dusty AGB stars, especially mid-infrared monitoring observations, are strongly desired.

In this study, we analyzed multi-epoch scan data of AKARI and WISE and produced long-term mid-infrared light curves of AGB stars. Known oxygen-rich (O-rich) AGB stars and OH/IR stars in our Galaxy were selected for this analysis. One technical issue was the difference of photometric systems of AKARI and WISE. We carefully estimated fluxes at 18 microns by using WISE W3 (12 microns) and W4 (22 microns) data and compared with AKARI L18W (18 microns) data. Finally, we obtained 18-micron light curves with at least 4 epochs of 169 O-rich AGB stars and 35 OH/IR stars. Its time coverage is more than 1300 days. Those are the longest and largest mid-infrared light curves of AGB stars.

Based on these light curves, as well as variability data at other wavelengths, we determined the variability amplitude at 18 microns for 169 O-rich AGB stars and 28 OH/IR stars.

We found that 1) there is a strong correlation between the 18-micron amplitude and W3-W4 color, and 2) this relationship is independent of the variability period and their pulsation mode. Therefore, this correlation indicates that stars with stronger variability show stronger dust mass loss, and the variability amplitude is the most important parameter for the dust supply mechanism.

Furthermore, we constructed models in which only the stellar temperature and luminosity were varied, to identify the stellar parameter changes that significantly affect the variability amplitude. The radiative transfer code DUSTY was used for this calculation. As a result the variability amplitude at 18 microns is not dependent on variation of stellar temperature, but strongly affected by the rate of luminosity change. Therefore, the correlation between the 18-micron amplitude and the infrared color suggests that the stellar luminosity change is the most important factor for the dust formation around AGB stars.

There are no detailed theoretical models to explain this correlation. A possible explanation is that AGB stars with larger variation of luminosity have larger region where the temperature decreases during the pulsation, and the larger size of the temperature-decreasing region causes more amount of dust formation.

For the next step, we have a plan of long-term mid-infrared monitoring of dusty AGB stars using the TAO (The University of Tokyo Atacama Observatory) 6.5-m telescope. Since MIMIZUKU, the mid-infrared

©2021. Japan Geoscience Union. All Right Reserved.

instrument for the TAO 6.5-m telescope, has high-precision monitor observation capability, we can obtain mid-infrared light curves with sufficient number of epochs. In addition, we will be able to obtain time variation data of mid-infrared spectra including silicate and alumina features. They may be helpful information to understand the detailed process of the dust formation. TAO will start science operations in 2022.

Keywords: dust, AGB star, mid-infrared

©2021. Japan Geoscience Union. All Right Reserved.

The birth environment and current location of the Solar system in the Galactic disc, using Milky-Way simulations and radioactive isotopes

*Yusuke Fujimoto[1]

1. Earth and Planets Laboratory, Carnegie Institution for Science

Formation mechanisms of the Solar system and exoplanetary systems that harbor life have been one of the hottest topics. The birth environment of the early Solar system 4.6 Gyr ago has been investigated using meteorites, which contain the oldest solids formed in the Solar protoplanetary disc. Materials from near-Earth asteroids by recent sample-return projects such as JAXA's Hayabusa-2 and NASA's OSIRIS-REx will give us more information about the Solar birth environment. At the same time, many nearby exoplanets have been discovered so far, and after the first observation of a protoplanetary disc of the exoplanetary system HL Tau, many observational and theoretical works have attempted to understand planet formation in the Solar neighborhood. However, we need to be aware of the fundamental issue of a 4.6 Gyr gap between the Solar system formation and the present-day planet formation. It is that the Solar birth environment could be quite different from the current local environment. For example, if the Solar system formed closer to the center of the Galaxy than it is today, the primordial gas of the Solar system was easily abundant in metals because it was a place where star formation and subsequent supernova (SN) explosions, which enriched the interstellar medium (ISM), were active (then the metals played an important role in such as a radiative cooling and chemical reaction of the ISM). Moreover, the morphology of the Galaxy should have changed for 4.6 Gyr. Therefore, it should be noted that the formation process of the Solar system discussed using meteorites and asteroids can be different in space and time from the planet formation in the vicinity of the present-day Solar system. To bridge the gap, I am investigating the evolution of the Galaxy for 4.6 Gyr and trajectories of the Solar system and other planetary systems from their birthplace to the current positions within the evolving Galactic disc.
In this presentation, I will show chemo-hydrodynamical simulations of the entire Milky Way galaxy, including ejections of short-lived radioisotopes (SLRs) such as 26Al and 60Fe from stellar winds and SNe. To understand the birthplace of the early Solar system and its environment in the Galactic disc, we measure the distribution of SLR ratios over star particles in the simulated galaxy and compare them with the initial abundance ratios of SLRs in the early Solar system observed in meteorites. We find that the Solar initial abundance ratios are well in the normal range and that the SLRs are abundant in newborn stars because star formation is correlated on galactic scales so that ejecta preferentially enrich atomic gas that will subsequently be accreted onto existing giant molecular clouds or will form new ones. We conclude that in terms of 26Al and 60Fe the birth environment of the Solar system is not atypical in the Galaxy (Fujimoto, Krumholz & Tachibana 2018, MNRAS, 480, 4025).
In addition, to understand the Solar local interstellar environment in the present-day Galaxy, we perform another galaxy simulation that represents the current state of the Milky Way, and compare it with astronomical and geological observations: galactic-scale distributions of 26Al seen in all-sky gamma-ray maps and detection of live 60Fe in deep-sea archives and Antarctic snow. We find that the current location of the Solar system in the Galactic disc is near the edges of spiral arms and lie inside kpc-scale bubbles that are created by multiple generations of star formation in the arm (Fujimoto, Krumholz, Inutsuka, Boss & Nittler 2020, MNRAS, 498, 5532).

Keywords: Galactic disc, meteorites, gamma-rays, hydrodynamics, massive stars, short-lived radioactive isotope

©2021. Japan Geoscience Union. All Right Reserved.

©2021. Japan Geoscience Union. All Right Reserved.

Mutual Relation among the Circummultiple Structure, the Circumstellar Disk, and the Outflow: the Young Multiple IRAS 16293-2422 Source A Case

*Yoko Oya[1]

1. The University of Tokyo

In these years, high capabilities in observational researches have opened new avenues in the star formation study. Various substructures in the vicinity of young stellar objects have recently been revealed, and their roles in the planet formation process are being discussed. As well, their origins are of great interesting. Especially, the formation of disk/envelope systems is closely related with the outflow launching via the angular momentum of the gas.
In this presentation, we report our ALMA observations for the Class 0 protostellar source IRAS 16293-2422. This source is a binary consisting of Source A and Source B, where Source A itself is a multiple source. We detected the substructure in the 1-mm and 3-mm dust continuum emission, tracing the protostars A1 and A2 in Source A. As well, we revealed the circummultiple structure surrounding Source A and the circumstellar disk of the protostar A1. Their kinematic structures traced by the $C^{17}O$ and H_2CS lines are reproduced by simple physical models.
We also delineated an outflow structure near its origin point in the SO line. The northwest-southeast outflow shows a rotating motion. Comparing the specific angular momenta of the outflow and the disk/envelope structures, we found that the outflow can extract the angular momentum from the circumstellar disk. Understanding their mutual relation will provide us with an essential clue to the disk formation process in this young multiple source.

Keywords: Interstellar Medium, Low-mass Protostar, Protostellar Disk, Multiple

©2021. Japan Geoscience Union. All Right Reserved.

Investigating the impact of X-rays on the molecular abundances of envelopes and disks around low-mass protostars with ngVLA

*Shota Notsu[1], Nami Sakai[1], Hideko Nomura[2], Ewine F. van Dishoeck[3], Catherine Walsh[4], Arthur D. Bosman[5]

1. Star and Planet Formation Laboratory, RIKEN Cluster for Pioneering Research, 2. Division of Science, National Astronomical Observatory of Japan, 3. Leiden Observatory, Faculty of Science, Leiden University, 4. School of Physics and Astronomy, University of Leeds, 5. Department of Astronomy, University of Michigan

Water has been used to study dynamical properties of star-forming regions, and it is also one of key molecules in chemical evolutions. Water destruction by X-rays has been proposed to explain the low water gas fractional abundances in the inner warm envelopes and disks around several low-mass protostars (e.g., Stauber et al. 2006), but the detailed chemistry, including the nature of alternative oxygen carriers, is not yet understood.
Recently, we computed the chemical composition of low-mass protostar envelopes using a gas-grain chemical reaction network (e.g., Walsh et al. 2015), with various X-ray luminosities of the central protostars. We aimed to understand the impact of X-rays on the composition of low-mass protostar envelopes, focusing specifically on water and related oxygen bearing species. According to our calculations, X- ray induced chemistry strongly affects the abundances of water and related species such as O, O_2. In addition, the fractional abundances of HCO^+ and CH_3OH, which have been considered to be tracers of the water snowline (e.g., van’ t Hoff et al. 2018a,b), significantly increase/decrease within the water snowline, respectively, as the X-ray fluxes become larger.
Moreover, the fractional abundances of some other dominant molecules, such as NH_3, are also affected by strong X-ray fields, especially within their own snowlines. Future molecular line observations with ngVLA will be expected to constrain the inner gas abundances of CH_3OH, HCO^+, and NH_3, creating a more complete picture of the oxygen chemistry and opening a window into the independent nitrogen chemistry.

Keywords: astrochemistry, protostars, protoplanetary disks, snowline, ngVLA, molecules

©2021. Japan Geoscience Union. All Right Reserved.

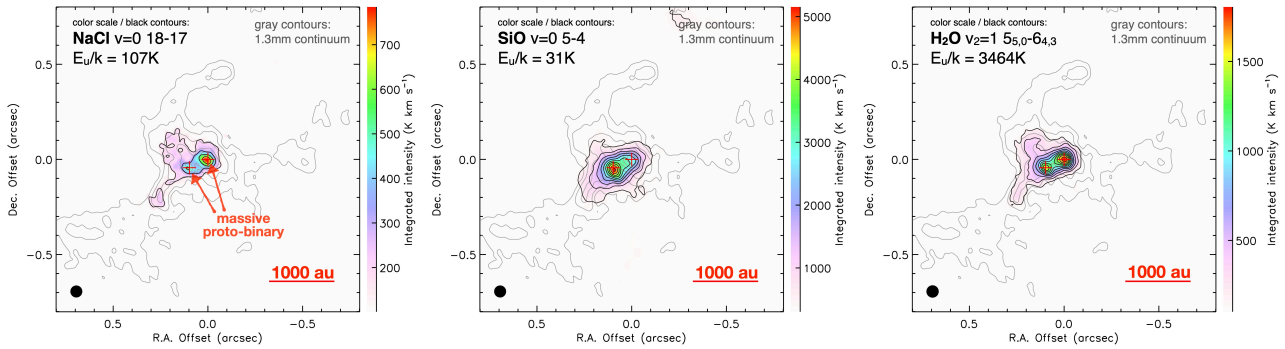
Hot Salty Disks around Massive Protostars: A New Connection from Star-Formation Observation to Meteoritics?

*Kei Tanaka[1,2]

1. University of Colorado Boulder, 2. National Astronomical Observatory of Japan

Massive stars (>10 solar mass, >10,000 solar luminosity) play significant roles in controlling the dynamical and chemical evolution of the interstellar medium in galaxies by intense radiation, stellar winds, and supernovae. Even at the formation stage, the radiation of massive protostars is already powerful, heating the surrounding gas (>1000 au) to over 100 K and producing a variety of chemical species, including complex organic molecules. Such regions/phases of massive protostars, so-called the “hot cores,” have been studied as an important test bed of astrochemistry. Using the Atacama Large Millimeter/submillimeter Array (ALMA), we conduct high-resolution observations toward the massive proto-binary system IRAS 16547-4247, and investigate the innermost structures down to the scale of 100 au. We detect emission lines of sodium chloride (NaCl), silicon compounds (SiO, SiS), and vibrationally-excited water (H_2O v_2=1) associated with the twin protostellar disks (Tanaka et al. 2020, ApJL; see the figure). Gaseous refractory molecules are rarely found in star-forming regions, and this is the second detection of salt in protostellar systems. These newly-detected molecular lines exclusively probe the individual disks at the innermost region of 100 au, while typical hot-core molecules trace the envelope of the 1000 au scale (e.g., complex organic molecules). The presence of the gaseous refractory species, which are products of dust destruction, and the highly-excited water vapor with $E_u/k > 3000$ K indicates the hot and dynamic nature of massive protostellar disks. The “hot disk” is the new key to understanding massive star formation, and also has excellent potential for future research on metallic elements in star-forming regions. In particular, we expect that the observations of hot-disk lines will provide new insights into the origin of the oldest meteoritic inclusions, i.e., CAIs and chondrules, in the proto-solar nebula.

Keywords: star formation, ALMA observations, refractory species



©2021. Japan Geoscience Union. All Right Reserved.

[J] Oral | P (Space and Planetary Sciences)：P-CG Complex & General

Fri. Jun 4, 2021 1:45 PM - 3:15 PM JST | Fri. Jun 4, 2021 4:45 AM - 6:15 AM UTC | Ch.04 Zoom Room 04

[P-CG19] Origin and evolution of materials in space

convener:Aki Takigawa(Department of Earth and Planetary Science, The University of Tokyo), Hitoshi Miura(Graduate School of Science, Department of Information and Basic Science, Nagoya City University), Takafumi Ootsubo(National Astronomical Observatory of Japan, National Institutes of Natural Sciences), Hideko Nomura(Division of Science, National Astronomical Observatory of Japan), Chairperson:Yoko Oya(The University of Tokyo), Shota Notsu(Star and Planet Formation Laboratory, RIKEN Cluster for Pioneering Research)

Recent progress of astronomical observations, laboratory experiments, solar-system exploration, and theoretical work have enabled us to attempt to understand the origin and evolution of materials (dust and gas) in space. It is thus important to link further planetary material science and astronomy for a comprehensive understanding of dust and gas in space and their role in the evolution of galaxies, stars, and planetary systems. Infrared observations with future large satellites/telescopes, such as TMT, are suitable for the study of gas and dust, and are expected to bring a new frontier of gas/dust study. In this session, based on the latest results on astronomical observations (ALMA, etc.), experiments, and theoretical studies on materials in space, we discuss the next steps in science for materials in space to maximize the outcome of the observations with the future satellites/telescopes.

1:45 PM - 2:00 PM JST | 4:45 AM - 5:00 AM UTC

[PCG19-07] Measurability of CO isotopologue ratio in PPDs with ALMA

*Tomohiro Yoshida[1], Hideko Nomura[2], Kenji Furuya[2], Takashi Tsukagoshi[2] (1.Faculty of Science, Kyoto University, 2.Division of Science, National Astronomical Observatory of Japan)

2:00 PM - 2:15 PM JST | 5:00 AM - 5:15 AM UTC

[PCG19-08] Oxygen isotope exchange kinetics between amorphous silicate dust and CO gas: Implication for oxygen isotope evolution in the early Solar System

*Daiki Yamamoto[1,2], Shogo Tachibana[1,2], Noriyuki Kawasaki[3], Michiru Kamibayashi[2], Hisayoshi Yurimoto[3] (1.Institute of Space and Astronautical Science, Japan Aerospace eXploration Agency , 2.UTokyo Organization for Planetary Space Science, The University of Tokyo, 3.Department of Natural History Sciences, Hokkaido University)

2:15 PM - 2:30 PM JST | 5:15 AM - 5:30 AM UTC

[PCG19-09] On the crystallinity of silicate dust in evolving protoplanetary disks due to magnetically driven disk winds

*Sota ARAKAWA[1], Yuji Matsumoto[2], Mitsuhiko Honda[3] (1.National Astronomical Observatory of Japan, 2.Institute of Astronomy and Astrophysics, Academia Sinica, 3.Okayama University of Science)

2:30 PM - 2:45 PM JST | 5:30 AM - 5:45 AM UTC

[PCG19-10] **Crystallization of amorphous Mg-Fe silicate dust: Implications for thermal processes in the early Solar System**

*Ryosuke Sakurai[1], Kodai Kobayashi[2], Daiki Yamamoto[3], Aki Takigawa[1], Shogo Tachibana[3,4] (1.Department of Earth and Planetary Science, UTokyo, 2.Department of Natural History Sciences, Hokkaido Univ., 3.Department of Solar System Sciences, ISAS, JAXA, 4.UTokyo Organization for Planetary and Space Science (UTOPS))

2:45 PM - 3:00 PM JST | 5:45 AM - 6:00 AM UTC

[PCG19-11] A novel laboratory approach to studying photochemistry of liquid organic interfaces

★Invited Papers

*Tetsuya Hama[1], Naoki Numadate[1] (1.Komaba Institute for Science, The University of Tokyo)

3:00 PM - 3:15 PM JST | 6:00 AM - 6:15 AM UTC

[PCG19-12] Assessing the potential of biogenic gases as exoplanet biosignatures

★Invited Papers

*Yuka Fujii[1], Yu Komatsu[2], Alexis Gilbert[3], Sebastian Danielache[4], Mayuko Nakagawa[3] (1.National Astronomical Observatory of Japan, 2.Astrobiology Center, 3.Tokyo Institute of Technology, 4.Sophia University)

Measurability of CO isotopologue ratio in PPDs with ALMA

*Tomohiro Yoshida[1], Hideko Nomura[2], Kenji Furuya[2], Takashi Tsukagoshi[2]

1. Faculty of Science, Kyoto University, 2. Division of Science, National Astronomical Observatory of Japan

Detailed measurement of materials such as meteorites, solar wind, and water on the Earth reveals oxygen isotope anomaly in the solar system. Since the three-oxygen isotope diagram of the materials in the solar system falls along the one-slope line, it is presumed that mass-independent isotope fractionation played a key role. As the fractionation mechanism, isotope selective photodissociation of carbon monoxide (CO) in the presolar cloud and/or presolar nebula has been theoretically suggested. However, observational evidence remains insufficient.

In recent years, thanks to the progress in the astronomical instrument such as Atacama Large Millimeter/Sub-millimeter Array (ALMA), detailed observations of nearby protoplanetary disks have become possible. If the oxygen isotope anomaly observed in the present solar system was established in the presolar cloud or presolar nebula, the similar mechanism would be at work in protoplanetary disks, which we can observe with ALMA.

We discuss a method for directly measuring the CO isotopologue ratio in protoplanetary disks. CO gas in protoplanetary disks is generally observed as emission lines in radio. It is difficult to estimate the total amount of the CO gas because the line centers are optically thick for $^{12}C^{16}O$ and $^{13}C^{16}O$. Even so, the line wings can be optically thin, and it is possible to estimate the isotopologue column density ratio in principle.

First, we calculated the physical and chemical structure of a typical protoplanetary disk with chemical reaction networks. Second, we executed the one-dimensional radiative transfer simulation. Then, we simulate the ALMA observations of the protoplanetary disk. As a result, the CO isotopologue ratio can be constrained using the line wings with the observations in high spatial (~15 au) and velocity (~0.1 km/s) resolution if the disk is edge-on.

Keywords: protoplanetary disk, astrochemistry, oxygen isotope anomaly

©2021. Japan Geoscience Union. All Right Reserved.

Oxygen isotope exchange kinetics between amorphous silicate dust and CO gas: Implication for oxygen isotope evolution in the early Solar System

*Daiki Yamamoto[1,2], Shogo Tachibana[1,2], Noriyuki Kawasaki[3], Michiru Kamibayashi[2], Hisayoshi Yurimoto[3]

1. Institute of Space and Astronautical Science, Japan Aerospace eXploration Agency , 2. UTokyo Organization for Planetary Space Science, The University of Tokyo, 3. Department of Natural History Sciences, Hokkaido University

The oxygen isotopic compositions of primitive Solar System materials exhibit mass-independent variation as a result of O isotope exchange between different O isotope reservoirs, such as primitive solid materials and disk gas in the early Solar System (e.g., Yurimoto and Kuramoto, 2004; McKeegan et al., 2011). Oxygen-16-rich CO and -poor H_2O gas would be produced through self-shielding of CO gas in the Sun’s parent molecular cloud or in the early Solar System (Yurimoto and Kuramoto, 2004; Lyons and Young, 2005). The O isotope exchange between three major oxygen isotope reservoirs (primitive solid materials, CO, and C H_2O) would thus be responsible for the O isotope variation within extraterrestrial materials.

Amorphous silicate dust is recognized as primitive solid materials in the early Solar System (e.g., Nuth et al., 2005). Oxygen isotopic exchange kinetics between amorphous silicates and H_2O gas has been experimentally investigated in our previous studies (Yamamoto et al., 2018, 2020), and the gas-phase O isotope exchange kinetics between CO and H_2O was discussed by Alexander (2004). However, O isotope exchange between amorphous silicates and CO gas has not yet been examined. In this study, we performed O isotope exchange experiments between amorphous silicate with forsterite (Mg_2SiO_4) stoichiometry (hereafter amorphous forsterite) and low-pressure CO gas.

The O isotope exchange experiments between amorphous forsterite dust (80 nm in average diameter) (Yamamoto et al., 2018) and ^{18}O-enriched CO gas (>95 atom% ^{18}O) were performed at 803, 853, and 883 K under low-pressure CO gas condition (P_{CO} = 0.3 Pa) for 3–177 hours using a gold-mirror vacuum furnace (Yamamoto et al., 2018, 2020) equipped with a gas flow system. The gas species in the furnace were monitored by a quadrupole mass spectrometer (QMS). Oxygen isotope measurements were conducted by secondary ion mass spectrometry (Cameca ims-1280HR) using the analytical procedure described in Yamamoto et al. (2020).

The heated samples are expected to remain amorphous under the heating conditions (Yamamoto and Tachibana, 2018), and their oxygen isotopic compositions [$^{18}O/(^{18}O + {}^{16}O)$] ($f^{18}O$) increased almost linearly with time. The QMS analysis showed that the partial pressure of $H_2{}^{18}O$ was more than three orders of magnitude lower than P_{CO} (< ~1 ×10^{-4} Pa). The $f^{18}O$ of heated samples was much larger than that expected for the O isotope exchange between amorphous forsterite and $H_2{}^{18}O$ in the furnace (< ~1 ×10^{-4} Pa) (Yamamoto et al., 2018). We thus conclude that O isotope exchange occurred between amorphous forsterite and $C^{18}O$. The linear increase of $f^{18}O$ with time cannot be explained by a three-dimensional spherical diffusion equation (Yamamoto et al., 2018; 2020), suggesting that O isotope exchange reaction is governed by gas dissolution into the amorphous structure and isotope exchange process between dissolved CO and structural oxygen atoms. The reaction timescale between amorphous forsterite and CO is about 1–2 order of magnitude smaller than that with H_2O at the same T-P condition (Yamamoto et al., 2018). Despite the slow O isotope exchange rate of amorphous forsterite with CO, the O isotope

©2021. Japan Geoscience Union. All Right Reserved.

exchange timescale for ~0.1 μm-sized amorphous forsterite dust with CO is 4–5 orders of magnitude shorter than the timescale of gas-phase CO-H_2O isotopic equilibrium at 803–883 K and $P_{CO} = P_{H2O}$ ~ 0.1 Pa in the protosolar disk (Alexander, 2004). This implies that amorphous forsterite dust would accelerate CO-H_2O isotopic equilibrium through isotope exchange of amorphous forsterite with both CO and H_2O, and the gas-phase isotope equilibrium timescale would be determined by the timescale of O isotope exchange between amorphous forsterite dust and CO (e.g., ~1 yr at 800–900 K). In other words, the oxygen isotope equilibrium in the protosolar disk is governed by the rate of oxygen isotope exchange between amorphous dust and CO in the mid- to low-temperature region (~800–1200 K).

Keywords: amorphous silicate, oxygen, isotope exchange, kinetics, protosolar disk

©2021. Japan Geoscience Union. All Right Reserved.

On the crystallinity of silicate dust in evolving protoplanetary disks due to magnetically driven disk winds

*Sota ARAKAWA[1], Yuji Matsumoto[2], Mitsuhiko Honda[3]

1. National Astronomical Observatory of Japan, 2. Institute of Astronomy and Astrophysics, Academia Sinica, 3. Okayama University of Science

Understanding the process of radial mixing in protoplanetary disks is of great importance in the context of star and planet formation in the solar and extrasolar systems. In particular, the radial distribution of crystalline silicate dust particles in disks is the key to understanding the material mixing process from astronomical observations (e.g., Honda et al. 2006; Maaskant et al. 2015). In protoplanetary disks, dust particles are radially transported by three processes, namely, advection, diffusion, and the radial drift of dust particles. The effects of these processes in viscous accretion disks are studied so far (e.g., Gail 2001; Pavlyuchenkov & Dullemond 2007).
Recent observations of protoplanetary disks by ALMA revealed that the disk structure (e.g., rings, gaps, and spirals) formed in the early stage of disk evolution. The magnetically driven disk wind (e.g., Suzuki et al. 2010) is one of the candidates to create observed structures, and the effects of disk winds on the evolution of dust and gas are investigated in previous studies (e.g., Takahashi & Muto 2018).
Here we calculate the radial distribution of crystalline silicate dust particles in evolving protoplanetary disks due to magnetically driven disk winds. We found that the radial distribution of the crystallinity strongly depends on the timescales of viscous evolution, the radial drift of dust particles, and wind mass loss, as the structure of gas and dust also depends on these timescales (e.g., Takahashi & Muto 2018). The crystallinity of dust particles may relate to the structure of protoplanetary disks.

Keywords: Protoplanetary disk, Dust, Crystallinity, Magnetically driven disk wind

©2021. Japan Geoscience Union. All Right Reserved.

Crystallization of amorphous Mg-Fe silicate dust: Implications for thermal processes in the early Solar System

*Ryosuke Sakurai[1], Kodai Kobayashi[2], Daiki Yamamoto[3], Aki Takigawa[1], Shogo Tachibana[3,4]

1. Department of Earth and Planetary Science, UTokyo, 2. Department of Natural History Sciences, Hokkaido Univ., 3. Department of Solar System Sciences, ISAS, JAXA, 4. UTokyo Organization for Planetary and Space Science (UTOPS)

The least metamorphosed chondrites contain amorphous silicate with a wide range of FeO content in their matrices (e.g., Vollmer et al., 2020). Infrared astronomical observation has shown that amorphous silicate is present as a major dust component in protoplanetary disks. The observation also indicates that the thermodynamically unstable amorphous silicate dust crystallized in the disks due to annealing. The presence of amorphous silicate in the least metamorphosed chondrites suggests that there was amorphous silicate dust that avoided thermal processes in the Sun’s protoplanetary disk and within chondrite parent bodies. The amorphous silicate should therefore be used to constrain quantitatively the dust thermal evolution in the Sun’s protoplanetary disk and the temperature-time condition of chondrite parent bodies if the crystallization kinetics of amorphous silicate is known. The crystallization kinetics of forsterite-like amorphous silicate has been well investigated by Yamamoto and Tachibana (2018), but that of FeO-bearing amorphous silicate, commonly found in pristine chondrites, has not been fully understood. In this study we conducted crystallization experiments of FeO-bearing amorphous silicate following Yamamoto and Tachibana (2018).

Amorphous Mg-Fe silicate nanoparticles with a composition similar to the solar abundance (Mg : Fe : Si ~ 1 : 1 : 1) were synthesized with a radio-frequency induction thermal plasma method at Nisshin Engineering Co. Ltd. The synthesized particles with the average diameter of ~70 nm mainly consisted of olivine-like amorphous silicate (Mg#=Mg/(Mg+Fe)~51 at.%, (Mg+Fe)/Si~1.9), but also included a contaminant of amorphous silicate powder with SiO2-rich composition and a tiny amount of crystalline olivine (Mg#~51 at.%) and metallic iron. The synthesized particles were heated in a vacuum at 580–630˚C for 0.5–162 h. The starting material and the heated samples were analyzed by FE-SEM-EDS, FE-EPMA, XRD, FT-IR, and Raman spectroscopy to determine their morphology, chemical compositions, microstructures, and crystallization degrees.

The XRD analysis shows that olivine crystals with the same composition as the main part of the starting material within an error range crystallized from the amorphous silicate through heating. It also shows that the metallic iron disappeared in the first 30 minutes of heating, probably incorporated into the amorphous silicate as FeO. The broad peaks attriubuted to amorphous material at wavelength of 10 and 18 μm in the infrared absorption spectrum decreased, and sharp peaks attributed to olivine crystals appeared in the 8–13 μm wavelength region as the heating duration increased. The SiO2-rich contaminants, most likely the product synthesized prior to the starting material of this study, did not crystalize under the present experimental condition, and its presence in the sample can be ignored in the following discussion. The crystallization degrees of samples heated for various durations were obtained based on the absorption features in the wavelength range of 8–13 μm. The timescales of crystallization of the synthesized amorphous silicate are estimated to be ~1.1, ~3.6, and ~15 h at 580, 610, and 630˚C, respectively, by applying the Johnson-Mehl-Avrami equation. These timescales are shorter than those for crystallization of amorphous forsterite (Yamamoto and Tachibana, 2018). The activation energy for crystallization of amorphous olivine was estimated to be 330.5±10.7 kJ/mol, which is smaller than that for amorphous forsterite in vacuum (414 kJ/mol; Yamamoto and Tachibana, 2018). These results imply that

©2021. Japan Geoscience Union. All Right Reserved.

crystallization is promoted by increasing FeO concentration in the amorphous silicate.

The time-temperature-transition diagram for crystallization of amorphous forsterite and olivine (Mg#~51 at.%) indicates that the timescale required for crystallization of amorphous Mg-Fe silicate is 3–4 orders of magnitude shorter than amorphous forsterite in the early Solar System and within a planetesimal. This lowers the upper limit of temperature for FeO-bearing amorphous silicate to preserve its amorphous nature within 1 million years in protoplanetary disks and planetesimals would be ~600 K, which is ~100 K lower than for amorphous FeO-free silicates.

Keywords: amorphous silicate, crystallization, kinetics, early Solar System, protoplanetary disk, meteorite parent body

©2021. Japan Geoscience Union. All Right Reserved.

A novel laboratory approach to studying photochemistry of liquid organic interfaces

*Tetsuya Hama[1], Naoki Numadate[1]

1. Komaba Institute for Science, The University of Tokyo

Surface and interfacial photochemistry of organic molecules have become increasingly of interest in the field of terrestrial atmospheric chemistry. In the Earth, surface-active organics such as fatty acids are ubiquitous, which cover the surfaces of oceans, lakes, cloud and fog droplets, and atmospheric aerosol particles. Rossignol et al. recently reported that, although fatty acids are believed to be photochemically inert in the actinic region, complex volatile organic compounds are produced during illumination of an air-water interface coated solely with a monolayer of nonanoic acid [$CH_3(CH_2)_7COOH$] [1, 2]. The authors suggest that, when nonanoic acid is present in coatings at a water-air interface, it weakly absorbs ultraviolet light at wavelengths present in sunlight at Earth’ s surface and yields hydroxyl (OH) and nonyl radicals.

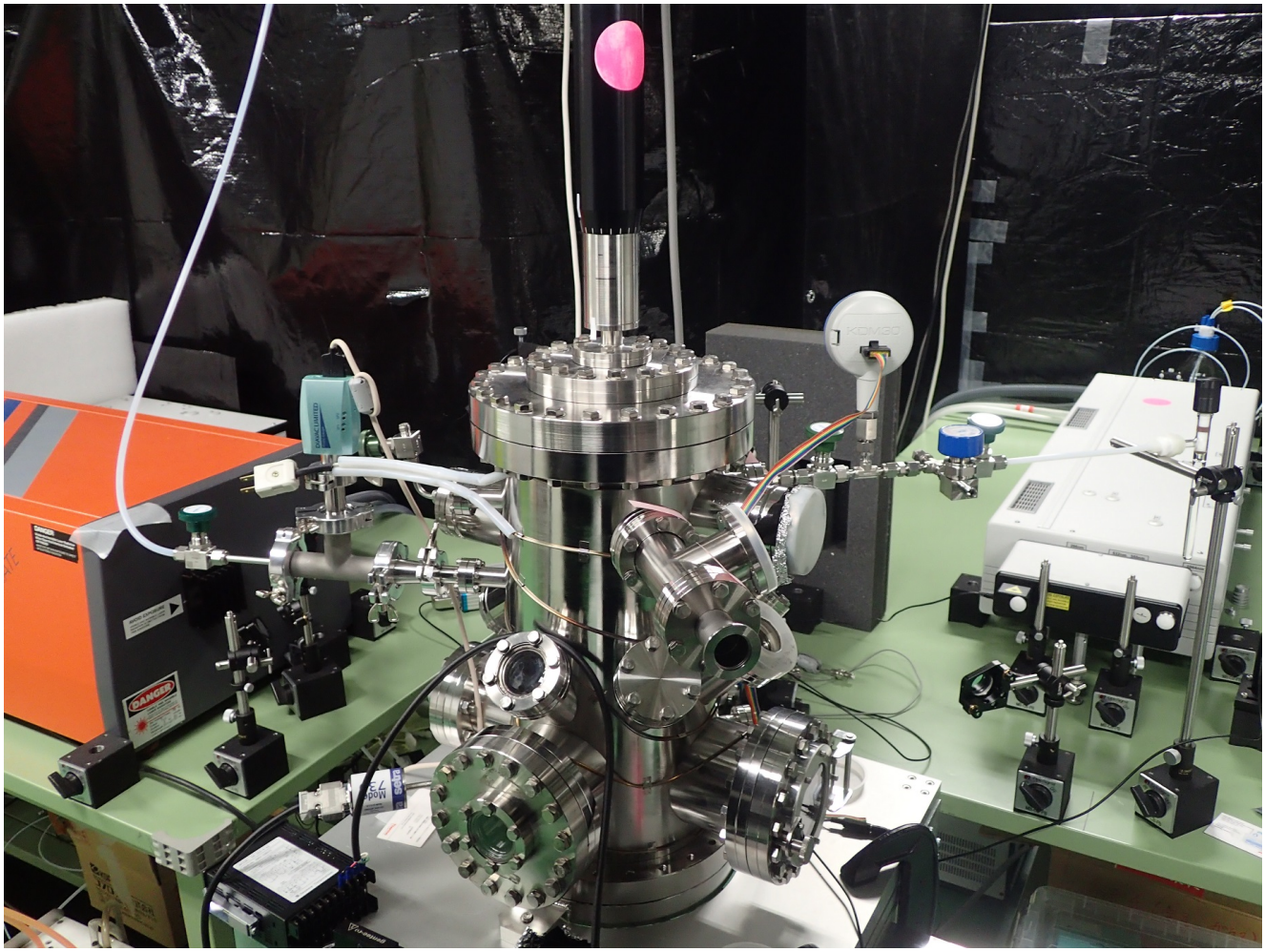
This previous study emphasizes the requirement to understand the elementary processes of photochemistry occurring on liquid organic interfaces. However, direct detection of primary photoproducts represented by radicals is technically challenging. Conventional methods suitable for detection of radicals such as resonance enhanced multi photon ionization (REMPI) generally require ultrahigh-vacuum conditions (10^{-4} Pa for REMPI), whereas liquid organic compounds intrinsically have high vapor pressures (1 Pa for nonanoic acid), which prevents us from performing direct detection of radicals.

We are currently working on developing a new type of experimental setup to study the interface photochemistry of liquid organic with high vapor pressure. Laser-induced fluorescence is employed to detect primary photoproducts desorbing from the liquid organic interface. In this talk, we show preliminary results that direct photolysis of liquid nonanoic acid [$CH_3(CH_2)_7COOH$] leads to the formation of OH radicals. The present technique can be also useful to study the chemistry in planetary atmospheres, as well as high pressure environments in protoplanetary disks.

Figure caption. Photographs of the new experimental setup for studying photochemistry of liquid organic interfaces.

[1] Rossignol et al., Science 353, 699 (2016).
[2] Vaida. Science 353, 650 (2016).

©2021. Japan Geoscience Union. All Right Reserved.



©2021. Japan Geoscience Union. All Right Reserved.

Assessing the potential of biogenic gases as exoplanet biosignatures

*Yuka Fujii[1], Yu Komatsu[2], Alexis Gilbert[3], Sebastian Danielache[4], Mayuko Nakagawa[3]

1. National Astronomical Observatory of Japan, 2. Astrobiology Center, 3. Tokyo Institute of Technology, 4. Sophia University

Searching for the signs of life on exoplanets is one of the major goals of modern astronomy. The proposed approaches such as transit spectroscopy, high-contrast imaging, and high-resolution spectroscopy will eventually allow us to access the spectra of a few nearby temperate terrestrial planets at the broad range of wavelengths from ultraviolet to mid-infrared ranges. A key to finding life on exoplanets is to detect the spectral features of biogenic gases. Earth’ s biosphere emits various gases including O2, CH4, and C5H8. In this talk, we discuss their detectability and the challenges in identifying the biological origin. Accumulation of a molecule in an atmosphere given the surface flux depends on the atmospheric properties (thickness, composition) and the boundary conditions including the ultraviolet spectrum. We examine the stability of O2 and CH4 as a function of surface flux under various conditions using a photochemical model (atmos; e.g. Kasting et al. 1984, Pavlov et al., 2001) and discuss the conditions in which their spectral features become detectable and how to distinguish from non-biological scenarios. We also qualitatively assess the stability of more complex volatile organic compounds and study their spectral fingerprints.

Keywords: Exoplanets, Earth-like planets, Planetary atmospheres

©2021. Japan Geoscience Union. All Right Reserved.

[J] Oral | A (Atmospheric and Hydrospheric Sciences)：A-AS Atmospheric Sciences, Meteorology & Atmospheric Environment

Fri. Jun 4, 2021 9:00 AM - 10:30 AM JST | Fri. Jun 4, 2021 12:00 AM - 1:30 AM UTC | Ch.07 Zoom Room 07

[A-AS07] Weather, Climate, and Environmental Science Studies using High-Performance Computing

convener:Hisashi Yashiro(National Institute for Environmental Studies), Takuya Kawabata(Meteorological Research Institute), Tomoki Miyakawa(Atmosphere and Ocean Research Institute, The University of Tokyo), Koji Terasaki(RIKEN Center for Computational Science), Chairperson:Hisashi Yashiro(National Institute for Environmental Studies)

High-performance computing(HPC) is one of the fundamental research tools supporting Today's meteorology, climate change research, and environmental sciences. Cutting-edge simulation studies have been carried out using supercomputers such as the Earth Simulator and the K computer. These big computers have contributed to an expansion of the range of feasible simulations, including higher resolution, wider computational domains, more ensemble sizes, and the use of more sophisticated physical processes. Supercomputers have also made significant progress in data science, with research into data assimilation techniques using high-frequency high-density observations and the combined use of simulation and Artificial Intelligence (AI). The supercomputer Fugaku is scheduled to begin full operation in fiscal 2021, and it is expected to produce many new research results with its world-beating computing performance.
This session calls for research topics in the atmospheric and hydrospheric studies using supercomputers, such as numerical modeling, big-data analysis, data assimilation, and AI. The participants can share future perspectives on atmospheric science research using HPC and the challenges to be addressed.

9:00 AM - 9:15 AM JST | 12:00 AM - 12:15 AM UTC

[AAS07-01] Atmospheric large eddy simulation with DALES on Fugaku

★Invited Papers

*Fredrik Jansson[1], Martin Janssens[1,2], Jisk Attema[3], Johanna Grönqvist, Franziska Glassmeier[1], Yousuke Sato[4], Masaki Satoh[5], Pier Siebesma[1] (1.Delft University of Technology, 2.Wageningen University & Research, 3.Netherlands eScience Center, 4.Faculty of Science, Hokkaido University, 5.Atmosphere and Ocean Research Institute, The University of Tokyo)

9:15 AM - 9:30 AM JST | 12:15 AM - 12:30 AM UTC

[AAS07-02] Big Data Assimilation: Real-time Demonstration Experiment of 30-second-update Forecasting in Tokyo in August 2020

*Takemasa Miyoshi[1], Takumi Honda[1], Arata Amemiya[1], Shigenori Otsuka[1], Yasumitsu Maejima[1], James David Taylor[1], Hirofumi Tomita[1], Seiya Nishizawa[1], Kenta Sueki[1], Tsuyoshi Yamaura[1], Yutaka Ishikawa[1], Shinsuke Satoh[2], Tomoo Ushio[3], Kana Koike[4], Erika Hoshi[4], Kengo Nakajima[5] (1.RIKEN, 2.NICT, 3.Osaka University, 4.MTI Ltd., 5.University of Tokyo)

9:30 AM - 9:45 AM JST | 12:30 AM - 12:45 AM UTC

[AAS07-03] 1000-member 18-km-mesh SCALE-LETKF experiment with conventional observations in summer 2020

*Arata Amemiya[1], Takemasa Miyoshi[1] (1.RIKEN Center for Computational Science)

9:45 AM - 10:00 AM JST | 12:45 AM - 1:00 AM UTC

[AAS07-04] Progress in Tropical Weather and Climate Prediction with Global Storm-Resolving Models

★Invited Papers

*Falko Judt[1] (1.National Center for Atmospheric Research)

10:00 AM - 10:15 AM JST | 1:00 AM - 1:15 AM UTC

[AAS07-05] **A 1000-member 14-km mesh global ensemble experiment to target typhoon FAXAI (2019)**

*Yohei Yamada[1], Masuo Nakano[1], Tomoki Miyakawa[2], Chihiro Kodama[1], Ying-Wen Chen[2], Hisashi Yashiro[3], Tomoe Nasuno[1], Masaki Satoh[2] (1.Japan Agency for Marine-Earth Science and Technology, 2.Atmosphere and Ocean Research Institute, The University of Tokyo, 3.National Institute for Environmental Studies)

10:15 AM - 10:30 AM JST | 1:15 AM - 1:30 AM UTC

[AAS07-06] A 1024-Member Data Assimilation and Forecast Experiment with NICAM-LETKF Using Fugaku: A Heavy Rainfall Event in Kyushu in July 2020

*Koji Terasaki[1], Takemasa Miyoshi[1] (1.RIKEN Center for Computational Science)

Atmospheric large eddy simulation with DALES on Fugaku

*Fredrik Jansson[1], Martin Janssens[1,2], Jisk Attema[3], Johanna Grönqvist, Franziska Glassmeier[1], Yousuke Sato[4], Masaki Satoh[5], Pier Siebesma[1]

1. Delft University of Technology, 2. Wageningen University & Research, 3. Netherlands eScience Center, 4. Faculty of Science, Hokkaido University, 5. Atmosphere and Ocean Research Institute, The University of Tokyo

DALES is an atmospheric large-eddy simulation program used for research and education. It simulates atmospheric processes including turbulence, convection, clouds, precipitation, and radiative effects. DALES stands for Dutch Atmospheric Large Eddy Simulator.

We have ported DALES to the Fugaku supercomputer. We report on our experiences with porting the code and running the model on the new A64FX architecture. Using DALES, we investigate the organization of shallow cumulus clouds, and how it depends on the atmospheric conditions and simulation parameters such as domain size and resolution. The high performance of Fugaku and fast inter-node communication makes it possible to simulate large domains or to run simulations at very high resolution.

Keywords: large eddy simulation, Fugaku, shallow cumulus, cloud organization

©2021. Japan Geoscience Union. All Right Reserved.

Big Data Assimilation: Real-time Demonstration Experiment of 30-second-update Forecasting in Tokyo in August 2020

*Takemasa Miyoshi[1], Takumi Honda[1], Arata Amemiya[1], Shigenori Otsuka[1], Yasumitsu Maejima[1], James David Taylor[1], Hirofumi Tomita[1], Seiya Nishizawa[1], Kenta Sueki[1], Tsuyoshi Yamaura[1], Yutaka Ishikawa[1], Shinsuke Satoh[2], Tomoo Ushio[3], Kana Koike[4], Erika Hoshi[4], Kengo Nakajima[5]

1. RIKEN, 2. NICT, 3. Osaka University, 4. MTI Ltd., 5. University of Tokyo

The Japan’s Big Data Assimilation (BDA) project started in October 2013 and ended its 5.5-year period in March 2019. Here, we developed a novel numerical weather prediction (NWP) system at 100-m resolution updated every 30 seconds for precise prediction of individual convective clouds. This system was designed to fully take advantage of the phased array weather radar (PAWR) which observes reflectivity and Doppler velocity at 30-second frequency for 100 elevation angles at 100-m range resolution. By the end of the 5.5-year project period, we achieved less than 30-second computational time using the Japan’s flagship K computer, whose 10-petaflops performance was ranked #1 in the TOP500 list in 2011, for past cases with all input data such as boundary conditions and observation data being ready to use. The direct follow-on project started in April 2019 under the Japan Science and Technology Agency (JST) AIP (Advanced Intelligence Project) Acceleration Research. We continued the development to achieve real-time operations of this novel 30-second-update NWP system for demonstration at the time of the Tokyo 2020 Olympic and Paralympic games. The games were postponed, but the project achieved real-time demonstration of the 30-second-update NWP system at 500-m resolution using a powerful supercomputer called Oakforest-PACS operated jointly by the Tsukuba University and the University of Tokyo. The additional developments include parameter tuning for more accurate prediction and complete workflow to prepare all input data in real time, i.e., fast data transfer from the novel dual-polarization PAWR called MP-PAWR in Saitama University, and real-time nested-domain forecasts at 18-km, 6-km, and 1.5-km to provide lateral boundary conditions for the innermost 500-m-mesh domain. A real-time test was performed during July 31 and August 7, 2020 and resulted in the actual lead time of more than 27 minutes for 30-minute prediction with very few exceptions of extended delay. Past case experiments showed that this system could capture rapid intensification and decays of convective rains that occurred in the order of less than 10 minutes, while the JMA nowcasting did not predict the rapid changes by its design. This presentation will summarize the real-time demonstration during August 25 and September 7 when Tokyo 2020 Paralympic games were supposed to take place.

Keywords: Numerical Weather Prediction, Data Assimilation, Phased Array Weather Radar, Big Data, Real Time, Demonstration Experiment

©2021. Japan Geoscience Union. All Right Reserved.

1000-member 18-km-mesh SCALE-LETKF experiment with conventional observations in summer 2020

*Arata Amemiya[1], Takemasa Miyoshi[1]

1. RIKEN Center for Computational Science

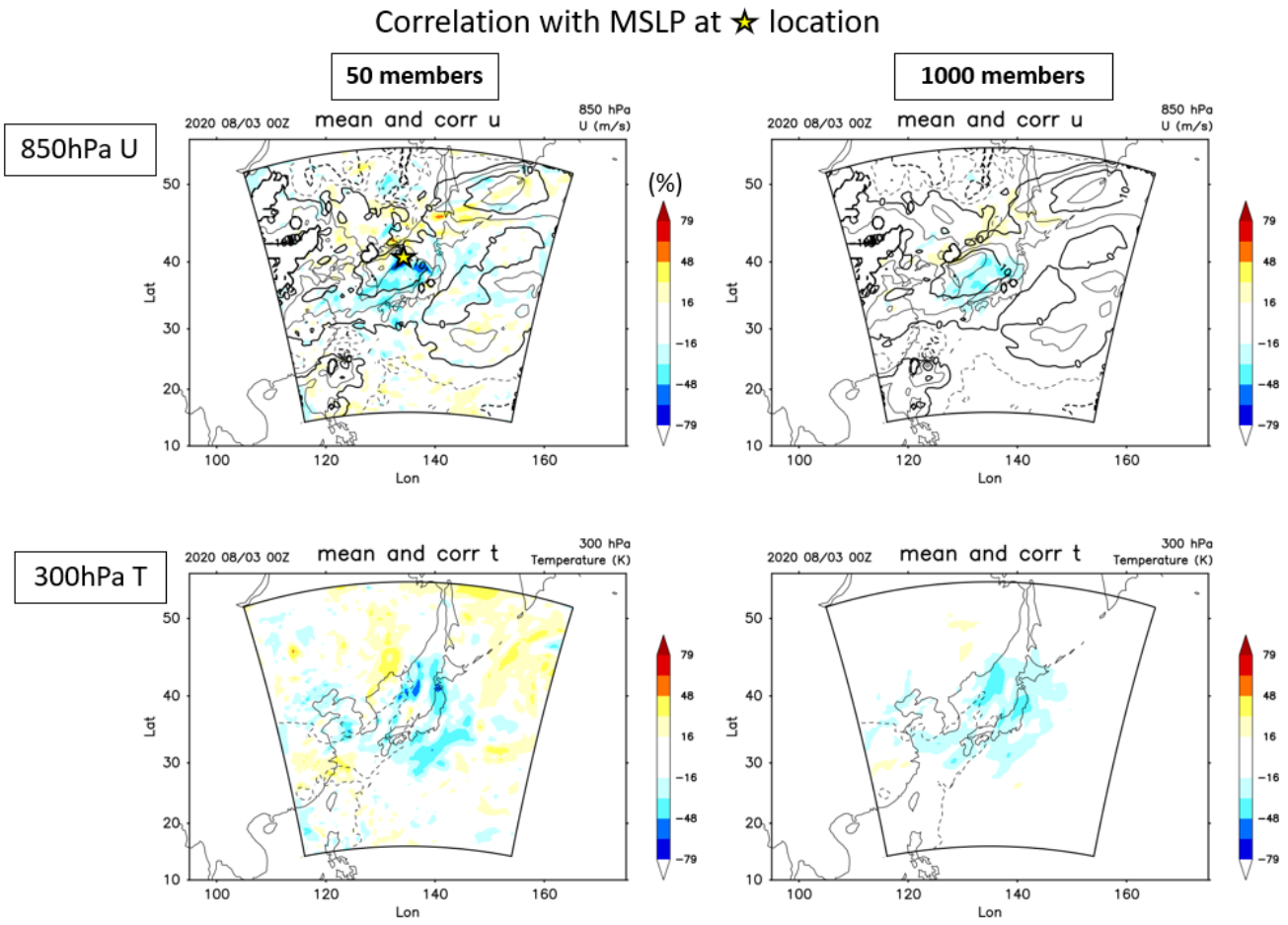
Advances of high-performance computing technologies have enabled us to study ensemble simulations with unprecedently large ensemble sizes. For example, a recent study performed a 1000-member convective-scale ensemble forecast experiment to examine the forecast error properties (Necker et al. 2020). Ensemble-based data assimilation such as the local ensemble transform Kalman filter (LETKF; Hunt et al. 2007) with a large ensemble size is also an important topic to study. The K computer played an important role in early works of such large ensemble data assimilation (Miyoshi et al. 2014; 2015, Kondo and Miyoshi 2016). More recently, 1024-member data assimilation with the 3.5-km resolution global model (Nonhydrostatic Icosahedral Atmospheric Model; NICAM) was performed on the supercomputer Fugaku (Yashiro et al. 2020). The previous studies demonstrated the advantage of a large ensemble in idealized experiments, but it is still unclear if the advantage is also true in the real situation, where imperfections are included in the observation and model, and in representing the observation errors. This study examines the advantage of a large ensemble of 1000 members in the LETKF in a real case with conventional observations in the Japan region in summer 2020.

We used the SCALE-LETKF system (Lien et al. 2017) composed of the 18-km resolution Scalable Computing for Advanced Library and Environment-Regional Model (SCALE-RM, Nishizawa et al. 2015) and the LETKF. The conventional observation dataset known as PREPBUFR used in NCEP Global Data Assimilation System (GDAS) is assimilated every 6 hours. For the lateral and surface boundary conditions, NCEP Global Forecasting System (GFS) data is used. In this study, we run the SCALE-LETKF with ensemble sizes up to 1000. The covariance inflation and localization parameters are fixed regardless of the ensemble size, so that we focus on the qualitative impact on the analysis. For each experiment with a different ensemble size, the model is initialized at 0000 UTC 1 August 2020, with NCEP GDAS field superposed with bandpass-filtered random temperature perturbations. The analyses at 0000 UTC 3 August are investigated.
The spatial and cross-variable correlation signals become clearer as the ensemble size increases (Figure 1). The analysis RMSE relative to the observations is significantly reduced for most variables and vertical levels with larger ensemble sizes. The first-guess RMSE is reduced as well, implying that the analysis field of the previous step is improved in a physically consistent manner.
However, we observed some undesirable behaviors as well. The analysis RMSE relative to surface pressure observations increased with larger ensemble sizes, suggesting that the LETKF fail to alleviate the surface pressure bias. An additional experiment with 1000-member LETKF without vertical localization did not show improvement of the analysis for most variables, on the contrary to the theoretical expectation. The possible cause of this behavior is the systematic model and observation biases. The treatment of those biases would be important to achieve the full potential of the LETKF with a large ensemble size. The results of further experiments will be discussed in the presentation.

Acknowledgement: The computation for this study was performed using Oakforest-PACS through HPCI System Research Project (Project ID: hp150019).

©2021. Japan Geoscience Union. All Right Reserved.

Keywords: Data Assimilation, Numerical weather forecasting, Big data



©2021. Japan Geoscience Union. All Right Reserved.

Progress in Tropical Weather and Climate Prediction with Global Storm-Resolving Models

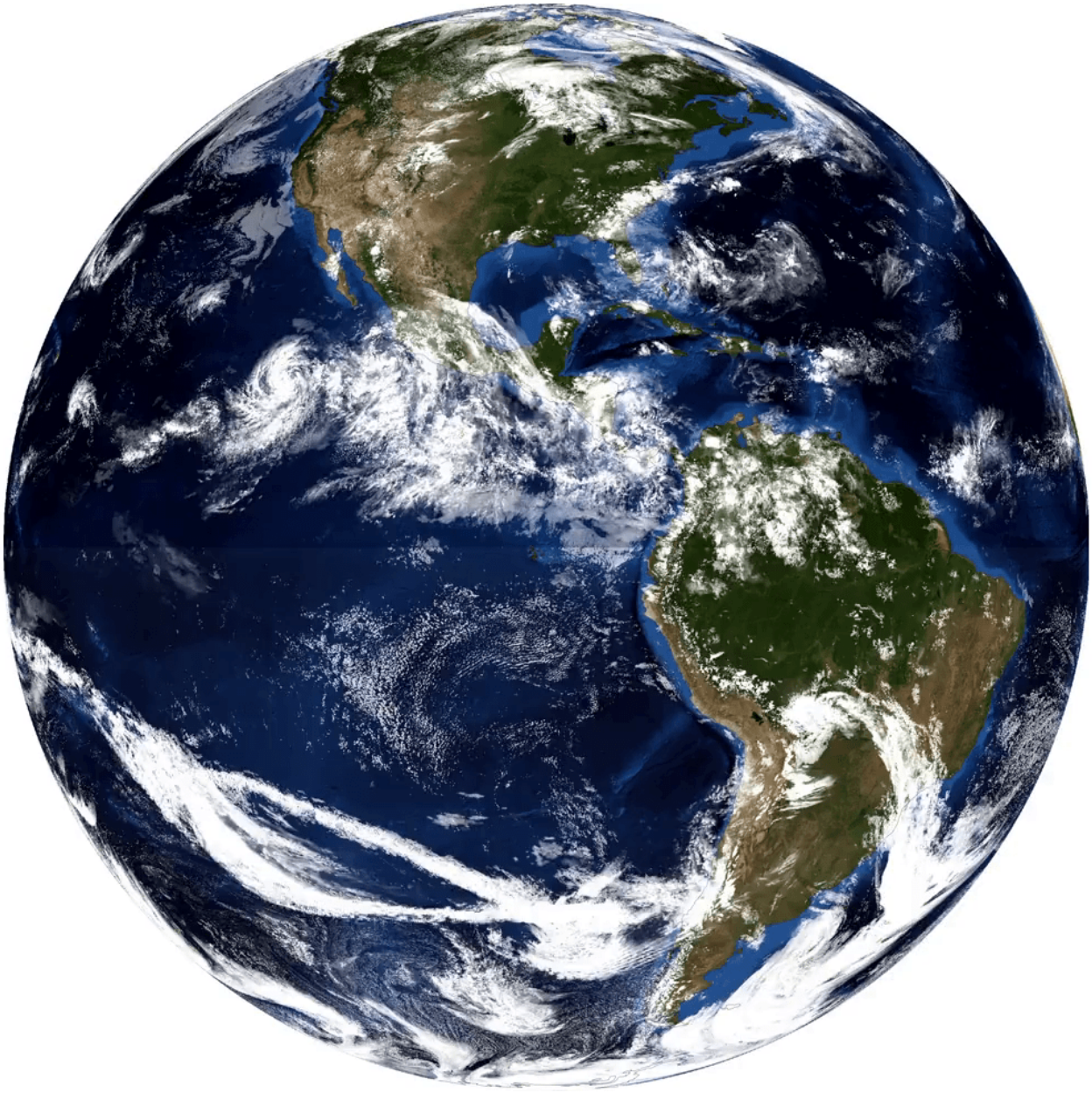
*Falko Judt[1]

1. National Center for Atmospheric Research

Despite advances in many areas, current-generation global weather and climate models struggle with simulating the tropical atmosphere. For example, current models have difficulties with capturing the extreme winds of tropical cyclones, and they are unable to properly simulate equatorial waves and tropical rainfall variability. It has long been hypothesized that these shortcomings are the consequence of inadequate model resolution and the need to parameterize deep convection. Unfortunately, a thorough assessment of this hypothesis has not been possible because of the tremendous computing resources required to run and analyze global models with horizontal resolution < 5 km (i.e., the resolution that is necessary to explicitly simulate convective storms). Yet as computing power has been increasing, limitations are easing, and it is now possible to produce global storm-resolving simulations and assess their benefits. Here we demonstrate that global storm-resolving models are indeed a game changer in simulating the tropical atmosphere. For example, global storm-resolving models capture the intensity of tropical cyclones, and they produce realistic equatorial waves. Nonetheless, a model intercomparison indicates that global storm-resolving models have unique biases, and further improvement is necessary to unleash the models' full potential.

Keywords: Tropical meteorology, Tropical cyclones, Global storm-resolving model, High-resolution model, Global cloud-resolving model

©2021. Japan Geoscience Union. All Right Reserved.



©2021. Japan Geoscience Union. All Right Reserved.

A 1000-member 14-km mesh global ensemble experiment to target typhoon FAXAI (2019)

*Yohei Yamada[1], Masuo Nakano[1], Tomoki Miyakawa[2], Chihiro Kodama[1], Ying-Wen Chen[2], Hisashi Yashiro[3], Tomoe Nasuno[1], Masaki Satoh[2]

1. Japan Agency for Marine-Earth Science and Technology, 2. Atmosphere and Ocean Research Institute, The University of Tokyo, 3. National Institute for Environmental Studies

A thousand members ensemble experiment on the Supercomputer Fugaku was conducted by a nonhydrostatic icosahedral atmospheric model (NICAM) with a 14-km mesh, which was targeted to Typhoon Faxai of which the genesis time is 18UTC 4 September 2019. Ensemble simulations started from different initial dates from 26 August 2019 to 4 September (10 days). NICAM-LETKF JAXA Research Analysis (NEXRA) was used as the initial atmospheric condition of the ensemble experiment. The NEXRA provided 100 perturbed atmospheric conditions for each initial date. The total number of ensemble members was 1000 in the present study. The sea surface temperature was calculated by a slab ocean model, which was nudged to NOAA OI SST V2.1. The ensemble experiments ran for about 30 days. We simply regarded a simulated typhoon generated from 00UTC 3 September to 18UTC 7 September within 140E-170E as a Faxai-like typhoon.
In the ensemble experiment, 391 members reproduced the Faxai-like typhoon. Focusing on impact of lead time on the reproducibility of the genesis time and intensity, fewer number of ensemble members with the short lead time reproduced the Faxai-like typhoon than that of members with the long lead time. This is a possible reason why the short lead time is insufficient for a vortex being intensified, which may become a typhoon. As for tracks of the Faxai-like typhoon, these tracks differed between members of which even experiments started from the same initial date. The variations were more prominent in the long lead time experiments than those of the short lead time experiments.

Keywords: Large ensamble simulation, high resolution global nonhydrostatic model, Typhoon Faxai 2019

©2021. Japan Geoscience Union. All Right Reserved.

A 1024-Member Data Assimilation and Forecast Experiment with NICAM-LETKF Using Fugaku: A Heavy Rainfall Event in Kyushu in July 2020

*Koji Terasaki[1], Takemasa Miyoshi[1]

1. RIKEN Center for Computational Science

Recently, the occurrence of severe heavy rainfall has been increasing. More accurate predictions are essential to reduce the risk of disasters caused by heavy rainfall. In July 2020, heavy rainfall caused severe disasters in Japan. At that time, heavy rainfall occurred across a wide area of western and eastern Japan, and total precipitation amounts reached more than half of the annual average in some parts of Kyushu from 3 to 14 July 2020. This study aims to investigate the predictability and cause of this heavy rainfall event. We use a global numerical weather prediction system composed of the NICAM (non-hydrostatic icosahedral atmospheric model: Satoh et al. 2014) and the LETKF (local ensemble transform Kalman filter: Hunt et al. 2007; Miyoshi and Yamane 2007). The NICAM-LETKF has been optimized for Fugaku to perform at high resolution and large ensemble sizes.
We performed ensemble data assimilation and forecast experiments using the NICAM-LETKF with 1,024 members and 56-km-horizontal resolution using 2,048 nodes of Fugaku. The results show that the large ensemble size contributes to significantly more accurate analysis compared with a typical ensemble size of less than 100. In addition, 1,024-member ensemble forecasts capture the probability of heavy rainfall in Kyushu about 5 days before it happens, although 10-day-lead forecast is difficult. Ensemble-based lag-correlation analyses with the large ensemble size show very small sampling errors in the correlation patterns and show that the moist air inflow in the lower troposphere and the location of a trough in the upper troposphere play an essential role in causing the heavy rainfall in Kyushu.

Keywords: Data assimilation, Fugaku, Large ensembles, Predictability

©2021. Japan Geoscience Union. All Right Reserved.

[J] Oral | A (Atmospheric and Hydrospheric Sciences)：A-AS Atmospheric Sciences, Meteorology & Atmospheric Environment

Fri. Jun 4, 2021 10:45 AM - 12:15 PM JST | Fri. Jun 4, 2021 1:45 AM - 3:15 AM UTC | Ch.07 Zoom Room 07

[A-AS07] Weather, Climate, and Environmental Science Studies using High-Performance Computing

convener:Hisashi Yashiro(National Institute for Environmental Studies), Takuya Kawabata(Meteorological Research Institute), Tomoki Miyakawa(Atmosphere and Ocean Research Institute, The University of Tokyo), Koji Terasaki(RIKEN Center for Computational Science), Chairperson:Takuya Kawabata(Meteorological Research Institute)

High-performance computing(HPC) is one of the fundamental research tools supporting Today's meteorology, climate change research, and environmental sciences. Cutting-edge simulation studies have been carried out using supercomputers such as the Earth Simulator and the K computer. These big computers have contributed to an expansion of the range of feasible simulations, including higher resolution, wider computational domains, more ensemble sizes, and the use of more sophisticated physical processes. Supercomputers have also made significant progress in data science, with research into data assimilation techniques using high-frequency high-density observations and the combined use of simulation and Artificial Intelligence (AI). The supercomputer Fugaku is scheduled to begin full operation in fiscal 2021, and it is expected to produce many new research results with its world-beating computing performance.
This session calls for research topics in the atmospheric and hydrospheric studies using supercomputers, such as numerical modeling, big-data analysis, data assimilation, and AI. The participants can share future perspectives on atmospheric science research using HPC and the challenges to be addressed.

10:45 AM - 11:00 AM JST | 1:45 AM - 2:00 AM UTC

[AAS07-07] Early results of the evaluation of the JRA-3Q reanalysis

★Invited Papers

*Yayoi Harada[1], Shinya Kobayashi[2], Yuki Kosaka[2], Jotaro Chiba[2], Takayuki Tokuhiro[2] (1.Meteorological Research Institute / Japan Meteorological Agency, 2.Office of Earth System Modeling / Numerical Prediction Division / Japan Meteorological Agency)

11:00 AM - 11:15 AM JST | 2:00 AM - 2:15 AM UTC

[AAS07-08] Quality assessment of the third Japanese Reanalysis for Three Quarters of a Century (JRA-3Q) during a pre-satellite era

*Hiroaki Naoe[1], Shinya Kobayashi[2], Yuki Kosaka[2], Jotaro Chiba[2], Takayuki Tokuhiro[2], Yayoi Harada[1] (1.Meteorological Research Institute / Japan Meteorological Agency, 2.Office of Earth System Modeling / Numerical Prediction Division / Japan Meteorological Agency)

11:15 AM - 11:30 AM JST | 2:15 AM - 2:30 AM UTC

[AAS07-09] Emulating rainfall-runoff-inundation model with deep convolutional neural network

*Masahiro Momoi[1], Shunji Kotsuki[2], Ryota Kikuchi[3], Satoshi Watanabe[4], Masafumi Yamada[5], Shiori Abe[6], Akira Watanuki[7] (1.DoerResearch Inc., 2.Center for Environmental Remote Sensing, Chiba University, 3.Office of Society Academia Collaboration for Innovation, Kyoto University, 4.School of Engineering, The university of Tokyo, 5.Disaster Prevention Research Institute, Kyoto University, 6.Mitsui Consultants Co., Ltd., 7.Civil Engineering & Eco-Technology Consultants Co.,Ltd.)

11:30 AM - 11:45 AM JST | 2:30 AM - 2:45 AM UTC

[AAS07-10] Microphysics dependency on the reproducibility of the MJO in the DYAMOND winter phase experiment on NICAM

★Invited Papers

*Tamaki Suematsu[1], Yohei Yamada[2], Chihiro Kodama[2], Tomoki Miyakawa[1], Hiroaki Miura[3], Masaki Satoh[1] (1.Atmosphere and Ocean Research Institute, The University of Tokyo, 2.Japan Agency for Marine-Earth Science and Technology, 3.Graduate School of Science, The University of Tokyo)

11:45 AM - 12:00 PM JST | 2:45 AM - 3:00 AM UTC

[AAS07-11] Global large ensemble simulations with a cloud-resolving atmosphere and eddy-resolving ocean model

*Ryusuke Masunaga[1], Tomoki Miyakawa[1] (1.Atmosphere and Ocean Research Institute, The University of Tokyo)

12:00 PM - 12:15 PM JST | 3:00 AM - 3:15 AM UTC

[AAS07-12] Comparison of stable water isotopes between the cloud-microphysical processes simulated by isotope-incorporated NICAM

*Masahiro TANOUE[1], Yuki Takano[2], Kei Yoshimura[3], Hisashi Yashiro[1] (1.National Institute for Environmental Studies, 2.Atmosphere and Ocean Research Institute, The University of Tokyo, 3.Institute of Industrial Science, the University of Tokyo)

Early results of the evaluation of the JRA-3Q reanalysis

*Yayoi Harada[1], Shinya Kobayashi[2], Yuki Kosaka[2], Jotaro Chiba[2], Takayuki Tokuhiro[2]

1. Meteorological Research Institute / Japan Meteorological Agency, 2. Office of Earth System Modeling / Numerical Prediction Division / Japan Meteorological Agency

The Japan Meteorological Agency (JMA) is conducting the third Japanese global atmospheric reanalysis named Japanese Reanalysis for Three Quarters of a Century (JRA-3Q) using the JMA operational data assimilation system that has been upgraded and improved since the Japanese 55-year Reanalysis (JRA-55) was conducted. Main points of improvement in the specifications of the data assimilation system are as follows (specifications of the JRA-55 data assimilation system are shown in parentheses for comparison): Vertical levels are increased up to 100 (60) layers; The top level of the system is 0.01 (0.1) hPa; The inner model resolution for 4D-Var is also increased up to TL319 (T106); Various parameterization schemes have been improved and several new schemes have been implemented. In addition, we use observations newly rescued and digitized by the ERA-CLIM and other projects as well as newly reprocessed and improved satellite observations. As for GNSS radio occultation, bending angle is assimilated up to 60 km (refractivity up to 30 km).

The early results show that both overestimation of precipitation in the tropics and dry bias in the middle troposphere are diminished compared with those in JRA-55, and the representation of diabatic heating rate is also improved. In addition, biases of surface heat fluxes and radiation fluxes at the top of the atmosphere are also reduced.

Keywords: Global long-term reanalysis, JRA-3Q, Evaluation

©2021. Japan Geoscience Union. All Right Reserved.

Quality assessment of the third Japanese Reanalysis for Three Quarters of a Century (JRA-3Q) during a pre-satellite era

*Hiroaki Naoe[1], Shinya Kobayashi[2], Yuki Kosaka[2], Jotaro Chiba[2], Takayuki Tokuhiro[2], Yayoi Harada[1]

1. Meteorological Research Institute / Japan Meteorological Agency, 2. Office of Earth System Modeling / Numerical Prediction Division / Japan Meteorological Agency

This study evaluates the latest Japanese Reanalysis for Three Quarters of a Century (JRA-3Q) conducted by the Japan Meteorological Agency (JMA), focusing on a semi-period of pre-satellite era (1960s and 1970s). JRA-3Q is the third Japanese global atmospheric reanalysis covering the period from late 1940s onward, and it is based on the JMA's operational system as of December 2018. The atmospheric model has a TL479 horizontal resolution and 100 vertical layers up to 0.01 hPa, and the core component of the JRA-3Q data assimilation system is the 6-hourly 4D-Var of the atmospheric state with a T319-resolution inner model. Three-dimensional daily-mean ozone distributions used in JRA-3Q were calculated using an off-line ozone transport model (MRI-CCM2, TL159L64) with a nudging scheme to assimilate Level 3 total column ozone (TCO) datasets which had originally produced from Level 2 TCO datasets for the period after 1979, and without a TCO nudging but bias-corrected for the period before 1978.
Because there are only few global-covered observational datasets during the pre-satellite era, evaluation of the JRA-3Q is mainly to conduct an intercomparison of other reanalysis datasets such as representation Japanese 55-year Reanalysis (JRA-55), a JRA-55's subset of atmospheric reanalysis assimilating conventional observations only (JRA-55C), and version 3 of the Twentieth Century Reanalysis (20CRv3), and also an intercomparison of JRA-3Q between the pre-satellite and satellite eras. Emphasis of this evaluation during the non-satellite era is placed on the representation of tropical circulation, the consistency in time of the reanalysed fields, detection of tropical cyclones, and the quality of the stratospheric water vapour and ozone. For example, the surface circulation over the tropical Africa is improved by means of reducing spurious anticyclonic circulation anomalies that were found in JRA-55. Stratospheric ozone is improved by the use of adequate ozone depletion substances, sea-surface temperature, and so on as well as the improvements of the ozone model. Although the atmospheric model can produce self-generated quasi-biennial oscillation (QBO) by introducing non-orographic gravity wave drag, the evaluation reveals that JRA-3Q has a shorter period of around one year in the middle stratosphere and diminished QBO amplitude in the lower stratosphere, indicating that representation of the QBO in JRA-3Q is not as good as that in JRA-55.

Keywords: Long-term Reanalysis , JRA-3Q, quality assessment of a pre-satellite era

©2021. Japan Geoscience Union. All Right Reserved.

Emulating rainfall-runoff-inundation model with deep convolutional neural network

*Masahiro Momoi[1], Shunji Kotsuki[2], Ryota Kikuchi[3], Satoshi Watanabe[4], Masafumi Yamada[5], Shiori Abe[6], Akira Watanuki[7]

1. DoerResearch Inc., 2. Center for Environmental Remote Sensing, Chiba University, 3. Office of Society Academia Collaboration for Innovation, Kyoto University, 4. School of Engineering, The university of Tokyo, 5. Disaster Prevention Research Institute, Kyoto University, 6. Mitsui Consultants Co., Ltd., 7. Civil Engineering & Eco-Technology Consultants Co.,Ltd.

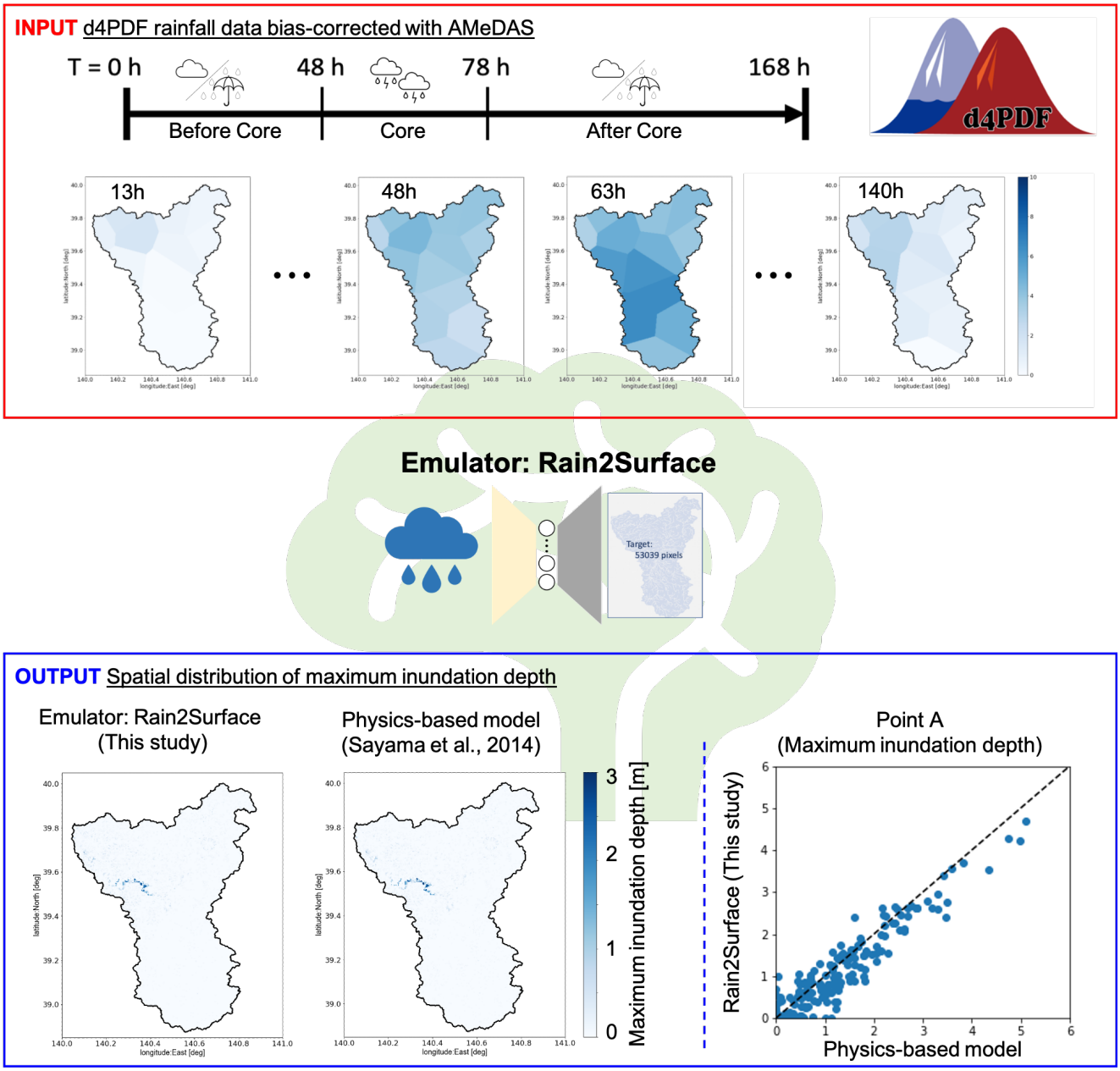
Predicting spatial distributions of maximum inundation depth for individual rainfall events is important to mitigate hydrological disasters induced by extreme precipitation. Physics-based rainfall-runoff-inundation (RRI) models, a mainstream for predicting hydrological disasters, need massive computation resource to employ model simulations. Here, this study aims to develop a computationally-inexpensive deep learning (hereafter, Rain2Surface) by emulating an RRI model. This study focuses around the Omono river in Akita prefecture and emulates prediction of the spatial distribution of maximum inundation depth from the spatial and temporal rainfall data for individual events.

The Rain2Surface is developed based on a deep convolutional neural network. We used hourly rainfall at 13 AMeDAS stations over seven days for input rainfall data, drawn from 50-ensemble of 30-years data from large-ensemble weather/climate predictions (d4PDF). The maximum inundation depth was simulated by Sayama et al. (2014)'s RRI model prior to the training. The Rain2Surface consists of two components. The first component extracts feature data from input rainfall data with one-dimensional convolutional layers and a fully-connected layer. The second component expands spatial distribution of maximum inundation depth from the feature data based on the two-dimensional transpose convolutional layers.

The prediction accuracy of the Rain2Surface was 20 cm for root mean square error (RMSE) and 0.93 for a coefficient of determination (γ) at a station with deep maximum inundation depth (hereafter, point A). The emulator provided more accurate predictions compared to our previous study (Kotsuki et al., 2020; RMSE = 29 cm, $\gamma = 0.89$) which used ensemble learning of multiple regularized regressions. This suggests that non-linear convolutional neural network effectively extracts feature required for the output inundation data from the input rainfall data. Kotsuki et al. (2020)'s approach needs to develop independent models for prediction spatial distributions of maximum inundation depth. In contrast, this study enabled to obtain spatial distribution of maximum inundation depth only by training single model, namely, Rain2Surface.

Keywords: d4PDF, rainfall-runoff-inundation, emulator, deep learning

©2021. Japan Geoscience Union. All Right Reserved.



©2021. Japan Geoscience Union. All Right Reserved.

Microphysics dependency on the reproducibility of the MJO in the DYAMOND winter phase experiment on NICAM

*Tamaki Suematsu[1], Yohei Yamada[2], Chihiro Kodama[2], Tomoki Miyakawa[1], Hiroaki Miura[3], Masaki Satoh[1]

1. Atmosphere and Ocean Research Institute, The University of Tokyo, 2. Japan Agency for Marine-Earth Science and Technology, 3. Graduate School of Science, The University of Tokyo

As part of participating in the DYAMOND (DYnamics of the Atmospheric general circulation Modeled On Non-hydrostatic Domains) winter phase model intercomparison project, we conducted a set of 40-days integrations on a convection-permitting model, NICAM (Nonhydrostatic ICosahedral Atmospheric Model) at 3.5 km horizontal resolution and 78 vertical layers using Fugaku. The simulations were done in two different microphysics settings, one optimized for the reproducibility of the MJO (MJO-tuned) in subseasonal integrations, and another optimized for high resolution model intercomparison project (High Res MIP)-type experiments.

In this study, we examined the microphysics dependency of the reproducibility of an MJO event from late January 2020 to mid February 2020, which was included in the integration period. The comparison of the two simulation results revealed that both settings successfully reproduce the eastward movement of convective system of the MJO to the dateline in the first 20 days of the integration. However, past 20 days of the integration, convective activities were maintained near the date-line, as in the observation, only for the MJO-tuned setting. The preliminary analyses on the simulation results indicate that the differences in the two settings arise from the contrasts in the type of convective systems that compose the simulated MJOs. A discussion on the physical interpretation of these differences will be given from the mean states that are achieved by the two model settings.

Keywords: DYAMOND, Madden-Julian Oscillation, NICAM

©2021. Japan Geoscience Union. All Right Reserved.

Global large ensemble simulations with a cloud-resolving atmosphere and eddy-resolving ocean model

*Ryusuke Masunaga[1], Tomoki Miyakawa[1]

1. Atmosphere and Ocean Research Institute, The University of Tokyo

Global large ensemble simulations over several months with a cloud-resolving (14 km resolution or finer) atmosphere, eddy-resolving (0.1 degrees resolution) ocean model, and their coupled system have become feasible thanks to the development of high-power supercomputer “Fugaku”. This is an unprecedented opportunity to explore the roles of the interaction between mesoscale atmospheric convections and ocean eddies on the global climate system.
Atmospheric convection over the tropical region can yield anomalous atmospheric circulations over the globe. Meanwhile, recent studies have shown that mesoscale ocean perturbations can trigger deep atmospheric convections, and thus exert remote and basin-scale impacts on the atmospheric circulation. Thus, it is of great importance to explore the role of the mesoscale air-sea interaction by using a global atmosphere-ocean coupled system.
We are assessing performance and utility of the high-resolution coupled system by comparing it with a lower-resolution (with a 0.25 degrees resolution ocean component) system. The representation of the mesoscale ocean features over the midlatitude regions are substantially improved in the high-resolution coupled system. Furthermore, the climatic drift in sea-surface temperature tends to be suppressed over the subtropical region, in particular the North Atlantic. These improvement in the surface ocean state can lead to better representation in the atmospheric state and better sub-seasonal to seasonal forecasts.

©2021. Japan Geoscience Union. All Right Reserved.

Comparison of stable water isotopes between the cloud-microphysical processes simulated by isotope-incorporated NICAM

*Masahiro TANOUE[1], Yuki Takano[2], Kei Yoshimura[3], Hisashi Yashiro[1]

1. National Institute for Environmental Studies, 2. Atmosphere and Ocean Research Institute, The University of Tokyo, 3. Institute of Industrial Science, the University of Tokyo

Stable water isotopes (SWIs) (δ^{2}H and δ^{18}O) show large spatial-temporal variability throughout the cloud process and large-scale transportation of atmospheric water vapor. However, there is some room for discussion of the effect of cloud-microphysics and large-scale transportation of water vapor on the variability of SWIs. Here, we incorporated SWI tracer into the Nonhydrostatic Icosahedral Atmospheric Model (NICAM) and investigated the contribution of cloud-microphysical processes to the variability of isotope ratios in precipitation and vapor. NICAM' s physical process can cover from low spatial resolution to high spatial resolution, and we can conduct simulations with two types of experimental setting; cloud-system-resolving-mode and general-circulation-mode (CRM-mode and GCM-mode). In the CRM-mode simulations, we used the single-moment bulk cloud microphysics scheme with six water categories (Tomita, 2008) for the cloud process, but did not use any convective parameterization scheme. In the GCM-mode simulations, we used the Arakawa-Schubert-type convective parameterization scheme and the large-scale condensation scheme as the cloud process with two water categories. We conducted an AMIP-type climate experiment from 1979 to 2000 using both settings with about 223 km of horizontal mesh resolution and 78 vertical layers, using 40 cores of the supercomputer Fugaku. The simulated δ^{18}O values of precipitation and water vapor showed the latitude effect pattern (high δ^{18}O in low latitude region, low δ^{18}O in high latitude region), but those values in the CRM-mode were slightly lower than those in the GCM-mode. The simulated precipitation δ^{18}O in the CRM-mode was lower in high altitude or inland regions compared with those in the GCM-mode. Besides, the precipitation d-excess, defined by δ^{2}H $-8*\delta^{18}$O, in the CRM-mode shows large spatial variability compared with the GCM-mode. These results indicates that the CRM mode show more larger spatial-temporal variability, meaning that the cloud-microphysical process is important for the large spatial-temporal variability of SWI. Although this study set the low spatial resolution, we will conduct these simulations with finer spatial resolution and a more extended simulation period.

Keywords: NICAM, Stable water isotopes, cloud microphysical process

©2021. Japan Geoscience Union. All Right Reserved.

[J] Oral | A (Atmospheric and Hydrospheric Sciences)：A-OS Ocean Sciences & Ocean Environment

Fri. Jun 4, 2021 9:00 AM - 10:30 AM JST | Fri. Jun 4, 2021 12:00 AM - 1:30 AM UTC | Ch.09 Zoom Room 09

[A-OS15] Ocean circulation and material cycle in coastal seas

convener:Naoki Furuichi(Fisheries Technology Institute, Japan Fisheries Research and Education Agency), Akihiko Morimoto(Ehime University), Kazuhiko Ichimi(Faculty of Agriculture, Kagawa University), Daisuke Takahashi(Tokai University), Chairperson:Naoki Furuichi(Fisheries Technology Institute, Japan Fisheries Research and Education Agency), Akihiko Morimoto(Ehime University), Tomaso Esposti Ongaro(Istituto Nazionale di Geofisica e Vulcanologia, Italy), Sakshi Ramesh Shiradhonkar (Department of Environment Systems, University of Tokyo)

Coastal seas have high biodiversity and high productivity, while various environmental problems such as eutrophication, red tide, and hypoxia are caused by human activity. In order to understand material cycle and various phenomena and to maintain sustainable environment in the coastal seas, interdisciplinary research is needed. In the present session, we invite researchers who are interested in physical phenomena, material cycle, biological responsive dynamics, and their interactions in the coastal seas. Neither study area nor study method is confined. We welcome presentations of wide-range topics to communize our knowledge in the coastal seas.

9:00 AM - 9:15 AM JST | 12:00 AM - 12:15 AM UTC

[AOS15-01] Intrusion of lower water into a coastal bay driven by a tropical storm

*Hajime Nishigaki[1], Kiyoshi Tanaka[2], Chul-hoon Hong[3] (1.Faculty of Science and Technology, Oita University, 2.Atmosphere and Ocean Research Institute, The University of Tokyo, 3.Division of Marine Production System Management, Pukyong National University)

9:15 AM - 9:30 AM JST | 12:15 AM - 12:30 AM UTC

[AOS15-02] Estimating the transport and settlement distribution of abalone larvae in the Otsuchi bay using high-resolution particle tracking model

*Yoshimasa Matsumura[1], Takashi T Sakamoto[1], Yuki Minegishi[1], Jun Hayakawa[1], Kosei Komatsu[1], Kiyoshi Tanaka[1], Koji Hamasaki[1], Tomohiko Kawamura[1] (1.Atmosphere and Ocean Research Institute, University of Tokyo)

9:30 AM - 9:45 AM JST | 12:30 AM - 12:45 AM UTC

[AOS15-03] Study on 3D oceanic transport of coral larvae in reef areas on the northwest coast of Okinawa Main Island

*Kimika Takeyasu[1], Yusuke Uchiyama[1], Xu Zhang[1], Kosei Matsushita[1], Satoshi Mitarai[2] (1.Graduate School of Engineering, Kove University, 2.Okinawa Institute of Science and Technology Graduate University)

9:45 AM - 10:00 AM JST | 12:45 AM - 1:00 AM UTC

[AOS15-04] Numerical study on wave breaking and refection processes on steep bottom slope

*Tsuyoshi Kaneko[1], Yoshihiro Ohmura[2], Naoki Furuichi[2], Shinya Saeki[1] (1.Aratani Civil Engineering Consultants CO.,LTD., 2.Japan Fisheries Research and Education Agency)

10:00 AM - 10:15 AM JST | 1:00 AM - 1:15 AM UTC

[AOS15-05] Operation and observations of the Autonomous Ocean Vehicle (AOV) around Japan coasts

*Kohei Ino[1], Shinji Sugiyama[1], Takahiro Kon[1], Rika Nozawa[1], Chikara TSUCHIYA[1] (1.Hydrographic and Oceanographic Department, Japan Coast Guard)

10:15 AM - 10:30 AM JST | 1:15 AM - 1:30 AM UTC

[AOS15-06] Influence of observational missing on harmonic constants analyzed by the least squares method

*Chikara TSUCHIYA[1], Kohei INO[1], Takahiro KON[1], Rika NOZAWA[1], Shinji SUGIYAMA[1] (1.Hydrographic and Oceanographic Department, Japan Coast Guard)

Intrusion of lower water into a coastal bay driven by a tropical storm

*Hajime Nishigaki[1], Kiyoshi Tanaka[2], Chul-hoon Hong[3]

1. Faculty of Science and Technology, Oita University, 2. Atmosphere and Ocean Research Institute, The University of Tokyo, 3. Division of Marine Production System Management, Pukyong National University

Water circulations and exchanges in coastal bays are important process for fishery as well as for oceanography. In Otsuchi Bay, located in the Sanriku ria coast on the eastern coast of northeastern Japan facing the North Pacific, we are monitoring water properties such as temperature (Tanaka et al. 2017).

A significant temperature change was recorded in August 2016 after the center of typhoon Lionrock (the 16th typhoon in 2016) passed by just near Otsuchi Bay. The change was dominant at 25 m depth, which is close to the bottom there. The temperature dropped abruptly by about 8ºC and undulated for following several days. Meanwhile, the temperature at 5 m depth had a small time change. These suggest that the water motion is trapped by the bottom.

In order to understand the dynamic process, a numerical experiment is made to represent the effect of the tropical storm on the ocean. The numerical model is the Princeton Ocean Model (POM) with horizontal resolution of 1/10º ×1/12º and 52 vertical levels. The area lies in 30º–45ºN and 135º–150ºE with a realistic topography but the maximum depth is limited to 1500 m. Initially, the ocean has a horizontally uniform vertical stratification representing summer condition and has no motion. It is driven by surface wind stress and atmospheric pressure imitating typhoon Lionrock as in the manner of Hong and Yoon (2003).

In the numerical result, the storm drives upper motions similar to the inertial oscillation described in Gill (1982). In the lower layer below 200 m depth, the velocity has opposite direction to the upper velocity. This flow pattern can be explained by the internal gravity lee waves with near-inertial period and vertical structure of the first baroclinic mode that is driven by a moving storm. In the open ocean, the temperature or density change is dominated by the mechanical mixing by the wind forcing. The contribution of the vertical motion in the lee waves and that of the Ekman vertical motion seem both minor.

The temperature change at the corresponding point in the numerical model is compared to the observation in Otsuchi Bay. They show quite similar time changes despite the forcing in the model is simple. Near the coast, vertical displacement of the thremocline is significantly larger than that in the open ocean. It is suggested that the vertical displacement of the thermocline is generated by the lower flow in the baroclinic near-inertial waves going up and down along the bottom slope, which is similar to the case of the internal tide generation.

References

Hong CH and Yoon JH, 2003. JGR, 108.
Gill AE, 1982. Atmosphere-ocean dynamics, Chap 9.11.
Tanaka K et al., 2017. JO, 73.

Keywords: typhoon, inertial oscillation, internal gravity waves, bottom slope

©2021. Japan Geoscience Union. All Right Reserved.

Estimating the transport and settlement distribution of abalone larvae in the Otsuchi bay using high-resolution particle tracking model

*Yoshimasa Matsumura[1], Takashi T Sakamoto[1], Yuki Minegishi[1], Jun Hayakawa[1], Kosei Komatsu[1], Kiyoshi Tanaka[1], Koji Hamasaki[1], Tomohiko Kawamura[1]

1. Atmosphere and Ocean Research Institute, University of Tokyo

Abalone is an important fishery resource in the Sanriku coast. In the present study the dispersal and settlement of abalone larvae in the Otsuchi bay was investigated using a three-dimensional particle tracking system driven by a state-of-the-art high resolution ocean circulation model. The velocity field was simulated by the multi-level nested version of COCO (an ocean general circulation model developed at AORI, University of Tokyo) driven by climatological forcing. The horizontal grid spacing of the inner-most domain focusing the Otsuchi bay is approximately 14 m, in which complex geometry of the bay boundary includes artificial objects such as an embankment are resolved.

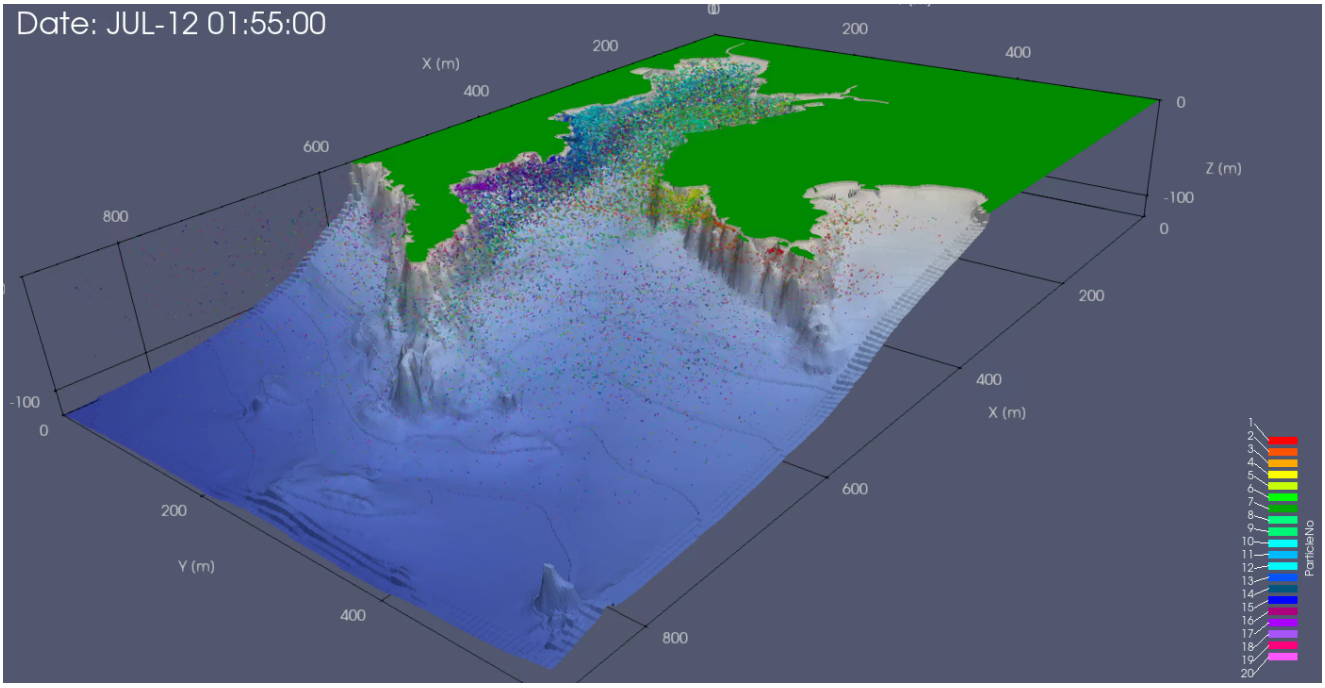
The particles that represent eggs and larvae of abalone were continuously released in 5 minutes interval from 20 spawning points located along the 10 m bathymetry contour. The trajectory of each particle was integrated by summation of advection by three-dimensional velocity field, vertical turbulent dispersion represented by random-walk, the Stokes drift estimated from a drifting buoy, and settling velocity of abalone eggs/larvae observed in still water. The modeled larvae particle is supposed to acquire the ability to settle on ground suitable for survival (i.e., habitat of coralline algae) in 4 days after the release, while the particles that failed to settlement in 14 days die and removed from the calculation. The integration was performed from Jul. 1st to Oct. 30th and total 4,216,320 particles were released.

The simulated distribution of settlement is consistent with our knowledge from observation, particularly at the northeast bank of the bay. The settlement distribution map shows that the mound near the southern tip at the bay mouth is a *hot-spot* of abalone settlement, which has not been confirmed in reality yet. It also exhibits substantial settlement along the southern coast outside the bay, that implies the possibility of connectivity of abalone over the bays in the Sanriku coast within a few generations.

In the present simulation the effect of Stokes drift caused by swell directing from the bay mouth to interior was not significant since the modeled particles were not suspended near the surface for long time. On the other hand, tidal current might play important role for abalone settlement since the number of particles successfully settled inside the bay was doubled in an experiment where the velocity field was 24-hour averaged.

Keywords: Particle tracking, Otsuchi bay, abalone larvae

©2021. Japan Geoscience Union. All Right Reserved.



©2021. Japan Geoscience Union. All Right Reserved.

Study on 3D oceanic transport of coral larvae in reef areas on the northwest coast of Okinawa Main Island

*Kimika Takeyasu[1], Yusuke Uchiyama[1], Xu Zhang[1], Kosei Matsushita[1], Satoshi Mitarai[2]

1. Graduate School of Engineering, Kove University, 2. Okinawa Institute of Science and Technology Graduate University

In recent years, coral bleaching has occurred extensively over the world ocean due primarily to high water temperatures. Mesophotic corals that inhabit in intermediate depth at about 30-150m depth are expected to survive during bleaching events and to reseed shallow water corals afterward. In particular, in Okinawa, Japan, mesophotic coral ecosystems (MCEs) have been reported to serve as a refuge to preserve genotypic diversity of bleaching-sensitive corals (Sinniger et al,. 2017). Connectivity of larval populations between different habitats has been a key element that determines the area to be conserved for desirable coral ecosystems. Coral larvae generally behave passively to the surrounding currents and are transported by the advective and dispersive effects of ambient ocean currents. Numerical ocean circulation models enable us to quantity connectivity with more detailed spaciotemporal network structures than genetic approaches. Previous numerical connectivity studies around the Ryukyu Islands and Okinawa Main Island have investigated rather large-scale coral connectivity with primary attention to horizontal migration of coral larvae (e.g., Uchiyama et al., 2018). However, short-distance, coastal scale transport has been recognized to be much more responsible for maintaining high connectivity.

This study aims at quantifying short-distance and vertical connectivity of coral larvae in reef areas on the northwest coast of Okinawa Main Island. Because both short-distance and vertical larval transports are influenced pronouncedly by complex nearshore topography, a very high-resolution 3-D circulation model is required. Therefore, we develop a quadruple nested high-resolution synoptic ocean modeling at a lateral spatial resolution of 50m based on the JCOPE2-ROMS downscaling system (Kamidaira et al., 2017), coupled with an offline 3-D Lagrangian particle-tracking mode that mimics coral larval transport. After validations of the developed model, short-distance horizontal coral connectivity across reef areas on the northwest coast was successfully evaluated. Furthermore, a series of Lagrangian particle release experiments was conducted for identifying vertical coral migration and thus 3-D connectivity required for preservation of MCEs. In the experiments, particles were released from two depths, 2m (shallow corals) and 30m (mesophotic corals) with sink areas that are vertical divided into three depth zones, 0-10m (shallow corals), 30-40m (upper mesophotic corals), 40-100m (lower mesophotic corals). Horizontal connectivity of shallow corals is characterized by prevailing northward transport and entrainment in topographic kinks in particular on the south side of Motobu Peninsula located near the center of the model domain. The intermediate depth of ~10m receive a substantial number of larvae originated from shallow and mesophotic spawning sites, suggesting that mesophotic coral be sustained by the regional 3-D larval network.

©2021. Japan Geoscience Union. All Right Reserved.

Numerical study on wave breaking and refection processes on steep bottom slope

*Tsuyoshi Kaneko[1], Yoshihiro Ohmura[2], Naoki Furuichi[2], Shinya Saeki[1]

1. Aratani Civil Engineering Consultants CO.,LTD., 2. Japan Fisheries Research and Education Agency

Wave breaking, reflection, and wave-induced currents are thought to play important roles in forming nearshore environment and distributions of fish or bivalve larvae. In this study, we investigated the features of wave breaking and reflection processes over steep bottom slope under several conditions of wave height and wave period, using a vertically two-dimensional numerical model. The numerical experiments reproduced several types of wave breaking processes, i.e., plunging, surging, and non-breaking, and demonstrated that the reflection coefficient increases with increasing bottom slopes and decreasing wave steepness (ratio of wave height to wave length). On the basis of the calculated results, we proposed a formulation for estimating the reflection coefficient under regular wave condition.

Keywords: wave breaking, reflection coefficient, breaker type

©2021. Japan Geoscience Union. All Right Reserved.

Operation and observations of the Autonomous Ocean Vehicle (AOV) around Japan coasts

*Kohei Ino[1], Shinji Sugiyama[1], Takahiro Kon[1], Rika Nozawa[1], Chikara TSUCHIYA[1]

1. Hydrographic and Oceanographic Department, Japan Coast Guard

Japan Coast Guard has been operating Autonomous Ocean Vehicle (AOV), which is Wave Glider made by Liquid Robotics and equipped with a GNSS antenna, an ADCP, a weather station, a wave sensor and a CTD, since 2016. We operate the AOV for one year in five square kilometer area for continuous meteorological and oceanographic observation and provide the observed data via our web site. The AOV moves forward by converting wave energy to propulsion and utilizes solar energy as a power source for sensors. In this presentation, we report the problems and improvements of the continuous long-term observation involved with the limited propulsion force and power source. In addition, we present GNSS observation for precisely determining the chart datum and observation of a typhoon.

Keywords: Wave Glider, Ocean Observation, Platform

©2021. Japan Geoscience Union. All Right Reserved.

Influence of observational missing on harmonic constants analyzed by the least squares method

*Chikara TSUCHIYA[1], Kohei INO[1], Takahiro KON[1], Rika NOZAWA[1], Shinji SUGIYAMA[1]

1. Hydrographic and Oceanographic Department, Japan Coast Guard

Japan Coast Guard operates GNSS observations using Autonomous Ocean Vehicles (AOVs) in order to determine the chart datum precisely using tidal time series of that period is more than one year. The obtained time series can have long observational missing because AOVs may locate out of the planning area due to the limitation of the driving force and power supply of the AOV. In this study, a necessary condition of the observation period to obtain reliable harmonic constants by analyzing responce of the harmonic constants by the harmonic analysis based on the least squares method to the duration of missing values is discussed.

Keywords: Tide, Wave Glider

©2021. Japan Geoscience Union. All Right Reserved.

[J] Oral | A (Atmospheric and Hydrospheric Sciences)：A-OS Ocean Sciences & Ocean Environment

Fri. Jun 4, 2021 10:45 AM - 12:05 PM JST | Fri. Jun 4, 2021 1:45 AM - 3:05 AM UTC | Ch.09 Zoom Room 09

[A-OS15] Ocean circulation and material cycle in coastal seas

convener:Naoki Furuichi(Fisheries Technology Institute, Japan Fisheries Research and Education Agency), Akihiko Morimoto(Ehime University), Kazuhiko Ichimi(Faculty of Agriculture, Kagawa University), Daisuke Takahashi(Tokai University), Chairperson:Naoki Furuichi(Fisheries Technology Institute, Japan Fisheries Research and Education Agency), Akihiko Morimoto(Ehime University), Tomaso Esposti Ongaro(Istituto Nazionale di Geofisica e Vulcanologia, Italy), Sakshi Ramesh Shiradhonkar (Department of Environment Systems, University of Tokyo)

Coastal seas have high biodiversity and high productivity, while various environmental problems such as eutrophication, red tide, and hypoxia are caused by human activity. In order to understand material cycle and various phenomena and to maintain sustainable environment in the coastal seas, interdisciplinary research is needed. In the present session, we invite researchers who are interested in physical phenomena, material cycle, biological responsive dynamics, and their interactions in the coastal seas. Neither study area nor study method is confined. We welcome presentations of wide-range topics to communize our knowledge in the coastal seas.

10:45 AM - 11:00 AM JST | 1:45 AM - 2:00 AM UTC

[AOS15-07] Observation of a river front using drones

*Kentaro Takami[1], Shinichiro Kida[2], Atsuhiko Isobe[2] (1.Kyushu University Interdisciplinary Graduate School of Engineering Sciences, 2.Research Institute for Applied Mechanics, Kyushu University)

11:00 AM - 11:15 AM JST | 2:00 AM - 2:15 AM UTC

[AOS15-08] Behavior of suspended particulate matter and Bottom boundary layer processes off Fukushima Prefecture

*Naoki Furuichi[1], Hideki Kaeriyama[2], Koichi Sugimatsu[1] (1.Fisheries Technology Institute, Japan Fisheries Research and Education Agency , 2.Fisheries Research Institute, Japan Fisheries Research and Education Agency)

11:15 AM - 11:30 AM JST | 2:15 AM - 2:30 AM UTC

[AOS15-09] Long-term trends of oxygen concentration in the waters in bank and shelves of the southern Japan Sea

*Tsuneo Ono[1] (1.Fisheries Research and Education Agency)

11:30 AM - 11:45 AM JST | 2:30 AM - 2:45 AM UTC

[AOS15-10] Interannual variations of nutrient concentrations and the mechanisms of nutrient supply in the western Seto Inland Sea

*Sohei Ogawa[1], Naoki Yoshie[1], Hidezirou Ohnishi[1] (1.Center for Marine Environmental Studies, Ehime University)

11:45 AM - 12:00 PM JST | 2:45 AM - 3:00 AM UTC

[AOS15-11] Standing stock and species composition of planktonic copepods occurred in Harima Nada in the eastern Seto Inland Sea, Japan

*Hamazaki Yuya[1], Hitomi Yamaguchi[1], Kuninao Tada[1], Kazuhiko Ichimi[1] (1.Graduate school of Agriculture Kagawa University)

12:00 PM - 12:05 PM JST | 3:00 AM - 3:05 AM UTC

[AOS15-12] Discussion

Observation of a river front using drones

*Kentaro Takami[1], Shinichiro Kida[2], Atsuhiko Isobe[2]

1. Kyushu University Interdisciplinary Graduate School of Engineering Sciences, 2. Research Institute for Applied Mechanics, Kyushu University

A river front is known to form between seawater and riverine water. To understand the physical process of river water dispersing to the ocean in coastal areas, it is necessary to clarify the spatial structure and temporal changes of the river front. In this study, we imitated remote sensing observations of a river front using drones by observing the river front reproduced within a rotating tank. The rotating tank is circular and rotates at a constant speed. After introducing river water into the tank, images were taken with a visible camera and an infrared camera from above and with an underwater camera near the outlet. The visible images showed the river water forming a bulge and a flow along the wall that branches off from the bulge. The infrared images showed vortices forming within the bulge. The underwater images showed river water mixing with seawater below. Since bathymetry is often shallow and river water can be in contact with the bottom, we plan to investigate river plumes that are influenced by bathymetry and examine their behavior.

Keywords: River front, Drones, Infrared camera, Rotating tank

©2021. Japan Geoscience Union. All Right Reserved.

Behavior of suspended particulate matter and Bottom boundary layer processes off Fukushima Prefecture

*Naoki Furuichi[1], Hideki Kaeriyama[2], Koichi Sugimatsu[1]

1. Fisheries Technology Institute, Japan Fisheries Research and Education Agency , 2. Fisheries Research Institute, Japan Fisheries Research and Education Agency

Sediment matter suspension and dispersion processes are thought to play important roles in forming marine benthic ecosystems, including those of demersal fishes. We investigated the behavior of suspended particulate matter on the shelf slope areas off Fukushima, focusing on the relationships with bottom boundary layer (BBL) processes, based on field observations and numerical simulations. Field observations were conducted using Laser In-Situ Scattering and Transmissometry (LISST)-100X/200X in the coastal region off Fukushima and nearby prefectures, and the vertical profiles of the volumetric concentration of particles and particle size distribution were obtained. The observations showed that the volumetric concentration of particles near the seabed increases considerably at many stations located near shelf slopes, where the total water depth is 100–200 m. We frequently observed that particles with a radius of less than 100 μm were dominant in this high turbidity layer; BBL thickness ranged from 10–100 m, and the volumetric concentration decreased significantly above the BBL compared to that within the BBL. To understand the mechanism behind the observed results, we conducted a vertical one-dimensional numerical experiment on tidal BBL processes and particulate matter behavior. The experiments demonstrated that the tidal current efficiently developed the BBL and that the vertical distribution of particle concentration was strongly controlled by the balance between tide-induced turbulent mixing and the settling of particles. These results suggest that BBL thickness and turbulence processes are important factors determining the distribution of particulate matter concentration.

Keywords: particulate matter dynamics, bottom boundary layer, turbulence, particle size distribution

©2021. Japan Geoscience Union. All Right Reserved.

Long-term trends of oxygen concentration in the waters in bank and shelves of the southern Japan Sea

*Tsuneo Ono[1]

1. Fisheries Research and Education Agency

Many studies have investigated oxygen decrease in Japan Sea Proper Water (JSPW), but we must also investigate oxygen decrease in shallow waters above JSPW to assess socio-economic impact of deoxygenation in Japan Sea. In this study, histrical oxygen data in the waters of three continental shelves and a bank off the Japan coastof Japan Sea, off-Awashima area (AW), Wakasa Bay (WB), East of Tsushima Straight (ETS), and Yamato Bank (YB), were collected from public database and analyzed to assess the temporal variation of oxygen in each region from 1960s to 2000s. Significant decreasing trends of oxygen were detected in the waters below 150 m depth in WB and YB, and below 300 m in AW, in the summer season. Deoxygenation siginal was more extensive in summer ETS, where a deoxygenation trend was detected throughout the water column from the bottom to the sea surface. These are the first evidences that reveals occurrence of ocean deoxygenation in the continental shelves of Japanese waters.
Detailed analysis indicated that oxygen decreases in AW, WB, and YB were consequence of the upward propagation of the deoxygenation signal from JSPW, while that of ETS was caused by horizontal propagation of deoxygenation signal fromthe East China Sea.Assuming that the observed trend will continue in future, it is predicted that part of the subsurface water in the summerTsushima Strait area in the summer season will reach the general sublethal threshold of oxygen (134 umol·kg^{-1}, Vaquer-Sunyer and Duarte, 2008) by the end of this century.

Keywords: Ocean deoxygenation, Japan Sea, continental shef, coastal area

©2021. Japan Geoscience Union. All Right Reserved.

Interannual variations of nutrient concentrations and the mechanisms of nutrient supply in the western Seto Inland Sea

*Sohei Ogawa[1], Naoki Yoshie[1], Hidezirou Ohnishi[1]

1. Center for Marine Environmental Studies, Ehime University

The mechanism of nutrient supply in the Bungo Channel part of the Western Seto inland Sea is not only from terrestrial regions by the inflow of river water, but also from the offshore regions caused by entering the bottom intrusion of the Kuroshio subsurface water into the Bungo Channel (Takeoka 2020). In the Hoyo Strait which is a narrow strait sandwiched between the Sada-misaki Peninsula and Saganoseki Peninsula and located in the northernmost in the Bungo Channel, sea water is strongly mixed horizontal and vertical with the strong tidal current. For these reasons, it can be said that the nutrient concentration around Sada-misaki is representative of the nutrient concentration in most parts of the western Seto Inland Sea, including the Bungo Channel and Iyo-nada. In this study, we investigated the relationship between seasonal and interannual variations of the nutrient concentration around Sada-misaki and variations of chlorophyll concentration, and the relationship between variations of the nutrient concentration and nutrient supplies from terrestrial and offshore regions. We have used a lot of data such as Dissolved inorganic nitrogen (DIN), dissolved inorganic phosphorus (DIP), and dissolved inorganic silicon (DISi) and chlorophyll concentration, which has been monitored daily at the cape of Sada-misaki from 2004 by joint research of Ehime University CMES and Misaki Fisheries Cooperative, Meteorological data from AMEDAS, first-class river flow and nutrient concentration data from the Ministry of Land, Infrastructure, Transport and Tourism and multi-layered water temperature data from the Uwa Seawater Temperature System, and analyze comprehensively. As a result, the seasonal variations of nutrient concentrations at the cape Sada-Misaki had the minimum values in the spring, which were quite different form typical variations in the mid-latitude offshore regions with the minimum values in the summer. This is because the nutrient supplies more than necessary from the both terrestrial and offshore regions from late May to September associated with the rainy and typhoon seasons in Japan. The nutrient supply from the terrestrial region through the river discharge was controlled by the amount of precipitation around Kyusyu Island. On the other hand, the nutrient supply from the offshore region was controlled by the intensity of the bottom intrusion of the Kuroshio subsurface water which was enhanced by flowing due to density difference which caused by the fresh water discharge from the inside of the Seto Inland Sea. In addition, biological production in Western Seto Inland Sea is controlled by DIN. In such area, phytoplankton breeding was further promoted for the next three months in the year when a large amount of DIN flowed due to rainfall in August. In recent years, decreasing trend of nutrient concentrations observed in the Eastern Seto Inland Sea, but it didn’t occur around Sada-misaki including the Bungo Channel and Iyo-nada.

Keywords: the inflow of river water, the bottom intrusion, Precipitation

©2021. Japan Geoscience Union. All Right Reserved.

Standing stock and species composition of planktonic copepods occurred in Harima Nada in the eastern Seto Inland Sea, Japan

*Hamazaki Yuya[1], Hitomi Yamaguchi[1], Kuninao Tada[1], Kazuhiko Ichimi[1]

1. Graduate school of Agriculture Kagawa University

In the Seto Inland Sea, Japan, fish catches have been declining since the latter 1980s. One of the causative factors may be a decrease in primary production due to oligotrophic water, followed by a decrease in zooplankton community, which is a prey for fish. Detailed surveys for zooplankton have not been carried out in the Seto Inland Sea since the 2000s. As there is a definite lack of data set about zooplankton, we cannot clarify the cause of the decrease in catch. In this study, we carried out annual observations for the species composition and biomass of planktonic copepods, which play an important role as secondary producers in the ocean, in Harima Nada in the eastern Seto Inland Sea.

Monthly samplings were conducted at Stn. NH from April 2019 to December 2020. Ten liters of the seawater samples were collected using a water sampler at 0, 10, 20 m depth. Planktonic copepods were concentrated with a 100 μm mesh size of plankton net. Adult individual was identified to the genus level under a microscope and the total number (abundance: inds./m^3) was calculated. The head-chest length was also measured and converted into biomass (mgC/m^3). Chlorophyll a concentration of the seawater was also measured by fluorometry.

The genus *Paracalanus*, *Oithona*, and *Microsetella* occurred as predominate species of copepods. The total abundance and the biomass was in the range of 0.02 - 6.28 $\times 10^4$ inds./m^3 and 0.05 - 30.9 mgC/m^3, respectively. Both of them were 2 - 10 times higher in summer-autumn than in winter-spring. The seasonal variation of abundance and biomass of copepods was similar to that of Chl a concentration (0.36 - 9.1 μg/L), indicating that the dynamics of copepods depend on the amount of prey organisms. Comparing the abundance and biomass of copepods in 1980 (Uye et al., 1987) and in 1994 (Uye and Shimazu, 1997) with the survey of this study, the abundance was similar, but the biomass tended to decrease. In addition, *Paracalanus* spp. still occurred as a dominant species throughout the year, but *Calanus* spp., relatively large species, was significantly reduced. It was considered that the abundance of planktonic copepods has not decreased, however, the biomass has been decreasing due to the decrease in large size of species.

Uye S, Kuwata H and Endo T (1987) J Oceanogr Soc Japan, **42**, 421-434

Uye S and Shimazu T (1997) JO, **53**, 529-538

Keywords: the Seto Inland Sea, zooplankton, copepod, seasonal variation

©2021. Japan Geoscience Union. All Right Reserved.

[J] Oral | A (Atmospheric and Hydrospheric Sciences) | A-OS Ocean Sciences & Ocean Environment

[A-OS15] Ocean circulation and material cycle in coastal seas

convener:Naoki Furuichi(Fisheries Technology Institute, Japan Fisheries Research and Education Agency), Akihiko Morimoto(Ehime University), Kazuhiko Ichimi(Faculty of Agriculture, Kagawa University), Daisuke Takahashi(Tokai University), Chairperson:Naoki Furuichi(Fisheries Technology Institute, Japan Fisheries Research and Education Agency), Akihiko Morimoto(Ehime University), Tomaso Esposti Ongaro(Istituto Nazionale di Geofisica e Vulcanologia, Italy), Sakshi Ramesh Shiradhonkar (Department of Environment Systems, University of Tokyo)

Fri. Jun 4, 2021 10:45 AM - 12:05 PM Ch.09 (Zoom Room 09)

Coastal seas have high biodiversity and high productivity, while various environmental problems such as eutrophication, red tide, and hypoxia are caused by human activity. In order to understand material cycle and various phenomena and to maintain sustainable environment in the coastal seas, interdisciplinary research is needed. In the present session, we invite researchers who are interested in physical phenomena, material cycle, biological responsive dynamics, and their interactions in the coastal seas. Neither study area nor study method is confined. We welcome presentations of wide-range topics to communize our knowledge in the coastal seas.

12:00 PM - 12:05 PM

[AOS15-12]Discussion

©Japan Geoscience Union

[J] Oral | A (Atmospheric and Hydrospheric Sciences)：A-OS Ocean Sciences & Ocean Environment

Fri. Jun 4, 2021 3:30 PM - 5:00 PM JST | Fri. Jun 4, 2021 6:30 AM - 8:00 AM UTC | Ch.11 Zoom Room 11

[A-OS17] Chemical and Biological Oceanography

convener:Kazuhiro Misumi(Environmental Science Research Laboratory, Central Research Institute of Electric Power Industry), Sayaka Yasunaka(Japan Agency for Marine-Earth Science and Technology), Chairperson:Kazuhiro Misumi(Environmental Science Research Laboratory, Central Research Institute of Electric Power Industry), Sayaka Yasunaka(Japan Agency for Marine-Earth Science and Technology)

This session invites presentations on a wide variety of topics related to chemical and biological oceanography.

3:30 PM - 3:45 PM JST | 6:30 AM - 6:45 AM UTC

[AOS17-01] A new SI traceable silicon standard solution for certification of nutrients CRM and measurement of silicate in seawater, part two

*Michio Aoyama[1,2], Chikako Cheong[3], Tsutomu Miura[3], Takeshi Fujii[4], Hitoshi Mitsuda[4], Tomomi Sone[5], Hiroshi Uchida[1], Akihiko Murata[1] (1.Research Institute of Global Change, The Japan Agency for Marine-Earth Science and Technology , 2.Center for Research in Isotopes and Environmental Dynamic, Faculty of Life and Environmental Sciences, University of Tsukuba, 3.National Metrology Institute of Japan (NMIJ), National Institute of Advanced Industrial Science and Technology (AIST), 4.Laboratory for Instrumentation and Analysis, KANSO CO., LTD., 5.MARINE WORKS JAPAN LTD.)

3:45 PM - 4:00 PM JST | 6:45 AM - 7:00 AM UTC

[AOS17-02] Spatio-temporal variability of subsurface Chl-a maximum in the world ocean

*Sayaka Yasunaka[1], Tsuneo Ono[2], Kosei Sasaoka[1], Kanako Sato[1] (1.Japan Agency for Marine-Earth Science and Technology, 2.Japan Fisheries Research and Education Agency)

4:00 PM - 4:15 PM JST | 7:00 AM - 7:15 AM UTC

[AOS17-03] **Improvements of ocean biogeochemical simulation of the North Pacific Ocean due to an enhanced horizontal resolution of an ocean model**

*Hiroyuki Tsujino[1], Toyama Katsuya[1], Hideyuki Nakano[1], Shiro Nishikawa[2], Toru Sugiyama[2], Haruka Nishikawa[2], Yoichi Ishikawa[2] (1.Japan Meteorological Agency / Meteorological Research Institute, 2.Japan Agency for Marine-Earth Science and Technology)

4:15 PM - 4:30 PM JST | 7:15 AM - 7:30 AM UTC

[AOS17-04] A modeling study on distribution of dissolved Zinc in the North Pacific

*Kiminori Sugino[1], Akira Oka[1] (1.Atmosphere and Ocean Research Institute, The University of Tokyo)

4:30 PM - 4:45 PM JST | 7:30 AM - 7:45 AM UTC

[AOS17-05] Geographical variation of Sr/Ca in skipjack tuna (*Katsuwonus peamis*) collected from Northwestern Pacific Ocean

*Shohgo Kawashima[1], Takaaki Itai[1] (1.The University of Tokyo)

4:45 PM - 5:00 PM JST | 7:45 AM - 8:00 AM UTC

[AOS17-06] Discussion about marine chemistry and biology

*Kazuhiro Misumi[1] (1.Environmental Science Research Laboratory, Central Research Institute of Electric Power Industry)

A new SI traceable silicon standard solution for certification of nutrients CRM and measurement of silicate in seawater, part two

*Michio Aoyama[1,2], Chikako Cheong[3], Tsutomu Miura[3], Takeshi Fujii[4], Hitoshi Mitsuda[4], Tomomi Sone[5], Hiroshi Uchida[1], Akihiko Murata[1]

1. Research Institute of Global Change, The Japan Agency for Marine-Earth Science and Technology , 2. Center for Research in Isotopes and Environmental Dynamic, Faculty of Life and Environmental Sciences, University of Tsukuba, 3. National Metrology Institute of Japan (NMIJ), National Institute of Advanced Industrial Science and Technology (AIST), 4. Laboratory for Instrumentation and Analysis, KANSO CO., LTD., 5. MARINE WORKS JAPAN LTD.

A new SI traceable silicon standard solution for certification of nutrients CRM and measurement of silicate in seawater was established (A-OS27-02, JpGU, 14th July 2020). This standard solution was produced by a dissolution technique with an alkaline solution and a silicon standard solution having a mass fraction of 1000 mg Si kg^{-1} was prepared. In June 2019 we produced 300 bottles of exp64 solution and a nominal mass fraction of solution prepared in June 2019 was 999.3 mg Si kg^{-1} and the certified mass fraction of this solution was 999.3 mg Si kg^{-1} ±2.8 mg Si kg^{-1} by a technology consulting system of AIST. In January 2021 we also produced 998 bottles of exp94 solution and the certified mass fraction of exp94 will be given by a technology consulting system of AIST in February 2021 again. The expanded uncertainty was 0.3 % for exp64 and this was better than the 0.5 % of NIST and Merck silicon standard solutions.

As a standard solution, homogeneity and long term stability are also essential. The homogeneity measurement result of the exp64 solution was 0.08 % in August 2019 and that of the exp94 solution was 0.07 % in January 2021. It is presumed that the long term stability might be theoretically good for a long period from a view of the chemical composition. No significant change in silicate concentration has been observed in the results of comparison between exp64 solution and certified reference materials of nutrients of lot CF of KANSO and NMIJ 7603-a.Long term storage experiment will be started soon. A small problem on production by the dissolution technique with an alkaline solution was found during our production experiments. We expected that silicon dioxide of which purity is 99.999 % should be reacted with sodium carbonate and a reaction rate of this might be very close to 100 %, however, measured silicate mass fraction showed that a reaction rate ranged from 99.29 % to 99.92 %. We need to seek the reasons for a little bit low reaction rate. We also did density measurements as a part of quality control of the production of this new silicon standard solution because we found a negative relationship between reaction rate and total mass after reaction by a dissolution technique with an alkaline solution.

This SI traceable silicon standard solution is already used to certify of nutrient CRM and is used to measure silicate concentration in seawater on the cruises of JAMSTEC worldwide. This new silicon standard solution will be provided to the coming ” IOCCP-JAMSTEC Inter-laboratory Comparison Exercise of a Certified Reference Material (CRM) for Nutrients in Seawater” , too.

Keywords: silicon standard solution, seawater, silicon, SI traceable, certified reference material

©2021. Japan Geoscience Union. All Right Reserved.

Spatio-temporal variability of subsurface Chl-a maximum in the world ocean

*Sayaka Yasunaka[1], Tsuneo Ono[2], Kosei Sasaoka[1], Kanako Sato[1]

1. Japan Agency for Marine-Earth Science and Technology, 2. Japan Fisheries Research and Education Agency

Chl-a concentration in ocean often retains its maximum value in subsurface layer. Using satellite retrieval of ocean surface Chl-a concentration, basin-wide spatial distribution and temporal variation of surface Chl-a has been described by many studies, while that of subsurface Chl-a has not been clarified yet. Here, we collects in-situ observation data of Chl-a concentration, and clarify the spatio-temporal variability of subsurface Chl-a concentration in the world ocean. Subsurface Chl-a maximum was stably observed in the subtropics and tropics (Figure 1). Depth of the subsurface Chl-a maximum is similar to the euphotic layer, but deeper than the euphotic layer in subtropics and shallower in tropics. Seasonal increase of oxygen below the mixed layer implied substantial biological new production. In El Niño years, subsurface Chl-a concentration in the equatorial Pacific is higher in the middle to east and lower in the west, which is opposite from surface.

Keywords: chlorophyll a, subsurface maximum, oxygen oversaturation

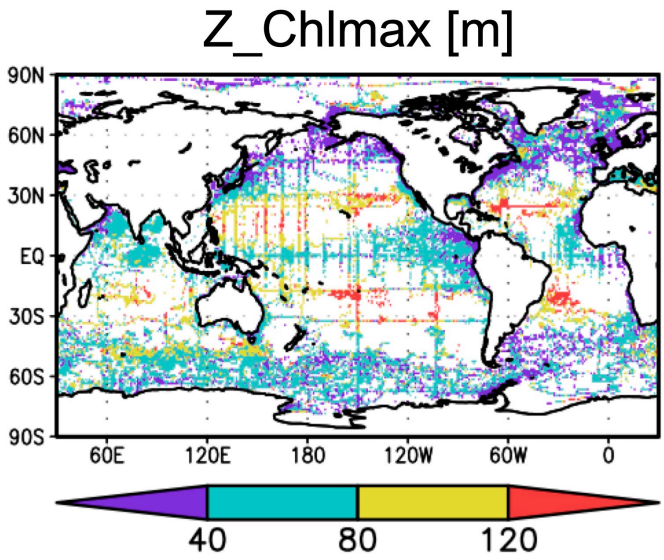


Figure 1: Depth of the Chl-a maximum in more than 70,000 profiles.

図1：約7万個のプロファイル毎に求めたクロロフィルa極大深度

©2021. Japan Geoscience Union. All Right Reserved.

Improvements of ocean biogeochemical simulation of the North Pacific Ocean due to an enhanced horizontal resolution of an ocean model

*Hiroyuki Tsujino[1], Toyama Katsuya[1], Hideyuki Nakano[1], Shiro Nishikawa[2], Toru Sugiyama[2], Haruka Nishikawa[2], Yoichi Ishikawa[2]

1. Japan Meteorological Agency / Meteorological Research Institute, 2. Japan Agency for Marine-Earth Science and Technology

The earth system model used by MRI for a series of CMIP6 experiments adopted a low-resolution ocean component whose grid size is around 100 km. Considering a possibility of using higher ocean model resolution in future projection experiments, we embedded a 10-km resolution North Pacific Ocean model into the global ocean model used for CMIP6 and conducted an ocean biogeochemical simulation following OMIP protocols to evaluate its overall performance. Changes of the simulated biogeochemical fields in the North Pacific Ocean due to the enhanced horizontal resolution are studied by comparing between high and low resolution simulations. Enhancing the model horizontal resolution in the North Pacific Ocean does not make major impacts on globally integrated surface carbon flux budgets, but it brings about improvements in local distributions of dissolved inorganic carbon and surface fluxes. Specifically, more anthropogenic carbon is stored in the Kuroshio recirculation gyre as inferred from observations, insufficient outgassing in annual mean surface carbon flux is improved in the subpolar and the eastern tropical coastal regions. Primary productivity is enhanced in the subtropics presumably owing to the presence of mesoscale eddies. Most of these improvements are caused by those of physical fields. The present assessment would motivate use of high resolution models in the future projection experiments of ocean biogeochemical fields in the North Pacific Ocean.

Keywords: ocean biogeochemical model, ocean carbon circulation

©2021. Japan Geoscience Union. All Right Reserved.

A modeling study on distribution of dissolved Zinc in the North Pacific

*Kiminori Sugino[1], Akira Oka[1]

1. Atmosphere and Ocean Research Institute, The University of Tokyo

In the ocean, Zinc is a trace metal and exists in smaller amounts than the more abundant elements. Zn, like Fe, has been recognized as an important element for biological activities and biogeochemistry in the ocean. It has been clarified from studies in the 1980s that the distribution of dissolved Zn in the global ocean is similar to that of Si. However, while Si distribution in the ocean is controlled by diatom shell made of opal, Zn exists only about 1-3% in diatom shell. Since Zn is incorporated into organic matter, its distribution should be similar to that of Phosphate, a representative nutrient; however, this is not the case. Therefore, the mechanism of coupling between Zn and Si has been discussed. In recent years, the GEOTRACES program has led to a rapid increase in observational data on dissolved Zn in the ocean, which has accelerated the discussion of the dissolved Zn cycle process in the ocean. From model-based experiments, Vance et al.(2017) proposed the Southern Ocean hypothesis; excessive Zn uptake by phytoplankton in Southern Ocean causes Zn-depleted surface water masses and this anomaly is transported northward into the interior ocean, resulting in a distribution similar to that of Si. In this model-based experiment, the Zn was assumed to be coupled with the P model, and was independent of the Si model. The results showed that the correlation between Zn and Si was better than the correlation between Zn and P, despite the fact that Zn was associated with P and the model was independent of Si, supporting the Southern Ocean hypothesis. However, observational data from Kim et al.(2017) showed that the correlation between Zn and Si was broken in the North Pacific. This was not discussed in Vance et al.(2017), which focused on the coupling relationship between Zn and Si in the global ocean. Based on this finding that the Southern Ocean hypothesis of Vance et al.(2017) is not sufficient for the distribution of Zn in the North Pacific, this study aimed to clarify the process of Zn cycle that causes the decoupling of Zn and Si distributions in the North Pacific by using a model. In our model, the basic model setting of Zn was the same as that of Vance et al.(2017). Additional experiments based on the Southern Ocean hypothesis which assumed different Zn uptake rates from previous studies were also conducted. However, no improvement in the distribution of Zn in the North Pacific was observed in any case, indicating that additional processes are required to reproduce the high Zn concentration in the North Pacific. We conducted the next experiment based on the discussion in Kim et al.(2017) where the trace metal source from the North Pacific continental shelf is incorporated. We tested whether Zn-Si decoupling appears in the North Pacific by applying large Zn source onto the continental shelves of the Sea of Okhotsk and the Bering Sea. We found that Zn-Si decoupling was reproduced in all cases wherever the source of Zn was specified. In conclusion, our studies suggest that high Zn outflow from the coastal regions in the North Pacific might cause the Zn-Si decoupling in the North Pacific.

Keywords: GEOTRACES, Zinc, Silica, Ocean biogeochemical model, Marine chemistry

©2021. Japan Geoscience Union. All Right Reserved.

Geographical variation of Sr/Ca in skipjack tuna (*Katsuwonus peamis*) collected from Northwestern Pacific Ocean

*Shohgo Kawashima[1], Takaaki Itai[1]

1. The University of Tokyo

The trace element level of skipjack tuna (Katsuwonus pelamis, n=219) collected from various region of North Western Pacific Ocean (NPOW) was measured to analyze controlling factor of trace elements. The latitudinal migration of this species is useful to assess geographical difference from tropical equatorial region to Kuroshi-Oyashio transition region. Through the analysis of relative standard deviation, body size dependence, seasonal variation, regional variation, and elemental correlation, we could characterize homeostatic power of each element, and classified regional variation trend. There were several unique findings from this approach : (i) despite different biochemical function, major essential trace metals, e.g., Mn, Fe, Co, Cu, Zn, Mo, and Se, were mutually correlated, (ii) Zn shows poor correlation to the other essential metals, (iii) strong body size dependence is observed for Hg, Ca, Sr, Mo. (iv) simple mass balance model is useful to estimate muscular Hg level combining metabolic and behavioral data by archival tag, (v) the ratio of Sr/Ca plausibly reflect fine bone in muscle tissue shows strong linear correlation except for near equatorial ocean showing lower shift. Among these, the geographical variation of Sr/Ca in the bone of migratory fish has not been reported, thereby clarifying underlining mechanism is important.
The mean Sr/Ca of eight regions of NWPO is as following: 3.1 ±0.4 (south of Kamchatka Peninsula, n=19), 3.8 ±1.0 (off-Sanriku, n=25), 3.7 ±0.8 (off-Izu, n=18), 3.5 ±0.6 (off-Kochi, n=75), 4.1 ±0.2 (near Guam, n=9), 3.3 ±0.6 (East China Sea, n=55), 3.2 ±0.6 (Japan sea, n=9), 7.5 ±1.5 (equatorial region, n=8). The Sr/Ca in equatorial region is significantly higher than the other regions ($p < 0.01$). In the seawater, the level of these elements is constant with Sr/Ca ratio being 8.4 to 8.6 mmol/mol (Villiers ,1999). Considering reported distribution coefficient of Sr into Ca [Kd = (Sr/Ca)solid/(Sr/Ca)solution] which is insensitive to the pH is 0.27, expected Sr/Ca in bone equilibrated with seawater is 2.16 (Fujino, 1975). This indicated that Sr/Ca in bone of skipjack tuna is hard to explain by precipitation from seawater, particularly equatorial region. Unlike otholith, bone material likely affected by dietary intake. Dominant calcifying planktonic organism is coccolithophorid and foraminifera. The former forms calcite with Sr/Ca being 2.0 to 2.4 mmol/mol (Stoll and Schrag, 2000), while latter form aragonite with the mode value of Sr/Ca being 15 mmol/mol (Graham et al., 1982). Hence, preferential feeding of aragonite is a possible mechanism of high Sr/Ca in equatorial region. The other possible Sr rich diet is acantharea (radiorarean protozoa) which has the unique SrSO4 shell. This species mainly inhabit from mid-latitudes to the tropical, and it is known that their abundance increases relatively in oligotrophic waters. Although further approach is needed to distinguish these contribution, biomonitoring of migratory species can be useful tool of regional ecological structure in ocean.

Keywords: Skipjack, trace elements, North Western Pacific Ocean, ecology, Sr/Ca

©2021. Japan Geoscience Union. All Right Reserved.

Discussion about marine chemistry and biology

*Kazuhiro Misumi[1]

1. Environmental Science Research Laboratory, Central Research Institute of Electric Power Industry

In this slot, we will discuss about talks presented in this session and briefly introduce studies presented in the poster session.

©2021. Japan Geoscience Union. All Right Reserved.

[J] Oral | A (Atmospheric and Hydrospheric Sciences)：A-CG Complex & General

Fri. Jun 4, 2021 9:00 AM - 10:30 AM JST | Fri. Jun 4, 2021 12:00 AM - 1:30 AM UTC | Ch.11 Zoom Room 11

[A-CG39] Science in the Arctic Region

convener:Tetsu Nakamura(Faculty of Environmental Earth Science, Hokkaido University), Jun Ono(Japan Agency for Marine-Earth and Science and Technology), Rigen Shimada(Japan Aerospace Exploration Agency), Tomoki Morozumi(Research Faculty of Agriculture, Hokkaido University), Chairperson:Tetsu Nakamura(Faculty of Environmental Earth Science, Hokkaido University), Jun Ono(Japan Agency for Marine-Earth and Science and Technology), Tomoki Morozumi(Research Faculty of Agriculture, Hokkaido University), Rigen Shimada(Japan Aerospace Exploration Agency)

The Arctic and circumpolar region is the key area for the study of global change because the anthropogenic impact is projected to be the largest in this area due to the complicated feedback processes of the nature. A number of international and interdisciplinary research projects have been conducted for the studies on the land-atmosphere-ocean-cryosphere system. In order to understand the feedback processes occurring in the Arctic and to project the global warming in the future, we need to establish the intense observational network and to exchange the knowledge and information by combining the different scientific communities under the common interest of the Arctic. The objectives of this session are 1) to exchange our knowledge on the observational facts and integrated modelling and 2) to deepen our understanding on wide range of natural sciences related to the Arctic and the circumpolar region. Studies on humanities, social sciences, and interdisciplinary fields are also welcomed.

9:00 AM - 9:15 AM JST | 12:00 AM - 12:15 AM UTC

[ACG39-01] Rapid Arctic warming enhances Eurasian heat wave and East Asian heavy rainfall

*Tetsu Nakamura[1], Tomonori Sato[1] (1.Faculty of Environmental Earth Science, Hokkaido University)

9:15 AM - 9:30 AM JST | 12:15 AM - 12:30 AM UTC

[ACG39-02] Seasonal and long-term variations in the top of the atmosphere shortwave radiation over the Arctic

*Michinari Amma[1], Tadahiro Hayasaka[1] (1.Graduate School of Science, Tohoku University)

9:30 AM - 9:45 AM JST | 12:30 AM - 12:45 AM UTC

[ACG39-03] Machine learning prediction of wildfire over the Republic of Sakha, Russia

*Teppei J Yasunari[1,2,3], Ichigaku Takigawa[4,5], Kyu-Myong Kim[6], Akira Takeshima[7] (1.Arctic Research Center, Hokkaido University, 2.Global Station for Arctic Research, GI-CoRE, Hokkaido University, Sapporo, Japan, 3.Center for Natural Hazards Research, Hokkaido University, 4.RIKEN Center for Advanced Intelligence Project, 5.Institute for Chemical Reaction Design and Discovery (WPI-ICReDD), Hokkaido University, 6.NASA Goddard Space Flight Center, 7.Department of Civil Engineering, The University of Tokyo)

9:45 AM - 10:00 AM JST | 12:45 AM - 1:00 AM UTC

[ACG39-04] Recent Fire Trends in the Arctic Region under Climate Change

*Hiroshi Hayasaka[1] (1.Arctic Research Center, Hokkaido University)

10:00 AM - 10:15 AM JST | 1:00 AM - 1:15 AM UTC

[ACG39-05] Thaw subsidence and frost heave after 2018-20 wildfires around Batagay detected by InSAR and field observation

*Kazuki Yanagiya[1], Masato Furuya[2], Go Iwahana[3,4], Petr Danilov[5] (1.Graduate School of Science, Hokkiado University, 2.Department of Earth and Planetary Sciences, Hokkaido University, 3.International Arctic Research Center, University of Alaska Fairbanks, 4.Arctic Research Center, Hokkaido University, 5.Institute of Northern Applied Ecology North-Eastern Federal University in Yakutsk)

10:15 AM - 10:30 AM JST | 1:15 AM - 1:30 AM UTC

[ACG39-06] Detection of surface displacement caused by permafrost in Lena river delta using Sentinel-1 InSAR

*Ryuji Yamaguchi[1] (1.Department of Natural History Sciences, Graduate School of Science, Hokkaido University)

Rapid Arctic warming enhances Eurasian heat wave and East Asian heavy rainfall

*Tetsu Nakamura[1], Tomonori Sato[1]

1. Faculty of Environmental Earth Science, Hokkaido University

In 2020 Eurasia has experienced unprecedented warm conditions long-lasting from winter to summer. Especially in Siberia marked heat wave were observed as record breaking hot temperature 38.0 ℃ at Verkhoyansk in 20 June. At the same time in East Asia heavy rainfall was observed in southern China and western Japan, where severe flood affected large area and caused human live and economic damages. Rapid warming over the Arctic region as twice speed of the global mean surely induces increase of heat waves over the Eurasia. Concerning the considerable increase of heavy rainfall over the East Asia in the recent years, such rapid Arctic warming may also affect on East Asian rainfall. Here we study relationship between the heat wave and heavy rainfall occurred in eastern edge of the Eurasian continent. Both of the atmospheric internal variability and externally forced anomalies possibly cause the heat wave and the heavy rainfall. Especially the latter, because mainly due to the anthropogenic global warming, has anticipating warning of increase of severe disasters over those regions continuously to the future.

Keywords: Rapid Arctic warming, Heat wave, Heavy rainfall events

©2021. Japan Geoscience Union. All Right Reserved.

Seasonal and long-term variations in the top of the atmosphere shortwave radiation over the Arctic

*Michinari Amma[1], Tadahiro Hayasaka[1]

1. Graduate School of Science, Tohoku University

The Arctic region has recently experienced significant climate changes such as a decrease in sea ice extent and a decrease in snow cover. Sea ice and snow cover have high albedo, and these changes significantly impact shortwave radiation. Cloud is also essential in the variability of shortwave radiation. Therefore, it is necessary to quantitatively evaluate the effects of clouds, sea ice, and snow cover.

The recent decrease in sea ice extent has been linked to a decrease in the upward shortwave radiation at the top of the atmosphere over the Arctic ocean (Hartmann and Ceppi, 2014; Pistone et al., 2014). Besides, cloud variability on shortwave radiation variation is negligible (Pistone et al., 2014). Most of these previous studies have focused on annual mean or summer to analyze the long-term variation in shortwave radiation. However, the seasonal variability of sea ice and snow cover in the Arctic is large. It is necessary to evaluate the long-term variation in shortwave radiation in each season. This study analyzes the long-term variation in shortwave radiation in each season from 2001 to 2019 using satellite observation data.

The upward shortwave radiation had been a downward trend over the entire Arctic region from 2001 to 2012, and the sizeable inter-annual variability after 2012. The variability is different for land and ocean. Over the ocean, the upward shortwave radiation decreased from 2001 to 2007, and sizeable inter-annual variability after 2007. It relates to an increase in the sea ice variability after 2007. The sea ice extent decreased sharply in 2007. In March 2008, there was a sharp increase in the one-year ice fraction (Richer-Menge and Druckenmiller, 2020). Thus, it seems to cause an increase in sea ice variability. The shortwave cloud radiative effect increased after 2007, and it weakens the decline in shortwave radiation. Over the land, it seems to be attributed to the increase in the snow cover extent's inter-annual variability after 2012.

Seasonal variability is different between land and ocean. Sea ice extent is maximum in March and minimum in September. Snow cover extent is maximum in February and minimum in August. The upward shortwave radiation is maximum in June over the ocean and in May over the land. Besides, since the variability of sea ice, snow cover, and cloud is different each month, the months with the largest variations in upward shortwave radiation also vary from year to year. Therefore, it is necessary to pay attention to seasonal changes in sea ice, snow cover, and clouds to understand the long-term variation in shortwave radiation.

Keywords: shortwave radiation, sea ice, snow cover, cloud

©2021. Japan Geoscience Union. All Right Reserved.

Machine learning prediction of wildfire over the Republic of Sakha, Russia

*Teppei J Yasunari[1,2,3], Ichigaku Takigawa[4,5], Kyu-Myong Kim[6], Akira Takeshima[7]

1. Arctic Research Center, Hokkaido University, 2. Global Station for Arctic Research, GI-CoRE, Hokkaido University, Sapporo, Japan, 3. Center for Natural Hazards Research, Hokkaido University, 4. RIKEN Center for Advanced Intelligence Project, 5. Institute for Chemical Reaction Design and Discovery (WPI-ICReDD), Hokkaido University, 6. NASA Goddard Space Flight Center, 7. Department of Civil Engineering, The University of Tokyo

In this study, we carried out machine learning (ML) prediction for the nation-averaged monthly mean datasets over the Republic of Sakha in Russia during 2003 and 2019. We used the Aqua and Terra MODIS averaged fire pixel count (FPC; https://feer.gsfc.nasa.gov/) data for objective variables. For explanatory variables, we selected the Aqua MODIS Snow Cover Fraction (SCF; https://nsidc.org/data/MYD10CM) and many atmospheric and land variables from NASA's MERRA-2 (Modern-Era Retrospective analysis for Research and Applications, Version 2: https://gmao.gsfc.nasa.gov/reanalysis/MERRA-2/) re-analysis data (total 170 variables). The FPC and SCF data were re-gridded to the MERRA-2 grid spacing in advance. All the data were then averaged over the Republic of Sakha with the nation mask data by Natural Earth, using SPRING (SPeroidal coordinates Regridding Interpolation table Generator: http://hydro.iis.u-tokyo.ac.jp/~akira/page/tmp/2020Feb_nations/). To assess the impact of removing small-scale fires on prediction performance, we prepared four fire datasets: all the data, and data only considering FPC equal to or greater than 5, 10, 20 counts per MERRA-2 grid, M2G, in which we treated the months with no corresponding fire data as zero fire. For the explanatory variables, we also made the time-lagged data from zero to six months for each variable to take pre-fire information into account, which was then all standardized (i.e., we used a total of 1190 explanatory variables for ML). We implemented ML prediction by three Linear Regression (LR) methods (ordinary LR; penalized LR: Lasso and Ridge) and three non-linear ensemble methods (Extra Trees, Random Forest, and Gradient Boosting). The data during July 2003 and December 2014 and during January 2015 and December 2019 were used for training and test, respectively.

Both the ordinary LR and Ridge methods did not predict the test data at all. Those methods likely induced overfitting to the training data because of too high R^2 scores. Lasso mitigated the overfitting to the training data and improved the test data's performance, but the scores were still not increased (R^2 of 0.45-0.48). All the non-linear ensemble methods showed much better results than those of the linear forms. Significantly, Random Forest and Gradient Boosting methods outperformed the others. The highest R^2 score was 0.75 by Gradient Boosting with the fire data, including FPC equal to or greater than ten counts/M2G. In this case, the permutation importance showed the top 5 variables dominant in the following order: "cloud area fraction for middle clouds" (lag 0), "transcom planetary boundary layer height" (lag 1), "lifting condensation level" (lag 0), "fractional area of wilting zone" (lag 0), and "in cloud optical thickness of low clouds" (lag 0). In the non-linear methods, the fire data, including all the fire data, showed worse performance than the other fire data, which was similar to what Yasunari et al. (in preparation) discussed over a large area of Siberia.

Keywords: wildfire, machine learning, Siberia, Russia, prediction, Arctic

©2021. Japan Geoscience Union. All Right Reserved.

Recent Fire Trends in the Arctic Region under Climate Change

*Hiroshi Hayasaka[1]

1. Arctic Research Center, Hokkaido University

Recent studies[1-4]have revealed the weather conditions for large-scale fires in the Arctic. As the westerlies meandered and the high-pressure system developed at upper air, fires were activated under the temperate (cTe) moved from the south. This report analyzes recent fire activity in the Arctic region (Northern Hemisphere (> 50 N, 0-180 E & W) north of latitude 50 N). The number of hotspots (HS) in the summer (JJA) 19 years (2002-2020) detected by MODIS (Moderate Resolution Imaging Spectroradiometer) was about 3.98 million, and the Arctic region was divided into 288 grid cells (cell size: 2.5 N, 10 E & W). The annual average fire density of each grid (Number of hotspots (HSs): $10^3 km^{-2} year^{-1}$) was calculated to identify active fire areas in the Arctic.

Based on the analysis results, we identified active fire areas and examined the relationship between climate change and fire. Figure 1 shows the distribution of the annual average fire density. Active fire areas in the Arctic region were found from Central Siberia to western Canada, where 84% of all HSs were detected. In this report, the results of analysis of fire activity of the entire Arctic region and three major research areas with particularly active fire activity (1. Krasnoyarsk (57.5-65 N, 90-120 E), 2. N. Sakha (62.5-70 N, 120-150 E), and 3. Alaska (62.5-70 N, 130-160 W)) were reported.

Major analysis results:

1. The very active fires in the Krasnoyarsk area occurred on July 23, 2019, under the presence of warm air masses (cTe = 290 K) moved from south related to the westerly meandering and the development of high pressure at upper air.

2. The average number of fires (HS) in the Arctic region (> 50 N) was about 210,000 per year, and the number of fires north of latitude 60 degrees north was about 110,000. HS of the largest fire year, 2012, reached about 370,000.

3. In 2019 and 2020, fires in north latitude 60-70 degrees were active, with about 200,000 and 180,000 annually.

4. The largest fire year in the Krasnoyarsk area (1. Krasnoyarsk in Figure 1) was 2019, with approximately 130,000 HS, about 4.3 times the average.

5. The number of fires (HS) in northern Sakha was remarkable, about 65,000 in 2019 and about 80,000 in 2020, and were 3-4 times the average.

6. The average fire location in northern Sakha for 19 years was 65.2 N. The total number of fires in 2019 was about 66,000, and their average fire location was 67.2 N and it was within the Arctic Circle.

7. The number of HSs in Alaska was about 110,000 in 2004 and about 60,000 in 2005.

8. Alaska's average fire location for 19 years was 65.3 N. The highest average fire position was 66.4

©2021. Japan Geoscience Union. All Right Reserved.

degrees.

9. The weather conditions during the active fire period in the three major research areas were westerly meandering, formation of an anticyclone system, and northward movement of the warm air masses from the south. It was similar to the results of recent studies[1-4].

10. The recent fire activity described above may indicate the impact of climate change on Arctic fires and is one piece of evidence of the impact of climate change.

References:

1. H. Hayasaka, H. L. Tanaka, P. A. Bieniek, Synoptic-scale fire weather conditions in Alaska, Polar Science, 10-3, 217-226, 2016.

2. H. Hayasaka, K. Yamazaki, and D. Naito, Weather Conditions and Warm Air Masses in Southern Sakha During Active Forest Fire Periods, J. Disaster Res., 14-4, 641-648, 2019.

3. H. Hayasaka, K. Yamazaki, and D. Naito, Weather Conditions and Warm Air Masses during Active Fire-periods in Boreal Forests, Polar Science, 22, 1-8, Article 100472, 2019.
4. H. Hayasaka, G. V. Sokolova , A. Ostroukhov and D. Naito, Classification of Active Fires and Weather Conditions in the Lower Amur River Basin, Remote Sens. 12(19), 3204, 2020.

Keywords: hotspot, climate change, warm air mass, westerlies, meandering

©2021. Japan Geoscience Union. All Right Reserved.

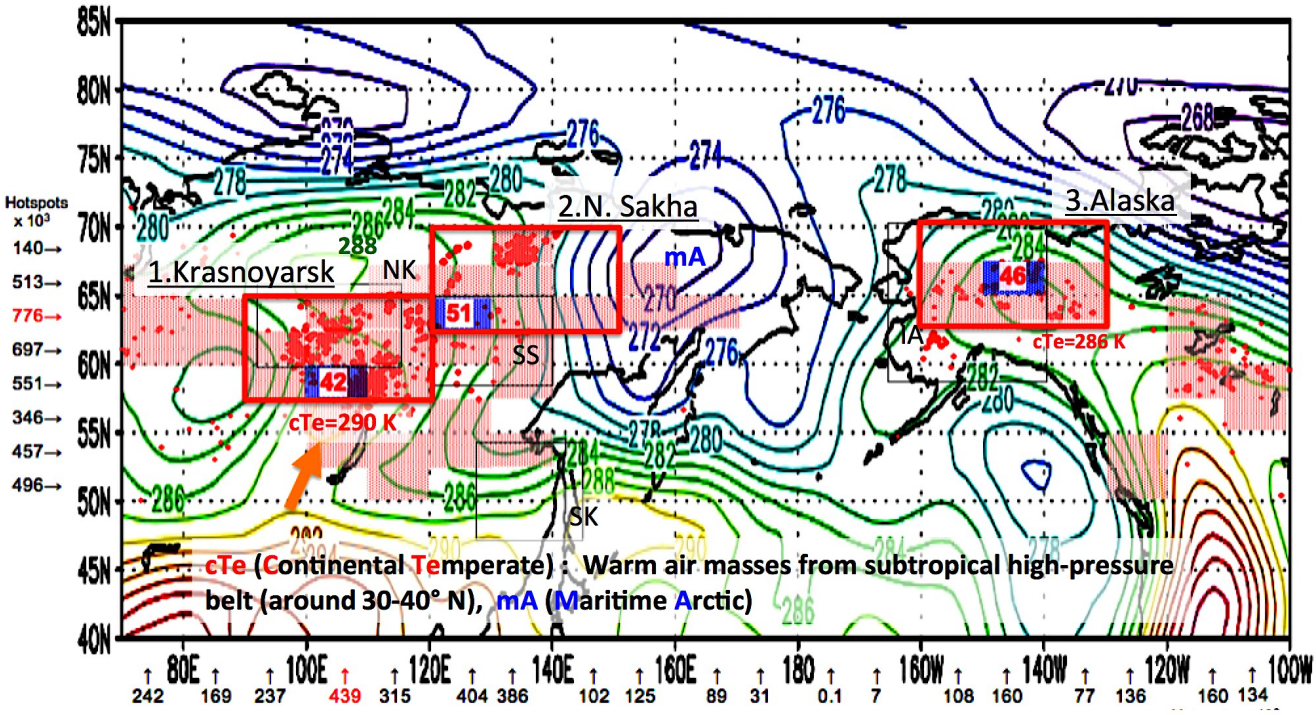


Figure 1. Map of active fire areas in the Arctic region (70° E-100° W, > 50° N).
High fire density grid cell (>10 (HSs 10^{-3} km^{-2} year^{-1})) are shown by rectangle with red dot pattern.
Top three very high fire density grid cells (>40) are shown by purple rectangle with their values.
Values with arrow at X and Y axis total number of hotspots (HSs) of their zone (50-70° N and 0-180° E & W).
Red dots are HSs on July 23, 2019. Contour line shows temperature (deg. K) at 850 hPa.
Three major study areas (rectangle with red line): 1.Krasnoyarsk, 2.N. Sakha, 3.Alaska.
NK, SS, SK, IA: previous study areas. Base map from NOAA Physical Sciences Laboratory.

©2021. Japan Geoscience Union. All Right Reserved.

Thaw subsidence and frost heave after 2018-20 wildfires around Batagay detected by InSAR and field observation

*Kazuki Yanagiya[1], Masato Furuya[2], Go Iwahana[3,4], Petr Danilov[5]

1. Graduate School of Science, Hokkiado University, 2. Department of Earth and Planetary Sciences, Hokkaido University, 3. International Arctic Research Center, University of Alaska Fairbanks, 4. Arctic Research Center, Hokkaido University, 5. Institute of Northern Applied Ecology North-Eastern Federal University in Yakutsk

The Arctic experienced numerous wildfires last year, and from June to August 2020, satellite data revealed record releases of carbon dioxide from wildfires. Peatland, in the Arctic, contains large amounts of organic carbon, and their discharge to the atmosphere can create positive feedbacks to further increase air temperature. Furthermore, wildfires burn the surface vegetation layer that acts as a thermal insulator, and it accelerates the thawing of permafrost over years to decades. Although the thaw depth can recover together with the recovery of surface vegetation, the massive segregated ice is not recoverable once it melted.

Around our study area of Batagay, Sakha Republic, Eastern Siberia, Sentinel-2 optical satellite image showed an increase of the burned area in 2019-20. Also, in June 2020, the highest daily maximum temperature of 38.0 degrees Celcius was recorded in Verkhoyansk, 55 km west of Batagay. To reveal the amount of fire-induced permafrost thawing, we used the remote-sensing technique called InSAR (Interferometric Synthetic Aperture Radar). InSAR can create the ground deformation map over those fire sites and detect deformation signals on a scale of several cm. Besides, we conducted a field observation in September 2019 for validations: 1) installed a soil thermometer and soil moisture meter; 2) established a reference point for leveling and first survey; 3) measured the thawing depth with a frost probe.

We analyzed two types of InSAR images, one for seasonal deformations and another for long-term deformations over a year. For seasonal ground deformations immediately after the fire, we mainly analyzed Sentinel-1 images. Sentinel-1 is the ESA's C-band SAR satellite, which has a short imaging interval of 12 days. Because of its shorter wavelength, vegetation changes can easily lose coherence and prevented us from detecting ground deformation signals in some pairs immediately after the fire. However, after the end of September, we detected displacements approaching toward the satellite line-of-sight direction at the fire sites. It indicates uplift signals due presumably to frost heave at the fire scar.

For long-term deformations over one year, we used ALOS2 images derived by JAXA's L-band SAR satellite. In the previous studies in Alaska, the ground deformation signal immediately after the fire could not be detected due to the coherence loss in the pairs derived from pre-fire and post-fire SAR images. Indeed, we could not detect deformation signals at the fire scars from the June pairs derived before and after the fire. However, the January pairs and March pairs, both of which were acquired before and after the fire, showed relatively high coherence even in the fire scar. We interpret that, because the studied Verkhoyansk Basin is very dry and has little snow cover, the microwaves could penetrate the snow layer, which allowed us to detect deformation signals even in winter. Yanagiya and Furuya (2020) validated the consistency of the winter uplift signal for the 2014 fire site. InSAR images indicated clear subsidence signals by as much as 15 cm. On the other hand, at the fire sites near Batagaika mega slump, we detected frost heave signals in the burned year and subsidence signals after the next to the burned year. To investigate the specific ground deformation at the two fire sites near Batagaika mega slump, we also

©2021. Japan Geoscience Union. All Right Reserved.

analyzed the SM1 high spatial resolution data (3 m) of ALOS2 taken in 2020-21. We validated the deformation signals with the thawing depth, the time series of ground temperature, and high-resolution optical images of WorldView-2.

Keywords: InSAR, ALOS2, Sentinel-1, permafrost, wildfire, Thermokarst

©2021. Japan Geoscience Union. All Right Reserved.

Detection of surface displacement caused by permafrost in Lena river delta using Sentinel-1 InSAR

*Ryuji Yamaguchi[1]

1. Department of Natural History Sciences, Graduate School of Science, Hokkaido University

Lena River Delta at 72° N, in Sakha Republic, Russia, is extensively underlain by permafrost, which is vulnerable to ongoing global warming. The impact of permafrost thawing spans from regional problems such as changes in surface topography and damages on infrastructure, to global problems such as the possible feedback of greenhouse gas emission. Direct monitoring of permafrost over a wide spatial coverage with fine resolution is infeasible. However, seasonal freeze-thaw cycle and inter-annual changes in permafrost can generate measurable surface displacements. Some previous studies report surface displacement signals in an island composing Lena River Delta by using In Situ measurement and satellite InSAR data. There are, however, few studies that comprehensively examined the surface deformation over the entire area in Lena River Delta.

InSAR can map surface displacements by taking phase differences at the same pixel locations, using two radar imaginaries. It has the advantage of high spatial resolution, wide spatial coverage, and no need to set any ground-based instruments. In this study, we examined surface displacements over Lena River Delta from March 2019 to December 2020 by InSAR, using radar image of Sentinel-1 launched by ESA.

As result, we detected larger inter-annual subsiding velocity in some islands than it around them, such as Kharadang Island, Dyanglakh Island, and Sobo-Sise Island all composed by Yedoma. The difference of subsidence between in the islands and around them are about 0.5-1.5 cm/year (LOS).

©2021. Japan Geoscience Union. All Right Reserved.

[J] Oral | A (Atmospheric and Hydrospheric Sciences)：A-CG Complex & General

Fri. Jun 4, 2021 10:45 AM - 12:15 PM JST | Fri. Jun 4, 2021 1:45 AM - 3:15 AM UTC | Ch.11 Zoom Room 11

[A-CG39] Science in the Arctic Region

convener:Tetsu Nakamura(Faculty of Environmental Earth Science, Hokkaido University), Jun Ono(Japan Agency for Marine-Earth and Science and Technology), Rigen Shimada(Japan Aerospace Exploration Agency), Tomoki Morozumi(Research Faculty of Agriculture, Hokkaido University), Chairperson:Tetsu Nakamura(Faculty of Environmental Earth Science, Hokkaido University), Jun Ono(Japan Agency for Marine-Earth and Science and Technology), Tomoki Morozumi(Research Faculty of Agriculture, Hokkaido University), Rigen Shimada(Japan Aerospace Exploration Agency)

The Arctic and circumpolar region is the key area for the study of global change because the anthropogenic impact is projected to be the largest in this area due to the complicated feedback processes of the nature. A number of international and interdisciplinary research projects have been conducted for the studies on the land-atmosphere-ocean-cryosphere system. In order to understand the feedback processes occurring in the Arctic and to project the global warming in the future, we need to establish the intense observational network and to exchange the knowledge and information by combining the different scientific communities under the common interest of the Arctic. The objectives of this session are 1) to exchange our knowledge on the observational facts and integrated modelling and 2) to deepen our understanding on wide range of natural sciences related to the Arctic and the circumpolar region. Studies on humanities, social sciences, and interdisciplinary fields are also welcomed.

10:45 AM - 11:00 AM JST | 1:45 AM - 2:00 AM UTC

[ACG39-07] Research progresses of PAWCs (Pan-Arctic Water-Carbon Cycles) focusing on water-carbon cycles in northern Eurasia

★Invited Papers

*Tetsuya Hiyama[1], Hotaek Park[2], Tomonori Sato[3], Hiroki Mizuochi[4], Akihiko Ito[5], Kazuhito Ichii[6], Yoshihiro Iijima[7] (1.Institute for Space-Earth Environmental Research, Nagoya University, 2.Japan Agency for Marine-Earth Science and Technology, 3.Graduate School of Environmental Science, Hokkaido University, 4.Geological Survey of Japan, National Institute of Advanced Industrial Science and Technology, 5.Center for Global Environmental Research, National Institute for Environmental Studies, 6.Center for Environmental Remote Sensing, Chiba University, 7.Graduate School of Bioresources, Mie University)

11:00 AM - 11:15 AM JST | 2:00 AM - 2:15 AM UTC

[ACG39-08] PMIP4/CMIP6 last interglacial simulations using three different versions of MIROC: importance of vegetation

*Ryouta O'ishi[1], Wing-Le Chan[1], Ayako Abe-Ouchi[1,2,3], Sam Sherriff-Tadano[1], Rumi Ohgaito[3], Masakazu Yoshimori[1] (1.Atmosphere and Ocean Research Institute, the Universitoy of Tokyo, 2.National Institute of Polar Research, 3.Japan Agency for Marine–Earth Science and Technology)

11:15 AM - 11:30 AM JST | 2:15 AM - 2:30 AM UTC

[ACG39-09] Future projection of greenhouse gas emissions due to permafrost degradation with a global land surface model

*Tokuta Yokohata[1], Kazuyuki Saito[2], Go Iwahana[3], Katsumasa Tanaka[1,4] (1.National Institute for Environmental Studies, 2.Japan Agency for Marine-Earth Science and Technology, 3.University of Alaska, Fairbanks, 4.Laboratoire des Sciences du Climat et de l'Environnement (LSCE), Commissariat à l'énergie atomique et aux énergies alternatives (CEA))

11:30 AM - 11:45 AM JST | 2:30 AM - 2:45 AM UTC

[ACG39-10] Record high Pacific Arctic seawater temperatures and delayed sea ice advance in response to episodic atmospheric blocking

*Tsubasa Kodaira[1], Takuji Waseda[1], Takehiko Nose[1], Jun Inoue[2] (1.The University of Tokyo, 2.NIPR)

11:45 AM - 12:00 PM JST | 2:45 AM - 3:00 AM UTC

[ACG39-11] Laboratory experiments of ice floe formation under wave motions

*Yasushi Fujiwara[1], Tomotaka Katsuno[1], Takuji Waseda[1], Takehiko Nose[1], Tsubasa Kodaira[1] (1.Graduate School of Frontier Sciences, the University of Tokyo)

12:00 PM - 12:15 PM JST | 3:00 AM - 3:15 AM UTC

[ACG39-12] Experimental research on wave attenuation in the Marginal Ice Zone

*Tomotaka Katsuno[1], Yasushi Fujiwara[1], Takuji Waseda[1], Takehiko Nose[1], Tsubasa Kodaira[1] (1.Graduate School of Frontier Sciences, University of Tokyo)

Research progresses of PAWCs (Pan-Arctic Water-Carbon Cycles) focusing on water-carbon cycles in northern Eurasia

*Tetsuya Hiyama[1], Hotaek Park[2], Tomonori Sato[3], Hiroki Mizuochi[4], Akihiko Ito[5], Kazuhito Ichii[6], Yoshihiro Iijima[7]

1. Institute for Space-Earth Environmental Research, Nagoya University, 2. Japan Agency for Marine-Earth Science and Technology, 3. Graduate School of Environmental Science, Hokkaido University, 4. Geological Survey of Japan, National Institute of Advanced Industrial Science and Technology, 5. Center for Global Environmental Research, National Institute for Environmental Studies, 6. Center for Environmental Remote Sensing, Chiba University, 7. Graduate School of Bioresources, Mie University

Research progresses of PAWCs (Pan-Arctic Water-Carbon Cycles) will be introduced. The purpose of PAWCs is to integrate atmospheric- terrestrial water and carbon cycles across atmosphere –biosphere –hydrosphere –cryosphere in the region. To achieve this goal, we are developing a water traceable integrated model (WTIM), which can calculate spatiotemporal variations in the atmospheric moisture transport, moisture flux convergence, precipitation, vegetation condition, permafrost degradation, and river discharge, with important boundary conditions of the Arctic sea ice extent. We also estimate spatiotemporal variations of water-covered area and vegetation condition in northern Eurasia, using satellite remote sensing data and WTIM products with the help of spatiotemporal data fusion technics. The water-covered (inundation) map will be used for improvement of the estimation of methane emission from wetlands.

Keywords: atmospheric water cycle, terrestrial water cycle, greenhouse gas flux

©2021. Japan Geoscience Union. All Right Reserved.

PMIP4/CMIP6 last interglacial simulations using three different versions of MIROC: importance of vegetation

*Ryouta O'ishi[1], Wing-Le Chan[1], Ayako Abe-Ouchi[1,2,3], Sam Sherriff-Tadano[1], Rumi Ohgaito[3], Masakazu Yoshimori[1]

1. Atmosphere and Ocean Research Institute, the Universitoy of Tokyo, 2. National Institute of Polar Research, 3. Japan Agency for Marine–Earth Science and Technology

We carry out three sets of last interglacial (LIG) experiments, named lig127k, and of pre-industrial experiments, named piControl, both as part of PMIP4/CMIP6 using three versions of the MIROC model: MIROC4m, MIROC4m-LPJ, and MIROC-ES2L. The results are compared with reconstructions from climate proxy data. All models show summer warming over northern high-latitude land, reflecting the differences between the distributions of the LIG and present-day solar irradiance. Globally averaged temperature changes are −0.94 K (MIROC4m), −0.39 K (MIROC4m-LPJ), and −0.43 K (MIROC-ES2L). Only MIROC4m-LPJ, which includes dynamical vegetation feedback from the change in vegetation distribution, shows annual mean warming signals at northern high latitudes, as indicated by proxy data. In contrast, the latest Earth system model (ESM) of MIROC, MIROC-ES2L, which considers only a partial vegetation effect through the leaf area index, shows no change or even annual cooling over large parts of the Northern Hemisphere. Results from the series of experiments show that the inclusion of full vegetation feedback is necessary for the reproduction of the strong annual warming over land at northern high latitudes. The LIG experimental
results show that the warming predicted by models is still underestimated, even with dynamical vegetation, compared to reconstructions from proxy data, suggesting that further investigation and improvement to the climate feedback mechanism are needed.

Keywords: Paleoclimate, General Circulation Model, Polar amplification

©2021. Japan Geoscience Union. All Right Reserved.

Future projection of greenhouse gas emissions due to permafrost degradation with a global land surface model

*Tokuta Yokohata[1], Kazuyuki Saito[2], Go Iwahana[3], Katsumasa Tanaka[1,4]

1. National Institute for Environmental Studies, 2. Japan Agency for Marine-Earth Science and Technology, 3. University of Alaska, Fairbanks, 4. Laboratoire des Sciences du Climat et de l'Environnement (LSCE), Commissariat à l'énergie atomique et aux énergies alternatives (CEA)

To date, the treatment of permafrost in earth system models has been simplified due to the prevailing uncertainties in the processes involving frozen ground. In this study, we improved the modeling of permafrost physical processes in a state-of-the-art earth system model (MIROC) by taking into account some of the relevant physical properties of soil such as changes in the thermophysical properties due to freezing (https://doi.org/10.1186/s40645-020-00380-w). As a result, the improved version of the model was able to reproduce a more realistic permafrost distribution at the southern limit of the permafrost area by increasing the freezing of soil moisture in winter. The improved modeling of permafrost processes also had a significant effect on future projections. Using the conventional formulation, the predicted cumulative reduction of the permafrost area by year 2100 was approximately 60% (40–80% range of uncertainty from a multi-model ensemble) in the RCP8.5 scenario, while with the improved formulation, the reduction was approximately 35% (20–50%). Our results indicate that the improved treatment of permafrost processes in global climate models is important to ensuring more reliable future projections. In addition, the processes of greenhouse gas (GHG) emissions due to permafrost degradation are not considered in many earth-system models. Therefore, we developed a model to diagnose that processes by using the output of earth system models (https://doi.org/10.1186/s40645-020-00366-8). The model called PDGEM (Permafrost Degradation and GHG Emission Model) describes the thawing of the Arctic permafrost including the Yedoma layer due to climate change and the GHG emissions. Our model simulations show that the total GHG emissions from permafrost degradation in the RCP8.5 scenario was estimated to be 31-63 PgC for CO2 and 1261-2821 TgCH4 for CH4 (68th percentile of the perturbed model simulations, corresponding to a global average surface air temperature change of 0.05–0.11 ˚C), and 14-28 PgC for CO2 and 618-1341 TgCH4 for CH4 (0.03–0.07 ˚C) in the RCP2.6 scenario. An advantage of PDGEM is that geographical distributions of GHG emissions can be estimated by combining a state-of-the-art land surface model featuring detailed physical processes with a GHG release model using a simple scheme, enabling us to consider a broad range of uncertainty regarding model parameters. In regions with large GHG emissions due to permafrost thawing, it may be possible to help reduce GHG emissions by taking measures such as restraining land development.

Keywords: Climate change, Future projection, Permafrost degradataion, Carbon cycle

©2021. Japan Geoscience Union. All Right Reserved.

Record high Pacific Arctic seawater temperatures and delayed sea ice advance in response to episodic atmospheric blocking

*Tsubasa Kodaira[1], Takuji Waseda[1], Takehiko Nose[1], Jun Inoue[2]

1. The University of Tokyo, 2. NIPR

Arctic sea ice is rapidly decreasing during the recent period of global warming. One of the significant factors of the Arctic sea ice loss is oceanic heat transport from lower latitudes. For months of sea ice formation, the variations in the sea surface temperature over the Pacific Arctic region were highly correlated with the Pacific Decadal Oscillation (PDO). However, the seasonal sea surface temperatures recorded their highest values in autumn 2018 when the PDO index was neutral. It is shown that the anomalous warm seawater was a rapid ocean response to the southerly winds associated with episodic atmospheric blocking over the Bering Sea in September 2018. This warm seawater was directly observed by the R/V Mirai Arctic Expedition in November 2018 to significantly delay the southward sea ice advance. If the atmospheric blocking forms during the PDO positive phase in the future, the annual maximum Arctic sea ice extent could be dramatically reduced.

Keywords: Pacific Arctic Region , Atmospheric Blocking, PDO

©2021. Japan Geoscience Union. All Right Reserved.

Laboratory experiments of ice floe formation under wave motions

*Yasushi Fujiwara[1], Tomotaka Katsuno[1], Takuji Waseda[1], Takehiko Nose[1], Tsubasa Kodaira[1]

1. Graduate School of Frontier Sciences, the University of Tokyo

Arctic sea ice is rapidly reducing, and an increasing trend of the wave height in the Arctic sea has been reported. Therefore, there is an increasing demand for improved modeling of wave-ice interactions. When seawater is frozen under wave effects, frazil crystals consolidate to form circular floes called pancake ice. The floe size is an important parameter in the sea ice thermodynamics and wave attenuation, but the knowledge of the relation between wave parameters and floe sizes is very limited. Shen et al.'s (2001, 2004) theory and experiments suggest that the floe size is limited by the tensile failure due to wave orbital motion. This leads to the scaling law $D/L \propto a^{-0.5}$, where D, L, and a are floe diameter, wavelength, and wave amplitude, respectively. However, the experimental data to support their theory is rather limited. To deepen the understanding of wave-ice interaction processes under controlled conditions, we conducted laboratory experiments using a newly built wave tank (8m x 1.5m x 1.0m with 0.6m water depth) with a freezing facility.

The experiments were conducted with freshwater, supposing that the difference in material and thermodynamic properties from seawater would not qualitatively alter the processes. To reproduce the ice floe formation processes in our wave tank, we cooled the water while monochromatic waves of various periods and amplitudes are continuously produced. Due to continuous agitation by waves, ice formed as numerous thin pieces of 1~5 cm size, and the pieces consolidated to form floes with raised ridges similar to observed pancake ice. The sizes of the floes were relatively uniform in each case. Representative floe sizes were objectively estimated from ridges detected by image processing.

The floes were larger with longer waves and smaller with larger wave amplitudes, both of which were consistent with Shen's model. However, the floe sizes normalized with wavelength showed stronger dependence on wave amplitudes. This result suggests a need for a new model of ice floe formation. Also, the results imply the presence of upper and lower limits of a for floes to form. These results, together with the experimental results of wave attenuation by the ice floes, will be useful for a simple description and understanding of wave-ice interactions in the marginal ice zone.

Keywords: wave-ice interaction, laboratory experiment, pancake ice

©2021. Japan Geoscience Union. All Right Reserved.

Experimental research on wave attenuation in the Marginal Ice Zone

*Tomotaka Katsuno[1], Yasushi Fujiwara[1], Takuji Waseda[1], Takehiko Nose[1], Tsubasa Kodaira[1]

1. Graduate School of Frontier Sciences, University of Tokyo

The coverage of sea ice in the Arctic sea is decreasing. This leads to an increase in wave height and sea failure. Between the open water and solid ice, the wave propagates to the Marginal Ice Zone (MIZ) and ice floes attenuate waves. However, the mechanism of wave attenuation under sea ice is not clear.

Wave attenuation under ice cover is investigated. Waves generated in the open-water area attenuate while propagating over the ice-covered area, but the mechanism of attenuation is still unclear, and various formulations are proposed. For example, in some models, wave energy is dissipated in the viscous boundary layer right beneath the horizontally immobile thin ice layer (e.g., Weber, 1987). In such cases, the spatial decay scale is proportional to $f^{-3.5}$, where f is the wave frequency. In other models, the ice is represented as a viscous layer with a finite thickness (e.g., Lamb, 1932), and wave energy is dissipated throughout the ice layer. This leads to the decay scale proportional to f^{-5}. Furthermore, these models consider ice as a continuous layer and do not take floe size into account. Unclear is a floe-to-wavelength ratio at which this approximation breaks down.

The experiment facility was built in the Kashiwa campus, the University of Tokyo. A wave tank with a dimension of 8m x 1.5m x 1.0m (0.6m water depth), with a plunger-type wavemaker and a beach at each end, is located in a freezer room. Surface displacement was measured with low-cost ultrasonic wave gauges, which were developed using modules of microcomputers and rangefinders. The experiments were conducted with freshwater, supposing that the difference in material and thermodynamic properties from seawater would not qualitatively alter the processes.

Using the ice floes produced under various wave forcings, we measured the propagating waves with various frequencies using an array of ultrasonic wave gauges. The results suggest that waves do not exponentially decay when the wavelength is shorter than or similar to floe sizes. It is suggested that the inertia of ice floes can no longer be neglected and that wave reflection and scattering become important at this scale. On the other hand, when waves are longer than floe sizes, the attenuation property is insensitive to floe sizes, suggesting the validity of representing ice as a continuous layer. In such cases, the decay scale followed f^{-3} to $f^{-3.5}$, which suggests the applicability of the dissipation model through the viscous boundary layer. However, the effective viscosity estimated from the measurements was greater than the molecular viscosity by more than one order of magnitude, so further investigation of the dissipation process is needed.

Keywords: wave attenuation, wave-ice interaction, wave ice tank, pancake ice

©2021. Japan Geoscience Union. All Right Reserved.

[J] Oral | A (Atmospheric and Hydrospheric Sciences)：A-CG Complex & General

Fri. Jun 4, 2021 1:45 PM - 3:15 PM JST | Fri. Jun 4, 2021 4:45 AM - 6:15 AM UTC | Ch.11 Zoom Room 11

[A-CG39] Science in the Arctic Region

convener:Tetsu Nakamura(Faculty of Environmental Earth Science, Hokkaido University), Jun Ono(Japan Agency for Marine-Earth and Science and Technology), Rigen Shimada(Japan Aerospace Exploration Agency), Tomoki Morozumi(Research Faculty of Agriculture, Hokkaido University), Chairperson:Tetsu Nakamura(Faculty of Environmental Earth Science, Hokkaido University), Jun Ono(Japan Agency for Marine-Earth and Science and Technology), Tomoki Morozumi(Research Faculty of Agriculture, Hokkaido University), Rigen Shimada(Japan Aerospace Exploration Agency)

The Arctic and circumpolar region is the key area for the study of global change because the anthropogenic impact is projected to be the largest in this area due to the complicated feedback processes of the nature. A number of international and interdisciplinary research projects have been conducted for the studies on the land-atmosphere-ocean-cryosphere system. In order to understand the feedback processes occurring in the Arctic and to project the global warming in the future, we need to establish the intense observational network and to exchange the knowledge and information by combining the different scientific communities under the common interest of the Arctic. The objectives of this session are 1) to exchange our knowledge on the observational facts and integrated modelling and 2) to deepen our understanding on wide range of natural sciences related to the Arctic and the circumpolar region. Studies on humanities, social sciences, and interdisciplinary fields are also welcomed.

1:45 PM - 2:00 PM JST | 4:45 AM - 5:00 AM UTC

[ACG39-13] Impacts of Riverine Carbon and Nutrient Delivery on Arctic Ocean Acidification

*Yuanxin Zhang[1], Michiyo Yamamoto-Kawai[1], Eiji Watanabe[2] (1.Tokyo University of Marine Science and Technology, 2.Japan Agency for Marine-Earth Science and Technology)

2:00 PM - 2:15 PM JST | 5:00 AM - 5:15 AM UTC

[ACG39-14] Spreading of aragonite undersaturated water in the Canada Basin of the Arctic Ocean

*Haruka Tsujimoto[1], Michiyo Yamamoto-Kawai[1], Yuanxin Zhang[1] (1.Tokyo University of Marine Science and Technology)

2:15 PM - 2:30 PM JST | 5:15 AM - 5:30 AM UTC

[ACG39-15] Glacier and whale monitoring with an Ocean-Bottom Seismometer at the calving front

*Evgeny A. Podolskiy[1], Yoshio Murai[2], Naoya Kanna[3], Shin Sugiyama[4] (1.Arctic Research Center, Hokkaido University, 2.Institute of Seismology and Volcanology, Faculty of Science, Hokkaido University, 3.Atmosphere and Ocean Research Institute, University of Tokyo, 4.Institute of Low Temperature Science, Hokkaido University)

2:30 PM - 2:45 PM JST | 5:30 AM - 5:45 AM UTC

[ACG39-16] Cloud radiative effect on the 2019 major surface melt area expansion over the Greenland ice sheet

*Masashi Niwano[1,2], Akihiro Hashimoto[1], Teruo Aoki[2,1], Satoshi Hirose [3], Rigen Shimada[4], Motoshi Nishimura[2], Masahiro Hori[5] (1.Meteorological Research Institute, 2.National Institute of Polar Research, 3.New Chitose Aviation Weather Station, Japan Meteorological Agency, 4.Earth Observation Research Center, Japan Aerospace Exploration Agency, 5.School of Sustainable Design, University of Toyama)

2:45 PM - 3:00 PM JST | 5:45 AM - 6:00 AM UTC

[ACG39-17] Mass loss of the Greenland ice sheet until the year 3000 simulated with the model SICOPOLIS

*Ralf Greve[1,2], Christopher Chambers[1], Reinhard Calov[3] (1.Institute of Low Temperature Science, Hokkaido University, Sapporo, Japan, 2.Arctic Research Center, Hokkaido University, Sapporo, Japan, 3.Potsdam Institute for Climate Impact Research, Member of the Leibniz Association, Potsdam, Germany)

3:00 PM - 3:15 PM JST | 6:00 AM - 6:15 AM UTC

[ACG39-18] Supraglacial lakes evolution on Tracy and Heilprin Glaciers, northwestern Greenland

*YEFAN WANG[1,2], Shin Sugiyama[1] (1.Institute of Low Temperature Science, Hokkaido University, 2.Graduate School of Environmental Science, Hokkaido University)

Impacts of Riverine Carbon and Nutrient Delivery on Arctic Ocean Acidification

*Yuanxin Zhang[1], Michiyo Yamamoto-Kawai[1], Eiji Watanabe[2]

1. Tokyo University of Marine Science and Technology, 2. Japan Agency for Marine-Earth Science and Technology

Introduction

Rapid environmental changes are happening in the Arctic Ocean, such as extensive sea ice retreat, seawater warming, ocean acidification (OA). The effect of climate change on land also affects the Arctic Ocean by increasing riverine biogeochemical delivery (carbon and nutrient) via runoff increase, permafrost thaw, and tree-line advance[1]. Changes in riverine delivery of carbon and nutrient may affect the primary production, air-sea CO_2 fluxes, and OA significantly. It was revealed that aragonite undersaturation (caused by OA) has been continued for more than one decade since 2006 in the surface waters of Arctic Ocean[2]. However, it is still unclear to what extent the delivery of riverine biogeochemical fluxes (R_BGC) has an impact on OA, as well on primary production and marine ecosystem in the Arctic Ocean.

Data & Method

By using a Pan-Arctic Sea Ice-Ocean Model (COCO) coupled to an Arctic and North Pacific Model for Lower-trophic Marine Ecosystem with Carbonate Chemistry (Arctic NEMURO-C), we conducted sensitivity experiments to understand the impact of riverine biogeochemical delivery on OA (including indexes of pH, aragonite saturation state: Ω_{Ar}) in several Arctic sub-regions for 1979-2018. Four experiments are composed of 1. Without R_BGC, 2. With only R_Carbon (Riverine TA and DIC fluxes), 3. With only R_Nut (Riverine Nitrate and Silicate fluxes), 4. With R_BGC. Monthly climatological riverine carbon and nutrient data were obtained from the Arctic Great Rivers Observatory (ArcticGRO). Monthly climatological freshwater fluxes known as R-ArcticNET were obtained from the Arctic Ocean Model Inter-comparison Project (AOMIP).

Results & Discussion

Compared with result in the case 1 (Without R_BGC case: only riverine freshwater fluxes were involved), it is found that R_BGC increases pH and Ω_{Ar} in waters shallower than ~100 m in almost the whole Arctic Ocean. In surface waters of the central Arctic (latitude > 83°N), mean positive anomalies for 1989-2018 in pH and Ω_{Ar} by R_BGC are ~0.01 and ~0.06, respectively, which is mostly due to delivery of R_Carbon in this region where the effect of R_Nut delivery is negligible.

Relatively large increases in pH and Ω_{Ar} by R_BGC are found in surface waters near the coastal regions, where large rivers enter into the Arctic Ocean, as well along the Lomonosov Ridge, which reflects the distribution pattern of transpolar drift that transports river waters further into the central Arctic. The largest positive anomalies of pH and Ω_{Ar} by R_BGC are found in the surface waters of Laptev Sea and Kara Sea where simulation with R_BGC causes a higher pH by ~0.1 and higher Ω_{Ar} by ~0.1. In these seas, delivery of R_Nut attributes up to ~20% of pH increment and ~10% of Ω_{Ar} increment, which is a consequence of enhanced primary productivity by the riverine nutrient supply.

References:

[1] Terhaar et al., (2019). Global Biogeochemical Cycles, 33, 1048–1070.

[2] Zhang, Y. et al., (2020). Geophysical Research Letters, 47, e60119.

©2021. Japan Geoscience Union. All Right Reserved.

Keywords: Ocean Acidification, Riverine Fluxes, Model Simulation, Arctic Ocean

©2021. Japan Geoscience Union. All Right Reserved.

Spreading of aragonite undersaturated water in the Canada Basin of the Arctic Ocean

*Haruka Tsujimoto[1], Michiyo Yamamoto-Kawai[1], Yuanxin Zhang[1]

1. Tokyo University of Marine Science and Technology

In the Canada Basin of the Arctic Ocean, aragonite undersaturation has been observed in the surface and subsurface layers. Ocean acidification and freshening cause surface undersaturation, while the advection of acidified Pacific-origin water causes subsurface undersaturation. In this study, we investigate the vertical distribution of aragonite saturation state in the Canada Basin from 2003 to 2019, estimate the change in thickness and volume of undersaturated water, and discuss the contributing factors.

The thickness of unsaturated water increased significantly in both the surface and subsurface layers. The volume of unsaturated water increased 11-fold in the surface layer and 1.5-fold in the subsurface layer from 2003 to 2019. Our analysis shows that the increase in the surface layer was mainly caused by freshening in the mid-2000s, but by ocean acidification after 2016. In the subsurface layer, ocean acidification accounts for 76% of the volume increase, and the expansion of Pacific-origin water explains the remaining 24%. These results indicate that the volume of aragonite unsaturated water in the Canada Basin has increased significantly, and ocean acidification is a major factor.

©2021. Japan Geoscience Union. All Right Reserved.

Glacier and whale monitoring with an Ocean-Bottom Seismometer at the calving front

*Evgeny A. Podolskiy[1], Yoshio Murai[2], Naoya Kanna[3], Shin Sugiyama[4]

1. Arctic Research Center, Hokkaido University, 2. Institute of Seismology and Volcanology, Faculty of Science, Hokkaido University, 3. Atmosphere and Ocean Research Institute, University of Tokyo, 4. Institute of Low Temperature Science, Hokkaido University

Recently, a lot has been learned about glacier dynamics from monitoring seismicity of glacial origin, including calving, crevassing, basal processes, and subglacial hydrology. Near glacier calving fronts, surface seismic stations are noisy, primarily due to crevassing and wind, are hazardous to maintain, and can be lost due to iceberg calving. To circumvent these issues, we have pioneered and applied ocean-bottom seismology to the calving front of a tidewater glacier in northwest Greenland. We present details of this multi-purpose experiment and describe the technical challenges, noise analysis, and examples of recorded seismo-acoustic data. This includes tide-modulated seismicity with thousands of icequakes per day and the first near-source (~200–640 m) underwater record of a major kilometer-scale calving event in Greenland, which generated a glacial earthquake that was detectable ~420 km away. At the same time, our approach offers a unique opportunity to monitor the acoustic presence of such poorly studied endemic Arctic animals as narwhals.

Keywords: Ocean Bottom Seismometer, glacier, cryoseismology, Greenland, whales, acoustics

©2021. Japan Geoscience Union. All Right Reserved.

Cloud radiative effect on the 2019 major surface melt area expansion over the Greenland ice sheet

*Masashi Niwano[1,2], Akihiro Hashimoto[1], Teruo Aoki[2,1], Satoshi Hirose [3], Rigen Shimada[4], Motoshi Nishimura[2], Masahiro Hori[5]

1. Meteorological Research Institute, 2. National Institute of Polar Research, 3. New Chitose Aviation Weather Station, Japan Meteorological Agency, 4. Earth Observation Research Center, Japan Aerospace Exploration Agency, 5. School of Sustainable Design, University of Toyama

During the summer of 2019, exceptional surface melt occurred over the Greenland ice sheet (Tedesco and Fettweis, 2020; Sasgen et al., 2020). In the previously reported major surface melt event in 2012, clouds played an important role in enhancing surface melt area through the cloud radiative effect (CRE) (Niwano et al., 2015, 2019). In the present study, we utilize the state-of-the-art high resolution (5 km and 1 hour) polar regional climate model NHM-SMAP (Niwano et al., 2018) to investigate CRE on the 2019 summer ice sheet surface melt area expansion. Another previous major surface melt event occurred in 2002 is also investigated. Our NHM-SMAP clear-sky sensitivity simulations based on the method by Niwano et al. (2019) indicates that clouds were responsible for a 0.6%, 3.0%, and 0.4% increase in JJA (June, July, and August) surface melt area extent during 2002, 2012, and 2019, respectively. The smaller atmospheric humidity in 2019, relative to 2012, over the ice sheet despite higher July air temperature anomalies (Tedesco and Fettweis, 2020) affected the contrasting results between 2012 and 2019. However, on the days when the seasonally maximum surface melt areas are estimated (28 June 2002, 12 July 2012, and 30 July 2019, respectively), CRE enhanced surface melt areas by 24.7%, 14.0%, and 26.0%, respectively. These suggest that seasonal frequency and intensity of CRE-induced surface melt events differ considerably year by year.

References:

Niwano, M., Aoki, T., Matoba, S., Yamaguchi, S., Tanikawa, T., Kuchiki, K., and Motoyama, H. (2015): Numerical simulation of extreme snowmelt observed at the SIGMA-A site, northwest Greenland, during summer 2012, The Cryosphere, 9, 971-988. https://doi.org/10.5194/tc-9-971-2015

Niwano, M., Aoki, T., Hashimoto, A., Matoba, S., Yamaguchi, S., Tanikawa, T., Fujita, K., Tsushima, A., Iizuka, Y., Shimada, R., and Hori, M. (2018): NHM–SMAP: spatially and temporally high-resolution nonhydrostatic atmospheric model coupled with detailed snow process model for Greenland Ice Sheet. The Cryosphere, 12, 635-655. https://doi.org/10.5194/tc-12-635-2018

Niwano, M., Hashimoto, A., and Aoki, T. (2019): Cloud-driven modulations of Greenland ice sheet surface melt. Sci. Rep., 9, 10380. https://doi.org/10.1038/s41598-019-46152-5

Sasgen, I., Wouters, B., Gardner, A.S., King, M. D., Tedesco, M., Landerer, F. W., Dahle, C., Save, H., and Fettweis, X. (2020): Return to rapid ice loss in Greenland and record loss in 2019 detected by the GRACE-FO satellites. Communications Earth & Environment, 1, 8. https://doi.org/10.1038/s43247-020-0010-1

©2021. Japan Geoscience Union. All Right Reserved.

Tedesco, M., and Fettweis, X. (2020): Unprecedented atmospheric conditions (1948–2019) drive the 2019 exceptional melting season over the Greenland ice sheet. The Cryosphere, 14, 1209–1223. https://doi.org/10.5194/tc-14-1209-2020

Keywords: Greenland ice sheet, surface melt, cloud radiative effect, polar regional climate model, NHM-SMAP

©2021. Japan Geoscience Union. All Right Reserved.

Mass loss of the Greenland ice sheet until the year 3000 simulated with the model SICOPOLIS

*Ralf Greve[1,2], Christopher Chambers[1], Reinhard Calov[3]

1. Institute of Low Temperature Science, Hokkaido University, Sapporo, Japan, 2. Arctic Research Center, Hokkaido University, Sapporo, Japan, 3. Potsdam Institute for Climate Impact Research, Member of the Leibniz Association, Potsdam, Germany

The Coupled Model Intercomparison Project Phase 6 (CMIP6) is a major international climate modelling initiative. As part of it, the Ice Sheet Model Intercomparison Project for CMIP6 (ISMIP6) was devised to assess the likely sea-level-rise contribution from the Greenland and Antarctic ice sheets until the year 2100. This was achieved by defining a set of future climate scenarios by evaluating results of CMIP5 and CMIP6 global climate models (GCMs, including MIROC) over and surrounding the Greenland and Antarctic ice sheets. These scenarios were used as forcings for a variety of ice-sheet models operated by different working groups worldwide (Goelzer et al. 2020, doi: 10.5194/tc-14-3071-2020; Seroussi et al. 2020, doi: 10.5194/tc-14-3033-2020).

Here, we use the model SICOPOLIS to carry out extended versions of the ISMIP6 future climate experiments for the Greenland ice sheet until the year 3000, employing a hybrid shallow-ice-shelfy-stream dynamics. For the atmospheric forcing (anomalies of surface mass balance and temperature) beyond 2100, we sample randomly the ten-year interval 2091-2100, while the oceanic forcing (prescribed retreat due to ocean thermal forcing) beyond 2100 is kept fixed at 2100 conditions. Twelve experiments are for the pessimistic, "business as usual" pathway RCP8.5 (CMIP5) / SSP5-8.5 (CMIP6), and two are for the optimistic RCP2.6 (CMIP5) / SSP1-2.6 (CMIP6) pathway that represents substantial emissions reductions. Results are shown in Fig. 1. For the control run with a constant, 1960-1989 average climate, the ice sheet is stable until the year 3000. For RCP8.5/SSP5-8.5, it suffers a severe mass loss, which amounts to ~1.8 m SLE (sea-level equivalent), or ~25% of its entire mass, for the twelve-experiment mean, and ~3.5 m SLE (~50% of the entire mass) for the most sensitive experiment. For RCP2.6/SSP1-2.6, the mass loss is limited to a two-experiment mean of ~0.28 m SLE. Climate-change mitigation during the next decades will therefore be an efficient means for limiting the contribution of the Greenland ice sheet to sea-level rise in the long term.

Keywords: Greenland, Ice sheet, Climate change, Sea-level rise, Modelling

©2021. Japan Geoscience Union. All Right Reserved.

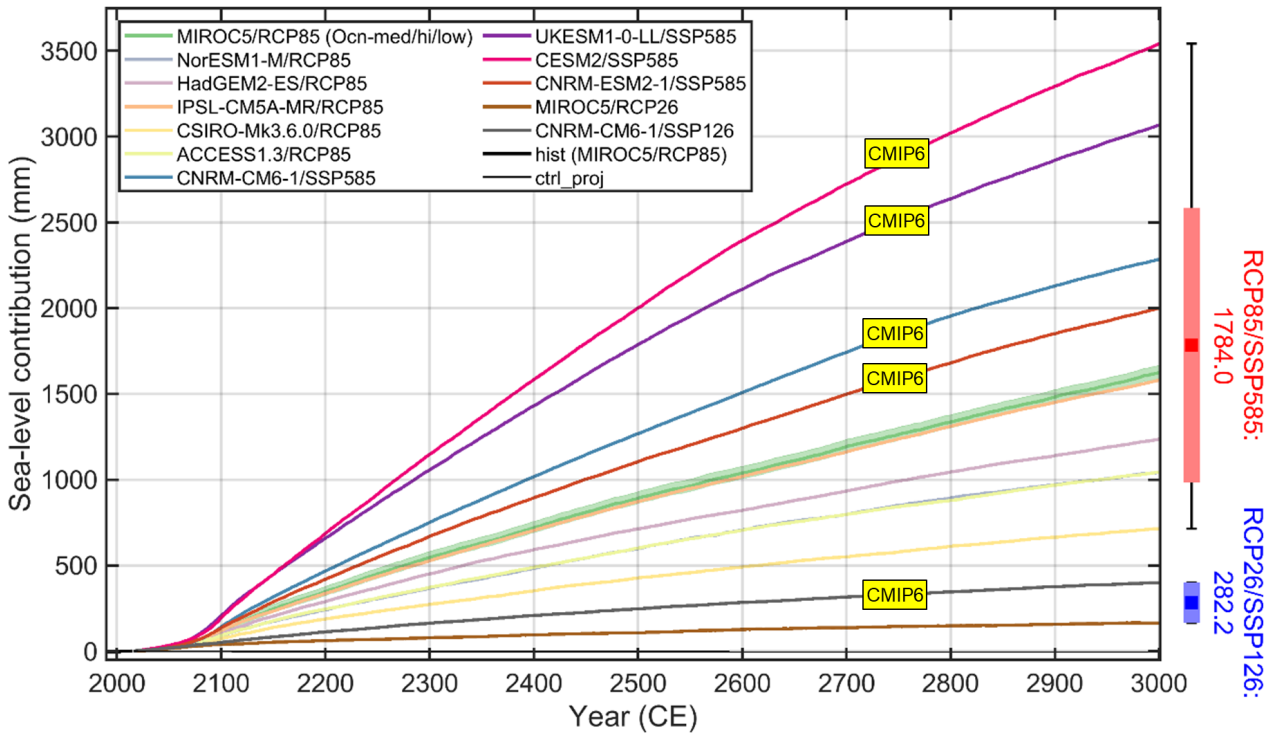


Figure 1: Mass loss (expressed as sea-level contribution) of the Greenland ice sheet under the RCP8.5/SSP5-8.5 and RCP2.6/SSP1-2.6 forcings. SSP5-8.5 and SSP1-2.6, marked by “CMIP6”, produce stronger mass losses than RCP8.5 and RCP2.6 (CMIP5, unmarked), respectively.

©2021. Japan Geoscience Union. All Right Reserved.

Supraglacial lakes evolution on Tracy and Heilprin Glaciers, northwestern Greenland

*YEFAN WANG[1,2], Shin Sugiyama[1]

1. Institute of Low Temperature Science, Hokkaido University, 2. Graduate School of Environmental Science, Hokkaido University

Supraglacial lakes are widely distributed near the margin of the Greenland ice sheet during the melt season. Generally, they form when meltwater ponds in ice surface depressions, and influence ice surface melt by lowing the albedo. Drainage of lake water into the glacier bed reduces basal friction and causes ice flow acceleration. Therefore, studying the evolution of supraglacial lakes sheds new light on understanding the effect of meltwater on the ice sheet. Here, we report a satellite-based study on supraglacial lakes on Tracy and Heilprin, marine-terminating glaciers in northwest Greenland (Fig. 1). Although these two glaciers have similar dimensions and flow into the same fjord, Inglefield Bredning, lakes on the glaciers exhibit remarkably different behaviors.

Taking advantage of Google Earth Engine (GEE), we compiled about 300 Sentinel-2 level-1C (S2) scenes at 10 m resolution, covering the two glaciers with sun elevation angles greater than 20˚. These S2 scenes cover the period from May to August during 2016–2020. Glacier masks were generated in this study to eliminate sea and land areas from the analysis. By the integrated random forest algorithm in GEE, we distinguished water pixels from the glacier surface for all the selected S2 scenes. The water body smaller than 5 pixels and narrower than 2 pixels were removed by assuming they are slush or streams rather than lakes.

For both of the glaciers (Fig. 2), relatively small lakes (< 0.5 km^2) account for the vast majority (> 95%) of all observed over the five-year period. Lakes larger than 0.5 km^2 were distributed mostly in higher altitude (> 400 m a.s.l). Although the basin areas of Heilprin and Tracy glaciers are similar (653.45 km^2 and 538.82 km^2), lake surface area on Heilprin glacier (21.13 km^2) was three times greater than that on Tracy glacier (6.87 km^2). Considering water tend to store in flat and slower-moving ice, we attribute the smaller lake area on Tracy to its faster ice speed (1740 m a^{-1} in 2014) and steeper surface slope (4.0˚) as compared to these of Heilprin glacier (1360 m a^{-1} in 2014 and 3.1˚). Despite the difference in the lake areas, temporal patterns were similar during the observation period. In general, lakes began formation in the middle of May, which was followed by substantial increase in area from middle of June. After reaching a maximum thereafter, the lake area decreases in August. Due to annual variations in meteorological conditions, the area peaked in different timing every year. In 2016, 2019, and 2020, lake area reached peak values between late June and beginning of July. In 2017 and 2018, however, the peaks were observed later in late July because of cold summer temperature (Fig. 3). A possible impact of lake drainage on the ice dynamics is under investigation using ice velocity time series.

Keywords: Greenland, supraglacial lake, remote sensing

©2021. Japan Geoscience Union. All Right Reserved.

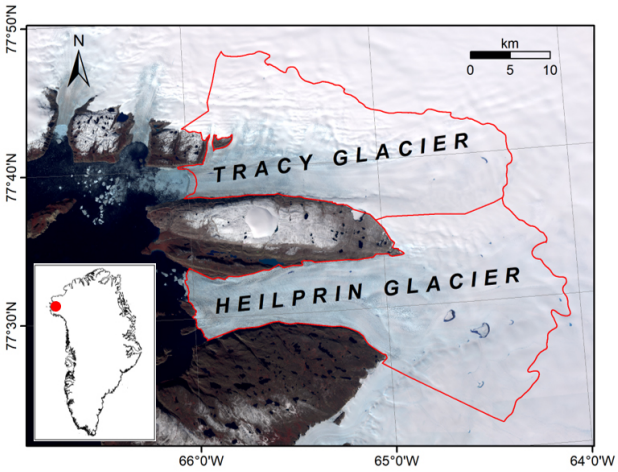


Fig. 1. Map of the study glaciers

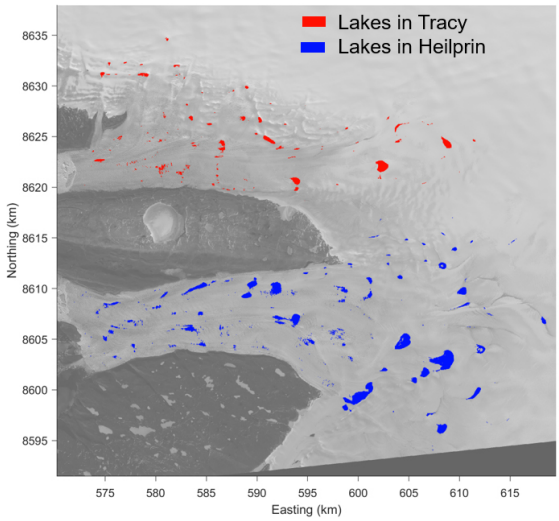


Fig. 2. 2016-2020 superimposed water pixels in the study glaciers

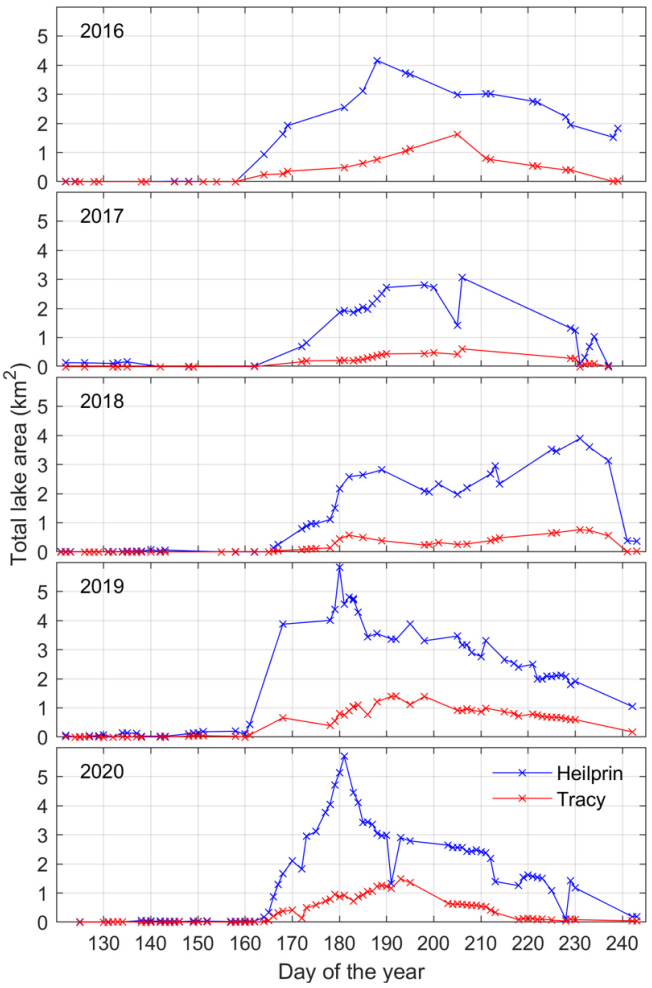


Fig. 3. Evolution of lake area for Heilprin and Tracy glacier during melt season in 2016-2020

©2021. Japan Geoscience Union. All Right Reserved.

[J] Oral | H (Human Geosciences)：H-GG Geography

Fri. Jun 4, 2021 3:30 PM - 5:00 PM JST | Fri. Jun 4, 2021 6:30 AM - 8:00 AM UTC | Ch.16 Zoom Room 16

[H-GG01] Use and management of natural resources and environment: Dialogues between earth and social sciences

convener:Gen Ueda(Graduate School of Social Sciences, Hitotsubashi University), Yoshinori OTSUKI(Institute of Geography, Graduate School of Science, Tohoku University), Takahisa Furuichi(Forest and Forest Products Research Institute), Toru Sasaki(Miyagi University of Education), Chairperson:Gen Ueda(Graduate School of Social Sciences, Hitotsubashi University), Yoshinori OTSUKI(Institute of Geography, Graduate School of Science, Tohoku University), Toru Sasaki(Miyagi University of Education)

(Language of the session is Japanese and English with no priority.) In this session, the situation and history of use, changes and management of natural resources and environment from various regions under diverse socio-economic and natural conditions are reported. Findings from local-scale fieldwork and feedbacks on their methodology and/or research concepts are particularly encouraged to be shared and discussed. The session also welcomes abstract submissions that include dialogues between earth and social sciences, including human-ecological perspectives. A variety of research topics are covered: local knowledge of natural resources and environment, environmental and climatic history, environmental geography, environmental degradation through resource use and/or management, effects of climate change, related socio-economic changes and adaptation for livelihood security, political ecology, and issues for overcoming gaps in linking between local and broader-scale (national, regional and global) studies.

3:30 PM - 3:45 PM JST | 6:30 AM - 6:45 AM UTC

[HGG01-01] Disaster Adaptive Strategy in a Flood-Prone area in Sri Lanka: A Case Study of Response and Recovery of Hard Rain and Flood Disaster

*Tsuchida Ryo[1] (1.Graduate School of Advanced Integrated Studies in Human Survivability, Kyoto University)

3:45 PM - 4:00 PM JST | 6:45 AM - 7:00 AM UTC

[HGG01-02] Is it possible to achieve economic development and environmental improvement?

*Toru Sasaki[1] (1.Miyagi University of Education)

4:00 PM - 4:15 PM JST | 7:00 AM - 7:15 AM UTC

[HGG01-03] Changes in "Tajima Cattle System" in Ojiro, Kami Town, Hyogo Prefecture: How to Continue to Nurture "Unique Cattle Here?"

*DAICHI KOHMOTO[1] (1.Nara University of Education)

4:15 PM - 4:30 PM JST | 7:15 AM - 7:30 AM UTC

[HGG01-04] Human and Physical Aspects in Geography: Research Issues on Natural Resources and Environment

*Gen Ueda[1], Yoshinori OTSUKI[2], Takahisa Furuichi[3] (1.Graduate School of Social Sciences, Hitotsubashi University, 2.Graduate School of Science, Tohoku University, 3.Forest and Forest Products Research Institute)

4:30 PM - 4:45 PM JST | 7:30 AM - 7:45 AM UTC

[HGG01-05] **Geographical implications of disturbed forest and degraded landscape from historical and present perspectives in Japan**

*Takahisa Furuichi[1,2,3], Hiromu Daimaru[1], Wataru Murakami[1], Takashi Okamoto[1], Toru Sasaki[3], Gen Ueda[4] (1.Forest and Forest Products Research Institute, 2.University of the Sunshine Coast, 3.Miyagi University of Education, 4.Graduate School of Social Sciences, Hitotsubashi University)

4:45 PM - 5:00 PM JST | 7:45 AM - 8:00 AM UTC

[HGG01-06] Biomagnetic monitoring investigations of the spatial distribution of atmospheric fine magnetic particles:
case study of the Toyama-shi area, Japan

*Hiroki Shibata[1], Kazuo Kawasaki[1], Keiji Horikawa[1] (1.University of Toyama)

Disaster Adaptive Strategy in a Flood-Prone area in Sri Lanka: A Case Study of Response and Recovery of Hard Rain and Flood Disaster

*Tsuchida Ryo[1]

1. Graduate School of Advanced Integrated Studies in Human Survivability, Kyoto University

The purpose of this study is to identify the actual situation and challenges of flood response and recovery in Ratnapura city, Sabaragamuwa Province through the case of May 1913 and May 2017 flood disaster, focusing on hard rains and floods in southwestern Sri Lanka. Through these cases, the paper describes the socio-economic and disaster prevention system in Sri Lanka in both years, and suggest disaster adaptation strategies for future disaster prevention and mitigation.
Based on the field survey, in the case of 2017, the author revealed that the response and recovery were based on religious places and local and kinship relations. While in the case of 1913, it was revealed that the response and recovery were based on institutions, multiple actors, local relations, and natural resources under the colonial era by analyzing the municipal official document. On the other hand, in the 2017 case, it was found that 1)the timing of evacuation was difficult, 2)the economic burden was chronic, and 3)there were problems in the integration and communication of information between central and local. In contrast, in the 1913 case, it was revealed that 1)material resources were scarce, 2)control by local officials was weak, and security was unstable due to rumors and looting.
From these findings, it can be concluded that the utilization of diverse local communities and resources and the enhancement of local relationships are necessary for disaster adaptation strategies in disaster prevention policies.

Keywords: Sri Lanka, Hard Rain and Flood Disaster, Adaptive Strategy

©2021. Japan Geoscience Union. All Right Reserved.

Is it possible to achieve economic development and environmental improvement?

*Toru Sasaki[1]

1. Miyagi University of Education

In this study, we reconstruct the case study on the mechanism of desertification in Inner Mongolia as one story. On that basis, I would like to clarify that economic development and environmental improvement in Inner Mongolia are in a trade-off relationship. On that basis, I would like to examine whether there is a trade-off between economic development and environmental improvement in Inner Mongolia. And I would like to argue that the current environmental policy of China is the spatial transfer of environmental pollution on a global scale.

Keywords: Economic Development, Environmental Improvement, Natural Resource, Inner Mongolia, China

©2021. Japan Geoscience Union. All Right Reserved.

Changes in "Tajima Cattle System" in Ojiro, Kami Town, Hyogo Prefecture: How to Continue to Nurture "Unique Cattle Here?"

*DAICHI KOHMOTO[1]

1. Nara University of Education

a

Keywords: livestock industry, hilly and mountainous area, small agricultural management, sustainability, local food, consumer education

©2021. Japan Geoscience Union. All Right Reserved.

Human and Physical Aspects in Geography: Research Issues on Natural Resources and Environment

*Gen Ueda[1], Yoshinori OTSUKI[2], Takahisa Furuichi[3]

1. Graduate School of Social Sciences, Hitotsubashi University, 2. Graduate School of Science, Tohoku University, 3. Forest and Forest Products Research Institute

After the discussion on the "Himalayan dilemma" and Neo-Malthusian pessimism that relates population growth with environmental degradation (e.g. Ives and Messerli 1989), the Boserupian optimism advanced the “More People, Less Erosion” hypothesis that population growth and agricultural intensification stopped soil erosion and realized environmental conservation, taking semi-arid Kenya as an example (Tiffen et al. 1994). This has stimulated a variety of arguments on its exceptionality (Boyd and Slaymaker 2000), challenges of soil erosion science including the scale issue (Boardman 2006), and more recent examination (e.g. Duriaux-Chavarría et al. 2020). Scientific understanding has also stressed that human-environmental dynamics in semi-arid areas are unpredictable and complex, and that a simple pessimistic / optimistic dichotomy is inappropriate. The scientific knowledge may resonate with indigenous knowledge (Dahlberg and Blaikie 1999), and it has evolved interdisciplinarily into the theme of community-based soil conservation (Peterson et al. 2018, Karaya et al. 2021).

If scientific knowledge is based on the dichotomy of pessimism / optimism, the argument may either deny "environmentally destructive" indigenous knowledge or confirm and idealize "environmentally conservationist" indigenous knowledge: this may affect development and conservation policies. From the perspective of human geography and social science, this presentation examines the validity of the above dichotomy and seeks jcollaboration with physical geography and earth science.

Time scale is a relevant issue. In rural East Africa, it is very difficult to retroactively gather longitudinal information on social phenomena with high time resolution and analyze their relationship with the slope process. However, as evidenced by an analysis of aerial photographs and satellite images of the research area on the Meru Mountain flanks in northeastern Tanzania (Ueda 2011), the area proportion of home gardens with perennial crops increased from 31.2% in 1962 to 51.2% in 1987, then it shrank to 27.7% by 2008 (seasonal cropland expanded). This non-linear land use / cover change is related to ever-ongoing land subdivision due to population growth and land inheritance, and the fluctuating international market conditions of cash crops. The relationship between the socio-economic factors captured on such a time scale and the slope process is one of the themes to be examined.

References

Boardman, J. 2006. Soil erosion science: Reflections on the limitations of current approaches. *Catena*, 68(2-3), 73-86.

Boyd, C., and Slaymaker, T. 2000. Re-examining the “more people less erosion” hypothesis: Special case or wider trend. *Natural Resource Perspective*, 63(November), 1-6.

Dahlberg, A. C., and Blaikie, P. M. 1999. Changes in landscape or in interpretation? Reflections based on the environmental and socio-economic history of a village in NE Botswana. *Environment and History*, 5(2), 127-174.

Ives, J. D. and Messerli, B. 1989. *The Himalayan Dilemma*. United Nations University, Routledge.

Karaya, R. N., Onyango, C. A., and Ogendi, G. M. 2021. A community-GIS supported dryland use and cover change assessment: The case of the Njemps flats in Kenya. *Cogent Food and Agriculture*, 7(1), 1872852.

©2021. Japan Geoscience Union. All Right Reserved.

Peterson, R. B., Kapiyo, R. A., Campbell, E. M., and Nyabua, P. O. 2018. Gully Rehabilitation Trusts: Fighting soil erosion through community participation in western Kenya. *Journal of Rural Studies*, 58, 67-81.
Tiffen, M., Mortimore, M., & Gichuki, F. 1994. *More People, Less Erosion: Environmental Recovery in Kenya*. John Wiley & Sons.
Ueda, G. 2011. Land subdivision and land use change in the frontier settlement zone of Mount Meru, Tanzania. *African Study Monographs*. Supplementary issue, 42, 101-118.

Keywords: Population, Environment, Scale, Methodology

©2021. Japan Geoscience Union. All Right Reserved.

Geographical implications of disturbed forest and degraded landscape from historical and present perspectives in Japan

*Takahisa Furuichi[1,2,3], Hiromu Daimaru[1], Wataru Murakami[1], Takashi Okamoto[1], Toru Sasaki[3], Gen Ueda[4]

1. Forest and Forest Products Research Institute, 2. University of the Sunshine Coast, 3. Miyagi University of Education, 4. Graduate School of Social Sciences, Hitotsubashi University

Japanese mountain forests were most intensively disturbed in the period from the end of Edo to the middle of Meiji eras. From the end of the Meiji era to the post WWII, overuse of mountain forest resources occurred extensively, causing disturbance of mountain slopes and resulted in frequent landslides and floods. Especially in the Tokai and Chugoku regions, growth of population during the modern era (17th century onward) caused expansion of disturbed mountain forests (i.e. bare mountains) especially in granite areas. Chiba (1956) called them as ’*hageyama*’ with its definition that is ‘forests that have lost their normal functions’, so that we here call them ‘defunctionalized forests’. Field data suggest that defunctionalized forests (*hageyama*) also appeared on granite mountains in the Tohoku region during the modern era. Indeed, we have found at present landslide sites on granite mountains in the Chugoku and Tohoku regions evidence showing that regolith materials supplied and accumulated in the modern era (most probably when defunctionalized forests dominated mountain slopes in the areas) have the significant influence on the present landslides.

On the other hand, after intensive afforestation during the post WWII, Japanese forests have long faced a paucity of maintenance works due to multiple reasons, including an increase in inexpensive imported timbers, a decline in domestic timber prices, and insufficiency of human resources who sustain the forest industry. Consequently, trees have not been harvested, resulting in the situation that Japanese forests have never been richer and wider in history. Presently in 2017, plantation forests occupy 45% of the Japanese forests and the paucity of maintenance work of the plantation forests has caused an increase in tree density, which has led to a decline of the economic value of the timber, changes in pleasant landscape of *satoyama*. This situation is widely recognized as ‘degradation’ of the forest. However, in a geomorphological perspective, evidence has not been clearly presented for showing the increase in landslides as tree density increases. Studies rather suggest that forest maintenance work, that often promotes construction of mountain roads, inevitably disturb soil layers which should have negative impacts on slope stability. Kadomura (1991) focused on the Japanese climatic environment under which climax vegetation will be forest, and defined ‘degraded landscapes’ in Japan as a landscape where forest is not easily restored. In this definition, plantation forest is not recognized as ‘degraded landscape’, regardless of its quality.

Forests are presumably an environment that includes not only trees but also, at least, soil layers. Some people recognize degradation of forest based on the economic value of timbers or the cultural value of the scenery of *satoyama*. But others, such as Chiba and Kadomura, would see degradation at the scale of landscape that represents the functions or system of the forest environment. Geography may have an advantage to study ‘degradation’ of mountain forests, because, ‘degradation’ occurs spatially and temporally in combination of human intervention and physical processes.

Chiba T, 1956. *A research on Hageyama*. The Agriculture and Forestry Association, Tokyo, 237pp.

©2021. Japan Geoscience Union. All Right Reserved.

Kadomura H, 1991. Introduction to Degraded Landscape Stuides. In: *Degraded Landscapes in Japan* (ed. Kadomura H.), Report of Grant-in-Aid for Co-Operative Research, 5-32.

Keywords: defunctionalized forest (hageyama), degraded landscape, landslide, economic value, satoyama

©2021. Japan Geoscience Union. All Right Reserved.

Biomagnetic monitoring investigations of the spatial distribution of atmospheric fine magnetic particles: case study of the Toyama-shi area, Japan

*Hiroki Shibata[1], Kazuo Kawasaki[1], Keiji Horikawa[1]

1. University of Toyama

Magnetic biomonitoring techniques have been shown to be rapid, cost-effective and useful methods for investigating spatial distribution of air pollution. Particulate matter in the atmospheric pollution contains measurable magnetic concentrations. Magnetite is known to be a major magnetic mineral in particulate matter and can have potentially large impacts on human health. Here environmental magnetic results are reported for the materials deposited on the Japanese flowering cherries (*Prunus* subgenus *Cerasus*) at Toyama city, Toyama, Japan. Stepwise isothermal remanet magnetization tests show that measurable magnetic particles are present on leaves at all sites. Further, details rock magnetic analyses indicate that the main magnetic mineral is single-domain partially oxidized magnetite, and the magnetic mineralogy on leaves' surface is consistent throughout the study area. Higher saturation isothermal remanent magnetization (SIRM) intensity is observed at northern parts of the city, which is coincident with the urban area. Elemental analysis showed a positive correlation between SIRM intensity and Fe. In addition, positive correlations were found in As, Sb and Cr that could be related to the combustion process of automobiles and the wear of brake pads. These results indicate that magnetic biomonitoring using the leaves of the Japanese flowering cherry can be a rapid and cost-effective method for studying the spatial distribution of fine magnetite derived from local industrial activities, and therefore it should be considered for application elsewhere in the country.

Keywords: Environmental magnetism, Japanese flowering cherry, Atmospheric magnetic particles

©2021. Japan Geoscience Union. All Right Reserved.

[J] Oral | H (Human Geosciences)：H-GM Geomorphology

Fri. Jun 4, 2021 9:00 AM - 10:30 AM JST | Fri. Jun 4, 2021 12:00 AM - 1:30 AM UTC | Ch.14 Zoom Room 14

[H-GM03] Geomorphology

convener:Tsuyoshi Hattanji(Faculty of Life and Environmental Sciences, University of Tsukuba), Masayuki Seto(Fukushima Future Center for Regional Revitalization, Fukushima University), Chairperson:Tsuyoshi Hattanji(Faculty of Life and Environmental Sciences, University of Tsukuba)

The main subject of this session is the whole range of themes relating to geomorphology, especially geomorphic processes, landform development and its relation to environmental changes, geomorphological hazards and their mitigation and reports of recent events of disaster occurred in Japan, various kind of hazard maps, relationships among geomorphic processes, other natural phenomena and human activities, and various techniques of geomorphological measurements and automatic landform classification. Japanese can be used in this session.

9:00 AM - 9:15 AM JST | 12:00 AM - 12:15 AM UTC

[HGM03-01] Uplift-induced drainage divide migration and channel reorganization:Laboratory model experiment

*Akimasa Sakashita[1], Noritaka Endo[1] (1.Kanazawa university)

9:15 AM - 9:30 AM JST | 12:15 AM - 12:30 AM UTC

[HGM03-02] Adjustment timescales of channel width and hillslope angle to accelerated uplift: Insights into a basin-scale steady state

*Naoya Takahashi[1], J Bruce H Shyu[2], Yuki Matsushi[3], Ryoga Ohta[4], Shinji Toda[5] (1.Department of Earth Science, Graduate school of Science, Tohoku University, 2.Department of Geosciences, National Taiwan University, 3.Disaster Prevention Research Institute, Kyoto University, 4.Graduate school of Science, Kyoto University, 5.International Research Institute of Disaster Science, Tohoku University)

9:30 AM - 9:45 AM JST | 12:30 AM - 12:45 AM UTC

[HGM03-03] **Development of “steady-state” landforms in geomorphic experiments and the concept of “threshold hillslope”**

*Shunji Ouchi

9:45 AM - 10:00 AM JST | 12:45 AM - 1:00 AM UTC

[HGM03-04] Causes of concentrated revetment damage in the Hatto River in eastern Tottori Prefecture during the heavy rains in western Japan in July 2018

*Yoshinori Kodama[1], Taishi Sugimoto (1.Faculty of Agriculture, Tottori Univ.)

10:00 AM - 10:15 AM JST | 1:00 AM - 1:15 AM UTC

[HGM03-05] Initiation factors of an incised meandering river in steep mountainous terrain: a case study of the Higashigouchi River with high-angle bedding plane

*Takuma Watakabe[1], Hikaru Osawa[2], Noriyuki Arai[3], Issei Doi[3], Yosuke Yamakawa[2] (1.Kansai Research Center, Forestry and Forest Products Research Institute, 2.Mountain Science Center, Univ. of Tsukuba, 3. Disaster Prevention Research Institute, Kyoto University)

10:15 AM - 10:30 AM JST | 1:15 AM - 1:30 AM UTC

[HGM03-06] Generation of Terrain Classification Data for Ground Vulnerability Assessment Using 30m DEM by Digital Terrain Analysis

*Junko Iwahashi[1], Dai Yamazaki[2], Takayuki Nakano[1], Ryo Endo[1] (1.GSI of Japan, 2.Institute of Industrial Science, The University of Tokyo)

Uplift-induced drainage divide migration and channel reorganization:Laboratory model experiment

*Akimasa Sakashita[1], Noritaka Endo[1]

1. Kanazawa university

A drainage divide, the boundary of a drainage basin, is modified by external forcing, changing its position and elevation along with reorganization of the channel. Non-uniform uplift is a common factor as forcing, and a key for reconstruction and prediction of past and future landforms in tectonically complicated regions such as Japan, but its detailed dynamics are not still well understood. Here, we observed divide migration and channel reorganization caused by non-uniform uplift, through a laboratory model experiment. The experimental tank has two outlets, so two neighboring drainage basins are formed by supplying misty artificial rainfall. We exerted tilting uplift as non-uniform uplift with linearly varying uplift rate.

During uplift activities, the basin under the downstream increasing of uplift did not show a large change of landform, while the basin of upstream increasing of uplift showed the increase in riverbed gradient, but the drainage divide between the two basin was stable. After the uplift ceased, the divide shifted, resulting in the increase in area and the decrease in riverbed gradient of the basin which has been influenced by the upstream increasing uplift. During the landform change, the shape of river varied by modifying its bend (curvature). Because we conducted only one experimental run so far, more data is needed to derive a general law.

Keywords: fluvial morphology, drainage divide

©2021. Japan Geoscience Union. All Right Reserved.

Adjustment timescales of channel width and hillslope angle to accelerated uplift: Insights into a basin-scale steady state

*Naoya Takahashi[1], J Bruce H Shyu[2], Yuki Matsushi[3], Ryoga Ohta[4], Shinji Toda[5]

1. Department of Earth Science, Graduate school of Science, Tohoku University, 2. Department of Geosciences, National Taiwan University, 3. Disaster Prevention Research Institute, Kyoto University, 4. Graduate school of Science, Kyoto University, 5. International Research Institute of Disaster Science, Tohoku University

River morphology is dictated by various factors, such as substrate properties and climate, and changes in the boundary conditions trigger river adjustment to the new boundary conditions.

A sustained increase in rock uplift rate drives changes in river morphology. Studies of transient landscapes are crucial to understand the style and timescale of river adjustment to accelerated uplift. Channel slope, width, and hillslope angle play important roles in controlling river erosion rate, and their relationships with active tectonics have been examined in detail. While adjustment time of channel slope can be estimated empirically and theoretically based on knickpoint travel time, those of channel width and hillslope angle are poorly understood because they are difficult to constrain in an actual landscape. This study presents a method to estimate adjustment timescales of width and hillslope angle and apply the method to rivers around the Yunodake fault, an active normal fault in Fukushima, northeastern Japan.

We focused on channel slope (k_{sn}: Normalized channel steepness), channel width, hillslope angle and examined their variation along the trunk streams. Rivers flowing across the fault contained slope-break knickpoints. The lower channel reaches had larger k_{sn} than reaches upstream of the knickpoints, suggesting these rivers are now adjusting to the accelerated relative uplift rates of the Yunodake fault. We measured bankfull width using a laser range finder. Although channel width increases with drainage area at a steady state, the observed channel width for three trunk streams did not follow such scaling relations. As for hillslope angle, we mapped hillslopes adjacent to the trunk streams and examined its along-trunk variation of hillslope angles using 5m-DEM provided from the Geospatial Information Authority of Japan. The result showed hillslopes downstream were steeper than those upstream, and there were transitional zones at the middle of the rivers where hillslope angles gradually increased toward the downstream side. We analyzed the ^{10}Be concentrations of detrital sand taken from the trunk streams to determine basin-averaged denudation rates and then calculated knickpoint travel speed using the resulting denudation rates. Based on the observations of channel and hillslope morphology and the knickpoint travel speed, we will discuss the adjustment timescales of channel width and hillslope angles and their significance in terms of a basin-scale steady state.

Keywords: Bedrock river, erosion, stream power model, cosmogenic nuclide

©2021. Japan Geoscience Union. All Right Reserved.

Development of “steady-state” landforms in geomorphic experiments and the concept of “threshold hillslope”

*Shunji Ouchi

The development of experimental landforms by uplift and rainfall erosion starting from a flat surface at the ground level commonly progresses to the steady-state, in which erosion attains equilibrium with uplift to keep relatively stable height and similar landforms. The sequence of this process of landform development can be divided into 3 stages, namely, the valley encroaching stage (stage 1), the mountain growth stage (stage 2), and the dynamic equilibrium stage (stage 3). In stage 1 fluvial erosion with the development of valley systems proceeds and average height of the uplifted area increases linearly with uplift at a slightly lower rate. Valleys continue to develop into stage 2, in which slopes grow high enough to induce slope failures and sediments produced by slope failures are quickly carried away through valley systems. Mountains grow, but the rate of surface rise in the uplifted area gradually declines in this stage. The average height then stops continuously increasing in stage 3 and starts to change around a certain height as maintaining similar landforms.

Two runs of experimental landform development, with the same uplift rate (0.36 mm/h for 960 hours) and different rainfall intensity (40 - 50 and 80 - 90 mm/h) on the same material (a mixture of fine sand and kaolinite 10 : 1 by weight and permeability of 10^{-3} cm/s order), showed the common process to reach steady-state landforms. The same serrate shape of graphs showing the change in average height of the uplifted area indicates the way how similar average height and landforms are maintained through stage 3, although the difference in rainfall intensity resulted in the development of different landforms, a higher massive mountain and lower separated ridges. The periodic rapid decrease followed by the gradual increase in average height of the uplifted area apparently reflects the observed cyclic occurrence of landslide concentration and the following period of uplift with basic erosion by sporadic slope failures and fluvial transportation. The repetition of this process works to limit the average surface height within a certain range and to keep landforms similar during stage 3. This interpretation of the process to maintain steady-state landforms seems to nicely fit in with the concept of threshold hillslope model of landscape evolution, which explains steady state landscapes in tectonically active mountain belts from the balance between rates of uplift and river incision through adjustment of landslide erosion rates on threshold hillslopes. The average value of *cell slope* steeper than the angle of repose of dry material used in the experiments (ca., 34˚), which is designated as *mean cell slope of steeper cluster* here, can be assumed to indicate the readiness of slopes to collapse. The parameter, *cell slope*, is defined as the gradient of the steepest line connecting two points among four vertices of a grid cell, and is considered to represent the slope gradient of each grid. The values of *mean cell slope of steeper cluster* in stage 3 of both runs, which changed with time (and uplift) as shown also by serrate shaped graphs, are plotted within a relatively narrow band of 45˚ - 54˚, suggesting that *mean cell slope of steeper cluster* in the dynamic equilibrium stage may represent the inherent threshold hillslope of the material used in these runs, regardless of rainfall intensity. The values of *mean cell slope of steeper cluster* in 11 other runs of experiments with the same material under various experimental conditions are all within the range of 45˚- 60˚ after slope failures become dominant in the erosion process, regardless of uplift rate, rainfall intensity, width of depositional area, and permeability adjusted by the degree of compaction. This suggests that *mean cell slope of steeper cluster* of 45˚- 60˚ is to represent the threshold hillslope proper to the 10 : 1 mixture of fine sand and kaolinite. Expressing the threshold hillslope in an area by an average value with a certain range is considered more appropriate than by a particular slope gradient. This is because defining a

©2021. Japan Geoscience Union. All Right Reserved.

particular threshold hillslope in the area is impractical even in the simplified experiment due to the diversity in conditions of individual slopes. Slope conditions, such as shape and size, the behavior of infiltrated water, and local condition of material, are more or less different on each slope; and moreover, the nature and magnitude of triggering events can be different at each time. If *mean cell slope of steeper cluster* increases into the range of threshold hillslope, landslide concentration would possibly occur, and this possibility or frequency would increase as the value of this parameter increases towards the upper limit.

Keywords: geomorphic experiment, steady state, permeability, fluvial erosion, slope failures, threshold hillslope

©2021. Japan Geoscience Union. All Right Reserved.

Causes of concentrated revetment damage in the Hatto River in eastern Tottori Prefecture during the heavy rains in western Japan in July 2018

*Yoshinori Kodama[1], Taishi Sugimoto

1. Faculty of Agriculture, Tottori Univ.

Introduction

The Hatto River, which flows through the eastern part of Tottori Prefecture, originates from Mt. Hyonosen (1,509 m.a.s.l.) with a river channel length of 39.1 km and a basin area of 417.3 km^2. Due to the heavy rains in western Japan in July 2018, revetments were damaged at five locations 18 to 20 km from the confluence of the Sendai River. The purpose of this study is to clarify the river channel shape in the Hatto River, especially the transition of gravel bars, and to consider the cause of the concentration of revetment damage points in the 2018 flood.

Method

Using aerial photographs of the Geospatial Information Authority of Japan and satellite images of Google Earth Pro, the gravel bars of the Hattou River was investigated. The shooting years were 1947, 1964, 1976 (including some 1975), 1995, 2013, and 2018, and the distributions of water bodies, gravel bars, vegetation, and exposed bedrock were plotted. The front edges of the gravel bars were determined from the distribution pattern of the gravel bars and represented by a red line with dipping direction. In addition, the area ratio of gravel bars and vegetation in the river channel was calculated by dividing it into 0 to 8 km (downstream), 8 to 16 km (middle stream), and 16 to 24 km (upstream) section.

Results and discussions

According to changes in the shape of gravel bars and changes in the area ratio of gravel bars and vegetation, the number of gravel bars that occupied about 50% in 1947 and 1964 decreased to 35% in 1976, and in 1995, as low water channel excavation work and high flood plain construction progressed, most of the artificial flood plain became vegetation areas. After that, the area ratio of the gravel bars decreased to less than 20%. Instead, vegetation increased to about 50%. As for the longitudinal changes, it was clarified that the area ratio of the gravel bars is higher toward the upstream and the area ratio of vegetation is higher toward the downstream. This is a manifestation of the downstream decrease in the amount of bedload per unit width.

The longitudinal distribution of the position of the front edge of the gravel bars and the frequency distribution classified by the length of the front edge of the gravel bars were analyzed by upper, middle, and downstream, and their transitions were investigated. As a result, 56 gravel bars were certified in 1947 over almost the entire area, and the half-wavelength of the gravel bars was about 50 to 1,250 m, and most of them were 50 to 350 m. In the period of high economic growth, the number of gravel bars gradually decreased in 1964 and decreased to 31 in 1976. In 1995, only 5 gravel bars were found. It is thought that the cause is low waterway construction work.

However, the number increased to 18 in 2013 and 33 in 2018, and many short gravel bars with half wavelengths of 100 to 300 m were observed. Especially in the upstream section of 2018, the number of gravel bars recovered to almost the same state as in 1947. Moreover, the short gravel bars with a half wavelength of 50 to 350 m were outstanding. It is thought that this is a reflection of the fact that the number of low-water channel excavation works has decreased and gravel has been transported from the upstream side. The five revetment damage points found at 18 to 20 km are near the downstream end of the gravel bar recovery section, and many short wavelength gravel bars were found. In general, gravel bars

©2021. Japan Geoscience Union. All Right Reserved.

have a short wavelength in the early stage of formation, and the wavelength becomes longer with time to reach a steady state. In short-wavelength bar, the angle of collision of the water flow with the riverbank becomes large and local scouring occurs, which is the cause of the concentration of revetment damage.

Conclusion

Due to the river improvement work after the high economic growth period, the gravel bar of the Hatto River was hardly seen around 1995. However, in the 2010s, a short-wavelength gravel bar was restored from the upstream side, increasing the angle of collision of the water stream with the riverbank and inducing damages to the revetment. This is the cause of the concentration of revetment damage observed in the Hatto River in the flood in July 2018. In the future, it is expected that short-wavelength gravel bars will be formed as the recovery section of the gravel bars extends downstream, and there is a high possibility that revetment damage will occur in the vicinity, so it is necessary to pay close attention.

Keywords: short wave-length gravel bars, concentrated revetment damage, the heavy rains in western Japan in July 2018, low water channel construction work, recovery of gravel bars, aerial photo interpretation

©2021. Japan Geoscience Union. All Right Reserved.

Initiation factors of an incised meandering river in steep mountainous terrain: a case study of the Higashigouchi River with high-angle bedding plane

*Takuma Watakabe[1], Hikaru Osawa[2], Noriyuki Arai[3], Issei Doi[3], Yosuke Yamakawa[2]

1. Kansai Research Center, Forestry and Forest Products Research Institute, 2. Mountain Science Center, Univ. of Tsukuba, 3. Disaster Prevention Research Institute, Kyoto University

This study reports conditions of initiation of an incised meandering river running through a steep mountainous terrain in Higashigouchi River in the watershed of Ooi River, Shizuoka prefecture, central Japan. The Higashigouchi River is underlain by Late Cretaceous accretionary complex called by Shimanto Belt, including shale, sandstone, shale-dominated interbedded shale and sandstone, and sandstone-dominated interbedded shale and sandstone. Bedding of these strata trends NE–SW and dips more than 50˚ to the northwest, which broadly corresponds to the flow direction of the Higashigouch River. Channel meandering develops at 2-6 km in streamwise distance from the confluence with the Ooi River, with a shorter wavelength than that of the Ooi river and without meander cutoff. The type of riverbed in the Higashigouchi River changes in four types: bedrock exposure zone, giant boulder zone, gravel cover zone, and strath terrace covered by thin sediment cover. Channel width in the meandering segment is narrower than the other segments, mostly showing within 30 m. Channel gradient in most of the segment ranges from 0.02 to 0.04. The geological structure shows marked changes along the meandering segment where shale-dominated interbedded shale and sandstone dominate. The streamflow runs alternately through areas with comprehensive geological structure and areas where the bedding trends NW–SE and dips more than 50˚ to the northeast. Rock strength in the meandering segment is similar to the other segments. Therefore, these results imply that the initiation of incised meander in the steep mountainous terrain with high-angle bedding planes is influenced by internal factors within the catchment that are changes of geological structure and channel gradient.

Keywords: Incised meandering river, Geological structure, Accretionary complex

©2021. Japan Geoscience Union. All Right Reserved.

Generation of Terrain Classification Data for Ground Vulnerability Assessment Using 30m DEM by Digital Terrain Analysis

*Junko Iwahashi[1], Dai Yamazaki[2], Takayuki Nakano[1], Ryo Endo[1]

1. GSI of Japan, 2. Institute of Industrial Science, The University of Tokyo

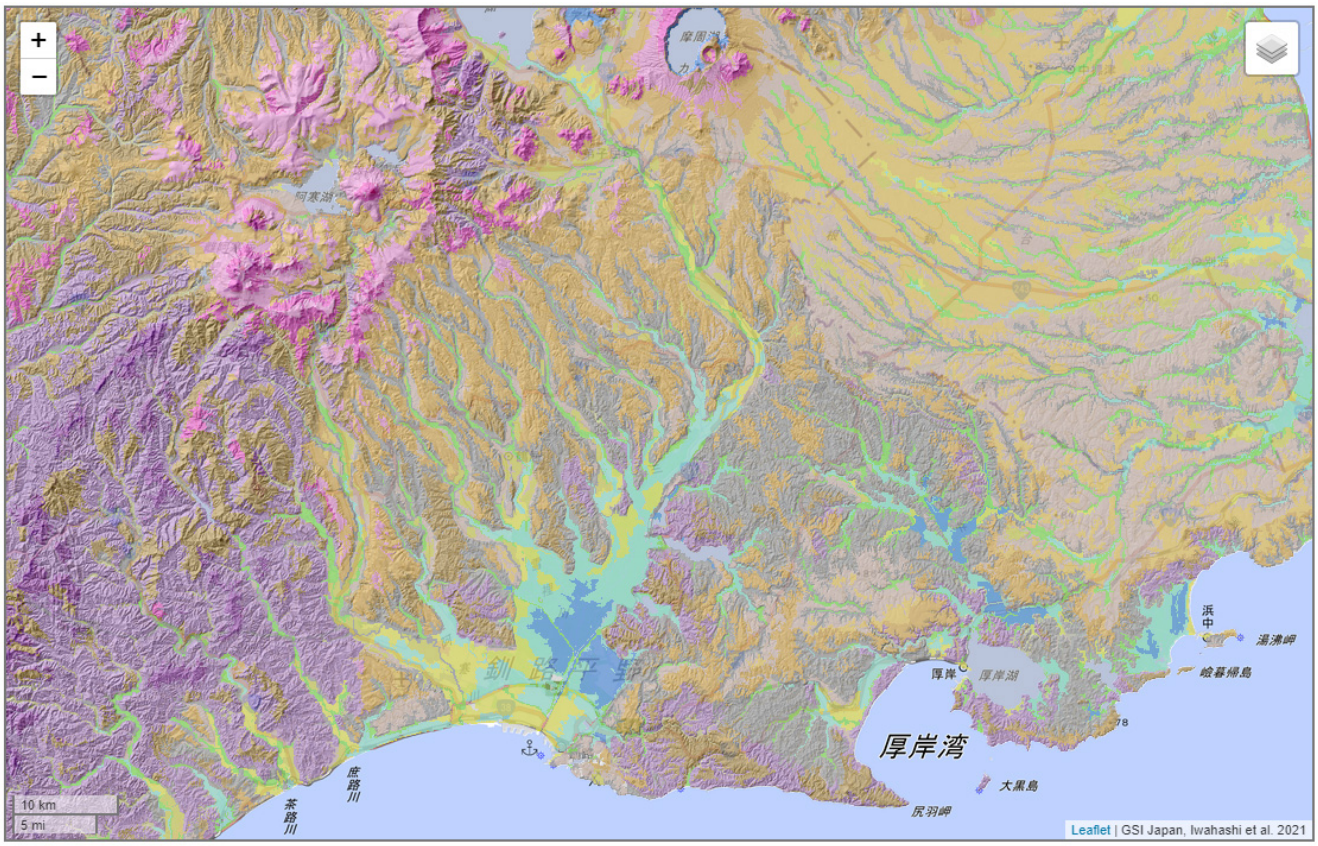
Digital terrain analysis aims at modeling and estimating various phenomena that are known to be related to topography, using either the terrain measurements (physical quantities such as slope gradient) themselves calculated from a Digital Elevation Model (DEM), or a map that combines these quantities and zones slopes with similar shapes (terrain characteristics). The purpose of this project is to model and estimate various phenomena that are known to be related to topography, and to produce useful data for such modeling and estimation. For example, the risk of slope failure and landslides, the susceptibility of the ground to shaking, the type of soil, the susceptibility to snow avalanches, etc. are known to be related to topography.

In this study, a terrain classification map was created using the Japanese 30-m DEM by calculating the slope gradient, surface texture, and local convexity, which have been found to be effective in zoning medium terrain from previous studies, and the newly added HAND (height above the nearest drainage). The method was simple and reproducible. Using raster images of terrain measurements, the study area was divided into polygons, zoned by clustering with the average value of each terrain measurements in the polygon region as the representative value, and grouped by terrain type in comparison with existing geological maps, landform classification maps, and the distribution of landslides and collapses. The 30-m GeoTIFF file of this classification map and the shape file containing intermediate results such as terrain measurements as attributes are available from the GSI website (https://gisstar.gsi.go.jp/Japan_terrain/).

Through comparison with existing landform classification maps by experts and comparison with areas where shallow landslides and floods have occurred in recent years, this presentation will provide an explanation of the points reached, areas that need improvement, and prospects. In addition, the authors are currently working on the publication of similar data using a global 90-m DEM. This effort will also be presented.

Keywords: Digital Elevation Model, terrain classification, ground vulnerability, landslide, DEM

©2021. Japan Geoscience Union. All Right Reserved.



Classification of topography using 30 m DEM of Japan (portion)

©2021. Japan Geoscience Union. All Right Reserved.

[J] Oral | H (Human Geosciences)：H-GM Geomorphology

Fri. Jun 4, 2021 10:45 AM - 12:15 PM JST | Fri. Jun 4, 2021 1:45 AM - 3:15 AM UTC | Ch.14 Zoom Room 14

[H-GM03] Geomorphology

convener:Tsuyoshi Hattanji(Faculty of Life and Environmental Sciences, University of Tsukuba), Masayuki Seto(Fukushima Future Center for Regional Revitalization, Fukushima University), Chairperson:Masayuki Seto(Fukushima Future Center for Regional Revitalization, Fukushima University)

The main subject of this session is the whole range of themes relating to geomorphology, especially geomorphic processes, landform development and its relation to environmental changes, geomorphological hazards and their mitigation and reports of recent events of disaster occurred in Japan, various kind of hazard maps, relationships among geomorphic processes, other natural phenomena and human activities, and various techniques of geomorphological measurements and automatic landform classification. Japanese can be used in this session.

10:45 AM - 11:00 AM JST | 1:45 AM - 2:00 AM UTC

[HGM03-07] Analysis of step-structure affecting Cs and sediment transport at hillslope scale

*Seigo Fujiwara[1], Yuichi Onda[2], Yoshifumi Wakiyama[3], Toshiaki Anzai[4], Hiroaki Kato[2] (1.Master Program in Geosciences, Degree Programs in Life and Earth Sciences, University of Tsukuba, 2.Center for Research in Isotopes and Environmental Dynamics, University of Tsukuba, 3.Institute of Environmental Radioactivity, Fukushima University, 4.School of Life and Environmental Sciences, University of Tsukuba)

11:00 AM - 11:15 AM JST | 2:00 AM - 2:15 AM UTC

[HGM03-08] Lithological Controls on Mechanisms of Shallow Landslides Triggered by an Extreme Rainfall Event:

Comparative Survey on Hillslopes underlain by Granite and Granodiorite in the Northern Abukuma Mountains

*Arihito Kondo[1], Yuki Matsushi[2], Yoshinori OTSUKI[1] (1.Institute of Geography, Graduate School of Science, Tohoku University, 2.Disaster Prevention Research Institute, Kyoto University)

11:15 AM - 11:30 AM JST | 2:15 AM - 2:30 AM UTC

[HGM03-09] Reconstructing the transition of hillslope denudation in granite watersheds using cosmogenic nuclides: quantifying the anthropogenic impacts on soil coverage in the Tanakami Mountains, central Japan

*Ryoga Ohta[1,2], Yuki Matsushi[3], Hiroyuki Matsuzaki[4] (1.Graduate School of Science, Kyoto university, 2.JSPS Research Fellow DC, 3.Disaster Prevention Research Institute, Kyoto University, 4.Micro Analysis Laboratory, Tandem Accelerator, The University of Tokyo)

11:30 AM - 11:45 AM JST | 2:30 AM - 2:45 AM UTC

[HGM03-10] Distribution of infilling rates in hollows estimated from radiocarbon dates and high-resolution DEMs -A case study of granitic mountain slopes in Hiroshima City, Hiroshima Prefecture-

*Wataru Koga[1], Tsuyoshi Hattanji[2], Takahisa Furuichi[3], Shoji Doshida[4], Yasushi Tanaka[5] (1.University of Tsukuba graduate school of Life and Environmental Science, 2.University of Tsukuba department of Life and Environmental Science, 3.Forestry and Forest Products Research Institute, 4.National Research Institute of Fire and Disaster, 5.Komazawa University Faculty of Letters)

11:45 AM - 12:00 PM JST | 2:45 AM - 3:00 AM UTC

[HGM03-11] Paleoenvironment in Lake Olgoy, Mongolia based on the anaylses of sediment from the paleoshoreline

*Yuma Shibuya[1] (1.KANAZAWA UNIVERSITY)

12:00 PM - 12:15 PM JST | 3:00 AM - 3:15 AM UTC

[HGM03-12] 3D geomorphological analysis method for sea cliff: A case study of Miocene sedimentary rocks in Yonaguni Island

*Hayate Kimura[1], Toshihiko Ichihara[2], Hironobu Kan[1] (1.Graduate School of Integrated Sciences for Global Society, Kyushu University, 2.Sedimentary Environments Research)

Analysis of step-structure affecting Cs and sediment transport at hillslope scale

*Seigo Fujiwara[1], Yuichi Onda[2], Yoshifumi Wakiyama[3], Toshiaki Anzai[4], Hiroaki Kato[2]

1. Master Program in Geosciences, Degree Programs in Life and Earth Sciences, University of Tsukuba, 2. Center for Research in Isotopes and Environmental Dynamics, University of Tsukuba, 3. Institute of Environmental Radioactivity, Fukushima University, 4. School of Life and Environmental Sciences, University of Tsukuba

Kawamata Town, Fukushima Prefecture was designated as a special decontamination area due to the Fukushima Daiichi Nuclear Power Plant accident in 2011, and decontamination activities were carried out in 2014. During the decontamination activities, the surface layer of 5 cm of soil with high Cs-137 concentration was stripped by heavy machinery, and coarse granitic sand was applied. In the decontaminated area, many step-structure microterracettette were observed during strong rainfall. Furthermore, the amount of sediment discharge was reduced in the decontaminated area compared to the pre-decontaminated area. Thus, it is necessary to elucidate the microterracettette structures that are considered to affect sediment transport.

This study was conducted in rainfall experiments and USLE plots (22.13 m long ×5 m wide) in Yamakiya area of Kawamata Town, Fukushima Prefecture, which is a decontaminated area, and in Tsukidate City, Fukushima Prefecture, which is an un-decontaminated area. The purpose of this study is to elucidate the Cs-137 and sediment transport process at hillslope scale by using the observation of Cs-137 and sediment discharge, surface change, and RFID (Radio Frequency IDentification) tags. Surface runoff and sediment discharge were observed at the lower end of the plot, and Cs-137 concentration and sediment discharge were measured. Surface changes were calculated from 3D data obtained by Unmanned Aerial Vehicle - Structure from Motion (UAV-SfM). The shear stress of surface flow was estimated from the distance of sediment movement with different particle sizes using RFID tags. In addition, a scraper plate survey was conducted in the microterracettette area in the un-decontaminated plot to analyze the relationship between sediment transport and Cs-137 discharge according to the depth distribution of Cs-137.

In field tests, the accuracy of the surface change map in the field test was 0.1 cm in mean error and 0.3 cm in standard deviation error compared with laser survey. The surface change showed microterracettettes above the rill erosion area during large rainfall events, and large sediment discharge was observed during these events. Microterracettettes were formed in both decontaminated and un-decontaminated plots.

In rainfall experiments, UAV-SfM survey and RFID tags were used to obtain the surface change map and the transport distance of soil particles. Two types of RFID tags were used: one with a small particle size with a median value of 2.8 mm and the other with a large particle size with a median value of 3.9 mm. Comparing the results between the agricultural and sand plots with a slope of 5˚, where the slope length and slope were the same and the distance from the top of the slope at the location where the RFID tag was placed was the same, the surface change was more pronounced at the lower end of the sand plot, where rill erosion occurred. It was found that the traveled RFID tags distance was longer in the agricultural plot, suggesting that surface flow was also generated at the top of the slope.
The terracettes were shown to be formed in the middle of the inter-rill area (upper part) and the rill area (lower part). Furthermore, the terracettes were formed in a wider area in the agricultural soil plot than in

©2021. Japan Geoscience Union. All Right Reserved.

the sand plot.

In conclusion, the contribution of sediment discharge in the sand plot is linear, while that in the agricultural plot is a wider area. Furthermore, terracette is more likely to form when the slope is greater than 5˚ and the rainfall intensity is greater than 130 mm/hr, and terracettes are likely to form in agricultural plots. In addition, the terracette is formed in the middle of the inter-rill area (upper part) and the rill area (lower part). In addition, field tests showed that terracette can form even at low rainfall intensity, but require a certain level of flow rate.

Keywords: soil erosion, surface change, UAV-SfM, Cs-137, decontamination activity

©2021. Japan Geoscience Union. All Right Reserved.

Lithological Controls on Mechanisms of Shallow Landslides Triggered by an Extreme Rainfall Event:

Comparative Survey on Hillslopes underlain by Granite and Granodiorite in the Northern Abukuma Mountains

*Arihito Kondo[1], Yuki Matsushi[2], Yoshinori OTSUKI[1]

1. Institute of Geography, Graduate School of Science, Tohoku University, 2. Disaster Prevention Research Institute, Kyoto University

The bedrock lithology dictates physical characteristics and production rates of regolith, which leads to characteristic regolith depending on the bedrock lithology. Differences in the properties of regolith cause different hydro-geomorphological processes through rainwater infiltration, which influences the differences in the mechanism of shallow landslides caused by extreme rainfall. Due to the extreme rainfall caused by typhoon in 2019, shallow landslides occurred extensively in the northern Abukuma Mountains which were underlain by granitoids. It has been pointed out that granodiorite slope area has a lower spatial landslide density than granite slope area, but many shallow landslides occurred in the slope area underlain by granodiorite in the Kitakami belt. In this presentation, we point out that the differences in mechanical and hydraulic properties of the shallow subsurface structures of slopes would make differences in the mechanism of shallow landslides in the slope area underlain by granite and granodiorite bedrock.

The shallow subsurface structures on the slopes were revealed by observation at the field, cone penetration test, geotechnical test in the laboratory. Pore water pressure fluctuations due to rainfall were revealed by hydrological monitoring using tensiometers.
On the granite slopes, the soil-layer has a small Nc value (Nc < 5). It has also high permeability and low water retention, suggesting it has high drainage capacity. The weathered bedrock beneath the soil-layer is rather hard (Nc > 10). Thus, there is a mechanical and hydraulic discontinuity between the soil-layer and the weathered bedrock. The results of hydrological monitoring suggests the infiltrated rainwater is likely to be easily drained above the weathered bedrock. Therefore, a sliding surface would often be formed near the discontinuity. However, a sliding surface does not often form because the drainage capacity of the soil-layer is high.
On the other hand, there is no clear mechanical and hydraulic difference in the soil-layer on the granodiorite slopes. However, there is a discontinuity in the soil-layer at which mechanical and hydraulic properties slightly change. According to a result of hydrological monitoring, a lateral infiltration flow that causes an increase in pore water pressure occurs near the slight discontinuity. The increase in pore water pressure causes a cohesion to decrease, which leads to the formation of sliding surfaces. Moreover, the shearing resistance angle is low value at the potential sliding surface. This may have promoted occurring shallow landslides on the gentle slope area.

These facts suggests that the shallow subsurface structures in the slopes are different with bedrock lithology. It is also possible that the difference in the shallow subsurface structures on the slopes make a difference in the characteristic of shallow landslides triggered by extreme rainfall.

Keywords: Shallow landslide, Shallow subsurface structure, Granitic rock, Abukuma mountains

©2021. Japan Geoscience Union. All Right Reserved.

Reconstructing the transition of hillslope denudation in granite watersheds using cosmogenic nuclides: quantifying the anthropogenic impacts on soil coverage in the Tanakami Mountains, central Japan

*Ryoga Ohta[1,2], Yuki Matsushi[3], Hiroyuki Matsuzaki[4]

1. Graduate School of Science, Kyoto university, 2. JSPS Research Fellow DC, 3. Disaster Prevention Research Institute, Kyoto University, 4. Micro Analysis Laboratory, Tandem Accelerator, The University of Tokyo

We quantify the anthropogenic acceleration of hillslope denudation by cosmogenic ^{10}Be measurements in detrital sand from watersheds with different hillslope coverage. We then reconstruct the anthropogenic environmental change through the detailed analysis of sediment cores obtained at the outlet of the watershed where significantly affected by human impact on hillslope coverage.
The investigated granite watersheds are located in the Tanakami mountains, about 20 km to the southeast of Kyoto, Japan. The present watersheds can be categorized into three types: 1) kept forested and naturally soil-mantled watersheds without significant human impact, 2) devastated and still bedrock-exposed watersheds, and 3) artificially reforested and thin soil coverage watersheds. The ^{10}Be concentration in forested watersheds indicates higher varying values (4.8×10^4–8.9×10^4 atoms g^{-1}). Assuming steady-state denudation, the non-impacted natural watersheds in this area have been denuded at rates ranging from 1.4×10^2–2.6×10^2 g^{-1} m^{-2} yr^{-1}. Whereas ^{10}Be concentration in devastated or reforested watersheds show lower constant values (1.9×10^4–4.0×10^4 atoms g^{-1}). Once the soil layer on hillslope have been thoroughly removed, the current fluvial sediment originates from the uppermost part of the saprolite. The ^{10}Be concentration in sample can not recover in the 10^2–10^3 yr timescale. Thus, the difference in ^{10}Be concentration can be explained by mass loss from hillslope due to the human impact. In the case of Tanakami Mountains, the thickness of removed material from hillslopes should have reached from 0.57±0.14–2.04±0.31 m for the past few hundred years since initiation of overexploitation on the forest resources.
Sediment that was washed away from hillslope due to the anthropogenic impact is widely distributed and filled the channel around the outlet of Tenjin watershed which is located in west side of Tanakami mountain. The depth profile of ^{10}Be in the sediment core collected at the point show gradually degrease forested watershed level (5.8×10^4 atoms g^{-1}) at bottom (2723–2490 cal BP) to devastated watershed level (2.6×10^4 atoms g^{-1}) at surface, changeling as repeatedly increases and decreases. The tendency emerged at the layer dated around 918–793 cal BP. The upper layer of that, charcoals that dated older than the lower samples were included in the layers (3000–2426 cal BP, 4289–4091 cal BP). Once the sediment produced from the upper part of the saprolite by freeze and thawing in winter and eroded by surface erosion in monsoon, ^{10}Be concentration in sediment should be getting lower. While, during heavy rainfall events, the remaining soil layers with organic material in watershed should be eroded, resulting in a temporary increase in the ^{10}Be concentration with reversals in ^{14}C age in the sediment. The anthropogenic deforestation must have progressed from the front to the interior. Our results indicate that if we continue to overexploit forest resources to a tipping point that vegetation recovery can not keep up the condition, the soil mantled on hillslope will be completely removed and will not be able to return to its original state.

Keywords: physical geography, human impact, tipping-points, cosmogenic nuclide, radiocarbon dating

©2021. Japan Geoscience Union. All Right Reserved.

Distribution of infilling rates in hollows estimated from radiocarbon dates and high-resolution DEMs -A case study of granitic mountain slopes in Hiroshima City, Hiroshima Prefecture-

*Wataru Koga[1], Tsuyoshi Hattanji[2], Takahisa Furuichi[3], Shoji Doshida[4], Yasushi Tanaka[5]

1. University of Tsukuba graduate school of Life and Environmental Science, 2. University of Tsukuba department of Life and Environmental Science, 3. Forestry and Forest Products Research Institute, 4. National Research Institute of Fire and Disaster, 5. Komazawa University Faculty of Letters

Hollows are generally infilled by soil creep or rockfall from upper slopes after shallow landslide occurs. Although many studies have focused on the temporal variation of landforms around valley heads and hollows under various regional settings, few studies have focused on the relationship between topographic parameter and infilling rates in each valley. Radiocarbon dates of charcoal in valley-head sediment were analyzed for granitic mountains of Hiroshima City where many shallow landslides occurred due to the heavy rainfall on August 20, 2014. Total 22 samples of charcoal were collected from 5 valley heads. In addition, the topographic parameters such as slope gradient and size of source area were measured using a 1 m-DEM before and after the shallow landslides. Furthermore, infilling rates at the valley heads were estimated from the calibrated radiocarbon ages and the pre-landslide depth of the samples. The calibrated radiocarbon ages ranged from about 350 to 1600 cal BP. This result suggests that the timing of the previous landslide event varied by valley. The estimated infilling rates of the valley heads ranged from about 0 to 3.5 mm/yr. When focusing on the middle to downstream parts of the valley heads, the infilling rates tend to increase with increasing source-area size. The infilling rates also tend to increase with increasing surface roughness of the source area, which is an index of rock exposure on ground surface. There was also a positive correlation between the infilling rates and the grain size of ground surface. Furthermore, the maximum grain size of mobile debris by overland flow was 10 cm or less at the middle to downstream parts of the valley heads under the assumption of heavy rainfall of 75 - 100 mm/h. These results suggest that the pre-landslide infilling rates were not spatially uniform and that the infilling proceeds faster at the downstream section of valley heads because large cobbles and boulders can accumulate downstream, except for some sites with intense human impacts.

Keywords: valley head, shallow landslide, radiocarbon dating, 1-m DEM, granite

©2021. Japan Geoscience Union. All Right Reserved.

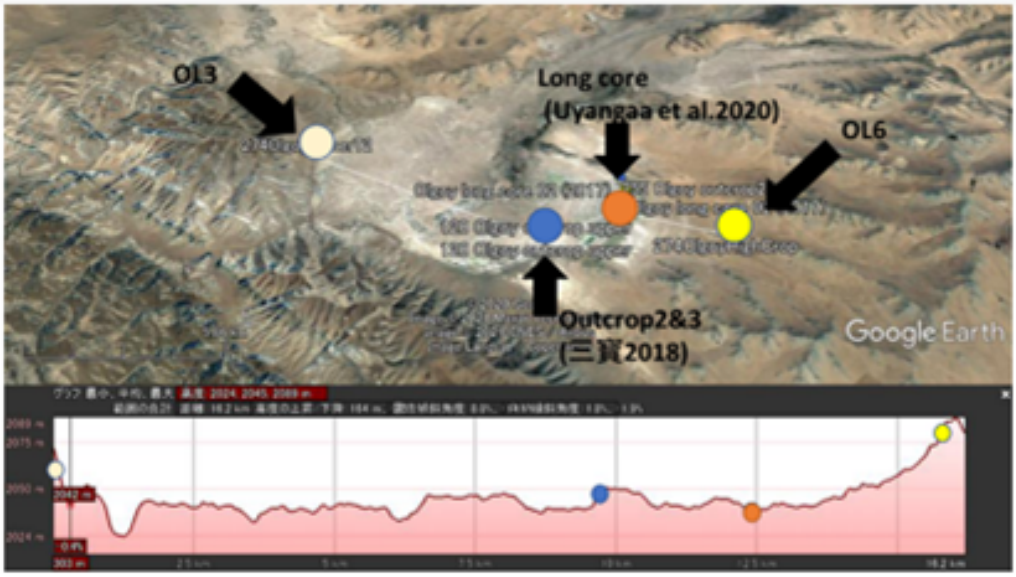
Paleoenvironment in Lake Olgoy, Mongolia based on the anaylses of sediment from the paleoshoreline

*Yuma Shibuya[1]

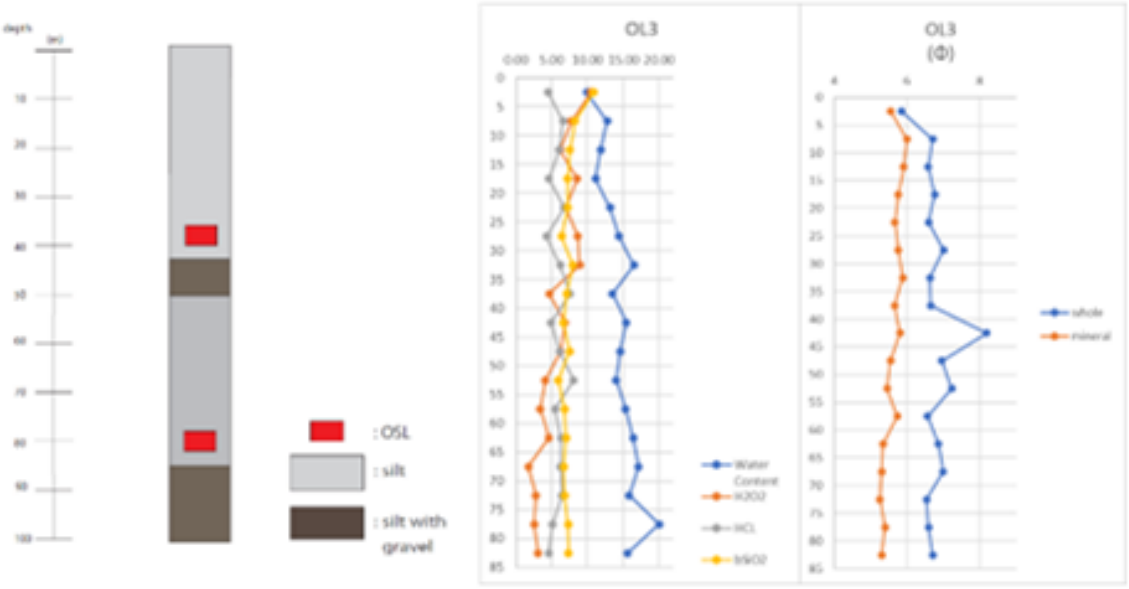
1. KANAZAWA UNIVERSITY

In recent years, environmental change due to global warming become a social threat. One of the serious problems is drought. In arid southern part of Mongolia, lakes are shrinking nowadays. We conducted a study in Lake Olgoy in Mongolia to reconstruct the fluctuation in lake levels and paleoenvironments by analyses of paleolake deposit collected from the outcrops.
10.5 m core was collected from Lake Olgoy in 2017, and anlysed to investigate environmental fluctuations. Age dating of this long core has produced two different age axes: One is by OSL dating and the other is radiocarbon dating (Igarashi 2019). Both results form linear relationships but the results by radiocarbon dating is older than OSL dating. However, since both graphs show linear relationships, the age estimate by OSL has a potential to correlate long core and outcrop sediment. Heavy inflows in the past have been implicated in previous study of Lake Olgoy (Matsumura et al. 2018). However, the scale and time of the water influx events are unknown.
To address lake level changes by the change of water influx, we analyzed samples (OL3&L6) from the paleoshoreline of Lake Olgoy and compared them to the results from the Long core (Uyangaa et al. 2020). Both OL3 and OL6 samples are located higher than the present lake level. Sediment samples were obtained by trenching. OL6 is located the highest within the paleoshoreline trenches and is considered to reflect the period of maximum lake level.
Based on OSL ages of OL3 and the Long core, OL3 sediment is correlated to around 280 cm depth in the Long core. Similar data fluctuations were also found in the analytical results of OL3 and the 280 cm depth of the Long Core. Since this similarity confirms the OL3 sediment is lake sediment, the lake level at that time was reconstructed as high as the altitude of the locality.
As for the OSL age of OL6, we found that it can be correlated to 450 cm depth of the Long Core. When similar fluctuation in sediment analytical results is searched, OL6 is correlated with the 850 cm depth section of the Long Core, different from the estimate by the OSL age. The 850 cm depth of the Long Core was dated as about 45,000 years ago. This is the period when the Long Core analysis suggests that the thawing of the permafrost caused a large amount of water to flow into the area. Therefore, we assume correlation to the 850 cm depth would be more plausible, and this period is considered to be the time when the huge amount of water flowed into Olgoy Lake and reached the maximum lake level.

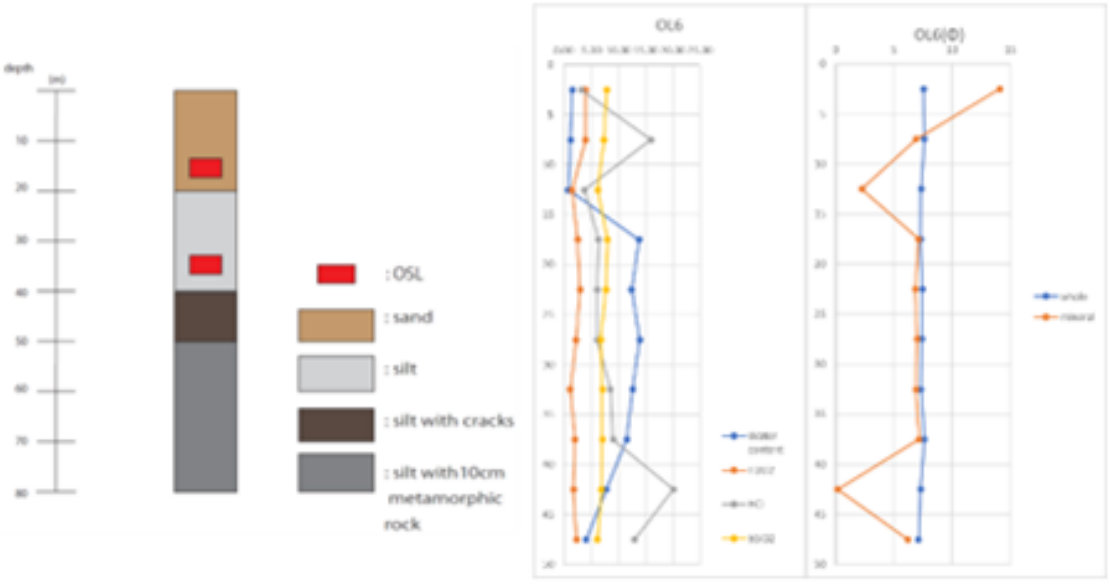
©2021. Japan Geoscience Union. All Right Reserved.



図① Olgoy 湖の断面図とサンプリング場所



図② OL3 の柱状図と分析結果



図③ OL6 の柱状図と分析結果

©2021. Japan Geoscience Union. All Right Reserved.

©2021. Japan Geoscience Union. All Right Reserved.

3D geomorphological analysis method for sea cliff: A case study of Miocene sedimentary rocks in Yonaguni Island

*Hayate Kimura[1], Toshihiko Ichihara[2], Hironobu Kan[1]

1. Graduate School of Integrated Sciences for Global Society, Kyushu University, 2. Sedimentary Environments Research

The sea cliffs are the zones hard to research geomorphologically because there are difficult to approach and survey. The topographic change has been measured in the areas of high cliff erosion rate with the development of surveying methods using the aerial laser scanner and the small UAV. However, there have been few applications in the sea cliff of low erosion rate. In this study, we investigated the geomorphological analysis method suitable for the unaccessible sea cliffs and performed the analysis as an example of the Miocene sedimentary rocks in Yonaguni Island.

Phantom4 RTK (DJI) was utilized to obtain aerial photographs. The photographs were taken in two steps. First step is to capture whole coastal zone by automatic control with the camera facing down. Second step is to capture the cliff face manually with the camera facing the cliff to obtain the high-resolution model. Metashape Professional (Agisoft) was used for SfM-MVS processing. The lithology of the cliffs was classified in the model based on the observations in the accessible coastal zones. The geomorphological analysis using the general Digital Elevation Model (DEM) isn’ t suitable for the cliff face. We created the geomorphological data sets suitable for 3D analysis by using the 3DCAD software Rhinoceros (McNeel). The profiles created by calculating the intersection of the mesh model and an arbitrary face represented the complex shape of the cliff including the overhang zones. The cliff face DEM was created by transforming the coordinates of the model, which the detailed shape of the cliff was visualized and quantified.

By calculating the slope and longitudinal curvature of the cliff face DEM (5cm meshed grid), the correspondence between the cliff face shape and the lithology was quantified. In the cliffs consisting of the tidal deposits, the tendency of roughness of the cliff face and the weathering and erosional process depends on the lithology. Therefore, in Yonaguni Island the lithology of the sedimentary rocks is considered to control the recession process of the sea cliff. The geomorphological analysis method adopted in this study is effective for the sea cliffs composed of the sedimentary rocks.

Keywords: Drone, RTK-UAV, SfM-MVS, Photogrammetry, DEM, Yaeyama Group

©2021. Japan Geoscience Union. All Right Reserved.

[J] Oral | H (Human Geosciences)：H-SC Social Earth Sciences & Civil/Urban System Sciences

Fri. Jun 4, 2021 9:00 AM - 10:30 AM JST | Fri. Jun 4, 2021 12:00 AM - 1:30 AM UTC | Ch.15 Zoom Room 15

[H-SC05] CCUS (Carbon Dioxide Capture, Utilization, and Storage) for Climate Mitigation

convener:Masao Sorai(Institute for Geo-Resources and Environment, National Institute of Advanced Industrial Science and Technology), Ziqiu Xue(Research Institute of Innovative Tech for the Earth), Masaatsu Aichi(Graduate School of Frontier Sciences, University of Tokyo), Yoshihiro Konno(The University of Tokyo), Chairperson:Masao Sorai(Institute for Geo-Resources and Environment, National Institute of Advanced Industrial Science and Technology)

The prevention of the global warming, which is the urgent challenge facing the world, requires the full-out efforts of science and technology. This session focuses on the CCUS (Carbon Dioxide Capture, Utilization, and Storage) as one of the useful countermeasures for the CO2 emission reduction. The session covers various scientific phenomenon caused by the capture and storage of CO2, CO2 utilization, and CO2-EOR/EGR, along with the discussion about the latest R&D developments of each method for the environmental impact assessment, safety assessment, the measuring, monitoring and verification (MMV), and public acceptance. The main theme is the recognition of key issues toward the practical use of CCUS, in addition to the deepening of our knowledge about the CO2 behavior on the underground.

9:00 AM - 9:15 AM JST | 12:00 AM - 12:15 AM UTC

[HSC05-01] Progresses of Nano-Scale Study on CO2 Utilization and Storage

*Yunfeng Liang[1] (1.The University of Tokyo)

9:15 AM - 9:30 AM JST | 12:15 AM - 12:30 AM UTC

[HSC05-02] Molecular Dynamics Study on Coal Matrix Swelling Characteristics by CO2, N2, and CO2–N2 Mixture

*Jinrong Cao[1], Yunfeng Liang[1], Yoshihiro Masuda[1], Ziqiu Xue[2], Toshifumi Matsuoka[3] (1.Department of Systems Innovation, The University of Tokyo, 2.Research Institute of Innovative Technology for the Earth, 3.Emeritus Professor, Kyoto University)

9:30 AM - 9:45 AM JST | 12:30 AM - 12:45 AM UTC

[HSC05-03] Wettability of CO_2/Water/Mineral Systems: Comparison of Water-wet and CO_2-wet systems by thermodynamics and molecular dynamics

*Masashige Shiga[1,2], Masaatsu Aichi[1], Masao Sorai[2] (1.The University of Tokyo, 2.AIST)

9:45 AM - 10:00 AM JST | 12:45 AM - 1:00 AM UTC

[HSC05-04] Coupled chemical osmosis and rock deformation: Numerical investigations and their comparison with experimental results

*Shogo Hirota[1], Tomochika Tokunaga[1], Ziqiu Xue[2], Takayuki Miyoshi[2,3], Hyuck Park[2] (1.Department of Environmental Systems, Graduate School of Frontier Science, the University of Tokyo, 2.Research Institute of Innovative Technology for the Earth, 3.Geological Carbon Dioxide Storage Technology Research Association)

10:00 AM - 10:15 AM JST | 1:00 AM - 1:15 AM UTC

[HSC05-05] Evaluation of Caprock Sealing Performance in Saline Aquifer Storage

*Yuuki Shigeoka[1], Haruki Nishiyama[1], Hiroshi Kinoto[1], Yukiko Shoji[2], Takaomi Tobase[2] (1.J-POWER Business Survice Corporation, 2.Electric Power Development Co.)

10:15 AM - 10:30 AM JST | 1:15 AM - 1:30 AM UTC

[HSC05-06] Recent advances in value of information analysis and application to geological CO_2 storage

*Takashi Goda[1], Kozo Sato[1], Takahiro Nakajima[2,3] (1.School of Engineering, The University of Tokyo, 2.Geological Carbon Dioxide Storage Technology Research Association, 3.Research Institute of Innovative Technology for the Earth)

Progresses of Nano-Scale Study on CO2 Utilization and Storage

*Yunfeng Liang[1]

1. The University of Tokyo

In this presentation, I’ll show some of our recent progresses in application of molecular simulation in CO2 utilization and geo-sequestration, including: (i) modeling CO2-water-mineral wettability; (ii) modeling CO2 mineralization; (iii) replacement of methane from methane hydrate by CO2; (iv) phase behavior in CO2-based enhanced oil recovery (EOR)) ; and (v) study on the stability of CO2 foam films.

For the wettability, I’ll review state-of-art studies on CO2-water-mineral systems, and show that it is possible to reproduce the CO2-water-mineral wettability at a wide range of pressures using molecular dynamics simulations. For CO2 mineralization, I’ll present the first-principles molecular dynamics study of carbonation and hydrolysis reactions on the newly-cleaved quartz surface. For utilization of CO2 in the development of methane hydrate, I’ll discuss the influence of adding N2 to CO2 on the process of replacing CH4 in methane hydrate.

For utilization of CO2 in EOR, I’ll show how to calculate the phase behavior involved with the oil and the injected CO2. For development of the CO2 foam, I’ll first present stability of CO2 foam with Sodium Dodecyl Sulfate (SDS), and show the effect of surfactant concentration, temperature, and pressure. After that, I’ll briefly explain our study on screening and optimizing the molecular structure of surfactants to improve the CO2 foam performance. Finally, I’ll present outlook on nanoscale study in CO2 utilization and geo-sequestration.

©2021. Japan Geoscience Union. All Right Reserved.

Molecular Dynamics Study on Coal Matrix Swelling Characteristics by CO2, N2, and CO2–N2 Mixture

*Jinrong Cao[1], Yunfeng Liang[1], Yoshihiro Masuda[1], Ziqiu Xue[2], Toshifumi Matsuoka[3]

1. Department of Systems Innovation, The University of Tokyo, 2. Research Institute of Innovative Technology for the Earth, 3. Emeritus Professor, Kyoto University

CO2 sequestration in coal seams is an economically viable option to reduce carbon emissions. Coalbed methane (CBM) is CH4 stored in the nanopores of the coal matrix. CO2 Enhanced CBM (CO2-ECBM) is considered prospective technology that can not only meet the increasing world energy resource demands but also ease greenhouse gas emissions by injecting CO2 into the coal seams. The injected CO2 is capable of promoting CH4 production. In the meantime, coal seams possess huge potentials for geological CO2 sequestration. However, the replacement process of CH4 in the coal matrix and the swelling/shrinkage of the coal matrix are poorly understood. Therefore, in this work, the molecular dynamics simulation study is presented considering the recovery of CH4 in the coal matrix and swelling of the coal matrix using CO2, N2, and CO2–N2 mixture, three different displacement schemes.

We quantify the amount by monitoring the density profiles. The results show that recovery of CH4 and swelling of the coal matrix are different in three displacement schemes. The use of CO2 injection obtained the highest recovery of CH4 inside the coal matrix. Meanwhile, coal matrix swelling is also quite severe. On the other hand, the use of CO2–N2 mixture injection yielded an increase of CH4 recovery as compared with the case of injecting pure N2. The coal matrix swelling is not severe. Also, there might be coal matrix shrinkage during the pure N2 displacement case. This work should shed light on the swelling of the coal matrix and recovery of CH4 during CO2, N2, and CO2–N2 mixture injection in coal seams.

©2021. Japan Geoscience Union. All Right Reserved.

Wettability of CO_2/Water/Mineral Systems: Comparison of Water-wet and CO_2-wet systems by thermodynamics and molecular dynamics

*Masashige Shiga[1,2], Masaatsu Aichi[1], Masao Sorai[2]

1. The University of Tokyo, 2. AIST

CO_2 capture and storage (CCS) is expected to be one of the important methods for reducing CO_2 emissions into the atmosphere. In CCS, the wettability of CO_2/water/mineral system is an important physical property that directly affects the storage potential and sealing performance. The contact angle is commonly used as an evaluation index of wettability. Therefore, many experimental measurements and simulations have been performed so far. The contact angle is modeled by Young's equation based on the balance of the energy of the three interfaces (CO_2/water interfacial tension, water/mineral interfacial energy, CO_2/mineral interfacial energy).
On the other hand, since it is not easy to measure and calculate the energy of the solid-liquid interface, it is difficult to make quantitative discussions such as estimating the value of the contact angle and identifying the influential factors. A better understanding of the structure and energy of solid-liquid interfaces is necessary to improve the model.
In this study, we focused on differences of these structure and energy between water-wet system and CO_2 -wet system. We performed molecular dynamics simulation to analyze the structure of the solid/fluid interface and calculate the adsorption free energy. As a result, the presence or absence of an adsorption film of the wetting phase was mentioned as a remarkable difference in the interfacial structure, and it was shown that the crucial factor was the salvation forces (structural forces) of the mineral surface.

Keywords: wettability, interface, contact angle, thermodynamics, molecular dynamics

©2021. Japan Geoscience Union. All Right Reserved.

Coupled chemical osmosis and rock deformation: Numerical investigations and their comparison with experimental results

*Shogo Hirota[1], Tomochika Tokunaga[1], Ziqiu Xue[2], Takayuki Miyoshi[2,3], Hyuck Park[2]

1. Department of Environmental Systems, Graduate School of Frontier Science, the University of Tokyo, 2. Research Institute of Innovative Technology for the Earth, 3. Geological Carbon Dioxide Storage Technology Research Association

Groundwater flow and solute transport in mudstone is generally considered to be very slow, and hence, mudstone formations are expected to perform as effective seal layers for carbon capture and storage (CCS) project. In the low-permeable, muddy formations, coupling processes such as chemical osmosis and poroelastic behavior can affect groundwater flow, solute transport, and rock deformation. Some mudstones are known to behave as semipermeable membranes. This is because the negative charges on the surface of clay minerals retard the transport of charged particles in narrow pores. In such mudstones, chemo-osmotic flow occurs by the concentration gradient (e.g., Marine and Fritz, 1981), and in some cases, pressure buildup can reach to about 20 MPa (Neuzil, 2000). In addition, pore pressure change may induce the deformation of porous medium. The purpose of this research is to evaluate the effect of chemical osmosis on the deformation and pressure behavior in mudstone based on both laboratory experiments and numerical simulations.

In the laboratory experiments, core samples with 50 mm diameter and 30 mm height were prepared from the mudstone of the Oganomachi Formation, collected from Saitama prefecture. The core samples were kept in NaCl solution with the same total dissolved ion concentrations of pore water (less than 0.1 g/L) under hydrostatic pressure at the beginning of the experiments. The lateral and the upper surfaces were sealed by silicon rubber while the lower surface was in contact with the NaCl solution of which concentration was kept at about 10 g/L. The circumferential strains of the sample were measured by the optical fiber strain sensor attached helically on the lateral surface of the sample. The measurements were continued for more than 200 hours and the temperature was controlled almost constant throughout the experiments.

A numerical model to calculate chemo-osmotic and poroelastic processes was used to compare numerical simulation results with the experimental ones. The governing equations were based on a set of equations describing groundwater flow and diffusion including chemical osmosis process (Malusis et al., 2012) and those describing poroelastic effect (e.g., Wang, 2000), and pore pressure, concentration, and rock deformation were calculated. The calculated domain, boundary conditions and initial conditions were set to be the same as those of the laboratory experiments, for example, calculated domain was a cylinder with 50mm in diameter and 30mm in height, the upper and lateral surfaces were set to be no-flow and no solute flux boundary, and the lower surface was set to be constant pressure (0 kPa) and constant concentration (about 10 g/L). All the surfaces were set to be strain-free boundaries.

In the laboratory experiments, the continuous contraction was observed, and was interpreted to be caused by the osmotic flow and induced deformation by pressure decrease in the sample. The amount of contraction near the bottom was larger than that near the upper surface. The maximum 130 $\mu\varepsilon$ was measured near the lower surface.

The effects of the parameters variation on the strain behavior were evaluated through numerical

©2021. Japan Geoscience Union. All Right Reserved.

simulation, and the appropriateness of the model to explain the overall behavior of the samples was discussed by comparing the laboratory experimental results and the numerical simulations.

Keywords: chemical osmosis, poroelasticity, mudstone, seal layer

©2021. Japan Geoscience Union. All Right Reserved.

Evaluation of Caprock Sealing Performance in Saline Aquifer Storage

*Yuuki Shigeoka[1], Haruki Nishiyama[1], Hiroshi Kinoto[1], Yukiko Shoji[2], Takaomi Tobase[2]

1. J-POWER Business Survice Corporation, 2. Electric Power Development Co.

A saline aquifer storage consists of a reservoir and a caprock layer overlying on the reservoir. It is possible to evaluate the storage performance of the reservoir by predicting the pressure rise and the spread of the CO_2 plume due to CO_2 injection using numerical analysis. In generally, numerical analysis for evaluating the storage performance of a reservoir, only the reservoir is modeled, and caprock is treated as an impermeable boundary. In this research, numerical analysis was performed using the analytical model that models both the caprock layer and the reservoir. Then, the sealing performance of the caprock was evaluated based on the analysis results.
The analysis model was created with reference to the storage site of the CCS project in operation. At the storage site, there are two types of seal layers as caprocks, and their physical property values are as follows.
Seal-A: Absolute permeability $1.0\times10^{-16}m^2$, Porosity 0.04
Seal-B: Absolute permeability $1.0\times10^{-21}m^2$, Porosity 0.01
In this research, two cases were carried out. As the caprock, the Seal-A was applied in Case-1 and the Seal-B was applied in Case-2. In the analyses, CO_2 was injected into the reservoir to predict the pressure response inside the caprock and the spread of the CO_2 plume in the reservoir. TOUGH-2/ECO2N was used in the numerical analyses.
As the result, slight CO_2 penetration into the caprock in the Case-1 (Seal-A), and no penetration in the Case-2 (Seal-B) were predicted.
It is considered that a more appropriate storage design will be possible by evaluating not only the storage performance of the reservoir but also the sealing performance of the caprock.

Keywords: Carbon dioxide Capture and Storage, Reservoir Simulation, Seal Performance Evaluations

©2021. Japan Geoscience Union. All Right Reserved.

Recent advances in value of information analysis and application to geological CO_2 storage

*Takashi Goda[1], Kozo Sato[1], Takahiro Nakajima[2,3]

1. School of Engineering, The University of Tokyo, 2. Geological Carbon Dioxide Storage Technology Research Association, 3. Research Institute of Innovative Technology for the Earth

The value of information (VOI) analysis provides an objective means for evaluating the cost-effectiveness of gaining additional information for decision making under uncertainty, and some attempts have been made in the literature to apply the VOI analysis to the context of geological CO_2 storage. In recent years, mostly motivated by applications to health economic evaluations, there have been significant progresses in developing efficient computational methods to estimate the expected value of information, which have been shown to work well even for complicated nonlinear models consisting of many input random variables. Such developments can lower the barrier to use of the VOI analysis in practical operations of geological CO_2 storage.

In this talk we start from an introduction to the VOI analysis; we define three classes of information (perfect information, partial perfect information, and sample information) and derive the expected value which each class of information brings to decision making under uncertainty. Here we confirm that the expected values of partial perfect information and sample information (abbreviated as EVPPI and EVSI, respectively) are defined as nested expectations mathematically, which make it difficult to construct an efficient estimator for them. Then we move on to an overview of recent developments in the methodology for the EVPPI and EVSI estimation. Finally, through a simple two-alternative decision problem on which site to store CO_2, we demonstrate the following items: how three classes of information are related each other, how the expected value of information can be estimated efficiently in comparison with the classical method, and which points we should be cautious about in practical use.

Keywords: geological CO2 storage, decision making under uncertainty, value of information, multilevel Monte Carlo methods, Bayesian inference

©2021. Japan Geoscience Union. All Right Reserved.

[J] Oral | H (Human Geosciences)：H-SC Social Earth Sciences & Civil/Urban System Sciences

Fri. Jun 4, 2021 10:45 AM - 12:15 PM JST | Fri. Jun 4, 2021 1:45 AM - 3:15 AM UTC | Ch.15 Zoom Room 15

[H-SC05] CCUS (Carbon Dioxide Capture, Utilization, and Storage) for Climate Mitigation

convener:Masao Sorai(Institute for Geo-Resources and Environment, National Institute of Advanced Industrial Science and Technology), Ziqiu Xue(Research Institute of Innovative Tech for the Earth), Masaatsu Aichi(Graduate School of Frontier Sciences, University of Tokyo), Yoshihiro Konno(The University of Tokyo), Chairperson:Masaatsu Aichi(Graduate School of Frontier Sciences, University of Tokyo)

The prevention of the global warming, which is the urgent challenge facing the world, requires the full-out efforts of science and technology. This session focuses on the CCUS (Carbon Dioxide Capture, Utilization, and Storage) as one of the useful countermeasures for the CO2 emission reduction. The session covers various scientific phenomenon caused by the capture and storage of CO2, CO2 utilization, and CO2-EOR/EGR, along with the discussion about the latest R&D developments of each method for the environmental impact assessment, safety assessment, the measuring, monitoring and verification (MMV), and public acceptance. The main theme is the recognition of key issues toward the practical use of CCUS, in addition to the deepening of our knowledge about the CO2 behavior on the underground.

10:45 AM - 11:00 AM JST | 1:45 AM - 2:00 AM UTC

[HSC05-07] Downhole Deformation Monitoring with High-Spatial-Resolution Distributed Strain Measurement in Optical Fiber during Water Injection Test

*Rasha Amer[1,2], Ziqiu Xue[1,2], Tsutomu Hashimoto[1,2], Takeya Nagata[1,2] (1.Geological Carbon Dioxide Storage Technology Research Association, 2.Research Institute of Innovative Tech for the Earth)

11:00 AM - 11:15 AM JST | 2:00 AM - 2:15 AM UTC

[HSC05-08] Advantages of Helically Wound optic-fiber Cables on VSP records

*Takayuki Miyoshi[1], Takahiro Nakajima[1], Ziqiu Xue[1] (1.Geological Carbon Dioxide Storage Technology Research Association / Research Institute of Innovative Technology for the Earth)

11:15 AM - 11:30 AM JST | 2:15 AM - 2:30 AM UTC

[HSC05-09] Numerical Simulation of Geophysical Changes based upon CO_2 Geological Storage and Leakage

*Yuki Kano[1,2], Tsuneo Ishido[1,2] (1.Geological Carbon Dioxide Storage Technology Research Association, 2.National Institute of Advanced Industrial Science and Technology)

11:30 AM - 11:45 AM JST | 2:30 AM - 2:45 AM UTC

[HSC05-10] Numerical simulation of electromagnetic exploration for CO_2 monitoring in horizontal multi-layered earth

*Haruhito Takuma[1], Takumi Ueda[1], Takahiro Nakajima[2,3] (1.Waseda University, 2.Geological Carbon Dioxide Storage Technology Research Association, 3.Research Institute of Innovative Technology for the Earth)

11:45 AM - 12:00 PM JST | 2:45 AM - 3:00 AM UTC

[HSC05-11] Observation of self-potential changes around a metal casing due to the injection of low pH solution in laboratory experiments

*Takuya Horikawa[1,2], Masao Sorai[1,2] (1.Geological Carbon Dioxide Storage Technology Research Association, 2.CO2 Geological Storage Research Group, GREEN, GSJ, AIST)

12:00 PM - 12:15 PM JST | 3:00 AM - 3:15 AM UTC

[HSC05-12] **Developing a science-based, quantitative approach for distinguishing CO2 injection-induced earthquakes from natural earthquakes**

*Takeshi Tsuji[1], Chanmaly Chhun[1], Tatsunori Ikeda[1], James Mori[2] (1.Department of Earth Resources Engineering, Kyushu University, 2.Kyoto University)

Downhole Deformation Monitoring with High-Spatial-Resolution Distributed Strain Measurement in Optical Fiber during Water Injection Test

*Rasha Amer[1,2], Ziqiu Xue[1,2], Tsutomu Hashimoto[1,2], Takeya Nagata[1,2]

1. Geological Carbon Dioxide Storage Technology Research Association, 2. Research Institute of Innovative Tech for the Earth

Introduction:

The fluids are injected into the subsurface around the world for various purposes which may induce a ground surface deformation due to the subsurface pressure buildup, Without the continuous strain data from the deep deformation to the surface, it is not easy to correlate the subsurface pressure changes with surface deformation, the distributed fiber optic strain sensing DFOSS tool could provide accurate deformation measurements at relatively low cost and permanent monitoring technique, In this study (DFOSS) was used to measure strain profile during a water injection test, where we installed two different fiber cables behind the casing in the three wells with different distances from the injection well, aiming to confirm the strain sensitivity of the fiber cables to the fluid migration behaviors.

Data:

As a part of the R&D project commissioned to the Geological Carbon Dioxide Storage Technology Research Association by the New Energy and Industrial Technology Development Organization (NEDO) and the Ministry of Economy, Trade, and Industry (METI) of Japan. A pilot water injection test was conducted in Mobara site /Chiba prefecture on January 2020, the water injected in a new injection well with depth 247m and the strain monitoring in there monitoring well with depth 180, 300, and 240m and distance from the injection well 5.5, 5.7 and 16.6 respectively.

Method:

DFOSS was used to measure strain profile in three shallow wells during water injection tests which carried out on March 2020, two different fiber cables installed behind the casing in the three wells with different distances from the injection well. the combined strain profile, pressure, and lithological heterogeneity analysis were conducted.

Result and Discussion:

The results suggested the strain measurements by the two different cables were almost the same, and there was no big difference in geomechanical deformation among the wells despite the distance to the injection well. From the combined strain profile, pressure, and lithological heterogeneity analysis, the strain responses under, within, and upper the injection zone has been successfully interpreted and the delayed strain response appeared at 6 m upper the injection zone was resulted from the pressure breakdown. the distributed strain fiber successfully could detect the deformation at the mud-sand alternation in high spatial resolution.

Keywords: Water injection test, Distributed Fiber Optic Strain Sensing DFOSS, Geomechanical deformation, Lithological heterogeneity, Pressure breakdown

©2021. Japan Geoscience Union. All Right Reserved.

Advantages of Helically Wound optic-fiber Cables on VSP records

*Takayuki Miyoshi[1], Takahiro Nakajima[1], Ziqiu Xue[1]

1. Geological Carbon Dioxide Storage Technology Research Association / Research Institute of Innovative Technology for the Earth

Geological CO2 storage is a promising technology to mitigate the global warming. The injected carbon dioxide underground needs to be monitored properly during/after injection periods. Some CO2 geosequestration projects conducted the repeated 3D seismic surveys to visualize the plume of injected CO2. However, due to the high cost, number of surveys had to be limited. The fiber-optic distributed acoustic sensing (DAS) for vertical seismic profiles (VSP) has quite high potential for more frequent surveys with low cost. The DAS is now widely used in exploration community as a novel technology. The small dimension of the fiber cables enables installation behind the casing, which increases availability of space of injection wells. Some indicate that the DAS records have less sensitivity than the conventional geophones, which requires more source efforts to achieve high signal-to-noise ratio (SNR). Another disadvantage of DAS is no sensitivity for waves incident laterally. The Helically Wound fiber-optic Cables (HWC) are recently developed in order to capture these waves.

To evaluate performance of a HWC, we installed the straight optic-fiber cable (STC) and the HWC in the vertical well of 250 m and cemented together along the tubing. Another vertical well of 880 m deep with metal casing had the same STC cemented behind the casing. All fibers were spliced together in one stroke and were connected to DAS interogator at the site. Also the downhole 4 of 3C geophones were put down in the 880 m well from 100 m to 700 m with interval of 7.5 m, which needed 21 levels of measurement. The P-vibroseis truck swept at the traffic road along the survey line of 2 km beside the site. The excited elastic waves from the offset of 90 m to 1350 m were recorded by optic fibers and geophones simultaneously.

From our field measurements, we revealed that (1) DAS records were noisier than geophone records, but 5-20 times more sweeps were enough to obtain geophone equivalent records; (2) The HWC records showed about twice higher SNR than the STC records in some offset of sweeps; and (3) the amplitude decay in HWC records were moderated significantly.

Keywords: Geological CO2 storage, Optic Fiber, DAS, HWC, VSP

©2021. Japan Geoscience Union. All Right Reserved.

Numerical Simulation of Geophysical Changes based upon CO_2 Geological Storage and Leakage

*Yuki Kano[1,2], Tsuneo Ishido[1,2]

1. Geological Carbon Dioxide Storage Technology Research Association, 2. National Institute of Advanced Industrial Science and Technology

For the monitoring of Carbon Capture and Storage (CCS), a variety of geophysical data will be useful to perceive the behavior of injected CO_2 and to detect a leakage if occurs. Since required monitoring period will be substantially long, cost-effective monitoring methods are desirable. To design such monitoring plan, it is necessary to predict whether and where observable changes will appear due to CO_2 migration in a quantitative way.
In this presentation, we will report the results of numerical simulations of changes in geophysical observables based upon hypothetical CO_2 geological storage and leakage calculations. Calculated geophysical data includes seismic reflection, microgravity and seafloor surface displacement. The results indicate that the location of observable changes and detection possibility of a leakage in early stages.
A 3D model was built representing an inshore saline aquifer below the seabed of 20-m water depth. A high-permeable sandstone layer located at about 1 km below the seabed is considered to be the reservoir. A low-permeable seal layer is overlaid by a secondary aquifer and seal, and a top Quaternary sediment. CO_2 is injected into the reservoir at a rate of 0.4 Mt/year for 50 years. Numerical simulations of the injection period and following shut-in period were carried out for a no leakage case and a few cases where a leakage took place. A hypothetical fault was supposed to be the leakage path and assumed to open at the end of the injection. Fluid flow simulations were carried out using the "STAR" reservoir simulation code (Pritchett, 1995; Pritchett, 2002) with the "SQSCO2" equations of state package (Pritchett, 2008), and then geophysical data was calculated using STAR’s "Geophysical Postprocessor" (Pritchett, 2003; Ishido et al., 2011; Ishido et al., 2015).
This presentation is based on results obtained from a project (JPNP18006) commissioned by the New Energy and Industrial Technology Development Organization (NEDO) and the Ministry of Economy, Trade and Industry (METI) of Japan.

References
Ishido, T., Tosha, T., Akasaka, C., Nishi, Y., Sugihara, M., Kano, Y. and Nakanishi, S. (2011): Changes in geophysical observables caused by CO_2 injection into saline aquifers. Energy Procedia 4, 3276-3283.
Ishido, T., Pritchett, J.W., Nishi, Y., Sugihara, M., Garg, S.K., Stevens, J.L., Tosha, T., Nakanishi, S., Nakao, S. (2015): Application of Various Geophysical Techniques to Reservoir Monitoring and Modeling. Proc. World Geothermal Congress, Melbourne, Australia, 19-25 April 2015.
Pritchett, J.W. (1995): STAR-a geothermal reservoir simulation system. Proc. World Geothermal Congress, Florence, 853-858.
Pritchett, J.W. (2002): STAR User’s Manual Version 9.0, SAIC Report Number 02/1055
Pritchett, J.W. (2003): Verification and Validation Calculations Using the STAR Geophysical Postprocessor Suite. SAIC Report Number 03/1040; 2003.
Pritchett, J.W. (2008): New "SQSCO2" equation of state for the "STAR" code, SAIC

Keywords: CO2 geological Storage, CO2 Leakage, Numerical simulation, Geophysical monitoring

©2021. Japan Geoscience Union. All Right Reserved.

Numerical simulation of electromagnetic exploration for CO_2 monitoring in horizontal multi-layered earth

*Haruhito Takuma[1], Takumi Ueda[1], Takahiro Nakajima[2,3]

1. Waseda University, 2. Geological Carbon Dioxide Storage Technology Research Association, 3. Research Institute of Innovative Technology for the Earth

In this study, we focused on the issue of CO_2 injection monitoring, and developed a calculation program and conducted numerical simulations for the monitoring by electromagnetic survey method for a three-dimensional transmitter-receiver configuration in a horizontal multilayer structure. The accuracy of the program for the horizontal multi-layered structure was confirmed by verifying the analytical and numerical solutions of the magnetic field response at the surface of the homogeneous earth, and the simulation was carried out for the horizontal multi-layered structure model with a shielding layer above the CO_2 reservoir.

In the monitoring, the seismic reflection survey (seismic survey) is the main method. In addition to the method, gravity survey and electromagnetic survey are also being considered. Electromagnetic survey has the advantage of being less costly than seismic reflection surveys. Moreover, this survey can monitor resistivity, as opposed to the seismic velocity (density) structure in seismic reflection surveys.

For these reasons, we investigate the possibility of monitoring the CO_2 injection model in CCS under different conditions by varying the transmitter arrangement and transmission frequency in the application of frequency-domain electromagnetic (FDEM) method. The magnetic field and its rate of change due to CO_2 injection were calculated under a total of nine conditions by combining the transmitter locations and frequencies.
The FDEM method is simpler in principle and analysis than the time-domain electromagnetic method, but the primary field, which does not include the influence of the subsurface structure, and the secondary field, which is the response of the subsurface structure, cannot be acquired separately. The amplitude of the total field is the magnitude of the response itself, which can be expressed by adding up the transmitted field as the primary field and the field due to the resistivity structure of the subsurface as the secondary field. The primary field is often known, so when estimating the resistivity structure, the secondary field is the value obtained by removing the effect of the primary field from the total field. The electromagnetic field is measured by amplitude and phase, and can be regarded as a complex number, but its imaginary component contains only the response of the earth. In this study, the amplitude of the imaginary component of the total field response was used to calculate the magnetic field response and its rate of change due to the subsurface resistivity structure. Based on these data, we evaluated the effects of CO_2 injection layer and shielding layer with high and low resistivity and discussed CO_2 injection monitoring by electromagnetic exploration method.

Keywords: electromagnetic exploration, CCS, FDEM, horizontal multi-layered earth

©2021. Japan Geoscience Union. All Right Reserved.

Observation of self-potential changes around a metal casing due to the injection of low pH solution in laboratory experiments

*Takuya Horikawa[1,2], Masao Sorai[1,2]

1. Geological Carbon Dioxide Storage Technology Research Association, 2. CO2 Geological Storage Research Group, GREEN, GSJ, AIST

In geological CO_2 storage and geothermal exploration, it is important to monitor the changes of subsurface fluid for a long time. Passive geophysical exploration techniques, e.g., self-potential (SP) method and gravity method, have advantages of cost and operation effort compared to the active techniques. The SP method is a technique for measuring the potential difference between two measurement points that spontaneously generated. The SP anomalies are caused by a variety of factors, including fluid flow (streaming potential) and changes in the redox condition (redox potential). It is well known that negative SP anomalies are observed near a conductor, e.g., a metal casing, when the conductor connects regions with different redox environments. This phenomenon is can be interpreted qualitatively by the “geobattery” model. Ishido et al. (2013) showed by a numerical experiment that injection and migration of CO_2 caused the change of the redox environment around the bottom of the metal casings and a potential variation of up to 80 mV was observed in injection wells, observation wells, and their surroundings. Therefore, the SP method is a promising and effective technique for sensing the approach of CO_2 to the well and the risk of leakage from the well. However, few experiments, regardless of in a laboratory or a field, have been performed to focus on the potential changes of the conductor coincided with injection or migration of CO_2.

A decrease in the pH of the groundwater due to the dissolution of CO_2 is thought to be one of the causes of the potential change in the conductor. In this study, we made the experimental sandbox using glass beads and a steel rod shown in Figure 1, and measured the potential of the rod while injecting solutions with different pH around the bottom of the rod. At the beginning of the experiment, the sandbox was saturated mostly with the solution of KCl 0.1 M, and its pH was almost 6.3. Next, the potential difference was measured between the rod and the reference electrode, placed on the opposite side of the rod, with a digital multimeter. Finally, the pH of the injected solution was adjusted to 2 ~ 6 by adding HCl into the KCl solution, and the potential of the rod was measured while injecting the solutions first from higher pH ones. Figure 2 is the experimental result, and shows that the potential dropped drastically by 170 mV or 500 mV coincided with the injection of the solution with pH 5 or 4.

This presentation is based on results obtained from a project commissioned by the New Energy and Industrial Technology Development Organization (NEDO) and the Ministry of Economy, Trade and Industry (METI) of Japan.

Keywords: self potential method, geobattery, redox potential, carbon dioxide capture and storage

©2021. Japan Geoscience Union. All Right Reserved.

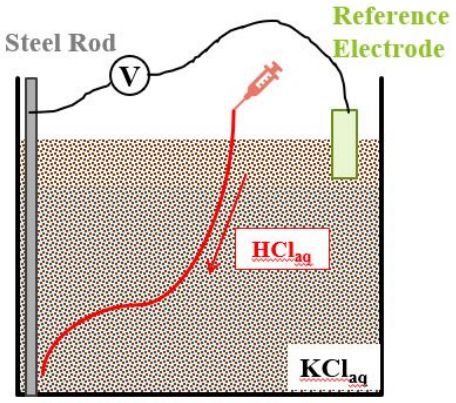


Figure 1. Schematic of the experimental apparatus.

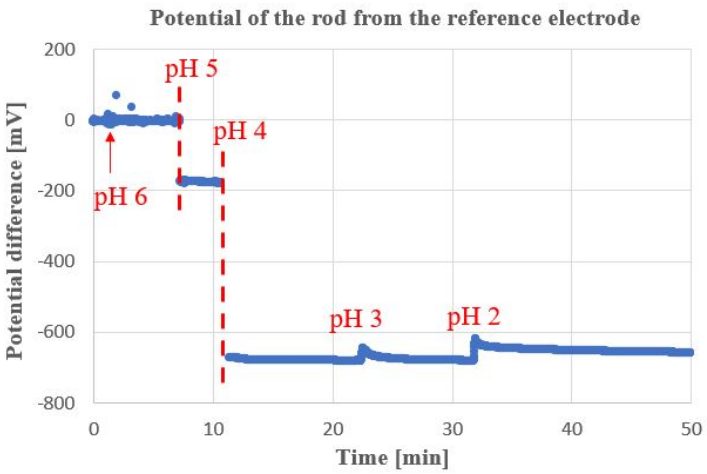


Figure 2. Experimental results.

©2021. Japan Geoscience Union. All Right Reserved.

Developing a science-based, quantitative approach for distinguishing CO2 injection-induced earthquakes from natural earthquakes

*Takeshi Tsuji[1], Chanmaly Chhun[1], Tatsunori Ikeda[1], James Mori[2]

1. Department of Earth Resources Engineering, Kyushu University, 2. Kyoto University

In countries located at plate convergent margins (e.g., Japan), many natural earthquakes occur every day. To obtain a public understanding of CO2 storage projects, we need to develop a method for distinguishing between natural earthquakes and those induced by CO2 injection. For example, the 2004 Mw 6.8 Chuetsu earthquake occurred close to the Nagaoka CO2 storage site during gas injection, but we could not quantify whether or not the earthquake was due to CO2 injection. The earthquake generation can be evaluated mainly based on the following parameters: pore pressure, effective stress, frictional coefficient of the fault plane, and shear stress across the fault. If the shear stress is larger than the frictional force of the fault, earthquakes will likely occur. During CO2 injection, while the frictional coefficient, effective stress, and shear stress could be almost constant, only pore pressure is varied. Therefore, the pore pressure could be an important factor in evaluating induced seismicity.

We have recently developed an approach to monitor the spatiotemporal pore pressure in wide areas (Nimiya et al., 2017; Andajani et al., 2020). Using this method, we identified the natural pore pressure variation due to rainfall, snowmelt, and remote earthquakes. On the other hand, we can also estimate changes in pore pressure during the CO2 injection using reservoir simulation (i.e., CO2-water fluid flow simulation). To distinguish between CO2 injection-induced earthquakes and natural earthquakes, we compared (1) the natural pore pressure variations and (2) the variation due to CO2 injection.

This study simulated pore pressure changes at the Nagaoka CO2 storage and compared these changes with estimated natural seasonal fluctuations in pore pressure (Chunn and Tsuji, 2020). Changes in pore pressure due to CO2 injection were clearly distinguished from those due to rainfall and snowmelt. The simulated pore pressure increase near the seismogenic fault area was much smaller than the seasonal fluctuations related to precipitation and stress increases caused by remote earthquakes. The lateral extent of the pore pressure increase was probably insufficient to influence seismogenic faults. We also demonstrated that large pore pressure changes due to distant earthquakes could trigger slip on seismogenic faults. This approach is simple, but the method is based on numerical stress calculations ; thus, we can quantitatively interpret the earthquake around the CO2 injection site. The approach will be useful at other CO2 sequestration sites and geothermal operations. We should consider the shear stress and poroelastic behaviors due to CO2 injection in this way to provide more quantitative evaluations of possible earthquake triggering. .

References:

1) Andajani, R. D., T. Tsuji, R. Snieder, and T. Ikeda (2020), Spatial and temporal influence of rainfall on crustal pore pressure based on seismic velocity monitoring, Earth, Planets and Space, 72:177, doi:10.1186/s40623-020-01311-1.

2) Chhun, C., and T. Tsuji (2020), Pore pressure analysis for distinguishing earthquakes induced by CO2

©2021. Japan Geoscience Union. All Right Reserved.

injection from natural earthquakes, Sustainability, 12, 9723; doi:10.3390/su12229723

3) Nimiya, H., T. Ikeda, and T. Tsuji (2017), Spatial and temporal seismic velocity changes on Kyushu Island during the 2016 Kumamoto earthquake, Science Advances, Vol. 3, no. 11, e1700813, doi:10.1126/sciadv.1700813.

Keywords: Induced seismicity, natural earthquake, Pore pressure, CO2 storage, Monitoring, Reservoir simulation

©2021. Japan Geoscience Union. All Right Reserved.

[J] Oral | H (Human Geosciences)：H-SC Social Earth Sciences & Civil/Urban System Sciences

Fri. Jun 4, 2021 1:45 PM - 3:15 PM JST | Fri. Jun 4, 2021 4:45 AM - 6:15 AM UTC | Ch.15 Zoom Room 15

[H-SC05] CCUS (Carbon Dioxide Capture, Utilization, and Storage) for Climate Mitigation

convener:Masao Sorai(Institute for Geo-Resources and Environment, National Institute of Advanced Industrial Science and Technology), Ziqiu Xue(Research Institute of Innovative Tech for the Earth), Masaatsu Aichi(Graduate School of Frontier Sciences, University of Tokyo), Yoshihiro Konno(The University of Tokyo), Chairperson:Yoshihiro Konno(The University of Tokyo)

The prevention of the global warming, which is the urgent challenge facing the world, requires the full-out efforts of science and technology. This session focuses on the CCUS (Carbon Dioxide Capture, Utilization, and Storage) as one of the useful countermeasures for the CO2 emission reduction. The session covers various scientific phenomenon caused by the capture and storage of CO2, CO2 utilization, and CO2-EOR/EGR, along with the discussion about the latest R&D developments of each method for the environmental impact assessment, safety assessment, the measuring, monitoring and verification (MMV), and public acceptance. The main theme is the recognition of key issues toward the practical use of CCUS, in addition to the deepening of our knowledge about the CO2 behavior on the underground.

1:45 PM - 2:00 PM JST | 4:45 AM - 5:00 AM UTC

[HSC05-13] Development of a biological impact database on marine organisms

*Jiro Suekuni[1], Keisuke Uchimoto[1], Yuji Watanabe[1], Ziqiu Xue[1] (1.Research Institute of Innovative Technology for the Earth)

2:00 PM - 2:15 PM JST | 5:00 AM - 5:15 AM UTC

[HSC05-14] Numerical estimation of leakage suppression using CO_2 hydrate on the oceanic field scale

Takuya Wako[1], Yosuke Sawano[1], *Toru Sato[1] (1.University of Tokyo)

2:15 PM - 2:30 PM JST | 5:15 AM - 5:30 AM UTC

[HSC05-15] Numerical simulation of seafloor ground deformation during CO_2 underground storage using gas hydrate

*Sayuri Kimoto[1], Kento Uehira[1] (1.Kyoto University)

2:30 PM - 2:45 PM JST | 5:30 AM - 5:45 AM UTC

[HSC05-16] **Experimental Study on Formation Behavior of CO2 Hydrate in a Flow Field Assuming Carbon Dioxide Storage in Subseabed**

*Yuichi Magara[1], Taku Nishimura[1], Yoshihiro Konno[1], Yusuke Jin[2], Takaomi Tobase[3] (1.Graduate School of Frontier Science, the University of Tokyo , 2.National Institute of Advanced Industrial Science and Technology, 3.Electric Power Development Co.,Ltd.)

2:45 PM - 3:00 PM JST | 5:45 AM - 6:00 AM UTC

[HSC05-17] Cost analysis of CO_2 transportation in CCS deployed in Japan

*Hirotaka Isogai[1], Corey Adam Myers[2], Takao Nakagaki[2], Takeshi Myoi[3], Junichi Shimizu[3] (1.Department of Modern Mechanical Engineering, Waseda University , 2.Faculty of Waseda University, 3.Geological Carbon Dioxide Storage Technology Research Association / Research Institute of Innovative Technology for the Earth)

3:00 PM - 3:15 PM JST | 6:00 AM - 6:15 AM UTC

[HSC05-18] Consideration about public consensus building of CCS

*Takaomi Tobase[1] (1.Electric Power Development Co., Ltd.)

Development of a biological impact database on marine organisms

*Jiro Suekuni[1], Keisuke Uchimoto[1], Yuji Watanabe[1], Ziqiu Xue[1]

1. Research Institute of Innovative Technology for the Earth

When CO_2 leaks from the seabed into the sea, the CO_2 concentration in seawater increases and pCO_2 rises. This result affects marine organisms. In assessing the potential environmental impact of leaked CO_2, which is required by law, it is important to collect data on the relationship between pCO_2 and biological impact, and organize them into a usable form. In this study, we developed a biological impact database for the purpose of searching and managing data on the biological impact of CO_2. When developing the system, we first defined the system requirements. This includes consideration of data volume, search items, search time, maintainability, and so on. We also aimed for an easy-to-use interface. In addition, graphing function was installed in the system using search results so that the impact threshold level can be confirmed on the screen. In parallel with the development of the database system, impact data were extracted from various papers related to biological impacts and inputted into the database. The species to be stored in the database were selected in consideration of various stakeholders. As a result, 150 lethal records and 661 sub-lethal records were collected. Biological impact is determined by a pCO_2 value and exposure time. Therefore, the lethal index was organized as LC50 and LT50 that are ΔpCO_2 (pCO_2 increment from the natural state) and exposure time, respectively, for half of the organisms to be killed . Although various items related to sublethal impact have been reported, in this database they have been classified into eight categories: growth, life and death, proliferation, metamorphosis, hatching, infection, malformation, and behavior. As the sublethal index, LnRR and Hedges' d were calculated to allow mutual comparison between the categories. LnRR is the logarithmic of the ratio of a variable in a category between the control group and the experimental group, and Hedges' d is another index calculated from the average value, the number of samples, and the standard deviation of both the control and experimental groups. Environmental impact assessment has a step to describe the biological composition of the target sea area. Based on the results obtained in this step, the information required for the target sea area can be searched and extracted from this database. By combining ΔpCO_2 distribution estimated from a simulation calculating leaked CO_2 dispersion based on a leakage scenario with the results from the database, it is possible to predict an area of biological impacts caused by CO_2 leakage. In addition, the results obtained from the biological impact database can be used to select organisms and items that should be focused on in monitoring.

Keywords: Database, Sub-seabed CO2 storage, Marine monitoring, CO2 leakage

©2021. Japan Geoscience Union. All Right Reserved.

Numerical estimation of leakage suppression using CO_2 hydrate on the oceanic field scale

Takuya Wako[1], Yosuke Sawano[1], *Toru Sato[1]

1. University of Tokyo

CO_2 capture and storage is a promising strategy against global warming. Although there is concern about the risk of CO_2 leakage from deep saline aquifers, it is expected that leaking CO_2 forms gas hydrate and this hydrate formation suppresses the CO_2 leakage. When the water depth of a storage site is large: say, about 400 m or more, leaked CO_2 changes its form to gas hydrate, which may block CO_2 rise in the sandy seabed sediment. Therefore, hydrate formation in the sub-seabed sand sediments is one of key factors in lowering the risk of CO_2 leakage and it is important to know conditions under which CO_2 leakage is suppressed by hydrate formation.

On the other hand, using this leakage trap mechanism, it is also possible to store CO_2 in the form of gas hydrate without a cap rock in the sub-seabed geological formation. To estimate the sealing effect of CO_2 hydrate against CO_2 leakage beneath the seafloor, it is necessary to evaluate the permeability of the stratum after CO_2 hydrate forms.

In this study, numerical simulations of hydrate formation in sand sediment are conducted for CO_2 injected in the sub-seabed geological formation. When modelling CO_2 hydrate formation, it is assumed that the hydrate forms on the CO_2-water interface and on the surface of the sand particles after CO_2 plume front passes by during its rise. Permeability reduction during hydrate formation was modelled using the results of microscale hydrate simulations with the phase field model and lattice Boltzmann method in the literature.

First, the processes of CO_2-water two-phase flow and CO_2 hydrate formation in the sand sediment under the experimental conditions are analysed by the present numerical model. Simulation results are compared with the experimental data, so that unknown parameters in the models are determined by parameter-fitting.

Simulation results suggest that the total hydrate formation rate is higher near the boundary of the reaction vessel, and CO_2 hydrate is mainly distributed near the boundary of the reaction vessel due to the cooling effect of the temperature-controlled boundary. Furthermore, it is also indicated that CO_2 hydrate formation on the hydrate film behind the gas front makes the most important contribution to the high CO_2 hydrate saturation near the boundary; on the contrary, CO_2 hydrate formation on the gas front and on the surface of the sand particles behind the gas front only have has a very small effect on CO_2 hydrate saturation in the sand sediment. Therefore, on the basis of the analysis above, we can draw the conclusion that the sharp permeability reduction of the sand sediment during CO_2 injection is mainly caused by the part of CO_2 hydrate formation on the hydrate film behind the CO_2 plume front, which is likely to exist between the sand particles and occupy the pore space of the sand sediment, resulting in blockage of the gas flow.

Then, this numerical method was applied to 3D realistic geological formation to simulate whether hydrate seal is formed to block the leakage of CO_2 and to store CO_2 safely in the form of gas hydrate in the reservoir scale. The results from numerical simulations showed that the formation of a CO_2 hydrate layer

©2021. Japan Geoscience Union. All Right Reserved.

could block the upwards migrating CO_2 under most conditions of injection depth, seafloor depth, seafloor temperature, and injection rate, while in some cases, CO_2 leaks before hydrate forms to occupy the pore space enough to block the leakage. Therefore, it is important to choose storage sea sites: particularly, absolute permeability.

Acknowledgement
This work has been conducted under “Sustainable CCS project” by the Ministry of the Environment, Government of Japan.

Keywords: Sub-seabed CO2 storage, Geological formation, CO2 hydrate formation, Numerical simulation, Reservoir scale

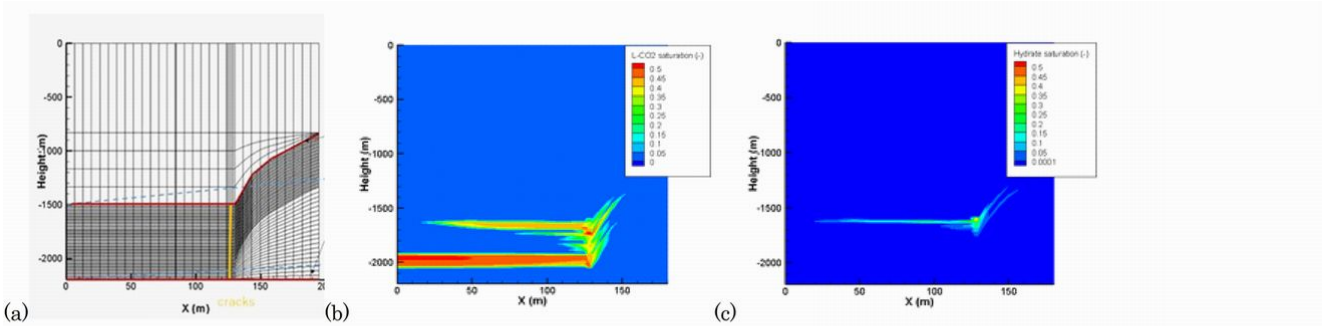


Figure : Grid distribution (a) and contour maps of liquid CO2 saturation (b) and CO2 hydrate (c) 300 years after the start of leakage. The seafloor depth of the ocean basin is 1500 m, the seafloor temperature is 3 degree Celsius, the geothermal gradient is 3 degree per 100 m, the absolute permeabilities of the sand layer, the mud layer and the fault are 10^{-14} m², 10^{-16} m², and 10^{-13} m², and the leakage rate is 10000 ton/year.

©2021. Japan Geoscience Union. All Right Reserved.

Numerical simulation of seafloor ground deformation during CO_2 underground storage using gas hydrate

*Sayuri Kimoto[1], Kento Uehira[1]

1. Kyoto University

A carbon dioxide sequestration method (CCS) using gas hydrate has recently been proposed, in which CO_2 is stored underground in the form of CO_2-hydrate. In this method, CO_2 and seawater will react under the gas hydrate equilibrium conditions, namely, high pressure and low temperature conditions so that CO_2 is stored as a solid in a chemically stable condition. It is possible that CO_2 is stably stored compared with a conventional method using supercritical CO_2 injection. In addition, the suitable geological area for the storage would be large since the caprock is not necessary.

In the present study, two-phase fluid–solid coupled analysis has been conducted to reproduce the ground deformation during CO_2 underground storage a hydrate. Solid phase (soil, hydrate) and two liquid phases (CO_2, water) are dealt with in the numerical analysis. An elasto-viscoplastic constitutive models are used for CO_2 hydrate-bearing sediment. As a capillary pressure- saturation relation, van Genuchten model is used. Finite element method and Newmark’ s β method is used as a discretization in space and time, respectively.

As a simulation example, the mechanical stability of the ground by CO_2 liquid injection is examined, assuming a hydrate seal layer with a thickness of 2 m is formed in the seafloor ground at a water depth of 1000 m. Simulation results will be discussed regarding to the change of water pressure, CO_2 liquid pressure, saturation, effective stress, and the soil deformation during CO_2 liquid injection.

Akaki, T., Kimoto, S. and Oka, F., Chemo-thermo-mechanically coupled seismic analysis of methane hydrate-bearing sediments during a predicted Nankai Trough Earthquake, Int. J. for Numerical and Analytical Methods in Geomechanics, Vol. 40, pp. 2207–2237, DOI: 10.1002/nag.2527, 2016.
Akaki, T., Kimoto, S. and Oka, F., Chemo-thermo-mechanically coupled seismic analysis of methane hydrate-bearing sediments during a predicted Nankai Trough Earthquake, Int. J. for Numerical and Analytical Methods in Geomechanics, Vol. 40, pp. 2207–2237, DOI: 10.1002/nag.2527, 2016

Kimoto, S., Yoshimoto, M. and Takuco, G., Creep Behavior of CO_2 Hydrate-bearing Sand and its Simulations by an Elasto-viscoplastic Constitutive Model, JSMS, Vol. 68, No. 11, pp. 812-817, 2019 (in Japanese).

Keywords: A carbon dioxide capture and storage, gas hydrate, ground deformation, numerical simulation

©2021. Japan Geoscience Union. All Right Reserved.

Experimental Study on Formation Behavior of CO2 Hydrate in a Flow Field Assuming Carbon Dioxide Storage in Subseabed

*Yuichi Magara[1], Taku Nishimura[1], Yoshihiro Konno[1], Yusuke Jin[2], Takaomi Tobase[3]

1. Graduate School of Frontier Science, the University of Tokyo , 2. National Institute of Advanced Industrial Science and Technology, 3. Electric Power Development Co.,Ltd.

In order to realize CO2 underground storage in Japan, we propose CO2 storage in subseabed using CO2 hydrate in addition to storage in aquifers. In this method, it is expected that injected CO2 will form hydrate during its rising process and become a seal layer by clogging pores. Therefore, caprock is unnecessary in this method, and it is expected that the storage site will be expanded and the storage cost will be reduced. However, there is a concern about CO2 leakage due to the lack of the sealing ability of CO2 hydrate.

In this study, liquid CO2 was injected into the Toyoura sand core under pressure and temperature conditions simulating the water depth of 600 m and the seabed depth of 150 m below the seafloor. We investigate whether the CO2 hydrate could yield a sealing function as a caprock.

In our previous experiment, liquid CO2 was injected into a short core (200 mm in height and 50 mm in diameter) at the same rate as the rising rate due to buoyancy. Due to the limitation of core volume, liquid CO2 could not be injected continuously; thus, it was injected intermittently. CO2 hydrate formation was confirmed about 36 hours after the start of injection. After confirming the CO2 hydrate formation, liquid CO2 was injected again. The pressure near the core inlet suddenly increased, and blockage by CO2 hydrate was confirmed. However, the method of intermittent injection of liquid CO2 is different from the actual field operation, which assumes continuous injection.

In this study, we investigate hydrate formation behaviors and sealing function in the flow field by injecting liquid CO2 continuously using a long core (734 mm in height and 50 mm in diameter). CO2 hydrate formation was confirmed around the upstream side of the core about 17.5 hours after the start of injection. After the first hydrate formation around the upstream side of the core, hydrate formation was also confirmed downstream of the core. However, blockage due to hydrate formation was not confirmed. The result indicates that hydrate was formed heterogeneously. In addition, a phenomenon that seemed to be a redistribution of hydrate with time was observed.

Keywords: Storage in subseabed, CO2 Hydrate, Sealing ability

©2021. Japan Geoscience Union. All Right Reserved.

Cost analysis of CO_2 transportation in CCS deployed in Japan

*Hirotaka Isogai[1], Corey Adam Myers[2], Takao Nakagaki[2], Takeshi Myoi[3], Junichi Shimizu[3]

1. Department of Modern Mechanical Engineering, Waseda University , 2. Faculty of Waseda University, 3. Geological Carbon Dioxide Storage Technology Research Association / Research Institute of Innovative Technology for the Earth

Carbon dioxide capture and storage (CCS) is regarded as an integral technology to meet net CO_2 neutrality in Japan and abroad. The technology can be divided into three major activities: capture of CO_2 from emission sources, transportation of CO_2 to a storage site, and injection of CO_2 into an appropriate underground geological formation. In Japan, the transportation of CO_2 captured at a power plant in Kyoto to the existing storage site in Hokkaido is planned to be demonstrated within a few years. One of the barriers to a rapid deployment of CCS is recognized as the high costs. Discussion of cost has historically focused on CO_2 capture, primarily because CO_2 transport by onshore pipeline is a mature and relatively cheap activity. In Japan and coastal Europe area where onshore pipelines are far less deployed than US, a mixture of geology, geography, regulations, and public opinion make CO_2 transport by ship a promising method as shown in hub and cluster system. The available data on cost of transport by ship is difficult to merge with existing data on CO_2 capture and injection because of imprecise definitions of the boundaries of each activity. In this study, the cost of CO_2 transport is calculated as part of a complete CCS chain to eliminate issues of boundary selection. Transport by ship and pipeline are evaluated in the context of Japan to provide a clear comparison. The cost of transport is reported per unit of avoided CO_2.

For both the pipeline and ship-based transport methods, it is assumed that the emission source is either a GW-class supercritical pulverized coal-fired power plant (SCPC) or a natural gas combined cycle power plant (NGCC). In both cases, an amine-based CO_2 capture system is retrofitted to existing power plant. For pipeline transport, captured CO_2 is compressed to the supercritical state and is transported via onshore pipeline with intermediate boosters. The injection site is assumed to be operated from onshore though actual injection occurs at sea, similar to JCCS' Tomakomai CCS demonstration facility. The pipeline cost estimate is broadly based on the "FE/NETL CO_2 Transport Cost Model" by NETL with various location factors modified to account for differences between the US and Japan. The results of the cost estimation are corroborated by comparison with multiple existing CO_2 pipeline projects. In all cases, pipeline transport costs are OPEX-dominated so long as the operation period is long to some extent (typically >20 years). Countries and localities with experience with pipelines show markedly lower costs due to the shorter permitting period, calling into question the applicability of pipeline transport in Japan. For transport by ship, the liquefaction of CO_2 at around triple point, intermediate storage at port, loading to the ship, transport by ship, unloading, and conditioning prior to injection are considered. It is assumed that CO_2 injection occurs at sea. The cost of ships and at-sea injection facilities are based on previously reported engineering analyses. The several conditioning steps applied to CO_2, especially conditioning chilled and liquefied CO_2, incurs a large electricity burden which means that the cost and CO_2 intensity of electricity are important factors in determining the cost per unit of avoided CO_2. At short transport distances, the cost for maintenance and repair of facilities also account for a large portion of the total cost. At longer transport distances, fuel costs become an increasingly large portion of total cost and the balance between ship speed and the number of ships gain importance. The results in this study are corroborated by comparison with cost estimates from literatures. Regardless of transport type, it was found that the SCPC case has a higher sensitivity of CO_2 transportation cost on the CO_2 avoided cost compared with NGCC case due to the difference in the amount of CO_2 captured and emission.

©2021. Japan Geoscience Union. All Right Reserved.

Keywords: pipeline, ship transportation, CO_2 avoided cost, hub and cluster

©2021. Japan Geoscience Union. All Right Reserved.

Consideration about public consensus building of CCS

*Takaomi Tobase[1]

1. Electric Power Development Co., Ltd.

The main issues to implement CCS in our society are considered as follows.
To reduce uncertainty in the storability evaluation of the CO2 reservoirs.
To realize cost reduction of CCS.
To development of storage sites.
To build public consensus for CCS.
This paper focuses on the consensus building. According to previous studies, citizens in Japan know little about CCS. On the other hand, some people who have a deep interest in environmental problems are skeptical about CCS.In order to promote the consensus building for CCS, the understanding of the people must also be secured in addition to acceptance of local citizens.I consider the consensus building of CCS from three viewpoints of necessity, appropriateness and validity.

Keywords: CCS, social consensus building, necessity, appropriateness, validity

©2021. Japan Geoscience Union. All Right Reserved.

[J] Oral | H (Human Geosciences)：H-DS Disaster geosciences

Fri. Jun 4, 2021 9:00 AM - 10:30 AM JST | Fri. Jun 4, 2021 12:00 AM - 1:30 AM UTC | Ch.17 Zoom Room 17

[H-DS09] Tsunami and tsunami forecast

convener:Hiroaki Tsushima(Meteorological Research Institute, Japan Meteorological Agency), Chairperson:Hiroaki Tsushima(Meteorological Research Institute, Japan Meteorological Agency)

This session discusses issues related to improving real-time and long-term prediction accuracy of tsunami from earthquakes, landslides, and volcanoes, which include such as a better understanding of tsunami dynamics, new real-time tsunami observing systems deployed in the open ocean and coastal waters, methodologies of more rapid and accurate prediction during tsunami emergencies, more extensive and accurate inundation maps, and long-term tsunami potential forecast.

9:00 AM - 9:15 AM JST | 12:00 AM - 12:15 AM UTC

[HDS09-01] Rapid magnitude estimation using long-period components of seismic waves

*Takahito Nishimiya[1], Akio Katsumata[2] (1.Meteorological Research Institute, Japan Meteorological Agency, 2.University of Toyama)

9:15 AM - 9:30 AM JST | 12:15 AM - 12:30 AM UTC

[HDS09-02] Validation of Tsunami Run-up Simulation Using Observed Tsunami Heights in the Sendai Plain after the 2011 Tohoku Tsunami

*Yoshinori Shigihara[1], Yuuki Eguchi[1], Tsuyoshi Tada[1] (1.Department of Civil and environmental Engineering, National Dedense Academy)

9:30 AM - 9:45 AM JST | 12:30 AM - 12:45 AM UTC

[HDS09-03] Numerical simulations for the 2006 and 2007 Kuril tsunamis

*Keiji Akai[1], Toshitaka Baba[2] (1.Graduate School of Engineering, Tokushima University, 2.Graduate School of Science and Technology, Tokushima University)

9:45 AM - 10:00 AM JST | 12:45 AM - 1:00 AM UTC

[HDS09-04] Causes and Solutions of Computational Instability in Tsunami Calculations by Finite Difference Method for Nonlinear Long Wave Equations

*Masaaki MINAMI[1] (1.Meteorological Research Institute)

10:00 AM - 10:15 AM JST | 1:00 AM - 1:15 AM UTC

[HDS09-05] Tsunami waveform analysis of 1929 Grand banks landslide tsunami

*Tatsuya Nakagaki[1], Yuichiro Tanioka[2] (1.Graduate school of Science, Hokkaido University, 2.Hokkaido University)

10:15 AM - 10:30 AM JST | 1:15 AM - 1:30 AM UTC

[HDS09-06] Development of automatic tsunami-detection method based on continuous analysis of offshore tsunami waveforms

*Hiroaki Tsushima[1], Naotaka YAMAMOTO CHIKASADA[2] (1.Meteorological Research Institute, Japan Meteorological Agency, 2.National Research Institute for Earth Science and Disaster Resilience)

Rapid magnitude estimation using long-period components of seismic waves

*Takahito Nishimiya[1], Akio Katsumata[2]

1. Meteorological Research Institute, Japan Meteorological Agency, 2. University of Toyama

The Japan Meteorological Agency (JMA) usually uses estimations of hypocenter and magnitude for the tsunami forecast to issue tsunami warning as soon as possible. JMA-magnitude (M_J) that JMA estimates rapidly is almost the same as M_W up to around 8 on average. However, when a magnitude is more than 8 such as the 2011 off the Pacific coast of Tohoku Earthquake, M_J is underestimated due to the saturation of amplitude-magnitude.
JMA uses several countermeasures for judging the M_J underestimation. The long-period components monitor of seismic waves is one of them, which is to monitor peak-amplitudes of composite displacements filtered with bandpass of 100s to 500s at broadband seismograph stations (JMA,2013). JMA can recognize that an earthquake has greater *M* from an empirical formula for the long-period components monitor, even if M_J is underestimated. The formula which was made using only the 2011 off the Pacific coast of Tohoku Earthquake and the Tokachi–oki Earthquake in 2003, is consist of a peak-amplitude and an epicentral distance.
We think that the long-period component monitor would be applicable also for detection of a tsunami earthquake which has the long source rupture duration because the pass band of 100s to 500s is long enough compared with the rupture durations of tsunami earthquakes.
We showed that M_J underestimated the size of tsunami earthquakes by 1 or more magnitude unit compared with M_W (in Seismological Society Fall Meeting 2020). It can even be under 7. In this study we try to reconstruct an empirical formula for the long-period components monitor so as to adapt it to earthquakes in the latter of *M*6 and above. We will also show results in the case that the reconstructed formula is applied to tsunami earthquakes.
Acknowledgement: We used NIED F-net data.

Keywords: tsunami earthquake, magnitude

©2021. Japan Geoscience Union. All Right Reserved.

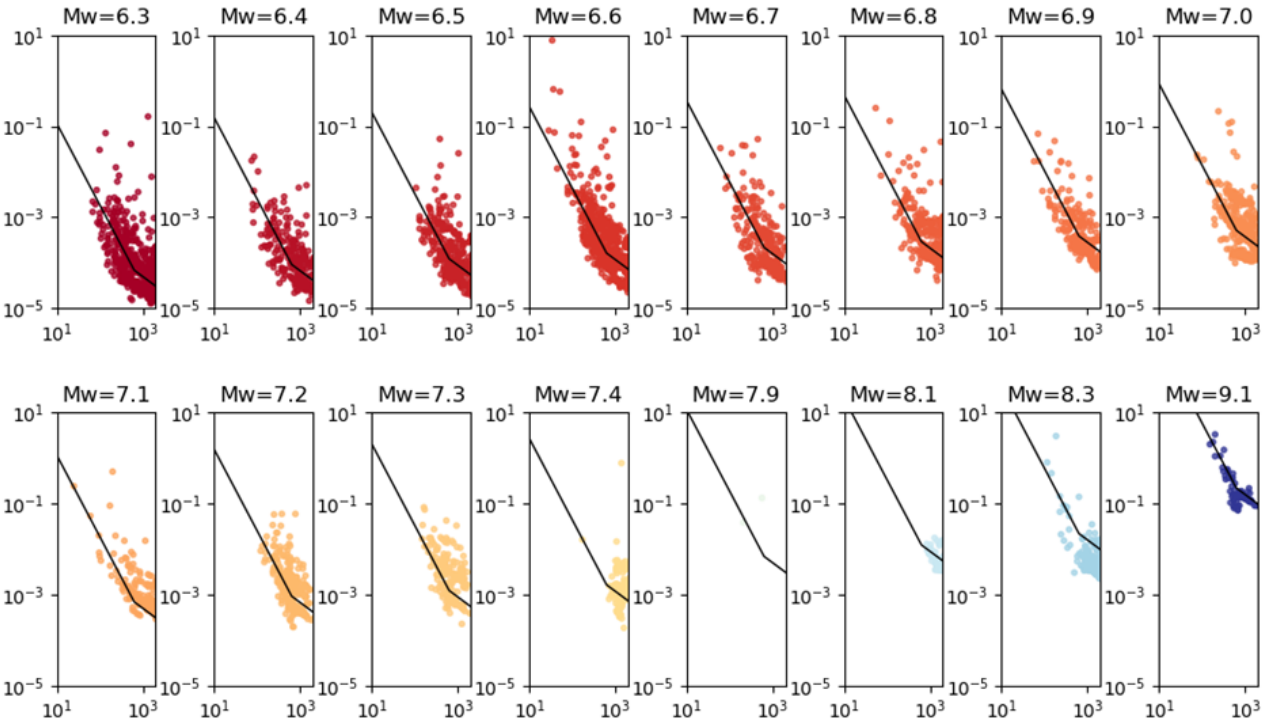


Figure: Obtained empirical formula from observational data

The vertical lines show composit peak-amplitude of long-period component obtained from seismic wave in m.
The horizontal lines show hypocentral distance in km.
The solid lines show empirical formula (preliminary).
The color-coded circles for each M_W show peak-amplitudes obtained from observed seismic waves.

©2021. Japan Geoscience Union. All Right Reserved.

Validation of Tsunami Run-up Simulation Using Observed Tsunami Heights in the Sendai Plain after the 2011 Tohoku Tsunami

*Yoshinori Shigihara[1], Yuuki Eguchi[1], Tsuyoshi Tada[1]

1. Department of Civil and environmental Engineering, National Dedense Academy

The accuracy of tsunami run-up simulations is important for predicting tsunami damage and taking countermeasures against it. The accuracy of numerical tsunami models has been verified by comparing them with analytical solutions and hydraulic experiments. On the other hand, the validation of numerical tsunami models should be done by comparing with field scale observations. The purpose of this study is to establish a new method to validate the tsunami run-up simulation by using the trace height data obtained from the survey in the Sendai Plain during the 2011 Tohoku Tsunami.
Since the tsunami trace height data measured in the field survey in the Sendai Plain was discrete, we created a continuous tsunami height distribution by using the spatial interpolation method. As a result of comparing several interpolation methods, the Natural Neighbor method was able to produce the most realistic tsunami height distribution. Thus, we were able to obtain the tsunami trace height data that existed uniformly in the whole inundation area, which enabled us to evaluate the tsunami inundation simulation without being affected by the bias of the survey points. Next, new indexes were proposed to compare the observed and simulated values, and the validity of the tsunami run-up model was confirmed. In determining the index, we considered that the index should be able to evaluate the entire inundation area without bias. Using the proposed indexes, the computational conditions that ensure the validity of the tsunami run-up simulation were investigated. As a result, the topographic resolution and the availability of topographic information were the most important factors to change the tsunami behavior.

Keywords: tsunami run-up simulation, tsunami trace height, Validation

©2021. Japan Geoscience Union. All Right Reserved.

Numerical simulations for the 2006 and 2007 Kuril tsunamis

*Keiji Akai[1], Toshitaka Baba[2]

1. Graduate School of Engineering, Tokushima University, 2. Graduate School of Science and Technology, Tokushima University

Numerical simulations for the 2006 and 2007 Kuril tsunamis

Keiji Akai and Toshitaka Baba

Tokushima Univ.

During the tsunami caused by the 2006 Kuril earthquake, the maximum amplitude arrived at the Japan coast after lifting the tsunami warning. Accurate predictions for far-field tsunamis lasting a long time are vital in lifting the tsunami warning. The 2006 Kuril earthquake was followed by an outer-rise earthquake (the 2007 Kuril earthquake) two months later. The 2007 Kuril earthquake also caused a significant tsunami. In this study, we calculated the tsunamis of the 2006 and 2007 Kuril earthquakes and compared observations by DART systems.

Fault models to calculate for the 2006 and 2007 tsunamis were based on Fujii and Satake (2008)'s models estimated by inversion analysis. For the 2006 earthquake, we used three fault models: the two models of them consisting of eight sub-faults and the other consisting of ten sub-faults. For the 2007 earthquake, we used two fault models consisting of six sub-faults. We calculated crustal displacement at the seafloor using the fault models and an analytical solution in the half-space homo-elastic medium. We applied the horizontal movement effect and the Kajiura filter to the seafloor displacement to estimate the initial sea surface displacement. The tsunami governing equations were the linear and nonlinear long-wave equations with the effects of dispersion, elastic loading, and seawater density stratification. The grid interval of the bathymetric data is 5 minutes re-sampled by GEBCO. The computed tsunami waveforms were compared at DART stations.

The numerical simulations predicted the arrival times, the amplitudes of the first waves, and the later phases with high accuracy for the 2006 tsunami. However, for the 2007 tsunami, the prediction was not as accurate as of the simulation for the 2006 tsunami. We will continue the investigations by such as changing fault models and using long calculation time.

Keywords: tsunami

©2021. Japan Geoscience Union. All Right Reserved.

Causes and Solutions of Computational Instability in Tsunami Calculations by Finite Difference Method for Nonlinear Long Wave Equations

*Masaaki MINAMI[1]

1. Meteorological Research Institute

When solving the nonlinear long wave equation by the finite difference method, which is commonly used in tsunami numerical simulations. The calculation may become unstable and the results may diverge even though the CFL condition is satisfied. When considering the issuance and updating of tsunami warnings using real-time simulations, such calculation failures can be fatal. Therefore, in order to eliminate such calculation instability, the evaluation of the difference equation and the calculation condition were examined, and the method to prevent calculation instability was verified.
First of all, the author has been examining the difference of time difference equation of friction term in nonlinear long wave equation (MINAMI 2020JpGU etc.), and examined the discretization error and computational stability of four difference methods, (1)Explicit (2)Semi-implicit(combined) (3)Semi-implicit(simple) (4)Full-implicit. Among them, Semi-implicit (simple) and Full-implicit are better in computational stability. However, many of the current tsunami models use Semi-implicit (combined) with various conditions. Therefore, in this paper, we evaluate the computational conditions in the TUNAMI-N2 model (Imamura et al. 2006, etc.).
In the TUNAMI-N2 model, Semi-implicit (combined) is used, and the following four conditions are added to the calculation: 1. If the total water depth is less than 0.1 cm before the flux calculation, the flux for that time step is set to zero. 2. If the total water depth is less than 1 cm when calculating the friction term, it is rounded up to 1 cm. 3. When the total water depth is less than 0.1cm, the advection term is not calculated (even when the total water depth is more than 0.1cm, only the upwind term is not calculated if the total water depth on the upwind side is less than 0.1cm). 4. If the calculated flux is smaller than 10^-10m, set the flux to zero.
As a result, even with the above conditions, there were cases where the semi-implicit (combined) produced large errors in the calculations, as shown in Fig. 1. This is a case where the flux converges to near zero when solved continuously, but at this time, due to the difference in the way the friction term is differentiated, the flux does not converge to zero and the positive and negative directions are reversed. When this inversion of the flux direction occurs, the upwind direction of the upwind difference is switched when calculating the advection term, and the upwind value that should be referenced is switched. This was found to be the cause of the time evolution and enlargement of the error. It is possible to avoid these problems by changing the numerical values of the above conditions, but this means that the advection term and the friction term disappear when the water depth is small, which also increases the error.
In addition, the instability of the calculation at the edge of the computational domain was also verified. In the finite difference method for tsunami computation, the method using the characteristic curve of progressive long wave (Goto and Ogawa 1982) is often adopted. This method assumes linear long waves, and if there is a shallow water mesh at the edge of the computational domain, the influence of friction and advection terms increases and the error becomes large. Therefore, frictional forces were also considered in the calculation at the boundary, the error was found to be small (Fig. 2). The water depth in the experiment is uniform, and the results are compared with the calculation using the periodic boundary condition.
From the above verification, it was confirmed that when solving the nonlinear long wave equation by the

©2021. Japan Geoscience Union. All Right Reserved.

finite difference method, it is possible to perform more stable calculations than before by using a more implicit difference equation for the friction term and by performing more appropriate processing at the edge of the calculation domain.

Keywords: Tsunami Calculations, Computational Instability, Nonlinear Long Wave Equations

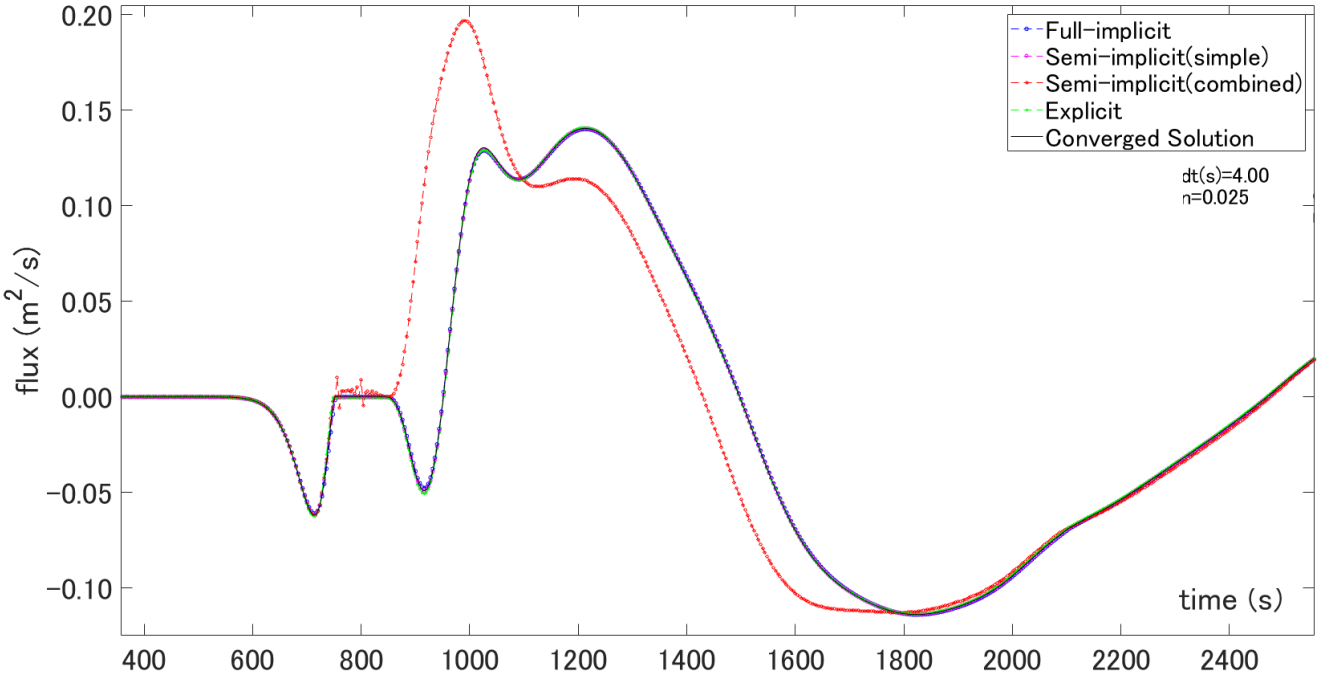


Fig 1. Case of instability using Semi-implicit(combined)

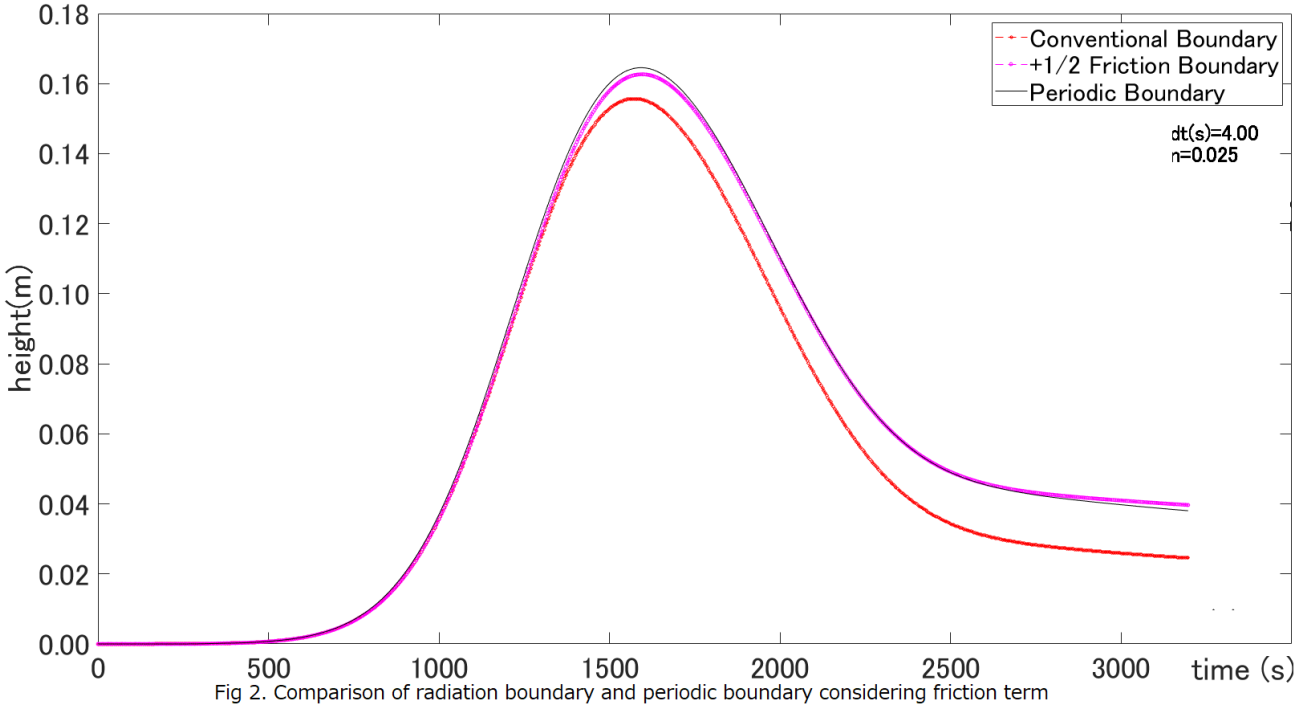


Fig 2. Comparison of radiation boundary and periodic boundary considering friction term

©2021. Japan Geoscience Union. All Right Reserved.

Tsunami waveform analysis of 1929 Grand banks landslide tsunami

*Tatsuya Nakagaki[1], Yuichiro Tanioka[2]

1. Graduate school of Science, Hokkaido University, 2. Hokkaido University

Large submarine landslides sometimes generated tsunamis causing the catastrophic disaster along the local coastal area. One of the most famous submarine landslide tsunamis is the 1929 Grand Banks tsunami generated off the east coast of Canada. On November 18th, 1929, the Grand Banks earthquake (Mw7.2) occurred, and tsunami struck the southern coast of Burin Peninsula in the east coast of Canada. Soon and some hours later of the earthquake, twelve intercontinental telegraph cables installed at the ocean bottom near the source area were cut one after another. This suggested that the cables were cut by submarine landslides. Previous seismological studies indicated that the earthquake was also generated by the single force, probably by the landslide. The tide gauge station in Halifax, Canada observed the tsunami waveform. In this paper, we try to model this tsunami waveform by the numerical simulation of both landslide and tsunami.

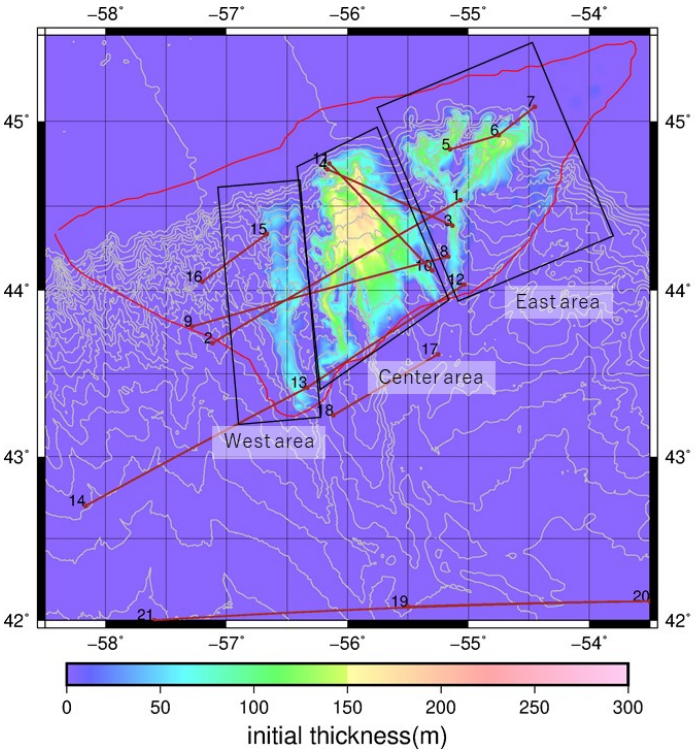
We assume that the landslides occurred at the continental slope which was located at the landward from the cut position and timing of telegraph cables by the submarine landslide. We also assume that those landslides occurred along the several submarine valleys in the continental slope. We calculate the submarine landslide tsunami with two-steps approach. The first step is mass movement calculation, and next step is tsunami calculation based on the result of first step. In the first step we used the Tsunami Squares method, which is not only a simple and effective method to calculate the time-dependent mass movement but also easy to introduce the effect of landslide propagation and start time difference of landslide for each point. In the next step, we calculate the tsunami propagation with finite different method. Time-dependent change of mass thickness in first step is treated as tsunami source.

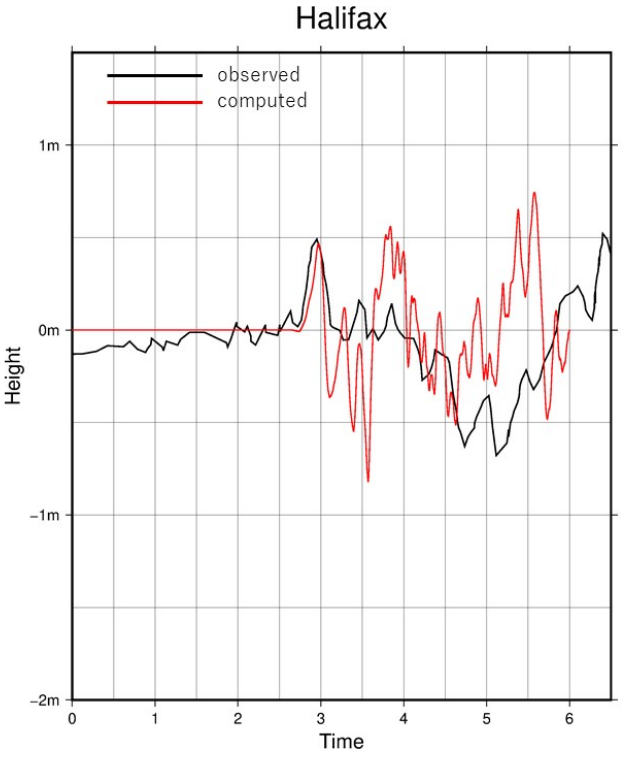
The landslide mass distribution is estimated by comparing the computed and observed waveform at Halifax tide gauge. We put masses on three area based on the previous studies. In the figure, colors show the initial mass height distribution, brown line around the colors show the mass area, dots and number are the cable cut position and position name, points from 1 to 16 were cut immediately after the earthquake. For reproducing the first wave, masses in west and center area collapse all at once, and in east should collapse at 10 minutes after of west and center.

The waveform is shown in figure, black line is observed waveform and red is calculated one. The first wave is well recreated in sight of arrival time, amplitude and wavelength, but large negative pulse appears only in simulated waveform. We should improve our model by changing frictional parameters to reproduce the tsunami waveform at Halifax.

Keywords: landslide tsunami, 1929GrandBanks Earthquake

©2021. Japan Geoscience Union. All Right Reserved.





©2021. Japan Geoscience Union. All Right Reserved.

Development of automatic tsunami-detection method based on continuous analysis of offshore tsunami waveforms

*Hiroaki Tsushima[1], Naotaka YAMAMOTO CHIKASADA[2]

1. Meteorological Research Institute, Japan Meteorological Agency, 2. National Research Institute for Earth Science and Disaster Resilience

Large tsunamis can be generated by not only earthquakes but also natural phenomena. For example, in the 1998 Papua New Guinea earthquake, it was pointed out that the tsunami was amplified by a submarine landslide. When the non-seismic tsunamis are generated offshore, the offshore tsunami observation is effective for early and direct tsunami detection. In Japan, dense offshore tsunami observation networks such as S-net and DONET are in operation, and it has been shown that an optimal interpolation method that is one of the data-assimilation techniques is effective to estimate the present tsunami-wavefield from the ocean-bottom pressure gauge (OBPG) data of these networks without earthquake information (e.g., Maeda et al., 2015). In these methods, the time history of the observed data is gradually incorporated into the tsunami propagation model during the successive analysis. On the other hand, if the time series data are directly used in a single analysis and the time history information is explicitly incorporated, the wavefield is more strongly constrained and the ability of tsunami monitoring may be improved. In this study, we are investigating a method for automatic detection of tsunamis by simple analysis of tsunami waveforms (time series data).

Our method is inspired by the GRiD MT (Tsuruoka et al., 2009), which automatically estimates the origin time, hypocenter location, moment tensor (MT) solution, and magnitude from seismic waveforms. First, in advance of tsunamigenic phenomena, a sea surface element wave source is distributed in the sea area to be monitored, and the Green's function of the tsunami waveform at the OBPGs is obtained by tsunami numerical calculation. Then, assuming that the tsunami is generated at one elemental source, the initial sea-surface displacement at any elemental source is estimated from the observed tsunami waveforms at multiple stations, and the variance reduction (VR) between the observed and theoretical waveforms is calculated. This is done for all the elemental wave sources. This successive analysis is carried out at temporal intervals to monitor the spatio-temporal distribution of VR, and the time and location of tsunami generation are detected based on the increase of VR.

The method was tested by synthetic tests in the sea area along the Japan Trench. A Gaussian distribution (size: ~10 km) is used as an elemental wave source from off the Etorofu Island to off the Boso Peninsula. The data length of the OBPG waveform used for the inversion is 15 minutes before the time of analysis execution. The analysis is conducted every minute from 15 minutes before to 15 minutes after the true origin time. Our method was applied to the synthetic observations of the S-net OBPGs that were computed by assuming a 50-km-long and 25-km-wide fault model near the trench. The results showed that the VR was maximum (about 0.3) at the elemental source nearest the true fault location at the timing consistent with the true source time, indicating the possibility of detection by our method. In the future, we will examine the effect of the difference of the target tsunami source and the real observation noise on the performance of our method.

Acknowledgments: This work was partially supported by JSPS KAKENHI Grant Number JP18K04674.

©2021. Japan Geoscience Union. All Right Reserved.

Keywords: Tsunami, non-seismic tsunami, Automatic detection

©2021. Japan Geoscience Union. All Right Reserved.

[J] Oral | H (Human Geosciences)：H-CG Complex & General

Fri. Jun 4, 2021 3:30 PM - 5:00 PM JST | Fri. Jun 4, 2021 6:30 AM - 8:00 AM UTC | Ch.15 Zoom Room 15

[H-CG25] Human social activities and earth and planetary sciences

convener:Kazuo Amano(Center for Spatial Information Science, The University of Tokyo), Takashi Oguchi(Center for Spatial Information Science, The University of Tokyo), Kayoko Yamamoto(University of Elctro-Communications), Masaki Ito(Institute of Industrial Science, the University of Tokyo), Chairperson:Kayoko Yamamoto(University of Elctro-Communications), Kazuo Amano(Center for Spatial Information Science, The University of Tokyo)

This session has expanded the scope of "Social Media and Earth and Planetary Sciences" which has been held over the past nine years and in which many innovative research results appeared, was renamed last year in consideration of the recent development of SNS. In this revised version unlimited to the use of SNS, presentations aimed at the development of earth and planetary sciences in relation to human social activities, such as the use of navigation systems and behavior support systems, are also targeted. We also welcome lectures on human geography related to the natural environment and human activities, and social use of crustal resources such as stone materials.

3:30 PM - 3:45 PM JST | 6:30 AM - 6:45 AM UTC

[HCG25-01] Significance of international webinars on Earth and Planetary Science: Cases of Geography and Geomorphology

*Takashi Oguchi[1] (1.Center for Spatial Information Science, The University of Tokyo)

3:45 PM - 4:00 PM JST | 6:45 AM - 7:00 AM UTC

[HCG25-02] Utilization of Digital Infrastructure Concerning Disaster Countermeasures in Japan

*Kayoko Yamamoto[1] (1.University of Elctro-Communications)

4:00 PM - 4:15 PM JST | 7:00 AM - 7:15 AM UTC

[HCG25-03] An Environmental Learning Support System Incorporating the Life Cycle Concept

*Kayoko Yamamoto[1], Akira Shirato[1] (1.University of Elctro-Communications)

4:15 PM - 4:30 PM JST | 7:15 AM - 7:30 AM UTC

[HCG25-04] Information exchange for earth science major graduates of a university by using Zoom

*Kazuo Amano[1,2], Satoshi Kanaguri[2] (1.Center for Spatial Information Science, The University of Tokyo , 2.Amano Geological Laboratory Japan)

4:30 PM - 4:45 PM JST | 7:30 AM - 7:45 AM UTC

[HCG25-05] How the Relationship between Society and Researchers Changes after the COVID-19 Disaster considering Rapid Spread of Online Technology

*Masaki Ito[1] (1.Institute of Industrial Science, the University of Tokyo)

4:45 PM - 5:00 PM JST | 7:45 AM - 8:00 AM UTC

[HCG25-06] Discussion

Significance of international webinars on Earth and Planetary Science: Cases of Geography and Geomorphology

*Takashi Oguchi[1]

1. Center for Spatial Information Science, The University of Tokyo

The global spread of COVID-19 has made it difficult to hold face-to-face international research meetings, and international webinars became more frequent as a supplementary activity. This is also the case with Earth and Planetary Science. Because such webinars have increased rapidly in a short period of time, they have been done by trial and error. Therefore, it is meaningful to consider the future of international webinars for science. This presentation first introduces the contents of international webinars on Geography and Geomorphology in which the author participated as an invited speaker or a coodinator. Then, the scientific significance and future prospects of international webinars is discussed.

Keywords: Webinars, Scientific significance

©2021. Japan Geoscience Union. All Right Reserved.

Utilization of Digital Infrastructure Concerning Disaster Countermeasures in Japan

*Kayoko Yamamoto[1]

1. University of Elctro-Communications

According to the White Paper on Disaster Management 2018, among disaster countermeasures such as “self-help”, “mutual help” and “public help”, the most fundamental method is “self-help” which is a countermeasure individually conducted. It is important for each individual to have a high disaster prevention awareness in everyday life in order to minimize the damage through countermeasures, as rescue teams are not able to immediately reach all disaster victims during a disaster. Therefore, it is important to enhance the government's “ability to inform” and the public’s “ability to become aware” by widely and appropriately providing disaster information, accurately grasping hazardous areas as well as evacuation centers in case of a disaster before it occurs, and accumulating disaster information with location information. In order for this to lead to “mutual help” and “public help”, sufficient accumulation and sharing of disaster information within the local community including residents, corporations and the local government are essential during normal times.
On the other hand, in recent years in Japan, a cloud computing society where the internet can be reached from various information tools has been established, and Japan has entered the age of Internet of Things (IoT) and Internet of Everything (IoE) in which various things can be connected to the internet. The society mentioned above is able to efficiently gather and accumulate disaster information as local knowledge made up of knowledge from the experience and everyday life of residents as well as the expertise based on scientific findings through the effective use of Information and Communication Technology (ICT).
The present study focused on social media and GIS of ICT as a digital infrastructure, which play important roles in disaster countermeasures. The present study also introduced development cases of the system developed integrating these, and presented the utilization potential as a digital infrastructure.
Additionally, Twitter, which is the most-used social media platform for disaster countermeasures in Japan, was focused on, and its utilization cases during the Heavy Rain Disaster in Western Japan in 2018 were considered as well as the utilization potential of Twitter as a familiar digital infrastructure in disaster countermeasures was indicated.
As the reality and virtual spaces are closely related and integrated in super-smart societies such as Japan, everyday events in either space influences the other space. Therefore, if a disaster in reality occurs, the transmission and reception of disaster-related information in the virtual space using various information communication methods such as mass media and social media start almost simultaneously. While this can lead to real activities such as evacuation, relief and support, it can also cause problems such as confusion due to information overload. Therefore, the issue is how to make the information circulating in the virtual space and especially on social media efficiently and effectively aid in the rescue and support activities in the reality space.
In order to solve such an issue, it is necessary to not only set rules for the utilization of social media but also to sift through information and share only the necessary information to the affected local governments and those involved in the rescue and support activities. In doing this, if the social media GIS for disaster information system and the function of social media mapping of the spatiotemporal information system are utilized, the essential information can be efficiently consolidated on the digital map of Web-GIS. Additionally, while the present study indicated the utilization potential of Twitter alone during disasters, the same utilization potential of other social media platforms based on their characteristics should be considered.

©2021. Japan Geoscience Union. All Right Reserved.

Furthermore, various information communication methods including verbal calls in addition to ICT are necessary in order to prevent people who are vulnerable to disasters from becoming people who are also vulnerable to information. Though prompt evacuation may not be realized, due to the normalcy bias where an individual has the “I’m okay” mentality during disasters, finding a way to effectively use ICT to encourage individuals to evacuate is an issue. It is necessary for individuals who are not used to using ICT to familiarize themselves with utilizing it in their daily life.

Keywords: Information and Communication Technology (ICT), Digital Infrastructure, Geographic Information Systems (GIS), Social Media, Disaster Countermeasures

©2021. Japan Geoscience Union. All Right Reserved.

An Environmental Learning Support System Incorporating the Life Cycle Concept

*Kayoko Yamamoto[1], Akira Shirato[1]

1. University of Elctro-Communications

According to Ilgin et al. (2010) and United State Environmental Protection Agency (EPA, 2012), life cycle assessment (LCA, also known as life cycle analysis) is a methodology for assessing environmental impacts associated with all the stages of the life cycle of a commercial product, process or service. For example, in the case of a manufactured product, environmental impacts are assessed from raw material extraction and processing (cradle), through the product's manufacture, distribution and use, to the recycling or final disposal of the materials composing it (grave). Studies on LCA involve a thorough inventory of the energy and materials that are required across the industry value chain of the product, process or service, and calculates the corresponding emissions to the environment. Thus, LCA assesses cumulative potential environmental impacts, and it aims to document and improve the overall environmental profile of the product.
Regarding the environmental education scene, efforts to incorporate the life cycle concept into the learning program have been occasionally seen (Hondo, 2008).The significance of incorporating the life cycle concept in environmental learning is that, first, learners can more easily make specific connections between daily consumer activities and environmental problems, and recognize that their own behavior choices are deeply involved with global environmental problems, by learning about the life cycle concept. Second, learners can quantitatively compare and determine the environmental impact, which tends to be qualitatively assessed, by learning about the direct assessment and analysis method of the environmental impact called the LCA.
Based on the above, the present study aims to develop an e-learning system to support environmental learning based on the life cycle concept. The present study can be summarized in the following 3 points.
(1) An e-learning system, which is made up of 3 parts including text-based learning materials, quizzes to review the content of the learning materials, and CO2 emission simulation, was designed and developed with the purpose of supporting environmental learning. Users that were expected to be from a wide range of age groups were recruited, and the system was operated and evaluated.
(2) The operation period of this system was 1 month. Based on the results of questionnaire survey for users, it was evident that the quiz function and the simulation function of CO2 emission contributed to the efficiency in environmental learning, and the format of the e-learning system was effective and helpful for environmental learning. Addition-ally, with the users' awareness related to environmental conservation before and after using the system, significant changes in awareness were seen in areas such as behavioral intention, sense of urgency and sense of connection. On the other hand, there were no major changes in awareness concerning the sense of effectiveness, responsibility and feasibility, and there was also no desirable change for a sense of burden.
(3) According to the access analysis of the log data during the operation period, it was revealed that 62% of the total access numbers were from mobile devices. Therefore, it was effective to prepare an interface optimized for mobile devices enabling users to use the system from their smartphones and tablet PCs.

Keywords: Environmental Learning, Life Cycle Assessment (LCA), Life Cycle Concept, Environmental Education, Sustainable Development Goals (SDGs), E-learning System

©2021. Japan Geoscience Union. All Right Reserved.

Information exchange for earth science major graduates of a university by using Zoom

*Kazuo Amano[1,2], Satoshi Kanaguri[2]

1. Center for Spatial Information Science, The University of Tokyo , 2. Amano Geological Laboratory Japan

In Japan as well, COVID-19 has become widespread since the beginning of 2020, making it impossible to hold study groups and seminars that are crowded with people at one venue. Under such circumstances, we started the online seminar "Forum Earth" in May 2020. The graduates of the Department of Earth Sciences, Faculty of Science Ibaraki University, one of the local national universities, were targeted for this forum. The reason for starting the forum was to respond to the desire to study professionally even after becoming a member of social world from a graduate. We used Zoom as a tool, but we also used various SNS such as Facebook, Twitter, and Note in conjunction with it. The themes related to nature and society such as natural disasters, hot spring resources and the Anthropocene were selected. At the same time, a book about the history of the earth was read in turns. After graduating from the university, it is considered that the seminar was exciting for participants of various levels who are active in various fields. In this lecture, we will also discuss the effects and issues of online seminars for working adults.

Keywords: online seminar, Zoom, SNS

©2021. Japan Geoscience Union. All Right Reserved.

How the Relationship between Society and Researchers Changes after the COVID-19 Disaster considering Rapid Spread of Online Technology

*Masaki Ito[1]

1. Institute of Industrial Science, the University of Tokyo

The COVID-19 disaster, which began in 2020, has brought about a rapid global shift to the online, and it has become common for researchers to conduct lectures, academic conferences, and various meetings online via Zoom or YouTube. On the other hand, face-to-face meetings and on-site surveys are restricted, and the skill sets required of researchers in terms of external relations have changed dramatically. On the positive side, many researchers have developed online communication skills, allowing them to disseminate information more actively than ever before. In this talk, I will review such examples and discuss how researchers should interact with a society. In particular, based on the author's own online experiences, the possibility of such information dissemination will be discussed.

Keywords: Online Communication, COVID-19 disaster

©2021. Japan Geoscience Union. All Right Reserved.

[J] Oral | H (Human Geosciences) | H-CG Complex & General

[H-CG25] Human social activities and earth and planetary sciences

convener:Kazuo Amano(Center for Spatial Information Science, The University of Tokyo), Takashi Oguchi(Center for Spatial Information Science, The University of Tokyo), Kayoko Yamamoto(University of Elctro-Communications), Masaki Ito(Institute of Industrial Science, the University of Tokyo), Chairperson:Kayoko Yamamoto(University of Elctro-Communications), Kazuo Amano(Center for Spatial Information Science, The University of Tokyo)

Fri. Jun 4, 2021 3:30 PM - 5:00 PM Ch.15 (Zoom Room 15)

This session has expanded the scope of "Social Media and Earth and Planetary Sciences" which has been held over the past nine years and in which many innovative research results appeared, was renamed last year in consideration of the recent development of SNS. In this revised version unlimited to the use of SNS, presentations aimed at the development of earth and planetary sciences in relation to human social activities, such as the use of navigation systems and behavior support systems, are also targeted. We also welcome lectures on human geography related to the natural environment and human activities, and social use of crustal resources such as stone materials.

4:45 PM - 5:00 PM

[HCG25-06]Discussion

©Japan Geoscience Union

[J] Oral | S (Solid Earth Sciences)：S-GD Geodesy

Fri. Jun 4, 2021 9:00 AM - 10:30 AM JST | Fri. Jun 4, 2021 12:00 AM - 1:30 AM UTC | Ch.22 Zoom Room 22

[S-GD01] Geodesy and Global Geodetic Observing System

convener:Koji Matsuo(Geospatial Information Authority of Japan), Yusuke Yokota(Institute of Industrial Science, The University of Tokyo), Toshimichi Otsubo(Hitotsubashi University), Chairperson:Koji Matsuo(Geospatial Information Authority of Japan), Akihisa Hattori(The Graduate University for Advanced Studies)

Geodesy is a discipline that aims to define a Terrestrial Reference Frame for accurate positioning in the Earth and monitor/understand the Earth system through precise measurements of the Earth's shape, gravity, and rotation, as well as their temporal evolutions. In this session, we call for wide range of papers concerned with geodesy and its application to geoscience. Topics of interest will include but not limited to recent advances in measurement techniques, data analysis, numerical modeling or theoretical studies of geodesy. This session also welcomes topics of interdisciplinary studies on geoscience using ground-based geodetic techniques (spirit leveling, absolute/relative gravimeter, strain meter and so on) or space geodetic techniques (GNSS, VLBI, SLR, DORIS, GRACE, satellite altimetry and so on). In addition, we also provide a forum for discussing GGOS (Global Geodetic Observing System) related observation programs, advancements of geodetic techniques, collaboration among various organizations in the world.

9:00 AM - 9:15 AM JST | 12:00 AM - 12:15 AM UTC

[SGD01-01] The Airborne Gravity Survey for Development of a New Precise Gravimetric Geoid Model in Japan

*Masahiro Nakashima[1], Kento Iio[1], Yasuhiro Iitsuka[1], Shinobu Kurihara[1], Kumikazu Ochi[1], Shuichi Omori[1], Tokuro Kodama[1], Masato Kuroyanagi[1], Masami Handa[1], Koji Matsuo[1] (1.Geospatial Information Authority of Japan)

9:15 AM - 9:30 AM JST | 12:15 AM - 12:30 AM UTC

[SGD01-02] Accuracy evaluation of airborne gravity data by the three-dimensional least-squares collocation method

*Koji Matsuo[1] (1.Geospatial Information Authority of Japan)

9:30 AM - 9:45 AM JST | 12:30 AM - 12:45 AM UTC

[SGD01-03] Introduction of Absolute Quantum Gravimeter (AQG)

*Masato KUROYANAGI[1], Masami HANDA[1], Tokuro KODAMA[1], Shinobu KURIHARA[1], Kumikazu OCHI[1], Hiroaki YAMAMOTO[1], Shuichi OMORI[1], Kento IIO[1], Masahiro NAKASHIMA[1], Yasuhiro IITSUKA[1] (1.Geospatial Information Authority of Japan)

9:45 AM - 10:00 AM JST | 12:45 AM - 1:00 AM UTC

[SGD01-04] GRACE/GRACE-FO Observed Mass Change Patterns of Antarctica Extracted by ICA Method

*SHI TIANYAN[1], Yoichi Fukuda[1], Koichiro Doi[1], Jun'ichi Okuno[1] (1.Department of Polar Science, Gradualate University for Advanced studies School of Multidisciplinary Sciences)

10:00 AM - 10:15 AM JST | 1:00 AM - 1:15 AM UTC

[SGD01-05] Gravity observations at Jang Bogo Station, Antarctica, and the scale factor calibrations of different type relative gravimeters

*Yoichi Fukuda[1], Jun'ichi Okuno[1], Koichiro Doi[1], Choon-ki Lee[2] (1.National Institute of Polar Research, 2.Korea Polar Research Institute)

10:15 AM - 10:30 AM JST | 1:15 AM - 1:30 AM UTC

[SGD01-06] Parallel observation with superconducting gravimeters TT70 #011 and iGrav #028 at Matsushiro, Japan (2016–2018)

*Yuichi Imanishi[1], Hiroshi Ikeda[2] (1.Earthquake Research Institute, The University of Tokyo, 2.KEK)

The Airborne Gravity Survey for Development of a New Precise Gravimetric Geoid Model in Japan

*Masahiro Nakashima[1], Kento Iio[1], Yasuhiro Iitsuka[1], Shinobu Kurihara[1], Kumikazu Ochi[1], Shuichi Omori[1], Tokuro Kodama[1], Masato Kuroyanagi[1], Masami Handa[1], Koji Matsuo[1]

1. Geospatial Information Authority of Japan

The gravimetric geoid model is constructed by combining the satellite gravity data and the terrestrial gravity data (land and shipborne measurements), the altimetry-derived marine gravity data. The satellite gravity data is used to determine the long wavelength components of the geoid undulations, while the terrestrial gravity data and the altimetry-derived marine gravity data are used to determine the medium and short wavelength components. Several attempts have been made to improve the accuracy of the gravimetric geoid model in Japan, such as adding new satellite gravity data and improving the method of computing gravimetric geoid model (Kuroishi, 2009; Matsuo and Kuroishi, 2020). However, due to the lack of land gravity data in mountainous areas and the low accuracy of shipborne marine gravity data in coastal areas, large discrepancies between the gravimetric geoid models and GNSS/leveling geoid heights occur in these areas (Matsuo, 2017; Matsuo and Kuroishi, 2020). In addition, most of the land gravity data was observed more than 30 years ago, and the observation locations are often obtained from maps. This inaccuracy in location information may cause errors in the gravimetric geoid model.
Therefore, in order to solve these problems, the Geospatial Information Authority of Japan (GSI) has started airborne gravity survey since 2019. The airborne gravity survey can efficiently collect homogeneous gravity data for everywhere, even in mountainous or coastal areas. Since the aircraft is equipped with a GNSS receiver, it is possible to obtain position data with centimeter accuracy. Furthermore, the obtained data has the advantage of higher spatial resolution (spatial wavelength about 10km) than the satellite gravity data. The plan is to collect the airborne gravity data for all over Japan except for the outlying islands by 2023 and to build a precise gravimetric geoid model accurate to 3 cm by combining the airborne gravity data with existing gravity data in 2024.

As of December 2020, approx. 50% of data collection of planned survey lines are completed. Comparing the airborne gravity data with EGM2008 model gravity data, there is a tendency of large gravity difference in some mountainous and coastal areas. In particular, there are gravity differences of over 10 mGal in Kashimanada Sea, Osaka Bay, and Akaishi Mountain Range. It is assumed that the airborne gravity could detect the certain gravity which is not covered by EGM2008.
In this presentation, we will report the progress of the measurement, design of survey lines, data processing, and quality assessment.

References
1) Kuroishi, Y. (2009). Improved geoid model determination for Japan from GRACE and a regional gravity field model, Earth Planets Space 61, 807–813.
2) Matsuo, K., Kuroishi, Y. (2020). Refinement of a gravimetric geoid model for Japan using GOCE and an updated regional gravity field mode, Earth Planets Space 72, 33.
3) Matsuo, K. (2017). Development of a precise gravimetric geoid model for constructing new national height reference system, Heisei 29 nendo kokudo koutsu sho kokudo gijutsu kennkyukai ronbunshu 277 –282. (Japanese).

©2021. Japan Geoscience Union. All Right Reserved.

Keywords: Airborne gravity survey, Geoid, Gravity

©2021. Japan Geoscience Union. All Right Reserved.

Accuracy evaluation of airborne gravity data by the three-dimensional least-squares collocation method

*Koji Matsuo[1]

1. Geospatial Information Authority of Japan

The Geospatial Information Authority of Japan (GSI) has been conducting a nationwide airborne gravity survey since 2019, with the aim of developing a highly accurate gravimetric geoid model for Japan. The target accuracy of the geoid model is about 3 cm. To achieve this, it is necessary to obtain airborne gravity data with an accuracy of 1-2 mGal. Commonly, the accuracy evaluation of the airborne gravity data is done by “cross-over validation” and “comparison with Global Geopotential field Models (GGMs)”. The cross-over validation is a method to evaluate the quality of airborne gravity data by comparing the gravity values at the intersection of multiple survey lines with similar flight altitudes. This method allows us to evaluate the internal consistency (repeatability) of airborne gravity data, it cannot evaluate the absolute certainty of the observed gravity values. On the other hand, the comparison with GGMs can evaluate the absolute certainty of airborne gravity data in principle, but it may be insufficient to perform a precise evaluation of airborne gravity data because the spatial resolution and accuracy of GGMs are not high enough for this use. In this study, we evaluate the absolute accuracy of airborne gravity data by the three-dimensional least-squares collocation (3D-LSC) method. Here, we use both surface gravity data and a GGM (EGM2008). The evaluation areas are the Kanto and Chubu regions. The airborne gravity surveys there were conducted using a TAGS-7 gravimeter, in which the spacings of each main line and validation line are set to 10 km and 50 km, respectively. The flight altitudes were about 5000 m in the Kanto region and about 3000 m in the Chubu region, respectively. Since the quality of surface gravity data is low in coastal ocean zones, we perform the evaluation only over the land area. Consequently, while the RMS of the difference between the airborne gravity data and the EGM2008-derived gravity values are 2.47 mGal in the Kanto region and 3.16 mGal in the Chubu region, that between the airborne gravity data and the 3D-LSC-estimated gravity values are 1.49 mGal in the Kanto region and 1.35 mGal in the Chubu region. Considering that the accuracy of the surface gravity data used is approximately 1.1 mGal (Matsuo and Kuroishi, EPS 2020), it can be said that the accuracy of the airborne gravity data is approximately 1 mGal according to the principle of error propagation. In conclusion, it is confirmed that our airborne gravity data has an accuracy of 1 mGal level and will be useful for developing a 3 cm-accurate geoid model for Japan.

Keywords: Geodesy, Gravity, Geoid

©2021. Japan Geoscience Union. All Right Reserved.

Introduction of Absolute Quantum Gravimeter (AQG)

*Masato KUROYANAGI[1], Masami HANDA[1], Tokuro KODAMA[1], Shinobu KURIHARA[1], Kumikazu OCHI[1], Hiroaki YAMAMOTO[1], Shuichi OMORI[1], Kento IIO[1], Masahiro NAKASHIMA[1], Yasuhiro IITSUKA[1]

1. Geospatial Information Authority of Japan

The Geospatial Information Authority of Japan (GSI) introduced an Absolute Quantum Gravimeter (AQG) made by Muquans in France for the first time in Japan.
AQG is a gravimeter based on atomic interferometry, which measures the gravitational acceleration by dropping an object freely as well as a conventional absolute gravimeter FG5 does. The difference between FG5 and AQG is that AQG drops Rubidium atoms cooled down below 2 μK while FG5 drops a reflective test mass. In particular, FG5 has easily worn moving mechanical parts that make it unsuitable for long-term continuous measurement. On the other hand, AQG which does not have any moving mechanical parts unlike FG5 enables long-term continuous measurement with low maintenance. In addition, AQG is easy to set up and the adjustment for measurement is done almost automatically by the software, so that even unexperienced engineers can start measurement immediately.
In this presentation, the features of the newly installed AQG will be introduced and the results of comparison with the gravity values measured by FG5 will be reported.

Keywords: AQG, FG5, gravity

©2021. Japan Geoscience Union. All Right Reserved.

GRACE/GRACE-FO Observed Mass Change Patterns of Antarctica Extracted by ICA Method

*SHI TIANYAN[1], Yoichi Fukuda[1], Koichiro Doi[1], Jun'ichi Okuno[1]

1. Department of Polar Science, Gradualate University for Advanced studies School of Multidisciplinary Sciences

Antarctica is one of the most rapidly mass changing areas with poor field observation data. Considering the dominant uncertainty in Glacial Isostatic Adjustment (GIA) effects for the Antarctic Ice Sheet (AIS) mass balance, we analyze mass change patterns of Antarctica qualitatively using a statistics-based blind source separation method named Independent Component Analysis (ICA). We extract the 6 leading independent components using gravimetric data derived from the Gravity Recovery and Climate Experiment (GRACE) mission and GRACE Follow-On (GRACE-FO) mission. The results show that the whole continental mass changes can be effectively separated into several spatial patterns that could be dominated by different physical processes. Although the hidden independent physical processes cannot be completely separated, some significant signals such as glacial melting components, snow accumulation components, periodic climatic components, and GIA effects could be determined without introducing any external information. We also found that the time period of the employed datasets has a direct impact on ICA results. This suggested that some impacts of extreme events, such as rapid increases of snowfall in the late 2000s might cause dramatic changes spatially and temporally. In general, ICA provides a special view for a better understanding of AIS mass changes and specific regional researches.

Keywords: GRACE, GRACE-FO, ICA, Antarctica, GIA

©2021. Japan Geoscience Union. All Right Reserved.

Gravity observations at Jang Bogo Station, Antarctica, and the scale factor calibrations of different type relative gravimeters

*Yoichi Fukuda[1], Jun'ichi Okuno[1], Koichiro Doi[1], Choon-ki Lee[2]

1. National Institute of Polar Research, 2. Korea Polar Research Institute

We conducted gravity observations using FG5-210 absolute gravimeter (AG) and LCR D-58 relative gravimeter, at Korean Jang Bogo Station (JBS), in 2019-2020 Austral summer season.

The AG measurements were successfully done at two points named JBSAG1 and JBSAG2, and obtained about 19000 and 14400 drops of data, respectively, with the measurement precisions better than 0.4 μGal (1 μGal=10^{-8} ms^{-2}). In addition, the relative gravity measurements were conducted at 10 newly established gravity points in JBS to supplement the absolute gravity points.

In JBS, superconducting gravimeter (SG) observation with iGrav-021 has been continued since 2016. Since SG is a relative gravimeter, the calibration of the scale factor is essential for long-term gravity monitoring. Moreover, D-58 is also required the scale factor calibration as well. To calibrate the scale factors of these gravimeters, we first estimated the iGrav-021scale factor by the parallel observations with the FG5-210. And then the D-58 scale factor were indirectly estimated by the parallel observations with iGrav-021. This procedure worked well, and these calibrations should ensure the accurate gravity monitoring in the future.
Since we have already reported the details about the AG measurements at the 2020 JpGU meeting, we will mainly report the results of relative gravity measurements and the scale factor calibrations in this paper.

Keywords: Absolute gravimeter, Superconducting gravimeter, LaCoste D-type gravimeter , Scale factor calibration, Jang Bogo Station

©2021. Japan Geoscience Union. All Right Reserved.

Parallel observation with superconducting gravimeters TT70 #011 and iGrav #028 at Matsushiro, Japan (2016–2018)

*Yuichi Imanishi[1], Hiroshi Ikeda[2]

1. Earthquake Research Institute, The University of Tokyo, 2. KEK

We made a parallel observation by means of two superconducting gravimeters, TT70 (#011) and iGrav (#028) at Matsushiro, Japan from May 2016 through July 2018, with the main purpose of characterizing the instrumental performance of the iGrav as well as training of its operator. In August 2017, the position and orientation of the iGrav were changed in the room, and at the same time the feedback control of iGrav was changed from Run to Medium Feedback.
Regarding long-term trends of the recordings, both gravimeters showed gravity increase in the two years of experiment. Difference between the recordings from the two gravimeters was very close to being linear with respect to time except just after the installation and the position change of iGrav. The linear rate of the difference was 10.7 μGal/year (in the first year) and 11.3 μGal/year (in the second year). Assuming that the rate of instrumental drift of the TT70 was about 18 μGal/year (gravity increasing), the drift rate of iGrav was about 7 μGal/year.
The fact that the difference between the two gravimeters was almost perfectly linear with respect to time implies that they produced almost identical gravity recordings of long-periodic gravity changes. Our result shows that the iGrav, sometimes regarded as a simplified version of the superconducting gravimeter, has a precision to 0.1 μGal in months and 0.01 μGal in days.

Keywords: superconducting gravimeter, Matsushiro, instrumental drift

©2021. Japan Geoscience Union. All Right Reserved.

[J] Oral | S (Solid Earth Sciences)：S-GD Geodesy

Fri. Jun 4, 2021 10:45 AM - 12:15 PM JST | Fri. Jun 4, 2021 1:45 AM - 3:15 AM UTC | Ch.22 Zoom Room 22

[S-GD01] Geodesy and Global Geodetic Observing System

convener:Koji Matsuo(Geospatial Information Authority of Japan), Yusuke Yokota(Institute of Industrial Science, The University of Tokyo), Toshimichi Otsubo(Hitotsubashi University), Chairperson:Masahiro Nakashima(Geospatial Information Authority of Japan), Yuji ITOH(Earthquake Research Institute, The University of Tokyo)

Geodesy is a discipline that aims to define a Terrestrial Reference Frame for accurate positioning in the Earth and monitor/understand the Earth system through precise measurements of the Earth's shape, gravity, and rotation, as well as their temporal evolutions. In this session, we call for wide range of papers concerned with geodesy and its application to geoscience. Topics of interest will include but not limited to recent advances in measurement techniques, data analysis, numerical modeling or theoretical studies of geodesy. This session also welcomes topics of interdisciplinary studies on geoscience using ground-based geodetic techniques (spirit leveling, absolute/relative gravimeter, strain meter and so on) or space geodetic techniques (GNSS, VLBI, SLR, DORIS, GRACE, satellite altimetry and so on). In addition, we also provide a forum for discussing GGOS (Global Geodetic Observing System) related observation programs, advancements of geodetic techniques, collaboration among various organizations in the world.

10:45 AM - 11:00 AM JST | 1:45 AM - 2:00 AM UTC

[SGD01-07] Absolute Gravity Measurements at Teshikaga in 2019 and 2020

*Yuichi Imanishi[1], Ryuichi Nishiyama[1], Kazunari Nawa[2] (1.Earthquake Research Institute, The University of Tokyo, 2.AIST)

11:00 AM - 11:15 AM JST | 2:00 AM - 2:15 AM UTC

[SGD01-08] Reading value dependence of scale factors for LaCoste & Romberg relative gravimeters

*TAMAKI WAKABAYASHI[1], Takahito Kazama[1], Yoichi Fukuda[2], Yuki Abe[3], Shin Yoshikawa[4], Takahiro Ohkura[4], Yuichi Imanishi[5], Ryuichi Nishiyama[5], Keigo Yamamoto[6] (1.Graduate School of Science, Kyoto University, 2.National Institute of Polar Research, 3.Hot Springs Research Institute of Kanagawa Prefecture, 4.Aso Volcanological Laboratory, Kyoto University, 5.Earthquake Research Institute, The University of Tokyo, 6.Disaster Prevention Research Institute, Kyoto University)

11:15 AM - 11:30 AM JST | 2:15 AM - 2:30 AM UTC

[SGD01-09] Vertical Movements of GEONET sites in Niigata region (Part 2)

*Seiichi Shimada[1], Yuka Ito[1], Masaatsu Aichi[1], Takemu Seki[2], Tomochika Tokunaga[1] (1.Graduate School of Frontier Sciences, The University of Tokyo, 2.Department of Systems Innovation, Faculty of Engineering, The University of Tokyo)

11:30 AM - 11:45 AM JST | 2:30 AM - 2:45 AM UTC

[SGD01-10] An Apparent Reduction of Crustal Activity before the Great East Japan Earthquake

*Yasushi Harada[1], Yuka Murai[1] (1.School of Marine Science and Technology, Tokai University)

11:45 AM - 12:00 PM JST | 2:45 AM - 3:00 AM UTC

[SGD01-11] Early afterslip of the 2011 Tohoku-Oki sequence estimated by the GNSS carrier phase to fault slip approach

*Yusuke Tanaka[1], Yusaku Ohta[1], SHINICHI MIYAZAKI[2] (1.Tohoku University, 2.Kyoto University)

12:00 PM - 12:15 PM JST | 3:00 AM - 3:15 AM UTC

[SGD01-12] **Crustal subsidence as the elastic response to the SWJ heavy rain in 2020**

*Kosuke Heki[1], Syachrul Arief[2] (1.Department of Earth and Planetary Sciences, Faculty of Science, Hokkaido University, 2.Indonesia Geospatial Information Agency)

Absolute Gravity Measurements at Teshikaga in 2019 and 2020

*Yuichi Imanishi[1], Ryuichi Nishiyama[1], Kazunari Nawa[2]

1. Earthquake Research Institute, The University of Tokyo, 2. AIST

Absolute gravity measurements were conducted at the Teshikaga Observatory, Hokkaido University in 2019 and 2020, with the main purpose of providing temporal gravity changes for calibrating the instrumental drift of the Superconducting Gravimeter iGrav #17. Temporal drift of the Rubidium clock for the absolute gravimeter as well as an offset of the built-in barometer was also measured and taken into account in determining gravity acceleration. The final estimates of the mean gravity value at Teshikaga were 980 518 908.41 μGal (2019) and 980 518 906.56 μGal (2020).

Keywords: absolute gravimeter, superconducting gravimeter, instrumental drift, Teshikaga

©2021. Japan Geoscience Union. All Right Reserved.

Reading value dependence of scale factors for LaCoste & Romberg relative gravimeters

*TAMAKI WAKABAYASHI[1], Takahito Kazama[1], Yoichi Fukuda[2], Yuki Abe[3], Shin Yoshikawa[4], Takahiro Ohkura[4], Yuichi Imanishi[5], Ryuichi Nishiyama[5], Keigo Yamamoto[6]

1. Graduate School of Science, Kyoto University, 2. National Institute of Polar Research, 3. Hot Springs Research Institute of Kanagawa Prefecture, 4. Aso Volcanological Laboratory, Kyoto University, 5. Earthquake Research Institute, The University of Tokyo, 6. Disaster Prevention Research Institute, Kyoto University

Campaign relative gravity measurement is one of the most useful methods to understand spatiotemporal mass variations in volcanoes. The relative gravity value obtained with a spring-type portable relative gravimeter can be expressed as g = f(x), where x and f indicate the reading value (corresponding to the elongation of the spring) and the conversion function provided by the gravimeter's manufacturer. For the accurate estimation of the relative gravity values, the conversion function has been calibrated using a scale factor (SF; denoted by S) to be g = S * f(x). The SF value can be calculated as the ratio of the absolute gravity difference to the relative one, which are both measured between any two gravity points.

SF has been conventionally regarded as a constant value for each gravimeter, but several studies have been discussing the existence of the time variation in SF these days. For example, Onizawa (2019) pointed out that the SF value of a Scintrex CG5 gravimeter depends on its reading value linearly (i.e., S = S(x)). He also found the time variation in the SF associated with the instrumental drift of the reading value (i.e., S = S(x(t))). However, SF values have not been calibrated for LaCoste & Romberg gravimeters sufficiently, even though they are often used in and around volcanic areas. In order to observe actual spatiotemporal gravity variations due to volcanic activity, S(x) should be determined for each LaCoste gravimeter in advance and its effect should be corrected from the collected gravity data accurately.

Therefore, we calibrated SF values for spring-type relative gravimeters belonging to Kyoto University, to discuss the reading value dependence of the SF values. We first collected the reading values at four gravity points (Ishioka, Kyoto, Aso and Sakurajima) using three LaCoste gravimeters (LC-G534, LC-G605 and LC-G680) and one Scintrex gravimeter (CG5-150241330) in September 2020. We then converted the reading values to the gravity values using the conversion functions provided for the corresponding gravimeters, and subtracted the effects of short-period tide and instrumental height/drift from the obtained gravity values. We finally calculated the SF value as the ratio of the absolute gravity difference to the relative one for each gravimeter and each pair of the gravity points; we here utilized the absolute gravity values at four gravity points measured in 2018 and 2020.

The SF values of four gravimeters were calculated to be in the range of 0.9991 to 1.0003. We also found that the SF values of each gravimeter vary linearly to the reading value of the corresponding gravimeter. By fitting a regression line to the distribution of the SF value to the reading value, the rate of the SF variation to the reading value was estimated for each gravimeter as follows. LC-G534: -2.15 +/- 0.91, LC-G605: -7.09 +/- 0.93, LC-G680: -7.20 +/- 0.92, CG5-150241330: +10.82 +/- 0.90 [E-7 /mGal]. In the case of the LC-G534 and LC-G680 gravimeters, the SF values expected from the regression lines were found to be consistent with those determined in 2018 (Kazama et al., 2019). From these respects, we succeeded in quantifying the linear dependence of the SF on the reading value for the LaCoste gravimeters. In contrast, the past SF value for the CG5 gravimeter (Kazama et al., 2019) differed from the regression line obtained in this study, and the difference exceeded the 95% confidence interval of the

©2021. Japan Geoscience Union. All Right Reserved.

regression line. This result may imply the existence of the SF’ s higher-order dependence on the reading value in the case of the CG5 gravimeter, so we should determine the SF variation with the wider range of the reading value in our future study.

Keywords: gravity, scale factor, relative gravimeter, absolute gravimeter, volcano

©2021. Japan Geoscience Union. All Right Reserved.

Vertical Movements of GEONET sites in Niigata region (Part 2)

*Seiichi Shimada[1], Yuka Ito[1], Masaatsu Aichi[1], Takemu Seki[2], Tomochika Tokunaga[1]

1. Graduate School of Frontier Sciences, The University of Tokyo, 2. Department of Systems Innovation, Faculty of Engineering, The University of Tokyo

We have present on the vertical movements in Niigata region, at the 2018 Meeting of the Geodetic Society of Japan titled “Vertical movements of GEONET sites in Niigata region” and at the 2019 Meeting of the Geodetic Society of Japan titled “The characteristics of the vertical movements in Niigata region caused by the groundwater usage for snow melting and the quaternary paleoenvironment”, and reported on the vertical variations of uplift and subsidence due to the post-seismic crustal deformations of the 2011 Great East Japan Earthquake, on annual variations mainly due to the usage of groundwater for snow melting, on the secular ground subsidence due to the usage of groundwater, which varies depending on the observation sites, and on the possibility that the difference of the vertical variations among the observation sites caused by the pumping groundwater for snow melting depends on the geology of the aquifer and the layer above it. In this presentation we report that the subsequent studies have revealed that a subsidence may also be observed caused by the pumping of groundwater for the agriculture usage in summer in some of the observation sites and years. Moreover, we will also present the characteristics of the significant land subsidence that has observed by the groundwater pumping for the usage of the melting of heavy snowfall during the period of December 2020 and February 2021, and that has not been seen in the last 10 years, comparing with the subsidence in winter so far.

Keywords: Niigata region, Vertical movements, GNSS, GEONET

©2021. Japan Geoscience Union. All Right Reserved.

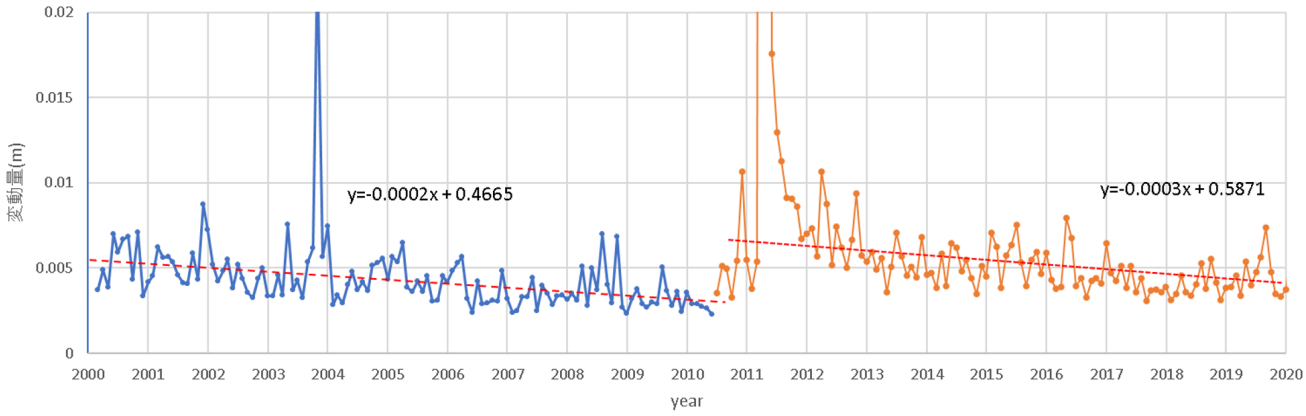
An Apparent Reduction of Crustal Activity before the Great East Japan Earthquake

*Yasushi Harada[1], Yuka Murai[1]

1. School of Marine Science and Technology, Tokai University

We used F3 solutions of GEONET(GSI) from 2000 to 2020, and calculated displacement vectors of about 1300 GNSS sites. First we created grid files for 3-components of the displacement vectors, and created animations for the deformation of Japan for the 3-components. We also calculated the length of the displacement vectors to investigate overall amount of crustal activity distribution of Japan. We noted the significant changes of regions where the length of the displacement relatively small and those changes of pattern are partly related to the previous block model of Japan. To quantify the long-term change of the crustal activity, we summed up every length of the displacement vectors, and made a time-series plot of the amount of crustal activity of Japan (See figure). The 10 years term decreasing trends are noted both before and after the Great East Japan Earthquake. It is natural that the decreasing trend appeared after the earthquake, but we found 10 years term decreasing trend for the crustal deformation of whole Japan even before the great earthquake. The rate of decrease is about 50% higher for after the earthquake than before. Further analyses are needed to be specify the cause of the reduction of the crustal activity before very large earthquake like the Great East Japan Earthquake.

Keywords: GEONET, The Great East Japan Earthquake, Reduction of Crustal Activity



©2021. Japan Geoscience Union. All Right Reserved.

Early afterslip of the 2011 Tohoku-Oki sequence estimated by the GNSS carrier phase to fault slip approach

*Yusuke Tanaka[1], Yusaku Ohta[1], SHINICHI MIYAZAKI[2]

1. Tohoku University, 2. Kyoto University

Time scale of few minutes to half day is remained shadow zone of current GNSS analysis. This is mainly due to difficulty of separation between deformation and other error factors such as atmospheric delay. And, actually very few previous studies analyzed deformation and/or fault slip with this time scale, for example early postseismic process. Using coordinate time series for observation is also obstruction for quantitative evaluation of parameter separation, since positioning analysis is originally independent from source of deformation, i. e. fault slip. Regarding these problems, we are developing broadband fault slip monitoring based on alternative approach, the GNSS carrier phase to fault slip approach. This method, which we call PTS (Phase To Slip), relates fault slip directly to relative change of GNSS carrier phase. As PTS method estimates all unknown parameters in parallel, we can evaluate their separation and discuss its improvement comprehensively.

In this study, we tried to continuously estimate coseismic and early postseismic slip of the 2011 Tohoku-Oki sequence. In the analysis, we used 1 Hz carrier phase data of 66 GEONET sites around east Japan. Then we estimated spatio-temporal evolution of slip from 05:00 to 06:56 (UTC) on 2011 March 11. As a result, PTS estimated aseismic slip increase in time after the mainshock. We obtained slip areas around downdip side of the assumed fault zone, which is below coastal region of Iwate, Miyagi, Fukushima and Ibaraki. We also obtained slip area around off Iwate and Aomori. All of them is adjacent to the mainshock rupture, and well intersect with early afterslip area estimated by normal positioning such as Munekane (2012). On the other hand, slip amount is about 0.4 to 0.5 m in maximum and equivalent seismic moment reached M_w7.47 in 33 minutes after the mainshock. These amounts seem to be slight larger than estimations by normal positioning. Additionally, our results show earlier slip increase around Fukushima and Ibaraki. This is also an unprecedented characteristic.

Our results indicate capability of the PTS method for broadband fault slip monitoring, which includes early postseismic process. In the presentation, first we will discuss robustness and reliability of our results. Then, we will focus on comparison of the estimations based on the PTS and normal positioning. Additionally, we evaluate O-C fitness and accuracy of parameter separation quantitatively in the dimension of carrier phase, which is used as observation in the PTS.

©2021. Japan Geoscience Union. All Right Reserved.

Crustal subsidence as the elastic response to the SWJ heavy rain in 2020

*Kosuke Heki[1], Syachrul Arief[2]

1. Department of Earth and Planetary Sciences, Faculty of Science, Hokkaido University, 2. Indonesia Geospatial Information Agency

Stationary weather fronts lying along the southwestern Japan (SWJ) often bring disastrous heavy rains in early summer. Here we study three past heavy rain episodes in 2017 July, 2018 July, 2019 August, and the latest episode in 2020 July, and study lithospheric deformation due to the rainwater loads. The water loads depress the land surface and let crust subside, and we study them using the F5 solutions of the GEONET station coordinates using methods used to study the 2019 typhoon Hagibis (Zhan et al., 2021 JGR submitted). After applying a network filter to remove common mode errors, we confirmed subsidence of 1-2 cm in multiple regions where severe flood occurred. Such subsidence was observed to recover with a time constant of 1-2 days reflecting rapid drain of rainwater to ocean due to large topographic slope and proximity to the sea. In Zhan et al. (2021), we estimated the distribution of surface water from crustal subsidence data using the Green’ s function for a point load. We then found that topographic concavity of GNSS stations in Japan (tend to be installed along valleys and within basins) causes overestimation of the water mass. In this study, we focus more on the correlation between subsidence of GNSS stations and precipitation at nearby rain gauges in a long time series. We will highlight following issues, (1) time constant of rainwater staying in situ, (2) difference in crustal response to rainwater load between GNSS stations with different topographic and geologic settings, (3) contribution of rain loads to day-to-day variabilities of vertical position of GNSS stations.

Keywords: vertical crustal movement, SWJ heavy rain, loading

©2021. Japan Geoscience Union. All Right Reserved.

[J] Oral | S (Solid Earth Sciences)：S-GD Geodesy

Fri. Jun 4, 2021 1:45 PM - 3:15 PM JST | Fri. Jun 4, 2021 4:45 AM - 6:15 AM UTC | Ch.22 Zoom Room 22

[S-GD01] Geodesy and Global Geodetic Observing System

convener:Koji Matsuo(Geospatial Information Authority of Japan), Yusuke Yokota(Institute of Industrial Science, The University of Tokyo), Toshimichi Otsubo(Hitotsubashi University), Chairperson:Yuichi Aoyama(National Institute of Polar Research), Shun-ichi Watanabe(Hydrographic and Oceanographic Department, Japan Coast Guard)

Geodesy is a discipline that aims to define a Terrestrial Reference Frame for accurate positioning in the Earth and monitor/understand the Earth system through precise measurements of the Earth's shape, gravity, and rotation, as well as their temporal evolutions. In this session, we call for wide range of papers concerned with geodesy and its application to geoscience. Topics of interest will include but not limited to recent advances in measurement techniques, data analysis, numerical modeling or theoretical studies of geodesy. This session also welcomes topics of interdisciplinary studies on geoscience using ground-based geodetic techniques (spirit leveling, absolute/relative gravimeter, strain meter and so on) or space geodetic techniques (GNSS, VLBI, SLR, DORIS, GRACE, satellite altimetry and so on). In addition, we also provide a forum for discussing GGOS (Global Geodetic Observing System) related observation programs, advancements of geodetic techniques, collaboration among various organizations in the world.

1:45 PM - 2:00 PM JST | 4:45 AM - 5:00 AM UTC

[SGD01-13] An Update of Daily Coordinate Product Estimated by the New Analysis Strategy of GEONET

*Naofumi Takamatsu[1], Hiroki Muramatsu[1], Chiaki Kato[1], Keitaro Ohno[1], Satoshi Abe[1], Tomoaki Furuya[1], Yohei Hiyama[1] (1.GSI of Japan)

2:00 PM - 2:15 PM JST | 5:00 AM - 5:15 AM UTC

[SGD01-14] Development of coordinate calculation strategy for GEONET station using multi GNSS PPP aiming future management scheme of the national coordinate

*Hiroyuki Nakagawa[1], Satoshi ABE[1], MURAMATSU Hiroki[1], Naofumi Takamatsu[1] (1.The Geospatial Information Authority of Japan)

2:15 PM - 2:30 PM JST | 5:15 AM - 5:30 AM UTC

[SGD01-15] On the performance of sidereal filter for 30-sec kinematic GPS to mitigate multipath errors

*Yuji ITOH[1], Yosuke Aoki[1] (1.Earthquake Research Institute, The University of Tokyo)

2:30 PM - 2:45 PM JST | 5:30 AM - 5:45 AM UTC

[SGD01-16] Development and assessment of the low-cost multi frequencies GNSS receiver and logger system

*Yusaku Ohta[1] (1.Research Center for Prediction of Earthquakes and Volcanic Eruptions, Graduate School of Science, Tohoku University)

2:45 PM - 3:00 PM JST | 5:45 AM - 6:00 AM UTC

[SGD01-17] Optimization of water vapor analysis using ship-borne GNSS measurement

*Yoshinori Shoji[1] (1.The Second Laboratory of Observation and Data Assimilation Research Department, Meteorological Research Institute)

3:00 PM - 3:15 PM JST | 6:00 AM - 6:15 AM UTC

[SGD01-18] Developmental status of Omni-SLR for small-size, low-cost SLR system

*Toshimichi Otsubo[1], Hiroshi Araki[2], Yusuke Yokota[3], Koichiro Doi[4], Hiroo Kunimori[5], Mihoko Kobayashi[1], Ryo Tsukagoshi[1], Masato Tomomatsu[1], Takehiro Matsumoto[6] (1.Hitotsubashi University,

2.National Astronomical Observatory of Japan, 3.University of Tokyo, 4.National Institute of Polar Research, 5.National Institute of Information and Communications Technology, 6.Japan Aerospace Exploration Agency)

An Update of Daily Coordinate Product Estimated by the New Analysis Strategy of GEONET

*Naofumi Takamatsu[1], Hiroki Muramatsu[1], Chiaki Kato[1], Keitaro Ohno[1], Satoshi Abe[1], Tomoaki Furuya[1], Yohei Hiyama[1]

1. GSI of Japan

Geospatial Information Authority of Japan has operated a dense GNSS observation network system, named GEONET, which consists of more than 1,300 CORS covering most region of Japan. The daily coordinate of each site from 1996 is calculated by the 4th analysis strategy developed in 2009 and is provided as the “F3 solution” via FTP site. Nowadays, F3 solution is vital infrastructure not only for crustal deformation monitoring but also for location based service and various scientific activities. We are now developing the new strategy that can deal with GPS Block III satellites and are aligned to ITRF2014. The resultant solution, named “F5 solution”, were released on March 24th, 2020 as a preliminary edition. In our presentation, we will give an overview of our new strategy and show the major improvement points; introduction of global network analysis for the reference coordinate determination and troposphere modelling update.

Keywords: GNSS, GEONET

©2021. Japan Geoscience Union. All Right Reserved.

Development of coordinate calculation strategy for GEONET station using multi GNSS PPP aiming future management scheme of the national coordinate

*Hiroyuki Nakagawa[1], Satoshi ABE[1], MURAMATSU Hiroki[1], Naofumi Takamatsu[1]

1. The Geospatial Information Authority of Japan

With the improvement of accuracy and real-time property of satellite positioning technologies, private companies are starting to provide many kind of GNSS positioning services. These services adopts their own system to refer geodetic frameworks, which might cause confusion and trouble in future since combination of them possibly brings inconsistency of positioning results. In addition, Japan is located in the region of active plate motion on the earth and suffers stable crustal motion as well as episodic large crustal motion caused by earthquakes and volcanic activities. Under these circumstances, in order for many positioning services to rapidly get positions consistent with national coordinate system, it is required to develop the system that properly manages the fundamental positional information as a national framework including its temporal variation, and that timely provides to positioning service providers and those users needing for the information.

The GSI focused on the precise point positioning (PPP) technologies using plural satellite positioning systems (multi-GNSS) for monitoring the spatial-temporal change of Japanese geodetic framework in detail. From 2020, the GSI started the research project to development of the positioning method to monitor the coordinates of GEONET stations nationwide using multi-GNSS PPP. The scheme is: First, using mixed RINEX observation data of IGS stations globally distributed, we estimate precise orbit of GPS, CLONASS and QZSS satellites, their clocks and so on by post-processing. Then, using them, the time-series of the coordinates of GEONET stations nationwide are derived by PPP-AR. The preliminary comparison of the coordinates for the six IGS stations included GEONET between PPP results and IGS daily solutions, they showed high consistency with in the repeatability.

In our presentation, we plan to report the present situation of the research and the result of detailed comparison of PPP solution and IGS daily solution as well as the comparison between PPP solution and GEONET operational solution for all the GEONET stations processed.

Keywords: multi GNSS, PPP, GEONET

©2021. Japan Geoscience Union. All Right Reserved.

On the performance of sidereal filter for 30-sec kinematic GPS to mitigate multipath errors

*Yuji ITOH[1], Yosuke Aoki[1]

1. Earthquake Research Institute, The University of Tokyo

1. Introduction

The noise level of kinematic Global Positioning System (GPS) coordinates is much higher than that of static daily coordinates. Therefore, it needs to be improved to capture details of small sub-daily tectonic deformation. One of the dominant error sources of kinematic GPS is multipath, which is the delay of carrier-phase due to reflection on the ground and other objects around the antenna. The sidereal filter is a well-known method to mitigate multipath effects by exploiting the repeatability of the geometrical relationship between GPS constellation and reflective bodies around the antenna. Many studies have investigated the characteristics of multipath and performance of the sidereal filter, but most of them focused only on seismic frequency and ignored longer periods. Their analyses are possibly contaminated with other error sources, including atmospheric disturbances, because they usually have employed Precise Point Positioning. With the increasing interest in applying kinematic GPS to subdaily postseismic deformation studies, we investigate the characteristics of multipath errors and the performance of sidereal filter using 30-sec kinematic coordinates with a length of nearly five days in an environment mostly free from atmospheric disturbances.

2. Method

We employ the differential positioning to focus on the multipath effect as error sources. A baseline we use consists of two GNSS sites, POTS and POTM. The approximate baseline length is 3 m, short enough to cancel most atmospheric and ionospheric disturbances. We obtain kinematic coordinates between 01 January 2019 and 31 December 2019. We split the year-long time series into 430770-seconds-long blocks, an integer multiple of the sub-sidereal satellite repeat period 86154 seconds estimated by a previous study. First, we assess the repeatability of kinematic coordinates, fundamental in applying the sidereal filter, by computing the correlation coefficient between arbitrary two blocks out of 73 blocks in total. We also calculate the correlation coefficient of two blocks after lowpass filtering with several different cut-off periods between 100 and 20,000 seconds to examine if longer-period fluctuations have better temporal repeatability than shorter-period fluctuations. Next, we apply a sidereal filter by subtracting a time series of one block from its neighbor. We also employ a lowpass-filtered sidereal filter to test if the performance of the sidereal filter is improved by discarding short-period fluctuations.

3. Results and Discussion

Correlation of lowpass-filtered time series with the longer cut-off period is generally better. However, in most pairs of blocks, variance reduction by sidereal filtering is largest when applying the lowpass filter to the sidereal filter with the cut-off period of 500 seconds, not with the longest one among tested. It is because longer-period fluctuations have smaller amplitudes. We find several peaks of power spectral density (PSD) at a period between 500 and 100,000 seconds. The standard (i.e., non-lowpass-filtered) sidereal filtering efficiently mitigates them, whereas it does not mitigate but enhance PSD fluctuations with periods shorter than 500 seconds. These data analyses suggest that this short-period fluctuation of kinematic coordinates is less likely due to multipath. It is also supported by a simple multipath model from the reflection at a horizontal surface beneath the antenna. Our results recommend lowpass filtering to the sidereal filter, which previous studies have empirically done. Because the cut-off period should depend on

©2021. Japan Geoscience Union. All Right Reserved.

each site's physical environment and other error sources contaminate the data, a careful design of the sidereal filter is required in its application to postseismic deformation studies.

Keywords: Kinematic GPS, Multipath, Sidereal filter

©2021. Japan Geoscience Union. All Right Reserved.

Development and assessment of the low-cost multi frequencies GNSS receiver and logger system

*Yusaku Ohta[1]

1. Research Center for Prediction of Earthquakes and Volcanic Eruptions, Graduate School of Science, Tohoku University

Observation of crustal deformation by GNSS is quite important to understand the strain accumulation near the active fault and the volcanic activities. On the other hand, the cost of the GNSS observation system for geodetic purpose is still expensive, which is an impediment to improving the density of the observation sites. In contrast, low-cost GNSS chips have been introduced for purposes other than the geodetic applications. Therefore, the purpose of this study is to develop a new GNSS observation system for long-term continuous observation and campaign observation using these consumer-use GNSS chips and to evaluate its performance.

We adopted the ublox ZED-F9P chips as the core GNSS engine. The F9P is a multi-band GNSS module. The module enables precise navigation and automation of moving industrial machinery. In contrast, there are few prior examples of the use of ZED-F9P for observation of the crustal deformation. Thus, we developed an observation system that combines ZED-F9P and Rasberry Pi. The developed system can record the GNSS carrier phase and pseudo range data. The ZED-F9P can supplement GPS L2C signals, but it does not support L2P signals. Therefore, there is a problem that the number of satellites in the L2 band is reduced when analyzing only GPS.

For comparison, signals from the antennas at the AOBL site, which is observed at Tohoku University, were split and recorded simultaneously by the Leica GRX1200+GNSS, a receiver for geodetic observations, and the developed system. As a tentative result, the carrier phase data for one day recorded by the developed system and conventional geodetic receiver system were analyzed by PPP of GIPSY-OASIS to obtain the daily coordinate values. We only sed GPS satellite system. We calculated the standard deviation of the time series between DOY 29 to 41 in 2021. The calculated SD was 5.3mm, 2.9mm, and 10.6mm for EW, NS, and UD component, respectively. In contrast, the result from conventional geodetic receiver system was 2.3mm, 1.6mm, and 7.4mm for EW, NS, and UD component, respectively. It should be caused by the lack of the L2P signal. In the presentation, the observation system developed in more detail will be discussed.

Keywords: GNSS, Low-cost GNSS

©2021. Japan Geoscience Union. All Right Reserved.

Optimization of water vapor analysis using ship-borne GNSS measurement

*Yoshinori Shoji[1]

1. The Second Laboratory of Observation and Data Assimilation Research Department, Meteorological Research Institute

1.Vertical positioning error and PWV error
GNSS analysis is affected by various factors such as interference with reflected waves (multipath), clock error, antenna phase center variation (PCV). It is expected that the kinematic positioning which treats the three-dimensional position of each GNSS antenna as a time variation parameter will be more affected than the static positioning. It is said that the error of vertical coordinates and the error of precipitable water (PWV) are inversely proportional (Beutler et al. 1988, Shoji et al. 2000). In the statistical comparison for a GEONET station "02P212" for eight months from May to December 2019, when there was a vertical positioning error of about 7 cm, a PWV error of about 1 mm occurred (Figure not shown). In this study, we examined the relationship between PWV error and vertical positioning error, and considered the optimum method for analyzing PWV from ship-borne GNSS measurements.

2.Vertical positioning error in kinematic GNSS analysis
We performed 10Hz GNSS observation at a fixed GNSS station at the Meteorological Research Institute for 16 days from December 1 to 16, 2020, performed kinematic positioning and static positioning while changing analysis frequency and analysis duration, and compared the vertical coordinates. As a result, it was found that the vertical coordinates by kinematic positioning tend to be higher than the static positioning solution within the range of about 1 to 2 cm. It was also found that the longer the analysis time and the higher the analysis frequency, the stronger the tendency.

3.Comparison of PWV obtained from ship-borne GNSS measurements with JMA’s meso-scale objective analysis and radiosonde observation
From October 20th to November 22nd, 2020, we carried out 10Hz GNSS observations on the two cargo ships "Wakanatsu" and "Ryunan". RTKLIB ver.2.4.2 was used for GNSS analysis. GNSS analysis was performed by changing the analysis frequency in the range of 0.1 to 30 seconds and increasing the analysis time from 0.5 to 8.5 hours in 1-hour units. As a result of comparison with PWV expressed in JMA’s operational meso-analysis (MA) (Figure 1), the tilt of the regression line tended to become smaller as the analysis time became longer. The lower the analysis frequency, the stronger the tendency. When the analysis time is less than 1 hour, the convergence of the solution is insufficient and the standard deviation (SD) becomes large. Considering BIAS and SD, it can be said that among the tried conditions, the 1.5-hour analysis at 2-second intervals has the highest degree of agreement with MA. We also compared GNSS PWV obtained by 2-sec interval analysis adopted on a GNSS observation data recorded on an observation vessel “Ryo-fu Maru” with radiosonde observations launched from the vessel. The slope of the regression line, BIAS, RMS, and SD (standard deviation), all showed a slightly higher degree of agreement in the 1.5-hour analysis than the 8-hour analysis, which shares the similar characteristics with the comparison against MA.

Acknowledgement
We thank "RYUKYU KAIUN KAISHA" for their support on “Wakanatsu” observation and "KAGOSHIMA NIYAKU KAIRIKU UNYU" and "MINAMINIHON KISEN" for their support on “Ryuunan” observation.

©2021. Japan Geoscience Union. All Right Reserved.

This study was partly supported by JSPS KAKENHI Grant Number 20H02420.
RTKLIB ver. 2.4.2 (Takasu 2013) was used for GNSS analysis.
GEONET observation data were acquired from the ftp server of the Geospatial Information Authority of Japan (GSI) in RINEX format.
MADOCA real-time prod- uct was provided by JAXA via the Internet (https://ssl.tksc.jaxa.jp/madoca/public/public_index_en.html).

References

Beutler, G., I. Bauersima, W. Gurtner, M. Rothacher, T. Schildknecht, and A. Geiger, Atmospheric refraction and other important biases in GPS carrier phase observation, in Atmospheric Effects on Geodetic Measurements, Monograph, 12, pp. 15–43, School of Surveying, Univ. of New South Wales, Kensington, Australia, 1988.
Shoji, Y., H. Nakamura, K. Aonashi, A. Ichiki, H. Seko, and Members of GPS/MET Japan summer Campaign 1997 in Tsukuba (2000): Semi-diurnal and diurnal variation of errors in GPS precipitable water vapor at Tsukuba, Japan caused by site displacement due to ocean tidal loading, Earth Planets Space, 52, 685-690.
Takasu T (2013) RTKLIB 2.4.2 manual. http://www.rtklib.com/prog/ manual_2.4.2.pdf.

Keywords: GNSS, Kinematic positioning, Water vapor

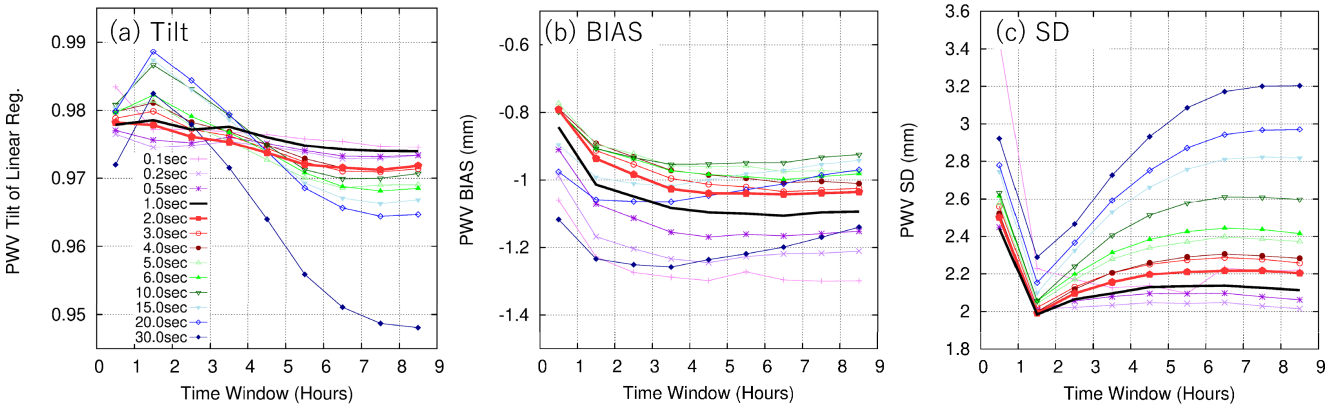


Figure 1. Statistical result of PWV comparison between ship-borne GNSS and MA. (a) Tilt of linear regression line, (b) BIAS, and (c) Standard deviation.

©2021. Japan Geoscience Union. All Right Reserved.

Developmental status of Omni-SLR for small-size, low-cost SLR system

*Toshimichi Otsubo[1], Hiroshi Araki[2], Yusuke Yokota[3], Koichiro Doi[4], Hiroo Kunimori[5], Mihoko Kobayashi[1], Ryo Tsukagoshi[1], Masato Tomomatsu[1], Takehiro Matsumoto[6]

1. Hitotsubashi University, 2. National Astronomical Observatory of Japan, 3. University of Tokyo, 4. National Institute of Polar Research, 5. National Institute of Information and Communications Technology, 6. Japan Aerospace Exploration Agency

Satellite laser ranging (SLR) is a geodetic technique to measure the ground-to-satellite distance very precisely. It is regarded one of the core geodetic techniques to measure the geometrical and gravitational shape of the Earth. Currently about 40 stations have been operational over the world. Despite the fact that the number of satellites equipped with retroreflectors is boosting, the number of the ground tracking stations remains almost the same for a couple of decades. It is because today’ s SLR systems are typically large and expensive, and therefore the compactness and low-cost are the key factors to strengthen the global SLR network.
We initiate a small project called Omni-SLR in 2020 to develop the first prototype system and demonstrate what can be achieved by a small low-cost SLR system.
We are currently designing the core part of Omni-SLR system. Key development elements include a nanosecond-pulse-width laser system, an optical design without Coude path, a lightweight telescope mount, an event timer, a coordinate monitoring system and operational software.

Keywords: Satellite Laser Ranging, Global Geodetic Observing System, Space Geodetic Techniques

©2021. Japan Geoscience Union. All Right Reserved.

[J] Oral | S (Solid Earth Sciences)：S-GD Geodesy

Fri. Jun 4, 2021 3:30 PM - 5:00 PM JST | Fri. Jun 4, 2021 6:30 AM - 8:00 AM UTC | Ch.22 Zoom Room 22

[S-GD01] Geodesy and Global Geodetic Observing System

convener:Koji Matsuo(Geospatial Information Authority of Japan), Yusuke Yokota(Institute of Industrial Science, The University of Tokyo), Toshimichi Otsubo(Hitotsubashi University), Chairperson:Yuto Nakamura(Hydrographic and Oceanographic Department, Japan Coast Guard), Hiroshi Takiguchi(Japan Aerospace Exploration Agency)

Geodesy is a discipline that aims to define a Terrestrial Reference Frame for accurate positioning in the Earth and monitor/understand the Earth system through precise measurements of the Earth's shape, gravity, and rotation, as well as their temporal evolutions. In this session, we call for wide range of papers concerned with geodesy and its application to geoscience. Topics of interest will include but not limited to recent advances in measurement techniques, data analysis, numerical modeling or theoretical studies of geodesy. This session also welcomes topics of interdisciplinary studies on geoscience using ground-based geodetic techniques (spirit leveling, absolute/relative gravimeter, strain meter and so on) or space geodetic techniques (GNSS, VLBI, SLR, DORIS, GRACE, satellite altimetry and so on). In addition, we also provide a forum for discussing GGOS (Global Geodetic Observing System) related observation programs, advancements of geodetic techniques, collaboration among various organizations in the world.

3:30 PM - 3:45 PM JST | 6:30 AM - 6:45 AM UTC

[SGD01-19] The Global Geodetic Observing System (GGOS) – infrastructure underpinning Earth science -

*Basara Miyahara[1], Laura Sánchez[2], Martin Sehnal[3] (1.GSI of Japan, 2.DGFI, Technical University of Munich, 3.BEV, Austrian Federal Office of Metrology and Surveying)

3:45 PM - 4:00 PM JST | 6:45 AM - 7:00 AM UTC

[SGD01-20] GGOS Japan: 2019-2021 Topics

*Toshimichi Otsubo[1], Basara Miyahara[2], Shinobu Kurihara[2], Yusuke Yokota[3], Yu Takagi[2], Shun-ichi Watanabe[4], Hiroshi Takiguchi[5], Yuichi Aoyama[6], Koji Matsuo[2] (1.Hitotsubashi University, 2.Geospatial Information Authority of Japan, 3.University of Tokyo, 4.Hydrographic and Oceanographic Department, Japan Coast Guard, 5.Japan Aerospace Exploration Agency, 6.National Institute of Polar Research)

4:00 PM - 4:15 PM JST | 7:00 AM - 7:15 AM UTC

[SGD01-21] Activity of GGOS working group on DOIs for geodetic data sets from 2019 to 2021

*Yusuke Yokota[1], Toshimichi Otsubo[2], Basara Miyahara[3] (1.Institute of Industrial Science, The University of Tokyo, 2.Hitotsubashi University, 3.Geospatial Information Authority of Japan)

4:15 PM - 4:30 PM JST | 7:15 AM - 7:30 AM UTC

[SGD01-22] SLR/GNSS observations and co-location survey at the Shimosato Hydrographic Observatory

*Yuto Nakamura[1], Shun-ichi Watanabe[1], Noritsune Seo[2], Yusuke Yokota[3], Akira Suzuki[4], Haruka Ueshiba[4] (1.Hydrographic and Oceanographic Department, Japan Coast Guard, 2.Shimosato Hydrographic Observatory, 5th Regional Coast Guard Headquarters, 3.Institute of Industrial Science, University of Tokyo, 4.Geospatial Information Authority of Japan)

4:30 PM - 4:45 PM JST | 7:30 AM - 7:45 AM UTC

[SGD01-23] Current status of Ishioka VLBI station

*Haruka Ueshiba[1], Yu Takagi[1], Tomokazu Nakakuki[1], Saho Matsumoto[1], Kyonosuke Hayashi[1], Toru Yutsudo[1], Katsuhiro Mori[1], Tomokazu Kobayashi[1] (1.Geospatial Information Authority of Japan)

4:45 PM - 5:00 PM JST | 7:45 AM - 8:00 AM UTC

[SGD01-24] Development of Wideband Receiver for Nobel Ground-based Microwave Radiometer -field experiments of the new 16-58 GHz wide-band receiver-

*Ryuichi Ichikawa[1], Hideki Ujihara[1], Shinsuke Satoh[1], Yusaku Ohta[2], Basara Miyahara[3], Hiroshi Munekane[3], Taketo Nagasaki[4], Osamu Tajima[5], Kentaro Araki[6], Takuya Tajiri[6], Hiroshi Takiguchi[7], Takeshi Matsushima[8], Nobuo Matsushima[9], Tatsuya Momotani[10], Kenji Utsunomiya[10] (1.National Institute of Information and Communications Technology, 2.Tohoku University, 3.Geospatial Information Authority of Japan, 4.RIKEN, 5.Kyoto University, 6.Meteorological Research Institute, 7.Japan Aerospace eXploration Agency, 8.Kyushu University, 9.National Institute of Advanced Industrial Science and Technology, 10.Japan Weather Association)

The Global Geodetic Observing System (GGOS) –infrastructure underpinning Earth science -

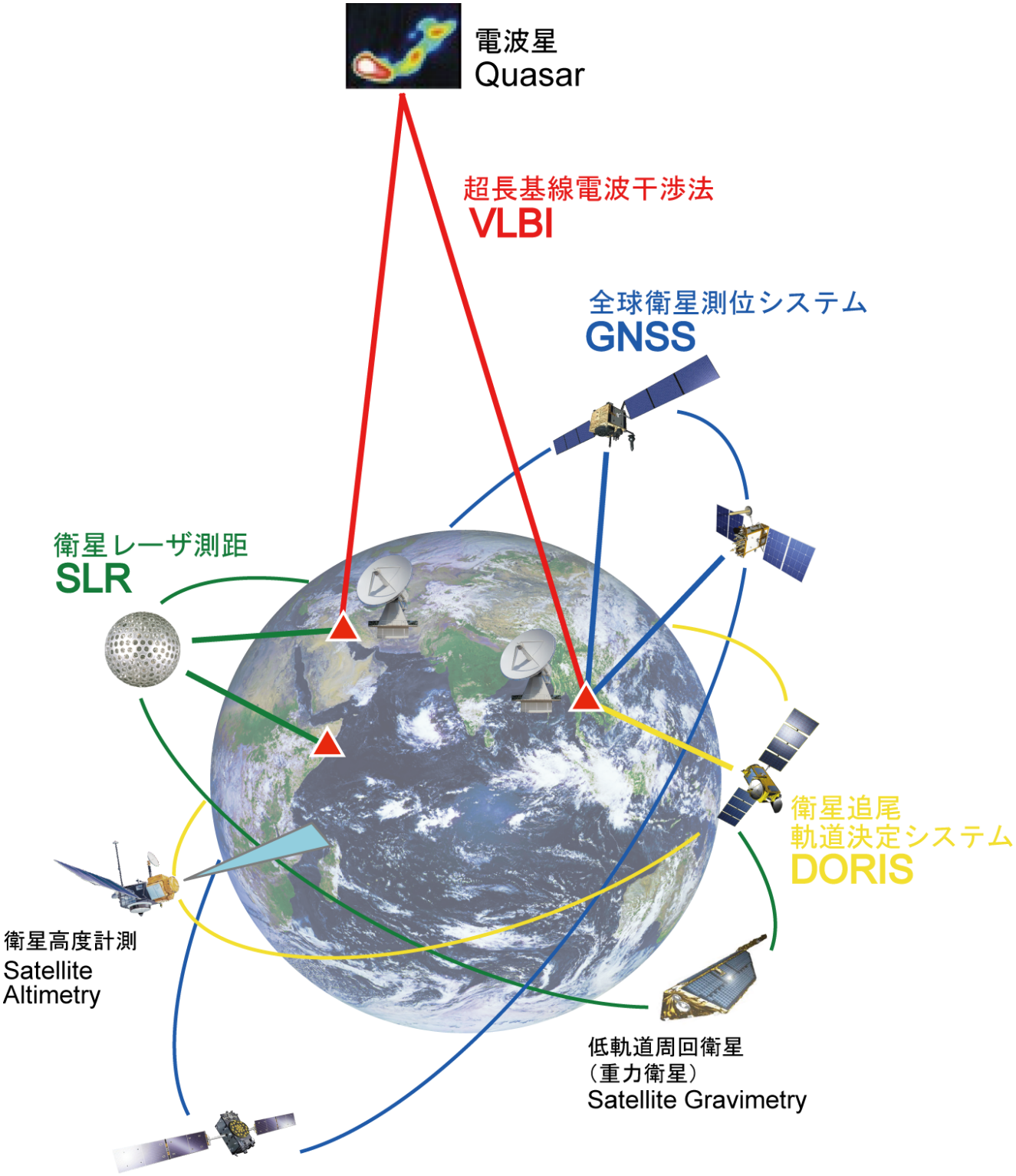
*Basara Miyahara[1], Laura Sánchez[2], Martin Sehnal[3]

1. GSI of Japan, 2. DGFI, Technical University of Munich, 3. BEV, Austrian Federal Office of Metrology and Surveying

The Global Geodetic Observing System (GGOS) is the contribution of Geodesy to the observation and monitoring of the Earth System. Geodesy is the science of determining and representing the shape of the Earth, its gravity field and its rotation as a function of time. A core element to reach this goal are stable and consistent geodetic reference frames, which provide the fundamental layer for the determination of time-dependent coordinates of points or objects, and for describing the motion of the Earth in space. Traditionally, geodetic reference frames have been used for surveying, mapping, and space-based positioning and navigation. With modern instrumentation and analytical techniques, Geodesy is now capable of detecting time variations ranging from large and secular scales to very small and transient deformations with increasing spatial and temporal resolution, high accuracy, and decreasing latency. GGOS has been working closely with components of International Association of Geodesy (IAG) to provide consistent and openly available observations of the spatial and temporal changes of the shape and gravity field of the Earth, as well as the temporal variations of the Earth’ s rotation. These efforts make available a global picture of the surface kinematics of our planet, including the ocean, ice cover, continental water, and land surfaces, as well as estimates of mass anomalies, mass transport, and mass exchange in the System Earth. Surface kinematics and mass transport together are the key to global mass balance determination, and are an important contribution to understanding the energy budget of our planet. In order to play its vital role, GGOS has following missions; a) to provide the observations needed to monitor, map, and understand changes in the Earth’ s shape, rotation, and mass distribution, b) to provide the global geodetic frame of reference that is the fundamental backbone for measuring and consistently interpreting key global change processes and for many other scientific and societal applications, c) to benefit science and society by providing the foundation upon which advances in Earth and planetary system science and applications are built. For the mission, GGOS works tighter with components of the IAG, more specifically, IAG Services, IAG Commissions and IAG Inter-Commission Committees. The IAG Services provide the infrastructure and products on which all contributions of GGOS are based, and the IAG Commissions and IAG Inter-Commission Committees provide expertise and support to address key scientific issues within GGOS. Together with the IAG components, GGOS provides the fundamental infrastructure underpinning Earth sciences and their applications.

Keywords: Global Geodetic Observing System, Global Geodetic Reference Frame, Earth Rotation, Earth's Gravity Field, International Association of Geodesy

©2021. Japan Geoscience Union. All Right Reserved.



©2021. Japan Geoscience Union. All Right Reserved.

GGOS Japan: 2019-2021 Topics

*Toshimichi Otsubo[1], Basara Miyahara[2], Shinobu Kurihara[2], Yusuke Yokota[3], Yu Takagi[2], Shun-ichi Watanabe[4], Hiroshi Takiguchi[5], Yuichi Aoyama[6], Koji Matsuo[2]

1. Hitotsubashi University, 2. Geospatial Information Authority of Japan, 3. University of Tokyo, 4. Hydrographic and Oceanographic Department, Japan Coast Guard, 5. Japan Aerospace Exploration Agency, 6. National Institute of Polar Research

Space geodetic techniques such as VLBI, SLR, GNSS and DORIS had competed eath other since the early age. With the 2015 UN resolution on geodetic reference frame, however, they are now regarded as a combined observing system because every technique has advantages and disadvantages.

As many as six different institutes have operated large-size geodetic systems with VLBI and/or SLR, which is unique to Japan. We therefore needed to have a coordinating board to strengthen the collaboration among the space-geodesy-related agencies.

This presentation will cover our achievement such as assembling our site list, hosting various domestic/international meetings, planning a special issue in a domestic journal, producing its leaflet and website. GGOS Japan also provides online and offline forums for timely issues, such as assigning Data DOI to geodetic dataset, submitting local tie for ITRF2020, etc.

Keywords: Global Geodetic Observing System, GGOS Japan, Space Geodetic Techniques

©2021. Japan Geoscience Union. All Right Reserved.

Activity of GGOS working group on DOIs for geodetic data sets from 2019 to 2021

*Yusuke Yokota[1], Toshimichi Otsubo[2], Basara Miyahara[3]

1. Institute of Industrial Science, The University of Tokyo, 2. Hitotsubashi University, 3. Geospatial Information Authority of Japan

The recognition has recently been established that scientific datasets should be shared on the basis of the FAIR principle [Willkinson et al., 2016]. Publishing data using digital object identifiers (DOIs) is the best practice for sharing data with FAIR. This is particular relevance to geodesy, as geodesy researchers are more involved in operational and data provision than researchers in other disciplines. Therefore, geodesy needs structured mechanisms that enable citation to data and data products.

To address these challenges and identify opportunities to improve coordination and advocacy within the geodesy community, the International Association of Geodesy of Geodesy (IAG) Global Geodesy Observation System (GGOS) has established working group on DOIs. This working group has been designated to establish best practices and advocate the consistent implementation of DOIs in all IAG services and the larger geodesy community.

< GGOS Working Group on DOIs for geodetic data sets:
https://ggos.org/about/org/co/dois-geodetic-data-sets/ >

In the discussions of the WG, geodetic data, data acquisition institutions, and existing data DOI assignment rules have been classified. Working group aims to build larger rules without damaging the existing framework. Also, the subject of particularly important discussion is the understanding and organization of DOI rules and author's framework according to the nature of the data (static data, dynamic data, processed data, raw data, etc.). It is expected that the report will be issued in the future without spending too much time.

Keywords: GGOS, DOI, geodesy data

©2021. Japan Geoscience Union. All Right Reserved.

SLR/GNSS observations and co-location survey at the Shimosato Hydrographic Observatory

*Yuto Nakamura[1], Shun-ichi Watanabe[1], Noritsune Seo[2], Yusuke Yokota[3], Akira Suzuki[4], Haruka Ueshiba[4]

1. Hydrographic and Oceanographic Department, Japan Coast Guard, 2. Shimosato Hydrographic Observatory, 5th Regional Coast Guard Headquarters, 3. Institute of Industrial Science, University of Tokyo, 4. Geospatial Information Authority of Japan

The Japan Coast Guard (JCG) operates Satellite Laser Ranging (SLR) observation at the Shimosato Hydrographic Observatory (SHO) since 1982. SLR observation results obtained at the SHO are submitted to the International Laser Ranging Service (ILRS), contributing to the development of the International Terrestrial Reference Frame (ITRF). SHO also conducts continuous GNSS observation at site “SMST”, which is one of the sites of the International GNSS Service (IGS). SHO, operating two types of space geodetic techniques, contributes to international geodetic frameworks such as the Global Geodetic Observing System (GGOS).

In order to construct a global earth-centered reference frame, it is necessary to link the reference frames obtained by using different space geodetic techniques. Thus, observation sites such as SHO that operate multiple space geodetic techniques, which function as co-location sites, are necessary for constructing a reference frame. At co-location sites, measurements using different techniques must be linked together by precisely determining the local tie between the reference points of the techniques.

In November 2020, the JCG and the Geospatial Information Authority of Japan (GSI), which has a prolonged experience of co-locating VLBI sites, have performed a co-location survey at the SHO to determine the local tie between the fixed point of the SLR telescope (SISL) and the GNSS station monument (SMST). In the survey, we mounted several targets on the SLR telescope, which we observed from four reference sites that were temporarily set around the observatory. To measure the fixed point of the SLR telescope, we rotated the telescope along the azimuth and the elevation axes at fixed intervals, observing the target positions for each rotation angle. The measured target positions form arcs around the rotation axes of the telescope, from which we can estimate the intersection of the axes (i.e., the fixed point of the SLR telescope). We also conducted levelling between the antenna reference point of the GNSS station and the center of the nasmyth mirror of the SLR telescope, which is the designed fixed point. For the calculation of the local tie, we used the software pyaxis (https://github.com/linz/python-linz-pyaxis), developed by Land Information New Zealand (LINZ).

In this presentation, we will present the results of the analyses of the SLR and GNSS data measured at the SHO. We will also show the methods of our co-location survey and the local tie calculation described above, and the estimated local tie vector.

Acknowledgements: Dr. Otsubo of the Hitotsubashi University has provided the SLR analysis software “C5++” and adjusted the data/parameters for SHO’s data analysis in this study.

©2021. Japan Geoscience Union. All Right Reserved.

Keywords: Satellite Laser Ranging, GNSS, Global Geodetic Observation System, Co-location survey

©2021. Japan Geoscience Union. All Right Reserved.

Current status of Ishioka VLBI station

*Haruka Ueshiba[1], Yu Takagi[1], Tomokazu Nakakuki[1], Saho Matsumoto[1], Kyonosuke Hayashi[1], Toru Yutsudo[1], Katsuhiro Mori[1], Tomokazu Kobayashi[1]

1. Geospatial Information Authority of Japan

The International VLBI Service for Geodesy and Astrometry (IVS) promotes VLBI Global Observing System (VGOS; Petrachenko et al., 2009), which is part of Global Geodetic Observing System (GGOS). The Ishioka VLBI observation station (Ishioka station) meets the VGOS requirements and participates in IVS international observations. The goals of VGOS are to achieve: 1-mm position accuracy on global scales, continuous measurements for time series of station positions as well as Earth Orientation Parameters, and turnaround time to initial geodetic results of less than 24 hours. To achieve these goals, the VGOS stations should be equipped with antennas with high slewing rate, receivers for broadband observations (2-14 GHz) and high speed recording systems up to 32 Gbps. Currently, because the number of VGOS stations is not sufficient, IVS conducts both of VGOS observations and legacy S/X observations. The Ishioka station participates in VGOS observations for several month every year and participates in legacy S/X observations for the rest of the period with switching its observation system.
The Ishioka Station uses two different types of receiver depending on a type of an observation: tri-band feed for S/X observations and QRFH for VGOS observations, and it is necessary to replace receivers when switching types of observations, which takes about one week. It is difficult to switch the observation type frequently. So the Geospatial Information Authority of Japan (GSI) improve the QRFH to be able to observe the S-band (2-3 GHz) to participate in S/X observations with it in 2020. By introducing superconducting filter, it became possible to receive signals in the S-band while suppressing strong RFI and fringes were detected in S/X test observations with domestic and international stations. Since July 2020, the Ishioka station has participated in IVS VGOS sessions with the improved QRFH and fringes were detected in them. For participation in IVS S/X sessions, it is necessary to convert the linearly polarized signal received with QRFH to circularly polarized signal to process the observation data at IVS correlators. To solve this obstacle, we will work on it.
Ishioka Geodetic Observation station is one of the GGOS sites which have a VLBI observation station (Ishioka Station) and GNSS stations. The GNSS station “ISHI” is one of IGS stations and its data is sent to them. As a GGOS site, GSI conducts co-location survey to determine the local tie vector between VLBI and GNSS on a regular basis. Since 2015, four co-location survey have been conducted at Ishioka. To contribute to construction of ITRF2020, GSI is preparing to submit the result of co-location survey in 2018 and 2020 to IERS (as of January 2020). This is the first time for Ishioka to submit the result of the co-location surveys.
This talk will summarize activitiese of the Ishioka Station as a VGOS station and a GGOS site.

Keywords: VLBI, Co-location

©2021. Japan Geoscience Union. All Right Reserved.

Development of Wideband Receiver for Nobel Ground-based Microwave Radiometer -field experiments of the new 16-58 GHz wide-band receiver-

*Ryuichi Ichikawa[1], Hideki Ujihara[1], Shinsuke Satoh[1], Yusaku Ohta[2], Basara Miyahara[3], Hiroshi Munekane[3], Taketo Nagasaki[4], Osamu Tajima[5], Kentaro Araki[6], Takuya Tajiri[6], Hiroshi Takiguchi[7], Takeshi Matsushima[8], Nobuo Matsushima[9], Tatsuya Momotani[10], Kenji Utsunomiya[10]

1. National Institute of Information and Communications Technology, 2. Tohoku University, 3. Geospatial Information Authority of Japan, 4. RIKEN, 5. Kyoto University, 6. Meteorological Research Institute, 7. Japan Aerospace eXploration Agency, 8. Kyushu University, 9. National Institute of Advanced Industrial Science and Technology, 10. Japan Weather Association

We are developing a next-generation microwave radiometer to be used in millimeter-wave spectroscopy for the high-resolution and high-precision monitoring of water vapor behavior. The new radiometer will be suitable for not only space geodetic techniques such as VLBI and GNSS, but also field measurements such as monitoring volcanic activities and cumulonimbus cloud generation. We assembled a room-temperature 20-30 GHz receiver without the cooling system in the middle of 2019 as a first step of our development. We implemented the new receiver into the 3.7 m dish at Okinawa Electromagnetic Technology Center, National Institute of Information and Communications Technology (NICT) and carried out first measurements using it for a validation test in October 2019. So far we have developed a new front-end module including the OMT and a new wideband feed by early December of 2020. The prototype of the complete receiver system has a wide-bandwidth feed of 16-58 GHz for measuring two frequency bands of 16-28 GHz (H_2O) and 50-58 GHz (O_2). We are now carrying out test measurement in order to evaluate the performance of the new receiver system. Although the experiment schedule for the validation of the new receiver is still uncertain owing to the COVID-19 pandemic, we are going to perform the experiments this fiscal year of 2020. After the validation measurements, we will install the receiver into the 90 cm dish or 1.8 m dish antenna and will start field measurements using the new receiver next fiscal year. Since the spatial resolution of the receiver depends on both dish size and distance between measurement site and object, we expect to detect various scales of water vapor behaviors. We will compare the results of the field experiments with those of tropospheric delay measurements using the low-cost multi-GNSS receivers and the GNSS Earth Observation Network (GEONET) System of the Geospatial Information Authority of Japan (GSI).

Keywords: Water Vapor, microwave radiometer, Wideband Receiver

©2021. Japan Geoscience Union. All Right Reserved.

[J] Oral | S (Solid Earth Sciences)：S-SS Seismology

Fri. Jun 4, 2021 9:00 AM - 10:30 AM JST | Fri. Jun 4, 2021 12:00 AM - 1:30 AM UTC | Ch.20 Zoom Room 20

[S-SS08] Fault Rheology and Earthquake Physics

convener:Shunya Kaneki(Disaster Prevention Research Institute, Kyoto University), Makiko Ohtani(Earthquake Research Institute, the University of Tokyo), Keishi Okazaki(Japan Agency for Marine-Earth Science and Technology), Keisuke Yoshida(Tohoku University), Chairperson:Keishi Okazaki(Japan Agency for Marine-Earth Science and Technology), Shunya Kaneki(Disaster Prevention Research Institute, Kyoto University)

The goal of this session is to integrate theoretical, experimental, observational, and numerical perspectives from various fields such as seismology, geodesy, geology, mineralogy, and so on, to define what is known about earthquake source processes and the physical and chemical elementary processes of faulting. This session welcomes studies that address such issues as pre-, co-, and post-seismic processes, the rheology of seismogenic faults and fault rocks, laboratory experiments on elementary processes, numerical models based on frictional laws, and estimates of the stress field in the seismogenic zones. We also welcome studies on fault-zone drilling projects and in situ stress measurements.

9:00 AM - 9:15 AM JST | 12:00 AM - 12:15 AM UTC

[SSS08-07] **New Split-Hopkinson pressure bar installed at Tohoku University to investigate pulverization during fault rupture.**

*Eranga Gayanath Jayawickrama[1], Takuma Sekiguchi[1], Jun Muto[1], Hiroyuki Nagahama[1], Hyung-Seop Shin[2] (1.Tohoku University Department of Earth Science, 2.Andong National University Department of Mechanical Design Engineering)

9:15 AM - 9:30 AM JST | 12:15 AM - 12:30 AM UTC

[SSS08-08] The role of fault zone heterogeneity in producing weak faults and promoting unstable slip

★Invited Papers

*John D Bedford[1,2], Daniel R Faulkner[2], Nadia Lapusta[3] (1.JAMSTEC, 2.Univ. of Liverpool, 3.Caltech)

9:30 AM - 9:45 AM JST | 12:30 AM - 12:45 AM UTC

[SSS08-09] Mechanical amorphization of synthetic fault gouges during rotary-shear friction experiments

*Shunya Kaneki[1], Kiyokazu Oohashi[2], Tetsuro Hirono[3], Hiroyuki Noda[1] (1.Disaster Prevention Research Institute, Kyoto University, 2.Graduate School of Sciences and Technology for Innovation, Yamaguchi University, 3.Graduate School of Science, Osaka University)

9:45 AM - 10:00 AM JST | 12:45 AM - 1:00 AM UTC

[SSS08-10] Friction experiments on volcanic glass-clay mixtures toward understanding the slip behavior of sediments near trench-arc system

*Hanaya Okuda[1,2], Takehiro Hirose[3], Asuka Yamaguchi[1,2] (1.Department of Ocean Floor Geoscience, Atmosphere and Ocean Research Institute, University of Tokyo, 2.Department of Earth and Planetary Science, Graduate School of Science, University of Tokyo, 3.Kochi Institute for Core Sample Research, Japan Agency for Marine-Earth Science and Technology)

10:00 AM - 10:15 AM JST | 1:00 AM - 1:15 AM UTC

[SSS08-11] Frictional properties of greenstone: Effects of the seamount subduction on earthquake generation

*Michiyo Sawai[1], Yuuto Yamauchi[1], Yasutaka Hayasaka[2], Kyuichi Kanagawa[1] (1.Chiba University, 2.Hiroshima University)

10:15 AM - 10:30 AM JST | 1:15 AM - 1:30 AM UTC

[SSS08-12] Rotary shear experiment for understanding frictional behavior of sandstone

*Hiromichi Yano[1], Takeshi Miyamoto[1], Tetsuro Hirono[1] (1.Department of earth and space science, Graduate School of Science, Osaka University)

New Split-Hopkinson pressure bar installed at Tohoku University to investigate pulverization during fault rupture.

*Eranga Gayanath Jayawickrama[1], Takuma Sekiguchi[1], Jun Muto[1], Hiroyuki Nagahama[1], Hyung-Seop Shin[2]

1. Tohoku University Department of Earth Science, 2. Andong National University Department of Mechanical Design Engineering

To investigate the effect of very large strain rates on rock deformation in analogs to the deformation very close to the rupture surface of large-scale faults, a new Split-Hopkinson pressure bar is installed at the Department of Earth Science, Tohoku University, Japan. The apparatus consists of a gas gun, four 20 mm diameter steel bars in a sequence of an impact bar, an incident bar, a transmitted bar, and a moment trap stationed at the end. The cylindrical core sample, placed between the two 1.5 m long incident and the transmitted bars, is compressed with a stress wave generated by the gas gun. The maximum launch velocity of the impact bar that has been tested so far in the apparatus is 23.36 m/s under a 1 MPa pressure, whereas the maximum pressure is 4 MPa. The strain, measured by the strain gauges attached at the center of each long bar, is acquired at a 1 MHz sampling rate recorded by a LabView program. The strain rate of the sample is calculated utilizing the reflected and transmitted stress waves recorded at the incident and transmitted bars, respectively. Preliminary tests conducted by granite cores with two diameters of 10 and 16 mm with the same lengths (i.e., length to diameter ratio is 1:1) are presented along with two standard metal samples (oxygen-free copper, and S45C) with the ratio of 1:2. The two metal samples generated strain rates of 2300 /s and 1480 /s at impact velocities of 23.36 and 19.06 m/s, respectively. The three granite cores with a diameter of 16 mm compressed with stress waves at impact velocities of 6.95, 10.2, and 16.12 m/s, showed several degrees of pulverization from broken yet bound by the jacket to complete powder with increasing strain rates from 370, 520, and 675 /s, respectively. The three cores with 10 mm diameter compressed under impact velocities of 6.9, 12.2 and, 15 m/s resulted in complete powder with generated strain rates of 700, 1350, and 1500 /s. This variation in the degree of pulverization has opened new insights to evaluate the energy consumed during pulverization of the rock specimens either via synchrotron facilities or by postmortem investigations. Hence, the utilization of the introduced apparatus has provided the opportunity to acquire detailed information of the energy consumed in a fault during earthquake rupture.

©2021. Japan Geoscience Union. All Right Reserved.

The role of fault zone heterogeneity in producing weak faults and promoting unstable slip

*John D Bedford[1,2], Daniel R Faulkner[2], Nadia Lapusta[3]

1. JAMSTEC, 2. Univ. of Liverpool, 3. Caltech

Large tectonic faults often appear frictionally weak when compared to laboratory measurements of frictional strength and display a range of fault slip behaviour, from aseismic creep to slow-slip to stick-slip. Fault zone heterogeneity if often qualitatively invoked to explain fault weakness and the spectrum of fault behaviour observed in nature; however the role of heterogeneity in controlling the mechanical behaviour of faults is poorly understood. Here we perform a series friction experiments at slow slip rates (0.3 to 3 microns/s) on faults comprised of heterogeneously distributed patches of weak, rate-strengthening gouge (clay) and strong, rate-weakening gouge (quartz). We systematically vary the size of the clay and quartz patches and find that these heterogeneous faults are significantly weaker and more unstable than homogenized mixtures of the two gouges. The heterogeneous faults also experience unstable stick-slip behaviour when the size of the quartz patch is sufficiently large. The observed weakening for the heterogeneous faults is greater than predicted if the strength evolution is assumed to be controlled by the relative sizes of the quartz and clay patches. This enhanced weakening is associated with the weaker clay patches promoting localized shear in the strong quartz patches resulting in slip at a lower overall shear stress than the compositionally equivalent homogeneous gouges. Our findings demonstrate how fault zone heterogeneity can cause the apparent weakness of many crustal faults and also reduce the frictional stability, which may lead to slow- or earthquake slip in nature.

Keywords: Fault zone heterogeneity, Friction, Fault weakening

©2021. Japan Geoscience Union. All Right Reserved.

Mechanical amorphization of synthetic fault gouges during rotary-shear friction experiments

*Shunya Kaneki[1], Kiyokazu Oohashi[2], Tetsuro Hirono[3], Hiroyuki Noda[1]

1. Disaster Prevention Research Institute, Kyoto University, 2. Graduate School of Sciences and Technology for Innovation, Yamaguchi University, 3. Graduate School of Science, Osaka University

Although mechanical amorphization of fault rocks and its possible effects on fault motion have been reported in both natural faults and laboratory experiments, the relationship between slip processes and generation rate of amorphous materials remains unclear. In this study, we performed rotary-shear friction experiments on quartz and kaolinite gouges under normal stresses of 1 or 3 MPa, at slip velocities of 0.001 or 1 m s^{-1}, with displacements of 1–100 m under room temperature and N_2 gas condition. Post-experiment XRD measurements revealed the occurrence of mechanical amorphization of both materials in some products after experiments. Microstructural observations demonstrated grain-size reduction, particle rounding, and generation of ultrafine particles (several tens to several hundreds of nanometers in diameter) within the localized slip zone with thickness of several tens to several hundreds of microns. The amount of amorphous materials generated is strongly dependent on total frictional work and mineralogy of fault gouge regardless of slip velocity, whereas the nominal dependence of amorphous content on seismic fracture energy and frictional power has no physical meaning. Estimated high amorphous content of up to 89 wt% indicates that mechanical amorphization may need to be considered for understanding dynamic mechanisms that affect strength of natural faults, such as thermo-chemical pressurization, fault lubrication by amorphous silica, and fault healing by pressure solution.

Keywords: Friction experiments, Fault gouge, Mechanical amorphization

©2021. Japan Geoscience Union. All Right Reserved.

Friction experiments on volcanic glass-clay mixtures toward understanding the slip behavior of sediments near trench-arc system

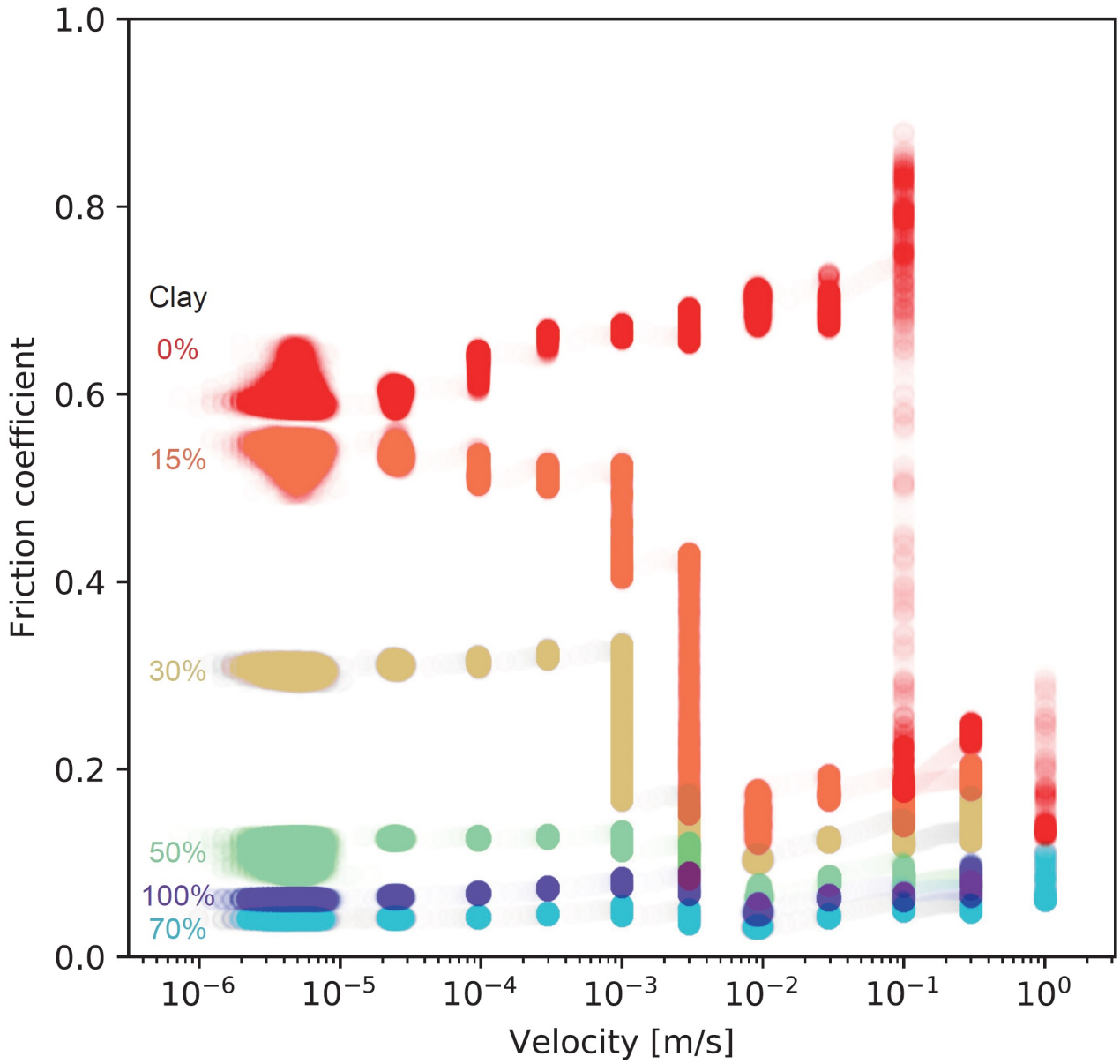
*Hanaya Okuda[1,2], Takehiro Hirose[3], Asuka Yamaguchi[1,2]

1. Department of Ocean Floor Geoscience, Atmosphere and Ocean Research Institute, University of Tokyo, 2. Department of Earth and Planetary Science, Graduate School of Science, University of Tokyo, 3. Kochi Institute for Core Sample Research, Japan Agency for Marine-Earth Science and Technology

Subduction of oceanic plate leads to produce magma beneath the upper plate, and forms island arc and volcanoes. Volcanic materials from such volcanoes deposit on the incoming oceanic plate and subduct at the trench as observed in the Nankai and the Barbados convergent margins. At the Nankai Trough, the subducting sediments comprise approximately 35% volcanic material (Scudder et al., 2018), and many volcanic ash layers are reported within the accretionary prisms (Screaton et al., 2009). The diagenetic reactions of volcanic glass in the volcanic materials to smectite stiffen surrounding sediments at the shallow subduction zone (e.g., White et al., 2011), and amorphous materials like volcanic glass are proposed to be frictionally weak (e.g., silica-gel lubrication; Goldsby & Tullis, 2002). In contrast, as clay minerals like smectite have low friction coefficients and easily induce a large slip (e.g., Faulkner et al., 2011), understanding frictional properties of volcanic glass-clay mixture is important to assess the slip behavior of sediments at a shallow subduction zone.
In this study, we performed a series of friction experiments on the volcanic glass-clay mixtures with different clay contents using a high-velocity rotary shear apparatus at Kochi Institute for Core Sample Research, Japan Agency for Marine-Earth Science and Technology (Tanikawa et al., 2012, 2015). All experiments were conducted at the velocity conditions ranged from 10 μm/sec to 1 m/sec under 5 MPa effective normal stress and 10 MPa pore fluid pressure conditions.
For the tests with 100% volcanic glass, friction coefficients of 0.6 to 0.75 were obtained when the velocities were from 10 μm/sec to 30 mm/sec, whereas the friction coefficients dynamically decreased at the velocity conditions higher than 100 mm/sec and dropped to 0.25 at the velocity of 1 m/sec. As the clay content increased, friction coefficients decreased down to 0.1 at the velocities slower than 300 μm/sec for the samples with >50% clay, and at the velocities faster than 1-3 mm/sec for those with >15% clay (Figure).
We found that the friction coefficient of volcanic glass is higher than that of smectite at all velocity conditions, and the velocity-strengthening behavior appears at 1-3 mm/sec that potentially suppresses the evolution to further fast slip rates. On the other hand, the clay content strongly affects the bulk friction coefficients such that the sediment with more than 15% clay easily induce a fast slip due to its low friction and velocity-weakening behavior at 1-3 mm/sec. These results indicate that the friction coefficient of the fault varies with depth depending on the amount of preserved volcanic glass at the shallowest part of the subduction zones such as the Nankai Trough: a fault may have a high frictional strength with velocity-strengthening behavior at a shallower depth due to the preservation of unaltered volcanic glass. Hence, a coseismic slip that is initiated at the seismogenic zone inhibit further slip speed as approaching toward the shallow part of the subductions zone. In contrast, the increase in clay content due to volcanic glass alteration weaken the volcanic ash layer. Such a layer may act as a weak plane to induce submarine landslides. Accordingly, the frictional property of volcanic glass-clay mixture has a strong influence on the fault slip behavior at shallow subduction zone as well as on the mass movement on the seafloor, and therefore plays an important role for tsunamigenesis.

©2021. Japan Geoscience Union. All Right Reserved.

Keywords: Volcanic glass, Subduction zone, Earthquake, Submarine landslide, Clay



©2021. Japan Geoscience Union. All Right Reserved.

Frictional properties of greenstone: Effects of the seamount subduction on earthquake generation

*Michiyo Sawai[1], Yuuto Yamauchi[1], Yasutaka Hayasaka[2], Kyuichi Kanagawa[1]

1. Chiba University, 2. Hiroshima University

Subducted seamounts are thought to generate large earthquakes by seamount geometry-related normal stress increase and to act as asperities (e.g., Cloos, 1992). There is also a possibility that they act as barriers for rupture propagation due to the large resistance on the subduction interface (e.g., Kodaira et al., 2000). On the other hand, since a seamount near the southern end of the Japan Trench has been mostly aseismic over the 80 years while many earthquakes have occurred in its adjacent areas, Mochizuki et al. (2008) suggested that the interplate coupling is weak there. In spite of many studies on subducting seamounts, frictional properties of seamount materials are still poorly understood. In this study, we conducted friction experiments to determine the friction parameter ($a-b$) (rate dependence of steady-state friction) and investigated how this parameter changes with temperature.

We conducted friction experiments on gouges of a greenstone from the Akiyoshi terrane in Yamaguchi, where a huge seamount with Carboniferous to Permian limestone accreted during the Permian time (e.g., Sano, 2006). Thin layer of greenstone underlying the limestone is distributed over 10 km along a fault. Experiments were conducted at a confining pressure of 150 MPa, a pore-water pressure of 100 MPa, temperatures of 25–200℃, and axial displacement rates changed stepwise among 0.1, 1 and 10 μm/s, by using a gas-medium, triaxial apparatus installed at Chiba University.

At temperatures ≦100℃ ($a-b$) value of the greenstone gouge is positive and does not change noticeably, while at temperatures ≧100℃ it decreases with increasing temperature, becoming ≈0 at 150℃ and negative at 200℃ where stick-slip was observed at 0.1 μm/s. Thus ($a-b$) value of the greenstone gouge changes from positive to negative with increasing temperature, i.e. with increasing depth. Our results suggest that a seamount may be a site of earthquake nucleation at depths where temperatures are higher than 150℃.

Keywords: seamount, subduction, friction, greenstone

©2021. Japan Geoscience Union. All Right Reserved.

Rotary shear experiment for understanding frictional behavior of sandstone

*Hiromichi Yano[1], Takeshi Miyamoto[1], Tetsuro Hirono[1]

1. Department of earth and space science, Graduate School of Science, Osaka University

Laboratory experiments are effective for understanding fault slip behavior during earthquakes, but few experiments have been conducted on sandstone. In order to understand the slip behavior of a sandy fault, we conducted rotary shear experiments of sandstone at wide range of slip rates (from 1.0 to 0.001 m/s). We also observed the cross sections and slip surface structures of the sheared samples by optical and electric microscopes. At the experiment of high slip rate (1.0 m/s), frictional coefficient oscillated unsteadily and the slip surface was intensively worn . At the experiment of low slip rate (under 0.1 m/s), frictional coefficient decreased exponentially and fault mirror was developed on the slip surface. Under microscopes, wildly worn surface and many large fragments (~10μm) were observed in the high-slip rate experiment sample. In contrast, mirror-like surface and spherical nanograins (diameter size 100 nm~) were observed in the low-slip rate sample. Roughness amplitude of the fault mirror was nearly same to that of fault mirror in natural fault. Therefore, we would suggest that frictional mechanism of sandy fault is strongly dependent on slip rate. At high slip rate, wearing of slip surface is dominant, and the frictional behavior is unsteady causing from the existence of fragments. At low slip rate, nanograin formation and wearing occurred and then the nanograins fill asperities on the slip surface making fault mirror. The frictional coefficient are relatively low and steady. These differences in mechanisms and the resultant frictional behaviors, depending on slip rate, could contribute to our understanding of rupture propagation and slip behavior along sandy fault such as splay fault in the Nankai Trough.

Keywords: Friction, Sandstone, Fault mirror

©2021. Japan Geoscience Union. All Right Reserved.

[J] Oral | S (Solid Earth Sciences)：S-SS Seismology

Fri. Jun 4, 2021 10:45 AM - 12:00 PM JST | Fri. Jun 4, 2021 1:45 AM - 3:00 AM UTC | Ch.20 Zoom Room 20

[S-SS08] Fault Rheology and Earthquake Physics

convener:Shunya Kaneki(Disaster Prevention Research Institute, Kyoto University), Makiko Ohtani(Earthquake Research Institute, the University of Tokyo), Keishi Okazaki(Japan Agency for Marine-Earth Science and Technology), Keisuke Yoshida(Tohoku University), Chairperson:Shunya Kaneki(Disaster Prevention Research Institute, Kyoto University), Keishi Okazaki(Japan Agency for Marine-Earth Science and Technology)

The goal of this session is to integrate theoretical, experimental, observational, and numerical perspectives from various fields such as seismology, geodesy, geology, mineralogy, and so on, to define what is known about earthquake source processes and the physical and chemical elementary processes of faulting. This session welcomes studies that address such issues as pre-, co-, and post-seismic processes, the rheology of seismogenic faults and fault rocks, laboratory experiments on elementary processes, numerical models based on frictional laws, and estimates of the stress field in the seismogenic zones. We also welcome studies on fault-zone drilling projects and in situ stress measurements.

10:45 AM - 11:00 AM JST | 1:45 AM - 2:00 AM UTC

[SSS08-13] Experimental evaluation of thermal maturation of carbonaceous materials under hydrous condition: As a proxy of frictional heating in a fault during an earthquake

*Keita Iwagaki[1], Tetsuro Hirono[1] (1.Department of Earth and Space Science, Graduate School of Science, Osaka University)

11:00 AM - 11:15 AM JST | 2:00 AM - 2:15 AM UTC

[SSS08-14] Overpressured subduction plate boundary caused by mantle-derived fluids: Evidence from noble gas isotope analysis on veins in subduction mélange

★Invited Papers

*Naoki Nishiyama[1], Hirochika Sumino[2], Kohtaro Ujiie[1] (1.University of Tsukuba, 2.The University of Tokyo)

11:15 AM - 11:30 AM JST | 2:15 AM - 2:30 AM UTC

[SSS08-15] Slip trace along an ancient plate boundary fault in the Shimanto accretionary, Hidakagawa Formation, Miyama Unit, Kii Peninsula, Japan: Organic geochemical and elemental approaches

*Ayana Shimamoto[1], Tetsuro Hirono[1], Tsuyoshi Ishikawa[2], Takeaki Ogawa[1] (1.Department of earth and space science, Graduate School of Science, Osaka University, 2.Kochi Institute for Core Sample Research, JAMSTEC)

11:30 AM - 11:45 AM JST | 2:30 AM - 2:45 AM UTC

[SSS08-16] Development of crystallographic preferred orientation during normal faulting in the Pleistocene Ryukyu Limestone

*Kaoru Inoue[1], Kohtaro Ujiie[2], Takayoshi Nagaya[3] (1.Graduate School of Life and Environmental Sciences, University of Tsukuba, 2.Faculty of Life and Environmental Sciences, University of Tsuku, 3.Graduate School of Science, The University of Tokyo)

11:45 AM - 12:00 PM JST | 2:45 AM - 3:00 AM UTC

[SSS08-17] Frictional experiments and numerical simulations for understanding the developing process of composite planar fabrics in faults

*Takeshi Miyamoto[1], Tetsuro Hirono[1], Akari Fuke[1], Satoshi Yukawa[1] (1.Graduate School of Science, Osaka University)

Experimental evaluation of thermal maturation of carbonaceous materials under hydrous condition: As a proxy of frictional heating in a fault during an earthquake

*Keita Iwagaki[1], Tetsuro Hirono[1]

1. Department of Earth and Space Science, Graduate School of Science, Osaka University

The thermal maturity of carbonaceous materials (CM) is often used for evaluation of the frictional heat recorded in faults. However, despite the fault is filled with water, the effect of water on the maturity of CM have not yet been investigated. Thus, in order to investigate the reactivity of thermal maturity of CM under hydrous condition, here we vacuum-sealed two types of CM (lignite, bituminous coal) in a glass tube with water and then performed heat treatments. We performed heat treatments with some different conditions of CM-water ratio (dry, 2:1, 1:4), target temperature (350, 700, 1050℃), and heating holding time (40 s, 1, 3, 5 h). The spectroscopic features by IR on the heated CMs with various conditions indicated no difference on the thermal breaking of aromatic C-H. Therefore, the thermal maturation of CM as a proxy for frictional heating in faults is not necessary to consider the presence of water.

Keywords: carbonaceous material, IR spectrometry

©2021. Japan Geoscience Union. All Right Reserved.

Overpressured subduction plate boundary caused by mantle-derived fluids: Evidence from noble gas isotope analysis on veins in subduction mélange

*Naoki Nishiyama[1], Hirochika Sumino[2], Kohtaro Ujiie[1]

1. University of Tsukuba, 2. The University of Tokyo

Overpressured fluids cause a weak subduction plate boundary and affect the degree of locking on the plate boundaries. The generation of fluid overpressure has been invoked for compaction disequilibrium and mineral dehydration through diagenetic and metamorphic processes of subducting sediments and altered oceanic crust (Hyndman & Peacock, 2003). The subduction mélange in the Shimanto accretionary complex, southwest Japan, preserves the quartz-calcite-filled shear veins and sigmoidal extension veins under fluid overpressure near the downdip limit of the thermally-controlled seismogenic zone. The shear veins record the repeated low-angle brittle thrusting under fluid overpressure, while the extension veins constitute the Riedel shear zones developed during subduction under vertical maximum principle stress. To examine the origin of overpressured fluids, we conducted fluid inclusion and noble gas analyses on the shear and extension veins.

The result of fluid inclusion analysis shows various fluid pressures ranging from lithostatic to hydrostatic pressures during the vein formation, which were associated with warm fluid infiltration. Helium isotope ratios ($^{3}He/^{4}He$) of shear veins and extension veins range 1.6-2.5 Ra and 1.6-2.3 Ra, respectively, indicating the presence of mantle helium (Ra is the $^{3}He/^{4}He$ ratio of air). Argon isotope ratios ($^{40}Ar/^{36}Ar$) and elemental ratios of heavy noble gases ($^{84}Kr/^{36}Ar$ and $^{130}Xe/^{36}Ar$) of the veins are similar to those of serpentinized mantle, suggesting that mantle helium originated from serpentinized mantle. Because the mantle-derived rocks such as peridotite and serpentinite are absent in the mélange, the results of noble gas analyses represent the infiltration of fluids from the serpentinized mantle into the mélange shear zone. The ratios of serpentinized mantle-derived fluids to the vein-forming fluids estimated by the $^{84}Kr/^{36}Ar$ and $^{130}Xe/^{36}Ar$ values are >64-94%, showing that the fluid supplied from the serpentinized mantle contributed to fluid overpressure in subduction plate boundary near the downdip limit of the seismogenic zone (Nishiyama et al., 2020). The infiltration of serpentinized mantle-derived fluids could contribute to the generation of tensile cracking during subduction-related deformation and brittle thrusting under fluid overpressure.

References

Hyndman, R.D., & Peacock, S.M. (2003), *Earth Planet. Sci. Lett.* 212, 417-432. doi: 10.1016/S0012-821X(03)00263-2.
Nishiyama, N., Sumino, H., & Ujiie, K. (2020), *Earth Planet. Sci. Lett.* 538, 116199. doi: 10.1016/j.epsl.2020.116199.

Keywords: Subduction fluids, Subduction plate boundary, Noble gas isotopes, mineral-filled vein

©2021. Japan Geoscience Union. All Right Reserved.

Slip trace along an ancient plate boundary fault in the Shimanto accretionary, Hidakagawa Formation, Miyama Unit, Kii Peninsula, Japan: Organic geochemical and elemental approaches

*Ayana Shimamoto[1], Tetsuro Hirono[1], Tsuyoshi Ishikawa[2], Takeaki Ogawa[1]

1. Department of earth and space science, Graduate School of Science, Osaka University, 2. Kochi Institute for Core Sample Research, JAMSTEC

In recent years, ancient plate boundary faults preserved in onland accretionary complexes have been investigated in order to understand the slip behavior earthquake along during plate subduction. In order to elucidate the characteristics and slip behavior of faults, we investigated the mélange unit in the Miyama Unit of the Hidakagawa Formation, which is exposed on the coast of the Mio area in Gobo, Wakayama, Japan. The unit is composed of sandstone, mudstone, chert, and altered basalt showing remarkable shear deformations, and some linear faults were developed. We collected samples from the main fault and its surrounding host rocks in the unit, and carried out microstructure observation, thermal background analysis using carbonaceous materials, and major- and trace-element concentration measurements. First, as a result of microstructure observation, we confirmed remarkable comminution in the primary slip zone compared to the surrounding cataclasites and host rocks. Next, as a result of Raman spectroscopic analysis of carbonaceous materials, the maximum temperature experienced host rock is estimated to 200 ℃ while primary slip zone is 400-900 ℃. Furthermore, as a result of major- and trace-element concentration analysis, the primary slip zone showed the decrease of quartz and the increase of plagioclase clearly compared to the host rock. Therefore, we carried out model calculation assuming albitization which is caused by metasomatism between host rock and high temperature fluid in the greenschist facies. The concentration change of elements in primary slip zone could be explained by albitization mediated by high temperature of 300 ℃ or higher. Accordingly, these results indicated that the mineral composition in the fault changed significantly due to the high temperature fluid generated during or immediately after an earthquake along plate boundary fault.

Keywords: Carbonaceous Materials, Spectroscopic analysis, trace elements

©2021. Japan Geoscience Union. All Right Reserved.

Development of crystallographic preferred orientation during normal faulting in the Pleistocene Ryukyu Limestone

*Kaoru Inoue[1], Kohtaro Ujiie[2], Takayoshi Nagaya[3]

1. Graduate School of Life and Environmental Sciences, University of Tsukuba, 2. Faculty of Life and Environmental Sciences, University of Tsuku, 3. Graduate School of Science, The University of Tokyo

Limestone is one of the major shallow crustal sedimentary rocks in seismically active area. The northwest-southeast striking Yonabaru Fault in Miyako Island, southern Ryukyu Arc has been thought to be an active fault because it displaced the Pleistocene Ryukyu Limestone derived from coral reef. We examined the fault rocks of the Yonabaru Fault at the southernmost part of Miyako Island, based on fieldwork and microstructural analysis using optical microscope and electron backscatter diffraction. The fault zone is ~50 m-thick and is composed of subvertical principal slip zones that sharply cut subhorizontal Ryukyu Limestone. The kinematic data obtained from the polished and lineated slip surfaces indicate the normal faulting in a northeast-southwest extension field. The principal slip zones are defined by the slip surfaces flanked by ~1-3 mm-thick zones composed of limestone fragments in the very fine-grained calcite matrix. The matrix calcite has monoclinic crystallographic preferred orientation(CPO) and shape preferred orientation(SPO). The EBSD map with grain boundaries defined by misorientation angles larger than 10˚ shows fine calcite grains and similar CPO patterns characterized by c-axes inclined against the shear direction, regardless of the degree of the misorientation angle within the grain. SPO is also marked by the alignment of inclined long axes at 60-70˚ to the shear direction. These CPO and SPO resemble those formed by dynamic recrystallization during the friction experiments on powdered calcite at seismic slip rates and the torsion experiments on Carrara marble at temperatures of 500-600 ℃. However, similar CPO was also obtained from dislocation glide in nano-crystalline gouge sheared at subseismic slip rates, which was enhanced at temperatures higher than 80 ℃. Our study demonstrates that intracrystalline deformation of calcite can occur during normal faulting at very shallow depths. Considering that crystal plasticity in calcite is strongly thermally activated, intracrystalline deformation of calcite observed in the principal slip zones may represent the past heat during normal faulting at very shallow depths and thus potentially an indicator of past seismic slip in the Ryukyu Limestone.

Keywords: Ryukyu Limestone, crystallographic preferred orientation, normal faulting

©2021. Japan Geoscience Union. All Right Reserved.

Frictional experiments and numerical simulations for understanding the developing process of composite planar fabrics in faults

*Takeshi Miyamoto[1], Tetsuro Hirono[1], Akari Fuke[1], Satoshi Yukawa[1]

1. Graduate School of Science, Osaka University

Many experimental works have previously performed to understand frictional properties of various kinds of rocks and minerals by using friction apparatus at various orders of sliding velocities ranging from nm/s to m/s. Some of them were conducted together with microscopic observation. However, friction experiments at wide range of velocities on a single type of rock or mineral have been rarely reported. Here we conducted friction experiments using powdered pyroclastic samples at velocities ranging from 0.0002 to 1 m/s, 1.5–3.0 MPa normal stress, and 10 m slip distance under dry and wet conditions. After experiments, we observed the thin sections of sheared samples. We also performed numerical simulation by using discrete element method (DEM) that focused on the changes of distances to adjacent particles (referred as CAP) and forces acting on particles during frictional slip. At higher velocities, the sample showed relatively drastic decrease of friction coefficient and boundary-parallel Y shears. In contrast, R_1 shears, oblique to shear direction, were observed in the samples at lower velocities. Numerical simulations at higher velocities of 0.1 and 1 m/s resulted in slip weakening and development of larger CAP lines parallel to boundary. At lower velocities, larger forces were concentrated locally. These results could imply that the development of composite planar fabrics during frictional slip has a dependency on slip velocity. Although pyroclastic samples we used contain much of volcanic glass, we could not identify the most efficient factor on the development of shear fabrics. Then, we tested frictional experiments using three kinds of quartz powders (supplied from Sigma-Aldrich, Wako, and Thermo Fisher Scientific) at 1 and 0.01 m/s slip rate and 2.0 MPa normal stress under dry condition. We also observed thin sections of sheared samples. At the case of experiment of 1 m/s velocity, friction coefficient was weakened drastically, whereas that of the experiment of 0.01 m/s velocity, it was almost at constant together with development of boundary parallel shear. We will show the preliminary result of friction experiments at wide ranging velocity using quartz supplied from Sigma-Aldrich together with the microscopic observation.

Keywords: friction experiment, numerical simulation, composite planar fabric

©2021. Japan Geoscience Union. All Right Reserved.

[J] Oral | S (Solid Earth Sciences)：S-SS Seismology

Fri. Jun 4, 2021 1:45 PM - 3:00 PM JST | Fri. Jun 4, 2021 4:45 AM - 6:00 AM UTC | Ch.20 Zoom Room 20

[S-SS08] Fault Rheology and Earthquake Physics

convener:Shunya Kaneki(Disaster Prevention Research Institute, Kyoto University), Makiko Ohtani(Earthquake Research Institute, the University of Tokyo), Keishi Okazaki(Japan Agency for Marine-Earth Science and Technology), Keisuke Yoshida(Tohoku University), Chairperson:Keisuke Yoshida(Tohoku University), Makiko Ohtani(Earthquake Research Institute, the University of Tokyo)

The goal of this session is to integrate theoretical, experimental, observational, and numerical perspectives from various fields such as seismology, geodesy, geology, mineralogy, and so on, to define what is known about earthquake source processes and the physical and chemical elementary processes of faulting. This session welcomes studies that address such issues as pre-, co-, and post-seismic processes, the rheology of seismogenic faults and fault rocks, laboratory experiments on elementary processes, numerical models based on frictional laws, and estimates of the stress field in the seismogenic zones. We also welcome studies on fault-zone drilling projects and in situ stress measurements.

1:45 PM - 2:00 PM JST | 4:45 AM - 5:00 AM UTC

[SSS08-18] Analysis of the source process of the 2016 Off Fukushima, Japan, crustal earthquake using land and seafloor observation data

★Invited Papers

*Hisahiko Kubo[1], Tatsuya Kubota[1], Wataru Suzuki[1], Takeshi Nakamura[2] (1.National Research Institute for Earth Science and Disaster Resilience, 2.Central Research Institute of Electric Power Industry)

2:00 PM - 2:15 PM JST | 5:00 AM - 5:15 AM UTC

[SSS08-19] **Determination of source parameters of the 2011 Tohoku-Oki earthquake from three-component pre-P gravity signals recorded by dense arrays in Japan**

*Nobuki Kame[1], Masaya Kimura[1], Shingo Watada[1], Akito Araya[1], Takashi Kunugi[2], Rongjiang Wang[3] (1.Earthquake Research Institute, the University of Tokyo, 2.National Research Institute for Earth Science and Disaster Resilience, 3.Helmholtz Centre Potsdam, GFZ German Research Centre for Geosciences)

2:15 PM - 2:30 PM JST | 5:15 AM - 5:30 AM UTC

[SSS08-20] Relative fluid pressure distribution around the 2000 Western Tottori Earthquake (M7.3) inferred from focal mechanism data of the aftershock

*Satoshi Matsumoto[1], Yoshihisa Iio[2], Shin'ichi Sakai[3], Aitaro Kato[4] (1.Institute of Seismology and Volcanology, Faculty of Sciences, Kyushu University, 2.Disaster Prevention Research Institute, Kyoto University, 3.The University of Tokyo III/GSII, 4.Earthquake Research Institute, University of Tokyo)

2:30 PM - 2:45 PM JST | 5:30 AM - 5:45 AM UTC

[SSS08-21] Intraslab repeating earthquakes beneath Japan; Implications for fluid-related embrittlement

*Junichi Nakajima[1], Akira Hasegawa[2] (1.Department of Earth and Planetary Sciences, Tokyo Institute of Technology, 2.Graduate School of Science, Tohoku University)

2:45 PM - 3:00 PM JST | 5:45 AM - 6:00 AM UTC

[SSS08-22] Intraplate repeating earthquakes in the Fukushima-Ibaraki border region following the 2011 Tohoku-Oki earthquake

*Rina Ikeda[1], Keisuke Yoshida[1], Ryo Takahashi[2], Toru Matsuzawa[1], Akira Hasegawa[1] (1.Tohoku University, 2.Japan Meteorological Agency)

Analysis of the source process of the 2016 Off Fukushima, Japan, crustal earthquake using land and seafloor observation data

*Hisahiko Kubo[1], Tatsuya Kubota[1], Wataru Suzuki[1], Takeshi Nakamura[2]

1. National Research Institute for Earth Science and Disaster Resilience, 2. Central Research Institute of Electric Power Industry

The 2016 off Fukushima earthquake (Mjma 7.4) occurred off Fukushima, northeast Japan on November 22, 2016 (JST). The moment tensor solution of F-net and the spatial distribution of the mainshock and its aftershocks indicate that this event was a shallow crustal normal-fault-type earthquake. Seismic and geodetic data for this earthquake were recorded not only by land observation networks but also by a seafloor observation network. In this study, we investigate the source process of this earthquake using seismic and geodetic data of land and offshore observation networks.

First, we estimate a rectangular fault model using land and seafloor geodetic data. For land geodetic data, we use two horizontal components of static displacements at stations of GEONET of GSI, which were obtained by differencing the preseismic and postseismic positions. For seafloor geodetic data, we use the uplift and subsidence spatial distribution, which was estimated from pressure waveform data at stations of S-net of NIED in Kubota et al. (2021, JpGU). Using these data, we estimate a rectangular fault with a uniform slip by the MCMC method. Unknown parameters are the spatial location of the rectangular fault (latitude, longitude, and depth), the fault mechanism (strike, dip, and rake), the fault length and width, and the slip value. For the geodetic Green’s functions, we calculate the theoretical static displacements assuming a homogeneous elastic half-space.

This analysis suggests the SE-dipping normal-fault-type fault model with a fault length of ~18 km, a fault width of ~13 km, and a slip of ~4 m. The top and bottom depth values of the estimated rectangular fault are ~3 km and ~9 km, respectively.

Then, we conduct the joint source inversion of near-field seismic and geodetic data. The spatiotemporal rupture history was estimated using the fully Bayesian multiple-time-window source inversion (Kubo et al. 2016). For near-field seismic data, we use velocity waveforms at stations of K-NET, KiK-net, and F-net of NIED. Their Green’s functions were calculated using the discrete wave number method and the reflection/transmission matrix method, with a 1-D layered velocity structure model. The 1-D velocity structure models were obtained for each station from the three-dimensional velocity structure model. For geodetic data and Green’s functions, we use the same ones as the investigation of the rectangular fault model. The assumed fault model in the source inversion is constructed by extending the rectangular fault model to cover the distribution of aftershocks. The horizontal location of the rupture starting point is set to the epicenter determined by JMA. The depth of the rupture starting point is set to the depth of the fault model at the epicenter of JMA.

The preliminary result of the source inversion suggests that large slips are found south-west of the rupture starting point and this large slip region is consistent with the rectangular fault model. These large slips were caused by the main rupture at 10-16 s after the rupture initiation, which propagated toward the southwest direction. The synthetic static displacements well match the observations, although the data fit of strong-motion waveforms is not good.

©2021. Japan Geoscience Union. All Right Reserved.

Keywords: The 2016 off Fukushima earthquake, Earthquake source process, Strong motion waveforms, Geodetic data, Seafloor observation network

©2021. Japan Geoscience Union. All Right Reserved.

Determination of source parameters of the 2011 Tohoku-Oki earthquake from three-component pre-P gravity signals recorded by dense arrays in Japan

*Nobuki Kame[1], Masaya Kimura[1], Shingo Watada[1], Akito Araya[1], Takashi Kunugi[2], Rongjiang Wang[3]

1. Earthquake Research Institute, the University of Tokyo, 2. National Research Institute for Earth Science and Disaster Resilience, 3. Helmholtz Centre Potsdam, GFZ German Research Centre for Geosciences

Dynamic earthquake rupture causes a mass redistribution around the fault, and the emitted propagating seismic waves are accompanied by bulk density perturbations. Both processes cause transient gravity changes before the arrival of P-waves. Such a pre-P gravity signal has been detected in previous studies on several huge earthquakes. However, the detections were limited to the signal's vertical component because of the high noise level in horizontal records. This study analyzed the dense tiltmeter array data in Japan to search for the signal's horizontal components from the 2011 Mw 9.1 Tohoku-Oki earthquake. Based on the synthetic waveforms for a realistic Earth model, we stacked the horizontal records and identified a signal that exceeded the noise level. We further performed a waveform inversion analysis to estimate the source parameters. The combination of the horizontal tiltmeter data and vertical broadband seismometer array data yielded a constraint on the earthquake's dip angle and magnitude in the ranges of 11.5˚-15.3˚ and 8.75-8.92, respectively. Our results indicated that the analysis of the three components of the pre-P gravity signal avoids the inherent trade-off problem between the dip angle and seismic moment in determining the source mechanism of shallow earthquakes. Pre-P gravity signals opened a new observation window for earthquake sources.

Keywords: earthquake pre-P gravity signal, determination of dip angle and moment for shallow earthquakes, earthquake prompt elastogravity signal

©2021. Japan Geoscience Union. All Right Reserved.

Relative fluid pressure distribution around the 2000 Western Tottori Earthquake (M7.3) inferred from focal mechanism data of the aftershock

*Satoshi Matsumoto[1], Yoshihisa Iio[2], Shin'ichi Sakai[3], Aitaro Kato[4]

1. Institute of Seismology and Volcanology, Faculty of Sciences, Kyushu University, 2. Disaster Prevention Research Institute, Kyoto University, 3. The University of Tokyo III/GSII, 4. Earthquake Research Institute, University of Tokyo

Aftershock activity following a large earthquake continues long time as expected to follow the modified Omori’ s law even if no earthquake detected before occurrence of the mainshock. Aftershock sequence might be attributed to stress change by the large earthquake and strength weakening. Fluid pressure in the crust might create strength weakening and induces seismic activity as suggested by numerous studies, being one of the important parameters to consider not only aftershock sequence but also crustal evolution involving fault zone development. Here, we estimated relative fluid pressure distribution around hypocentral area of the 2000 Western Tottori Earthquake (M7.3). By using precise focal mechanism data obtained from seismic observation just after and 17 years the mainshock occurrence. Especially, “0.1 Manten” hyper dense seismic observation conducted in 2017 has successfully detected event with widely magnitude range. We estimated the relative fluid pressure from discrepancy of nodal plane geometry of the focal mechanism from optimal fault plane under regional stress condition. The result showed heterogeneous distribution of the relative fluid pressure field. High pressure part was found beside the large co-seismic slip area, which might indicate fluid injection to the fault (fault valve model) and sustain it for 17 years. On the other hand, the pressure decrease with distancing from fault plane, showing possibility that it behave under diffusion process. These results suggest a scenario of fault maturing process.

Keywords: The 2000 Western Tottori Earthquake, Pore fluid pressure, aftershock activity

©2021. Japan Geoscience Union. All Right Reserved.

Intraslab repeating earthquakes beneath Japan; Implications for fluid-related embrittlement

*Junichi Nakajima[1], Akira Hasegawa[2]

1. Department of Earth and Planetary Sciences, Tokyo Institute of Technology, 2. Graduate School of Science, Tohoku University

Repeating earthquakes, or repeaters, are identical in location and geometry but occur at different times. Repeaters are most commonly found on creeping plate boundary faults, where seismic patches are loaded by surrounding slow slip. This study investigates whether repeating earthquakes occur in subducting slabs and finds the repeating earthquakes in the aftershock sequence of the 2003 Miyagi earthquake (M7.1). The occurrence of intraslab repeating earthquakes suggests that slow slip takes place even in the fault in the slab. In the presentation, we will talk about the systematic analysis of intraslab repeating earthquake beneath the Japanese Islands.

©2021. Japan Geoscience Union. All Right Reserved.

Intraplate repeating earthquakes in the Fukushima-Ibaraki border region following the 2011 Tohoku-Oki earthquake

*Rina Ikeda[1], Keisuke Yoshida[1], Ryo Takahashi[2], Toru Matsuzawa[1], Akira Hasegawa[1]

1. Tohoku University, 2. Japan Meteorological Agency

Since the 2011 M9 Tohoku-Oki earthquake, intense seismicity has continued around the Fukushima-Ibaraki prefectural border. Particularly in the northern part of Ibaraki prefecture, about M6 earthquakes occurred on March 19, 2011, and December 28, 2016. It was pointed out that the two earthquakes may have repeatedly ruptured the same location on the same fault (Fukushima et al., 2018; Uchide, 2017, JpGU). It is extremely rare for intraplate faults to have repeated earthquakes in such a short interval. It is important to investigate these cases to understand the intraplate earthquake cycle and the stress accumulation and release process. If repeated earthquakes were present in this seismicity, they would provide information about the aseismic slip that may occur within the earthquake cycle (Nadeau & Johnson, 1998). Therefore, the present study detected repeated earthquakes included in the small and medium-sized earthquakes during seismicity around the Fukushima-Ibaraki prefectural border. Many previous studies have used waveform cross-correlation to detect repeated earthquakes, but this method may mistake a group of nearby earthquakes for repeaters. In this study, we investigate the existence of repeated earthquakes based on the precise relocating hypocenters.

Using the Double-Difference method (Waldhauser & Ellsworth, 2002), we relocated hypocenters. Target is 45,988 earthquakes with $M_{JMA}>1$ that occurred from 2003 to October 31, 2018. The obtained hypocenter distribution showed a complex fault structure. However, there is one dominant planar structure with west-dipping in northern Ibaraki prefecture, on which the M6 earthquake probably occurred.

We detected repeated earthquakes by comparing the distances between the hypocenters of all earthquake pairs with their fault sizes. Specifically, we regarded an earthquake pair as a repeating earthquake pair when (1) the distance is less than the average fault radius, and (2) the magnitude difference is 0.5. The fault size was calculated assuming a circular fault with a stress drop of 20 MPa (Ikeda et al., 2020, JpGU). As a result, 181 seismic pairs were found, most of which were located in northern Ibaraki prefecture. The seismic waveforms of these possible repeating earthquake pairs were very similar even at nearby stations. Besides, the S-P arrival times of the earthquake pairs were very similar among different stations; the standard deviation was within 0±0.01 seconds for 112 pairs. Therefore, it is likely that these seismic pairs are repeated earthquakes.

Based on the empirical relationship by Nadeau & Johnson (1998), we estimated the amount of aseismic slip around repeated earthquakes and obtained a value of about 7 to 15 cm. Fukushima et al. (2018) estimated an anomalously high amount of afterslip, about several tens of cm, caused by the M6 earthquake in 2011. The value is about the same as those estimated from repeated earthquakes. The repeated earthquakes detected in this study may have been caused by the afterslip of the M6 earthquake.

Keywords: repeated earthquake, intraplate fault

©2021. Japan Geoscience Union. All Right Reserved.

[J] Oral | S (Solid Earth Sciences)：S-SS Seismology

Fri. Jun 4, 2021 3:30 PM - 4:45 PM JST | Fri. Jun 4, 2021 6:30 AM - 7:45 AM UTC | Ch.20 Zoom Room 20

[S-SS08] Fault Rheology and Earthquake Physics

convener:Shunya Kaneki(Disaster Prevention Research Institute, Kyoto University), Makiko Ohtani(Earthquake Research Institute, the University of Tokyo), Keishi Okazaki(Japan Agency for Marine-Earth Science and Technology), Keisuke Yoshida(Tohoku University), Chairperson:Keisuke Yoshida(Tohoku University), Yusuke Mukuhira(Institute of Fluid Science, Tohoku University)

The goal of this session is to integrate theoretical, experimental, observational, and numerical perspectives from various fields such as seismology, geodesy, geology, mineralogy, and so on, to define what is known about earthquake source processes and the physical and chemical elementary processes of faulting. This session welcomes studies that address such issues as pre-, co-, and post-seismic processes, the rheology of seismogenic faults and fault rocks, laboratory experiments on elementary processes, numerical models based on frictional laws, and estimates of the stress field in the seismogenic zones. We also welcome studies on fault-zone drilling projects and in situ stress measurements.

3:30 PM - 3:45 PM JST | 6:30 AM - 6:45 AM UTC

[SSS08-23] Urgent observation of seafloor crustal movement and installation of seafloor seismographs in preparation for future earthquakes off the east coast of Aomori Prefecture

*Takane Hori[1], Takeshi Iinuma[1], Fumiaki Tomita[1], Motoyuki Kido[2], Chie Honsho[3], Ryosuke Azuma[3], Chi-Hsien Tang[3], Yusaku Ohta[3], Ryoko Nakata[3], Ryota Hino[3], Masanao Shinohara[4], Shuichi Kodaira[1] (1.Research Institute for Marine Geodynamics, Japan Agency for Marine-Earth Science and Technology, 2.International Research Institute of Disaster Science, 3.Graduate School of Science, Tohoku University, 4.Earthquake Research Institute, The University of Tokyo)

3:45 PM - 4:00 PM JST | 6:45 AM - 7:00 AM UTC

[SSS08-24] Hotspots of Hypocenters Illuminated by a Newly-Developed Cross-Correlation-Based Hypocenter and Centroid Relocation Method

*Ta-Wei Chang[1], Satoshi Ide[1] (1.The University of Tokyo)

4:00 PM - 4:15 PM JST | 7:00 AM - 7:15 AM UTC

[SSS08-25] Microseismic Cloud Growth Process Mainly Controlled by *In-Situ* Stress During Hydraulic Stimulation

*Yusuke Mukuhira[1], Meihua Yang[5,1], Kyosuke Okamoto[4], Takuya ISHIBASHI[4], Yusuke Kumano[2], Hirokazu Moriya[3], Hiroshi Asanuma[4], Kangnan Yan[5,1], Justin Rubinstein[6], Yinhui Zuo[5], Markus O Häring[7] (1.Institute of Fluid Science, Tohoku University, 2.JAPEX Co., Ltd., 3.School of engineering, Tohoku University, 4.Fukushima Renewable Energy Institute, National Institute of Advanced Industrial Science and Technology, 5.State Key Laboratory of Oil and Gas Geology and Exploitation, Chengdu University of Technology, 6.United States Geological Survey, 7.Häring GeoProject)

4:15 PM - 4:30 PM JST | 7:15 AM - 7:30 AM UTC

[SSS08-26] Moment tensor analysis for numerous AEs induced by hydraulic fracturing in laboratory

Rui Tanaka[1], *Makoto Naoi[1], Youqing Chen[1], Kazune Yamamoto[1], Keiichi Imakita[1], Naofumi Tsutsumi[1], Akihiro Shimoda[1], Daiki Hiramatsu[1], Hironori Kawakata[2], Tsuyoshi Ishida[1], Eiichi Fukuyama[1], Hiroyuki Tanaka[3], Yutaro Arima[3], Shigehiro Kitamura[3], Daisuke Hyodo[3] (1.Kyoto University, 2.Ritsumeikan University, 3.JOGMEC)

4:30 PM - 4:45 PM JST | 7:30 AM - 7:45 AM UTC

[SSS08-27] AE events observed during loading velocity step change in large-scale gouge friction experiments

*Shun Watanabe[1], Eiichi Fukuyama[1,2], Futoshi Yamashita[2], Akihiro Shimoda[1] (1.kyoto university, 2.National Research Institute for Earth Science and Disaster Prevention)

Urgent observation of seafloor crustal movement and installation of seafloor seismographs in preparation for future earthquakes off the east coast of Aomori Prefecture

*Takane Hori[1], Takeshi Iinuma[1], Fumiaki Tomita[1], Motoyuki Kido[2], Chie Honsho[3], Ryosuke Azuma[3], Chi-Hsien Tang[3], Yusaku Ohta[3], Ryoko Nakata[3], Ryota Hino[3], Masanao Shinohara[4], Shuichi Kodaira[1]

1. Research Institute for Marine Geodynamics, Japan Agency for Marine-Earth Science and Technology, 2. International Research Institute of Disaster Science, 3. Graduate School of Science, Tohoku University, 4. Earthquake Research Institute, The University of Tokyo

A series of M5-class earthquakes occurred from November 6 to 7, 2020 off the coast of Aomori Prefecture, which is also in the vicinity of the rupture initiation point and slip area of the 1968 Tokachi-oki earthquake (Mw 8.2) and that of the 1994 Sanriku far offshore earthquake (Mw 7.7), raising concerns about the possibility of foreshocks. In addition, considering the fact that the 2011 off the Pacific coast of Tohoku earthquake was observed, it is necessary to understand and evaluate the state of fault slip and interplate coupling near the source area in order to discuss whether this activity will lead to the next M8 class earthquake. Therefore, it is necessary to obtain the crustal movement including slow slip with the highest possible temporal and spatial resolution. For this reason, we deployed a wave glider for observing seafloor crustal movement to acquire data at existing observation points, and conducted emergency observations by sharing a voyage scheduled for another purpose from the end of November in order to establish a new seafloor crustal movement observation point as soon as possible. In addition, the positioning of the newly established submarine crustal deformation observation station and the installation of ocean bottom seismographs to fill the gaps in the S-net observation network were carried out in February using a chartered vessel.

©2021. Japan Geoscience Union. All Right Reserved.

Hotspots of Hypocenters Illuminated by a Newly-Developed Cross-Correlation-Based Hypocenter and Centroid Relocation Method

*Ta-Wei Chang[1], Satoshi Ide[1]

1. The University of Tokyo

The location of earthquake occurrences has been extensively discussed for its importance. With the advances in methods of earthquake relocation, we now possess methods to determine earthquake centroids with lower uncertainties, using cross-correlation-based methods with data in regional distances. Hypocenters of earthquakes, on the other hand, are traditionally determine using onset picking of event waveforms, which tend to results in poorer resolution as compared to centroid locations. Here, by including an extra step to search for suitable window to perform cross-correlation on the onsets of waveforms, we developed a new cross-correlation-based relative hypocenter relocation method based on the Network Correlation Coefficient (NCC) method. After obtaining relative locations among hypocenters and centroids, we then perform a joint inversion to directly compare their relative locations under a unified coordinate. We have applied this methods to 3 regions that include repeating earthquakes, showing not only the repetitive rupturing of centroids for repeating events, but also the newly-illuminated hotspots of hypocenters, from which earthquakes growing into selective final sizes initiate. Joint hypocenter and centroid locations enables quick estimations of rupture developments without the need of slip inversion analyses. Uncertainties of the locations are estimated using bootstrap, where the 95% confidence intervals yielding sub-100 m error in both centroid and hypocenter locations for horizontal components under best station coverage and event availability. The results of these case studies point to some but limited correspondence between hypocenter and centroid locations or final event sizes, as well as complexity in hypocenter distributions even within repeating earthquakes where rupturing regions mostly overlap.

Keywords: Earthquake relocation, Repeating earthquakes

©2021. Japan Geoscience Union. All Right Reserved.

Microseismic Cloud Growth Process Mainly Controlled by *In-Situ* Stress During Hydraulic Stimulation

*Yusuke Mukuhira[1], Meihua Yang[5,1], Kyosuke Okamoto[4], Takuya ISHIBASHI[4], Yusuke Kumano[2], Hirokazu Moriya[3], Hiroshi Asanuma[4], Kangnan Yan[5,1], Justin Rubinstein[6], Yinhui Zuo[5], Markus O Häring[7]

1. Institute of Fluid Science, Tohoku University, 2. JAPEX Co., Ltd., 3. School of engineering, Tohoku University, 4. Fukushima Renewable Energy Institute, National Institute of Advanced Industrial Science and Technology, 5. State Key Laboratory of Oil and Gas Geology and Exploitation, Chengdu University of Technology, 6. United States Geological Survey, 7. Häring GeoProject

Forecasting the shape of the area deformed by hydraulic stimulation is essential for the design of an energy extraction system. Here we use microseismicity as a proxy for the area of deformation, given the limitation that aseismic deformation is not easily observed. Microseismic clouds caused by hydraulic stimulation are typically observed to be elongated in the direction of maximum principal stress. However, there are exceptions to this empirical relationship, and spatio-temporal evolution of microseismicity is not fully understood. We investigate the microseismic cloud growth process at the Basel, Switzerland geothermal site, focusing on the correlation with *in-situ* stress. We apply principal component analysis to examine the temporal evolution of the distribution of microseismicity. The smallest axis of the microseismic cloud is stable and nearly identical to the minimum horizontal stress. The largest axis of the seismicity dips during the stimulation, but after injection it is near- vertical. This observation suggests the microseismic cloud growth behavior was different before and after the stimulation, likely being correlated with the dynamic and static permeability tensors. The microseismic cloud grew radially within the plane perpendicular to the minimum horizontal stress. The radial growth is consistent with nearly identical maximum horizontal and vertical stress. We hypothesize that the microseismic cloud did not grow in the direction of least principal stress because the permeability is lower in this direction, while the microseismic cloud did grow parallel to the orientations of maximum and intermediate stresses. Based on these observations, we conclude that microseismic cloud growth is mainly controlled by *in-situ* stress given a wide distribution of fault orientations, as can be found in Basel. This study suggests that *in-situ* stress measurements taken before stimulation can be used to help forecast geothermal reservoir shapes.

Keywords: induced seismicity, Permeability, pore pressure, In-situ stress, Shape of reservoir

©2021. Japan Geoscience Union. All Right Reserved.

Moment tensor analysis for numerous AEs induced by hydraulic fracturing in laboratory

Rui Tanaka[1], *Makoto Naoi[1], Youqing Chen[1], Kazune Yamamoto[1], Keiichi Imakita[1], Naofumi Tsutsumi[1], Akihiro Shimoda[1], Daiki Hiramatsu[1], Hironori Kawakata[2], Tsuyoshi Ishida[1], Eiichi Fukuyama[1], Hiroyuki Tanaka[3], Yutaro Arima[3], Shigehiro Kitamura[3], Daisuke Hyodo[3]

1. Kyoto University, 2. Ritsumeikan University, 3. JOGMEC

Acoustic emission (AE) sensors are used to detect microseismic events in laboratory or observations for a relatively small area. Although AE sensors have sensitivity higher than seismometers, their characteristics, which depend on the sensor-setting conditions, are complicated, making it difficult to use their waveforms. In this study, we estimated seismic moment tensors by overcoming this problem for AEs induced by hydraulic fracturing in a laboratory. We also introduced a convolutional neural network to read first motion polarities, allowing us to estimate moment tensors (MT) of numerous AEs.

In the analysis, we used data obtained by the hydraulic fracturing experiments in laboratory that were conducted to investigate the influence of the viscosity of fracturing fluid. We used 10 Kurokami-jima granite samples with dimensions of 65 x 65 x 130 mm. A thermosetting acrylic region (~0.8 mPa·s viscosity at room temperature and pressure) containing a fluorescent compound was used as a fracturing fluid, allowing us to observe fluid penetration regions after the experiments. We also used resins with the addition of a thickener to adjust the viscosities to ~10, ~50, ~300, ~1000 mPa·s, each of which fractured two specimens. AE signals that occurred during the experiments were recorded by 24 AE sensors attached onto the specimens. We detected AE events, picked arrival times, and located their hypocenters by using automatic algorithms.

We inversely estimated MTs of the AEs from the P-wave first motion polarities and their amplitudes. To overcome the difficulties of using AE sensors, we investigated the sensor characteristics by the following procedure and corrected the effect. 1) We measured directivities of AE sensors before the experiments. 2) We conducted pulse radiation tests after attaching the sensors onto the specimen for each experiment, and the sensitivities of individual sensors and attenuation of the specimen were estimated from the amplitude data.

In each experiment, 3755–12,872 AEs occurred. To estimate MT solutions of the numerous AEs, we introduced an automatic reading procedure of P-wave first motions using a convolutional neural network. We trained the network by 68,152 waveforms for which their first motion polarities were manually read, and successfully read a total of 1,366,118 polarities by using the trained network. Finally, we obtained 54,727 MT solutions for the 10 experiments.

From the spatiotemporal distributions of observed AEs, we found two preparatory phases of hydraulic fracture before the breakdown (a rapid drop of the borehole pressure induced by a main hydraulic fracture). The first phase started at 10-30% of the breakdown pressure, where AEs occurred three-dimensionally surrounding a borehole, and their active region expanded with time towards the outside of the specimen. The MT solutions of these AEs corresponded to crack-opening events in various orientations, and we interpreted that this phase was induced by fluid penetration into pre-existing microcracks. The second phase began at 90–99% of the breakdown pressure. During this phase, a planar AE distribution newly emerged from the borehole and expanded along the maximum compression axis,

©2021. Japan Geoscience Union. All Right Reserved.

and MTs of these AEs corresponded to the crack-opening events on the AE-delineating plane. Those features are consistent with the expectation from the classical theory of hydraulic fracturing, so this phase likely corresponded to the main fracture formation. In this phase, shear events, which were rarely observed in the first phase, also occurred. Significant dependences on fluid viscosity were observed in the fluid penetration regions observed on the sliced specimen, borehole pressure at the main fracture initiation, and the fracture propagation speed in the second phase.

This study was financially supported by the Japan Oil, Gas and Metals National Corporation (JOGMEC), JSPS KAKENHI Grant Number 16H04614, and the Kyoto University Foundation.

Keywords: Acoustic Emission, Deep learning, Hydraulic fracturing

©2021. Japan Geoscience Union. All Right Reserved.

AE events observed during loading velocity step change in large-scale gouge friction experiments

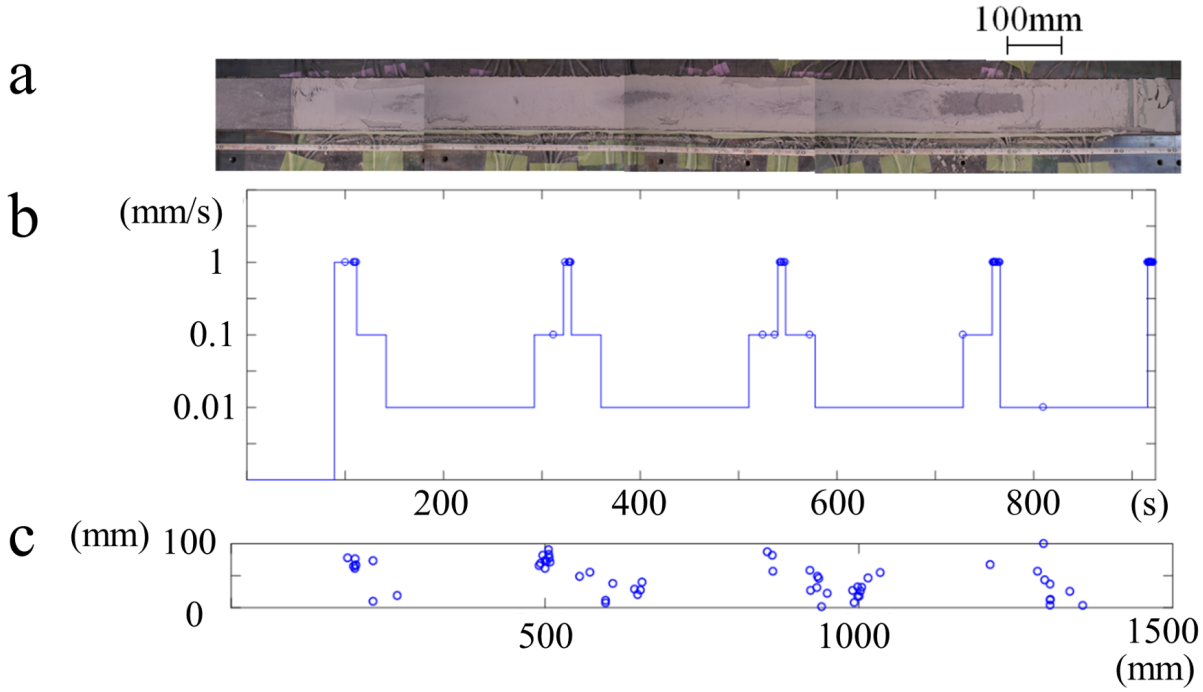
*Shun Watanabe[1], Eiichi Fukuyama[1,2], Futoshi Yamashita[2], Akihiro Shimoda[1]

1. kyoto university, 2. National Research Institute for Earth Science and Disaster Prevention

In recent years, hydraulic fracturing has been carried out to artificially crack the bedrock for oil and shale gas oil mining. Injection of fracturing fluids into the bedrock can increase the pore pressure, decrease the effective normal stress, and therefore decrease the fault strength, which may induce earthquakes. In this study, we conducted large-scale gouge friction experiments, in which the loading velocity was changed stepwise. We analyzed AE (Acoustic Emission) events that occurred during the experiments to investigate the effect of the loading velocity on the AE event occurrence (timing and location).
The experiment was carried out using a large biaxial rock friction apparatus at the National Research Institute for Earth Science and Disaster Resilience (NIED). Metagabbro was used as host blocks whose dimensions were L1.5 m x W0.5 m x H0.5 m for the top block and L2.0 m x W0.1 m x H0.5 m for the bottom block. These two blocks were stacked vertically, and the normal load was applied onto the top face of the top block. The shear load was applied onto the side face of the top block. Before each experiment, simulated gouge was distributed between the host blocks, so that the thickness of gouge layer was 3 mm (Fig.a). The gouge was made of the same metagabbro pieces by crushing them, so that the average particle size is 10 μm and the maximum particle size is 200 μm. All gouge used in an experiment was removed and new gouge was distributed before the next experiment. In the present study, we focus on four experiments (LB21-003 and LB21-004 with 3.3MPa normal stress and LB21-007 and LB21-008 with 6.5 MPa normal stress). The loading velocity was changed stepwise among 0.01 mm/s, 0.1 mm/s, and 1 mm/s (Fig.b). 16 AE sensors were installed on both side surfaces of the top block 70 mm away from the sliding surface with 180 mm intervals. We first picked up the time window when the AE events were detected by using InSite software (made by Applied Seismology Consulting Ltd), and then manually picked the P wave arrival times of all events. Their locations were estimated using the data of the four sensors with the earliest P wave arrival. The grid search method was used for the estimation of the hypocenter (x, y) and the origin time (t) that minimized $G = \Sigma|g_i|$, where $g_i = \{(x-x_i)^2 + (y-y_i)^2 + z_i^2\}^{1/2} / Vp-(t_i - t)$, x_i, y_i, and z_i are the location of the i-th sensor, and ti is the P wave arrival time at the i-th sensor. In this estimation, we assumed that the AE events occurred on the sliding surface and the P wave velocity Vp = 6919 (m/s), which was estimated from the physical properties of the host rock. The grid interval was 0.5 mm in the x and y directions and 0.1 μs in time. Furthermore, cross-correlation analysis was performed for events whose epicenter was not well determined. By utilizing the time difference with respect to those of well-located events, we could further reduce the error function G. The cross-correlation analysis should be effective for locating event whose P wave arrival is unclear.
Figure c shows the spatial distribution of AE events observed during the LB21-007 experiment. The AE events were clustered at four locations. It should be noted that the locations of the AE clusters were quite similar to each other in four all experiments . Because such a clustering was not observed in the rock-on-rock experiments without the gouge layer, the spatially-concentrated occurrences of the AE events should be relevant to the presence of the gouge layer. Figure b shows the temporal change in the number of the AE event, which suggests that most events occurred immediately after the loading velocity was increased to 1 mm/s. Statistical characteristic of the AE event clearly shows a positive correlation of the occurrence number with the loading velocity: averaged numbers of the AE events per unit displacement in LB21-007 were 0.17, 0.28, and 0.91 under the loading velocities of 0.01, 0.1, and 1 mm/s, respectively.

©2021. Japan Geoscience Union. All Right Reserved.

Keywords: rock friction experiment, acoustic emission, epicenter determination



©2021. Japan Geoscience Union. All Right Reserved.

[J] Oral | S (Solid Earth Sciences)：S-SS Seismology

Fri. Jun 4, 2021 9:00 AM - 10:30 AM JST | Fri. Jun 4, 2021 12:00 AM - 1:30 AM UTC | Ch.21 Zoom Room 21

[S-SS10] Active faults and paleoseismology

convener:Mamoru Koarai(Earth Science course, College of Science, Ibaraki University), Yoshiki Shirahama(Advanced Industrial Science and Technology, Geological Survey of Japan, Research Institute of Earthquake and Volcano Geology, Active Fault Research Group), Yoshiki Sato(Advanced Industrial Science and Technology, Geological Survey of Japan), Masayuki Yoshimi(Geological Survey of Japan, AIST), Chairperson:Mamoru Koarai(Earth Science course, College of Science, Ibaraki University), Yoshiki Shirahama(Advanced Industrial Science and Technology, Geological Survey of Japan, Research Institute of Earthquake and Volcano Geology, Active Fault Research Group)

Geologic and historic information on seismic cycles and on the magnitude and source faults of past earthquakes is essential information to understand future large earthquakes. The study of past faulting and seismicity is an important issue for an interdisciplinary community of seismologists, geologists, geomorphologists, archaeologists, and historians.

9:00 AM - 9:15 AM JST | 12:00 AM - 12:15 AM UTC

[SSS10-01] Introduction

9:15 AM - 9:30 AM JST | 12:15 AM - 12:30 AM UTC

[SSS10-02] Simultaneous rupturing of the Tanna fault and its branch faults in the Kita-Izu fault zone

*Ryuhei Oda[1], Daisuke Ishimura[1], Takehiko Suzuki[1] (1.Tokyo Metropolitan University)

9:30 AM - 9:45 AM JST | 12:30 AM - 12:45 AM UTC

[SSS10-03] Microtremor Array Observation across Active Faults in Ogasawara Iwo-To Island

*Takumi Murakoshi[1], Takayuki Kouno[2] (1.National Defense Academy, 2.Japan Air Self-Defense Force)

9:45 AM - 10:00 AM JST | 12:45 AM - 1:00 AM UTC

[SSS10-04] Rerationship between earthquake disaster and basement depth due to active faults in Iiyma City, Nagano Prefecture

*Mamoru Koarai[1], Keiichi Takami[1], Naoki Hashikami[1], Takayuki Nakano[2], Shigeki Senna[3] (1.Earth Science course, College of Science, Ibaraki University, 2.Geospatial Information Authority of Japan, 3.National Research Institute of Earth Science and Disaster Resilience)

10:00 AM - 10:15 AM JST | 1:00 AM - 1:15 AM UTC

[SSS10-05] Probing shallow region structure of Atotsugawa fault fracture zone with cosmic-ray muon detector

*Katsuya Yamazaki[1], Akimichi Taketa[2], Daisuke Ikeda[3], Kentaro Omura[4] (1.College of Engineering, Chubu University, 2.Earthquake Research Institute, the University of Tokyo, 3.Faculty of Engineering, Kanagawa University, 4.National Research Institute for Earth Science and Disaster Resilience)

10:15 AM - 10:30 AM JST | 1:15 AM - 1:30 AM UTC

[SSS10-06] The Quaternary fault outcrop of the Inagoe fault, Furukawa fault zone, in northern part of Gifu Prefecture, central Japan

*Tomonori Tamura[1], Kiyokazu Oohashi[1], Nagisa Maruo[1] (1.Graduate school of Sciences and Technology for Innovation, Yamaguchi University)

[J] Oral | S (Solid Earth Sciences) | S-SS Seismology

[S-SS10] Active faults and paleoseismology

convener:Mamoru Koarai(Earth Science course, College of Science, Ibaraki University), Yoshiki Shirahama(Advanced Industrial Science and Technology, Geological Survey of Japan, Research Institute of Earthquake and Volcano Geology, Active Fault Research Group), Yoshiki Sato(Advanced Industrial Science and Technology, Geological Survey of Japan), Masayuki Yoshimi(Geological Survey of Japan, AIST), Chairperson:Mamoru Koarai(Earth Science course, College of Science, Ibaraki University), Yoshiki Shirahama(Advanced Industrial Science and Technology, Geological Survey of Japan, Research Institute of Earthquake and Volcano Geology, Active Fault Research Group)

Fri. Jun 4, 2021 9:00 AM - 10:30 AM Ch.21 (Zoom Room 21)

Geologic and historic information on seismic cycles and on the magnitude and source faults of past earthquakes is essential information to understand future large earthquakes. The study of past faulting and seismicity is an important issue for an interdisciplinary community of seismologists, geologists, geomorphologists, archaeologists, and historians.

9:00 AM - 9:15 AM

[SSS10-01]Introduction

©Japan Geoscience Union

Simultaneous rupturing of the Tanna fault and its branch faults in the Kita-Izu fault zone

*Ryuhei Oda[1], Daisuke Ishimura[1], Takehiko Suzuki[1]

1. Tokyo Metropolitan University

The Kita-Izu fault zone, a 32 km-long NS striking sinistral strike-slip fault zone, is located in the northeastern part of the Izu Peninsula. A branch fault group showing NW-SE strike is distributed in the east side of the Tanna and Ukihashi-central faults. At the 1930 Kita-Izu earthquake, which is the latest event of the fault zone, surface ruptures of some branch faults were reported (Matsuda, 1972). This suggests the triggered slip on the branch faults by the Tanna fault activity. Consideration of a simultaneous rupturing of active faults is important for the mitigation of surface rupturing around active faults, the assessment of minor active faults around a high slip-rate active fault, and the development of fault topography. Thus, we clarified the detailed distribution and geometry of active faults in the northeastern part of the Izu Peninsula, based on the geomorphic interpretation using the high-resolution LiDAR DEMs. Then, we conducted drilling survey and tephra analysis and estimated the slip-rates of the branch faults. In addition, we calculated the coulomb failure function (delta CFF) that the Tanna fault gives to the branch fault. Based on the detailed distribution and geometry of active faults, slip-rates of the branch faults and the delta CFF, we discuss the simultaneous rupturing of the Tanna fault and its branch faults.

In this study, we divided branch faults into 3 types based on the geomorphic interpretation. The type 1 is a dextral strike-slip fault (mainly NW striking). The type 2 is a NW striking normal fault forming a graben structure, located in the southeast of the Lake Ashinoko. The type 3 is a mainly NW striking branch fault, showing vertical and little horizontal displacements. From drilling survey and tephra analysis, we identified 5 tephras in the cores, that is, Fuji-Hoei scoria tephra (AD1707 ; Machida and Arai, 2003), Kozushima-Tenjosan tephra (AD838 ; Machida and Arai, 2003), Fuji-Zunasawa scoria tephra (ca.3.0 ka ; Geological Survey of Japan, AIST, 2021), Amagi-Kawagodaira tephra (ca.3.2 ka ; Tani et al., 2013), and Kikai-Akahoya tephra (ca.7.2 ka ; Smith et al., 2013). Using the ages of tephras and accumulated vertical displacement along the branch faults, we estimated the vertical slip-rate of the YG fault (type 2) and the NM fault (type 3) to be 0.1-1.0 mm/yr.

Furthermore, we calculated the coulomb failure function (delta CFF) that the Tanna fault gives to the branch fault, and discussed whether the movement of the Tanna fault promotes or suppresses the activity of the branch fault. The value of delta CFF to the type 1 branch faults is positive, and it is highly possible that the Tanna fault activates the type 1. The value of delta CFF to the type 2 is negative, and it is unlikely that Tanna fault activates the type 2. However, there are similarities between normal faults in the Kuradake area, which ruptured at the 2016 Kumamoto earthquake and that in the Izu Tanna area. Therefore, as in the case of the 2016 Kumamoto earthquake (as described in Fujiwara et al., 2020), it is likely that the type 2 is activated by the dynamic stress change caused by the seismic shaking of the Tanna fault. The value of delta CFF to the type 3 (NM fault : locating in the area sandwiched between two type 1s) is negative, and it is unlikely that the Tanna fault activates the type 3. However, if the Tanna fault and type 1 faults, which are dextral faults, move simultaneously, there is a possibility of the co-movement of the rupturing of the NM fault and them. When the value of dextral displacement of the type 1 faults are 2-3 times of the value obtained from the empirical relationship of Wells and Coppersmith(1994), delta CFF to the type 3 is positive, in that case, it is likely that the Tanna fault activates the type 3.

In conclusion, it is possible that the Tanna fault movement activates branch faults in the Kita-Izu fault zone by various factors, such as delta CFF and dynamic stress change. Moreover, comparing between the

©2021. Japan Geoscience Union. All Right Reserved.

Izu and Kumamoto areas, there are similarities between active fault distributions and landform position. This may indicate the relationship between active fault development and geomorphology, geology and stress field.

Keywords: Kita-Izu fault zone, Tanna fault, branch fault, coulomb failure function (delta CFF), 2016 Kumamoto earthquake

©2021. Japan Geoscience Union. All Right Reserved.

Microtremor Array Observation across Active Faults in Ogasawara Iwo-To Island

*Takumi Murakoshi[1], Takayuki Kouno[2]

1. National Defense Academy, 2. Japan Air Self-Defense Force

Iwo-To is a seismic and tectonically active volcanic island located in Ogasawara, Tokyo, Japan. In 2020, more than 100 volcanic earthquakes occurred per day during a three-day observation period. Currently, seismic activity is still observed on this island. The Motoyama area, located on the east side of Iwo-To island is experiencing rapid crustal movement with uplift measuring 50– 100 cm per year (The handout of 147th Coordinating Committee for Prediction of Volcanic Eruption, 2020). Kaizuka et al. (1983) reported the presence of active faults at several locations in the western and northeastern parts of Iwo-To island. In the present study, a microtremor array survey was conducted from September 30–October 2, 2019, to investigate the ground properties and subsurface geometry near active faults in the northeastern part of Iwo-To island. Using two lines with lengths of 1,000 and 550 m that crossed the presumed active faults, 37 and 15 observations were made respectively. The intervals between the observation points were set at 10 m or 25 m near active faults and at 50 m in other locations. Using a seismometer (JU410, Hakusan Corporation, Japan) as the observation device, three components of horizontal and vertical directions were measured continuously for more than 15 min at each observation point at a sampling frequency of 100 Hz. The H/V spectral ratios of the acceleration waveform records of the three components of microtremors were used for analysis. To understand the characteristics of the ground properties and the spatial changes in the subsurface faults, we analyzed the spatial changes in the dominance period, amplitude, and shape of the H/V spectral ratio of the microtremors. The results were used to effectively detect the horizontal changes occurring during the predominant period of the microtremor H/V spectral ratio across the surface faults estimated from the geological map data.

Acknowledgments:
This observation in Iwo-to island was supported by Japan Maritime Self-Defense Force Atsugi Air Base and Iwoto Air Base.

Keywords: Ogasawara Iwo-To Island, Active fault , Microtremor, H/V Spectral Ratio

©2021. Japan Geoscience Union. All Right Reserved.

Rerationship between earthquake disaster and basement depth due to active faults in Iiyma City, Nagano Prefecture

*Mamoru Koarai[1], Keiichi Takami[1], Naoki Hashikami[1], Takayuki Nakano[2], Shigeki Senna[3]

1. Earth Science course, College of Science, Ibaraki University, 2. Geospatial Information Authority of Japan, 3. National Research Institute of Earth Science and Disaster Resilience

Iiyama City is located in the Iiyama Basin, which extends northeast-southwest along the Chikuma River in the northeastern part of Nagano Prefecture, and the western edge of the basin is bordered by the Western Edge Fault Zone of the Nagano Basin. The authors conducted leveling surveys and micro tremor survey in the center of Iiyama City area, and examined the relationship between the estimation of the shallow ground structure of Iiyama City area and past earthquake disasters, and the relationship with tectonic landforms and active structures.

Leveling survey was carried out with two survey lines crossing the low earthquake cliff with north-south direction caused by the 1847 Zenkoji Earthquake, and micro tremor survey were carried out at 11 points covering the target area around it. In the micro tremor survey, the depth at which the S wave velocity exceeds 300 m / s was used as the engineering base depth. On survey line 1 on the north side of the survey area, the relative height of the low cliff was about 1 m, and the displacement of engineering basement depth of the two points across the low cliff was about 5 m. On survey line 2 on the south side of the survey area, the relative height of the low cliff was about 80 cm, and the displacement of engineering basement depth of the two points across the low cliff was about 3 m. Assuming that the basement depth is contemporaneous, the displacement of the basement depth is larger than the relative height of the low cliff, which may indicate the accumulation of fault displacements that formed the low cliff.

In the area around Kita-Iiyama Station northwest of the Iiyama Castle Ruins, the basement depth is more than 15m lower than the surrounding area. The area around Kita-Iiyama Station was the area where the building damage caused by the 1847 Zenkoji Earthquake was remarkable. It can be considered that the earthquake damage was remarkable in the area where the soft ground was thickly deposited. The authors considered that the cause of the deep basement depth at the western edge of the Iiyama basin is likely to be due to structural movements such as back thrust associated with active faults.

Keywords: Zenkoji Earthquake, Earthquake disaster, basement depth, micro tremor, Iiyma City, active fault

©2021. Japan Geoscience Union. All Right Reserved.

Probing shallow region structure of Atotsugawa fault fracture zone with cosmic-ray muon detector

*Katsuya Yamazaki[1], Akimichi Taketa[2], Daisuke Ikeda[3], Kentaro Omura[4]

1. College of Engineering, Chubu University, 2. Earthquake Research Institute, the University of Tokyo, 3. Faculty of Engineering, Kanagawa University, 4. National Research Institute for Earth Science and Disaster Resilience

In this talk, I will introduce the method and the observation equipment of the subsurface density structure measurement using the cosmic ray muon observation system in the borehole, and report the measurement result in the borehole in the Atotsugawa fault zone in Hida city, Gifu prefecture in 2016 and the parameter estimation of the Atotsugawa fault.

Parameters such as fault strike, dip, width and density of fracture zones are important basic data for predicting seismic intensity and disaster scale of earthquakes. However, in order to obtain detailed information on these parameters using conventional methods, it is necessary to conduct extensive and spatially dense surveys. In this study, we have developed a method to survey the density structure of the subsurface including faults extensively by observation from a single point using a structure-viewing method using cosmic-ray muons, which has been actively studied in recent years.

In this method, the average density along the path is measured from the attenuation of cosmic-ray muons, which have high penetrating power. The muon attenuation does not depend on any properties other than the density of the penetrating material, and can be measured even in the surface layer of the earth's crust, which is highly heterogeneous. The penetrating power of cosmic-ray muons is so high that they can penetrate several kilometers underground, and can see through large structures such as faults and volcanoes. However, cosmic ray muons fly only from the sky, so until now, only structures that rise above the ground, such as volcanoes, could be observed.

In this study, we developed a compact instrument that can be installed in a borehole with a diameter of 15 cm in order to overcome this problem and to observe underground structures. The instrument has a limited directional resolution due to its small size. The measurement direction of the zenith angle is limited to one direction by a statistical method, and the azimuthal direction is resolved into eight directions. The instrument is installed in a borehole and the subsurface density structure is explored by moving the instrument in the depth direction, and the surrounding density structure including faults is measured extensively from one point to several hundred meters around.

Since 2016, we have measured the density structure up to 100 m underground using a borehole through the Atotsugawa fault in Hida City, Gifu Prefecture. As a result, we detected a low-density region in a direction consistent with past drilling survey records. Furthermore, we estimated the parameters such as the strike and dip of the fault using the measurement results.

Keywords: Muography, Fault, Borehole, Atotsugawa

©2021. Japan Geoscience Union. All Right Reserved.

The Quaternary fault outcrop of the Inagoe fault, Furukawa fault zone, in northern part of Gifu Prefecture, central Japan

*Tomonori Tamura[1], Kiyokazu Oohashi[1], Nagisa Maruo[1]

1. Graduate school of Sciences and Technology for Innovation, Yamaguchi University

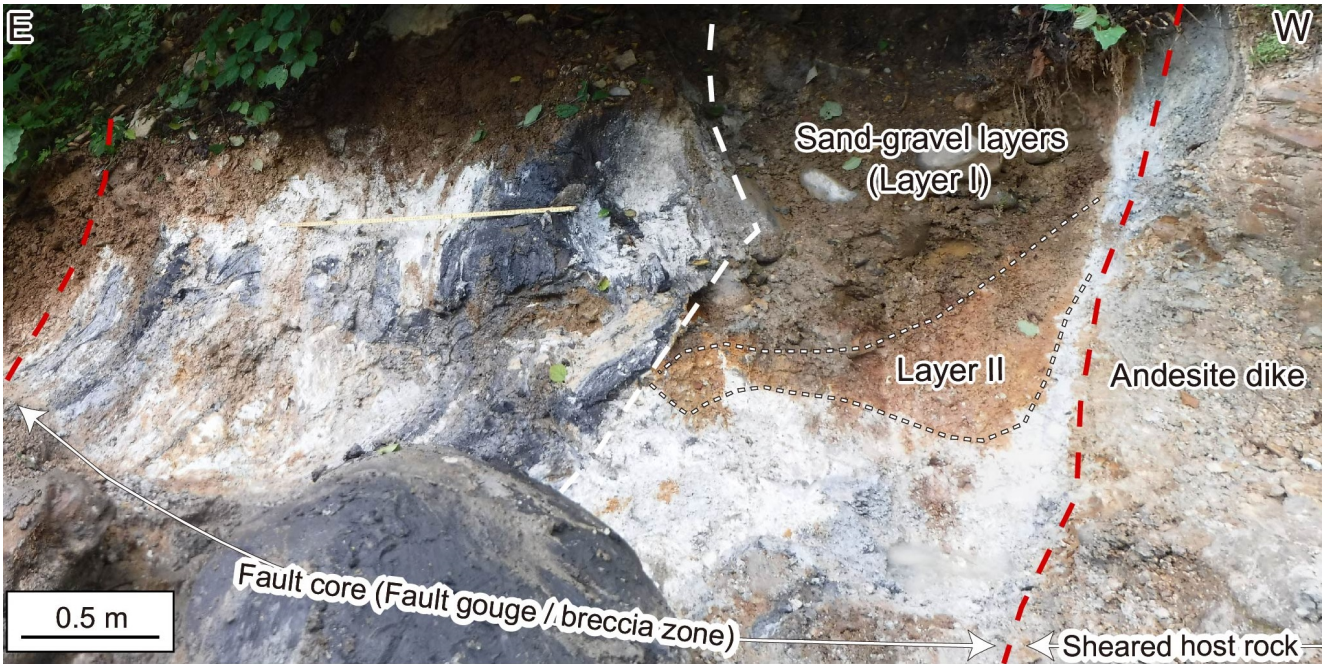
Inagoe fault, trending NE–SW ~ ENE–WSW and extending 13 km in length, is one of the Quaternary faults of the Furukawa fault zone located in Gifu Prefecture, Hida city (Suzuki and Sugito, 2010; Kumabara, 2019; Kumabara et al., 2019). Although the Quaternary fault outcrop was confirmed in the eastern part of the Inagoe fault (Research Group for the Active Faults of Gifu Prefecture, 2008), there are no reports on the direct evidences such as the Quaternary fault outcrop in the western extension of the Inagoe fault toward Kurigatani-gawa area by topographical studies (Suzuki and Sugito, 2010; Kumabara, 2019; Kumabara et al., 2019). This study reports the detail characteristics of the newly-found Quatrenary fault outcrop, and discuss the latest event in the western part of the Inagoe fault.

The 5-m-wide fault zone is composed of fault gouge and fault breccia, which is located on the fault trace detected by the topographical studies (Suzuki and Sugito, 2010; Kumabara, 2019; Kumabara et al., 2019). The approximate strike and dip of this fault zone are N55° E85° S, and composite planar fabrics containing P-foliation and R_1 shear shows dextral sense of shear in its fault gouge zone. While unconsolidated sand-gravel layers unconformably underlain by the fault zone, the partial layers were sandwiched within the fault zone. Major axis of the gravels adjacent to the fault gouge were oriented vertically, and striations on its surface were recognized. A humic soil was partially included in the sand-gravel layer; radiocarbon age of the humic soil sample showed AD 1527–1658 cal. BP.

This fault outcrop is located on the fault trace of the Inagoe fault as mentioned above, which strike coincides with direction of the fault trace. In addition, dextral sense of shear recognized by composite planar fabrics in the gouge zone was confirmed, which is consistent with the right-lateral tectonic landforms. These evidences indicate that this fault outcrop is thought to be the fault core of the Inagoe fault. Furthermore, sandwiched sand-gravel layers within the fault zone, vertical orientation of the gravels and striation on the surface of gravels suggest that the sand-gravel layers fell into tensile crack and deformed by the movement of the fault. This event is considered to be after AD 1527–1658 cal. BP because of the radiocarbon age. Historical earthquakes which occurred in northern Gifu prefecture include the AD 1586 Tensho earthquake, AD 1826 earthquake at Hida Ono-gun (M6.0), and AD 1855 Hida-Shirakawa and Kanazawa earthquake (M6.8) and AD 1858 Hietsu earthquake (Usami, 1987). Hence, we concluded that the latest event of the Inagoe fault may correspond to either of the historical earthquakes.

Keywords: Inagoe fault, Quaternary fault outcrop, Tectonic landforms, 1858AD Hietsu earthquake

©2021. Japan Geoscience Union. All Right Reserved.



©2021. Japan Geoscience Union. All Right Reserved.

[J] Oral | S (Solid Earth Sciences)：S-SS Seismology

Fri. Jun 4, 2021 10:45 AM - 12:15 PM JST | Fri. Jun 4, 2021 1:45 AM - 3:15 AM UTC | Ch.21 Zoom Room 21

[S-SS10] Active faults and paleoseismology

convener:Mamoru Koarai(Earth Science course, College of Science, Ibaraki University), Yoshiki Shirahama(Advanced Industrial Science and Technology, Geological Survey of Japan, Research Institute of Earthquake and Volcano Geology, Active Fault Research Group), Yoshiki Sato(Advanced Industrial Science and Technology, Geological Survey of Japan), Masayuki Yoshimi(Geological Survey of Japan, AIST), Chairperson:Yoshiki Sato(Advanced Industrial Science and Technology, Geological Survey of Japan), Masayuki Yoshimi(Geological Survey of Japan, AIST)

Geologic and historic information on seismic cycles and on the magnitude and source faults of past earthquakes is essential information to understand future large earthquakes. The study of past faulting and seismicity is an important issue for an interdisciplinary community of seismologists, geologists, geomorphologists, archaeologists, and historians.

10:45 AM - 11:00 AM JST | 1:45 AM - 2:00 AM UTC

[SSS10-07] Paleoseismic activity and slip rate of the Obitoke and Tenri faults in the Nara basin

★Invited Papers

*Hiroyuki Tsutsumi[1], Nobuhiko Sugito[2], Haruo Kimura[3], Shozo Kawashima[1], Toranosuke Morishima[1], Kaoru Taniguchi[4], Masashi Omata[4] (1.Department of Environmental Systems Science, Faculty of Science and Engineering, Doshisha University, 2.Faculty of Sustainability Studies, Hosei University, 3.Central Research Institute of Electric Power Industry, 4.Pasco Co.)

11:00 AM - 11:15 AM JST | 2:00 AM - 2:15 AM UTC

[SSS10-08] Distribution of amount of displacement along the Eastern Margin Fault System of Nara basin, Kinki District, Central Japan

*Taku Komatsubara[1] (1.Institute of Geology and Geoinformation, Advanced Industrial Science and Technology)

11:15 AM - 11:30 AM JST | 2:15 AM - 2:30 AM UTC

[SSS10-09] The Oldest Report of a Tsunami in Mexico in 1537 Based on Japanese Literature Is Erroneous

*Yutaka Hayashi[1] (1.Meteorological Research Institute, Japan Meteorological Agency)

11:30 AM - 11:45 AM JST | 2:30 AM - 2:45 AM UTC

[SSS10-10] Discovery of active faults on the coasts of Gulf of Suez and its significance

*Takashi Nakata[1], Steven G. Wesnousky[2], Hideaki Goto[1] (1.Hiroshima University, 2.University of Nevada, Reno)

11:45 AM - 12:15 PM JST | 2:45 AM - 3:15 AM UTC

[SSS10-11] Discussion

Paleoseismic activity and slip rate of the Obitoke and Tenri faults in the Nara basin

*Hiroyuki Tsutsumi[1], Nobuhiko Sugito[2], Haruo Kimura[3], Shozo Kawashima[1], Toranosuke Morishima[1], Kaoru Taniguchi[4], Masashi Omata[4]

1. Department of Environmental Systems Science, Faculty of Science and Engineering, Doshisha University, 2. Faculty of Sustainability Studies, Hosei University, 3. Central Research Institute of Electric Power Industry, 4. Pasco Co.

The eastern marginal fault of the Nara basin consists of a series of east-dipping reverse faults at the topographic boundaries between mountains and hills on the east and basins and lowlands on the west. This fault zone poses high seismic hazards to the central Kinki area but the probability of earthquake occurrence in the next 30 years is very loosely constrained. Since the 2019 academic year, we have conducted active fault mapping, slip rate estimation, and obtaining paleoseismic data of the fault zone under a 3-year research project, "Comprehensive Research Project for the Nara-bonchi-toen Fault Zone." In 2020, we conducted paleoseismic investigations at a few localities within the Nara basin. At Imaichi, Nara City, we carried out a GPR survey, trenching, and borehole drilling to identify geologic evidence for recent faulting on the Obitoke fault. At Yashima, Nara City, we excavated pits to radiometrically date faulted and un-faulted geomorphic surfaces by the Tenri fault. Besides, geologic cross-sections based on the "Database for Boreholes in the Kansai Area" clearly illuminate the deformation of lower terrace deposits by the Obitoke fault, which gives a dip-slip rate of 0.3-0.4 mm/yr of the fault.

Keywords: the eastern marginal fault of the Nara basin, Obitoke fault, Tenri fault, paleoseismic trenching, borehole data, paleoseismic activity

©2021. Japan Geoscience Union. All Right Reserved.

Distribution of amount of displacement along the Eastern Margin Fault System of Nara basin, Kinki District, Central Japan

*Taku Komatsubara[1]

1. Institute of Geology and Geoinformation, Advanced Industrial Science and Technology

1. Introduction

The eastern margin fault zone of Nara Basin is 55 km in length, N-S strike, reverse active fault from Yamashina Basin (Kyoto City) to southern end of Nara Basin. It had been thought to be divided into two segments by discontinuity of fault geomorphology, the segment boundary is located near Joyo City. The presenter tries to make clear fault segmentation and structural evolution by comparison of features and the amount of displacement of various geological and geomorphological horizons.

2.Geological and geomorphological horizons along fault zone

Five horizons are recognizable from old to young. 1) Base of the Miocene and upper boundary of the underground basement rocks in Nara Basin. 2) Base of the Osaka Group (approximately 2.5 Ma) 3) Base of the lower subgroup of Osaka Group (approximately 1.7 Ma) 4) Ma 1 to Ma 3 layers in the Osaka Group (approximately 0.9 to 1.0 Ma) 5) Ma 9 layer in the Osaka Group and higher terraces (approximately 0.2 to 0.4 Ma).

3. Elevation (amount of displacement) of horizons along the fault zone

Fig. 1 shows elevation of the horizons both uplifting side (Daigo Mountains, Joyo and Ide Hills and Yamato Plateau) and sinking side (Yamashina Basin, Kidukawa Lowland and Nara Basin) of faults. This figure indicates followings. 1) the amount of displacement of the base of Osaka Group is minimum in the southern part of the Kidukawa Lowland (around Inooka, Kyotanabe City to Ide town). 2) The amount of displacement of the base of the Miocene is about 1000 m around the Nara Basin, however the most of it had caused before Early Quaternary (by deposition of the lower subgroup of Osaka Group). On the other hand, the amount of displacement around Uji area during middle to late Quaternary (since Ma 0) reaches 500 m or more.

These facts suggest that the eastern margin fault zone of the Nara Basin is subdivided into two segments at the Inooka hill (southern part of the Kizukawa Lowland).

4. Future study

The presenter hopes to make a database for estimating the late Quaternary fault activity by gathering much more data on the date of terraces and stratigraphy of subsurface geology.

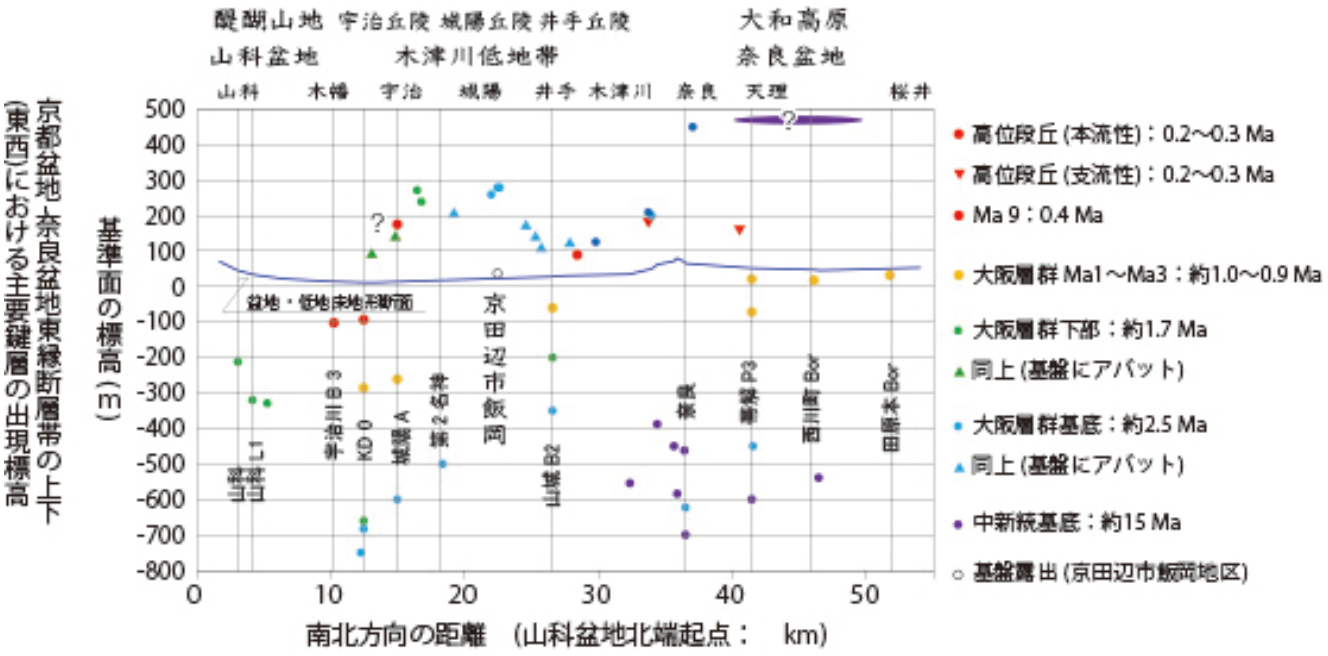
Reference

The Headquaters for Earthquake Research Promotion (2001) Long-term evaluation on the southern part of the Eastern Margin active fault zone of the Kyoto and Nara Basins (the Eastern Margin Fault zone of the

©2021. Japan Geoscience Union. All Right Reserved.

Nara Basin). (https://jishin.go.jp/regional_seismicity/rs_katsudanso/f075_kyoto_nara/)

Keywords: Active fault, Amount of displacement, Segmentation, Slip rate, Structural evolution



©2021. Japan Geoscience Union. All Right Reserved.

The Oldest Report of a Tsunami in Mexico in 1537 Based on Japanese Literature Is Erroneous

*Yutaka Hayashi[1]

1. Meteorological Research Institute, Japan Meteorological Agency

The dates and the magnitudes of the oldest phenomena in a certain area play important roles in estimating long-term seismicity in that area. However, in earthquake and tsunami catalogs, the older the historical records, the more difficult it is to ensure the reliability of the corresponding report. For example, widely used earthquake and/or tsunami catalogs in Japan (*e.g.* Usami *et al.*, 2013) listed the 1586 Peruvian earthquake as the oldest tele-tsunami record in Japan; however, this tsunami turned out to be incorrectly linked to a certain oral tsunami record in Japan (Hayashi *et al.*, 2018; Satake *et al.*, 2020). According to the world historical tsunami database (NCEI, 2017) and the Mexican tsunami catalog (Sá nchez and Farreras, 1993), the oldest historical tsunami record in Central America is the earthquake tsunami that occurred in Mexico in 1537; however, this record is flagged as doubtful one because this tsunami is reported by no authority outside Japan. I examined earthquake and tsunami catalogs and found the source of this suspicious data.
Imamura (1925) compiled the first part of the chronological table of major earthquakes in the world from Milne's (1912) earthquake catalog of the world. During this compilation, information on the tsunami caused by the 1531 Spain–Portugal earthquake was not copied. The chronological table was published almost annually until 1962, during which time the table was revised by Kawasumi (1958), who was the author in charge at the time. The remarks for the 1531 Spain–Portugal earthquake tsunami should have been added to that entry during the revision, but the text “tsunami existence” was erroneously added to the next entry for the 1537 Mexico earthquake. The source of the 1537 tsunami report turned out to be this miscopy.

References:
Hayashi *et al.* (2018): Negative effects of erroneous records of Japanese tsunami caused by the 1586 earthquake off the coast of Peru being included in the Technical Reports of the Japan Meteorological Agency. *Quart. J. Seis.*, **81**, 9:1-7. (in Japanese with English Abstract).
Imamura (1925): Sekai Dai-jishin Nendai-hyo Zen-hen. in Chronological Scientific Tables, **2**, 312–313 and 331–344. (in Japanese)
Kawasumi (1958): Sekai Dai-jishin Nendai-hyo Zen-hen. in Chronological Scientific Tables, **32**, Chi143–Chi149. (in Japanese)
Milne (1912): A catalogue of destructive earthquakes, A.D. 7 to A.D. 1899.
NCEI (2017): NGDC/WDS Global Historical Tsunami Database. DOI: 10.7289/ V5PN93H7
Sánchez and Farreras (1993): Catalog of Tsunamis on the Western Coast of Mexico. World Data Center A for Solid Earth Geophysics Publication, SE-50. (in Spanish and English)
Satake *et al.* (2020): History and features of trans-oceanic tsunamis and implications for paleotsunami studies. Earth-Sci. Rev., **202**, 103112.
Usami *et al.* (2013): Nihon Higai Jishin Soran 599–2012, ISBN 4130607596. (in Japanese)

Keywords: 1537 Mexico earthquake, false tsunami, miscopy, ” Chronological Scientific Tables”, 1531 Spain–Portugal earthquake tsunami

©2021. Japan Geoscience Union. All Right Reserved.

Discovery of active faults on the coasts of Gulf of Suez and its significance

*Takashi Nakata[1], Steven G. Wesnousky[2], Hideaki Goto[1]

1. Hiroshima University, 2. University of Nevada, Reno

We newly found active faults, which are widely developed across the alluvial fans on both banks of the Gulf of Suez. There are regional differences in the development of faults. In the northernmost part of the bay, NW-SE extending active faults with cumulative displacements across the alluvial fan, develop to the northwest of Suez and east of Ras Sudr. On the east bank of the central part of the Gulf of Suez, the low-lying mountains face the coast, and the alluvial fan is poorly developed. Here, active faults develop in the part of the boundary between low mountains and lowlands located near the coast. A part of the main rift boundary fault east of Al Tur has displaced the alluvial fan, and its activity cannot be completely denied. On the other hand, active faults are well developed on the west bank the central part of the Gulf of Suez. In the central part of the Gharib plain on the west bank, many normal fault-type active faults extending NNW-SSE parallel to the long axis of the Gulf of Suez are widely observed on the alluvial fans. In the southern part of the Gulf of Suez, on the eastern shore south of Al Tur, we find many short active faults across the alluvial fan, but few faults show evidence of cumulative displacement. On the other hand, on the west bank, a remarkable active fault develops to the west of Jemsa Bay. One of the most distinctive active fault developments in the Gulf of Suez area is observed in the Gharib plain on the west bank between Ras Abu Bakr and Ras Gharib. Many active faults extending parallel to each other with northeast-southwest strikes are found in the area. Most of them are normal fault-type active faults with a length less than 10 km long. They displace the old and new alluvial fans, indicating their cumulative activity. We recognized many small grabens that were bounded by fault scarps facing each. The mechanism solutions of 18 shallow earthquakes with magnitudes of 2.8-5.2 in the central and northern parts of the Gulf of Suez between 1983 and 2004 show mostly normal fault components (Morsy et al., 2011) that are consistent with the activity of the active faults in the study area. There is no study regarding the age of alluvial fans in this area, but the correlation of their age with the alluvial fans in the arid regions of the western United States (Hoeft and Frankel 2010) is attempted based on their surface structure characteristics. As a result, the alluvial fan correlated with Q3b (15.5 ±1.2ka) is vertically displaced by 1-3m, Q2c (92 ±9ka) 5-6m, and Q2b (137 ±25ka) 10-15m. The vertical slip rate is roughly estimated at 0.1 mm/year. Since about ten active faults with similar slip rates are recognized on land, the total slip rate of the active faults on land reaches almost 1 mm / year. We have no data regarding the dip of the mapped active faults, but from the source mechanism of the earthquakes in the area, we may consider that faults dip 50-60 degrees. Therefore the expansion rate across the Suez rift may become approximately 1 mm/year if we add the slip of the active faults at the bottom of Suez Bay. The Sharm El Sheikh earthquake (Mw6.6) occurred in 1969 on the seafloor near the west bank at the southern end of the Gulf of Suez, and it is predicted that hazardous earthquakes originating from newly discovered active faults may occur anytime.

Keywords: Gulf of Suez, active fault, ALOS 30 anaglyph

©2021. Japan Geoscience Union. All Right Reserved.

[J] Oral | S (Solid Earth Sciences) | S-SS Seismology

[S-SS10] Active faults and paleoseismology

convener:Mamoru Koarai(Earth Science course, College of Science, Ibaraki University), Yoshiki Shirahama(Advanced Industrial Science and Technology, Geological Survey of Japan, Research Institute of Earthquake and Volcano Geology, Active Fault Research Group), Yoshiki Sato(Advanced Industrial Science and Technology, Geological Survey of Japan), Masayuki Yoshimi(Geological Survey of Japan, AIST), Chairperson:Yoshiki Sato(Advanced Industrial Science and Technology, Geological Survey of Japan), Masayuki Yoshimi(Geological Survey of Japan, AIST)

Fri. Jun 4, 2021 10:45 AM - 12:15 PM Ch.21 (Zoom Room 21)

Geologic and historic information on seismic cycles and on the magnitude and source faults of past earthquakes is essential information to understand future large earthquakes. The study of past faulting and seismicity is an important issue for an interdisciplinary community of seismologists, geologists, geomorphologists, archaeologists, and historians.

11:45 AM - 12:15 PM

[SSS10-11]Discussion

©Japan Geoscience Union

[J] Oral | S (Solid Earth Sciences)：S-GL Geology

Fri. Jun 4, 2021 1:45 PM - 3:15 PM JST | Fri. Jun 4, 2021 4:45 AM - 6:15 AM UTC | Ch.23 Zoom Room 23

[S-GL22] Geochronology and Isotope Geology

convener:Takahiro Tagami(Graduate School of Science, Kyoto University), Yuji Sano(Division of Ocean and Earth Systems, Atmosphere and Ocean Research Institute, University of Tokyo),
Chairperson:Takahiro Tagami(Graduate School of Science, Kyoto University), Yuji Sano(Center for Advanced Marine Core Research, Kochi University)

Reliable reconstruction of geohistory is of primary importance to better envision the present and future of the Earth. Geochronology and isotope geology play major roles in the reconstruction. This session offers an opportunity to present the results of fundamental studies, including the developments / improvements of analytical methods and age calibration, as well as applications to the Earth and planetary materials. We particularly focus on: (1) radiometric dating, bio-stratigraphy, magneto-stratigraphy and stable isotopic time series that provide the age information, (2) radioisotopes and stable isotopes widely employed for analyzing the Earth and planetary systems and (3) hypothesis and numerical modeling that utilize / assimilate the age and isotopic data. We also welcome contributions that integrate a variety of relevant disciplines.

1:45 PM - 2:15 PM JST | 4:45 AM - 5:15 AM UTC

[SGL22-01] Inter-method comparison study between $^{40}Ar/^{39}Ar$ and unspiked K-Ar method for some young volcanic rocks

★Invited Papers

*Seiko Yamasaki[1], Daniel P. Miggins[2], Anthony A.P. Koppers[2] (1.Geological Survey of Japan, Advanced Industrial Science and Technology, 2.Oregon State University)

2:15 PM - 2:30 PM JST | 5:15 AM - 5:30 AM UTC

[SGL22-02] Sub-millimeter scale helium measurement for MORB glass

*Hidenori Kumagai[1], Keiko Sato[2,1,3], Ieyoshi Shimizu[1] (1.Japan Agency for Marine-Earth Science and Technology, 2.National Institute of Technology, Fukushima College, 3.Okayama, Univ. of Science)

2:30 PM - 2:45 PM JST | 5:30 AM - 5:45 AM UTC

[SGL22-03] Asteroid shower on the Earth-Moon system 0.8 billion years ago

*Kentaro Terada[1], Tomokatsu Morota[2], Mami Kato[3] (1.Department of Earth and Space Science, Graduate School of Science, Osaka University, 2.Graduate School of Science, The University of Tokyo, 3.MEISEI ELECTRIC CO., LTD)

2:45 PM - 3:15 PM JST | 5:45 AM - 6:15 AM UTC

[SGL22-04] Deciphering the earliest Earth history from nitrogen, a highly-siderophile-highly-volatile element

★Invited Papers

*Ko Hashizume[1], Osamu Ohtaka[2] (1.Faculty of Science, Ibaraki University, 2.Graduate School of Science, Osaka University)

Inter-method comparison study between $^{40}Ar/^{39}Ar$ and unspiked K-Ar method for some young volcanic rocks

*Seiko Yamasaki[1], Daniel P. Miggins[2], Anthony A.P. Koppers[2]

1. Geological Survey of Japan, Advanced Industrial Science and Technology, 2. Oregon State University

Recent $^{40}Ar/^{36}Ar$ and unspiked K-Ar studies have been successfully applied toward younger and younger samples. The unspiked K-Ar method enables the correction for the mass fractionated initial $^{40}Ar/^{36}Ar$ ratios to yield more accurate ages. In the $^{40}Ar/^{39}Ar$ method, initial $^{40}Ar/^{36}Ar$ ratios can be assessed by the use of an inverse isochron plot, resulting in higher precisions.

We conducted inter-method comparison between 40Ar/39Ar and unspiked K-Ar dating method for some young volcanic rocks. The age results by both methods agree within errors and consistent with stratigraphic relationships, as well as concordant with reported conventional K-Ar, Thermo Luminescence, Fission Track and ^{14}C ages. Some uncorrected ages show negative ages in both methods, but for all corrected age spectra we obtained positive ages. The calculated age differences between corrected and uncorrected ages are up to ~100 ka. We conclude that the initial argon correction is effective in dating younger samples, providing more robust ages for Quaternary samples

Keywords: Ar/Ar dating, unspiked K-Ar dating

©2021. Japan Geoscience Union. All Right Reserved.

Sub-millimeter scale helium measurement for MORB glass

*Hidenori Kumagai[1], Keiko Sato[2,1,3], Ieyoshi Shimizu[1]

1. Japan Agency for Marine-Earth Science and Technology, 2. National Institute of Technology, Fukushima College, 3. Okayama, Univ. of Science

Regardless of the recent extensive effort to reduce the contamination/interference of the atmospheric component at the noble gas analyses (e.g. Moreira et al., 2018), such contamination/interference of the atmospheric component were still commonly reported in the upper-mantle-derived samples. On the other hand, the authors have reported a preliminary single-grain helium isotope analysis for an olivine taken from an alkaline lava fragment sampled from low 3He/4He super-segment of Southwest Indian Ridge (Kumagai et al., Goldschmidt Conference, 2008). In the experiment, analytical uncertainty was not small mainly due to the more than 10% contribution of blank correction.

We will report in the presentation, our recent trials for MORB glass shards with sub-millimeter spatial resolution using an infrared laser probe; assembled by Marubun Co. using SDL-IFL-15 (JDF uniphase co.) of which wavelength is 1110nm and 0.2 mm of focusing diameter in ×5 optical magnification. In a preliminary trial, the MORB glass shard with thick color was immediately melted within 0.5 seconds with 2W power of the output. The released amount of He was sufficient to be detected by an old-generation noble gas mass spectrometer GVI5400He under 400 μA trap current condition; approx. 0.5mV output were recorded. The reduced volume of the extraction volume and mass spectrometer were also contributed to this output. Accumulated data set will be further reported.

Keywords: Laser probe, MORB glass, Helium isotope ratio

©2021. Japan Geoscience Union. All Right Reserved.

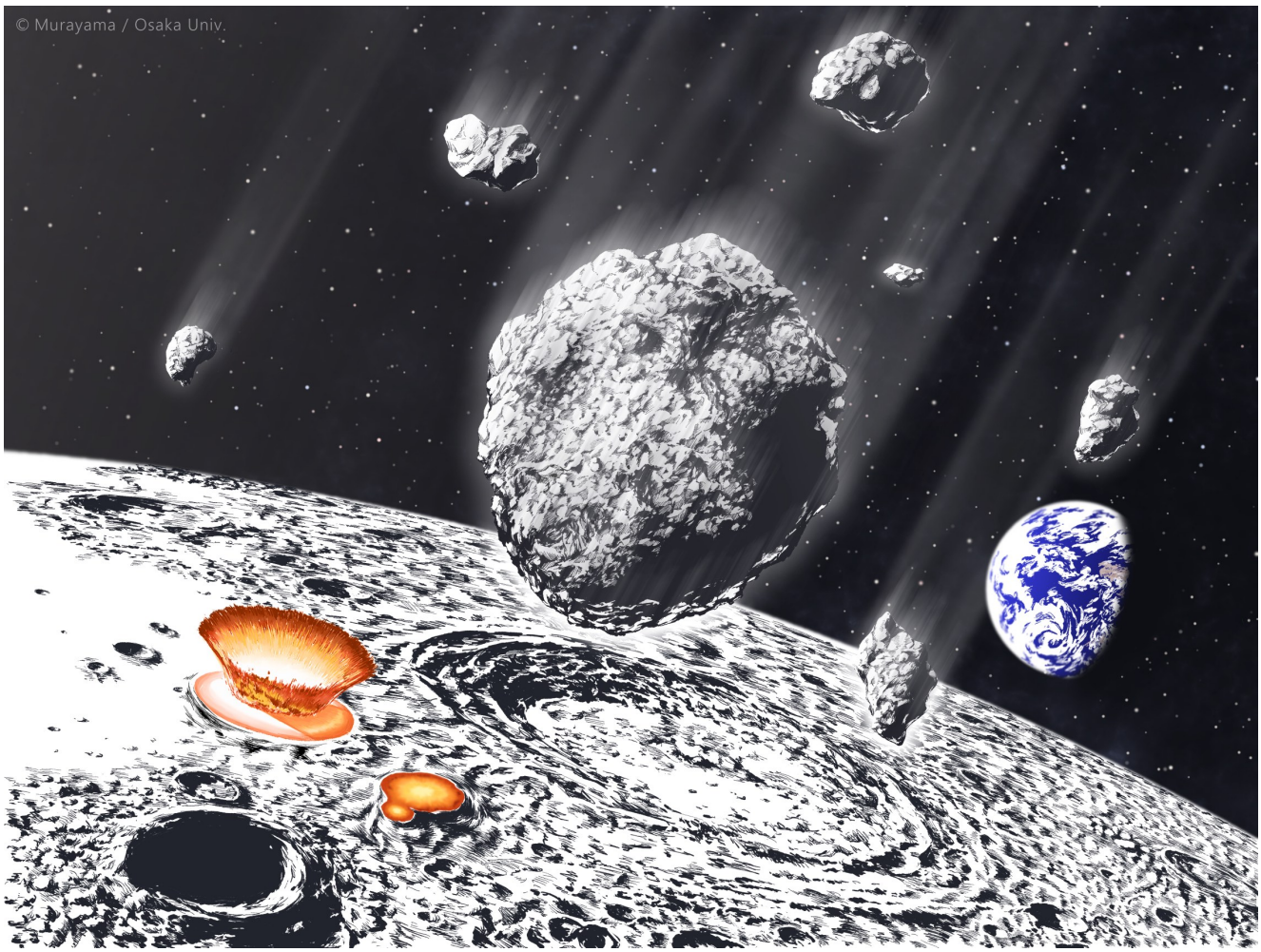
Asteroid shower on the Earth-Moon system 0.8 billion years ago

*Kentaro Terada[1], Tomokatsu Morota[2], Mami Kato[3]

1. Department of Earth and Space Science, Graduate School of Science, Osaka University, 2. Graduate School of Science, The University of Tokyo, 3. MEISEI ELECTRIC CO., LTD

We investigate the formation ages of 59 lunar craters with fresh morphologies and diameters greater than approximately 20 km and first find that 8-17 of 59 craters were formed simultaneously. Considering the radiometric ages of ejecta from Copernicus crater and impact glass spherules from various Apollo landing sites, we conclude that sporadic meteoroid bombardment occurred across the whole Moon at approximately 0.8 Ga. Based on crater scaling laws and collision probabilities with the Earth and Moon, we suggest that at least (4–5) ×10^16 kg of meteoroids, approximately 30–60 times more than the Chicxulub impact, must have plunged into the Earth.

Keywords: Crater Chronology, impact flux, Earth and Moon system, Lunar Orbiter KAGUYA



©2021. Japan Geoscience Union. All Right Reserved.

Deciphering the earliest Earth history from nitrogen, a highly-siderophile-highly-volatile element

*Ko Hashizume[1], Osamu Ohtaka[2]

1. Faculty of Science, Ibaraki University, 2. Graduate School of Science, Osaka University

Earth is generally considered to have been formed mainly from primitive chondrite-like building blocks. The differences in the elemental composition between chondrites and the bulk silicate Earth may provide information on the behaviors of elements during the accretion and differentiation stages of Earth. This study highlights the behaviors of the highly volatile elements, particularly nitrogen and carbon during the core formation, and by catastrophic impacts.

Keywords: Earliest Earth History, Nitrogen, Siderophile

©2021. Japan Geoscience Union. All Right Reserved.

[J] Oral | S (Solid Earth Sciences)：S-VC Volcanology

Fri. Jun 4, 2021 10:45 AM - 12:15 PM JST | Fri. Jun 4, 2021 1:45 AM - 3:15 AM UTC | Ch.25 Zoom Room 25

[S-VC28] Active Volcanism

convener:Yuta Maeda(Nagoya University), Takahiro Miwa(National research institute for earth science and disaster prevention), Takeshi Matsushima(Institute of Seismology and Volcanology, Faculty of Science, Kyushu University), Chairperson:Kohei Hotta(University of Toyama), Hiroshi Munekane(Geospatial Information Aurhotiry of Japan)

This session discusses various aspects of active volcanisms including, but not limited to, rec ent and historical eruptions, various phenomena associated with the volcanic activities, und erground structures of the volcanoes, and developments of new instruments based on geop hysical, geochemical, geological, and multidiscipline approaches. We also welcome studies o n understanding and predicting the transitions of the eruptive activities from observational, theoretical, and experimental approaches.

10:45 AM - 11:00 AM JST | 1:45 AM - 2:00 AM UTC

[SVC28-01] Reappraisal of the deformation model for Mt. Kusatsu-shirane and Mt. Asama

*Hiroshi Munekane[1] (1.Geospatial Information Aurhotiry of Japan)

11:00 AM - 11:15 AM JST | 2:00 AM - 2:15 AM UTC

[SVC28-02] Volcano monitoring based on InSAR Time-series Analysis

*Satoshi Miura[1], Morishita Yu[2], Yusaku Ohta[1], Tomotsugu Demachi[1], Micaela Colavita[1] (1.Graduate School of Science, Tohoku University, 2.Geospatial Information Authority of Japan)

11:15 AM - 11:30 AM JST | 2:15 AM - 2:30 AM UTC

[SVC28-03] **Evolution of Volcanic Deformation at Domuyo and Laguna del Maule, Southern Andes, Revealed by InSAR Time-series Analyses**

*Micaela Colavita[1], Satoshi Miura[1], Yu Morishita[2] (1.Graduate School of Science, Tohoku University , 2.Geospatial Information Authority of Japan)

11:30 AM - 11:45 AM JST | 2:30 AM - 2:45 AM UTC

[SVC28-04] Evaluation of volcanic activity using "Non-eruptive ground deformation"

*Masato Iguchi[1] (1.Sakurajima Volcano Research Center, Disaster Prevention Research Institute, Kyoto University)

11:45 AM - 12:00 PM JST | 2:45 AM - 3:00 AM UTC

[SVC28-05] The deformation source revealed from leveling surveys in Jigokudani valley, Tateyama volcano, Japan

*Kohei Hotta[1], Shigekazu Kusumoto[2], Hidenori Takahashi[1], Yuichi S. Hayakawa[3] (1.University of Toyama, 2.Kyoto University, 3.Hokkaido University)

12:00 PM - 12:15 PM JST | 3:00 AM - 3:15 AM UTC

[SVC28-06] Crustal structure around Kikai submarine caldera deduced from gravity anomaly

*Tomoko Hanyu[1], Satoshi Shimizu[1], Hiroto Yamaguchi[2], Yuiko Morita, Nobukazu Seama[2,1] (1.Kobe Ocean-Bottom Exploration Center, 2.Department of Planetology, Graduate School of Science, Kobe University)

Reappraisal of the deformation model for Mt. Kusatsu-shirane and Mt. Asama

*Hiroshi Munekane[1]

1. Geospatial Information Aurhotiry of Japan

In this study, the deformation model for the displacements around Mt. Kusatsu-shirane and Mt. Asama developed by Munekane (2020) is reappraised. The model by Munekane (2020) fit the observed displacements relatively well. However, there exists apparent correlations between some model parameters, which suggests the model contains redundant parameters. A current working model consists of 1) a deep dike in the northwest of Mt. Kusatsu-shirane, 2) a deep sill under the western frank of Mt. Asama, and 3) a shallow dike under the western frank of Mt. Asama. It is found that the intensities of 1) and 3) are correlated with the volcanic activities of each volcano.

Keywords: Mt. Ksatsu-Shirane, Mt. Asama, crustal deformation

©2021. Japan Geoscience Union. All Right Reserved.

Volcano monitoring based on InSAR Time-series Analysis

*Satoshi Miura[1], Morishita Yu[2], Yusaku Ohta[1], Tomotsugu Demachi[1], Micaela Colavita[1]

1. Graduate School of Science, Tohoku University, 2. Geospatial Information Authority of Japan

The Centre for the Observation and Modelling of Earthquakes Volcanoes and Tectonics (COMET), in the UK conducts the Looking Inside the Continents from Space (LiCS) project, which primarily aims at understanding how the continents deform at all spatial and temporal scales, with a focus on using observations of the earthquake deformation cycle to understand how seismic hazard is distributed in space and time. And the project develops an automated InSAR processing system, LiCSAR (Lazeckýet al., [1]) using the earth observing satellite Sentinel-1 by European Union (EU) and the European Space Agency (ESA). Morishita et al. [2] releases LiCSBAS, an open-source SAR interferometry (InSAR) time series analysis package that integrates with LiCSAR.

All programs of LiCSBAS are written in Python3 and a bash script controls the sequence of the steps such as downloading LiCSAR products, data conversion, down-sampling, propagation delay correction, masking and clipping, quality checking (QC), small-baseline inversion, error estimation, time-series masking, and filtering. It also includes plentiful tools to convert formats among float, GeoTIFF, KMZ, and text, to draw LOS displacement maps and time-series, to calculate 2.5-dimensional displacements (Fujiwara et al., [3]), and so on.

Applying LiCSBAS to Sakurajima volcano for the period from Aug., 2015 to Aug., 2020, the InSAR time-series analyses revealed the uplifting in the area along the NE coast of the island with the maximum rate of about 10 mm/year. Yamamoto et al. [4] derived the similar result using repeated precise leveling for the period from 1996 to 2010 and suggested a model of the pressurized magma reservoir beneath Aira caldera. The other characteristic obtained by the InSAR time-series analyses is the subsidence around the SE frank of the summit, where Morishita et al. [6] retrieved uplifting and eastward displacements due to the magma intrusion event in 2015 based on InSAR analysis and proposed a dike model beneath the Showa crater at a depth of 0.4–1.2 km.

Applying LiCSBAS to Kuchierabujima volcano for the period from 2015 to 2020, extensional LOS displacements are noticeable around the summit area both for ascending and descending tracks and suggesting the subsidence in the area. There have been three major eruptions in the last decade; Aug. 2014 (VEI1), May –Jun., 2015 (VEI3), and Oct. 2018 –Feb. 2019 (VEI3), when the overall eruptive activity resulted in the contractive deformation as mentioned above. The Japan Meteorological Agency reported that the extensional baseline length change started around Oct. 2019 suggesting a deeper pressure source. The InSAR results shows that the subsidence rate around the summit area slows down almost in the same period.

These two application examples suggest that the InSAR time series analysis is useful and effective in volcano monitoring.

References:
[1] Remote Sens. 2020, **12**, 2430; doi:10.3390/rs12152430. [2] Remote Sens. 2020, **12**, 424; doi:10.3390/rs12030424. [3] GRL, 2000, **27**, 2049–2052. [4] BVSJ, 2013, 58, 137-151. [5] GRL, 2016, **43**, 4197-4204.

©2021. Japan Geoscience Union. All Right Reserved.

Keywords: Volcanic activity, InSAR, ground deformation

©2021. Japan Geoscience Union. All Right Reserved.

Evolution of Volcanic Deformation at Domuyo and Laguna del Maule, Southern Andes, Revealed by InSAR Time-series Analyses

*Micaela Colavita[1], Satoshi Miura[1], Yu Morishita[2]

1. Graduate School of Science, Tohoku University , 2. Geospatial Information Authority of Japan

Introduction

“Los Andes” mountain range, in South America, hosts numerous volcanoes that present eruptive and non-eruptive activity. Recently, alarming episodes of unrest at Domuyo and Laguna del Maule volcanic complexes (DVC and MVC respectively) inferred from geophysical observations have been announced. According to Astort et al.[1] (2019), inflation has been recognized at DVC from 2014, while at MVC from 2007, both with rates that surpass 12 cm/year. Here, we follow up on the recent deformation using time-series analyses of InSAR images and estimate the source parameters by applying different models representing the magmatic system.

InSAR time-series analysis

InSAR time series and velocity estimates of surface deformation were obtained using an open-source SAR interferometry (InSAR) analysis package, LiCSBAS (Morishita et al.[2], 2020). It integrates with an automated Sentinel-1 InSAR processor, LiCSAR (Lazecký et al.[3],2020), that produces interferograms using GAMMA SAR and Interferometry software.
The LiCSAR frames processed for both DVC and MVC correspond to the IDs 018A_12668_131313 for the ascending orbit and 083D_12636_131313 for the descending orbit, covering a time interval of about six years, from October 2014 to January 2021, with a total amount of 660 and 835 interferograms, respectively.
From the LiCSBAS analysis for DVC, a large deformation area around the summit was recognized with mean velocity of 10 cm/year as for January 2021, lower than that in the previous studies (e.g. Astort et al.[1], 2019) and that has been almost constant or slowly decreasing since the start of 2020 as shown in the time-series. This could indicate the possible culmination of the period of unrest of the complex. The normalized LOS displacements were divided into four periods based on displacement rates: I) Jan-Dec 2015, II) Jan-Dec 2016, III) Jul 2017-Dec 2018, and IV) Jan-Dec 2019.
For MVC, we also recognize a large circular deformation area surrounding the summit in both the ascending and descending paths, with a mean velocity of ~21 cm/yr. Comparing the temporal evolution of LOS displacements with that of the DVC, we found that MVC presents a continuous growth almost at a constant rate through the years.

Model selection

For source model estimation we used Geodetic Bayesian Inversion Software (GBIS) which allows a rapid characterization of posterior probability density functions (PDFs) of model parameters (Bagnardi and Hooper[4], 2018). LOS displacement data from both satellite tracks were used, assuming different types of source models: point pressure (Mogi[5], 1958), rectangular dipping dike (Okada[6], 1985), prolate spheroid (Yang and Davis[7], 1988), and horizontal rectangular sill (Okada[6], 1985). We treated each of the periods independently and then compared the residuals obtained for each model and conclude that the lowest values were related to the horizontal sill model.

©2021. Japan Geoscience Union. All Right Reserved.

In the case of the DVC, no significant differences in the source locations, length (~10 km) and strike of the sill were found, in contrast with the depths that range between 7.9 and 8.8 km. The volume varies as 21, 41, 30 and 16 $\times 10^6$ m^3 from period I to IV respectively, supporting the assumption of the ending of the DVC episode of unrest due to the decreasing of the values in time.
Although for the MVC the location and depth (7 ±0.1 km) remained almost constant, the volume of the source increased from 25 to 39 $\times 10^6$ m^3. This could not only mean that the source of magma supply does not move but also it increases through time.

References

[1] Remote Sens. 2019, **11**, 2175; doi:10.3390/rs11182175
[2] Remote Sens. 2020, **12**, 424; doi:10.3390/rs12030424
[3] Remote Sens. 2020, **12**, 2430; doi:10.3390/rs121524300
[4] GGG. 2018, **19**, 2194-2211; doi: 10.1029/2018GC007585
[5] Bull. Earthq. Res. Inst. U. Tokyo. 1958, **36**, 99–134
[6] BSSA. 1985, **75(4)**, 1135-1154
[7] JGR: Solid Earth, 1988, **93(B5)**, 4249-4257

Keywords: InSAR, Volcano deformation, Volcanic unrest, Time-series, Source modeling

©2021. Japan Geoscience Union. All Right Reserved.

Evaluation of volcanic activity using "Non-eruptive ground deformation"

*Masato Iguchi[1]

1. Sakurajima Volcano Research Center, Disaster Prevention Research Institute, Kyoto University

Sakurajima volcano is one the active volcanoes in the world. In recent 65 years, it has repeated eruptions at the summit crater of Minamidake and Showa crater 500 m east of the Minamidake since October 1955. The eruptive activity stayed at the Minamidake from 1955 to 2005 with vulcanian eruption, strombolian eruption and continuous ash emission, and then the eruption center was shifted to the Showa crater in 2006. The eruption at the crater was mostly vulcanian type with more frequent, but smaller than the Minamidake crater. At the end of October 2017, the eruption center returned to the Minamidake and the following eruptive activity is divided into 6 episodes; 1) November 2017, 2) January 2018, 3) February –September 2018, 4) October 2018 –July 2019, 5) September 2019 –June 2020 and 6) after August 2020. Sequence of vulcanian eruptivity during the episodes is analyzed based on seismic, ground deformation, infrasound, SO_2 discharge rate and mass eruption rate from ash fall deposit. A characteristic inflation –deflation patter is identified in the ground deformation records. It corresponds to eruptive events (vulcanian type with significant air-shock of >10 Pa and less infrasonic type) with effusion of volcanic ash and non-eruptive phenomena associated with gas emission. Time series of volume change of pressure source inducing non-eruptive ground deformation (NEGD) are examined, comparing with volume change of pressure source by eruptive events, mass eruption of volcanic ash, and discharge rate of SO_2. The episode 5 has the largest number of vulcanian eruption and mass eruption of volcanic ash among the episodes. The sequence of the episode 5 was commenced by an eruption on September 3, 2019 and mostly terminated with a strong eruption, which ejected volcanic bomb up to a distance 3.3 km from the crater, on June 4, 2020. The activity of NEGD events is dominant in the initial stage of the episode and declines accompanying relatively larger ratio of effusion of volcanic ash. This characteristics is shown by partitioning of NEGD events in the total volume change of pressure source and apparent density which is defined by mass eruption of volcanic ash to the total volume change. The gas-rich magma is emitted in the initial stage in September 2019 to February 2020 and ash-rich magma is ejected in the latter stage during the period from March to June 2020. This is supported by SO_2 discharge rate of 2000 –4700 ton/day in the initial stage and 700 - 2600 ton/day in the latter stage. The transition of magma from gas-rich to ash-rich is identified during the episode 3, secondly active.

Keywords: Sakurajima volcano, ground deformation, volcanic gas

©2021. Japan Geoscience Union. All Right Reserved.

The deformation source revealed from leveling surveys in Jigokudani valley, Tateyama volcano, Japan

*Kohei Hotta[1], Shigekazu Kusumoto[2], Hidenori Takahashi[1], Yuichi S. Hayakawa[3]

1. University of Toyama, 2. Kyoto University, 3. Hokkaido University

Leveling surveys have been done in Jigokudani valley, Tateyama volcano, since 2015. Benchmarks, which were set along the walkway of the valley, showed subsidence up to 2.9 cm during the one-year period from September 2019 to September 2020. A dislocation source model by Okada (1992) was applied. Using a grid search method, optimal location, depth, dip, strike, length, width and opening/closing of the dislocation source, which minimize weighted residual sum of square of observation and calculation, were determined. A closing dike was located in southeast area of the valley at a depth of 50 m from surface. Its dip, strike, length, width and closing were 84˚ from horizontal, N128˚E, 300 m, 100 m and 86 cm, respectively. The deflation volume was 25,800 m^3. The location of the dike was near the gas chamber estimated by Seki et al. (2016) from AMT surveys. The dike was directing the Koya Jigoku (fumarolic areas) where the largest subsidence was detected and the new fumarolic areas at east side of the Koya Jigoku. The obtained dike might correspond to the hydrothermal fluid pass from the gas chamber to surface. Recent violent fumarolic activity in these fumarolic areas might lead deflation in the hydrothermal fluid pass. Applying the obtained dike to previous vertical deformation during 2015–2016, 2016–2017, 2017–2018 and 2018–2019, openings of the dike were obtained to be 29 cm, 10 cm, −97 cm and 1 cm, respectively. The deflation due to fumarolic activity started from 2017, but the deflation rate is not constant. This may be caused by changes in fumarolic activities and/or intrusion amount of thermal fluid from deeper level.

This study was supported by the Ministry of Education, Culture, Sports, Science and Technology (MEXT) of Japan, under its Earthquake and Volcano Hazards Observation and Research Program.

Keywords: Jigokudani valley, Tateyama volcano, leveling survey, dislocation source model

©2021. Japan Geoscience Union. All Right Reserved.

Crustal structure around Kikai submarine caldera deduced from gravity anomaly

*Tomoko Hanyu[1], Satoshi Shimizu[1], Hiroto Yamaguchi[2], Yuiko Morita, Nobukazu Seama[2,1]

1. Kobe Ocean-Bottom Exploration Center, 2. Department of Planetology, Graduate School of Science, Kobe University

Kikai caldera submarine volcano is located at south of Kyushu Island, southwest Japan. For imaging the subsurface crustal structure of this caldera, we have conducted the analysis of the gravity anomaly data. Gravity anomaly is cause by the density heterogeneity due to the difference in subsurface structure, therefore the marine gravity data provides an effective information for investigating three-dimensional crustal structure beneath the seafloor.

The free-air gravity anomaly around Kikai caldera was digitized from the free-air gravity anomaly map published by Japan Coast Guard (Onodera et al., 2009). Bouguer anomaly was calculated from free-air gravity anomalies following the method of Parker (1972). The densities of sea-water, sediment, upper crust, lower crust, and mantle were assumed as 1000, 2100, 2700, 3000, and 3300 kg/m^3, respectively. Interface between sea-water and sediment layer was assumed by the acoustic bathymetric data acquired with T/S Fukae-maru, Kobe university. Depth of the interface between upper crustal layer and lower crustal layer, and lower crustal layer and mantle were assumed based on the seismic refraction profile nearby the caldera (Nishizawa et al., 2017). The sediment thickness was not well defined in this area. Bouguer anomalies around Kikai caldera were calculated by subtracting the effects of each interface from the free-air gravity anomalies. Finally, we considered that the bouguer anomalies in this area were caused by the density contrast between the sediment layer and upper crustal layer.

Bouguer anomalies were observed in a range from -5 to 50 mGal around Kikai caldera. Bouguer anomalies with more than 20 mGal were mostly distributed along the caldera rims identified by Tatsumi et al. (2018), indicating the existence of high-density crust or crustal exposure to the seafloor. Bouguer anomalies with less than 15 mGal, which elongated to east-southeast, were observed in southeast area of the rims. Bouguer anomalies with less than 15 mGal were also appeared on whole of the central dome suggested by Tatsumi et al. (2018). The existence of low-density crust, thick sediment, or regional collapse of the crust were implied by the low value of the bouguer anomaly. We will discuss about detailed crustal structure around Kikai caldera in this presentation.

Keywords: Kikai caldera, gravity anomaly, crustal structure

©2021. Japan Geoscience Union. All Right Reserved.

[J] Oral | S (Solid Earth Sciences)：S-VC Volcanology

Fri. Jun 4, 2021 1:45 PM - 3:15 PM JST | Fri. Jun 4, 2021 4:45 AM - 6:15 AM UTC | Ch.25 Zoom Room 25

[S-VC28] Active Volcanism

convener:Yuta Maeda(Nagoya University), Takahiro Miwa(National research institute for earth science and disaster prevention), Takeshi Matsushima(Institute of Seismology and Volcanology, Faculty of Science, Kyushu University), Chairperson:Takao Ohminato(Earthquake Research Institute, Tokyo University), Yuta Maeda(Nagoya University)

This session discusses various aspects of active volcanisms including, but not limited to, rec ent and historical eruptions, various phenomena associated with the volcanic activities, und erground structures of the volcanoes, and developments of new instruments based on geop hysical, geochemical, geological, and multidiscipline approaches. We also welcome studies o n understanding and predicting the transitions of the eruptive activities from observational, theoretical, and experimental approaches.

1:45 PM - 2:00 PM JST | 4:45 AM - 5:00 AM UTC

[SVC28-07] Seismic structural imaging of shallow fluid supply beneath Mt. Ontake

*Yuta Maeda[1], Toshiki Watanabe[1] (1.Nagoya University)

2:00 PM - 2:15 PM JST | 5:00 AM - 5:15 AM UTC

[SVC28-08] Temporal variations in seismic scattering anomalies estimated by inversion of envelope widths of volcano-tectonic earthquakes at Taal volcano, Philippines.

*Miki Hamamoto [1], Hiroyuki Kumagai[1], Rudy Lacson[2] (1.Graduate School of Environmental Studies, Nagoya University, 2.PHIVOLCS (Philippine Institute of Volcanology and Seismology))

2:15 PM - 2:30 PM JST | 5:15 AM - 5:30 AM UTC

[SVC28-09] Attenuation characteristics of Hachijojima Island from twofold spectral ratio method using dense seismic observation

*Utako Watanabe[1], Hiroyuki Azuma[1], Yoshiya Oda[1] (1.Tokyo Metropolitan university)

2:30 PM - 2:45 PM JST | 5:30 AM - 5:45 AM UTC

[SVC28-10] Automatic Detection of First Arrival Time of Seismic Waves with the Fine-tuning: Applying to Observed Datas in Hachijojima

*Hikaru Kunimasa[1], HIROYUKI AZUMA[1], Yoshiya Oda[1] (1.Tokyo Metropolitan University)

2:45 PM - 3:00 PM JST | 5:45 AM - 6:00 AM UTC

[SVC28-11] Moment Tensors of Ring-Faulting at Active Volcanoes: Insights into Vertical-CLVD Earthquakes at the Sierra Negra Caldera, Galápagos Islands

*Osamu Sandanbata[1,2], Hiroo Kanamori[3], Luis Rivera[4], Zhongwen Zhan[3], Shingo Watada[2], Kenji Satake[2] (1.National Research Institute for Earth Science and Disaster Resilience, Ibaraki, Japan, 2.Earthquake Research Institute, the University of Tokyo, Tokyo, Japan, 3.California Institute of Technology, Pasadena, CA, USA, 4.Université de Strasbourg, CNRS, ITES UMR 7063, Strasbourg F-67084, France)

3:00 PM - 3:15 PM JST | 6:00 AM - 6:15 AM UTC

[SVC28-12] The 2019-2020 Nishinoshima activity inferred from seismic and infrasound observations in the island

*Takao Ohminato[1], Atsushi Watanabe[1] (1.Earthquake Research Institute, Tokyo University)

Seismic structural imaging of shallow fluid supply beneath Mt. Ontake

*Yuta Maeda[1], Toshiki Watanabe[1]

1. Nagoya University

1. Introduction

A fluid supply to shallow parts of hydrothermally active volcanoes is a key to understand phreatic eruption and preparation processes. Mt. Ontake has been extensively monitored by a dense network after the 2014 eruption, showing persistent seismicity and deflation. The magma supply system (Takagi and Onizawa 2016; Murase et al. 2016) and shallow resistivity structure (Abdallar and Mogi 2016) of this volcano were investigated, whereas previous seismic structural surveys have mainly focused on base regions (e.g., Ikami et al. 1986; Doi et al. 2013). In this study, we investigate a shallow seismic structure of Mt. Ontake using data after November 2017 when a dense summit station network was established.

2. Analysis

(1) P-wave velocity in the summit region

We first investigate a typical P-wave velocity in the summit region using intermediate-depth earthquakes which occur along the Pacific plate (~250 km deep) beneath Mt. Ontake. The first arrivals of these earthquakes are aligned from lower to higher altitude stations, and this upward propagation for ≧1500 m above sea level (asl.) is best approximated by a P-wave velocity V_p = 2600 m/s based on a semblance analysis, although the value slightly differed among events. This velocity is close to that of the southeastern flank estimated by a refraction survey of Ikami et al. (1986).

(2) A layered structure

We estimated hypocenters of 59 volcano-tectonic earthquakes in November 2017 using grid searches to minimize residuals of P- and S-phase arrival times. We examined three velocity models: (i) a uniform medium of V_p = 2600 m/s based on the analysis (1); (ii) a two-layer horizontally stratified medium of V_p = 2600 and 5900 m/s; and (iii) a three-layer horizontally stratified medium of V_p = 2600, 3900, and 5900 m/s, where we referred to the velocities of second and third layers in the southeastern flank (Ikami et al. 1986). We assumed an S-wave velocity $V_s = V_p/\sqrt{3}$, and conducted grid searches for layer boundary altitudes. The traveltime residuals were smallest when the second boundary is set at 1000 m asl., whereas two candidates for the first boundary (1900 and 2500 m asl.) showed almost equal and smallest residuals. We consider 1900 m to be more plausible because V_p = 2600 m/s is estimated for ≧1500 m asl. in (1).

(3) A reflection profile

We investigated a reflection profile of Mt. Ontake by stacking ambient noise autocorrelations of continuous 1-bit records from November 2017 to May 2020. We used a high-frequency (6-14 Hz) band to obtain high resolution images in shallow parts. The lag times were converted to depths using the velocity model obtained in (2). Results showed relatively intense reflectors down to ~4 km depths at stations close to craters, whereas most other stations show intense reflectors only to several hundred meters.

3. Discussion

The first boundary altitude estimated by (2) is close to that of old (<0.4 Ma) and new (>0.1 Ma) lavas, suggesting that V_p = 2600 and 3900 m/s represent typical velocities of them. At a similar altitude, several stations showed a possible reflector in (3).

The hypocenters estimated in (2) are distributed in 900-2100 asl., which are between deep (> 3000 m)

©2021. Japan Geoscience Union. All Right Reserved.

and shallow (500 m) sources of the deflation after 2014 estimated by Narita and Murakami (2018). The relatively intense reflectors below the craters imaged by (3) are close to this depth range. A possible interpretation to these results may be a fluid migration from the deep to shallow deflation sources, associated seismicity, and resultant cracks which may be seen as the reflectors.

Acknowledgements
This work was supported by JSPS KAKENHI Grant Number JP19K04016, and the Ministry of Education, Culture, Sports, Science and Technology of Japan, under its The Second Earthquake and Volcano Hazards Observation and Research Program. We used data from Japan Meteorological Agency, National Research Institute for Earth Science and Disaster Resilience, Nagano and Gifu Prefectures.

Keywords: Mt. Ontake, Seismic velocity structure, Reflection profile

©2021. Japan Geoscience Union. All Right Reserved.

Temporal variations in seismic scattering anomalies estimated by inversion of envelope widths of volcano-tectonic earthquakes at Taal volcano, Philippines.

*Miki Hamamoto [1], Hiroyuki Kumagai[1], Rudy Lacson[2]

1. Graduate School of Environmental Studies, Nagoya University, 2. PHIVOLCS (Philippine Institute of Volcanology and Seismology)

Volcano-tectonic (VT) earthquakes have frequently occurred at Taal volcano. We analyzed envelope widths (p) of VT earthquakes to investigate scattering and attenuation structures at this volcano. The envelope width is defined by the ratio of the peak amplitude to the cumulative amplitude in a high-frequency (5–10 Hz) envelope waveform. We performed inversion of p values to estimated spatial distributions of mean free path (l_0) and intrinsic attenuation (Q_i) at Taal. One-dimensional (1D) depth-dependent l_0 and Q_i structures were estimated by a previous study with a grid-search approach to fit observed envelope widths to those calculated with Monte Carlo envelope waveform simulations. Using these models as initial models and 224 VT earthquakes during 2011–2017 including those not used by the previous study, we performed inversion of p values with a damped least-squares method to estimate new 1D models, in which partial derivatives with respect to l_0 and Q_i in each layer were calculated with Monte Carlo simulations. Plots of the differences between observed p values and those calculated with the new 1D models (dp) in individual ray paths show that positive and negative values exist beneath a geothermal area in Main Crater and the eastern flank of Volcano Island, respectively. We thus assumed these two anomalies and estimated their l_0 and Q_i values from the new 1D models by inversion of dp values of all VT earthquakes. We also performed inversion of dp values of each earthquake to estimate temporal variations in l_0 and Q_i in the two anomalies. Our inversion results show smaller l_0 values or stronger scattering in the anomaly beneath the geothermal area in Main Crater without their temporal variations. In the anomaly beneath the eastern flank of Volcano Island, we found temporal variations in l_0 values, in which small l_0 values occurred when seismicity was high. This anomaly has been interpreted as an actively degassing magma body, and our estimated temporal variations may be caused by heterogeneous distributions of degassed bubbles and microlites in the magma as follows. An intense supply of volatile-rich magma into the magma reservoir produces stress changes in the surrounding medium, which induce more frequent VT earthquakes. The vesiculated magma with microlites ascends in the conduit, and releases degassed bubbles near the surface. This activates the magma convection in the conduit, and enhances heterogenous distributions of bubbles, microlites, and degassed magma, which result in small l_0 values in the anomaly beneath the eastern flank.

Keywords: Volcano-tectonic earthquake, Taal volcano, envelope width, scattering, inversion

©2021. Japan Geoscience Union. All Right Reserved.

Attenuation characteristics of Hachijojima Island from twofold spectral ratio method using dense seismic observation

*Utako Watanabe[1], Hiroyuki Azuma[1], Yoshiya Oda[1]

1. Tokyo Metropolitan university

In order to interpret volcanic phenomena correctly, it is necessary to understand subsurface structure. Hachijojima Island, the target of this study, is an active volcano being monitored 24 hours a day by JMA. However, the subsurface structure of Hachijojima Island has not been clarified with sufficient resolution. The attenuation characteristics are known to be highly correlated with the properties of magma. In this study, we aim to estimate the attenuation characteristics of Hachijojima Island by using twofold spectral ratio method.

Twofold spectral ratio method removes the source and site amplification characteristics by using multiple earthquake records observed at multiple stations, and extracts path characteristics, attenuation characteristics. The attenuation characteristics estimated by twofold spectral ratio method are average over the entire ray-path. In this study, we estimate the attenuation characteristics between seismic stations by selecting distant earthquakes whose ray-paths are almost same. Earthquake data observed by a dense seismic network of 46 stations in Hachijojima Island during the period 2019 September to 2020 March are used. In this study, we calculated the twofold spectral ratios for 13 station pairs in Nishiyama volcano and 3 pairs of stations in Higashiyama volcano.

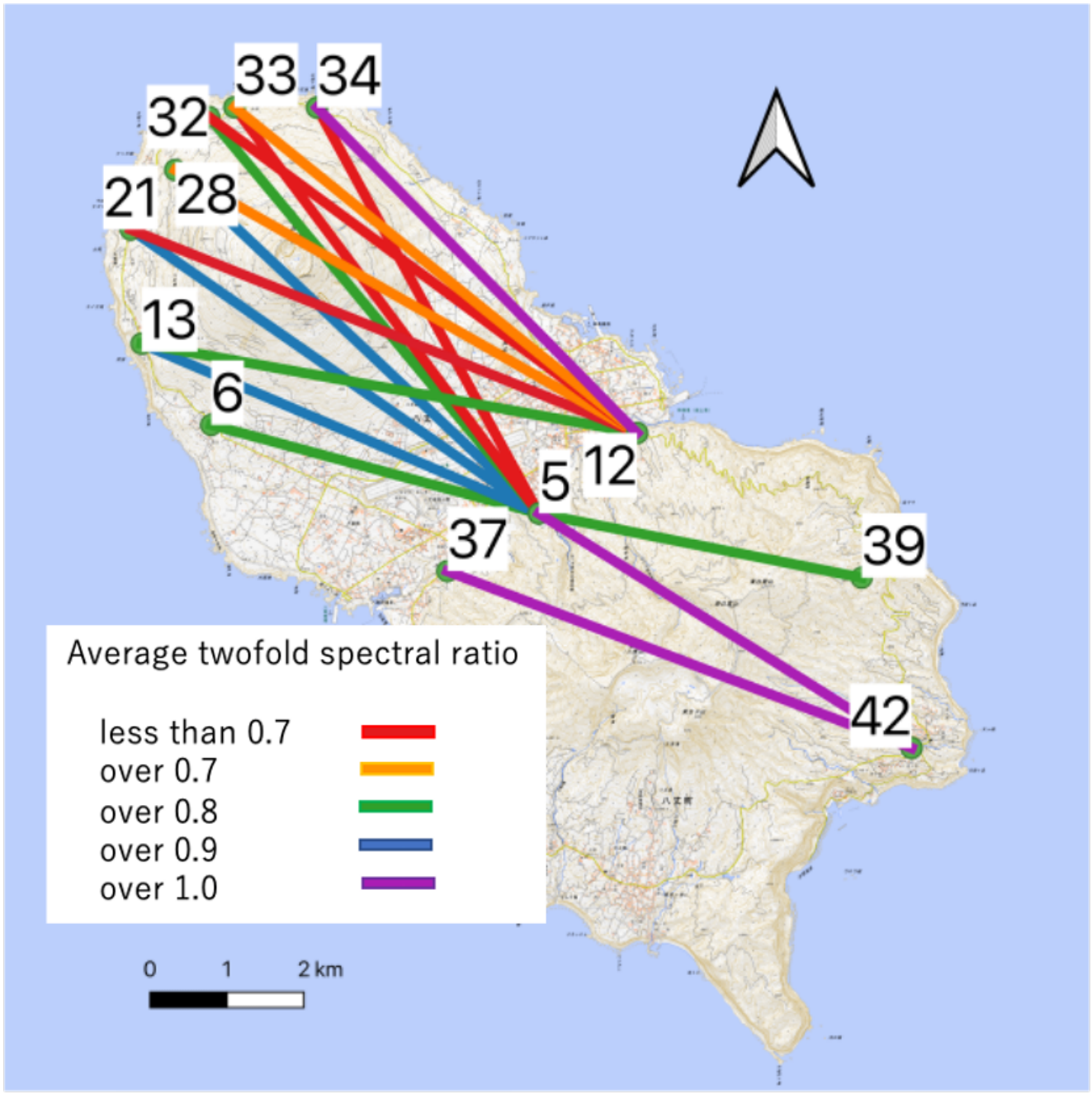
The figure represents average of twofold spectral rations (ATSR) from 3Hz to 10Hz. The numbers in the figure indicate station numbers. As shown in the figure, the ATSR of Mt.Nishiyama is relatively smaller than that of Higashiyama volcano, i.e., the attenuation is larger. This result is consistent with the fact that Nishiyama volcano is more active than Higashiyama volcano in the past 10,000 years.

The low seismic attenuation area is located in the same area as dike intrusion model (Kimata, et al., 2004) and the high seismic attenuation area is situated in the area of tuff cones and tuff rings formed by phreatomagmatic explosions (Sugihara and Shimada, 1998).

The high seismic attenuation regions in Nishiyama and Higashiyama volcanos roughly correspond to the low-velocity region of the velocity structure of Hagiwara and Watanabe (2019).

Keywords: hachijojima Island, attenuation, twofold spectral ratio method

©2021. Japan Geoscience Union. All Right Reserved.



©2021. Japan Geoscience Union. All Right Reserved.

Automatic Detection of First Arrival Time of Seismic Waves with the Fine-tuning: Applying to Observed Datas in Hachijojima

*Hikaru Kunimasa[1], HIROYUKI AZUMA[1], Yoshiya Oda[1]

1. Tokyo Metropolitan University

It was reported that volcanic activity has been getting active near Hachijojima recently (Kimura et al.,2002). In order to evaluate a risk of eruption, it is important to analyze underground structure. Among various techniques for analyzing underground structure, we aim to find understructure by technique using natural earthquake, such as natural earthquake tomography. Hence, we need many and accurate first arrivals of seismic waves generated by natural earthquakes to improve the accuracy of underground structure analysis. However, the number of earthquakes near Hachijojima is small due to low the volcanic activity. Therefore, we try to increase the number of earthquakes to improve the accuracy underground structure analysis.

we focus on deep learning. The recent development of the deep learning is leading innovations in various fields. However, it is necessary for deep learning to prepare a large-scale dataset. It takes vast time to prepare the dataset. In order to solve the problem, we use the method called fine-tuning. The fine-tuning is a method to retrain some parameters of a trained model with a small amount of data and enables to extract the features of that small amount of data efficiently. We aim for the increase of the number of earthquakes by the applications of the method to detection of first arrivals of seismic waves. Moreover, we also aim to make this detection automatically for labor saving.

We installed seismometers to observe seismic waves in Hachijojima. Then, we applied Generalized Seismic Phase Detection with Deep learning (GPD) (Ross et al., 2018) to these waves. GPD is a Convolutional Neural Network (CNN) model that was developed by group of California Institute of Technology. This model can classify waveform datas as P-wave or S-wave, noise.

When we applied GPD to observed waveform datas in Hachijojima, there were a lot of false detections. We thought two factors caused the false detections that GPD classified the waveform data which was not seismic wave as P-wave or S-wave. One is that noise caused by wind and sea wave interferes with observed waveform datas. The other is that the compatibility between the datas used for training of GPD and observed waveform datas.

To solve these problems, we applied fine-tuning for two intentions. One is learning noise waveforms. It could make the number of false detections of GPD small. The other is solving the compatibility between the datas used training for GPD and observed waveform datas in Hachijojima.
We evaluated the effects of fine-tuning by comparing the results of fine-tuning with manual detections in terms of the number of detections and the accuracy of detection time. As a result, sometimes we could reduce false detections and succeed in highly accurate detections, sometimes we couldn’ t.

Keywords: deep learning, fine-tuning, first arrival time of seismic wave, automatic detection

©2021. Japan Geoscience Union. All Right Reserved.

Moment Tensors of Ring-Faulting at Active Volcanoes: Insights into Vertical-CLVD Earthquakes at the Sierra Negra Caldera, Galápagos Islands

*Osamu Sandanbata[1,2], Hiroo Kanamori[3], Luis Rivera[4], Zhongwen Zhan[3], Shingo Watada[2], Kenji Satake[2]

1. National Research Institute for Earth Science and Disaster Resilience, Ibaraki, Japan, 2. Earthquake Research Institute, the University of Tokyo, Tokyo, Japan, 3. California Institute of Technology, Pasadena, CA, USA, 4. Université de Strasbourg, CNRS, ITES UMR 7063, Strasbourg F-67084, France

Large volcanic earthquakes ($M_w > 5$) with moment tensors (MTs) dominated by a vertical compensated-linear-vector-dipole (vertical-CLVD) component are sometimes generated by dip slip along a curved ring-fault system, which is often called *ring-faulting*. Ring-faulting causing vertical-CLVD earthquakes are known to be often associated with volcanic unrests at volcanic calderas (Shuler *et al.,* 2013, JGR). However, relating their MTs determined from long-period seismic records to ring-fault parameters has proved difficult. The objective of this study is to find a robust way of estimating ring-fault parameters based on their MT solutions obtained from the records.

We first model the MTs of idealized ring-faulting and decompose into three deviatoric components representing the vertical dip-slip (*DS*), vertical strike-slip (*SS*), and vertical-CLVD (*CLVD*) mechanisms, respectively (**Figure**). We then show that the *DS* component is indeterminate from long-period seismic waves owing to its little seismic excitation at a very shallow source depth (< ~5 km) (Kanamori & Given, 1981, PEPI), whereas the *SS* and *CLVD* components are resolvable from long-period seismic waves. Considering the limited resolvability of the MT, we propose a new method for estimating ring-fault parameters using the two resolvable components. The arc angle of ring fault can be inferred from the dominancy of the *CLVD* component, whereas the ring-fault orientation can be constrained from the azimuth of the tension- or pressure-axis of the *SS* component.

For validation, we study a vertical-CLVD earthquake (M_w 5.5 on October 22, 2005 in UTC) that occurred during the 2005 volcanic activity at the Sierra Negra caldera, Galápagos Islands. We conduct the MT inversion using long-period (80–200 s) seismic data at far-field (epicentral distance: 12.6˚–46.6˚). Even when we change the source location and depth, the *SS* and *CLVD* components are stably estimated, whereas the estimation of the *DS* component is quite unstable. This confirms the resolvability of the *SS* and *CLVD* components from the far-field long-period seismic data. By considering the two resolvable components, we estimate the ring-fault parameters, i.e., the arc angle and the orientation of ring fault, which are consistent with those identified by previous geodetic studies and field surveys. We also consider ring-fault parameters of two recent vertical-CLVD earthquakes (M_w 5.3 on June 26, 2018; M_w 5.1 on July 5, 2018) that took place during the 2018 activity at the caldera, revealing significant differences between the two earthquakes in terms of slip direction and location.

These results show the usefulness of our method for estimating ring-fault parameters of vertical-CLVD earthquakes, which enables us to examine the kinematics and structures below active volcanoes with ring faults that are distributed globally. A better understanding of such vertical-CLVD earthquakes will provide insights into rock-fluid interactions between fault systems of volcanic edifices and magmatic processes, potentially leading to assessments of volcanic hazards. We also discuss the insufficient seismic excitation

©2021. Japan Geoscience Union. All Right Reserved.

property of the ring-faulting at a shallow depth, and possible biases to the MT inversion caused by an isotropic source occurring nearby the ring-faulting.

Keywords: caldera, volcanic earthquake, ring fault, moment tensor

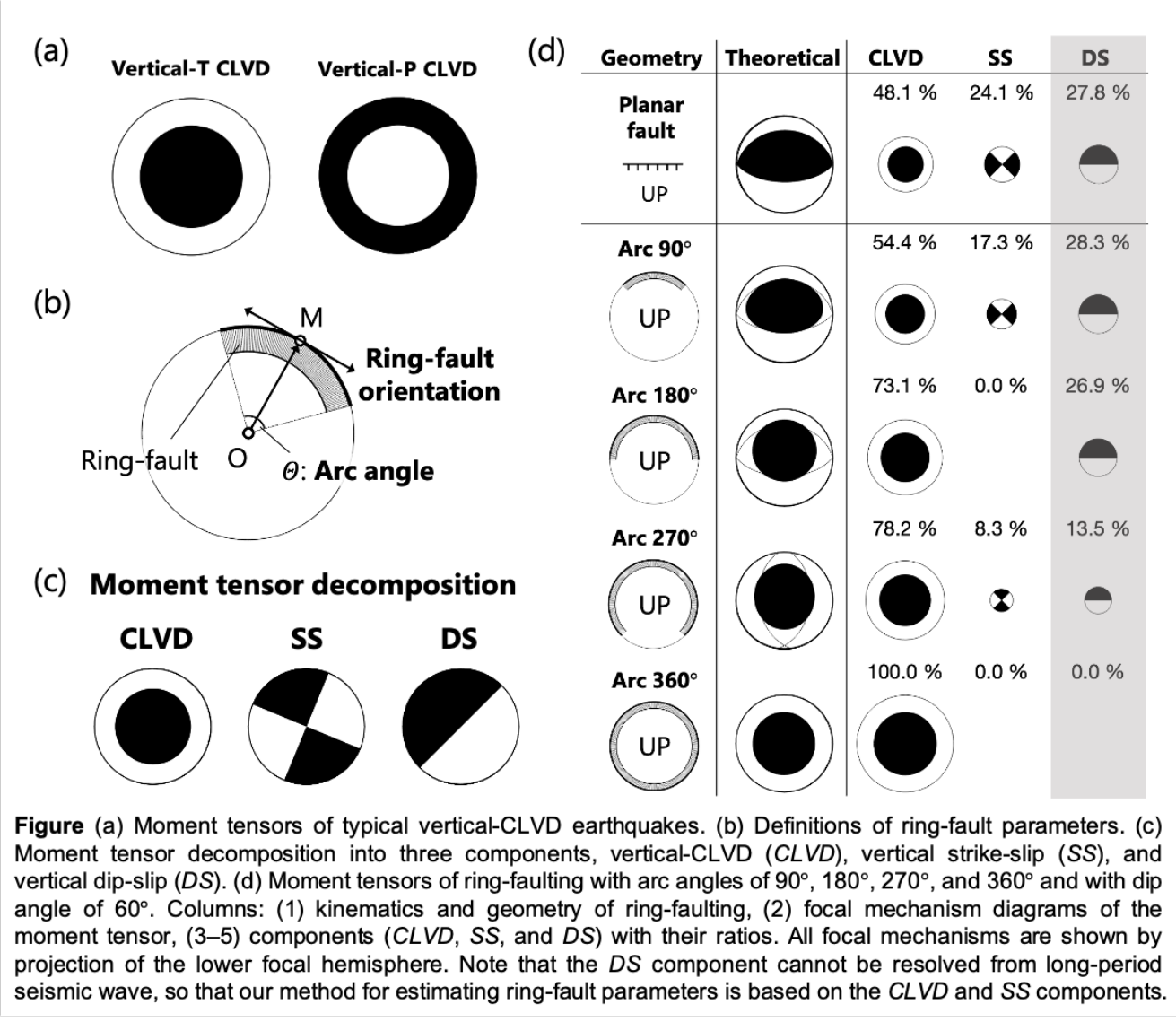


Figure (a) Moment tensors of typical vertical-CLVD earthquakes. (b) Definitions of ring-fault parameters. (c) Moment tensor decomposition into three components, vertical-CLVD (*CLVD*), vertical strike-slip (*SS*), and vertical dip-slip (*DS*). (d) Moment tensors of ring-faulting with arc angles of 90°, 180°, 270°, and 360° and with dip angle of 60°. Columns: (1) kinematics and geometry of ring-faulting, (2) focal mechanism diagrams of the moment tensor, (3–5) components (*CLVD*, *SS*, and *DS*) with their ratios. All focal mechanisms are shown by projection of the lower focal hemisphere. Note that the *DS* component cannot be resolved from long-period seismic wave, so that our method for estimating ring-fault parameters is based on the *CLVD* and *SS* components.

©2021. Japan Geoscience Union. All Right Reserved.

The 2019-2020 Nishinoshima activity inferred from seismic and infrasound observations in the island

*Takao Ohminato[1], Atsushi Watanabe[1]

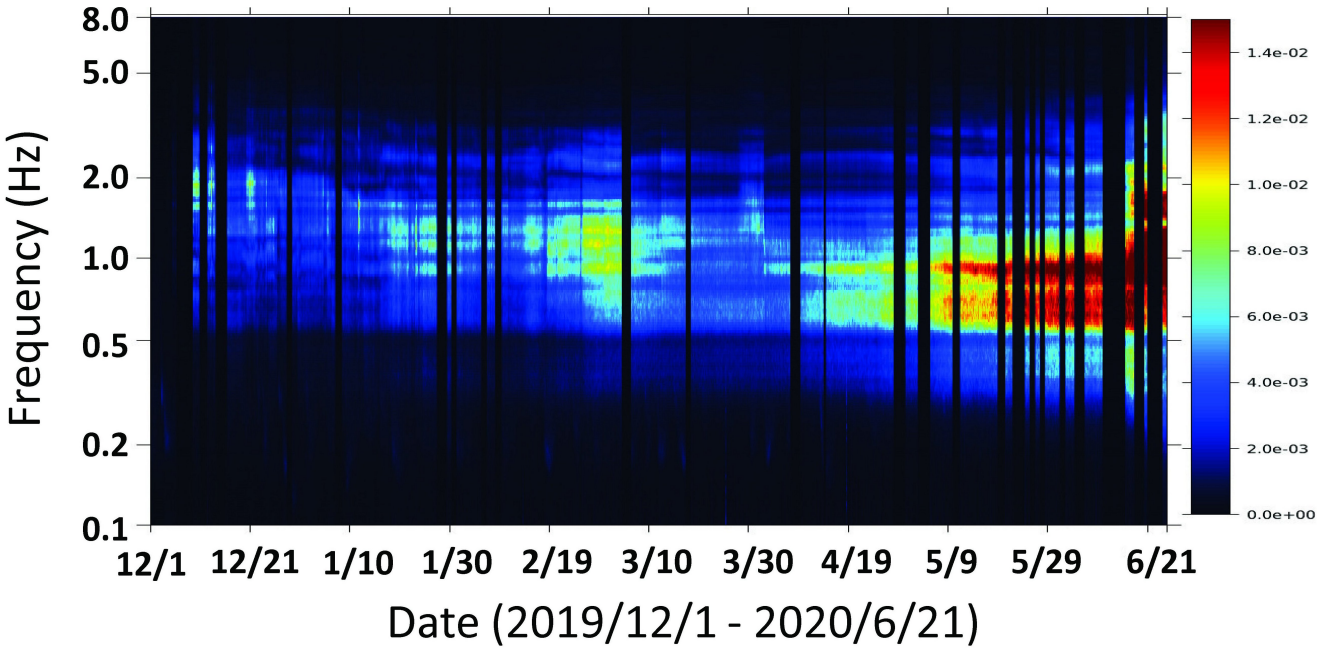
1. Earthquake Research Institute, Tokyo University

On Nishinoshima Island in Ogasawara Islands, volcanic activity began in November 2013. The activity started as a small submarine eruption and gradually shifted to the activity accompanying lava flow. By October 2014, most parts of the old Nishinoshima were covered by lava flow. The volcanic activity has continued since then, and can be divided into 4 terms: the 2013-2015 activity (1st term), the 2017 activity (2nd term), the 2018 activity (3rd term), and the 2019-2020 activity (4th term).
The first landing survey after 2013 was conducted in October 2016. Geological surveys, ejecta collection, installation of seismic and infrasound sensors, and biological surveys were carried out (Takeo et al., 2018, Maeno et al., 2018). The geophysical observation equipment was buried in the lava flow during the 2nd term activity, but valuable data in the early stage of the 2nd term were obtained.
In September 2019, the "2019 Nishinoshima Comprehensive Academic Survey" was conducted by the Ministry of the Environment. We participated in the landing survey and re-installed seismic and infrasound observation equipment. The fourth phase of activity, which began in December 2019, was dominated by multiple lava runoff, and reached its peak in June-July 2020, followed by a sudden decline at the end of July. The reinstalled equipment recorded the volcanic activity from the beginning of the 4th term to the time when it was swallowed by lava flow. In this report, we introduce the outline of the observation equipment and the characteristics of the seismic and infrasound data observed during the 4th period.
In the 2019 observation, we used almost the same equipment and methods as in the 2016 observation (Watanabe et al., 2017). It is solar-powered, and data is transmitted by satellite communication. Since it is difficult to send all the 80MB of daily data in real-time due to the limitation of costs and power, we decided to send compressed running spectra only. As a result, the daily amount of transmitted data was reduced to about 500 kB. The running spectrum is created daily and sent to Tokyo so that we can get an overview of volcanic activity by the next day. Collection of the unprocessed original waveform is also possible on request.
The 4th-period activity started as following. From around 12:00 on December 4, 2019, the high-frequency components of seismic signal began to increase. Satellite data also confirmed thermal anomalies at night. At this point, the magma is approaching the shallow part, but the magma outflow has not yet started. The seismic amplitude remarkably increased after 4:00 in the early morning the next day. The air-shocks began to occur after 5:00. These observations suggest that a small eruption started at the summit around this time. After 12:00 on December 5, the amplitude and frequency of occurrence of events increased sharply, and a large-amplitude ground shaking accompanied by air-shocks occurred at 16:13. Since the thermal anomaly increased rapidly after 15:00, it is possible that the event at 16:13 was an explosive eruption accompanied by the expansion of the lava flow outlet causing full-scale outflow.
The figure shows the running spectrum of the seismic waveform from December 1st to June 21st. Immediately after the start of the activity, the dominant frequency was 2Hz, but the dominant frequency gradually decreased to 0.5 to 1Hz by early June when the eruption rate began to increase sharply. In middle to late June, the dominant frequency shifted to the high-frequency side. The temporal variation of the eruption rate estimated from satellite data does not necessarily correspond to the temporal change in the seismic amplitude. As for the particle velocity of the horizontal components of the seismic waveform, the high-frequency component of 1.5 Hz or higher consistently points in the direction of the central active vent. The particle motion of the slightly low-frequency component of 0.5 to 1.5 Hz behaves differently. It

©2021. Japan Geoscience Union. All Right Reserved.

pointed slightly south of the central vent initially, and then gradually shifted to pointing to the north-south direction. These observations suggest that the high-frequency components correspond to continuous small eruptions at the central vent, while the lower frequency components may reflect the movement of fluids or pressure sources at depth. In the presentation, we will explain in more detail the transition of the 4th term activity estimated from the earthquake and infrasound waveforms.

Keywords: Nishino-shima, volcanic earthquakes, infrasound, satelite data transmission



©2021. Japan Geoscience Union. All Right Reserved.

[J] Oral | S (Solid Earth Sciences)：S-VC Volcanology

Fri. Jun 4, 2021 3:30 PM - 5:00 PM JST | Fri. Jun 4, 2021 6:30 AM - 8:00 AM UTC | Ch.25 Zoom Room 25

[S-VC28] Active Volcanism

convener:Yuta Maeda(Nagoya University), Takahiro Miwa(National research institute for earth science and disaster prevention), Takeshi Matsushima(Institute of Seismology and Volcanology, Faculty of Science, Kyushu University), Chairperson:Mie Ichihara(Earthquake Research Institute, University of Tokyo), Haruhisa Nakamichi(Sakurajima Volcano Research Center, Disaster Prevention Research Institute, Kyoto University)

This session discusses various aspects of active volcanisms including, but not limited to, rec ent and historical eruptions, various phenomena associated with the volcanic activities, und erground structures of the volcanoes, and developments of new instruments based on geop hysical, geochemical, geological, and multidiscipline approaches. We also welcome studies o n understanding and predicting the transitions of the eruptive activities from observational, theoretical, and experimental approaches.

3:30 PM - 3:45 PM JST | 6:30 AM - 6:45 AM UTC

[SVC28-13] Dike inflation process below Sakurajima volcano during the earthquake swarm of 15 August 2015

*Haruhisa Nakamichi[1] (1.Sakurajima Volcano Research Center, Disaster Prevention Research Institute, Kyoto University)

3:45 PM - 4:00 PM JST | 6:45 AM - 7:00 AM UTC

[SVC28-14] A preliminary report of a pilot experiment for the sustainable repeating seismic experiment in Aira Caldera, Japan.

*Tomoki Tsutsui[1], Takeshi Tameguri[1], Daisuke Miki[1], Masato Iguchi[1], Masanao Shinohara[2] (1.DPRI, Kyoto University, 2.ERI, University of Tokyo)

4:00 PM - 4:15 PM JST | 7:00 AM - 7:15 AM UTC

[SVC28-15] Temporal variation of b value of volcanic earthquakes associated with the 2008-2011 Shinmoe-dake eruption

*Jun Oikawa[1], Yasuhisa Tajima[2] (1.Earthquake Research Institute, University of Tokyo, 2.Nippon Koei)

4:15 PM - 4:30 PM JST | 7:15 AM - 7:30 AM UTC

[SVC28-16] Long-term base level variations of seismic power at Shinmoedake, revealing fluid migration prior to the 2011 and 2018 eruptions

*Mie Ichihara[1], Takao Ohminato[1], Minoru Takeo[1] (1.Earthquake Research Institute, University of Tokyo)

4:30 PM - 4:45 PM JST | 7:30 AM - 7:45 AM UTC

[SVC28-17] Waveform inversion of the ultra-long-period seismic event associated with a ground tilt motion during the eruption of Mt.Kusatsu-Shirane, Japan, on January 23, 2018

*Ryohei Takahashi[1], Yuta Maeda[1], Toshiki Watanabe[1] (1.Graduate School of Environmental Studies, Nagoya University)

4:45 PM - 5:00 PM JST | 7:45 AM - 8:00 AM UTC

[SVC28-18] Resistivity structure of Mt. Motoshirane, Japan, inferred from an audio-frequency magnetotelluric survey

*Honda Asami[1], Wataru Kanda[1], Takao Koyama[2], Shinichi Takakura[3], Yasuo Matsunaga[1], Tatsuji Nishizawa[1], Satoshi Ikezawa[2] (1.School of Science, Tokyo Institute of Technology, 2.Earthquake Research Institute, the University of Tokyo, 3.National Institute of Advanced Industrial Science and Technology (AIST))

Dike inflation process below Sakurajima volcano during the earthquake swarm of 15 August 2015

*Haruhisa Nakamichi[1]

1. Sakurajima Volcano Research Center, Disaster Prevention Research Institute, Kyoto University

An earthquake swarm associated with dike intrusion occurred beneath Sakurajima volcano on 15 August 2015. The hypocenters are distributed at depths of 0.3–1 km and 7:00–10:30, and at depths of 0.3–3 km and 10:30–12:00. At 12:00–24:00, the hypocenters are distributed in shallow and deep clusters at depths of 0.2–1 and 1.5–3.5 km, respectively. The T-axes of the deep cluster are distributed in the NW–SE direction. A 90° rotated pattern of strike-slip faulting is also observed at the deep cluster where the T-axes are distributed in the NE–SW direction. This reflects the change in the stress field due to the dike inflation during the earthquake generation, and indicates that the alteration of stress in the vicinity of the dike due to the dike inflation and VT earthquakes are induced by the stress exceeding the fracture strength of the rock. The results of this study are published in the following paper: Koike, M. and Nakamichi, H. (2021) Dike inflation process beneath Sakurajima volcano, Japan, during the earthquake swarm of August 15, 2015. Front. Earth Sci. doi:10.3389/feart.2020.600223. Please refer to the paper for details.

Keywords: Dike, Earthquake Swarm, Sakurajima Volcano

©2021. Japan Geoscience Union. All Right Reserved.

A preliminary report of a pilot experiment for the sustainable repeating seismic experiment in Aira Caldera, Japan.

*Tomoki Tsutsui[1], Takeshi Tameguri[1], Daisuke Miki[1], Masato Iguchi[1], Masanao Shinohara[2]

1. DPRI, Kyoto University, 2. ERI, University of Tokyo

A pilot experiment for a feasibility study of the sustainable repeating seismic experiments in Aira Caldera is presented. Aira Caldera locates in the south end of Kyushu island, Japan, and hosts Sakurajima Volcano at the south margin. Aira Caldera had erupted on 29ka with huge volume of pyroclastic material, however, the caldera is still active. Active ground deformations have been observed in the margin of the caldera, which suggests activity of the caldera associating with Sakurajima Volcano. Direct monitoring methods are necessary in order to assess level of volcanic activity in the caldera. The repeating seismic experiment has proposed as one of progressive methods to monitor underground volcanic activity of the caldera. Foundation and feasibility of new method is tested through the pilot experiment. The experiment contains airgun shooting as a seismic source in one side of the caldera and a seismic array as the receivers in another side of the caldera. The experiment was successful and provides what is enough for sustainability of the experiment. This research is supported by the safety research fund from Nuclear Regulation Authority.

Keywords: Aira Caldera, Monitoring method, Controlled source seismology

©2021. Japan Geoscience Union. All Right Reserved.

Temporal variation of b value of volcanic earthquakes associated with the 2008-2011 Shinmoe-dake eruption

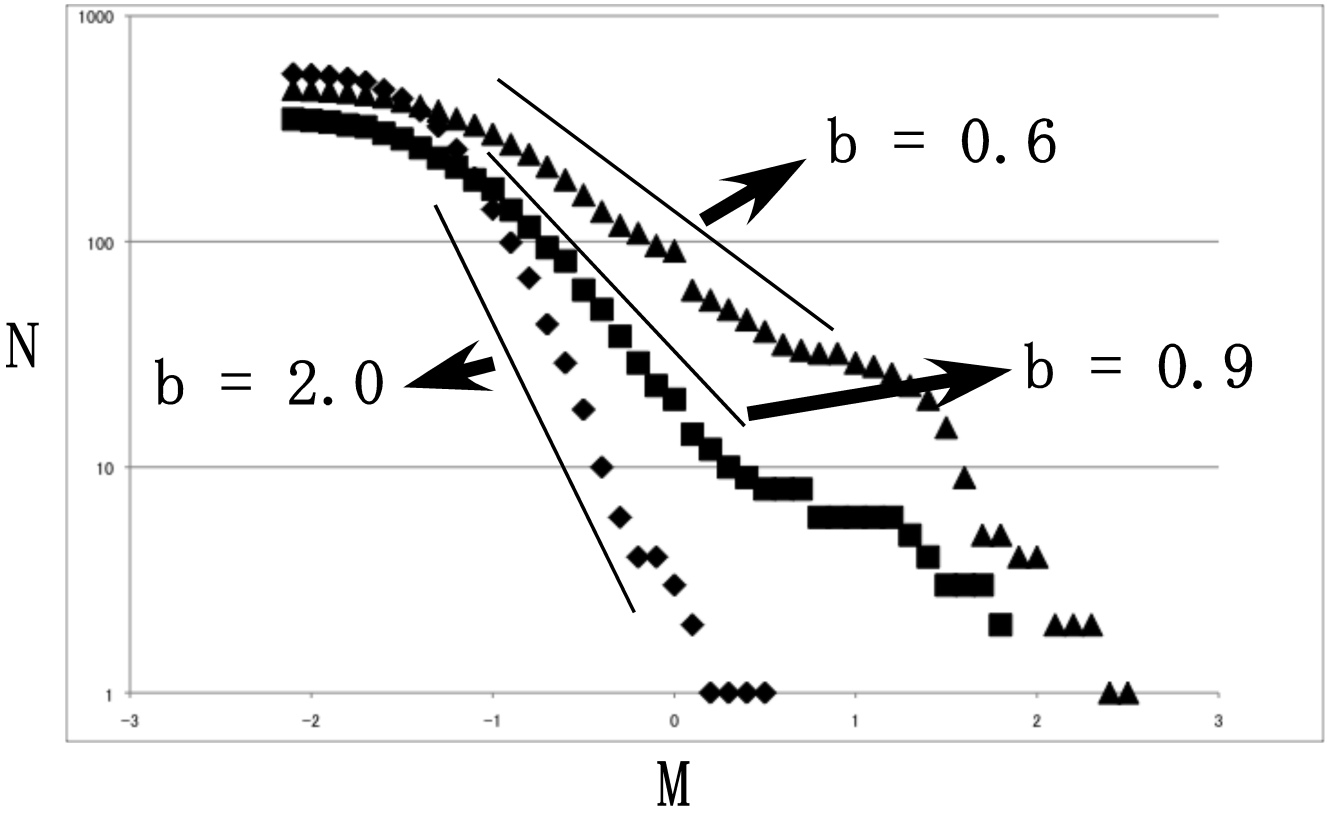
*Jun Oikawa[1], Yasuhisa Tajima[2]

1. Earthquake Research Institute, University of Tokyo, 2. Nippon Koei

The latest eruptive activity of Shinmoe-dake started on August 22, 2008 after 16 years dormancy. Subsequently, it erupted on March 30, April 17, May 27, June 27 and 28, and July 5 and 10, 2010. In 2011, the eruption started on January 19 and was followed by sub-Plinian eruption on 27 January. Eruptive activity gradually ceased since February 2 and moved to Vulcanian activities. It erupted in October 2017 and in March 2018. Eruptions continued until June 27. In this study, we investigate the change in b value for the seismic activity from just before the 2008 eruption to the 2011 eruption and estimate the temporal change in the properties of the region just below the summit crater.
Seismic activity around Shinmoe-dake is low before the 22 August eruption, where a seismic swarm continued since 3 days before the eruption. After the eruption, seismic activity became low, but the activity became higher again in December 2009 and continued until the January 2011 eruption. The figure shows the frequency-magnitude distribution of the earthquakes. The horizontal axis indicates the magnitudes (M) of earthquakes and the vertical axis is the cumulative number of earthquakes larger than M. Solid diamonds represent the seismic swarm before the 2008 eruption. Solid squares represent the seismic activity from just after the eruption to December 2008. Solid triangles show the seismic activity from January 2009 to just before the 2011 eruption. We applied the Gutenberg-Richter’s relation to the data to find b values for each period. The result is as follows: 2.0 just before the 2008 eruption, 0.9 after the eruption until December 2008 and 0.6 after that. This indicates that the volcanic activity field just below the summit crater is significantly different in nature from just before the 2008 eruption and after that. This indicates that the volcanic activity field just below the summit crater is significantly different in nature from just before the 2008 eruption and after that. For example, this difference can be interpreted as the activity to create a passage for volcanic fluid occurred immediately before the eruption, and then the activity occurred in the situation where the passage already existed.

Keywords: b value, volcanic earthquake, volcanic eruption

©2021. Japan Geoscience Union. All Right Reserved.



©2021. Japan Geoscience Union. All Right Reserved.

Long-term base level variations of seismic power at Shinmoedake, revealing fluid migration prior to the 2011 and 2018 eruptions

*Mie Ichihara[1], Takao Ohminato[1], Minoru Takeo[1]

1. Earthquake Research Institute, University of Tokyo

Shinmoedake is an active cone of the Kirishima Volcano Complex. It had two major magmatic eruptions in January 2011 and March 2018 after 300-year quiescence. Over a year before each event, significant inflation was reported from the GNSS observations, of which source was estimated about 7 km to the northwest of the crater and 8-10 km below the sea level (Nakao et al., 2013). Since the 2011 eruption, researchers have searched for other signs of magma migration before the eruptions. The long-term ambient-noise cross-correlation analyses were performed by Nishida et al. (2020) using seismic stations around the volcano. A gradual drop of seismic velocity was observed for one month before the 2011 eruption, but only at one pair of the stations closest to the crater. No significant velocity change was detected with the 2018 eruption. Kurihara et al. (2019) reported an increase of deep low-frequency earthquakes near Shinmoedake in correlation with the inflation before the 2011 eruption. However, they observed no corresponding sign associated with the 2018 eruption, either. On the other hand, the number of low-frequency earthquakes gradually increased while that of high-frequency events decreased at 10 km depth over half a year before the 2018 eruption (Yamada et al., 2019). It is still unclear when and how magma moved to the shallow depth beneath the Shinmoedake crater.

We investigated the long-term baseline variation of seismic power around Shinmoedake. We used the 1-7 Hz frequency bands, which were the main bands of seismic tremors associated with the eruptions (Ichihara and Matsumoto, 2017). Because the data were contaminated by noise from human activity in the daytime, we used two time-windows of 0:00-6:00 and 18:00-24:00 for each day. We collected the lowest 20 percentile of the power in the individual time windows at each station as the baseline.

The baseline variations generally correlated with the precipitation around the volcano. On the other hand, we found gradual increases of the base levels before the eruptions, which dominated the precipitation noises. The increases preceded four months before the 2011 eruption (since October 2010) and about a year before the 2018 eruption (since April 2017). In addition, the base level was high from July 2013 and January 2014, the beginning of which coincided with the restart of the extensions among the GNSS station pairs. As the base-level increases were significant at the closest stations to the crater, we infer that the source was at the shallow depth beneath it. We regard this seismic baseline analysis to reveal clear precursory signs for both the 2011 and 2018 eruptions. Although the same deep source resumed inflating and recovering right after both eruptions, they accompanied no such increase in the seismic powers. The baseline analysis will provide a simple and easy tool for monitoring fluid movement toward an eruption.

Keywords: Volcano, Tremor, Monitoring

©2021. Japan Geoscience Union. All Right Reserved.

Waveform inversion of the ultra-long-period seismic event associated with a ground tilt motion during the eruption of Mt.Kusatsu-Shirane, Japan, on January 23, 2018

*Ryohei Takahashi[1], Yuta Maeda[1], Toshiki Watanabe[1]

1. Graduate School of Environmental Studies, Nagoya University

We conducted waveform inversion of an ultra-long period (ULP; ~240 s) event associated with the phreatic eruption of Mt. Kusatsu-Shirane on 23 January 2018. We used broadband seismic and tilt records from three stations surrounding the eruption site. The horizontal components of the broadband seismic records were severely contaminated by tilt motions. We applied a waveform inversion algorithm that can take both translational and tilt motions into account. To reduce the number of free parameters, we assumed a tensile crack source and conducted grid searches for the centroid location and orientation of the crack. Among the six traces of the horizontal broadband seismic records, one trace (N.KSHV.BN) showed the maximum amplitude at a time different from the others. It is uncertain if this time difference is caused by true volcanic processes. Therefore, we used the following four datasets: (1) all the broadband seismic data (nine traces), (2) broadband seismic data excluding N.KSHV.BN (eight traces), (3) all the broadband seismic and tilt records (15 traces), and (4) all the broadband seismic and tilt records except for N.KSHV.BN. Waveform inversion results from each dataset consisted of two or three local minimum centroid locations with similar residuals between observed and synthetic waveforms, giving a total of 11 candidate sources. However, either the location, orientation, or size of most of these candidate sources was inconsistent with tilt records around active craters, locations of hydrothermal fluids expected from a resistivity structure, volcanically active regions, source depths, or surface crater locations. The most likely source is an N-S opening vertical crack near the eruptive craters. The source time function showed rapid inflation of 105 m3 of the crack, followed by a slow deflation starting at 9-12 s before the eruption onset. An interpretation is that a volcanic fluid migrated from depth to the surface through the estimated crack during the eruption.

This work was supported by JSPS KAKENHI Grant Number JP19K04016. We used data from National Research Institute for Earth Science and Disaster Resilience.

Keywords: ultra-long-period event, waveform inversion, Mt.Kusatsu-Shirane

©2021. Japan Geoscience Union. All Right Reserved.

Resistivity structure of Mt. Motoshirane, Japan, inferred from an audio-frequency magnetotelluric survey

*Honda Asami[1], Wataru Kanda[1], Takao Koyama[2], Shinichi Takakura[3], Yasuo Matsunaga[1], Tatsuji Nishizawa[1], Satoshi Ikezawa[2]

1. School of Science, Tokyo Institute of Technology, 2. Earthquake Research Institute, the University of Tokyo, 3. National Institute of Advanced Industrial Science and Technology (AIST)

Mt. Motoshirane is situated in the northwestern part of Gunma prefecture and is one of the pyroclastic cones of the Kusatsu-Shirane volcano. Its location is about 2 km south from Mt. Shirane, which hosts the Yugama crater. In 2018, some eruptions occurred from the Kagamiike-kita crater of Mt. Motoshirane. The eruptions were sudden phreatic explosions that resulted in casualties.
Since the most activities had occurred in the Yugama crater and its vicinity, few studies were conducted at Mt. Motoshirane. A broadband magnetotelluric (MT) survey carried out before the 2018 eruption revealed a low resistivity zone at a depth of ~2 km, but shallow structures, which include the explosion depths, were not well constrained due to the low-resolution at shallow depths (Matsunaga et al., 2020). X-ray diffraction analysis of the ash sampled of the 2018 eruption suggested that the source depth of the eruption reached the basement rocks (Yaguchi et al., 2019). Geological studies inferred that the basement rocks are exposed around the Kusatsu-Shirane volcano (Hayakawa, 1983). However, there is no information on the depth of the basement rocks below Mt. Motoshirane.
In this study, we conducted an audio-frequency magnetotelluric (AMT) survey to reveal the shallow structures around the craters erupted in 2018 and to clarify the shallow hydrothermal system of Mt. Motoshirane. The survey was conducted from September to October 2020, and five components of the electromagnetic field were measured at a total of 30 locations around the craters of the 2018 eruption. The distribution of apparent resistivity was calculated using det (Re Z), one of the rotational invariants of the impedance tensor, and tended to show high resistivities in the high frequencies and low resistivities in the low frequencies. In particular, some apparent resistivity maps at low frequencies showed low resistivity around the craters of the 2018 eruption.
We used a three-dimensional (3-D) inversion code using tetrahedral meshes (Usui, 2015; Usui et al., 2017) to accurately express the steep topography around the surveyed area. The obtained model was characterized by features similar to the apparent resistivity distribution: high resistivities in the shallow part of the pyroclastic cone and low resistivities in the deep part. To confirm the fitness to the data, we compared the model response function with the observed data using the phase tensor and the induction arrows. The calculated and observed data were consistent at most areas. However, a large difference between them was found on the east flank of the Mt. Motoshirane, which may have been caused by noise originating from man-made objects. We should further examine the data carefully.
In the presentation, we will show the inferred shallow structure of Mt. Motoshirane and interpret it based on the previous studies.

Keywords: Mt. Motoshirane, resistivity structure, audio-frequency magnetotelluric method, phreatic eruption, hydrothermal system

©2021. Japan Geoscience Union. All Right Reserved.

[J] Oral | S (Solid Earth Sciences)：S-TT Technology & Techniques

Fri. Jun 4, 2021 9:00 AM - 10:00 AM JST | Fri. Jun 4, 2021 12:00 AM - 1:00 AM UTC | Ch.18 Zoom Room 18

[S-TT35] Seismic monitoring and processing system

convener:Wataru Suzuki(National Research Institute for Earth Science and Disaster Resilience), Chairperson:Tsunehisa KIMURA(Schlumberger)

This session covers scientific and technical issues in seismic monitoring or data processing systems for earthquakes or explosions observation. This includes development or improvement of seismic observation networks, innovative techniques in observation and monitoring, cutting-edge data acquisition and processing techniques in geophysical explorations. Other topics related to geophysical observation are also welcome.

9:00 AM - 9:15 AM JST | 12:00 AM - 12:15 AM UTC

[STT35-01] Technological innovation of accelerometers with applications to seismometers

*Peiliang Xu[1] (1.Disaster Prevention Research Institute, Kyoto University)

9:15 AM - 9:30 AM JST | 12:15 AM - 12:30 AM UTC

[STT35-02] Concept of fail-safe seismograph with improved reliability

*Shinji SATO[1] (1.Railway Technical Research Institute)

9:30 AM - 9:45 AM JST | 12:30 AM - 12:45 AM UTC

[STT35-03] Extending the Range of Fiber-optic DAS Systems For Seismicity Monitoring

*Martin Horst Karrenbach[1], Victor Yartsev[1], Steve Cole[1], Richard Hooper[1] (1.OptaSense)

9:45 AM - 10:00 AM JST | 12:45 AM - 1:00 AM UTC

[STT35-04] Rapid Progress of Seismic Monitoring System using Optical Fiber and DAS Technology

*Tsunehisa KIMURA[1] (1.Schlumberger)

Technological innovation of accelerometers with applications to seismometers

*Peiliang Xu[1]

1. Disaster Prevention Research Institute, Kyoto University

Seismology is built on three basic disciplines: mathematics, physics and instrumentation. It is certainly true that any interpretations of earthquakes without a master knowledge on mathematics and physics do not make sense but could be nothing more than a story. On the other hand, data used to study the natural phenomena of earthquakes has to depend on seismic instrumentation. In this talk, we will focus on the most fundamental component of instruments for seismometers, namely, accelerometers. Since the first accelerometer was made around 1923 in America and the first strong motion seismometer was produced in 1933 by the National Coast and Geodetic Survey of the US, huge advance in hardware technology has been achieved, with a great number of patents on accelerometers worldwide, in particular, from Japan, the USA and Europe.

Unfortunately, there still exist a number of critical technological problems with accelerometry, which can be summarized as follows:

[1] with the increase of sampling rate, accelerations look like going up and down randomly and with an extremely large amplitude, depending on the noise of the original measurements. In other words, accelerations look like random noise. This phenomenon should be totally unacceptable physically. More precisely, the data from an accelerometer are not physical accelerations but totally random. One of such examples from a strong motion seismometer is shown in Fig. 1 (see Fig. 3 of Xu et al. 2021) in association with the 2013 Lushan Mw6.3 earthquake;

[2] if the sampling rate is sufficiently low, velocity and acceleration signals are distorted, the extent of which depend on that specific rate of sampling; and

[3] no velocimeters and accelerometers can produce correct and physically meaningful values of instantaneous velocity and acceleration for a moving object,

according to the recent patent application on accelerometry by Xu (2021). The same can be said about velocimetry, as also documented in Xu (2021).

In this talk, we will present a regularization method to compute velocity and acceleration and its apparatus, which have been shown to successfully solve the critical technological problems mentioned in the above and documented in the recent research paper by Xu et al. (2021) and a patent application under review by Xu (2021). Our patented research has shown that current technology of accelerometers can result in incorrect values of acceleration by a factor of several hundreds to thousands in terms of peak ground acceleration (PGA), depending on the noise level of the original measurements of accelerometers. An example is shown in Fig. 2 (see also Figs. 2 and 9 of Xu (2021) and Fig. 8 of Xu et al. (2021)). As a result of these researches, we expect a technological revolution in velocimetry and accelerometry. As a by-product or as a direct application of our research, seismometers expect an immediate technological innovation as well to produce physically meaningful raw data of velocity and/or acceleration.

©2021. Japan Geoscience Union. All Right Reserved.

P Xu, F Du, Y Shu, H Zhang, Y Shi (2021) Regularized reconstruction of peak ground velocity and acceleration from very high-rate GNSS precise point positioning with applications to the 2013 Lushan Mw6. 6 earthquake.
Journal of Geodesy 95, article number 17, doi.org/10.1007/s00190-020-01449-6

P Xu (2021) A regularization method to compute velocity and acceleration and its apparatus. Patent submitted on 13 Jan 2021

Keywords: accelerometry, velocimetry, seismometers, regularization, GNSS, waveform reconstruction of acceleration and velocity

©2021. Japan Geoscience Union. All Right Reserved.

P Xu, F Du, Y Shu, H Zhang, Y Shi (2021) Regularized reconstruction of peak ground velocity and acceleration from very high-rate GNSS precise point positioning with applications to the 2013 Lushan Mw6. 6 earthquake.
Journal of Geodesy 95, article number 17, doi.org/10.1007/s00190-020-01449-6

P Xu (2021) A regularization method to compute velocity and acceleration and its apparatus. Patent submitted on 13 Jan 2021

Figure 1: The accelerograms of the strong motion station at YAD, Sichuan, PR China (after Xu et al. 2021)

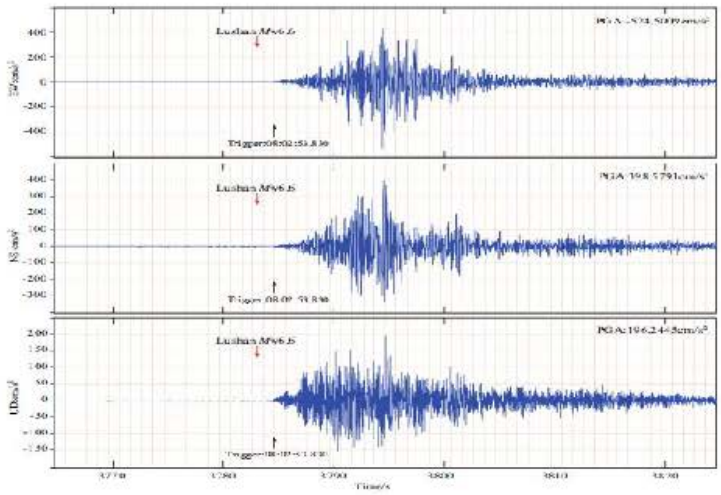
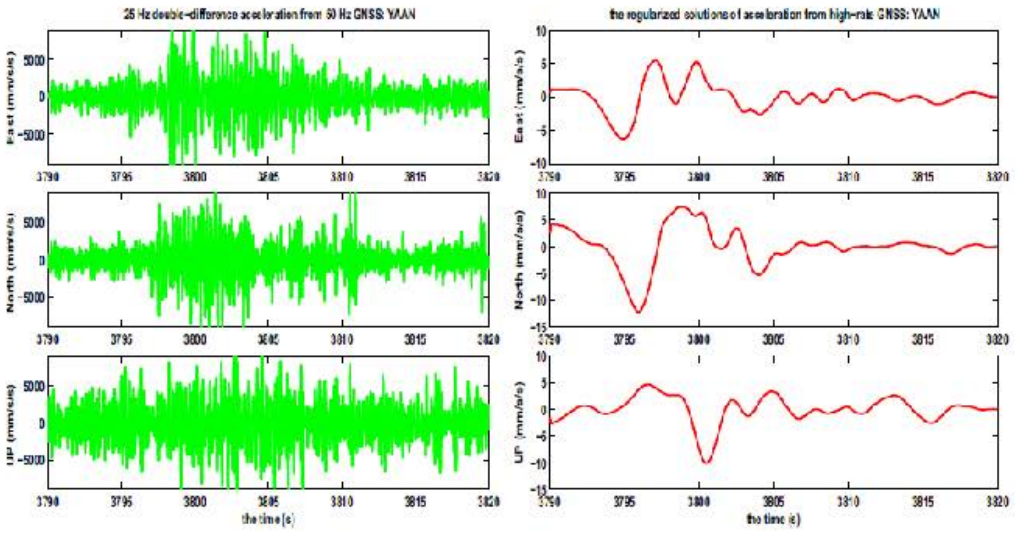


Figure 2: The reconstructed accelerograms from very high-rate GNSS measurements (after Xu et al. 2021 and Xu 2021)



©2021. Japan Geoscience Union. All Right Reserved.

Concept of fail-safe seismograph with improved reliability

*Shinji SATO[1]

1. Railway Technical Research Institute

The Earthquake Early Warning System for Shinkansen developed by the Railway Technical Research Institute in 1992 has observed various earthquakes. This system plays a certain role in ensuring the safety of the Shinkansen. In particular, the electric seismographs installed along the railway lines have the function of making train control decisions based on the earthquake information (epicenter, magnitude, seismic intensity scale, etc.) transmitted from other seismographs.

Currently, this system is using EEW of JMA and NIED’s ocean bottom seismographs in order to improve safety. Improving the reliability of seismographs managed by railway companies is an important issue in order to further enhance the robustness of this system. When the reliability improvement measures were considered to prevent malfunctions and extend the operating time, we decided that the adoption of fail-safe structure for seismograph.

The fail-safe seismograph has the same function as the train control judgment function by detecting P-wave and S-wave of the current seismograph. Since the calculated results are collated at the sampling interval, the information output from the fail-safe seismograph can be said to be highly reliable information. It can be said that not only the reliability of the hardware itself is improved, but also the output information is highly reliable. Currently, the Shinkansen uses a method of stopping trains by power supply cutting at substations. In the future, by connecting to railway signals and wireless train control systems, we believe that it will be possible to support a wider range of train control methods.

In the future, we will consider the details of the specifications and verify that fail-safe work as designed. After that, we plan to conduct test observations at the railway site to confirm whether reliability that exceeds the performance of the current seismograph can be ensured. Furthermore, as the number of parts increases, countermeasures against the cost increase of the seismograph are also an important issue. We plan to work with manufacturers and experts to find out in detail how to achieve high reliability at low cost.

Keywords: EEW, Seismograph, Fail safe, Fault tolerance , High Speed Train

©2021. Japan Geoscience Union. All Right Reserved.

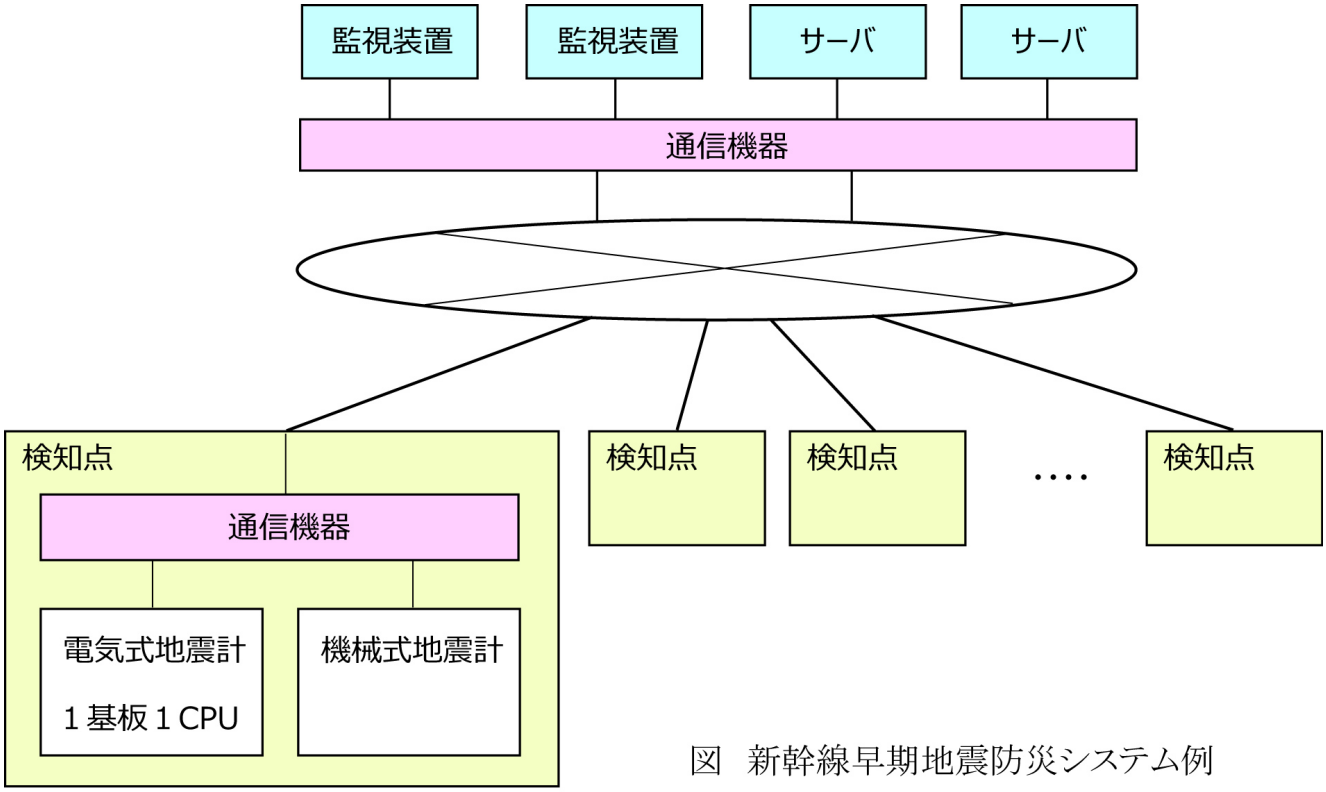


図　新幹線早期地震防災システム例

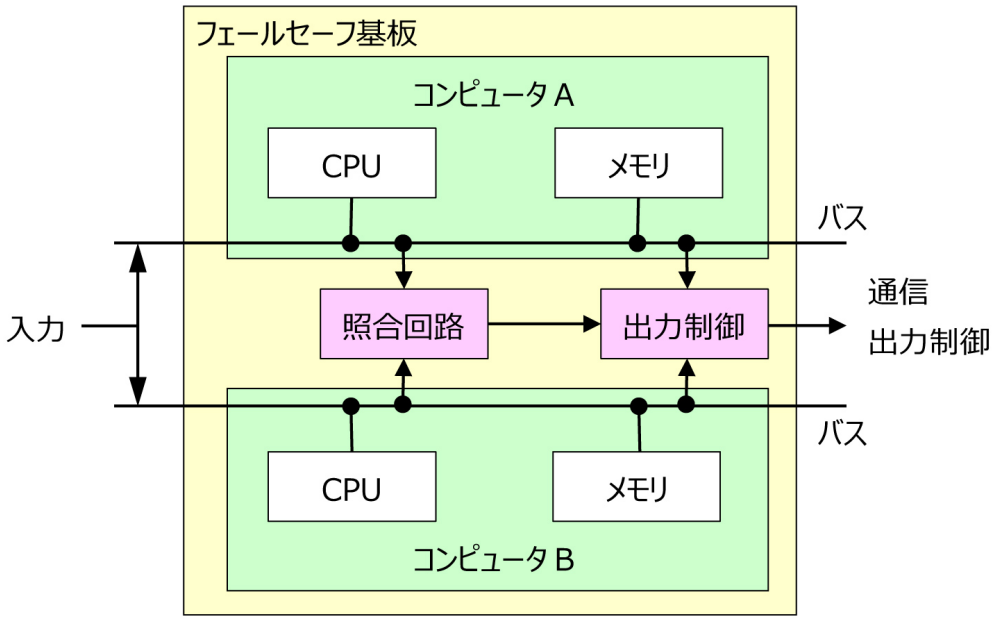


図　フェールセーフ基板の構造例

©2021. Japan Geoscience Union. All Right Reserved.

Extending the Range of Fiber-optic DAS Systems For Seismicity Monitoring

*Martin Horst Karrenbach[1], Victor Yartsev[1], Steve Cole[1], Richard Hooper[1]

1. OptaSense

Recent years show increased use of fiber-optic distributed strain sensing based on Rayleigh scattering for earthquake and induced seismicity measurements. For earthquake monitoring and early-warning often existing fiber-optic cable is used that happens to be installed on existing infrastructure for data transmission purposes. While the sensitivity is lower than compared to purpose-installed dedicate fiber installation, the cost savings are large. Deploying tens of thousands of sensor with the installation of a DAS system at a fiber network location allows to create large-N sensor networks that can enhance sensitivity through beam-forming and other processing techniques.

Typical ranges of current DAS systems have been limited to 30-50km. However, for practical purposes we would like to have larger sensor array lengths with fine sensor spacing, so that we can adapt the sensing geometry to specific detection, warning and scientific measurement purposes. Range-extending DAS technology is an active field of research and applications with circulators or amplifiers have been proposed and being tested. While these are certainly applicable to solve specific range problems, we focus on improving the range an unmodified fiber-optic cable installation. This allows us measure without modification to the installed infrastructure.

In an effort to prove long-range DAS sensing, we acquired seismicity data with a DAS system on an internet data cable on land. We demonstrated that this long-range DAS system is capable of supporting a long and dense sensing array to 100km with a channel spacing of 10m. We show examples of small local and regional earthquakes that were recorded and detected on this ad-hoc 100km sensing array.

Keywords: Distributed Fiber-optic Sensing, seismicity, earthquake, land-based

©2021. Japan Geoscience Union. All Right Reserved.

Rapid Progress of Seismic Monitoring System using Optical Fiber and DAS Technology

*Tsunehisa KIMURA[1]

1. Schlumberger

With the recent development of the Internet and mobile technology, the processing power of various consumer computers, especially data servers, and the capacity to hold data have been remarkably improved. Today, online conferences and lessons are becoming routine tasks, accelerating further advances in data servers. The rapid development of such technology also benefits seismic observations with new methods.

DAS (Distributed Acoustic Sensing) technology, which observes seismic waves using a long-range optical fiber as a distributed vibration sensor, began to be used in the oil and gas industry as a new geophysical exploration technology from around 2011. “heterodyne Distributed Vibration Sensing” (hDVS), which uses backscattered light with improved linearity, began to be used around 2014 [1)]. At the 2017 JpGU-AGU Meeting, we announced the third generation hDVS system completed in the latter half of 2016 [2)]. Compared to the second generation system, the S/N ratio of the data was improved and the data processing capacity was also improved, but the achievement was that the Optical Interrogator in the optical circuit section and the Processing Server in the data processing section were clearly separated, so that it was rationalization efforts. The performance improvement due to this was about double. At the time of 2016, the maximum capacity of one SATA or SAS type 3.5-inch HDD that can be purchased in general was 4TB, and the maximum capacity when eight units were configured in RAID 1 was 16TB. At that time, this amount of data storage was sufficient to record VSP continuously for several days. However, in recent years, the capacity of 16 TB has not been sufficient for one month of continuous recording using a long-distance optical fiber exceeding 10 km.

The clear separation of the optical circuit section and the data processing section, which is the main feature of the third-generation system, made the subsequent development aimed at improving performance relatively easy. The optical circuit section is equivalent to a so-called analog circuit, and its performance can only be improved by improving the coherency and stability of the laser module, speeding up the optical modulation, and improving the optical fiber technology, but the development speed is slow due to unique technology. On the other hand, the data processing unit corresponding to a digital circuit, that is, the server, is not much different from a general-purpose Internet-related server, and is expected to have a rapid improvement in performance due to the demand of high-speed data handlings.

hDVS Tier-3+ is a device that improves only the server part of the third generation system, the data processing capacity is improved by about 4 times, and the maximum capacity of data retention can be increased by 4 times with the advent of large capacity HDD. In other words, we were able to achieve a four-fold improvement in performance in four years. Due to this performance improvement, when the optical pulse rate is set to 1 kHz (1 ms sampling), the performance that can be recorded using a fiber with a length of 100 km can be achieved, which is the theoretical limit of the DAS device. An actual optical fiber has an optical loss, and in the case of a general communication fiber, the typical value of the loss is around 0.2 dB/km. Since the total optical loss that can be handled by current DAS equipment is about 10 dB, the actual limit is about 50 km.

©2021. Japan Geoscience Union. All Right Reserved.

The main improvements of hDVS Tier-3+ are shown below.

a)Achieved the maximum optical limit of about 50 km of the current optical fiber in DAS observation.
b)Observations up to 100 km are possible if the loss of optical fiber can be further reduced.
c)In addition to the standard mode (minimum gauge length 5m), a high-resolution mode has been added (minimum gauge length 1.5m).
d)The gauge length can be set as a parameter with many options from 1.5m to 300m.
e)4 types of high-pass filters can be selected and data in the low frequency range including 0.01Hz can be acquired.
f)By improving the data processing capacity, a higher optical pulse rate can be set and the S/N ratio of the data has improved.
g)Output in HDF5 format is possible in addition to SEGY.
h)Observation is possible at a maximum optical pulse rate of 20 kHz (sampling is possible at a minimum of 0.05 ms).
i)Improved reliability of hDVS Server and reduced noise.

With the advent of hDVS Tier-3 +, it has become possible to make more expansive observations that take advantage of DAS.

References:

1) Hartog, A. et al, The Optics of Distributed Vibration Sensing, 2nd EAGE Workshop on Permanent Reservoir Monitoring, July 2-5, 2013
2) Kimura, T., Progress of Seismic Monitoring System using Optical Fiber and DAS Technology, JpGU-AGU 2017 STT59-04

Keywords: DAS, hDVS, optical fiber, seismic monitoring, earthquake, tsunami

©2021. Japan Geoscience Union. All Right Reserved.

[J] Oral | S (Solid Earth Sciences)：S-CG Complex & General

Fri. Jun 4, 2021 10:45 AM - 12:15 PM JST | Fri. Jun 4, 2021 1:45 AM - 3:15 AM UTC | Ch.23 Zoom Room 23

[S-CG47] Evolution and movement of the crustal surface and application of geo- and thermochronology

convener:Noriko Hasebe(Institute of Nature and Environmental Technology, Kanazawa University), Shigeru Sueoka(Japan Atomic Energy Agency), Hiroyuki Tsutsumi(Department of Environmental Systems Science, Faculty of Science and Engineering, Doshisha University), Takahiro Tagami(Graduate School of Science, Kyoto University), Chairperson:Shigeru Sueoka(Japan Atomic Energy Agency)

The terrestrial earth surface is the habitat of humans and undergoes drastic changes caused by endogenic and exogenic processes. Establishing the chronology of the past changes/episodes is a key to understanding ongoing processes and to predict future physical environments. This session aims at comprehensive understanding of dynamics of the earth's surface, including crustal movements, uplift-denudation processes, and subsequent landform development occurred in various spatio-temporal scales. In addition to the thermochronological approach, it welcomes interdisciplinary studies based on, e.g., tectonic geomorphology, structural geology, geodetic observation, cosmogenic nuclides, numerical calculations, and analogue experiments.

10:45 AM - 11:15 AM JST | 1:45 AM - 2:15 AM UTC

[SCG47-01] Studies of tectonic geomorphology at the northeastern edge of the Tibetan plateau by the dating method with *in situ* terrestrial cosmogenic nuclides

★Invited Papers

*Yoshiki Shirahama[1] (1.Advanced Industrial Science and Technology, Geological Survey of Japan, Research Institute of Earthquake and Volcano Geology, Active Fault Research Group)

11:15 AM - 11:45 AM JST | 2:15 AM - 2:45 AM UTC

[SCG47-02] Denudation process of high-grade metamorphic nappe in eastern Nepal constrained by thermochronological inverse analysis

★Invited Papers

*Nakajima Toru[1], Tetsuo Kawakami[1], Hideki Iwano[2], Tohru Danhara[2], Harutaka Sakai (1.Division of Earth and Planetary Sciences, Graduate School of Science, Kyoto University, 2.Kyoto Fission-Track Co., Ltd.)

11:45 AM - 12:00 PM JST | 2:45 AM - 3:00 AM UTC

[SCG47-03] Toward the reconstruction of the uplift style of a volcanic arc: Insights from apatite fission-track thermochronometry of granitoids in the northern part of the Ou Backbone Range

*Shoma Fukuda[1], Shigeru Sueoka[1], Yuya Kajita[2], Saya Kagami[1], Tatsunori Yokoyama[1], Takahiro Tagami[2] (1.Japan Atomic Energy Agency, 2.Kyoto University)

12:00 PM - 12:15 PM JST | 3:00 AM - 3:15 AM UTC

[SCG47-04] Constraining thermal/denudation histories in the last 0.1 Myr using OSL thermochronometry applied to samples from deep boreholes -A case study in Rokko Mountains-

*Manabu Ogata[1], Georgina E King[2], Frédéric Herman[2], Shigeru Sueoka[1], Ryuji Yamada[3], Kentaro Omura[3] (1.Tono Geoscience Center, Japan Atomic Energy Agency, 2.Institute of Earth Surface Dynamics, University of Lausanne, 3.National Research Institute for Earth Science and Disaster Prevention)

Studies of tectonic geomorphology at the northeastern edge of the Tibetan plateau by the dating method with *in situ* terrestrial cosmogenic nuclides

*Yoshiki Shirahama[1]

1. Advanced Industrial Science and Technology, Geological Survey of Japan, Research Institute of Earthquake and Volcano Geology, Active Fault Research Group

Tibetan plateau has been growing up by the collision between Indian and Eurasian plates and expanding its area laterally. The marginal deformation of the plateau related to the lateral growth formed some major strike-slip faults; Altyn Tagh Fault, Kunlun Fault, and Haiyuan Fault, and many active thrusts and folds around those major faults. Understanding the development and slip rate of these faults and folds is important for revealing the growing process of the northeastern plateau. Due to the cold and dry climate of this region, old topographic surfaces are very well preserved because of the low erosion rate. However, until the 1990s, there were no suitable dating methods available, making quantitative analysis difficult. After the development of the surface exposure dating method using *in situ* terrestrial cosmogenic nuclides (TCN) in the late 1990s, the TCN dating method has been applied broadly to the geomorphological study of this region. The dating method made quantitative analyses to be conductable such as the estimation of average slip rate along the major strike-slip faults and has become an essential tool for the study of tectonics in the Tibetan plateau. This presentation introduces some examples of the applications of TCN in this region, mainly focusing on the author's research in the Kumkol and Gonghe basins, northeastern Tibet.

In the Kumkol basin near the closing area between Altyn Tagh Fault and Kunlun Fault at the northeastern margin of the plateau, there is a huge anticlinorium that consists of many thrusts and folds. The anticlinorium is covered with significantly deformed fluvial or fluvioglacial fans or terraces along the Pitileke river at the eastern part of the anticlinorium. Geomorphological studies and TCN dating for those tectonic landforms were applied to reveal the development and deformation rate of the anticlinorium. The formation age of the oldest terrace, T1 was determined 252 ±24 ka by depth profiling. As a result, the age and deformation of the T1 terrace give a maximum uplift rate of *c.* 1.0 mm/yr and a north-south horizontal shortening rate of 2.5-3.2 mm/yr of the anticlinorium, absorbing a part of shortening between Tibetan plateau and Qaidam basin.

Gonghe Basin, one of the inter-mountain basins at the northeastern margin of the plateau, is about 3200 m above sea level and located at the border of Qinghai Nan Shan and Heka Shan to its north and south, respectively. Previous researches reported that after the Yellow River filled the basin with over 500 m thick clastic sediments, it started to cut it down and formed many fluvial terraces. In order to reveal the filling process, pebbles of quartz were collected at nine points per about 50 m depth in the sediments from the fill top surface to the bottom of the valley, and burial dating by TCN was conducted. The ratio of ^{26}Al concentration to ^{10}Be yields a period since the sample completely shielded from cosmic rays. Calculated burial ages showed in remarkable stratigraphic order from top to bottom, suggesting an average deposition rate of about 70 mm/kyr. The fact indicates that the basin had been constantly filled since the late Miocene.

Keywords: tectonic geomorphology, active fault, in situ terrestrial cosmogenic nuclide, surface exposure dating, Tibetan plateau

©2021. Japan Geoscience Union. All Right Reserved.

©2021. Japan Geoscience Union. All Right Reserved.

Denudation process of high-grade metamorphic nappe in eastern Nepal constrained by thermochronological inverse analysis

*Nakajima Toru[1], Tetsuo Kawakami[1], Hideki Iwano[2], Tohru Danhara[2], Harutaka Sakai

1. Division of Earth and Planetary Sciences, Graduate School of Science, Kyoto University, 2. Kyoto Fission-Track Co., Ltd.

The Himalayan ranges are the most typical example of orogenic belt built by continent-continent collision, and a thermochronological method has been widely applied to the high-grade metamorphic rocks distributed in the Himalayas to understand the denudation history of the high-grade metamorphic rocks in collision setting over the geologic time-scale (10^6–10^7 yr). However, the detailed cooling history of the high-grade metamorphic rocks is still unknown, and there is little consensus on a tectonic process which primarily drove the denudation. This is because the thermochronological studies have been focused on the distribution of the cooling age along an elevation profile or an across-strike section of the Himalayas, and another approach is required to reconstruct the cooling history with high temporal-resolution.

In this study, the thermochronological inverse analysis was applied to the Higher Himalayan Crystalline (HHC) nappe and the underlying Lesser Himalayan sediments (LHS) distributed in eastern Nepal to elucidate the denudation process of the high-grade metamorphic rocks in collision setting over the geologic time-scale. New results of systematic fission-track (FT) age dating and FT length measurements of zircon and apatite were utilized in the thermochronological inverse analysis to reconstruct the time-temperature (*t-T*) paths in the temperature range of 60–350˚C. Eight *t-T* paths obtained along the across-strike section in eastern Nepal showed that the cooling process of the HHC nappe is characterized by following three aspects: 1) gradual cooling (<30℃/Myr) followed by rapid cooling (~150℃/Myr) and subsequent gradual cooling (gradual-rapid-gradual cooling: GRG cooling), 2) northward-younging of the timing of the rapid cooling since ca. 9 Ma, 3) gradual cooling followed by < 2 Myr rapid cooling in the frontmost part.

The observed FT ages and *t-T* paths were then compared with the FT ages and *t-T* paths obtained by forward calculations using 3-D thermokinematic models. In this study, following four thermokinematic models were designed to test the tectono-thermal models which have been proposed in the Central and Eastern Himalayas and to constrain the primary factor that drove the denudation in eastern Nepal: 1) The Flat MHT model in which the HHC nappe and the underlying LHS are denudated accompanied with the movement of the plate boundary fault (Main Himalayan Thrust: MHT) showing flat geometry, 2) the Flat-Ramp-Flat MHT model in which the HHC nappe and the underlying LHS are denudated in the same process as the former one, whereas the MHT shows the flat-ramp-flat geometry, 3) the Duplex 01-03 model in which the denudation of the HHC nappe and the underlying LHS are mainly controlled by the focused uplift associated with the growth of the Lesser Himalayan Duplex (the Duplex 01-03 model), and 4) the Splay Fault model in which the movement of the splay fault of the MHT mainly controls the enhanced denudation in the high-mountain range. Only the Flat-Ramp-Flat model could have reconstructed similar *t-T* paths and age distribution patterns which were obtained from inverse analyses. This suggests that the observed FT ages and *t-T* paths from the HHC nappe reflect a denudation process driven by the movement of the MHT showing a flat-ramp-flat geometry. The GRG cooling and the northward-younging of the timing of rapid cooling indicate that the flat-ramp-flat geometry of the MHT was established by ca. 9 Ma and has been stable thereafter. It is assumed that the denudation rate and its spatial distribution pattern have roughly been constant in eastern Nepal since ca. 9 Ma.

©2021. Japan Geoscience Union. All Right Reserved.

Keywords: continental collision zone, Himalayas, thermochronology, fission-track, denudation

©2021. Japan Geoscience Union. All Right Reserved.

Toward the reconstruction of the uplift style of a volcanic arc: Insights from apatite fission-track thermochronometry of granitoids in the northern part of the Ou Backbone Range

*Shoma Fukuda[1], Shigeru Sueoka[1], Yuya Kajita[2], Saya Kagami[1], Tatsunori Yokoyama[1], Takahiro Tagami[2]

1. Japan Atomic Energy Agency, 2. Kyoto University

In arc-trench systems, volcanisms, earthquakes, and orogenesis actively occur derived from the plate subduction. In principle, these deformations can be comprehended by estimating material properties and forces (Fukahata et al., 2019, Chigaku Zassi). However, to estimate responsibilities of crust (i.e., material property), and especially, stresses (i.e., force) are interactable issues, thus, we attempt to estimate stresses as a causal parameter, based on observed deformations under certain hypotheses or constraints such as responsibilities. Volcanic arcs are commonly identified in arc-trench systems, which are supposed to be formed by partial melting of crust due to dehydration of slab and heating of mantle wedges (e.g., Nakajima, 2016, Volc.). On the other hand, the quantitative development of vertical deformations (uplift/denudation) coinciding a volcanic arc formation has been poorly understood so far.

The Northeast (NE) Japan Arc is characterized by typical topographies of an island arc, where the Ou Backbone Range (OBR) is obviously located along the center as a volcanic arc. The formation process of the OBR has been investigated based on stratigraphy (Nakajima, 2013, INTECH), volcanic geology (Yoshida et al., 2013, Geol. Soc. Lon.), and structural geology (Sato, 1994, JGR). Those studies suggested the OBR was supposed to be uplifted rapidly, mainly because of the E-W compressive stress since the Quaternary, however, uplift/denudation histories of the OBR were not uncovered quantitatively. Developments of thermochronology in three decades enabled to quantitatively reconstruct uplift/denudation histories even for low relief mountains like in Japan Islands (Sueoka et al., 2016, Geosci. Front.). Thus, thermochronologic studies have been recently conducted in the NE Japan Arc based on low-temperature thermochronometers, such as apatite fission-track (AFT) (Fukuda et al., 2019, JAES:X) and (U-Th)/He (Sueoka et al., 2017, EPS; Fukuda et al., 2020, EPS) methods. As the latest one, Fukuda et al. (submitted) preformed AFT and apatite (U-Th)/He thermochronometric mapping at intervals of 1-few km across the southern part of the OBR. This study proposed that the OBR has possibly been uplifted in domal on geologic timescales. Hence, such implications of uplift style of the OBR in a typical island arc are expected to provide the deformation model for a general volcanic arc distributed in plate subduction boundaries as well as tectonic histories in the NE Japan Arc. For elucidating the mountain building process of the OBR on the 10^6 yrs. timescale, this study has conducted AFT mapping along the E-W traverses of the northern part of the OBR as a low-temperature thermochronometer (T_c of 90-120˚C: Ketcham et al., 1999, Am. Mineral.), also attempting to quantitatively constrain the uplift model based on the spatial pattern of obtained AFT ages across the OBR.
We newly conducted AFT dating for 7 localities of the Cretaceous-Miocene granitoids collected from the northern part of the OBR. The number of FTs and the U contents in apatites were determined by FT automated counting system (TrackScan Plus Professional) and laser ablation-inductively coupled plasma-mass spectrometer (Analyte G2: ArF 193nm excimer laser + Agilent 7700x: ICP-QMS), respectively, housed in Tono Geoscience Center, JAEA. These samples yielded AFT ages of the range of few tens to several Ma, implying that consistent with AFT data of previous study (Fukuda et al., submitted). Moreover, such younger ages of several Ma probably reflected uplift/denudation by the recent E-W

©2021. Japan Geoscience Union. All Right Reserved.

compressive stress accelerated since 6.5 Ma or 3-2 Ma (e.g., Nakajima, 2013). In this presentation, we will discuss the spatial pattern of AFT ages across the northern part of the OBR, and the uplift model of the overall OBR by integrated with previously reported ages in the south.

Keywords: Low-temperature thermochronology, Volcanic arc, Ou Backbone Range, Fission-track method, Uplift/denudation

©2021. Japan Geoscience Union. All Right Reserved.

Constraining thermal/denudation histories in the last 0.1 Myr using OSL thermochronometry applied to samples from deep boreholes -A case study in Rokko Mountains-

*Manabu Ogata[1], Georgina E King[2], Frédéric Herman[2], Shigeru Sueoka[1], Ryuji Yamada[3], Kentaro Omura[3]

1. Tono Geoscience Center, Japan Atomic Energy Agency, 2. Institute of Earth Surface Dynamics, University of Lausanne, 3. National Research Institute for Earth Science and Disaster Prevention

Optically stimulated luminescence (OSL) thermochronometry is a method for estimating the thermal histories in the ultra-low-temperature domain less than several tens of degree Celcius [1][2][3]. This method enables reconstructing the exhumation histories of a period over which rocks are exhumed by several hundred meters assuming a geothermal field. Application of OSL-thermochronometry is currently limited to regions that have experienced denudation rates higher than 5 mm/yr (assuming a general geothermal gradient in Japan; ~0.03℃/m); luminescence signals saturate before the rocks are exhumed to the surface in slowly-denuding regions. However, constraining the slow cooling histories may be possible if unsaturated samples are obtained from deep boreholes.

We apply OSL-thermochronometry to deep borehole cores drilled at the Rokko Mountains that have experienced moderate denudation rates (0.1-1.0 mm/yr). We used the Kabutoyama core collected by National Research Institute for Earth Science and Disaster Resilience [4][5]. The total length of Kabutoyama core is 1,313 m and we collected the samples at 408, 642, 818 and 1048 m for OSL thermochronometry. In this presentation, we will present the OSL thermochronometry results, and discuss landform development history based on these results and previous studies on uplift and denudation rates.

This study was carried out under a contract with METI (Ministry of Economy, Trade and Industry) as part of its R&D supporting program for advanced research on long-term stability of geological environment.

References:

[1] Herman et al. (2010). Earth and Planetary Science Letters, 297, 183-189.

[2] King et al. (2016). Quaternary Geochronology, 33, 76-87.

[3] Herman and King (2018). Elements, 14, 33-38.

[4] Yamada et al. (2012). Technical Note of the National Research Institute for Earth Science and Disaster Prevention, 371, 27p.

[5] Sueoka et al. (2010). Journal of Geography, 119, 84-101.

Keywords: optically stimulated luminescence, thermochronology

©2021. Japan Geoscience Union. All Right Reserved.

©2021. Japan Geoscience Union. All Right Reserved.

[J] Oral | S (Solid Earth Sciences)：S-CG Complex & General

Fri. Jun 4, 2021 9:00 AM - 10:30 AM JST | Fri. Jun 4, 2021 12:00 AM - 1:30 AM UTC | Ch.25 Zoom Room 25

[S-CG48] Volcanic roots

convener:Naofumi Aso(Tokyo Institute of Technology), Tsuyoshi Iizuka(University of Tokyo), Yohei Yukutake(Earthquake Research Institute, University of Tokyo), Chairperson:Naofumi Aso(Tokyo Institute of Technology), Tsuyoshi Iizuka(University of Tokyo), Yohei Yukutake(Earthquake Research Institute, University of Tokyo)

The magma transport system beneath volcanoes is a key to understand geodynamics and the evolution of the Earth. To understand the deep volcanic roots around the lower crust, including deep magma chambers, we need to integrate studies based on various approaches. For example, deep long-period earthquakes around the Moho beneath active volcanoes are interpreted to relate to magma, and therefore, it is important to investigate their seismicity and focal mechanisms. Physical understanding of these events will guide us to reveal the role of deep long-period earthquakes in the magma transport system. Also, high-resolution seismic or electrical resistivity imaging is essential to understand physical properties at the depths and to visualize the magma transport system. Besides, the petrological and geochemical properties of igneous rocks provide important information on the origin of magma and its evolutionary processes including fractional crystallization, assimilation, and mixing at the deeper part of the crust. In particular, microscale chemical and isotopic analyses of minerals with compositional zoning provide important constraints on the evolution of magma chambers. Also, experimental studies under the pressure and temperature conditions at the mantle wedge are essential for understanding magma generation. We welcome studies to understand volcanic roots from a variety of approaches including but not limited to the methods mentioned above.

9:00 AM - 9:15 AM JST | 12:00 AM - 12:15 AM UTC

[SCG48-01] Transcrustal magmatic mushes - implications for igneous differentiation and the heights of volcano edifices

★Invited Papers

*Jon Blundy[1] (1.University of Oxford)

9:15 AM - 9:30 AM JST | 12:15 AM - 12:30 AM UTC

[SCG48-02] Imaging the fossils of magma supplying system: Electrical resistivity structure of the Mt. Okue batholith

*Ayumu Okubo[1], Koki Aizawa[2], Takeshi Matsushima[2], Agnis Triahadini[1], Yuto Yamamoto[1], Haruto Tanabe[1], Mitsuru Utsugi[3], Ken'ichi Yamazaki[4], Ryokei Yoshimura[4], Shintaro Komatsu[4], Kana Araue[4], Ayako Namigishi[4], Yoshiko Teguri[5], Kaori Tsukamoto[5], Dan Muramatsu[1], Yuto Hayashida, Kosuke Takeishi[5], Miki Ogata[1], Haruna Watanabe[1], Kana Fujimori[1], Naoto Harada[1] (1.Department of Earth and Planetary Sciences, Graduate School of Science, Kyushu University , 2.Institute of Seismology and Volcanology, Faculty of Sciences, Kyushu University, 3.Aso Volcanological Laboratory, Institute for Geothermal Sciences, Graduate School of Science, Kyoto University, 4.Disaster Prevention Research Institute, Kyoto University, 5.JMA)

9:30 AM - 9:45 AM JST | 12:30 AM - 12:45 AM UTC

[SCG48-03] A three-dimensional electrical resistivity model beneath Azumayama Volcano, NE Japan

*Masahiro Ichiki[1], Toshiki Kaida[1], Takashi NAKAYAMA[1], Satoshi Miura[1], Mare Yamamoto[1], Yuichi Morita[2], Makoto Uyeshima[2] (1.Graduate School of Science, Tohoku University, 2.Earthquake Research Institute, The University of Tokyo)

9:45 AM - 10:00 AM JST | 12:45 AM - 1:00 AM UTC

[SCG48-04] Periodic activity of deep low-frequency earthquakes in Meakandake, Nikko and Yakedake

*Ryo Kurihara[1], Kazushige Obara[1] (1.Earthquake Research Institute, The University of Tokyo)

10:00 AM - 10:15 AM JST | 1:00 AM - 1:15 AM UTC

[SCG48-05] The diversity of focal mechanisms of volcanic deep low frequency earthquakes in Northeast Japan caused by spatiotemporal stress pattern

*Genki Oikawa[1], Naofumi Aso[1], Junichi Nakajima[1] (1.Tokyo Institute of Technology)

10:15 AM - 10:30 AM JST | 1:15 AM - 1:30 AM UTC

[SCG48-06] Low-frequency earthquakes in close vicinity of repeating earthquakes in the brittle upper crust of Hakodate, Hokkaido, northern Japan

★Invited Papers

*Keisuke Yoshida[1], Akira Hasegawa[1,2], Shinako Noguchi[2], Keiji Kasahara[2] (1.Tohoku University, 2.Association for the development of earthquake prediction)

Transcrustal magmatic mushes - implications for igneous differentiation and the heights of volcano edifices

*Jon Blundy[1]

1. University of Oxford

Chemical differentiation of igneous rocks in Earth’s crust is viewed traditionally through the prism of melt-rich magma chambers, wherein physical separation of crystals drives change in melt composition. Such crystal fractionation is central to interpretation of igneous geochemistry and crustal structure. Given the centrality of magma chambers to the interpretation of igneous geology it is surprising that geophysical studies of the crust beneath volcanoes find extensive regions of low melt-fraction crustal mush, but no suitably large chambers. As a result petrologists are moving away from the long-standing magma chamber paradigm to a concept of vertically-extensive, transcrustal magmatic systems that for most of their lifetimes exist in a partially molten or mushy state Transcrustal magmatic mushes (or hot zones) have a number of important implications for magma chemistry, the structure of the crust and the heights of volcanic edifices.

Chemical differentiation in hot zones occurs primarily by percolative reactive flow whereby melt chemistry is controlled (or ‘buffered’) by the mineralogy of the volumetrically-dominant crystalline mush through which melts pass, and the associated mineral-melt chemical reactions. Erupted mush fragments (plutonic xenoliths) testify texturally and chemically to such processes. Amphibole, formed by reaction between hydrous melts and clinopyroxene + plagioclase, is a common reaction product in xenoliths from arc volcanoes, accounting for the widespread evidence of ‘cryptic’ amphibole fractionation in arc magmas lacking amphibole phenocrysts.

Melt chemistry becomes fixed at the point at which magma segregates from the hot zone and ascends; this point is termed the ‘launch depth’. Chemically speaking, launch depths represent discrete points in P-T-X space on a multiple-saturation surface that is defined by the hot zone mush mineralogy. Thus, melts do not follow conventional liquid lines of descent (LLD), although LLD and multiple-saturation surfaces are often hard to distinguish chemically. Some magmas ascend from their launch depths to erupt at the surface, whereas others stall en route to form plutons. In both cases, little chemical differentiation occurs following launch, due to the inefficiency of crystal-liquid separation during ascent. However, the ascent path and rate do exercise important controls on magma textures.

Magma launch depth also exercises a first-order control on the heights of volcanic edifices above the surrounding base level. This is due to the density difference between buoyant magma and surrounding crust integrated over the vertical distance from the launch depth to the surface. At 30 well-characterised, long-lived volcanoes from a wide range of locations and tectonic settings (including Japan), the calculated volcanic edifice height points to a launch depth of 6 to 50 km. At each volcano studied the launch depth matches petrological (thermobarometry) and geophysical (seismic tomography, MT) constraints on the depth to the upper surface of the underlying hot zone. Although local factors, such as regional stresses or faults, facilitate magma ascent, over the approximately Myr lifetime of a single volcano, the equilibrium (isostatic) edifice height appears to be maintained. Modification of the volcanic edifice and/or changes in magma launch depth and chemistry perturb the equilibrium volcano height, and may lead to renewed growth. Thus, periods of increased edifice construction may be ascribed to episodes of erosion, deglaciation or sector collapse, or changes to hot zone architecture.

©2021. Japan Geoscience Union. All Right Reserved.

It is observed that, in general, more silicic melts are launched from shallower depths than more mafic melts, consistent with differentiation via percolative flow and the overall layered structure of the continental crust. The greatest (sub-Moho) launch depths are found at ocean islands, where mantle xenoliths have been recorded.

Keywords: Volcanoes, Crustal structure, Chemical differentiation

©2021. Japan Geoscience Union. All Right Reserved.

Imaging the fossils of magma supplying system: Electrical resistivity structure of the Mt. Okue batholith

*Ayumu Okubo[1], Koki Aizawa[2], Takeshi Matsushima[2], Agnis Triahadini[1], Yuto Yamamoto[1], Haruto Tanabe[1], Mitsuru Utsugi[3], Ken'ichi Yamazaki[4], Ryokei Yoshimura[4], Shintaro Komatsu[4], Kana Araue[4], Ayako Namigishi[4], Yoshiko Teguri[5], Kaori Tsukamoto[5], Dan Muramatsu[1], Yuto Hayashida, Kosuke Takeishi[5], Miki Ogata[1], Haruna Watanabe[1], Kana Fujimori[1], Naoto Harada[1]

1. Department of Earth and Planetary Sciences, Graduate School of Science, Kyushu University , 2. Institute of Seismology and Volcanology, Faculty of Sciences, Kyushu University, 3. Aso Volcanological Laboratory, Institute for Geothermal Sciences, Graduate School of Science, Kyoto University, 4. Disaster Prevention Research Institute, Kyoto University, 5. JMA

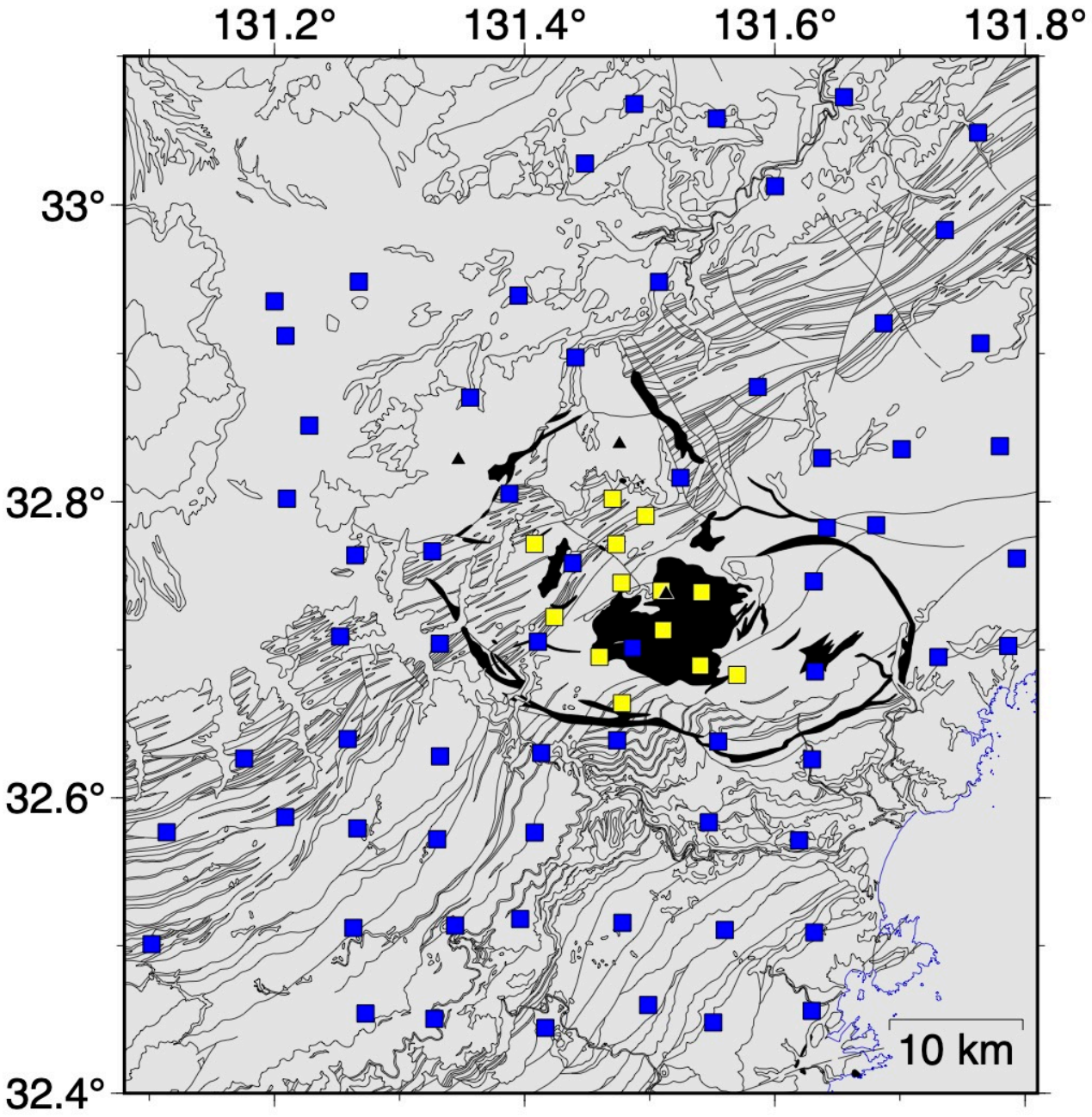
The shape of magma supplying system in the crust has been imagined by many studies. The classic image is that a single or multiple spheroids magma chambers are connected by dikes or narrow magma pathways. On the other hand, recent studies have suggested the magma system extends vertical column-shape in the crust (Cashman et al., 2017). The proposed system is that the majority of magma reservoirs were assumed to be mush state with the crystals content over 40-50 %. Several lenticular magma regions with low crystal content < 40-50 % are connected each other, and are totally surrounded by mush magma region. The mush magma is relatively immobile, while the low crystal content magma is considered to be highly mobile and eruptible. Although the column-like shape electrical conductors are frequently imaged beneath active volcanoes (e.g., Bertrand et al., 2012, 2013; Comeau et al., 2015; Aizawa et al., 2014), it is difficult to judge whether they correspond to the transcrustal ascending magma system or zone of other electrical conductive material, such as volatiles (e.g., Aizawa et al., 2014) and graphite (Bedrosian et al., 2018).
When magma reservoirs are completely solidified, they are imaged as electrical high-resistivity bodies (e.g., Aizawa et al., 2014, Bedrosian et al., 2018). In the area around Mt. Okue, Japan, a granitic batholith and surrounding ring dikes, which intruded 14 Ma and later, are exposed on the surface (Takahashi, 1984). The granitic batholith (33 x 23 km), which is a fossil of a magma reservoir, have little pore space and fracture, and is expected to show electrical high resistivity. The purpose of this study is to image the shape of fossils of the magma supplying system beneath Mt. Okue by estimating the subsurface resistivity structure.
We conducted 84 broadband MT observations around Mt.Okue in 2015, 2017 and 2020. As a preliminary analysis, we estimated the 1-D resistivity structure by using the MT response function (0.003125 s - 3276.8 s) obtained from 84 observations sites. The obtained response function suggest the validity of 1-D assumption up to the period of 1s, which correspond to the surface to the depth of about 5 - 15 km with 10^3 - 10^4 Ωm uniform resistivity. The 1-D structures of 84 sites show that the high-resistivity zone approximately correspond to the area inside of the ring dykes. In particular, the extremely high resistivity zone is located on the western region inside of the ring dykes. These extremely high resistivity zone have the thickness over 15 km, and may be interpreted as the root of the batholith. The zone of seismic swarm is located at the western rim of the high-resistivity zone, while little earthquakes occur inside of the high-resistivity zone. This is consistent with the idea that the high-resistivity batholith is hard to fail, and earthquakes occur around the batholith (Bedrosian et al., 2018). In the presentation, we will show the 3-D resistivity structure.

Acknowledgement
This work is supported by JSPS KAKENHI (JP20K04132), MEXT under its The Second Earthquake and

©2021. Japan Geoscience Union. All Right Reserved.

Volcano Hazards Observation and Research Program, and Earthquake Research Institute Joint Usage Program, the University of Tokyo (C002051).

Keywords: Batholith, Magma supplying system, Resistivity structure, Magnetotellurics method



The black colored areas show the distribution of the batholith and ring dike around Mt.Okue; Blue (in 2015 and 2017) and yellow (in 2020) squares show MT observation sites.

©2021. Japan Geoscience Union. All Right Reserved.

A three-dimensional electrical resistivity model beneath Azumayama Volcano, NE Japan

*Masahiro Ichiki[1], Toshiki Kaida[1], Takashi NAKAYAMA[1], Satoshi Miura[1], Mare Yamamoto[1], Yuichi Morita[2], Makoto Uyeshima[2]

1. Graduate School of Science, Tohoku University, 2. Earthquake Research Institute, The University of Tokyo

We propose a three-dimensional (3-D) electrical resistivity model beneath Azumayama Volcano, NE Japan. The 3-D model shows the conductor beneath Oana Crater indicating magma reservoir. The dimension of the conductor less than 3 Ωm is about 15 km×10 km×10 km. The top depth is about 3 km below sea level. The 67 % and 90 % confidence intervals of resistivity (CIR) for the region less than 3 Ωm are 0.2–5 Ωm and 0.02–70 Ωm, respectively. Two checkerboard resolution tests using 1 Ωm cubes of the side of 3 and 5 km in 1000 Ωm background medium show that the resistivity of 5 km cubes are correctly estimated, while that the resistivity of 3 km cubes are estimated to be 3 to 10 Ωm.

Assuming melt + rock complex, we test whether 67 % CIR is able to be explained quantitatively. In addition, we postulate dacitic melt in shallower part (e.g. 3 to 5 km) and mafic melt in deeper part (e.g. deeper than 5 km). The result is CIR cannot be explained in the shallower part condition even assuming a water-saturated (5.5 wt %) dacitic melt. Thus, we interpret the shallower part conductor consists of dacitic melt-silicic rock-hydrothermal fluid complex. On the other hand, CIR can be estimated by water-saturated (8 wt %) andesitic melt-mafic rock complex.

The Mogi inflation source determined from GNSS and tilt data is located near the top boundary of the conductor at a depth of 2.7–3.7 km (Seki et al., 2021, Q. J. Seismology, under review), which suggests that the ascent of hydrothermal fluids exsolved from the dacitic melt is interrupted by the impermeable roof. Assuming two phases of hydrothermal fluid and silicic rock, the resistivity at the inflation source corresponds to about 5 % of hydrothermal fluid fraction. The 5 % is percolation threshold porosity of effusive eruption (e.g. Colombier et al., 2017 EPSL). This indicates that the percolation threshold porosity characterizes the impermeable roof associated with the Mogi inflation source.

Keywords: magma reservoir, magnetotellurics, electrical resistivity, melt fraction, porosity, percolation threshold

©2021. Japan Geoscience Union. All Right Reserved.

Periodic activity of deep low-frequency earthquakes in Meakandake, Nikko and Yakedake

*Ryo Kurihara[1], Kazushige Obara[1]

1. Earthquake Research Institute, The University of Tokyo

In most volcanic regions, deep low-frequency (DLF) earthquakes occurred at a depth of 10–50 km. Activity patterns of DLF earthquakes are important to understand occurrence mechanisms of the earthquakes. We constructed a catalog of DLF earthquakes in 52 regions all over Japan from April 2004 to December 2018 using matched filter method and grouped based on the classification analysis (Kurihara and Obara, 2020). It was revealed that the temporal seismicity pattern of separated groups classified in each region can be typified as being either episodic or non-episodic. In the groups of episodic activity, swarms of DLF earthquakes sometimes occur. In the group of non-episodic activity, DLF earthquakes constantly occur without seismic rate change. Even in a region, temporal seismicity pattern is different for each group.

In the aspect of the interevent times of DLF earthquakes, periodic activity of DLF earthquakes were observed in episodic activity of Klyuchevskoy volcano in Kamchatka, Russia (Frank et al., 2018) and non-episodic activity of Mauna Kea volcano, Hawaii (Wech et al., 2020). This might be caused by the mechanisms such as second boiling (e.g. Wech et al., 2020). In this study, we investigated interevent times of DLF earthquakes in 52 regions using the catalog of DLF earthquakes.

In result, DLF earthquakes with constant interevent times were observed in the groups of episodic activity in Meakan, Nikko, and Yakedake. In Meakan, DLF earthquakes classified into two groups, Group 1 and Group 2. Episodic activities of DLF earthquakes were observed in both groups. In Group 1, swarms of DLF earthquakes lasted for approximately six months from November 2015 to April 2016 and the lasting period included repeating nine episodes of DLF earthquakes with durations of a few days at an interval of approximately two weeks. Upper limit of the magnitudes of DLF earthquakes in the episodes gradually grew. The interevent times of DLF earthquakes in each episode are larger than 1000 seconds and gradually became shorter and longer in the beginning half and the later half, respectively. In Group 2 of Meakan, each episode had long durations of approximately half a year and the magnitudes and interevent times gradually became larger in each episode.

In Nikko, DLF earthquakes were classified into 7 groups. In Group 1 of Nikko, episodic activities of DLF earthquakes were observed. 6 episodes has the durations of longer than 9 days out of 22 episodes. The interevent times of DLF earthquakes became shorter in the first day of each episode and gradually became longer in the later period.

In Yakedake, DLF earthquakes were classified into 5 groups. In Group 1 of Yakedake, very episodic activities were observed. In this group, DLF earthquakes with interevent times less than 1000 seconds were rarely observed from 2004 to 2018. In other words, periodic activities of DLF earthquakes were observed in each episode.

On the other hand, the characteristic interevent times were only observed in some groups with episodic activity such as Sakurajima except the above three regions. In other words, interevent times were random in other regions and do not have any characteristics unlike the above cases. A large number of DLF

©2021. Japan Geoscience Union. All Right Reserved.

earthquakes were detected in Fuji and they show mixed trend of episodic and non-episodic activity. Durations of most of the episodes in Fuji were less than few hours.
In conclusion, DLF earthquakes with constant interevent times occurred periodically in some episodic groups. On the other hand, DLF earthquakes do not have any characteristics in most groups of most regions which include both of non-episodic groups and episodic groups. Occurrence mechanisms of DLF earthquakes may not be explained by a single mechanism, but rather multiple causes because activity patterns of DLF earthquakes are greatly different from group to group.

Keywords: Deep low-frequency earthquake

©2021. Japan Geoscience Union. All Right Reserved.

The diversity of focal mechanisms of volcanic deep low frequency earthquakes in Northeast Japan caused by spatiotemporal stress pattern

*Genki Oikawa[1], Naofumi Aso[1], Junichi Nakajima[1]

1. Tokyo Institute of Technology

Deep low-frequency earthquakes (LFEs) in Northeast Japan occur actively beneath the active volcanoes at depths of 20–40 km. LFEs radiate low-frequency seismic waves, with most energy at 2–8 Hz, despite their small magnitudes (M < 2). Although many previous studies obtained various focal mechanisms with non-double-couple components and suggested physical process related to fluid movement, the universal physical process is poorly understood. Therefore, we comprehensively determine focal mechanisms of 264 LFEs for 26 volcanic regions in Northeast Japan using the S/P amplitude ratios. In addition, we investigate the relationship between the static stress change of large earthquakes and activity of LFEs by evaluating the similarity between stress tensors and moment tensors of LFEs. We calculate induced stress tensor orientations of both the 2008 Iwate-Miyagi earthquake and the 2011 Tohoku earthquake using “Coulomb 3.3” program (Toda et al., 2005; Lin et al., 2004).
Many of the obtained solutions have large double-couple component with small compensated linear vector dipole component. Considering that we determine focal mechanisms using the initial part of waveforms, this result suggests that the initial rupture process of LFEs is dominated by shear slip on the faults like ordinary earthquakes. Such source mechanisms can be explained by shear slip on the bending fault. We also find that plunge of the Null axis increases from 22º at 20 km depth to 41º at 40 km depth, which indicates that focal mechanisms change from dip-slip type to strike-slip type with depth. The differential stress change in the depth direction may be caused by the depth variation in physical properties such as Poisson’s ratio. In an extreme case of viscous fluid with high Poisson’s ratio, isotropic stress is produced, while in the other extreme case of elastic body with low Poisson’s ratio, the differential stress appears large, which results in the east-west compressional and vertically-tensional stress. With regard to the temporal stress change, we find that activity change and similarity between stress tensors and moment tensors of LFEs have some correlation. Their weak correlation suggests that the seismicity of LFEs is more or less sensitive to temporal stress change.

Keywords: low-frequency earthquakes, focal mechanisms

©2021. Japan Geoscience Union. All Right Reserved.

Low-frequency earthquakes in close vicinity of repeating earthquakes in the brittle upper crust of Hakodate, Hokkaido, northern Japan

*Keisuke Yoshida[1], Akira Hasegawa[1,2], Shinako Noguchi[2], Keiji Kasahara[2]

1. Tohoku University, 2. Association for the development of earthquake prediction

Pore pressure changes at depth affect fault strength and thus play an important role in the generation of earthquakes (e.g. Hubbert & Rubey 1959; Nur & Booker 1972; Rice 1992; Sibson 1992, 2020; Hasegawa 2017). The occurrence of deep low-frequency earthquakes (LFEs) is suggested to be closely related to fluid behaviour (e.g. Ukawa & Ohtake 1987; Hasegawa & Yamamoto 1994; Aso *et al*. 2013). In this study, we conducted a detailed investigation of an earthquake cluster distributed from the lower crust to the upper crust beneath Hakodate, Hokkaido, which included both semi-volcanic low-frequency earthquakes (LFEs) and regular earthquakes.

We first relocated the hypocenters of 212 earthquakes (MJMA 0.0–2.7) listed in the JMA unified catalogue from this region of Hakodate, Hokkaido, for the period from January 2003 to October 2018. Of these earthquakes, 189 and 23 were classified as LFEs and regular earthquakes, respectively, in the JMA unified catalogue. Relocated hypocenters clearly show that both the LFEs and regular earthquakes occurred close to each other in the brittle upper crust of this non-volcanic area, while only LFEs occurred in the lower crust. Inspection of the observed earthquake waveforms has shown that some of LFEs that occur in the shallow upper crust were misclassified as regular earthquakes in the JMA unified catalogue.

The observed differences between LFEs and regular earthquakes might be related to differences in pore pressure and/or fluid volume: larger pore pressure and/or fluid volume for LFEs than regular earthquakes. However, a reduction in effective normal stress alone cannot explain some characteristics of LFE waveforms, including their significant CLVD components and long-lasting high-amplitude codas. These characteristics may be explained by incorporating other fluid effects, such as fluid movement (Hasegawa & Yamamoto 1994), nonlinear self-excited oscillations induced by a fluid flow (Julian 1994), or oscillations of fluid-filled resonators (e.g. Kubotera 1974), which were proposed to explain the characteristics of volcanic long-period (LP) events.

Regular earthquakes that occur in close vicinity of LFEs have very similar waveforms and nearly overlapping source regions, which indicate that they reflect the repeated rupture of the same asperity patch on a fault. Temporally, the intervals between events in the repeating earthquake sequence were very short, thus suggesting that they were caused by a sudden increase in pore pressure. The deep cluster of earthquakes, composed of LFEs, in the lower crust seems to connect with a shallower cluster of earthquakes composed of both LFEs and regular earthquakes. As a whole, the earthquakes have a rod-like distribution extending from the bottom of the crust to near the surface and dipping slightly eastward. This continuous eastward-dipping zone that extends through the entire crust might represent a pathway of aqueous fluids originally sourced from the subducting slab.

Keywords: deep low frequency earthquakes, repeating earthquakes, fluid supply

©2021. Japan Geoscience Union. All Right Reserved.

[J] Oral | S (Solid Earth Sciences)：S-CG Complex & General

Fri. Jun 4, 2021 1:45 PM - 3:15 PM JST | Fri. Jun 4, 2021 4:45 AM - 6:15 AM UTC | Ch.21 Zoom Room 21

[S-CG49] Structure, evolution and deformation of island arcs associated with subduction processes

convener:Masahiro Ishikawa(Graduate School of Environment and Information Sciences Yokohama National University), Masanao Shinohara(Earthquake Research Institute, University of Tokyo), Makoto MATSUBARA(National Research Institute for Earth Science and Disaster Resilience), Tatsuya Ishiyama(Earthquake Research Institute, University of Tokyo), Chairperson:Masahiro Ishikawa(Graduate School of Environment and Information Sciences Yokohama National University), Makoto MATSUBARA(National Research Institute for Earth Science and Disaster Resilience)

Subduction processes such as accretion, back-arc-spreading, and arc-arc collisions have created overall architectures of the Japanese island arc through geologic time. Recent advances in seismic imaging by both passive and controlled source obtained onshore and offshore Japanese islands have successfully provided plenty of new informations on structural, mechanical, rheological and thermal properties of crust and upper mantle that have presumably strongly controls on active tectonics manifested by seismic activities, crustal deformation and other tectonic records in the overriding plate. Our goal in this session is to advance the understanding of overriding plate deformation in various timescales based on state-of-the-art results of observational and modeling studies encompassing both earthquake cycles and tectonic evolution of the Japanese island arc and other plate convergent margins. We welcome contributions from seismology, physical geology, geochemistry, tectonic geomorphology, and numerical and/or analogue geodynamic modeling on deformation processes associated with plate subduction processes and related feedbacks.

1:45 PM - 2:00 PM JST | 4:45 AM - 5:00 AM UTC

[SCG49-01] Cutoff depth and coseismic slip zone for the large earthquake along the Sea of Japan

*Makoto MATSUBARA[1], Tomoko Elizabeth Yano[1] (1.National Research Institute for Earth Science and Disaster Resilience)

2:00 PM - 2:15 PM JST | 5:00 AM - 5:15 AM UTC

[SCG49-02] Stress loading on offshore faults in the Sea of Japan due to the interplate processes along the northwest and southwest Japan arcs

*Akinori Hashima[1], Hiroshi Sato[1], Tatsuya Ishiyama[1], Andrew M. Freed[2], Thorsten W. Becker[3] (1.Earthquake Research Institute, The University of Tokyo, 2.Purdue University, 3.The University of Texas at Austin)

2:15 PM - 2:30 PM JST | 5:15 AM - 5:30 AM UTC

[SCG49-03] Crustal structure characteristics of the Japan Sea revealed by active source seismic survey

*Tetsuo No[1], Takeshi Sato[2], Shuichi Kodaira[1], Hiroshi Sato[3] (1.JAMSTEC, 2.Sapporo Regional Headquarters, JMA, 3.ERI, University of Tokyo)

2:30 PM - 2:45 PM JST | 5:30 AM - 5:45 AM UTC

[SCG49-04] Seismic structure from the forearc region off Miyagi to the central part of Northern Honshu arc, Japan, revealed by onshore-offshore seismic experiment

*Eiji Kurashimo[1], Hiroshi Sato[1], Takaya Iwasaki[2], Takashi Iidaka[1], Tatsuya Ishiyama[1], Masanao Shinohara[1], Hirokazu Ishige[3], Hidehiko Shimizu[3], Shinji Kawasaki[3], Susumu Abe[3], Naoshi Hirata[4] (1.Earthquake Research Institute, the University of Tokyo, 2.Association for the Development of Earthquake Prediction, 3.JGI, Inc., 4.National Research Institute for Earth Science and Disaster Resilience)

2:45 PM - 3:00 PM JST | 5:45 AM - 6:00 AM UTC

[SCG49-05] The upper crustal structure across the central part of the NE Japan Arc revealed from the 2019 onshore seismic refraction/wide-angle reflection profiling

*Takaya Iwasaki[1], Hiroshi Sato[2], Eiji Kurashimo[2], Hirokazu Ishige[3], Hidehiko Shimizu[3], Tatsuya Ishiyama[2], Takashi Iidaka[2], Masanao Shinohara[2], Shinji Kawasaki[3], Susumu Abe[3], Naoshi Hirata[4] (1.Association for the Development of Earthquake Prediction, 2.ERI, the University of Tokyo, Tokyo 113-0032, Japan, 3.JGI, Inc., 4.National Research Institute for Earth Science and Disaster Resilience)

3:00 PM - 3:15 PM JST | 6:00 AM - 6:15 AM UTC

[SCG49-06] **Crust and Mantle Structure of the Tohoku Region from the Viewpoint of Seismic Anisotropy**

★Invited Papers

*Motoko Ishise[1] (1.Earthquake Reseach Institute, University of Tokyo)

Cutoff depth and coseismic slip zone for the large earthquake along the Sea of Japan

*Makoto MATSUBARA[1], Tomoko Elizabeth Yano[1]

1. National Research Institute for Earth Science and Disaster Resilience

1. Introduction

The subduction of the Pacific (PAC) plate from the east makes Japanese Islands under compressional stress. The cutoff depth of the seismogenic zone (D90) is important to estimate the maximum size of the earthquake with the active faults. We relocate hypocenters with three-dimensional (3D) seismic velocity structure using airgun and estimate the cutoff depth of seismogenic zone for the crustal events beneath Sea of Japanese.

2. Data and Method

We relocated 1,918,174 events from October 2000 to December 2019 within 120-150E, 20-50N with 3D seismic velocity structure. We selected events with depths of 0-25 km to be considered as those related to the active faults. We investigated the index D90 as the lower limits of the seismogenic layer defined as the depth above which 90 % of the whole crustal events occurred from the surface. The size of area in which we count earthquake is +/-0.1 degree (approximately 10 km) in case of focusing the active faults and 0.20 degree (approximately 20 km) in case of focusing the area.

3. Result and discussion

We focus four large earthquakes, 2005 West Off Fukuoka prefecture, 2007 Noto-Hanto 2007 Chuetsu-oki, and 2019 Off Yamagata earthquakes. We calculate D90 for each earthquake using the earthquake catalog before the mainshock. Hypocenters determined with 3D seismic velocity structure are shifted to shallower where the shallow low-velocity zones are resolved such as beneath the hypocenters of 2007 Chuetsu-oki and 2019 Off Yamagata earthquakes, however those are shifted to deeper where the shallow zone are not resolved such as 2005 West Off Fukuoka prefecture and 2007 Noto Hanto earthquake. Hypocenter of the 2007 Chuetsu-oki earthquake is at depth of 9 km and coseismic slip zone reached 15 km depth (Aoi et al., 2008). These depths are extremely shallower than D90 as 25 km. The rupture area of the 2019 Off Yamagata prefecture earthquake reached 13 km depth and is above the D90 as 14 km. The hypocenter of the 2007 Noto Hanto earthquake is at 11 km depth and fault zone was estimated to 12 km (Hiramatsu et al., 2008). D90 estimated with hypocenters determined by 1D seismic velocity structure is 11 km however, D90 estimated with hypocenters determined by 3D seismic velocity structure is 12 km. D90 with 3D seismic velocity structure is below the fault zone. The hypocenter of the 2005 West Off Fukuoka prefecture earthquake is at 9 km depth and rupture zone is above the hypocenter. D90 is approximately 13 km

5. Conclusion

We obtain D90 estimated using hypocenters determined with 3D seismic velocity structure below the rupture zone of the large earthquakes beneath the Sea of Japan. It indicates that the D90 estimated using hypocenters determined with 3D seismic velocity structure is important since D90 estimated using 1D seismic velocity structure partly located within the rupture zone.

Keywords: cutoff depth of seismogenic zone, large earthquake, along Sea of Japan

©2021. Japan Geoscience Union. All Right Reserved.

©2021. Japan Geoscience Union. All Right Reserved.

Stress loading on offshore faults in the Sea of Japan due to the interplate processes along the northwest and southwest Japan arcs

*Akinori Hashima[1], Hiroshi Sato[1], Tatsuya Ishiyama[1], Andrew M. Freed[2], Thorsten W. Becker[3]

1. Earthquake Research Institute, The University of Tokyo, 2. Purdue University, 3. The University of Texas at Austin

In the Sea of Japan, several damaging earthquakes occurred such as the 1964 Niigata, the 1983 Sea of Japan, the 1993 Southwest Hokkaido earthquakes. In the coastal region, not only damages from strong motions but also risks of tsunamis are concerned. Recently, the distribution of possible source faults in the Sea of Japan from geophysical explorations. It is important to estimate the stress accumulation on these source faults for assessing seismic risks. In this study, we estimate stress loading due to the dominant interplate process along the Northeast and Southwest Japan arcs using our finite element model. The model is constrained by the data from the dense GPS observation network over the Japanese islands.

In our previous studies, we construct a 3-D finite element model including the Japanese islands. This model consists of the Eurasia, Pacific and Philippine Sea plates. The plate boundaries are determined by the previous studies based on distribution of the interplate earthquakes. The plate boundary shallower than depth of 80 km is divided into ~3000 subfaults to generate Green’ s functions. The model includes viscoelastic property in the asthenosphere to treat the long-term process.

Using the model, we obtain distribution of slip-rate deficit (locking) on the plate boundaries. Then, we calculate the Coulomb stressing rate on the source faults in the Sea of Japan. The long-term locking along the Nankai trough and the Kuril trench have strong influence on the Sea of Japan, resulting in the widely positive Coulomb stressing rate on the source faults along the north coast of from the Kyushu island to the central Japan and along the west coast of Hokkaido, which is bringing those faults forward to rupture. On the source faults along the west coast of Tohoku region, the Coulomb stressing rates was positive before the occurrence of the 2011 Tohoku-oki earthquake, but they have been negative since then. The effect of the Sagami trough is limited but can been seen on the source faults along the coast of Niigata and Hokuriku. In particular, the offshore region along the coast of Niigata and Aomori is transitional zone between the Tohoku-oki earthquake and the locking of the Nankai trough, and between the Tohoku-oki earthquake and the locking of the Kuril trench. It is important to make clear the contribution of their effects and verify them with the seismic activities.

Keywords: Stress loading, Northeast Japan arc, Southwest Japan arc, Source fault, Finite element method, Crustal deformation

©2021. Japan Geoscience Union. All Right Reserved.

Crustal structure characteristics of the Japan Sea revealed by active source seismic survey

*Tetsuo No[1], Takeshi Sato[2], Shuichi Kodaira[1], Hiroshi Sato[3]

1. JAMSTEC, 2. Sapporo Regional Headquarters, JMA, 3. ERI, University of Tokyo

Studies on the characteristics of the entire Japan Sea crustal structure have gradually accumulated (e.g. Ludwig et al., 1975), but surveys of the whole area sea have been slowed, due to issues such as exclusive economic zones and so on. However, some seismic surveys and studies on individual structures such as the Japan Basin, Yamato Basin, and Yamato Bank have been conducted.

We have been studying crustal structure with multichannel seismic reflection (MCS) survey and active source seismic survey using Ocean bottom seismographs (OBSs) from off western Hokkaido to off Tottori through several research projects since 2007. These surveys were carried out using Japan Agency for Marine-Earth Science and Technology (JAMSTEC) research vessels to acquire data with almost identical specifications. Some survey lines were integrated offshore and onshore seismic surveys in collaboration with the Earthquake Research Institute of the University of Tokyo. These studies are important not only for understanding the Japan Sea crustal structure, but also for researching damaging earthquakes along the coast of the Japan Sea and their source faults. Earthquake faults in the Japan Sea are influenced by structures related to the formation of the Japan Sea, such as active faults that originate from inversion tectonics (e.g. Okamura et al., 1995).

Most active faults and shallow seismic activities in the Japan Sea are distributed along the coast of the Japan Sea, in the region where continental crust is formed. However, seismic activity in the last 100 years and active faults off western Hokkaido to off Akita have in some cases been located at the boundary between continental and oceanic crust or in areas where the thickness of the oceanic crust is changing. Damaging earthquakes and source faults in the Japan Sea are not generated and distributed under the same crustal structures, but can be classified into several patterns. Therefore, it is necessary to consider the crustal structure where the faults are formed when studying source faults in the Japan Sea.

Next, we briefly describe the Japan Basin and the Yamato Basin. In the Japan Basin, P-wave velocity structure corresponds to that of standard oceanic crust, and MCS survey results clearly image a reflector that is presumed to be the Moho. Furthermore, reflective surfaces with good spatial continuity are imaged in the crust and uppermost mantle. At the eastern margin of the Japan Basin, shortening structures formed by east-dipping reverse faults are recognized, corresponding to areas of increasing crustal thickness. The Yamato Basin has a crustal thickness of about 12–16 km, which is about twice that of the Japan Basin (Sato et al., 2014, 2018, 2020). There is a high-velocity area with P-wave velocity of more than 7.2 km/s in the lowest part of the crust. The upper part of the crust is about 3 to 5 km thick with a steep velocity gradient, and the lower part of the crust is about 8 to 12 km thick with a slower velocity gradient. The P-wave velocity gradient in the crust approximates the velocity gradient of typical oceanic crust, but the thickness of the lower part of crust is larger than that of the oceanic layer 3. Conversely, the thickness of the crust at the southwestern edge of the Yamato Basin from off Hyogo to off Tottori is about 17 km, and the P-wave velocity structure characteristics in this region are no longer typical of oceanic crust.

Keywords: Japan Sea, Crustal structure, MCS, OBS

©2021. Japan Geoscience Union. All Right Reserved.

©2021. Japan Geoscience Union. All Right Reserved.

Seismic structure from the forearc region off Miyagi to the central part of Northern Honshu arc, Japan, revealed by onshore-offshore seismic experiment

*Eiji Kurashimo[1], Hiroshi Sato[1], Takaya Iwasaki[2], Takashi Iidaka[1], Tatsuya Ishiyama[1], Masanao Shinohara[1], Hirokazu Ishige[3], Hidehiko Shimizu[3], Shinji Kawasaki[3], Susumu Abe[3], Naoshi Hirata[4]

1. Earthquake Research Institute, the University of Tokyo, 2. Association for the Development of Earthquake Prediction, 3. JGI, Inc., 4. National Research Institute for Earth Science and Disaster Resilience

Northern Honshu is a typical island arc with a trench-arc-backarc basin. The 2011 Tohoku-Oki Earthquake (Mw9.0), that occurred on the Japan Trench off the eastern shore of northern Honshu, Japan, generated enormous crustal deformations. Detailed crustal structure and geometry of the fault is important to understand the crustal deformation and the process of earthquake occurrence. In the summer of 2019, an onshore-offshore integrated seismic survey was carried out along a 850 km long profile crossing the central part of Northern Honshu from Japan trench to the Yamato bank (Sato et al., 2020). Sato et al. (2020) presented seismic reflection image and tomography-derived velocity model along the onshore part of the survey line, on which 24 large energy shots and 1,667 receivers were set. Previous studies with use of active sources have revealed the velocity structure beneath the forearc region off Miyagi (e.g., Watanabe et al., 2006). However, seismic structure from the forearc region to Northern Honshu arc has not been resolved, even though this would provide key for understanding the crustal deformation and the process of earthquake occurrence. Onshore recording of the air gun shots is a useful to obtain a structure of the ocean–land transition zone. Twenty-four temporary seismic stations equipped with a 1.0-Hz three-component seismometer were deployed along our onshore survey line. The air gun shots in the forearc side were recorded by these temporary seismic stations. Refraction from the uppermost mantle beneath the forearc region of the Northern Honshu is recognized. Clear reflections from the Moho boundary are also recognized. To obtain the seismic structure from the forearc region to the central part of Northern Honshu, first arrival refraction tomography (Zelt and Barton, 1998) was applied. We picked first arrivals from the air gun shots in the forearc side into temporary seismic stations deployed along our onshore survey line. These arrival data were combined with first arrivals of 24 large energy shots obtained at 1,667 receivers. We also applied the seismic reflection technique to air-gun data recorded by onshore stations to obtain the reflection image beneath the forearc region. The tomography-derived P-wave velocity structure shows that low-velocity zones exist along the estimated deeper extension of the active faults. We obtained a seismic velocity model revealing good correlations with the surface geology along the profile. High-velocity zone (>7.0km/s) can be recognized deeper than ~25km beneath the forearc region of the Northern Honshu. Reflection image shows the reflector interpreted as the Moho beneath the forearc region at ~25 km depth.

Keywords: Northern Honshu, onshore-offshore seismic experiment, seismic tomography

©2021. Japan Geoscience Union. All Right Reserved.

The upper crustal structure across the central part of the NE Japan Arc revealed from the 2019 onshore seismic refraction/wide-angle reflection profiling

*Takaya Iwasaki[1], Hiroshi Sato[2], Eiji Kurashimo[2], Hirokazu Ishige[3], Hidehiko Shimizu[3], Tatsuya Ishiyama[2], Takashi Iidaka[2], Masanao Shinohara[2], Shinji Kawasaki[3], Susumu Abe[3], Naoshi Hirata[4]

1. Association for the Development of Earthquake Prediction, 2. ERI, the University of Tokyo, Tokyo 113-0032, Japan, 3. JGI, Inc., 4. National Research Institute for Earth Science and Disaster Resilience

In 2019, an extensive onshore-offshore seismic expedition was undertaken from the Japan Trench to the Yamato bank across the central part of the NE Japan arc (Sato et al., 2020a). The onshore seismic line in the NE Japan Arc was laid out from the Shonai Plain on the coast of the Sea of Japan to the Kitakami Mountains on the Pacific coast, crossing the Dewa Hills, Shinjo Basin, Ou Backbone Range and Kitakami River Valley from the west to the east. In the western part of the profile (from the Shonai Plain to the eastern boundary of the Shinjo Basin), seismic reflection and refraction/wide-angle reflection surveys were simultaneously carried out under the “Integrated Research Project on Seismic and Tsunami Hazards around the Sea of Japan” funded by MEXT (Sato et al., 2020b). A refraction/wide-angle reflection experiment in the eastern half of the profile, on the other hand, was supported by funds from MEXT under its 2nd Earthquake and Volcano Hazards Observation and Research Program and ERI, the University of Tokyo. The total length of the profile is about 155 km, on which 1,667 receivers were set to record 24 large energy shots. As seismic sources, we used explosives at 3 shot points and 4 vibroseis trucks with 150 stationary sweeps at the other 21 points.

In this paper, we present the first velocity structure model based on the ray-tracing technique. The travel-times from the above 24 shots were highly undulated except beneath the Kitakami Mts. The uppermost part of the crust from these data is composed of 4 layers of Vp=1.6-2.0, 1.8-3.5, 3.5-4.5 and 4.5-5.5km/s, respectively, representing sedimentary and volcaniclastic rocks. Their geometry shows significant change along the profile line. At the boundary of the Shinjo Basin and Dewa Hills, the upper 3 layers abruptly reduce in thickness from 5 to 1 km to the east. This position is almost consistent with the location of the Aosawa fault. In the Ou Backbone Range, the thickness of the above 3 layers is less than 1.5 km, but it again increases to 2-2.5 km beneath the Kitakami River Valley. As in the case of the Aosawa fault, the uppermost parts of the major faults developed around the profile are well correlated to the locations at which the sedimentary part shows abrupt change in thickness. Such complicated structure represents the crustal deformation associated with the Miocene backarc spreading of the Sea of Japan. In Kitakami Mts., on the other hand, the structure is very simple, where the 5.0-5.5 km/s layer is almost outcropped, showing marked contrast with highly deformed crust from the Shinjo Basin to the Kitakami River Valley. Such structural variation of the uppermost crust is well consistent with those from the tomographic analyses by Sato et al. (2020a) and Kurashimo et al. (2021).

The velocity of the crystalline part of the crust is about 5.8 km/s. Although the deeper part of the crust is not modelled as yet, weak arrivals beyond offsets of 40-50 km indicate that the crustal velocity increases to 6.3 km/s around at a depth of 8 km. In some shot records, later phases 0.2-0.5 s appearing behind the first arrivals in an offset range of 40-70 km suggest the existence of some velocity discontinuities within the crust.

References

Kurashimo et al., 2021. Seismic structure from the forearc region off Miyagi to the central part of Northern Honshu arc, Japan, revealed by onshore-offshore seismic experiment. submitted to 2021 JpGU Meeting.

©2021. Japan Geoscience Union. All Right Reserved.

Sato et al., 2020a. Seismic transect across the central part of Northern Honshu, Japan, 2020 JpGU-AGU Joint Meeting, MIS03-P05.
Sato et al., 2020b. Deep seismic reflection profiling across the Shonai and Shinjo basins, northern Honshu, Japan, 2020 Spring Meeting of JAPT, 016.

Keywords: NE Japan Arc, upper crustal structure, refraction/wide-angle reflection experiment, crustal deformation, the Sea of Japan, back arc spreading

©2021. Japan Geoscience Union. All Right Reserved.

Crust and Mantle Structure of the Tohoku Region from the Viewpoint of Seismic Anisotropy

*Motoko Ishise[1]

1. Earthquake Reseach Institute, University of Tokyo

Seismic anisotropy is closely related to stress fields, flow fields, and structural geometries, and thus provides useful information for understanding tectonics and dynamics of subduction zone. In this presentation, we present the results of azimuthal and radial anisotropy tomography analyses of the Tohoku region (Ishise et al., 2018) and show the characteristics of crustal and mantle anisotropy.

The main features of the azimuthal and radial anisotropy of the upper crust, lower crust, and upper mantle (mantle wedge) obtained by tomographic analyses and their interpretations are as follows:

Upper crust (0 and 10 km depths)

At a depth of 10 km, N–S-trending anisotropy (from NNW–SSE to N–S) is dominant in the Kitakami region, and NW–SE and NE–SW anisotropy coexist. At a depth of 0 km, both N–S- and EW-trending anisotropy are observed. The distribution of N–S-trending anisotropy is almost consistent with the distribution of earthquakes with N–S compression seismic mechanism and distribution of major active faults with N–S strike. In general, anisotropy in the upper crust is explained by regional stress fields, but in the Tohoku region, it is thought to be caused by regional tectonics and geological structure.

Beneath the land area, the forearc region shows radial anisotropy of $V_{PH} > V_{PV}$ and the backarc region show radial anisotropy of $V_{PH} < V_{PV}$, respectively. This distribution pattern suggests the existence of large-scale structure that separates the forearc region from the backarc region.

Lower crust (25 km depth)

E–W-trending azimuthal anisotropy is dominant beneath the inland area. The direction is almost coincides with the direction of motion of the PAC slab relative to the Okhotsk plate, and is presumed to reflect the plastic deformation and flow field of the lower crust caused by the subduction of the PAC plate.

The N–S-trending azimuthal anisotropy is zonally distributed beneath the coastal areas of the Pacific Ocean and Japan Sea. This anisotropy can be attributed to plastic flow in the N–S direction or the developed internal structure (such as laminated structure) orientated in the N–S direction. However, since it is unlikely that orthogonal deformation fields exist next to each other, the N–S anisotropy can be attributed to the geometry of the internal structure.

In addition, a characteristic zonal region with NW–SE azimuthal anisotropy is found beneath the Honjo-Sendai tectonic line. This may reflect the deep structure of the tectonic line.

The coastal regions indicating N–S azimuthal anisotropy shows distinct radial anisotropy of $V_{PH} > V_{PV}$, which suggests that the laminated structure has gentle slope. On the other hand, strong radial anisotropy of $V_{PH} < V_{PV}$ are observed beneath the inland area, suggesting that the lower mantle in the Tohoku region dose not have a horizontal layering structure.

©2021. Japan Geoscience Union. All Right Reserved.

Mantle wedge (deeper than 40 km)

N–S-trending azimuthal anisotropy is widely distributed beneath the land area. The direction is almost parallel to the strike of the iso-depth contours of the PAC slab, which suggests that the flow field in the mantle wedge would be controlled by the geometry of the PAC slab.

Radial anisotropy of $V_{PH} < V_{PV}$ is found beneath the land area, suggesting the presence of small scale convection (e.g., Honda and Yoshida, 2005). Although it is not clear, the areas around the active volcanoes indicate strong $V_{PH} < V_{PV}$ anisotropy.

In this study, the anisotropic features the upper crust, lower crust, and mantle wedge are presented and interpreted individually. As the next step, we aim to relate them and comprehensively interpret the anisotropic structure of the Tohoku region.

Keywords: seismic anisotropy, Tohoku region, tomography, tectonics

©2021. Japan Geoscience Union. All Right Reserved.

[J] Oral | S (Solid Earth Sciences)：S-CG Complex & General

Fri. Jun 4, 2021 3:30 PM - 5:00 PM JST | Fri. Jun 4, 2021 6:30 AM - 8:00 AM UTC | Ch.21 Zoom Room 21

[S-CG49] Structure, evolution and deformation of island arcs associated with subduction processes

convener:Masahiro Ishikawa(Graduate School of Environment and Information Sciences Yokohama National University), Masanao Shinohara(Earthquake Research Institute, University of Tokyo), Makoto MATSUBARA(National Research Institute for Earth Science and Disaster Resilience), Tatsuya Ishiyama(Earthquake Research Institute, University of Tokyo), Chairperson:Masanao Shinohara(Earthquake Research Institute, University of Tokyo), Tatsuya Ishiyama(Earthquake Research Institute, University of Tokyo)

Subduction processes such as accretion, back-arc-spreading, and arc-arc collisions have created overall architectures of the Japanese island arc through geologic time. Recent advances in seismic imaging by both passive and controlled source obtained onshore and offshore Japanese islands have successfully provided plenty of new informations on structural, mechanical, rheological and thermal properties of crust and upper mantle that have presumably strongly controls on active tectonics manifested by seismic activities, crustal deformation and other tectonic records in the overriding plate. Our goal in this session is to advance the understanding of overriding plate deformation in various timescales based on state-of-the-art results of observational and modeling studies encompassing both earthquake cycles and tectonic evolution of the Japanese island arc and other plate convergent margins. We welcome contributions from seismology, physical geology, geochemistry, tectonic geomorphology, and numerical and/or analogue geodynamic modeling on deformation processes associated with plate subduction processes and related feedbacks.

3:30 PM - 3:45 PM JST | 6:30 AM - 6:45 AM UTC

[SCG49-07] 3-D Crustal Shear Wave Velocity Model Derived from the Adjoint Tomography in the Central Japan

*Kota Mukumoto[1], Takeshi Tsuji[1] (1.Kyushu University)

3:45 PM - 4:00 PM JST | 6:45 AM - 7:00 AM UTC

[SCG49-08] Structure and deformation in the overlying plates of Japanese arcs

★Invited Papers

*Hiroshi Sato[1,2] (1.Earthquake Prediction Research Center, Earthquake Research Institute, The University of Tokyo, 2.Center for Integrated Research and Education of Natural Hazards, Shizuoka University)

4:00 PM - 4:15 PM JST | 7:00 AM - 7:15 AM UTC

[SCG49-09] Magmatic evolution of Cretaceous north Kyushu batholiths and its role in creation of crustal structure

*Masaaki Owada[1], Keisuke Eshima[1], Atsushi Kamei[2] (1.Graduate School of Science and Engineering for Innovation, Yamaguchi University, 2.Interdisciplinary Faculty of Science and Engineering, Shimane University)

4:15 PM - 4:30 PM JST | 7:15 AM - 7:30 AM UTC

[SCG49-10] The fate of the Philippine Sea slab in central Japan

*Kazuki Miyazaki[1], Junichi Nakajima[1], Nobuaki Suenaga[2], Shoichi Yoshioka[2,3] (1.Department of Earth and Planetary Sciences, Tokyo Institute of Technology, 2.Research Center for Urban Safety and Security, Kobe University, 3.Faculty of Science, Graduate School of Science, Kobe University)

4:30 PM - 4:45 PM JST | 7:30 AM - 7:45 AM UTC

[SCG49-11] Contrasting volcano spacing along SW Japan arc caused by difference in age of subducting lithosphere

★Invited Papers

*Takumi Matsumoto[1], Yoshiyuki Tatsumi[2,3], Nobuaki Suenaga[4], Shoichi Yoshioka[4,5], Katsuya Kaneko[5,3] (1.National Research Institute for Earth Science and Disaster Resilience, 2.Research Alliance for Human and Ocean Coevolution, Kobe University, 3.Kobe Ocean-Bottom Exploration Center, Kobe University, 4.Research Center for Urban Safety and Security, Kobe University, 5.Faculty of Science, Graduate School of Science, Kobe University)

4:45 PM - 5:00 PM JST | 7:45 AM - 8:00 AM UTC

[SCG49-12] The thermal structure of the Honshu arc crust deduced from seismic tomography

*Masahiro Ishikawa[1] (1.Graduate School of Environment and Information Sciences Yokohama National University)

3-D Crustal Shear Wave Velocity Model Derived from the Adjoint Tomography in the Central Japan

*Kota Mukumoto[1], Takeshi Tsuji[1]

1. Kyushu University

In Japan, most seismic velocity models for crust structure investigation have been estimated by ray tomography. This method has resolved the many interesting geological features related to the fluids, volcanic activities, earthquake faults, and interactions of the plates. The adjoint tomography that takes the advantage of full numerical seismic wave simulation and banana-doughnut sensitivity kernels has led to more accurate estimation and fine structures in the crustal and global seismic tomographic model. However, applications of the full waveform inversion have been limited. In this study, we estimated 3-D crustal S-wave velocity model based on the adjoint tomography in the Central Japan Island. The waveforms of 70 earthquakes were collected from 385 3-components high sensitivity seismometers (Hi-net). The phase shift between observed and synthetic seismograms filtered over the period range 10-30 sec was minimized by successively updating the velocity models from the initial model. After 21 iterations, the phase misfit was reduced by 11.3%. The estimated S-wave velocity model revealed the distinct low- and high-velocity anomalies related to the magmatic fluids, sedimentary basins, volcanoes, and lithologies. Based on the waveform comparisons between before and after the inversion, minimizing the phase misfit improves not only the phase misfit but also the amplitude differences. This means the constructive and destructive interference of the seismic wavefields was also improved. The first S-wave velocity model by applying the adjoint tomography to the Hi-net stations suggests the applicability of the waveform inversion to the Hi-net stations in Japan and opportunities to image heterogeneous crustal structures in the Japan Island.

Keywords: Adjoint tomography, Waveform inversion, Shear wave velocity structure

©2021. Japan Geoscience Union. All Right Reserved.

Structure and deformation in the overlying plates of Japanese arcs

*Hiroshi Sato[1,2]

1. Earthquake Prediction Research Center, Earthquake Research Institute, The University of Tokyo, 2. Center for Integrated Research and Education of Natural Hazards, Shizuoka University

The structure and deformation in Japanese arcs have been revealed last decades through densely distributed seismic, geodetic networks and deep seismic profiling. The M9.0 Tohoku-oki earthquake manifested the strong relationship between intraplate coupling and deformation of overlying plate. In the NE Japan arc, geological shortening deformation concentrated along the backarc continental crust. The shortening deformation was archived by reverse faulting of Miocene normal faults. Through the analysis of post M9.0 crustal deformation, Freed et al. (2017, EPSL) revealed the structure of overlying plate and wedge mantle, including the location of cold nose and thickness of overlying plate. Most of the geological shortening deformation occurs in the thin lithosphere (continental crust) between cold nose to the Sea of Japan oceanic crust underlaid by thick lithosphere. Through the recent seismic reflection profiling, the models of seismogenic source faults in and around the Sea of Japan were proposed (Sato et al., 2020: Abst. Seismol. Soc. Jpn). Reactivated reverse faults of Miocene normal faults shows moderate dip. Thrusts developed between oceanic and continental crust (No et al., 2014: EPSL) or along the margin of intra-continental backarc rift zones. Backarc continental rift zones are marked by thick post rift sediments and mafic lower crust. Thrusts along the backarc rift were produced by stress concentration along the rock boundary between mafic and felsic crust. Along the eastern part of Sea of Japan, the plate boundary between North American/Eurasia or Okhotsk/Amur is estimated. However, no suitable plate boundary faults were found by dense deep seismic profiling. Such plate convergence, if it exists, is accommodated in the wider zone of backarc in Northern Honshu. Through the saloon door opening of the Sea of Japan (Otofuji et al., 1985: Nature), counter clock-wise rotation of NE Japan was performed by strike-slip motion of the northern part of Itoigawa-Shizuoka tectonic line and Kanto tectonic line (Sato, 1994: GJR). High Vp lower crust underlaid along these intra-arc rift zones (Matsubara et al., 2017: JDR).

In SW Japan arc, basic structure of backarc is similar to NE Japan arc. Basic structure of rifted continental crust is marked by arc-parallel normal faults. The northward motion of Philippine Sea plate (PHS), mainly “hot” Shikoku basin” produced the large amount of NS-shortening in the backarc of SW Japan arc and formed the Shinji fold belts. This belt is marked by reverse faulting of older normal faults. Most of the NS-trending shortening terminated before Pliocene due to the northward subduction of PHS (Kimura et al., 2005: GSA Bull.). Change in motion of PHS from NNW to WNW, occurred at 1 Ma. This change created the reverse to right-lateral strike-slip faulting of Median Tectonic Line and asymmetric deformation of Izu collision zone. This westward motion of the PHS synchronized with main opening of the Okinawa trough associated with trench retreat and slab roll back.

Basic tectonic framework of Japanese arcs is strongly affected by the subduction of oceanic plates and slab behavior in the asthenosphere. Together with the change in coupling between the plate boundary, tectonic models of the overlying plate have to be constructed as a subduction system.

Keywords: overlying plates, deformation, Deep seismic profiling, Japanese arcs

©2021. Japan Geoscience Union. All Right Reserved.

Magmatic evolution of Cretaceous north Kyushu batholiths and its role in creation of crustal structure

*Masaaki Owada[1], Keisuke Eshima[1], Atsushi Kamei[2]

1. Graduate School of Science and Engineering for Innovation, Yamaguchi University, 2. Interdisciplinary Faculty of Science and Engineering, Shimane University

Understanding igneous activities in active continental margins could provide us useful information for the evolution of continental crusts. The geological and petrological data revealed that the Cretaceous granitoid batholiths in north Kyushu, the north Kyushu batholiths hereafter, were produced by partial melting of mafic lower crusts due to underplating of mantle derived mafic magmas as an acting heat source. The north Kyushu batholiths are characterized by episodic magmatism from 109 to 95 Ma, and consist mainly of hornblende-bearing granitoids with positive epsilon initial Nd values, and are locally associated with coeval high-Mg diorite. The batholiths would, therefore, play an important role to understand the growth of juvenile crust in an active continental margin due to the magmatic flare-up. We will address the geological and petrological features of the granitoids and related mafic rocks from the north Kyushu batholiths to unravel magmatic evolution and its role in the creation of crustal structure.
The host rocks of the western part of the north Kyushu batholiths are composed of the pre-Jurassic accretionary complexes with their high-P/T metamorphic facies and the Cretaceous low-P/T metamorphic rocks reaching up to granulite facies conditions. On the other hand, the Cretaceous shallow marine deposits are exposed as host rocks on the eastern part of batholiths. The magma plumbing system can be recognized in the small stocks on the eastern part of batholiths. The Shaku-dake diorite body, a member of the north Kyushu batholiths, intruding the shallow marine deposits possesses layered structures on the wall sides. The intrusive age of the diorite has been thought to be c. 106 Ma. The dioritic dikes and sills intruded the diorite body where the dikes and sills would provide the magmatic pulses to the Shaku-dake diorite body. The diorite magma was geochemically differentiated from high-Mg diorite to granodiorite through the process of assimilation and fractional crystallization. The Shikano-shima granodiorite occupied in the western part of the batholiths involves the hornblende gabbro as blocks that bears leucocratic patches or lenses geochemically resembling the Shikano-shima granodiorite. The results of melting experiment inferred that the hornblende gabbro was originally formed under the lower crust at pressure conditions more than 800 MPa during 120 to 103 Ma. The partial melting took place in the gabbro, then gave rise to the Shikano-shima granodiorite magma at the age of 104 Ma. The lower crust, 25–35 km in depth, beneath the north Kyushu batholiths is underlain by the P-wave structure with 6.5–7.0 km/s that corresponds to a hornblende-bearing gabbro. The region covering the north Kyushu batholiths locally shows positive Bouguer anomaly spots where some gabbro blocks are exposed on the surface. The areas distribution of the Shikano-shima granodiorite and the gabbro block are identical with the place of positive Bouguer anomaly. Therefore, the granodiorite magma probably ascended as a diapir from the lower crust accompanied by the source gabbro. Combined with the petrological study and the seismic structure, the upper crust was formed by the flare-up of intermediate to felsic magmas through the pathway as the dikes. In addition to this magma plumbing system, the granodiorite magmas originated from mafic lower crust would be ascended as diapirs to form the middle crust.

Keywords: North Kyushu batholiths, Cretaceous, Magmatic flare-up, Crustal structure

©2021. Japan Geoscience Union. All Right Reserved.

The fate of the Philippine Sea slab in central Japan

*Kazuki Miyazaki[1], Junichi Nakajima[1], Nobuaki Suenaga[2], Shoichi Yoshioka[2,3]

1. Department of Earth and Planetary Sciences, Tokyo Institute of Technology, 2. Research Center for Urban Safety and Security, Kobe University, 3. Faculty of Science, Graduate School of Science, Kobe University

The Philippine Sea slab beneath central Japan is believed to have started subducting at least 15Ma. Given a convergence rate of 3 cm/year, the Philippine Sea slab has subducted by 450 km. However, the slab shape determined by previous studies is shorter than the expectation. In this study, we explore the whereabouts of the subducted Philippine Sea slab using numerical calculations of slab subduction and seismic tomography.

The Philippine Sea slab is in contact with the Pacific slab beneath Kanto, and there is a possibility that the two oceanic slabs are interacting to form a complex shape. In this study, we used the numerical calculation program SSS (Torii and Yoshioka, 2007) to calculate the interaction of the Philippine Sea slab with the Pacific slab. When the Philippine Sea slab was subducted against the Pacific slab, which was prescribed as a highly viscous body, the subducted Philippine Sea slab was simulated either to lie on top of the Pacific slab or to bend in the opposite direction of the convergence. In the future, we will adjust the parameters to make the subduction calculation more realistic.

We plan to conduct seismic tomography in the Central Japan and compare the tomographic results with our calculations.

Keywords: Philippine Sea slab

©2021. Japan Geoscience Union. All Right Reserved.

Contrasting volcano spacing along SW Japan arc caused by difference in age of subducting lithosphere

*Takumi Matsumoto[1], Yoshiyuki Tatsumi[2,3], Nobuaki Suenaga[4], Shoichi Yoshioka[4,5], Katsuya Kaneko[5,3]

1. National Research Institute for Earth Science and Disaster Resilience, 2. Research Alliance for Human and Ocean Coevolution, Kobe University, 3. Kobe Ocean-Bottom Exploration Center, Kobe University, 4. Research Center for Urban Safety and Security, Kobe University, 5. Faculty of Science, Graduate School of Science, Kobe University

The SW Japan arc built by subduction of the Philippine Sea (PHS) plate exhibits uneven distribution of volcanoes: thirteen Quaternary composite volcanoes form in the western half of this arc, Kyushu Island, while only two in the eastern half, Chugoku district.
In the non-volcanic forearc of the eastern half of this arc spring out characteristic deep-seated fluids referred to as the Arima-type brines possessing high Cl contents, high Li/Cl ratios. Such geochemical characteristics of these brines may be attributed to dehydration of the downgoing PHS oceanic crust. In addition, characteristic tectonic tremors and low-frequency earthquakes(LFEs) are observed in the Nankai subduction zone.
Here will be discussed based on the age of the subducted PHS plate inferred by reconstruction of plate motion, and calculation of temperature distribution along the sinking PHS plate beneath the Chugoku and Kyushu regions, and the behavior of water during subduction of the PHS plate. The calculation of 2D thermal structures in this study follows the previous models. We also used heat flow data from high-quality high-density Hi-net borehole and BSRs in addition to previously-used land boreholes and marine heat probes, resulting in the highdensity heat flow data to constrain the thermal structures.
Reconstruction of the PHS plate back to 14 Ma, together with examinations based on thermal structure models constrained by highdensity heat flow data and a petrological model for dehydration suggest that fluids are discharged actively at depths of 90–100 km in the hydrous layer at the top of the old (> 50 Ma), hence, cold lithosphere sinking beneath Kyushu Island. In contrast, the young (15–25 Ma) oceanic crust downgoing beneath Chugoku district releases fluids largely at shallower depths, i.e. beneath the nonvolcanic forearc, to cause characteristic tectonic tremors and LFEs and be the source of specific brine springs. Much larger amounts of fluids supplied to the magma source region in the western SW Japan arc could build more densely-distributed volcanoes.

Keywords: volcano, 2D thermal modeling, dehydration, heat flow

©2021. Japan Geoscience Union. All Right Reserved.

The thermal structure of the Honshu arc crust deduced from seismic tomography

*Masahiro Ishikawa[1]

1. Graduate School of Environment and Information Sciences Yokohama National University

Quantifying the thermal structure of the overlying plate is essential for understanding the nature of deformation of the island arc. In order to interpret seismic tomography into the thermal structure, it is important to accurately measure the temperature dependence of elastic wave velocity of lower crustal/upper mantle rocks and minerals. In this study, simultaneous measurements of ultrasonic compressional wave velocities (Vp), shear wave velocities (Vs), Vp/Vs ratio, and their temperature dependence were conducted on natural xenolith samples collected from the Honshu arc and sintered polycrystalline mineral samples at high temperature and high-pressure conditions representative of the lower crust and uppermost mantle of the island arc. The experimental results for each sample have shown a distinct negative temperature dependence of P and S wave velocities. The Vp/Vs ratio, on the other hand, depends heavily on the mineral compositions of rocks, not temperature. By extracting regions that are presumed to have the same lithology from the Vp/Vs tomography, Vp perturbations or Vs perturbations of the extracted regions can be interpreted as thermal perturbations. In this study, Vp or Vs in an arbitrary Vp/Vs range were extracted using the three-dimensional seismic tomography of Matsubara et al. (2019), and the thermal structure was estimated from the extracted velocity structure by comparing experimentally determined temperature dependence of Vp or Vs of the samples with Vp perturbations or Vs perturbations in the lower crust and uppermost mantle. An example of the estimated thermal feature is described below. To clarify the temperature perturbation of the lower crust of the NE Honshu arc in the east-west direction, P-wave velocities and S-wave velocities with a constant Vp/Vs were extracted from the seismic tomography of 20km depth. At the latitude of 39.75-40˚N, the lower crust of the Ou Backbone Range is estimated to be the hottest, because the extracted velocities of the P and S waves indicate the lowest velocities below the Ou Backbone Range. P-wave velocity and S-wave velocity increase toward Kitakami Lowland (141 ˚E) and Hachirogata (140 ˚E), and the feature suggest that the temperature of the lower crust decreases from the Ou Backbone Range to the east and west sides. The feature is common in the NE Honshu arc, but there are some differences and exceptions in the north-south direction. The detailed thermal structures and estimated temperatures will be discussed in our presentation.

Keywords: thermal structure, Honshu arc

©2021. Japan Geoscience Union. All Right Reserved.

[J] Oral | B (Biogeosciences)：B-CG Complex & General

Fri. Jun 4, 2021 9:00 AM - 10:30 AM JST | Fri. Jun 4, 2021 12:00 AM - 1:30 AM UTC | Ch.26 Zoom Room 26

[B-CG04] Decoding the history of Earth: From Hadean to the present

convener:Tsuyoshi Komiya(Department of Earth Science & Astronomy Graduate School of Arts and Sciences The University of Tokyo), Yasuhiro Kato(Department of Systems Innovation, Graduate School of Engineering, University of Tokyo), Katsuhiko Suzuki(Submarine Resources Research Center, Japan Agency for Marine-Earth Science and Technology), Kentaro Nakamura(Department of Systems Innovation, School of Engineering, University of Tokyo), Chairperson:Yoshida Satoshi(Department of Earth and Planetary Science, Graduate School of Science, The University of Tokyo), Tsuyoshi Komiya(Department of Earth Science & Astronomy Graduate School of Arts and Sciences The University of Tokyo)

The latest results of Earth's evolution and geological processes through 4.6 billion years from Hadean to Modern, based on various approaches including fieldworks, chemical analyses, experiments and computer simulation, will be presented. In this session, we aim to discuss and understand causal relationships and interplay among the evolution of Earth's deep interior, changes in the surface environments, and development and evolution of life. Wide-ranging topics are accepted.

9:00 AM - 9:15 AM JST | 12:00 AM - 12:15 AM UTC

[BCG04-01] Progress of the end-Permian oceanic anoxia in the pelagic Panthalassa

*Satoshi Takahashi[1], Rie Hori[2], Satoshi Yamakita[3], Yoshiaki Aita[4], Atsushi Takemura[5], Minoru Ikehara[6], Yujin Xiong[7], Simon W. Poulton[7], Paul B. Wignall[7], TAKAAKI ITAI[1], Hamish J. Campbell[8], Bernard K. Spörli[9] (1.Department of Earth and Planetary Science, University of Tokyo, 2.Department of Earth Sciences, Graduate School ofScience and Engineering, Ehime University , 3.Department of Earth Sciences, Faculty of Culture, Miyazaki University, 4.Department ofGeology, Faculty ofAgriculture, Utsunomiya University, 5.Geosciences Institute, Hyogo University ofTeacher Education, 6.Center for Advanced Marine Core Research, Kochi University, 7.School of Earth and Environment, University of Leeds, 8.GNS Science, 9.School of Environment, The University of Auckland)

9:15 AM - 9:30 AM JST | 12:15 AM - 12:30 AM UTC

[BCG04-02] Discovery of the Miocene ocean impact event

*Tatsuo Nozaki[1,2,3,4], Junichiro Ohta[2,4], Takaaki Noguchi[5], Honami Sato[6], Akira Ishikawa[7,1], Yutaro Takaya[8,1,4], Jun-Ichi Kimura[9], Qing Chang[9], Kazuhiko Shimada[10], Jun-ichiro Ishibashi[10], Kazutaka Yasukawa[2,4], Katsunori Kimoto[11], Koichi Iijima[1], Yasuhiro Kato[2,4,1] (1.JAMSTEC/SRRC, 2.Univ. of Tokyo, 3.Kobe Univ., 4.Chiba Tech, 5.Kyushu Univ., 6.Univ. of Padova, 7.Tokyo Tech, 8.Waseda Univ., 9.JAMSTEC/VERC, 10.Kyushu Univ, 11.JAMSTEC/ESS)

9:30 AM - 9:45 AM JST | 12:30 AM - 12:45 AM UTC

[BCG04-03] Geochemistry of the Kawame ferromanganese deposit in the Hayachine Belt: Implications for the oceanic environment in the Late Devonian

*Yusuke Kuwahara[1], Koichiro Fujinaga[2,3], Tatsuo Nozaki[4,3,5,2], Junichiro Ohta[3,2], Kazutaka Yasukawa[3,1,2], Kentaro Nakamura[1], Yasuhiro Kato[3,1,2,4] (1.Department of Systems Innovation, School of Engineering, The University of Tokyo, 2.Ocean Resources Research Center for Next Generation, Chiba Institute of Technology, 3.Frontier Research Center for Energy and Resources, School of Engineering, The University of Tokyo, 4.Research and Development Center for Submarine Resources, Japan Agency for Marine-Earth Science and Technology, 5.Department of Planetology, Graduate School of Science, Kobe University)

9:45 AM - 10:00 AM JST | 12:45 AM - 1:00 AM UTC

[BCG04-04] Paleovegetation changes reconstructed by terrestrial plant biomarker analyses in the sediments deposited across the Cenomanian/Turonian boundary in the Great Valley Sequence, northern California, USA

*Masashi A. Ikeda[1], Ken Sawada[2], Reishi Takashima[3], Hiroshi Nishi[4] (1.Graduate School of Science, Hokkaido University, 2.Department of Earth and Planetary Sciences, Faculty of Science, Hokkaido

University, 3.The Center for Academic Resources and Archives, The Tohoku University Museum, Tohoku University, 4.Institute of Dinosaur Research, Fukui Prefectural University)

10:00 AM - 10:15 AM JST | 1:00 AM - 1:15 AM UTC

[BCG04-05] Constraint on the Location of the Australasian Tektite Event based on the Thickness Distribution and Gravel Composition of the Ejecta Deposits across the Eastern Indochina

*Toshihiro Tada[1], Ryuji Tada[1,3,2], Paul A Carling[4], Wickanet Songtham[5], Praphas Chansom[5], Thuyên Lê Xuân[6], Toshihiro Kogure[2], Chang Yu[2], Eiichi Tajika[2] (1.Institute for Geo-Cosmology, Chiba Institute of Technology, 2.Department of Earth and Planetary Science, School of Science, The University of Tokyo, 3.Research Center for Earth System Science, Yunnan University, 4.School of Geography and Environmental Sciences, University of Southampton, 5.Northeastern Research Institute of Petrified Wood & Mineral Resources, Nakhon Ratchasima Rajabhat University, 6.Ho Chi Minh City University of Science)

10:15 AM - 10:30 AM JST | 1:15 AM - 1:30 AM UTC

[BCG04-06] **Paleoproterozoic magmatic flare-up of the Ubendian Belt, SW Tanzania: A crustal growth history events before the amalgamation of the Central African Shield**

*Ariuntsetseg Ganbat[1], Tatsuki Tsujimori[1,2], Nelson Boniface[4], Daniel Pastor-Galan[1,2,3], Shogo Aoki[5,6], Kazumasa Aoki[6] (1.Graduate School of Science, Tohoku University, 2.Center for Northeast Asian Studies, Tohoku University, 3.Frontier Research Institute for Interdisciplinary Sciences, Tohoku University, 4.Department of Geology, University of Dar es Salaam, 5.Graduate School of International Resource Sciences, Akita University, 6.Center for Fundamental Education, Okayama University of Science)

Progress of the end-Permian oceanic anoxia in the pelagic Panthalassa

*Satoshi Takahashi[1], Rie Hori[2], Satoshi Yamakita[3], Yoshiaki Aita[4], Atsushi Takemura[5], Minoru Ikehara[6], Yujin Xiong[7], Simon W. Poulton[7], Paul B. Wignall[7], TAKAAKI ITAI[1], Hamish J. Campbell[8], Bernard K. Spörli[9]

1. Department of Earth and Planetary Science, University of Tokyo, 2. Department of Earth Sciences, Graduate School ofScience and Engineering, Ehime University , 3. Department of Earth Sciences, Faculty of Culture, Miyazaki University, 4. Department ofGeology, Faculty ofAgriculture, Utsunomiya University, 5. Geosciences Institute, Hyogo University ofTeacher Education, 6. Center for Advanced Marine Core Research, Kochi University, 7. School of Earth and Environment, University of Leeds, 8. GNS Science, 9. School of Environment, The University of Auckland

The end-Permian mass extinction event (EPME) has been linked with the widespread development of oxygen-poor oceanic conditions. However, information on the spatial extent of anoxia in the Panthalassa super-ocean has been limited. This study reports oceanic redox records from the southern middle-latitude, pelagic Panthalassa across the EPME, based on a deep-sea chert succession (the Waiheke 1 section, WHK 1) from the North Island of New Zealand. Carbon isotope correlation between the study section and the GSSP section for the Permian-Triassic boundary (PTB) indicates that the EPME is recorded in a thin black claystone interbedded between siliceous siltstone beds in WHK 1. Pyrite dominated reactive iron, and high Fe/Al, U/Al and Mo/Al values occur in the black claystone bed and the overlying strata, which comprises the Permian-Triassic transition. These geochemical features suggest that anoxic-sulfidic water developed at that time. Similar redox variations across the EPME boundary have been reported from other Panthalassic deep-sea sections, suggesting widespread sulfidic waters during EPME. However, the onset of the shift to the oxygen-poor and/or sulfidic condition of WHK 1 postdates the change to anoxia in low latitude sections by up to a hundred kilo years. This finding implies the gradual expansion of oceanic anoxia from low to middle-high latitude oceanic regions during the Permian-Triassic transition. As an result of this expansion in ocean anoxia, a significant decrease in seawater trace metals such as Mo is inferred from the earliest Triassic strata of the studied section and other PTB sections. The pre-EPME ocean anoxia that occurred mainly in low latitude regions began after the first Siberian Traps eruption and during terrestrial de-vegetation trends, implying a terrestrial-marine linkage to severe environmental change. The more widespread anoxia at the EPME coincides with extreme global warming. This suggests that rising temperature and associated effects (e.g. change of ocean circulation, marine eutrophication intensified by terrestrial weathering) were critical triggers for ocean deoxygenation and the mass extinction event.

Keywords: Permian-Triassic boundary, Mass extinction, Ocean anoxia

©2021. Japan Geoscience Union. All Right Reserved.

Discovery of the Miocene ocean impact event

*Tatsuo Nozaki[1,2,3,4], Junichiro Ohta[2,4], Takaaki Noguchi[5], Honami Sato[6], Akira Ishikawa[7,1], Yutaro Takaya[8,1,4], Jun-Ichi Kimura[9], Qing Chang[9], Kazuhiko Shimada[10], Jun-ichiro Ishibashi[10], Kazutaka Yasukawa[2,4], Katsunori Kimoto[11], Koichi Iijima[1], Yasuhiro Kato[2,4,1]

1. JAMSTEC/SRRC, 2. Univ. of Tokyo, 3. Kobe Univ., 4. Chiba Tech, 5. Kyushu Univ., 6. Univ. of Padova, 7. Tokyo Tech, 8. Waseda Univ., 9. JAMSTEC/VERC, 10. Kyushu Univ, 11. JAMSTEC/ESS

Meteorite impacts have caused catastrophic perturbations to the global environment and mass extinctions throughout the Earth’ s history [1-3]. Here, we present petrographic and geochemical evidence of an impact ejecta layer, dating from about 11 Ma, in deep-sea clayey sediment in the Northwest Pacific [4]. This clay layer has high platinum group element (PGE) concentrations and features a conspicuous negative Os isotope anomaly ($^{187}Os/^{188}Os$ as low as ~0.2), indicating an influx of extraterrestrial material. It also contains abundant spherules that include pseudomorphs suggestive of porphyritic olivine as well as spinel grains with euhedral, dendritic and spherical forms and NiO contents as great as 23.3 wt%, consistent with impact ejecta. Osmium isotope stratigraphy suggests the most plausible depositional age of ~11 Ma (Miocene) for this layer, as determined by fitting with the seawater evolution curve. No large impact crater of this age is known on land, even within the relatively large uncertainty range of the relative Os age. Thus, we suggest that an unrecognized ocean impact event in the middle or late Miocene produced the impact ejecta layer of the Northwest Pacific. This unrecognized ocean impact event is possibly related to the latest and enigmatic mass extinction during the middle Miocene (11.6 Ma) [5].

[1] Alvarez et al. (1980) *Science*, **208**, 1095-1108. [2] Schulte et al. (2010) *Science*, **327**, 1214-1218. [3] Lowery et al. (2018) *Nature*, **558**, 288-291. [4] Nozaki et al. (2019) *Sci. Rep.*, **9**, 16111. [5] Raup and Sepkoski (1986) *Science*, **231**, 833-836.

Keywords: Ocean impact, Miocene, Ejecta layer, NW Pacific, Re-Os isotope, Platinum group element (PGE)

©2021. Japan Geoscience Union. All Right Reserved.

Geochemistry of the Kawame ferromanganese deposit in the Hayachine Belt: Implications for the oceanic environment in the Late Devonian

*Yusuke Kuwahara[1], Koichiro Fujinaga[2,3], Tatsuo Nozaki[4,3,5,2], Junichiro Ohta[3,2], Kazutaka Yasukawa[3,1,2], Kentaro Nakamura[1], Yasuhiro Kato[3,1,2,4]

1. Department of Systems Innovation, School of Engineering, The University of Tokyo, 2. Ocean Resources Research Center for Next Generation, Chiba Institute of Technology, 3. Frontier Research Center for Energy and Resources, School of Engineering, The University of Tokyo, 4. Research and Development Center for Submarine Resources, Japan Agency for Marine-Earth Science and Technology, 5. Department of Planetology, Graduate School of Science, Kobe University

It is widely accepted that hydrothermal ferromanganese sediment is a useful recorder of ocean chemistry. Because the ancient ferromanganese sediments were subducted and then accreted onto the continental crust, onshore hydrothermal ferromanganese deposits (termed umbers) are regarded as an important key to understand the chemistry of the ancient ocean. The Late Devonian umber, the oldest umber in Japan, can be observed at the Kawame Quarry in the Hayachine Belt, Northeast Japan. Here we investigate the bulk chemical composition and osmium isotopic composition ($^{187}Os/^{188}Os$) of the Kawame umber. In the presentation, we will report the geochemical features of the Kawame umber and $^{187}Os/^{188}Os$ of the Late Devonian seawater, and discuss their paleoceanographic implications.

Keywords: Umber, Accretionary complex, Osmium isotopic ratio

©2021. Japan Geoscience Union. All Right Reserved.

Paleovegetation changes reconstructed by terrestrial plant biomarker analyses in the sediments deposited across the Cenomanian/Turonian boundary in the Great Valley Sequence, northern California, USA

*Masashi A. Ikeda[1], Ken Sawada[2], Reishi Takashima[3], Hiroshi Nishi[4]

1. Graduate School of Science, Hokkaido University, 2. Department of Earth and Planetary Sciences, Faculty of Science, Hokkaido University, 3. The Center for Academic Resources and Archives, The Tohoku University Museum, Tohoku University, 4. Institute of Dinosaur Research, Fukui Prefectural University

The Cretaceous is known as the extreme greenhouse period attributed to the elevated atmospheric CO_2 concentration triggered by the superplume activity. The Oceanic Anoxic Events (OAEs) caused by the occurrences of the Large Igneous Plateaus (LIPs) in several times, especially in the mid-Cretaceous. Global environmental disturbance events have been extensively investigated in the ocean, but there have been few reports for terrestrial environmental variation during the OAE periods (e.g. Heimhofer et al., 2018). In the present study, we analyzed biomarkers of terrestrial plants in the sediments deposited across the Cenomanian/Turonian boundary (CTB) from the northern California, USA to reconstruct paleovegetation changes and to evaluate paleoecology of plants during environmental disturbance event.
We analyzed sedimentary rocks across the CTB in the Budden Canyon Formation, Great Valley Sequence (GVS), were collected from the North Fork Cottonwood Creek sections in northern California, USA. The sediments used correspond to the OAE2 intervals (1st build-up, Trough, 2nd build-up, Plateau, and Recovery phases), determined by $\delta^{13}C$ stratigraphy (Takashima et al., 2011). For the biomarker analysis, the extractions of crashed sediments were fractionated using silica-gel column and analyzed by GC-MS. By sterane and hopane ratios, we confirmed the high contribution of terrigenous matter input and low maturity of organic matter (vitrinite reflectance ca. 0.4% level; lignite to subbituminous coal rank) in the North Fork Cottonwood Creek section. The aromatic terpenoid-based angiosperm/gymnosperm index (ar-AGI) values tended to increase gradually until the Plateau phase, although it decreased temporarily during environmental disturbances (1st build-up and 2nd build-up). The coniferous vegetation index as retene / cadalene ratio-based higher plant parameter (HPP), consistently low until the Plateau phase, and then increased rapidly in the Recovery phase. The ratio of perylene to plant-derived aromatic terpenoids (Pery / arT), which is tentatively defined as an indicator of fungal biomass in terrestrial flora i.e. fungal activity, also declined during the Recovery phase. These results suggest that, in the western margin of the north America continent during the CTB, the environmental disturbance had a negative effect on the angiosperm, causing a temporary increase in gymnosperms, and that the vegetation changed drastically around the end of OAE2 due to the expansion of coniferous vegetation.

Keywords: Paleovegetation, biomarker, Great Valley Sequence, C/T boundary, Cretaceous

©2021. Japan Geoscience Union. All Right Reserved.

Constraint on the Location of the Australasian Tektite Event based on the Thickness Distribution and Gravel Composition of the Ejecta Deposits across the Eastern Indochina

*Toshihiro Tada[1], Ryuji Tada[1,3,2], Paul A Carling[4], Wickanet Songtham[5], Praphas Chansom[5], Thuyên Lê Xuân[6], Toshihiro Kogure[2], Chang Yu[2], Eiichi Tajika[2]

1. Institute for Geo-Cosmology, Chiba Institute of Technology, 2. Department of Earth and Planetary Science, School of Science, The University of Tokyo, 3. Research Center for Earth System Science, Yunnan University, 4. School of Geography and Environmental Sciences, University of Southampton, 5. Northeastern Research Institute of Petrified Wood & Mineral Resources, Nakhon Ratchasima Rajabhat University, 6. Ho Chi Minh City University of Science

Tektites are glass spherules formed by large impacts and reported from 4 strewn fields on the Earth. Australasian tektites distributed widely from Southeast Asia to Antarctica are considered to be formed by an impact event that occurred ca. 0.8 Ma in Southeast Asia (Australasian Tektite Event; AATE). This impact event is the youngest among large impact events. Because of its young age, it is expected that evidence of the impact (impact crater and ejecta deposits) is well preserved.
However, the biggest mystery is that no crater has been found yet despite intensive search efforts. The location of the impact has been considered as somewhere in Eastern Indochina, mainly based on the distribution of the tektites. For more precise constraints on the impact location, the distribution of the ejecta deposit is important since an ejecta deposit becomes thicker toward the impact location. The ejecta deposit of this impact event, however, has not been identified on the Indochina Peninsula. To identify the ejecta deposit of the AATE and clarify its distribution, we have conducted field surveys across a wide area of Eastern Indochina, including northeastern Thailand, central Vietnam, southern Laos, and northern Cambodia.
We identified the ejecta deposit associated with the AATE based on the in-situ occurrence of the tektite fragments (Tada et al. 2020 PEPS) and the discovery of shocked quartz grains with planar deformation features (PDFs) from the Quaternary deposit at Huai Om and HO06 sections in northeastern Thailand. PDFs were confirmed by the measurement of their orientation and SEM/TEM observations.
The ejecta deposit can be divided into three lithostratigraphic units (units 1–3 in ascending order). Unit 1 is composed of gravely silt to sand layers or a sandy gravel layer containing materials reworked from the local basement and occasionally showing cross-lamination. Unit 2 is a tektite-bearing breccia, and Unit 3 is a massive sand to silt layer. Unit 2 and 3 are laterally traceable in eastern Indochina. Based on their stratigraphy and lithological and sedimentological evidence, Unit 1 is probably fine ejecta carried by impact-induced winds. Unit 2 and 3 are considered to be the ejecta curtain deposit breccia and fallout fine ejecta. The thickness of Unit 2 increases toward southwestern Laos, where a breccia of over 9 m thick was found. The regression analysis of the distribution of the thickness of Unit 2, assuming that the log thickness is negatively correlated with log distance from a source area, indicates that the Bolaven Plateau area (15.2°N, 106.1°E) is the most probable impact site.
Unit 2 is composed of weathered basalt fragments, sandstone and mudstone fragments, and fragments of rounded quartzite gravels. This gravel composition of Unit 2 indicates that the target rock of the impact includes basalt, sedimentary rocks, and possibly river gravels. This estimation of the target rocks is consistent with the estimation of the impact site in southwestern Laos, where Neogene to Quaternary basalt lava and Mesozoic sedimentary rocks (mudstone, sandstone, and conglomerate) are widely distributed.
The result of this study strongly supports the hypothesis of Sieh et al. (2019) that the AATE occurred in the basalt field of the Bolaven Plateau, and the crater was buried by younger basalts that erupted after the

©2021. Japan Geoscience Union. All Right Reserved.

impact.

Keywords: Australasian Tektite, Impact, Ejecta

©2021. Japan Geoscience Union. All Right Reserved.

Paleoproterozoic magmatic flare-up of the Ubendian Belt, SW Tanzania: A crustal growth history events before the amalgamation of the Central African Shield

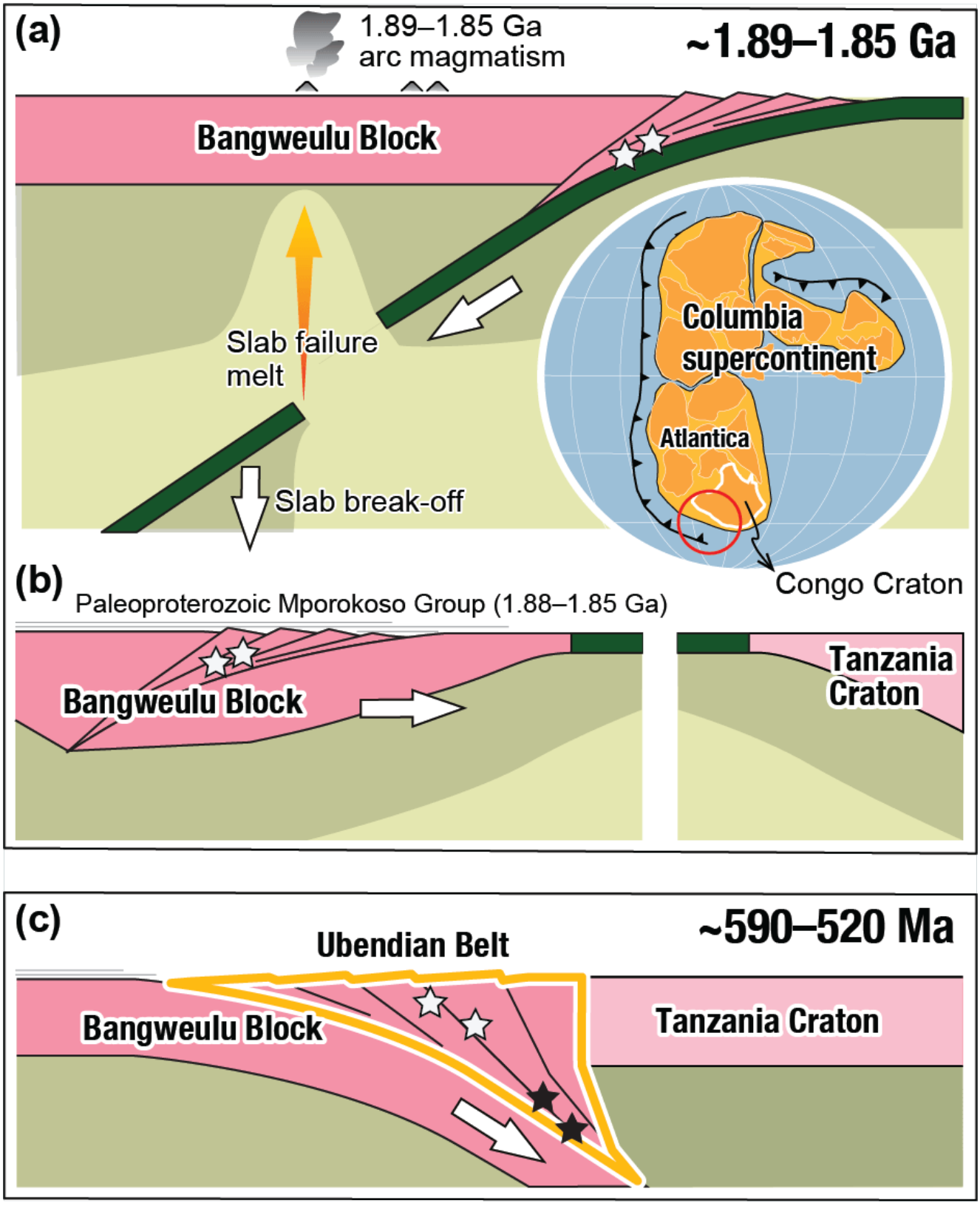
*Ariuntsetseg Ganbat[1], Tatsuki Tsujimori[1,2], Nelson Boniface[4], Daniel Pastor-Galan[1,2,3], Shogo Aoki[5,6], Kazumasa Aoki[6]

1. Graduate School of Science, Tohoku University, 2. Center for Northeast Asian Studies, Tohoku University, 3. Frontier Research Institute for Interdisciplinary Sciences, Tohoku University, 4. Department of Geology, University of Dar es Salaam, 5. Graduate School of International Resource Sciences, Akita University, 6. Center for Fundamental Education, Okayama University of Science

The Ubendian Belt (UDB) is a Paleoproterozoic orogeny between the Archean Tanzania Craton (TZC) and the Bangweulu Block (BWB), which are part of the Congo Craton assembled at ~1.8 Ga, forming the Central African Shield, during the amalgamation of the Columbia Supercontinent and the Gondwana assembly (Ganbat et al., 2021). This study presents the new LA-ICPMS zircon and apatite U–Pb ages, Hf-in-zircon isotope compositions, and whole-rock geochemistry for the metagranitoids from the Ufipa Terrane of the Western Ubendian Corridor of UBD and the BWB. LA-ICPMS zircon U–Pb ages confirmed magmatic events from 1.89 to 1.85 Ga. The metagranitoids of the Western Corridor of UBD and that of the BWB are compositionally similar and are contemporaneous. The geochemistry of 1.89–1.85 Ga metagranitoids and granoporphyries are suggested that they are originated from slab-failure magma. The melt derived from the mafic upper portion of the detached slab induced the partial melting of crust which can form felsic magmatism in the BWB and the UBD. The development of thick sediments (the Mporokoso Group) overlying the BWB implies a crustal extension after the Orosirian magmatic flare-up due to the slab failure. Zircons from two metagranitoids from the Northern Ufipa Terrane evidence the tectonothermal event at ~570 Ma. However, we found non-annealed Orosirian apatites in metagranitoids from the Southern Ufipa Terrane and the BWB, implying that the Neoproterozoic overprint in the Ufipa Terrane was heterogeneous. Zircon ε Hf(t) value and the model ages are indicate interaction with older crust underlying the BWB.

Keywords: Ubendian Belt, Slab-failure magmatism, Paleoproterozoic, U–Pb zircon geochronology

©2021. Japan Geoscience Union. All Right Reserved.



©2021. Japan Geoscience Union. All Right Reserved.

[J] Oral | B (Biogeosciences)：B-CG Complex & General

Fri. Jun 4, 2021 10:45 AM - 12:15 PM JST | Fri. Jun 4, 2021 1:45 AM - 3:15 AM UTC | Ch.26 Zoom Room 26

[B-CG04] Decoding the history of Earth: From Hadean to the present

convener:Tsuyoshi Komiya(Department of Earth Science & Astronomy Graduate School of Arts and Sciences The University of Tokyo), Yasuhiro Kato(Department of Systems Innovation, Graduate School of Engineering, University of Tokyo), Katsuhiko Suzuki(Submarine Resources Research Center, Japan Agency for Marine-Earth Science and Technology), Kentaro Nakamura(Department of Systems Innovation, School of Engineering, University of Tokyo), Chairperson:Toshihiro Tada(Chiba Institute for Technology, Institute for Geo-Cosmology), Tsuyoshi Komiya(Department of Earth Science & Astronomy Graduate School of Arts and Sciences The University of Tokyo)

The latest results of Earth's evolution and geological processes through 4.6 billion years from Hadean to Modern, based on various approaches including fieldworks, chemical analyses, experiments and computer simulation, will be presented. In this session, we aim to discuss and understand causal relationships and interplay among the evolution of Earth's deep interior, changes in the surface environments, and development and evolution of life. Wide-ranging topics are accepted.

10:45 AM - 11:00 AM JST | 1:45 AM - 2:00 AM UTC

[BCG04-07] Reconstruct BIF bearing volcano-sedimentary sequence of Neoproterozoic, El-Dabbah Formation, Central Eastern Desert, Egypt

*Shoichi Kiyokawa[1], TAISHI SUZUKI[1], Kenji Horie[2], Mami Takehara[2], Maher Dawoud[3] (1.Department of Earth and Planetary Sciences Faculty of sciences, Kyuushu University, 2.National Institute of Polar Research, 3. Menoufiya University)

11:00 AM - 11:15 AM JST | 2:00 AM - 2:15 AM UTC

[BCG04-08] Occurrence and geochemistry of the Eoarchean carbonate rocks: Deciphering the co-evolution of life and bioessential element contents in the seawater through geologic time

★Invited Papers

*Satoshi Yoshida[1], Yusuke Sawaki[1], Tsuyoshi Komiya[1] (1.Department of Earth Science & Astronomy, Graduate School of Arts and Sciences, The University of Tokyo)

11:15 AM - 11:30 AM JST | 2:15 AM - 2:30 AM UTC

[BCG04-09] Nanoscale analysis of trace elements in the Gunflint microfossils using a NanoSIMS: implication for the elemental cycle in the Paleoproterozoic biosphere

*Akizumi Ishida[1], Kouhei Sasaki[1], Takeshi Kakegawa[1], Naoto Takahata[2], Yuji Sano[2] (1.Department of Earth Science, Graduate school of Science, Tohoku University, 2.Atmosphere and Ocean Research Institute, the University of Tokyo)

11:30 AM - 11:45 AM JST | 2:30 AM - 2:45 AM UTC

[BCG04-10] Nitrogen isotope compositions of ca. 2.0 Ga Zaonega Formation in Russia: their constraints on Paleoproterozoic oceanic environments and microbial activities

★Invited Papers

*Kouhei Sasaki[1], Akizumi Ishida[1], Ko Hashizume[2], Takeshi Kakegawa[1] (1.Tohoku University, 2.Ibaraki University)

11:45 AM - 12:00 PM JST | 2:45 AM - 3:00 AM UTC

[BCG04-11] Upper Limit of the Activity of Anaerobic Microbial Ecosystem in the Early Earth

*Yasuto Watanabe[1], Eiichi Tajika[1], Kazumi Ozaki[2], Peng K Hong[3] (1.The University of Tokyo, 2.Toho University, 3.Chiba Institute of Technology)

12:00 PM - 12:15 PM JST | 3:00 AM - 3:15 AM UTC

[BCG04-12] The micro-scale speciation analyses of sulfur in the Ediacaran limestones: Implications for diagenetic mobilization of sulfur species

★Invited Papers

*Fumihiro Matsuura[1,2], Ryoichi Nakada[3], Yusuke Sawaki[4], Yuichiro Ueno[2,5,6], Masafumi Saitoh[7], Iori Kajitani[1], Tomohiro Usui[1,2] (1.Institute of Space and Astronautical Science, JAXA, 2.Earth-Life Science Institute, Tokyo Tech, 3.Kochi Institute for Core Sample Research, JAMSTEC, 4.Department of Earth Science and Astronomy Graduate School of Arts and Sciences, The University of Tokyo, 5.Institute for Extra-cutting-edge Science and Technology Avant-garde Research (X-star), JAMSTEC, 6.Department of Earth and Planetary Sciences, School of Science, Tokyo Tech, 7.Institut des sciences de la Terre, University of Lausanne)

Reconstruct BIF bearing volcano-sedimentary sequence of Neoproterozoic, El-Dabbah Formation, Central Eastern Desert, Egypt

*Shoichi Kiyokawa[1], TAISHI SUZUKI[1], Kenji Horie[2], Mami Takehara[2], Maher Dawoud[3]

1. Department of Earth and Planetary Sciences Faculty of sciences, Kyuushu University, 2. National Institute of Polar Research, 3. Menoufiya University

The El-Dabbah Group records a history of oceanic island arc accretion, collision, and collapse within the northern East African Orogeny during 770-570 Ma in Neoproterozoic.The El-Dabbah Group is an iron formation containing metavolcanic rocks in the Nubian Shield, Central Eastern Desert, Egypt. It preserves a sequence of relatively undeformed lower greenschist-facies rocks, overlain by subaerial sedimentary strata deposited in strike-slip basins (the Atsham Formation and the Hammamat Group). This formation includes a metavolcanics succession (>5500 m thick) containing three members, including coarse massive metavolcanic rock, pillow lavas, volcaniclastics with banded iron formation, and bedded volcaniclastic rock.At least 14 iron formations successions have been identified stratigraphically middle unit within 5500m thick volcaniclastic sequence at which are interbedded with greenish and black shales. Iron oxide beds most likely originated from dissolved Fe^{2+} sourced from oceanic arc volcanism, with repeated iron precipitation occurring during successive volcanically active periods. Four faulting were distinguished within the El-Dabbah area: (1) top-to-the-S low-angle thrusting; (2) NNE side down normal faulting; (3) sinistral displacement on north–south faults; and (4) WNE trend N-side-down normal faulting with the Hammamat Group. We obtained the crystallization ages of a granite (638.1 ±2.9 Ma) and a quartz porphyry (659.6 ±3.0 Ma). The detrital zircon age of the Hammamat Group show peaks at 650, 680, and 790 Ma. The El Dabbar Group formed several iron formations within relative proximal basin with hydrothermal section, which may be not related glacial condition.

Keywords: neoproterozoic, central East Desret, Banded Iron Formation

©2021. Japan Geoscience Union. All Right Reserved.

Occurrence and geochemistry of the Eoarchean carbonate rocks: Deciphering the co-evolution of life and bioessential element contents in the seawater through geologic time

*Satoshi Yoshida[1], Yusuke Sawaki[1], Tsuyoshi Komiya[1]

1. Department of Earth Science & Astronomy, Graduate School of Arts and Sciences, The University of Tokyo

Many geologists and biologists believe that the trace elements utilized in the metalloenzymes of life reflect the availability of trace elements in ancient ocean where those enzymes first appeared (e.g., Fraú sto da Silva and Williams, 2001). However, studies to estimate composition of paleoseawater have only been conducted in the last 20 years, so it is necessary to confirm whether the life and bioessential element contents in ocean actually co-evolved.

Geochemistry of banded iron formation (BIF) is commonly utilized to estimate surface environmental conditions such as seawater composition during the Archean. However, an estimation of ocean composition with BIF has some difficulties. For example, trace elements contents in a BIF depends not only these elements contents in ambient seawater but also sedimentary rates, involvement of detrital materials (e.g., Bau, 1993), kinetic effect originated from adsorption rate of element on iron-oxide (e.g., Byrne and Kim, 1990), and other interference elements such as Si (Konhauser et al., 2009). Another problem is that most of modern iron-rich sediments are formed near hydrothermal vents, so they don’t reflect the global seawater composition. Despite the problems with the estimation using the BIF, few studies have been conducted to estimate the concentrations of bio-essential elements in the paleoseawater using carbonate rocks, which also exist as chemical sedimentary rocks. This is because it was reported that the Eoarchean carbonate rocks could be formed secondary to igneous rocks due to an alteration (e.g., Rose et al., 1996).

Here, we estimated the concentrations of V, Co, Ni, and Zn in the Eoarchean seawater using carbonate rocks from Nulliak supracrustal rocks (ca. 3.9 Ga) and Isua supracrustal belt (ca. 3.8 Ga). The Nulliak and Isua carbonate rock used in this study have already been reported to be derived from chemical sedimentary rocks by Yoshida et al. (2021) and (2019; JpGU meeting), respectively.

We analyzed V, Co, Ni, and Zn contents of the whole rocks of the carbonate rocks with High-Resolution Inductively Coupled Plasma Mass Spectrometry (HR-ICP-MS).

We estimated bioessential element contents of the Eoarchean seawater using carbonate rocks, which are the least affected by silicification and contamination of detrital material reported by previous studies (Yoshida et al., 2019, 2021). Moreover, we compared these element contents in the Eoarchean carbonate rocks with those of modern carbonate rocks.

The secular change of V, Co, Ni, and Zn contents show that the Eoarchean seawater are enriched in transitional element than modern seawater. The estimation using the BIF reported by previous study is inconsistent with the results of this study because it suggests that V and Zn were more depleted in the Eoarchean ocean than later ocean (Robbins et al., 2013; Aoki et al., 2018). This discrepancy can be attributed to the fact that BIFs in the younger age were strongly influenced by hydrothermal fluids.

©2021. Japan Geoscience Union. All Right Reserved.

Nitrogenase is classified into V-Fe (Vnf), Mo-Fe (Nif), and Fe-Fe (Anf) types, and is thought to have existed as early as the Archean (e.g., Stüeken et al., 2015). Phylogenetic analysis of nitrogenase reported that Nif was the closest to the origin of nitrogenase (e.g, Boyd et al., 2011). This study suggests that nitrogenase and V content in the ocean didn’ t co-evolve. Cobalt is indispensable for the production of a vitamin B12 for prokaryote. On the other hand, eukaryotes have an ability to synthesize methionine independently of Co. Therefore, this study suggests that biological Co dependence and Co concentration in the ocean may have co-evolved. Nickel is an essential element for methanogen, which is considered to be one of the candidates for early life. This study indicates that the elemental requirements of methanogen may have co-evolved with ocean composition. These indicate that life and ocean composition co-evolve, but that evolution can also be driven by biological factors.

Keywords: Carbonate rocks, Bioessential elements, Isua supracrustal belt, Nulliak supracrustal rocks, Rare earth elements, Eoarchean

©2021. Japan Geoscience Union. All Right Reserved.

Nanoscale analysis of trace elements in the Gunflint microfossils using a NanoSIMS: implication for the elemental cycle in the Paleoproterozoic biosphere

*Akizumi Ishida[1], Kouhei Sasaki[1], Takeshi Kakegawa[1], Naoto Takahata[2], Yuji Sano[2]

1. Department of Earth Science, Graduate school of Science, Tohoku University, 2. Atmosphere and Ocean Research Institute, the University of Tokyo

In this study, we focused on elemental distributions of the Paleoproterozoic ‘Gunflint microfossil’ by using lateral high-resolution secondary ion mass spectrometry (NanoSIMS). Distributions of bioessential trace elements, such as phosphorus, iron, and molybdenum were newly measured together with biological major elements (such as carbon, nitrogen, and sulfur). The ‘Gunflint microfossil’ is a generic term for the group of microbial fossils found in the Gunflint Formation, Canada, which is a Paleoproterozoic sedimentary formation. The Gunflint microfossil has several types of morphology with size distributions from a few microns to a hundred-micron meter. Their morphological characteristics with carbon isotope compositions or distributions of organic elements determined by SIMS were reported in previous studies (e.g., Tyler & Barghoorn, 1954, Science; House et al., 2000, Geology; Wacey et al., 2013, PNAS; Williford et al., 2013, GCA). Although microscale analyses of major organic elements were performed in previous studies, bioessential trace elements that have crucial information to determine not only metabolic pathways and species of microfossils but also further implicate the elemental cycle in the biosphere at that time, have rarely been measured because of some technical difficulties.
In our research, we adopted and improved the acid treatment technic proposed by Grey and Sugitani (2009, Precam.Res.), and finally succeed to isolate ‘naked’ Gunflint microfossils from bulk cherty rocks without any destructions of microfossil structures (Sasaki et al., 2021, in prep.). In this research, we developed a new methodology to measure the depth-dependent elemental profile utilizing the sputtering effect of primary ion beam by NanoSIMS targeting such ‘naked’ microfossils without any matrix effect from minerals. As a result, we succeed to detect phosphorus and trace amounts of molybdenum directly from the organic part of Gunflint microfossils. This is the first report of the detection of organic phosphorus from the Paleoproterozoic microfossils and suggests that microbes in 1.9 billion years ago have already utilized phosphorus similar to modern life. This further implicates that life in this age had already been evolved and utilized phosphorus-based bio-structures and functions such as phospholipid membrane or ATP. In addition, detection of organic-related molybdenum from microfossils, which is the typical central metal of the nitrogen metabolizing enzyme, has the potential to prescribe a microbial activity and surrounding biosphere in that age.

Keywords: Gunflint Microfossils, Paleoproterozoic, NanoSIMS, phosphorus

©2021. Japan Geoscience Union. All Right Reserved.

Nitrogen isotope compositions of ca. 2.0 Ga Zaonega Formation in Russia: their constraints on Paleoproterozoic oceanic environments and microbial activities

*Kouhei Sasaki[1], Akizumi Ishida[1], Ko Hashizume[2], Takeshi Kakegawa[1]

1. Tohoku University, 2. Ibaraki University

Sedimentary rocks of organic-rich detrital sediments from 1.98 Ga Zaonega Formation, Russia are deposited at about the same time as the Lomagundi Jatuli Event that was one of the largest positive carbonate carbon isotope ($\delta^{13}C$) excursion in earth history and are also known to contain shungite (solidified petroleum-like material). It is a key stratum when considering the carbon cycle between the atmosphere, hydrosphere, and biosphere in the early Proterozoic era. The carbon isotope variability recorded in the Zaonega Formation has been linked to the nitrogen isotope variability, but it may be biased to the analytical sample and needs to be reassessed. The nitrogen isotope composition of sediments is more linked to microbial ecology than carbon isotopes, and more detailed nitrogen isotope analysis can constrain the early Proterozoic microbial ecosystems.

In this study, using stepwise combustion nitrogen isotope analysis for sedimentary rocks from Zaonega Formation, released amounts of carbon, nitrogen and argon, together with nitrogen isotope ratio ($\delta^{15}N$) and ^{40}Ar / ^{36}Ar ratio (Ar ratio) were calculated. By these results, host phase-dependent differences of nitrogen was estimated to presume the marine environment including the biological nitrogen cycle at that time. The analysis was performed on the greywacke and black shale samples. As a preliminary analysis, both greywacke and black shale samples were combusted from 400 ℃ to 800 ℃ in 50 ℃ steps, and finally at 1200 ℃ in oxygen atmosphere (fine step). From the results, it was clarified that major release of nitrogen and argon, or $\delta^{15}N$ gaps were observed at combustion temperatures of 400 ℃, 500 ℃, 600 ℃, 700 ℃ and 1200 ℃. Based on this preliminary analysis, a simplified version of released profiles and isotope compositions of N and Ar were measured in 9 samples of black shale after that (rough step).

Both greywacke and black shale samples showed similar releasing profiles in N and Ar. Major release of nitrogen and carbon were observed in the same temperature range (mainly 650-700 ℃) with $\delta^{15}N$ value of less than ~+4 ‰in both samples, suggesting that the host phase of nitrogen was the organic matter. On the other hand, a heavy $\delta^{15}N$ value of up to ~+12 ‰was obtained at the lower and higher temperature range than that of an organic matter. In addition, a higher Ar ratio was obtained in the same temperature range, suggesting that this nitrogen was hosted in clay minerals. The $\delta^{15}N$ value, up to ~+12 ‰, obtained in this study is the highest value reported in previous studies of the Zaonega Formation. Thus, the nitrogen in clay mineral have a high $\delta^{15}N$ value. This result suggests that the biological nitrogen cycle (BNC) in the oxidative environment may have been predominant in the land or shallow waters where clay is formed.

Nine black shale samples, evenly sampled from the bottom to the top of the core sample, were analyzed by rough step and $\delta^{15}N$ values were profiled to determine host phases of nitrogen and their sources in each sample. As a result, the $\delta^{15}N$ values of organic matter and clay minerals were clearly separated in the range of ~0 to ~+5 ‰and of ~+1 to ~+12 ‰, respectively. It shows that the nitrogen isotope ratio in the seawater nitrogen reservoir vary and became rich in ^{15}N over time. It can be interpreted that seawater gradually changed from a reducing environment to an oxidizing environment.

©2021. Japan Geoscience Union. All Right Reserved.

These profiles suggested that oxygen concentrations could be increased on land and ocean surfaces, which lead to the gradual development of the BNC in an oxidative environment. Such an environment may cause an increase in the supply of nutrient elements due to high weathering rate, in primary production in the photic zone and in variety of ecosystem due to the development of the chemocline. This study contributes to the elucidation of the peculiar marine environment of the Paleoproterozoic era.

Keywords: stepwise combustion analysis, Paleoproterozoic, Nitrogen isotope

©2021. Japan Geoscience Union. All Right Reserved.

Upper Limit of the Activity of Anaerobic Microbial Ecosystem in the Early Earth

*Yasuto Watanabe[1], Eiichi Tajika[1], Kazumi Ozaki[2], Peng K Hong[3]

1. The University of Tokyo, 2. Toho University, 3. Chiba Institute of Technology

The global marine primary production in the modern ocean is suggested to be limited by the supply of phosphorus from rivers (e.g. Tyrrell, 1999). However, in the early Earth before the onset of oxygenic photosynthesis, the global marine primary production is suggested to have been limited by the production of electron donors, including hydrogen (H_2), ferrous iron, and carbon monoxide (CO) (e.g. Kharecha et al., 2005). Under the anoxic conditions in early Earth, it is suggested that an hydrocarbon haze layer is formed in the upper atmosphere when the supply of electron donors is large enough. Because such a haze layer absorbs the UV-flux from the sunlight effectively (Wolf and Toon, 2010), it should affect the atmospheric photochemistry, hence the activity of anaerobic marine microbial ecosystem. However, the relationship between the biological activity and the formation of haze has not been demonstrated. Here, we employed a coupled model of one-dimensional photochemical model “Atmos” (Arney et al., 2016) and a marine microbial ecosystem model to elucidate the responses of the biological activities in the early Earth in association with the formation of haze for wide ranges of parameters (atmospheric CO_2 level, H_2 outgassing rate, Fe(II) upwelling rate, and burial efficiency of organic carbon).
We found that the primary productivity of anaerobic biosphere under the hazy atmosphere is around 1.0 GtC/yr, independent of the thickness of the haze layer and the atmospheric CO_2 level. In the hazy condition, formation rates of electron donors (H_2 and CO) in the atmosphere decreases with development of haze, hence the biogenic methane flux and the haze formation rate is decreased. As a result, the maximum level of primary productivity due to anaerobic ecosystem is achieved at the clear-sky condition close to the boundary of the formation of haze. Interestingly, this maximum level is always around 1.5 GtC/yr (~3% of the present marine gross primary production), independent of values of parameters we considered. Thus, this maximum level corresponds to the upper limit of the activity level of anaerobic ecosystem in the early Earth. Once the supply of electron donors increases to allow the activity of anaerobic ecosystem to reach this critical level, haze is formed in the atmosphere and the activity level of anaerobic ecosystem decreases to ~1.0 GtC/yr. This upper limit is broadly consistent with the previous estimates of the primary production in the early Earth based on independent methods (Kharecha et al. 2005; Canfield, 2006; Hao et al., 2020). Even after the evolution of the oxygenic photosynthesis, the upper limit of the activity level of anaerobic ecosystem is almost the same. Based on these results, the evolution of the surface environments and the marine primary productions in the early Earth system will be discussed.

Keywords: Archean, Biogeochemistry

©2021. Japan Geoscience Union. All Right Reserved.

The micro-scale speciation analyses of sulfur in the Ediacaran limestones: Implications for diagenetic mobilization of sulfur species

*Fumihiro Matsuura[1,2], Ryoichi Nakada[3], Yusuke Sawaki[4], Yuichiro Ueno[2,5,6], Masafumi Saitoh[7], Iori Kajitani[1], Tomohiro Usui[1,2]

1. Institute of Space and Astronautical Science, JAXA, 2. Earth-Life Science Institute, Tokyo Tech, 3. Kochi Institute for Core Sample Research, JAMSTEC, 4. Department of Earth Science and Astronomy Graduate School of Arts and Sciences, The University of Tokyo, 5. Institute for Extra-cutting-edge Science and Technology Avant-garde Research (X-star), JAMSTEC, 6. Department of Earth and Planetary Sciences, School of Science, Tokyo Tech, 7. Institut des sciences de la Terre, University of Lausanne

The Ediacaran period was characterized by an increase in atmospheric oxygen concentrations that was critical for the evolution of life. Oceanic sulfate concentration increases with the increase of atmospheric oxygen concentrations, and the oceanic sulfate concentration in paleo-ocean is inferred from sulfur isotopic compositions of sedimentary sulfates and pyrite, and sulfur concentrations of pyrite and carbonate associated sulfate (CAS). Sulfur isotopic composition of sedimentary pyrite has been known to express microbial activities which involve large sulfur isotope fractionation; however, in addition to the microbial processes, environmental factors such as sedimentation rate, redox condition, and iron availability have come to be known to have strong impacts on the isotopic composition and concentration of sedimentary pyrite. Besides, elucidating diagenetic impacts on the isotopic composition and concentration of CAS is necessary to reconstruct the paleo-oceanic sulfate concentration. Here, we conducted μ-XRF and S K-edge XANES analyses of limestones of the Ediacaran Doushantuo and Dengying formations using a drilling core samples collected from Three Gorges area, south China. The results show maximum 1237 ±315 ppm of abundant reduced organic sulfur species such as thiophenes and thiols were exclusively existing in the Dengying limestones. Given the low pyrite content in the Dengying limestones, lower than 100 ppm, the high organic sulfur contents indicate organic matter outcompeted iron to scavenge sulfide expelled from sulfate reducing microbes in sediments, which force us considering environmental factors as well as microbial process to interpret the oceanic sulfur cycling based on the isotopic composition of pyrite. The diagenetic impact on CAS was quantified by comparing contents of sulfur species in micrite and in sparite. High strontium content (>1%) and existence of celestine ($SrSO_4$) in sparite indicate the Dengying limestones used in this study were only suffered from marine diagenesis. Our results show the CAS content decreased from 277 ±288 ppm in micrite to 229 ± 138 ppm in sparite, which suggests CAS concentration decreased even during marine diagenesis in which porewater sulfate was mM level. Thus, we conclude the isotope and concentration of CAS in micrite are the most appropriate to extract the information of paleo-oceanic sulfate. Our micro-scale mapping of sulfur species revealed how oceanic sulfate in paleo-ocean was preserved and subsequently altered in the carbonate sediments, which provided us the ways to extract the most primary information of paleo-ocean from carbonate and interpret the paleo-oceanic sulfur cycling.

Keywords: carbonate associated sulfate, organic sulfur, diagenesis, sulfur cycling

©2021. Japan Geoscience Union. All Right Reserved.

[J] Oral | M (Multidisciplinary and Interdisciplinary)：M-IS Intersection

Fri. Jun 4, 2021 9:00 AM - 10:30 AM JST | Fri. Jun 4, 2021 12:00 AM - 1:30 AM UTC | Ch.16 Zoom Room 16

[M-IS11] Biogeochemistry

convener:Keisuke Koba(Center for Ecological Research, Kyoto University), Hideaki Shibata(Field Science Center fot Northern Biosphere, Hokkaido University), Naohiko Ohkouchi(Japan Agency for Marine-Earth Science and Technology), Youhei Yamashita(Faculty of Environmental Earth Science, Hokkaido University), Chairperson:Keisuke Koba(Center for Ecological Research, Kyoto University), Yoshiyuki Inagaki(Forestry and Forest Products Research Institute)

Biogeochemistry is an interdisciplinary study field including ecology, geochemistry, oceanography, limnology, hydrology, soil science, and environmental sciences. Respective researches have tended to be conducted separately so far. This session aims to provide a common platform for biogeochemists of different disciplines, which facilitates the interactive discussion and information exchanges for further development of biogeochemical studies

9:00 AM - 9:15 AM JST | 12:00 AM - 12:15 AM UTC

[MIS11-01] Source of dissolved black carbon in streams

*Youhei Yamashita[1,2], Daiki Kojima[2], Natsumi Yoshida[2], Hideaki Shibata[3,2] (1.Faculty of Environmental Earth Science, Hokkaido University, 2.Graduate School of Environmental Science, Hokkaido University, 3.Field Science Center for Northern Biosphere, Hokkaido University)

9:15 AM - 9:30 AM JST | 12:15 AM - 12:30 AM UTC

[MIS11-02] Biodegradation kinetics of different molecular-size classes of freshwater dissolved organic matter

*Yasuhiko T. Yamaguchi[1], Koichi Shimotori[2], Akio Imai[2], Yusuke Okazaki[3], Tomoyuki Ohara[1], Miho Nakamura[1], Shoichi Hichiri[1], Takahiro Okamoto[1], Kazuhide Hayakawa[1] (1.Lake Biwa Environmental Research Institute, 2.NIES Lake Biwa Branch Office, National Institute for Environmental Studies, 3.Institute for Chemical Research, Kyoto University)

9:30 AM - 9:45 AM JST | 12:30 AM - 12:45 AM UTC

[MIS11-03] Responses of phytoplankton biomass to river-borne nutrient flux in the coastal waters of Suruga Bay

*Tomoya Iwata[1], Yuri Amada[1], Akifumi Kitabatake[1], Nao Yonehara[1], Mizuho Shikata[1], Hiroshi Kobayashi[1], Mitsuhiro Toratani[3], Akira Tsukagoshi[2], Kenji Kato[2] (1.Faculty of Life and Environmental Sciences, University of Yamanashi, 2.Faculty of Science, Shizuoka University, 3.School of Engineering, Tokai University)

9:45 AM - 10:00 AM JST | 12:45 AM - 1:00 AM UTC

[MIS11-04] Investigation on the sources of arsenic and the formation process of arsenic-rich peat in groundwater level in Asia

*Thinh Van NGUYEN[1], Kuwahara Yoshihiro[1], Masaru Matsumoto[2], Thanh Dinh Xuan[3], Nguyen Dinh Nguyen[3], Myo Zaw[4] (1.Department of Environmental changes, Faculty of Social and Cultural Studies, Kyushu University, Fukuoka, 819-0395, Japan, 2.Institute of Tropical Agriculture, Kyushu University, Fukuoka, 819-0395, Japan, 3.Faculty of Geology, Hanoi University of Science, Vietnam National University, 334 Nguyen Trai, Thanh Xuan, Hanoi, Vietnam., 4.Graduate School of Integrated Sciences for Global Society, Kyushu University, Fukuoka, 819-0395, Japan)

10:00 AM - 10:15 AM JST | 1:00 AM - 1:15 AM UTC

[MIS11-05] Why is Rawanbuki large?

*Masaaki Chiwa[1], Yasuhiro Utsumi[1], Naoaki Tashiro[1], Yuko Yasuda[1,4], Ken'ichi Shinoduka[1,3], Ru Yang[1], Nao Nagano[1], Shusuke Murata[1], Takuma Nakamura[1], Kohei Yamauchi[1], Yuji Kabemura[1], Tatsuro Ando[2],

Hiroshi Sawamura[2] (1.Kyushu University Forest, 2.Ashoro Museum of Paleontology, 3.Fukuoka Institute of Technology, 4.Forest Research and Management Organization)

10:15 AM - 10:30 AM JST | 1:15 AM - 1:30 AM UTC

[MIS11-06] Comparison of litter decomposition rates and dissolved organic carbon fluxes in soils across global climatic gradient

*Kazumichi Fujii[1], Chie Hayakawa[2], Yoshiyuki Inagaki[1], Shinya Funakawa[3], Kosaki Kosaki[4] (1.Forestry and Forest Products Research Institute, 2.Utsunomiya University, 3.Kyoto University, 4.Aichi University)

Source of dissolved black carbon in streams

*Youhei Yamashita[1,2], Daiki Kojima[2], Natsumi Yoshida[2], Hideaki Shibata[3,2]

1. Faculty of Environmental Earth Science, Hokkaido University, 2. Graduate School of Environmental Science, Hokkaido University, 3. Field Science Center for Northern Biosphere, Hokkaido University

Pyrogenic carbon (PyC) is pyrolyzed product derived from incomplete combustion during biomass burning as well as fossil fuel combustion and plays an important role as carbon sink in the global carbon cycle. A major fraction of PyC produced with landscape fire is initially deposited to on-site soils. Atmospheric deposition of soot is also known to be important source of soil PyC. Transport of dissolved fraction of oxidized PyC in soil, defined as dissolved black carbon (DBC), to stream has been considered to be one of the important loss pathways of PyC in soil, while the mechanism is not well documented. We measured quantity and quality of DBC determined by a benzenepolycarboxylic acids method together with quantitative and qualitative parameters of bulk DOM in streams in Hokkaido University’ s Uryu Experimental Forest, Hokkaido, northern Japan, which catchments were not affected by landscape fire for at least 110 years. DBC having relatively less polycondensed signature occurred in the streams, irrespective of differences in watershed characteristics and seasons, suggesting that atmospheric deposition of PyC to the catchment is probably a major source of stream DBC. The DBC concentration was linearly related to the DOC concertation, irrespective of differences in watershed characteristics and seasons. Furthermore, an index of the polycondensation degree of DBC was correlated with qualitative parameters of bulk DOM. That is, the polycondensation degree of DBC was positively correlated with specific UV absorbance (SUVA) and DOC/DON ratio, while negatively correlated with spectral slope ratio (S_R) and fluorescence index. Such quantitative and qualitative relationships between DBC and bulk DOM imply that transfer mechanism from soils to streams is similar between thermally altered polycondensated DBC and higher plant derived high molecular weight aromatic DOM.

Keywords: Pyrogenic carbon, Dissolved black carbon, soot

©2021. Japan Geoscience Union. All Right Reserved.

Biodegradation kinetics of different molecular-size classes of freshwater dissolved organic matter

*Yasuhiko T. Yamaguchi[1], Koichi Shimotori[2], Akio Imai[2], Yusuke Okazaki[3], Tomoyuki Ohara[1], Miho Nakamura[1], Shoichi Hichiri[1], Takahiro Okamoto[1], Kazuhide Hayakawa[1]

1. Lake Biwa Environmental Research Institute, 2. NIES Lake Biwa Branch Office, National Institute for Environmental Studies, 3. Institute for Chemical Research, Kyoto University

Degradation of aquatic dissolved organic matter (DOM) is a major process of the global biogeochemical cycles. Molecular sizes of DOM have been suggested to have a strong relationship to DOM reactivity (the size-reactivity continuum model: Amon & Benner, 1996, Limnol. Oceanogr. 41:41-51; Benner & Amon, 2015, Annu. Rev. Mar. Sci. 7:185–205). Yet, details and mechanisms of the link still remain poorly understood. In this study, we investigated biodegradation kinetics of different molecular-size classes of natural DOM in a deep meso/oligotrophic lake (Lake Biwa, Japan) and an inflowing river to the lake (Yasu River) by long-term dark incubations of water samples (> 200 days). Changes of molecular size distribution of dissolved organic carbon (DOC) were quantified by a custom-made high-performance size-exclusion chromatograph with total organic carbon analyzer (HPSEC-TOC: Shimotori et al. 2016, Limnol. Oceanogr. Meth. 14:637-648). Two molecular size classes of DOC were identified by HPSEC-TOC: high-molecular-weight (HMW) DOC (weight-averaged molecular weights (M_w) ~ 150kDa) and low-molecular-weight (LMW) DOC (M_w ~ 2kDa). HMW DOC was all degraded within 200 days, while LMW DOC contained semi-labile (LMW SLDOC) and refractory (LMW RDOC) fractions in this time scale. Thus, the DOM examined in this study can be modeled by mixing of the three components (1. HMW DOC: ~10%, 2. LMW SLDOC: ~30%, 3. LMW RDOC: ~60%). HMW DOC showed higher degradation rates than LMW SLDOC (k-d: 0.02-0.04 and 0.01-0.02, respectively). LMW SLDOC and LMW RDOC showed almost the same M_w values (~2kDa). These results suggest that, while DOM reactivity significantly differs depending on its molecular size on a large MW scale (~150kDa vs ~2kDa), this relationship would not be applicable to the finer MW scale (within the LMW fraction).

Keywords: Aquatic environments, Dissolved Organic Matter, Molecular size, Lake Biwa, Microbes

©2021. Japan Geoscience Union. All Right Reserved.

Responses of phytoplankton biomass to river-borne nutrient flux in the coastal waters of Suruga Bay

*Tomoya Iwata[1], Yuri Amada[1], Akifumi Kitabatake[1], Nao Yonehara[1], Mizuho Shikata[1], Hiroshi Kobayashi[1], Mitsuhiro Toratani[3], Akira Tsukagoshi[2], Kenji Kato[2]

1. Faculty of Life and Environmental Sciences, University of Yamanashi, 2. Faculty of Science, Shizuoka University, 3. School of Engineering, Tokai University

Riverine transports of biogeochemical elements from watersheds can be an important flux that supports the downstream and coastal food webs. Thus, numerous studies have been performed to identify the linkage between terrestrial and coastal ecosystems through nutrient flux from lands to the oceans. However, the spatial and temporal patterns of coastal phytoplankton responses to river-borne materials, as well as the effect of tectonic and volcanic activity on riverine biogeochemical flux, have yet to be fully understood.

Here we present our empirical studies conducted in a Japanese watershed to show that volcanic-rock lithology strongly influences the biogeochemical characteristics of river-borne nutrients and thereby influence primary productivity in the coastal ecosystem. We performed the field sampling campaigns covering the whole area of Kano River watershed, central Japan, to measure discharge, nutrient concentrations, and other physico-chemical variables. The spatial analyses showed that streams and rivers flowing through the lava flow area of the southern east slope of Mt.Fuji (i.e., Mishima Lava) contained high concentrations of basalt-derived minerals (P, Si, V, etc.) and exhibited a significant quantitative contribution to their downstream flux from the entire watershed. Moreover, our coastal-monitoring surveys and batch-culture experiments showed that coastal phytoplankton biomass was fueled by such riverine biogeochemical flux. Furthermore, the satellite ocean color data showed that the spatial and temporal patterns of surface chlorophyll-a concentration tended to respond to nutrient inputs following rainfall and terrestrial runoff events.

On the basis of the obtained results, we emphasize that riverine-nutrient input is critically important to phytoplankton dynamics in this coastal ecosystem. We further discuss the implications of these findings on food web dynamics in coastal ecosystems under changing climate with more frequent storm runoff events.

Keywords: volcanic watershed, spring-fed river, biogeochemical flux, riverine nutrinets, phytoplankton, primary production

©2021. Japan Geoscience Union. All Right Reserved.

Investigation on the sources of arsenic and the formation process of arsenic-rich peat in groundwater level in Asia

*Thinh Van NGUYEN[1], Kuwahara Yoshihiro[1], Masaru Matsumoto[2], Thanh Dinh Xuan[3], Nguyen Dinh Nguyen[3], Myo Zaw[4]

1. Department of Environmental changes, Faculty of Social and Cultural Studies, Kyushu University, Fukuoka, 819-0395, Japan, 2. Institute of Tropical Agriculture, Kyushu University, Fukuoka, 819-0395, Japan, 3. Faculty of Geology, Hanoi University of Science, Vietnam National University, 334 Nguyen Trai, Thanh Xuan, Hanoi, Vietnam., 4. Graduate School of Integrated Sciences for Global Society, Kyushu University, Fukuoka, 819-0395, Japan

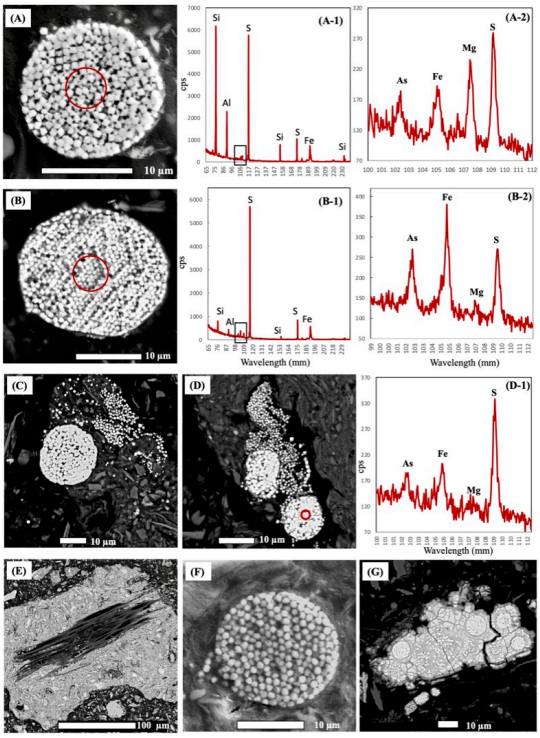
An estimation of more than 130 million people worldwide is exposed to drinking water with an excessive arsenic (As) content. High As concentrations in groundwater (for drinking purpose) were reported in the deltas in Bangladesh and Vietnam, such as Mekong delta –one of the biggest plain in Asia. Here, arsenic (As) concentration and major characteristics of the sediment cores in a shallow aquifer in Bangladesh and Vietnam were investigated using ICP-MS, XRD and ^{14}C-AMS chronology techniques. The results of the present study indicated that the peak concentrations of As (54.7 to 127 μg/g) were in some peat layers (at a depth of 7.5 –8.0 m in Bangladesh and ~23 m in Vietnam). Several types of iron (oxyhidr)oxides and framboidal pyrite, which contain As also were found in the peat samples **(Figure 1-A:G).** The high concentrations of As were in an exchangeable form, As-bearing iron crystalline and As-bearing organic materials. The isotope carbon analysis results revealed that As-rich peat layers in Bangladesh were formed in this area from 3170 to 3901 cal yrs BP, while those in Vietnam were formed from 5962 to 8361 cal yrs BP.

In addition, the original source and initial ecological condition of the As-rich peat sediments in the investigated areas will be clarified using molecular biological techniques, and biodiversity classification of diatoms. I will show the preliminary result of the DNA extraction from the As-rich peat samples, as well as the PCR results using primers of chloroplast loci, which will be used to identify the original plant of the peat. By using the ancient DNA templates of the samples, we expect to reveal the formation condition of the As-rich peat layers in the aquifer, which has not been clarified yet.

The microbial community of the sediment in Bangladesh was analyzed using PCR-DGGE technique. The 16S rRNA gene-based phylogenetic analysis revealed that the bacterial strains in the peats were mainly affiliated with genera *Acinetobacter, Enterobacter*, *Escherichia*, *Bacillus, Clostridiaceae* and *Acinetobacter* **(Figure 1-H)**. Under the permanent saturated condition, the As-rich peat layers should be considered as an important potential driver of the groundwater As in this area.
In the future, the diversity of the bacterial community and their roles on the As mobility under the differential condition of the aquifer, such as high salinity, will be discovered. The pilot experiment using real As-rich sediment and varied levels of intrusion salt will be expected to predict the changes of As concentration in groundwater under effects of sea-level rise in the investigated region.

Keywords: Arsenic contamination, Holocene groundwater, ancient plant, DNA sequencing, Microorganism, ICP-MS

©2021. Japan Geoscience Union. All Right Reserved.



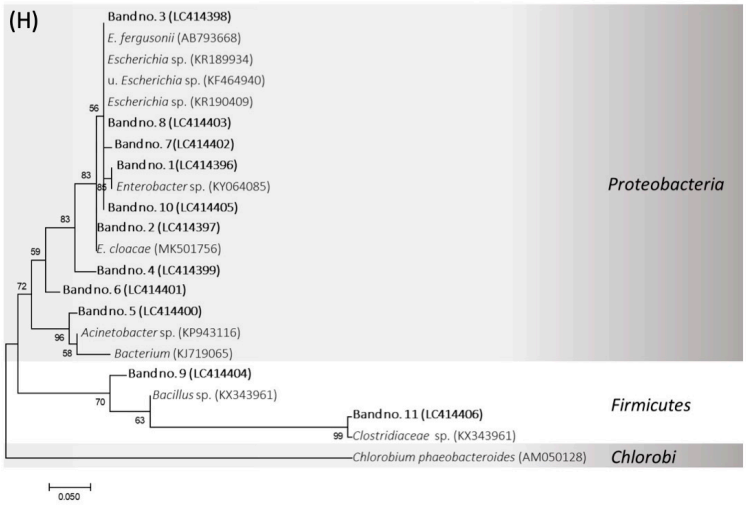


Figure. *(A, B, C, D) The framboidal pyrite and cluster pyrite grains (bright contrast) in the peat samples of this study; (A-1, A-2, B-1, B-2, D-1) The peak for As and major elements on framboidal pyrite surface using WDS technique on FE-EPMA; (E) The ancient plant debris in the peat layer samples; (F, G) Framboidal pyrite in surface sediment of mangrove forest in Vietnam* (Thinh et al. 2018); and *(H)* Phylogenetic tree based on 16S rRNA genes obtained from PCR-DDGE bands from environmental DNA samples from the organic-rich sediment

©2021. Japan Geoscience Union. All Right Reserved.

Why is Rawanbuki large?

*Masaaki Chiwa[1], Yasuhiro Utsumi[1], Naoaki Tashiro[1], Yuko Yasuda[1,4], Ken'ichi Shinoduka[1,3], Ru Yang[1], Nao Nagano[1], Shusuke Murata[1], Takuma Nakamura[1], Kohei Yamauchi[1], Yuji Kabemura[1], Tatsuro Ando[2], Hiroshi Sawamura[2]

1. Kyushu University Forest, 2. Ashoro Museum of Paleontology, 3. Fukuoka Institute of Technology, 4. Forest Research and Management Organization

1. Introduction

Rawanbuki, a variety of the Japanese butterbur Akitabuki (*Petasites japonicus* subsp. *giganteus*), is grown naturally along the Rawan and Moashoro Rivers, Hokkaido. Most Rawanbuki plants reach 2–3 m in height and 10 cm in diameter in two months, and these are much larger than those grown along other nearby rivers. However, the reason that Rawanbuki plants are extremely large remains unknown.
It is hypothesized that nutrients exported from upland areas stimulate the growth rates of Rawanbuki, resulting in them being extremely large. To test this hypothesis, three experiments were conducted: 1) an analysis of the stream water quality, 2) an evaluation of the growth and environmental conditions of Rawanbuki, including soil nutrients, and 3) a manipulation experiment to test fertilization effects on the growth of butterburs.

2. Methods

1) Stream water quality

Synoptic stream water sampling was conducted. The sampling was conducted every 1–3 months from August 2015 to July 2016. The samples were analyzed for electric conductivity (EC), major ions (Cl-, NO3-, SO42-, Na+, NH4+, K+, Mg2+, and Ca2+), and soluble reactive phosphorus (SRP).

2) Growth and environmental conditions of Rawanbuki

The growth of Rawanbuki and soil physicochemical properties were evaluated at three sites along the Rawan River (R1, R2, and R3) and at three sites along the tributary of the Toshibetsu River (T1, T2, and T3) as control sites. At each site, butterburs were harvested in these plots on June 2016 when most butterburs were fully grown. Stem height, stem diameter, leaf width, and the mass of the leaves and stems were measured. Soil physicochemical properties, such as water content, temperature, pH (H2O), EC, inorganic N pool, net N mineralization/nitrification rate, and available P pool, were also measured.

3) Manipulation experiment

Four different treatment plots [control (C), nutrient (N), water (W), and nutrient + water (N + W)] were established. Treatments were conducted for a growing period. After the treatments, all butterburs were harvested, and their stem height, stem diameter, leaf width, and the mass of the leaves and stems were measured.

3. Results and discussion

1) Stream water quality

Solute concentrations, including nitrate, soluble reactive phosphorus, and minerals, in the Rawan and Moashoro Rivers were much higher than those in the neighboring rivers (Toshibetsu and Ashoro Rivers). The underlying geology in the Rawan and Moashoro Rivers is very different from that in the Toshibetsu and Ashoro Rivers, and this geology can characterize the stream water quality in the Rawan River.

©2021. Japan Geoscience Union. All Right Reserved.

2) Growth and environmental conditions of Rawanbuki
Rawanbuki plants grown along the Rawan River is much larger than those along the Toshibetsu River. The high level of soil nutrients and water along the Rawan River may cause the extremely large Rawanbuki plants. Nutrient-rich conditions in the Rawan River likely result from upland stream water inflow.

3) Manipulation experiment
Manipulation experiment confirms the hypothesis that additional nutrients enhance the size of butterburs. Stem height and stem diameter were significantly greater for the nutrient-addition plots (N and N+W) than for the control (C) and water-addition plot (W).

4. Conclusion
The extremely large butterburs are caused by a large amount of nutrients exported from upland areas. These results are the first demonstration of the role of stream water nutrients in enlarging agricultural crops.

Suggested Reading
Chiwa, M. et al. Nutrients exported from upland stream water enlarge perennial biomass crops. Scientific Reports 11, 2200, doi:10.1038/s41598-021-81191-x (2021).

Keywords: Rawanbuki, stream water quality, Agricultural crops

©2021. Japan Geoscience Union. All Right Reserved.

Comparison of litter decomposition rates and dissolved organic carbon fluxes in soils across global climatic gradient

*Kazumichi Fujii[1], Chie Hayakawa[2], Yoshiyuki Inagaki[1], Shinya Funakawa[3], Kosaki Kosaki[4]

1. Forestry and Forest Products Research Institute, 2. Utsunomiya University, 3. Kyoto University, 4. Aichi University

Temperature and soil moisture are crucial factors regulating microbial litter decomposition. And precipitation is a driver of leaching of dissolved organic carbon (DOC) into the mineral soil and groundwater. We compiled decomposition rates of different substrates (forest leaf litter, maize leaf litter, moss litter, lichen litter, and cellulose) and DOC fluxes in the soil profiles. Litter decomposition rates increase with increasing annual mean air temperature, but response to temperature rise differs between substrates. Cellulose and maize leaf litter display a strong dependency to temperature, while slopes of forest, lichen, and moss litter decomposition rates related to temperature rise are smaller than cellulose and maize leaf litter. Forest litter decomposition rates and manganese lignin peroxidase activities increase with increasing litter manganese concentration relative to lignin concentration. DOC fluxes from the organic horizon increase with annual precipitation or C inputs, respectively, but the proportions of DOC flux relative to C inputs are highly variable. The proportions of DOC flux relative to C inputs increase with decreasing soil pH or with increasing lignin peroxidase activities, respectively. The responses of litter decomposition rates and leaching of dissolved organic matter to climate are affected by litter recalcitrance and soil properties as well.

Keywords: litter decomposition, dissolved organic matter, climate change, soil

©2021. Japan Geoscience Union. All Right Reserved.

[J] Oral | M (Multidisciplinary and Interdisciplinary)：M-IS Intersection

Fri. Jun 4, 2021 10:45 AM - 12:15 PM JST | Fri. Jun 4, 2021 1:45 AM - 3:15 AM UTC | Ch.16 Zoom Room 16

[M-IS11] Biogeochemistry

convener:Keisuke Koba(Center for Ecological Research, Kyoto University), Hideaki Shibata(Field Science Center fot Northern Biosphere, Hokkaido University), Naohiko Ohkouchi(Japan Agency for Marine-Earth Science and Technology), Youhei Yamashita(Faculty of Environmental Earth Science, Hokkaido University), Chairperson:Keisuke Koba(Center for Ecological Research, Kyoto University), Hideaki Shibata(Field Science Center fot Northern Biosphere, Hokkaido University)

Biogeochemistry is an interdisciplinary study field including ecology, geochemistry, oceanography, limnology, hydrology, soil science, and environmental sciences. Respective researches have tended to be conducted separately so far. This session aims to provide a common platform for biogeochemists of different disciplines, which facilitates the interactive discussion and information exchanges for further development of biogeochemical studies

10:45 AM - 11:00 AM JST | 1:45 AM - 2:00 AM UTC

[MIS11-07] Effects of understory vegetation removal on soil nitrogen availability and ectomycorrhizal community composition in a northern forest

*Karibu Fukuzawa[1], Takeshi Taniguchi[2], Masataka Nakayama[3] (1.Field Science Center for Northern Biosphere, Hokkaido University, 2.Arid Land Research Center, Tottori University, 3.Graduate School of Agriculture, Kyoto University)

11:00 AM - 11:15 AM JST | 2:00 AM - 2:15 AM UTC

[MIS11-08] Source identification of nitrate increased in forest streams during rainfall events

*Weitian Ding[1], Urumu Tsunogai[1], Fumiko Nakagawa[1], Hiroyuki Sase[2], Masayuki Morohashi[2], Hiroki Yotsuyanagi[2] (1.Graduate School of Environmental Studies, Nagoya University, 2.Asia Center for Air Pollution Research)

11:15 AM - 11:30 AM JST | 2:15 AM - 2:30 AM UTC

[MIS11-09] Chloride cycling in forested watersheds in the Shimanto River Basin

*Yoshiyuki Inagaki[1], Hisao Sakai[1], Atsushi Torii[1], Yoshiki Shinomiya[1], Kazumichi Fujii[1] (1.Forestry and Forest Products Research Institute)

11:30 AM - 11:45 AM JST | 2:30 AM - 2:45 AM UTC

[MIS11-10] To close the nitrogen budgets at a rice paddy

*Kentaro Hayashi[1] (1.Institute for Agro-Environmental Sciences, NARO)

11:45 AM - 12:00 PM JST | 2:45 AM - 3:00 AM UTC

[MIS11-11] Evaluation of global riverine N_2 and N_2O emissions using biogeochemical model

*Kazuya Nishina[1], Akihiko Ito[1] (1.NIES National Institute of Environmental Studies)

12:00 PM - 12:15 PM JST | 3:00 AM - 3:15 AM UTC

[MIS11-12] Footprint analysis on nutrient runoff from farmland in regions of Japan

*Azusa Oita[1], Yoshiya Touge[2], Taku Ishiro[3], Kaori Matsuoka[1], Yusuke Takata[1], Kentaro Hayashi[1] (1.National Agriculture and Food Research Organization, 2.Tohoku University, 3.Yokohama National University)

Effects of understory vegetation removal on soil nitrogen availability and ectomycorrhizal community composition in a northern forest

*Karibu Fukuzawa[1], Takeshi Taniguchi[2], Masataka Nakayama[3]

1. Field Science Center for Northern Biosphere, Hokkaido University, 2. Arid Land Research Center, Tottori University, 3. Graduate School of Agriculture, Kyoto University

Trees and understory vegetation compete with resources underground. Productivity of understory vegetation often corresponds to or larger than that of trees. *Sasa* dwarf bamboo (hereafter Sasa) is one of the major understory vegetation in cool-temperate forests in Japan. It is known that biomass and production of Sasa contribute much to those of ecosystems, but recently understory vegetation including Sasa decreases due to high pressure of deer browsing. On the other hand, most of terrestrial plants live symbiotically with mycorrhiza (e.g., grasses including Sasa with arbuscular mycorrhiza (AM), not all but most trees with ectomycorrhiza (EcM)). However, relationships between EcM colonization or EcM community composition and ecosystem functioning such as nitrogen (N) dynamics are not understood well despite its flexibility depending on stand structure and environmental factors. Decrease of understory vegetation living symbiotically with AM would change EcM dynamics and its relationship with N dynamics in forests. We manipulated removal of above ground understory Sasa and investigated soil N availability, soil physical and chemical properties, EcM colonization rate and EcM community composition before and after the Sasa removal (SR) to clarify the effects of Sasa decline on soil N dynamics and EcM dynamics. We expected that soil N availability increases due to reduced N uptake by Sasa and EcM colonization and composition change in environment without Sasa.
We established twelve plots of 8 m in radius surrounding mature oak (*Quecus crispula*) trees in cool-temperate forest covered with Sasa (S*asa senanensis*) in understory in Nakagawa Experimental Forest in northern Japan. We cut the above ground parts of Sasa and exported them to outside in June 2017 in six SR plots. We collected surface 10 cm soil in May 2017 (before SR) and September 2017 (after SR). We measured gravimetric soil water content, and soil inorganic N content, dissolved organic carbon (DOC) and dissolved organic N (DON) contents after soil extraction (soil:0.5M K_2SO_4=1:10). We measured microbial biomass C (MBC) and N (MBN) using chloroform fumigation method. We also collected root sample of oak surrounding target oak trees in October 2016 (before SR) and September 2017 (after SR). We observed 300 root tip per sample using stereomicroscope and counted EcM and non-EcM root tips. We further distinguish EcM to the types based on the observation of fungal sheath and recorded number. We calculated EcM colonization rate as the ratio of EcM root tips to the total. We extracted DNA of each EcM type and sequenced, then identified OTU (operational taxonomic unit) by homology analysis in nucleotide search. We tested EcM community structure and effects of SR and soil environments by non-metric multidimensional scaling (NMDS) and PerMANOVA.
There was no significant difference in soil inorganic N, DOC, DON contents, DOC/DON, MBC, MBN, and MBC/MBN between SR treatments. EcM colonization rate did not significantly differ between SR treatments. Regarding EcM composition, eleven and ten OTUs were identified before and after SR, respectively. Dominant OTUs throughout the observation period were *Helotiales*, *Russula*, and *Lactarius*. Community composition was not significantly different between SR treatments. In addition, SR or any soil environmental factors did not significantly affect the EcM community composition. Stable EcM community composition after SR would be attributable to stable soil environment after SR and slow response of root associated EcM community under situation that parent trees remained. Further, *Russula* and *Lactarius*, which were dominant even before SR, has been reported to be dominant in N-rich environment, suggesting the possibility that N status before SR in our site was not N limited. This study demonstrated

©2021. Japan Geoscience Union. All Right Reserved.

stable root associated EcM community composition and soil N dynamics after understory vegetation removal during relatively short period after the disturbance.

Keywords: oak, Sasa dwarf bamboo, ammonium, nitrate, root tip

©2021. Japan Geoscience Union. All Right Reserved.

Source identification of nitrate increased in forest streams during rainfall events

*Weitian Ding[1], Urumu Tsunogai[1], Fumiko Nakagawa[1], Hiroyuki Sase[2], Masayuki Morohashi[2], Hiroki Yotsuyanagi[2]

1. Graduate School of Environmental Studies, Nagoya University, 2. Asia Center for Air Pollution Research

Forest ecosystems are deficient in nitrogen in general. Excess loading of nitrogen, however, often leads to “nitrogen saturation” (Aber et al., 1989) in forest ecosystems from which significant quantify of nitrogen is eluted as nitrate. Enrichment of nitrate often caused environmental problems such as degradation of water quality, eutrophication, N_2O emission. Nakagawa et al. (2018) proposed to use the export flux of unprocessed atmospheric nitrate relative to the entire deposition flux (M_{atm}/D_{atm} ratio) in each forested catchment determined precisely using ^{17}O-excess of eluted nitrate as a new index for the nitrogen saturation stage. The concentration of nitrate in forest stream, however, often shows significant increase during rainfall. On the other hand, little is known about the variation in the concentration of unprocessed atmospheric nitrate in forest streams in response to the nitrate increase during rainfall. Therefore, we must clarify the source of nitrate that increased during rainfall, and quantify the impact of the changes in the concentration of unprocessed atmospheric nitrate in forest streams during rainfall on estimating M_{atm}/D_{atm} ratio.

In this study, we determined the changes in the concentration of unprocessed atmospheric nitrate in response to rainfall at Kaji River forest catchment (KJ) in Niigata Prefecture and at Ijira forest catchment (IJ1) in Gifu Prefecture, where unprocessed atmospheric nitrate and M_{atm}/D_{atm} ratio in the forest stream eluted from each catchment had been determined and reported. In the Kaji River forest catchment (KJ), in addition to routine water samples taken once every month from May 2017 to March 2020 at the forest stream, special water sampling campaign was conducted every hour on August 12, 2019 (n=24) and on October 22, 2019 (n=23) when the flow rate of the forest stream increased due to rainfall. In the Ijira forest catchment (IJ1), stream water samples were taken twice every month from May 2017 to December 2019, and the changes in the concentration of unprocessed atmospheric nitrate in response to the increases in nitrate concentration in response to precipitation were determined precisely. The concentration of nitrate in each sample was quantified using ion chromatography. The stable isotopic compositions including the ^{17}O-excess of dissolved nitrate were determined using Continuous-Flow Isotope Ratio Mass Spectrometry (CF-IRMS) system in Nagoya University (Tsunogai et al., 2010).

The nitrate concentrations in the stream water taken during the special water sampling campaign in the Kaji River catchment (KJ) increased in response to the increase in flow rate of stream water, from 30 μmol/L before the rainfall, to a maximum of 130 μmol/L. On the other hand, the $\Delta^{17}O$ values of nitrate decreased in response to the increase in nitrate concentration, showing linear relationship between the $\Delta^{17}O$ value and the reciprocal of nitrate concentration($p<0.001$). The $\Delta^{17}O$ value of the endmember obtained as the intercept of the linear regression line was +0.10 - +0.15‰, which was consistent with the $\Delta^{17}O$ values of nitrate in soil water (+0.10 - +0.20‰; Nakagawa et al., 2018). We concluded that the increase in nitrate concentrations in forest stream was caused by leaching of soil nitrate enriched in the riparian area due to the raising of the stream due to rainfall. The average concentration of unprocessed atmospheric nitrate in the stream during the rainfall were 1.7±0.2 μmol/L in August and 1.8±0.3 μmol/L in October, which corresponded with those determined in the forest stream determined through routine monitoring (1.6±0.3 μmol/L in August and 1.8±0.3 μmol/L in October). We concluded that the observed increases in nitrate in response to rainfall were caused by leaching of the remineralized nitrate produced through nitrification in soil. As a result, the increase in nitrate concentration in stream had little

©2021. Japan Geoscience Union. All Right Reserved.

impact on the elution of unprocessed atmospheric nitrate and thus M_{atm}/D_{atm} ratio.
In the Ijira Lake catchment (IJ1), similar enrichment of nitrate of nitrate (about 64.1 μmol/L, 2.5 times higher than the annual average), were observed in response to rainfall on August 12, 2018. In response to the increase, the concentrations of unprocessed atmospheric nitrate in stream water also increased to 3.4±0.4 μmol/L, from 1.5±0.2 μmol/L on July 31, 2018, and +1.2±0.1 μmol/L on August 31, 2018. We concluded that not only the increase in remineralized nitrate produced through nitrification in soil, but also the increase in unprocessed atmospheric nitrate was responsible for the increase in nitrate in the stream water during rainfall in IJ1.

Keywords: nitrogen saturation, forest stream, Matm/Datm ratio, rainfall, unprocessed atmospheric nitrate

©2021. Japan Geoscience Union. All Right Reserved.

Chloride cycling in forested watersheds in the Shimanto River Basin

*Yoshiyuki Inagaki[1], Hisao Sakai[1], Atsushi Torii[1], Yoshiki Shinomiya[1], Kazumichi Fujii[1]

1. Forestry and Forest Products Research Institute

The main sources of chloride input to forest ecosystems are sea salt and anthropogenic sources such as coal combustion. A long-term monitoring in forest watersheds in the Shimanto River Basin has shown that runoff of Cl^- is much larger than the input of Cl^- in bulk precipitation. In addition, Cl^- concentration in bulk precipitation and stream water was decreasing for 20 years. The information about Cl^- input by throughfall is required when we discuss the factors affecting Cl^- cycling in the forest watersheds. Objective of the study is that Cl^- input by throughfall in fir, Japanese cedar and hinoki cypress forests were quantified and that Cl budget of fir and planation forest watersheds were calculated to understand the possible role of dry deposition of Cl^-.

The input of Cl^- by throughfall in the fir, Japanese cedar, and hinoki cypress forests was, 1.75 $kmol_c\ ha^{-1}$,0.95 $kmol_c\ ha^{-1}$, and 0.82 $kmol_c\ ha^{-1}$, respectively, which is 2.9-fold, 1.6-fold and 1.4-fold larger than that in bulk precipitation, respectively (0.60 $kmol_c\ ha^{-1}$). The percentage of non- sea salt Cl^- in bulk precipitation and throughfall in fir, Japanese cedar and hinoki cypress was 1%, 17%, 11% and 11%, respectively. There are two main sources of non- sea salt Cl-; canopy exchange and anthropogenic sources. In the fir forest, leaching of K^+ is greater than other two forests (1.35 $kmol_c\ ha^{-1}$) and Cl^- was moved following K^+. Non-sea salt Cl^- input in early spring without K^+ leaching suggests the anthropogenic sources.

Input and output of Cl were determined for20 years from 2000 to 2019. The average of Cl^- input by bulk precipitation was 0.65 kmolc ha-1, and Cl^- runoff in the fir and plantation forest watersheds were 1.54 kmolc ha-1 and 1.17 kmolc ha-1, respectively. The ratio of Cl^- runoff to the Cl^- input was 2.4 and 1.8, respectively. When input of Cl- is calculated based on the results of throughfall, Cl^- input was larger than Cl^- runoff in the fir forest whereas Cl^- input was smaller than Cl^- runoff in the plantation. The Cl^- input in the fir forest was overestimated due to counting the canopy exchange of Cl^-. Input and output of Cl^- were determined from 2000 to 2009 and from 2010-2019. The ratio Cl^- input by bulk precipitation in the latter period to that in the former period was 0.76. The ratio in the Cl^- runoff in fir and plantation forests was 0.86, and 0.85, respectively. When we assume that input and output of Cl^- is equal, the result suggest that the contribution of Cl^- input by dry deposition was greater in the latter period.

Keywords: Chloride, Forest, Sea salt

©2021. Japan Geoscience Union. All Right Reserved.

To close the nitrogen budgets at a rice paddy

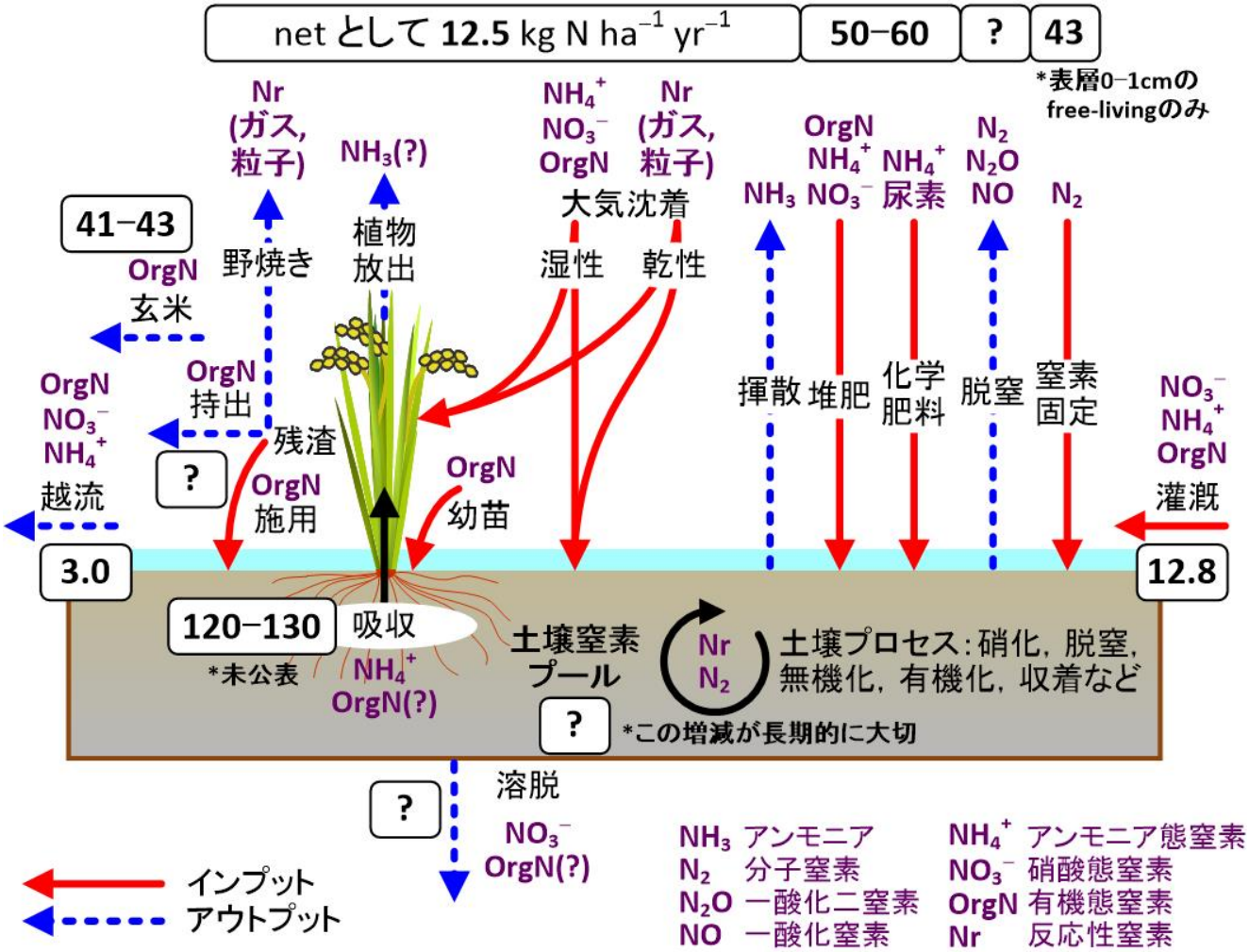
*Kentaro Hayashi[1]

1. Institute for Agro-Environmental Sciences, NARO

Input of chemical nitrogen (N) fertilizer to rice paddies to earn high rice yield can cause N pollution such as water pollution and eutrophication. In addition, the increasing atmospheric CO_2 levels and climate change can impact on the N cycling in rice paddies. For example, elevated CO_2 levels promote photosynthesis and then crop yield (CO_2 fertilization effect), whereas the relative deficiency in N and other nutrients reduces the fertilization effect and the protein composition. Warming can accelerate many biogeochemical N processes. To maintain the sustainability of rice paddies with respect to rice production and agro-ecosystems, accumulating knowledge of the N cycling in rice paddies and its response to environmental change is essential. Grasping N budgets (total input –total output = stock change) is fundamental when aiming to maintain soil fertility as a target of the sustainability. Closing the N budgets of rice paddies is to obtain reliable information of the N flows of all processes in rice paddies.
As shown in the figure, a variety of N processes exist in a rice paddy. The values in the figure were obtained from previous studies those correspond to single-cropping rice paddies in the Kanto region of Japan (unit: kg N ha^{-1} yr^{-1} as a flux). For rice paddies, there are several processes lacking in quantitative information of their flows, i.e., biological N fixation (BNF) as input to rice paddies and denitrification and ammonia (NH_3) volatilization as output from rice paddies. Quantitative information is particularly limited in BNF and denitrification with flows as dinitrogen (N_2). Both are microbial processes active in anaerobic conditions, and therefore submerged rice paddies are ideal environment for these processes. However, it is difficult to measure the atmosphere–rice paddy N_2 fluxes where 78% of the atmosphere is consisted of N_2. Although techniques using N-15 and membrane inlet mass spectrometry enable precise quantification of N_2 flows, they are still not suitable for field measurements. The two processes are often ignored in discussions even in the field of soil science. It is unfortunate to exclude them from the discussion only because of the difficultness in measurement. According to the presenter’ s research, the net free-living BNF (excluding symbiotic and associative BNF) of surface soil (1 cm thickness) in submerged rice paddy was estimated at ca. 40 kg N ha^{-1} in three months in the cropping season. Considering the associative BNF with rice plants, the total rate of 100 kg N ha^{-1} described in the past literature would be reasonable. Owing to the reduced fertilization in recent years with respect to environmental protection, application rates of chemical fertilizer to rice paddies are ca. 50 kg N ha^{-1} indicating an increase in relative contribution of BNF. Although few examples are available on denitrification in actual rice paddies, paddy soils have a strong dentification potential according to incubation studies. Measuring NH_3 volatilization is possible but limited number of studies have been conducted in Japan. Unelucidated processes remain such as the daytime NH_3 emissions in summer not ascribed to fertilization (Hayashi et al., 2017). Effects of elevated CO_2 levels and climate change on the N cycling in rice paddies are almost unknown. The CO_2 fertilization effect can increase rice yield in a short term, but that might accelerate nutrient uptake by rice plants and then reduce soil fertility in a long term. It may not be serious in Japan where fertilization and irrigation are carried out, whereas soil degradation might occur in the future in areas where organic farming and rain-fed cultivation are conducted. Thus, it is expected to elucidate each of the key N processes in rice paddies and its response to environmental changes, to connect the obtained knowledge, and to cooperatively work on synthetic research to enable model evaluation including the effects of agricultural management practices.

©2021. Japan Geoscience Union. All Right Reserved.

Keywords: Rice paddy, Biological nitrogen fixation, Denitrification, Elevated CO2 levels, Climate change, Paddy soil



©2021. Japan Geoscience Union. All Right Reserved.

Evaluation of global riverine N_2 and N_2O emissions using biogeochemical model

*Kazuya Nishina[1], Akihiko Ito[1]

1. NIES National Institute of Environmental Studies

A large amount of anthropogenic reactive nitrogen (Nr) is released to terrestrial ecosystems from chemical fertilizers by the Haber-Bosch process and fossil fuel combustion and the increase of wastewater due to urbanization. Anthropogenic Nr is absorbed and accumulated in terrestrial ecosystems and released to the atmosphere in gaseous forms via biotic and abiotic processes (i.e., nitrification and denitrification). In addition, with the movement of water, Nr is transported from the land to the ocean via rivers, causing eutrophication especially in coastal areas. During transport from land to ocean, some of the reactive nitrogen is released to the atmosphere as N_2 and N_2O through denitrification processes, but the flux is highly uncertain due to the limitations of difficult observation. For example, 190 Tg-N per year is denitrified from rivers according to the estimates presented in Gruber & Galloway (2009). This estimate was estimated using a global-scale distributed hydrological model by Seitzinger et al. (2005). In this study, spatial details are basin-based, and due to the lack of observations, there has not been sufficient validation of the observed data. In this study, we developed a global river denitrification model using a grid-based global river routing model. Using the observed data of inorganic nitrogen fluxes in the river mouths, the parameters related to denitrification were estimated by Bayesian inference with MCMC. In this study, we report the global inorganic nitrogen transport and river denitrification emissions (N_2, N_2O) from 1961 to 2010 using this model.

Keywords: Global nitrogen cycling, Riverine N2O emission

©2021. Japan Geoscience Union. All Right Reserved.

Footprint analysis on nutrient runoff from farmland in regions of Japan

*Azusa Oita[1], Yoshiya Touge[2], Taku Ishiro[3], Kaori Matsuoka[1], Yusuke Takata[1], Kentaro Hayashi[1]

1. National Agriculture and Food Research Organization, 2. Tohoku University, 3. Yokohama National University

Applied nutrients partly runoff into the hydrosphere along with soil due to soil erosion associated with rainfall, contributing to water pollution and eutrophication. Information on the quantitative relationship between nutrient runoff and consumption through the supply chains is needed to develop measures to prevent nutrient runoff throughout the food system. Nitrogen and phosphorus footprints quantify the loss of nitrogen and phosphorus to the environment due to resource consumption. This study aims to quantify the amounts of nitrogen and phosphorus runoff due to soil erosion caused by rainfall from croplands except for paddy fields in regions of Japan and link them to the consumption of agricultural crops excluding paddy rice in those regions based on a footprint analysis using an input-output table.

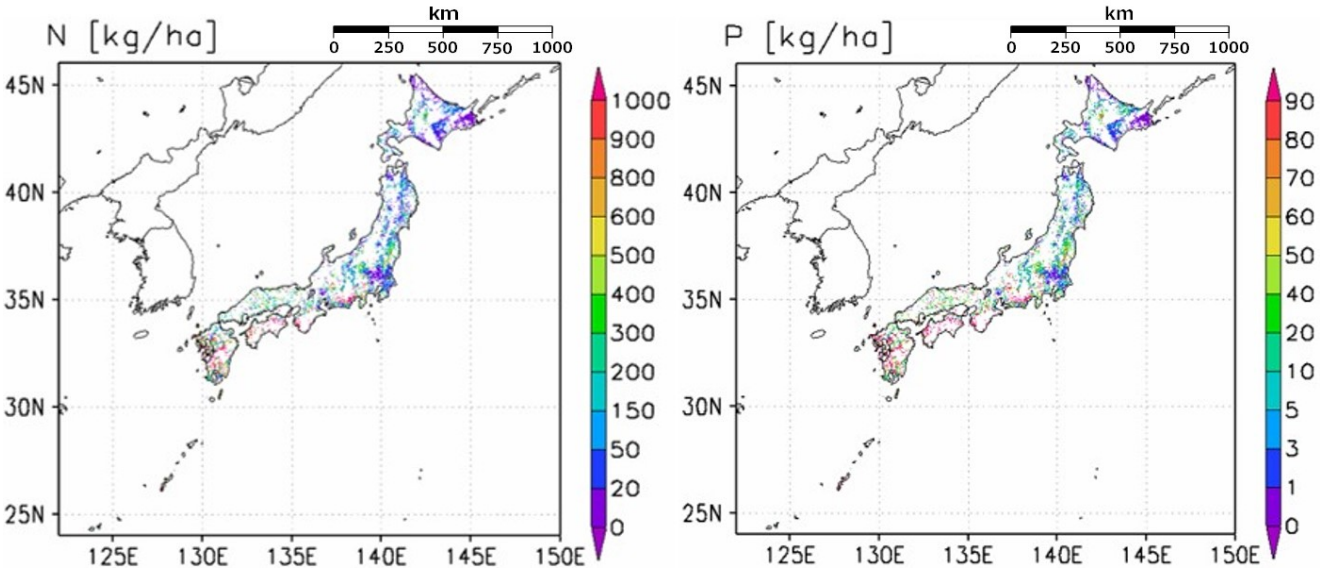
The amount of soil erosion from farmland except for paddy field in 2011 for each 1 km^2 grid cell was calculated using the Revised Universal Soil Loss Equation (RUSLE), a model for estimating soil erosion. Soil erosion from the paddy field was considered to be negligible due to its flatness. The RUSLE model describes the annual soil erosion rate, Y [t ha^{-1} $year^{-1}$] as the equation $Y = R \cdot K \cdot LS \cdot C \cdot P$ (1)where R is the rainfall-runoff erosivity factor [MJ mm ha^{-1} $hour^{-1}$ $year^{-1}$], K is the soil erodibility factor [t hour MJ^{-1} mm^{-1}], LS is the slope length and steepness factor [dimensionless], and C is the cover management factor [dimensionless], and P is the support practice factor [dimensionless]. R-values were obtained, following Udo (2019), by the number of annual rainfall events n, the kinetic energy per mm of rainfall given by the rainfall intensity I_i [mm $hour^{-1}$] at any rainfall event i [MJ ha^{-1} mm^{-1}], the rainfall amount r_i [mm], the maximum rainfall for 60 minutes I_{60i} [mm $hour^{-1}$] using the equation $R = \sum_{i=1}^{n}(0.119+0.0873 \log I_i)\, r_i I_{60i}$ (2). The Radar Automated Meteorological Data Acquisition System (1 km^2 grid cell resolution, hourly rainfall data) was used as the rainfall data. Here, snowfall was considered as rainfall. K-values for 383 sites were calculated using the data of the plow layer in the 4th round of the Basic Survey on the Soil Environment (1994–1998) and the two equations as in Taniyama (2003). From the obtained K-values, the values for each soil series group in the Comprehensive Soil Classification System of Japan First Approximation were determined. LS-values were estimated using the statistical formula of Kohyama *et al.* (2012) for LS values and the gradient degrees. The gradient degree was calculated as the average gradient degrees between 50 m grid cells of the farmland within each 1 km grid cells. The digital soil map of cultivated soil in Japan by the National Agriculture and Food Research Organization (NARO) was used for farmland data (100m resolution), and the Digital Map 50m Grid (elevation) by the Japan Map Center was used for elevation data. The cover management factor C was taken from Taniyama (2003) and Imai and Ishiwatari (2007) and averaged in each grid cell based on the NARO data. The support practice factor P was uniformly set to 1, following Kohyama et al. (2012).

We estimated the nitrogen and phosphorus content of each soil category from the Basic Survey on Soil Environment and calculated the annual runoff of nitrogen and phosphorus due to soil erosion for each 1 km^2 grid cell for the farmland except for the paddy field (Figure 1). On a country scale, the annual runoff was estimated at 656 Gg-N yr^{-1} and 96 Gg-P yr^{-1}. On a prefectural scale, the annual runoff of nitrogen and phosphorus was high in Shizuoka Prefecture, where the target area was relatively large and the slope was relatively high due to heavy rainfall; Hokkaido Prefecture, where the target area was more than 40% of the national total but the slope was moderate due to little heavy rainfall; and Kagoshima Prefecture, where the target area was relatively large, and the slope was moderate due to heavy rainfall.

©2021. Japan Geoscience Union. All Right Reserved.

By the JpGU conference, we plan to estimate the quantitative relationship between the consumption of food and other resources and the amount of nitrogen and phosphorus runoff in each region of Japan based on the analysis using the inter-prefectural input-output table for 2011, and resultant nitrogen and phosphorus footprints for each prefecture. The results of this study will contribute to the optimization of nutrient management in the entire food system by showing the important supply chains in nutrient runoff control.

Keywords: RUSLE model, nitrogen footprint, phosphorus footprint, input-output analysis



©2021. Japan Geoscience Union. All Right Reserved.

[J] Oral | M (Multidisciplinary and Interdisciplinary)：M-IS Intersection

Fri. Jun 4, 2021 1:45 PM - 3:15 PM JST | Fri. Jun 4, 2021 4:45 AM - 6:15 AM UTC | Ch.26 Zoom Room 26

[M-IS16] Paleoclimatology and paleoceanography

convener:Yusuke Okazaki(Department of Earth and Planetary Sciences, Graduate School of Science, Kyushu University), Hitoshi Hasegawa(Faculty of Science and Technology, Kochi University), Atsuko Yamazaki(Faculty of Science, Kyushu University), Akitomo Yamamoto(Japan Agency for Marine-Earth Science and TechnologyAtmosphere and Ocean Research Institute), Chairperson:Atsuko Yamazaki(Faculty of Science, Kyushu University)

Past environmental changes and events at interannual to tectonic timescale toward an understanding of Earth climate system by an integration of terrestrial and marine proxy studies and numerical modeling will be discussed. At JpGU2021, a series of presentations on "high-resolution" paleo data and model studies will be held. We welcome a variety of paleo-environmental studies from a wide range of background. We hope that this session will provide an opportunity to promote communication between participants from multidisciplinary field.

1:45 PM - 2:07 PM JST | 4:45 AM - 5:07 AM UTC

[MIS16-01] Recent progress of the microscale isotopic analytical technique of carbonate (MICAL) and the applications to the high resolution environmental analysis

★Invited Papers

*Toyoho Ishimura[1] (1.Graduate School of Human and Environmental Studies, Kyoto University)

2:07 PM - 2:30 PM JST | 5:07 AM - 5:30 AM UTC

[MIS16-02] Coral Sclerochronology: High-temporal resolution windows for Palaeoclimatology, Palaeocenography, and Palaeoecology

★Invited Papers

*Tsuyoshi Watanabe[1] (1.Hokkaido University /KIKAI Institute for coral reefs sciences)

2:30 PM - 2:45 PM JST | 5:30 AM - 5:45 AM UTC

[MIS16-03] **Hydroclimate seasonality during mid- to late Holocene transition: Evidence of East Asian Monsoon dynamics from fossil corals**

*Kevin Lariosa Garas[1,3,4], Tsuyoshi Watanabe[1,3], Atsuko Yamazaki[2,3], Tarou Komagoe[3] (1.Hokkaido University, 2.Kyushu University, 3.Kikai Institute for Coral Reef Sciences, 4.Mines and Geosciences Bureau-Philippines)

2:45 PM - 3:00 PM JST | 5:45 AM - 6:00 AM UTC

[MIS16-04] Reconstruction of Past Hawaiian Sea Surface Temperature (SST) Using Modern Coral Skeletal Sr/Ca ratio: Decadal Response to Trade Winds

*Ryohei Uchiyama[1], Tsuyoshi Watanabe[1,2], Taro Nojiri[3], Takaaki TK Watanabe[1,4], Samuel Kahng[5], Atsuko Yamazaki[1,2,6] (1.Graduate School of Science, Hokkaido University, 2.KIKAI Institute for Coral Reef Sciences, 3.Faculty of Science, Hokkaido University, 4.Universität zu Kiel, 5.University of Hawaii at Manoa, 6.Faculty of Science, Kyushu University)

3:00 PM - 3:15 PM JST | 6:00 AM - 6:15 AM UTC

[MIS16-05] High-spatiotemporal-resolution hindcast simulation for reproducing coral reef environments in Sekisei Lagoon, Okinawa, Japan

*Takashi Nakamura[1], Takafumi Sakuma[1] (1.School of Environment and Society, Tokyo Institute of Technology)

Recent progress of the microscale isotopic analytical technique of carbonate (MICAL) and the applications to the high resolution environmental analysis

*Toyoho Ishimura[1]

1. Graduate School of Human and Environmental Studies, Kyoto University

The stable carbon and oxygen isotopic compositions ($\delta^{13}C$ and $\delta^{18}O$) of carbonate, especially biological calcite (e.g. foraminifera and coral), are useful as environmental tracers to reconstruct paleoclimate and paleo-oceanic circulations. In recent studies, stable isotopic analyses for sub-100 micrograms of carbonate are needed to reconstruct high-resolution environmental fluctuations. To analyze the stable isotopic compositions of carbonate, however, more than 10 –400 micrograms of $CaCO_3$ are needed even with the latest methods. As a consequence, in case of foraminiferal study, we have had to prepare several to several tens of foraminiferal shells to determine the stable isotopic compositions, and the reported isotopic data of individual foraminiferal shells are limited to the taxa that have large and thick $CaCO_3$ shells (e.g. Uvigerina spp.). We could not utilize the $\delta^{13}C$ and $\delta^{18}O$ values of foraminifera for the sediments in which a limited number of small-sized shells are available, such as at high latitudes, in the deep sea around carbonate compensation depth, etc. If we can determine the isotopic compositions of individual small foraminifera, we can expand the area of the seafloor to which they can be applied.

Recently, Ishimura et al. (2004, 2008) have developed a stable carbon and oxygen isotopic analysis system for sub-microgram quantities of $CaCO_3$ (MICAL), and have applied it to the analysis of high-resolution environmental studies with collaborators in the field of paleoceanography, geology, biology, and fisheries sciences. By using the system we can determine the $\delta^{13}C$ and $\delta^{18}O$ values for almost all kinds of foraminifera, including foraminifera of the minimum size. We can apply the isotopic studies of foraminifera to seafloor sediments in which a limited numbers of small shells are available. In addition, in the case of large-sized calcareous foraminifera, we can determine the $\delta^{13}C$ and $\delta^{18}O$ differences between the fragments within a single shell. Foraminifera make their shells larger by adding new chambers at each growth stage, but little ecological information is known about foraminifera. High resolution isotopic analysis of $CaCO_3$ will be useful not only for paleoceanography, but also for ecological research, for example, high-resolution stable isotopic analysis of $CaCO_3$ to clarify the life history recorded in fish otolith. In this presentation, we will introduce the applications not only to the field of paleoenvironmental analysis, but also to the other scientific fields.

Keywords: microscale analysis, stable isotope, carbonate

©2021. Japan Geoscience Union. All Right Reserved.

Coral Sclerochronology: High-temporal resolution windows for Palaeoclimatology, Palaeocenography, and Palaeoecology

*Tsuyoshi Watanabe[1]

1. Hokkaido University /KIKAI Institute for coral reefs sciences

The daily and annual growth bands formed in biogenic carbonates such as coral skelerons and molluscan shells could serve as the high-temporal resolution archives for the environmental and/or physiological changes during their life span. We use skeletological and geochemical approaches to investigate the histories recorded in living and fossil specimens. Understanding the past climate variability and oceanographyic events in the tropical ocean is a high priority as long-term obsercation is very limited in these areas. Tropical shallow water corals could live up to several hundred years and the decadal to century-scale of climate and oceanic signals such as glocal warming, ocean acidification, El-nino Southern Oscillation (ENSO), anthropogenic CO_2 uptake, atmosphere, marine pollution, river discharge, and ocean circuration dynamics could be detected via reconstructing temperature, salinity, pH, nutrient, and chemical composition in seawater by using isotopes (e.g. oxygen, carbon, boron, lead, and nitrogen isotopes) and elemental (e.g. Sr/Ca, Mg/Ca, and Ba/Ca ratios) analysis along the growth direction.
Ocean acidification and rising atmospheric CO_2 with global warming are also predicted to severely damege the calcification processes of marine organisms and thus the sustinability of marine ecosystems in the near future. The skeletal density, extension rate, and calcification rate deduced from coral cores cuould be useful to estimate the response and acclimatization against such environmental changes during last few hundred years, and to predict the future of coral reefs and ecosystems exhibiting coral acclimation to warmer, more acidified, and polluted conditions.
On the other hand, such recent advance of microanalytical techniques also revealed large heterogeneity of these isotopic and elemental composition in nano to sub-micrometer scale of skeletal microstructures, which are difficult to explain simply by surrounding environmental changes, suggesting understanding biomineralization processes in cellular level with more complexity and plasticity are important to establish more reliable proxy for past environmental changes. I would like to introduce our recent and on-going researches applied on modern and fossil specimens in western pacific, Indian Ocean, and Caribbean Sea and also recent efforts to understand biomineralization process of coral reef dweller.

References
Yamazaki, et al. (2016) A 150-year variation of the Kuroshio transport inferred from coral nitrogen isotope signature, Paleooceanography
Yamazaki, et al. (2014) The coral d15N record of terrestrial nitrate loading varies with river catchment land use, Coral Reefs
Ohmori, et al. (2013) Lead concentration and isotopic composition in the Pacific sclerosponge (Acanthochaetetes wellsi) reflects environmental lead pollution, Geology
Sano et al. (2012) Past daily light cycle recorded in the strontium/ calcium ratios of giant clam shells, Nature Communication.
Watanabe, et al. (2011) Permanent El Niño during the Pliocene warm period not supported by coral evidence, Nature

Keywords: Coral skeleton, Sclerochronology, Isotope geochemistry, Carbonate geochemistry

©2021. Japan Geoscience Union. All Right Reserved.

Hydroclimate seasonality during mid- to late Holocene transition: Evidence of East Asian Monsoon dynamics from fossil corals

*Kevin Lariosa Garas[1,3,4], Tsuyoshi Watanabe[1,3], Atsuko Yamazaki[2,3], Tarou Komagoe[3]

1. Hokkaido University, 2. Kyushu University, 3. Kikai Institute for Coral Reef Sciences, 4. Mines and Geosciences Bureau-Philippines

Hydroclimate (SST, salinity and rainfall) associated with the East Asian summer and winter monsoon (EASM and EAWM) is reconstructed for the mid-to late Holocene transition using fossil corals in Kikai Island, Southern Japan. Here we present monthly-resolved Sr/Ca, $\delta^{18}Oc_{oral}$ and estimated $\delta^{18}O_{seawater}$ from modern (1989-2015AD), 3235, 4960 and 5712 years BP corals. The ocean condition in Kikai Island is modulated by the seasonal shift of monsoon circulation with warm (cool) sea surface temperature (SST), high (low) rainfall, low (high) salinity and negative (positive) $\delta^{18}O_{seawater}$ during EASM (EAWM). Modern coral and in-situ SST, salinity, $\delta^{18}O_{seawater}$ data were calibrated to demonstrate the sensitivity of the coral geochemical records to the monsoon-driven oceanographic response. Summer $\delta^{18}O_{coral}$ values at 5712 and 4960 years BP are lower than the coral data from 3232 years BP. The double negative $\delta^{18}O_{seawater}$ peaks in June and September at 5712 and 4960 years BP compared to the single negative peak at 3235 years BP, are indications of increased salinity and/or reduced rainfall from mid-to-late Holocene. The warm (cool) SST, low (high) salinity and negative (positive) $\delta^{18}O_{seawater}$ during the winter season are indicators of a weaker (stronger) EAWM during 4960 and 3235 (5712) years BP. The negative $\delta^{18}O_{seawater}$ from average winter values at 4960 and 3235 years BP are opposite to the value recorded at 5712 years BP. Weaker EAWM in recent decades is marked by negative winter $\delta^{18}O_{seawater}$ in the 26-year modern coral, which signals the increased winter rainfall.

Together with published $\delta^{18}O_{coral}$ records of previous studies from Southern Japan, we demonstrate the weakening of EASM rainfall from mid-to late Holocene. The coral-derived mean SST anomalies from northwestern Pacific and southwestern Indo-Pacific show that the expansion (contraction) of the northern margin of West Pacific Warm Pool (WPWP) may have influenced the northerly (southerly) position of the intertropical convergence zone (ITCZ) and the intensified (weakened) summer monsoon rainfall. Weak EAWM at 4960 and 3235 years BP and strong EAWM at 5712 years BP are consistent with the established winter monsoon records in East Asia. The decline of Sr/Ca and $\delta^{18}O_{coral}$ seasonalities from mid-to-late Holocene was caused by reduced seasonal ocean heating and monsoon convection, which led to the weakened state of EASM and EAWM. A wealth of paleoclimate records agrees that the complex interaction of the extent of WPWP, ITCZ position, tropical SST forcing, and Northern Hemisphere insolation changes have dominated the mechanism of highly varied EASM and EAWM intensities from mid-to late Holocene.

Keywords: East Asian monsoon, corals, hydroclimate, Holocene, seasonal variation

©2021. Japan Geoscience Union. All Right Reserved.

Reconstruction of Past Hawaiian Sea Surface Temperature (SST) Using Modern Coral Skeletal Sr/Ca ratio: Decadal Response to Trade Winds

*Ryohei Uchiyama[1], Tsuyoshi Watanabe[1,2], Taro Nojiri[3], Takaaki TK Watanabe[1,4], Samuel Kahng[5], Atsuko Yamazaki[1,2,6]

1. Graduate School of Science, Hokkaido University, 2. KIKAI Institute for Coral Reef Sciences, 3. Faculty of Science, Hokkaido University, 4. Universität zu Kiel, 5. University of Hawaii at Manoa, 6. Faculty of Science, Kyushu University

Fast-growing (1cm/year) reef corals provides high-resolution archives of changes in shallow marine environment. Geochemical proxies such as Sr/Ca ratio, have been used in tracking sea surface temperature (SST, ℃) for paleoclimate reconstructions in tropical regions (Beck *et al.*, 1992; Gagan *et al.*, 2000). Hawaiian Islands are located at the central region of North Pacific Ocean where distinct decadal to inter-decadal SST variability with limited influence from the continental/terrestrial factors (Mantua *et al.*, 1997; Di Lorenzo *et al.*, 2008). However, past climate reconstructions using Hawaiian coral skeletons are scarce, as well as only a few numbers of in-situ SST data exist. This study aims to fill the gap of decadal- to centennial-scale SST changes in north-central Pacific using coral geochemical approach.

Modern *Porites sp.* coral cores sampled at eastern and western side of Oahu Island, were used in this study. X-ray photo of the coral slabs were used to determine maximum growth axis as measurement line. Coral powders were obtained at 0.2mm intervals using a micro drill. Sr/Ca was analyzed using inductively coupled plasma optical emission spectrometer (ICP-OES). Age model for the Sr/Ca profile was made by anchoring the timing of maxima (minima) of Sr/Ca to the minima (maxima) of reference SST. For calibrating Sr/Ca for SST, skeletal Sr/Ca in eastern coral and satellite-based SST time series which was corrected by in-situ SST, were used. Applying the calibration result on Sr/Ca ratio in coral from eastern and western Oahu, long term SST records for each location were reconstructed and compared.

Sr/Ca ratio was highly correlated to reference SST, and the calibration result of coral Sr/Ca-SST from eastern Oahu coral was comparable to the previously reported values from other regions (Gagan, 2000; Swart, 2002; Corrège, 2006). The standard SST error (1 σ) was <1˚C, suggesting a reliable calibration of the high resolution (bi-weekly) Sr/Ca record. Applying the coral-based thermometry, SST variability was reconstructed from 1920s and 1950s in eastern and western Oahu respectively. Seasonal amplitude was subtracted to the reconstructed SST to show each long-term variability. The eastern and western Oahu SST records did not show covariance. Interestingly, the east-west SST difference during overlapping period showed decadal variability with an amplitude of approximately ±2℃, which could be correlated to northeastern winds intensity (m/s). The windward eastern (leeward western) SST were higher when northeastern winds were stronger (weaker). Based on the previous studies, the prevailing winds around the Hawaiian Islands is trade winds outflow from the northeastern subtropical high pressure (Sanderson *et al.*, 1993; Garza *et al.*, 2012), and the wind stress curl derived by the trade winds drives SST variation in the open ocean around the Hawaiian Islands (Xie *et al.*, 2001). In this study, SST variabilities in the two different local coastal areas were reconstructed, which demonstrated ocean responses to the trade winds. The long term SST reconstruction, which predates observation records suggested that the decadal-scale changes of trade wind intensity controls local SST variabilities.

Keywords: coral, Hawaii, Sr/Ca ratio, SST, Trade winds

©2021. Japan Geoscience Union. All Right Reserved.

High-spatiotemporal-resolution hindcast simulation for reproducing coral reef environments in Sekisei Lagoon, Okinawa, Japan

*Takashi Nakamura[1], Takafumi Sakuma[1]

1. School of Environment and Society, Tokyo Institute of Technology

Scleractinian corals provide high-resolution (monthly to weekly) climate and environmental records on the shallow-water tropical and subtropical ocean regions. The environmental parameters, such as temperature and salinity, are extracted from the coral skeleton as environmental proxies, such as skeletal $\delta^{18}O$, Sr/Ca and Mg/Ca. However, to convert the proxies to certain environmental parameters, the environment proxies should be calibrated with observation data. Because the proxies usually do not follow theoretical values due to biological activities, so-called vital-effect. Therefore, to convert the proxies to environmental parameters and to extend proxies extracted from the coral core to long-term environmental data, the environmental data on where coral cores are collected is required. However, available on-site past environmental data is very limited.

Recently some global/regional ocean analysis/reanalysis products, such as Global HYCOM (https://www.hycom.org/), JCOPE2M (Miyazawa et al., 2017; 2019), and JCOPE-T DA (Varlamov et al., 2015) are released. The latest Global HYCOM is 3 hourly products and available from 1994 to the present. The JCOPE2M is daily products and available from 1992 to present. The JCOPE-T DA is hourly products and available from 2018 to present. The analysis/reanalysis products might be a good option for extending the availability of environmental data. However, the products are not enough resolution for extract environments inside our target area, Sekisei lagoon, since the resolutions of the Global HYCOM, JCOPE2M and JCOPE-T DA are 1/12˚ (~9 km), 1/12˚ (~9 km) and 1/36˚ (~3 km), respectively.

For overcoming the problems, we conducted downscaling from global/regional products to the Sekisei lagoon area by multi-nested approach by using an ocean circulation model based on the Coupled-Ocean-Atmosphere-Wave-Sediment Transport (COAWST) Modeling System (Warner et al., 2010). A YAEYAMA1 is the coarsest grid which is 1.5 km grid resolution and covering the East-coast of Taiwan to Miyako Island. The YAEYAMA1 was downscaled from Global HYCOM between 1994 and 2018, and JCOPE-T DA between 2018 and present. The YAEYAMA1 is downscaled to YAEYAMA2 domain which is 300 m resolution and covering the entire Ishigaki Island and Iriomote Island, then that is finally downscaled to YAEYAMA3 domain which is 100 m resolution and covering Sekisei lagoon area by offline one-way nesting. Since the Global HYCOM products do not include tide, the tidal forcing by TPXO9-atlas global tidal solution (Egbert and Svetlana, 2002) was added to the boundaries produced by Global HYCOM products. Atmospheric forcing datasets are used Dynamical Regional Downscaling Using the JRA-55 Reanalysis (DSJRA-55; Kayaba et al., 2016) from 1994 to 2003, and Japan Meteorological Agency’ s Meso-Scale Model Grid Point Value (MSM-GPV) from 2004 to the present. By using this multi-nested model, we can obtain a long-term (1994 to present) high-spatiotemporal-resolution (hourly, 100-m grid resolution) dataset of temperature, salinity and water velocity around the Sekisei lagoon area.

Keywords: hindcast simulation, ocean circulation model, downscaling

©2021. Japan Geoscience Union. All Right Reserved.

[J] Oral | M (Multidisciplinary and Interdisciplinary)：M-IS Intersection

Fri. Jun 4, 2021 3:30 PM - 5:00 PM JST | Fri. Jun 4, 2021 6:30 AM - 8:00 AM UTC | Ch.26 Zoom Room 26

[M-IS16] Paleoclimatology and paleoceanography

convener:Yusuke Okazaki(Department of Earth and Planetary Sciences, Graduate School of Science, Kyushu University), Hitoshi Hasegawa(Faculty of Science and Technology, Kochi University), Atsuko Yamazaki(Faculty of Science, Kyushu University), Akitomo Yamamoto(Japan Agency for Marine-Earth Science and TechnologyAtmosphere and Ocean Research Institute), Chairperson:Yusuke Okazaki(Department of Earth and Planetary Sciences, Graduate School of Science, Kyushu University)

Past environmental changes and events at interannual to tectonic timescale toward an understanding of Earth climate system by an integration of terrestrial and marine proxy studies and numerical modeling will be discussed. At JpGU2021, a series of presentations on "high-resolution" paleo data and model studies will be held. We welcome a variety of paleo-environmental studies from a wide range of background. We hope that this session will provide an opportunity to promote communication between participants from multidisciplinary field.

3:30 PM - 3:52 PM JST | 6:30 AM - 6:52 AM UTC

[MIS16-06] Today’s drought extremes, little ice age wet extremes, and quiet 3 centuries in between: observations from Guatemalan varves, 1413±4 to 2015±0 CE

★Invited Papers

*Ikuko Kitaba[1], GPB15 Project Members (1.Ritsumeikan University)

3:52 PM - 4:07 PM JST | 6:52 AM - 7:07 AM UTC

[MIS16-07] Recognition of annual lamination and high-resolurion stable isotopic records of cascade-type tufa.

*Akira Murata[1], Hirokazu Kato[1], Akihiro Kano[1] (1.The University of Tokyo)

4:07 PM - 4:22 PM JST | 7:07 AM - 7:22 AM UTC

[MIS16-08] Effects of environmental changes on planktic foraminiferal shells assessed by the investigation of micro-X-ray CT.

*Shunichi Kinoshita[1], Quan Wang[2], Azumi Kuroyanagi[3], Masafumi MURAYAMA[4], Yurika Ujiie[5], Hodaka Kawahata[2] (1.Department of Geology and Paleontology National Museum of Nature and Science, 2.Atmosphere Ocean Research Institute, the University of Tokyo, 3.Tohoku University Museum, The Center for Academic Resources and Archives, Tohoku University, 4.Faculty of Agriculture and Marine Science, Kochi University, 5.Center for Advanced Marine Core Research, Kochi University)

4:22 PM - 4:37 PM JST | 7:22 AM - 7:37 AM UTC

[MIS16-09] Paleoenvironmental reconstruction of the North Pacific Subtropical Mode Water at the Last Glacial Maximum based on carbon- and oxygen-isotope composition of fossil brachiopod *Basiliola lucida*

*Haruna Sugazawa[1], Hideko Takayanagi[1], Yusuke Yokoyama[2], Takuya Itaki[3], Toshihiro Miyajima[2], Yasufumi Iryu[1] (1.Institute of Geology and Paleontology, Graduate School of Science, Tohoku University, 2.Atmosphere and Ocean Research Institute, The University of Tokyo , 3.Advanced Industrial Science and Technology)

4:37 PM - 5:00 PM JST | 7:37 AM - 8:00 AM UTC

[MIS16-10] Evaluation of proxy system models for stable water isotopes and introduction of their application to paleoclimate studies

★Invited Papers

*Okazaki Atsushi[1], Kei Yoshimura[2] (1.The Pennsylvania State University, 2.The University of Tokyo)

Today’s drought extremes, little ice age wet extremes, and quiet 3 centuries in between: observations from Guatemalan varves, 1413±4 to 2015±0 CE

*Ikuko Kitaba[1], GPB15 Project Members

1. Ritsumeikan University

Increased frequency of extreme weather events is considered to be closely linked to recent global warming. However, reliable meteorological data are available only since the industrial revolution, i.e., after the beginning of the present global warming. Before that, it is generally difficult to find geological archives that enable us to detect extreme weather events, which, in turn, prevents us from assessing the relationship between present global warming and instability of weather.

Sediment cores recovered from Lake Petexbatún (Guatemala) in 2015 (GPB15) are ideal materials for this purpose. Counts of their clear varves (annual laminae) and 29 ^{14}C dates for the last 600 years enabled us to establish a chronology with exceptionally high precision and accuracy. We then performed ultra-high resolution (on average, ca. 180 data points per varve, i.e. ca. 2 days interval) X-ray fluorescence scans of the cores. Changes in the Ca/Fe ratio, a proxy for precipitation –evaporation balance, show that long-term drying proceeded in parallel with contemporary warming. More importantly, amplitude of the estimated dryness has increased during the same interval, suggesting a dramatic change in the instability of the climate system. On the other hand, during the Little Ice Age (LIA, ca. 16th to 17th century CE), rainfall increased and became unstable (the frequency of extreme rainfall events increased). During the 300 year period from the LIA to the 1970’s, we were in the narrow window of the ‘stable’ climatic mode.

A clear increase of the both dryness and wetness oscillation amplitudes is only visible, and is very visible, in monthly data because impacts of spiky events are not suitably represented in long-term means. Strong weather extremes included in the climatic oscillation cannot be seen in the geo-archives at annual or lower resolution.

Keywords: Extreme weather, Climatic stability, Itrax XRF scanner, Varve

©2021. Japan Geoscience Union. All Right Reserved.

Recognition of annual lamination and high-resolurion stable isotopic records of cascade-type tufa.

*Akira Murata[1], Hirokazu Kato[1], Akihiro Kano[1]

1. The University of Tokyo

Tufas, which develop in freshwater environments in limestone areas, are excellent paleoclimate archives for terrestrial regions in temperate to subtropical zones. Because tufas develop annual laminations and grow at a rate of several millimeters per year, analyses can be done at high resolution. However, fluvial tufas, which develop in riverine water passages, do not continuously accumulate beyond 20-30 years due to changes in the flow path. On the other hand, cascade tufas, which develop under waterfalls, are expected to provide a longer continuous record like stalagmites. This study aimed to reconstruct past climatic conditions using this cascade tufa developed at Obaru beach in Tokunoshima, Kagoshima Prefecture.
Two samples of cascade tufas of 49 cm and 18 cm thick, respectively, were collected from the Obaru beach. Age model based on observation of thin section and X-ray CT scan images indicates that both samples have grown during the last ~200 years. Stable oxygen and carbon isotopes were measured for 1430 and 892 sub-samples respectively collected in 0.2 mm or 0.4 mm intervals. Two samples show a common decadal variability of the oxygen isotope time series, but lack trends reflected from the Global Warming. Time series of the oxygen isotopes reveals saw-tooth pattern of ~25-year cyclicity until late 1970s, and then generally increased. These trends positively correlated with the Pacific Decadal Oscillation (PDO). Oxygen isotopes of tufa are generally controlled by precipitation rather than temperature. Correlation with PDO will be examined with isotopic measurements of local rainwater samples. In addition, carbon isotopes of one sample has been decreasing since the 1960s, which may record the Suess effect of fossil fuel consumption.

Keywords: tufa, stable isotopic analyses, paleoclimate, Pacific Decadal Oscillation

©2021. Japan Geoscience Union. All Right Reserved.

Effects of environmental changes on planktic foraminiferal shells assessed by the investigation of micro-X-ray CT.

*Shunichi Kinoshita[1], Quan Wang[2], Azumi Kuroyanagi[3], Masafumi MURAYAMA[4], Yurika Ujiie[5], Hodaka Kawahata[2]

1. Department of Geology and Paleontology National Museum of Nature and Science, 2. Atmosphere Ocean Research Institute, the University of Tokyo, 3. Tohoku University Museum, The Center for Academic Resources and Archives, Tohoku University, 4. Faculty of Agriculture and Marine Science, Kochi University, 5. Center for Advanced Marine Core Research, Kochi University

Ocean acidification is in progress, and the main reason of this environmental problem is that the ocean has taken in about half of pCO_2 originating in human activity after the pre-industrial era. Various organisms living in the sea such as corals, coccolithophorids, and foraminifers produce their shells with carbonate ions which present in the seawaters around them. There are some evidences that the carbonate saturation state affects on the planktic foraminiferal shells, and it is known that the production rate of foraminiferal shells sensitively reacts to increasing of pCO_2. The size-normalized weight of foraminiferal shells is used to estimate the surface carbonate system. However, it is unsolved that which shell parameters has been reflect to size-normalized weight. It is considered ambiguously to be attributed to shell wall thickness or shell density, or both. Therefore, it is still unclear that the relationships between foraminiferal shell parameters and environmental ones, especially three-dimensional parameters such as shell volume (which could be reflect mean shell thickness) and density.
In this study, we measured the shell size-normalized weight, shell volume, and shell density of planktic foraminifer *Globigerinoides ruber* (white) in the core MD98-2196 to elucidate the relationship between those shell parameters and environmental parameters (pCO_2 and SST). We used high-resolution micro-X-ray computed tomography for assessed the shell volume and shell density. The results suggested that the shell size-normalized weight and shell volume might be negatively correlated to marine environmental parameters (pCO_2 and SST). In addition, these two parameters might be more affected by pCO_2 than SST. On the other hand, since the shell density showed no changes in 3-100ka, it could be interpreted to be constant. Thus, it is suggested that future ocean acidification and warming will cause negative effects on carbonate productivity of planktic foraminiferal even though it will not affect on shell density.

Keywords: atmospheric pCO_2, *Globigerinoides ruber*, shell density, shell volume, size-normalized weight, SST

©2021. Japan Geoscience Union. All Right Reserved.

Paleoenvironmental reconstruction of the North Pacific Subtropical Mode Water at the Last Glacial Maximum based on carbon- and oxygen-isotope composition of fossil brachiopod *Basiliola lucida*

*Haruna Sugazawa[1], Hideko Takayanagi[1], Yusuke Yokoyama[2], Takuya Itaki[3], Toshihiro Miyajima[2], Yasufumi Iryu[1]

1. Institute of Geology and Paleontology, Graduate School of Science, Tohoku University, 2. Atmosphere and Ocean Research Institute, The University of Tokyo , 3. Advanced Industrial Science and Technology

The North Pacific Subtropical Mode Water (STMW) is distributed along the southern side of the Kuroshio Current and the Kuroshio Extension in the western North Pacific Ocean. Long-term oceanographic data along the 137°E meridian south of Japan and profiling float CTD data from the International Argo Program showed that the STMW is absorbing a large amount of heat and CO_2 from the atmosphere to ocean, indicating that the STMW can serve as heat and CO_2 reservoir under recent global warming. Therefore, it is likely that the STMW has acted as an important positive/negative feedback on climate change at various time scales. However, a little is known about the behavior and changes in physical properties and chemical composition of the STMW on a long-term scale because instrumental data recording temporal variations of the STMW is limited to those after 1900’s. Consequently, proxy records of the past STMW are required to improve and deepen our knowledge about dynamics of the STMW and the associated feedback effect. It is known that modern brachiopod *Basiliola lucida* around the Ryukyu Islands is mainly living in a range of the STMW, namely on the shelf slope at water depths of 200–300 m and that carbon- and oxygen-isotope composition of this brachiopod shells is useful to reconstruct the dissolved inorganic carbon concentration and seawater temperature of the ambient seawater. In this study, we first show an optimal way to reconstruct secular variations in the physical properties and chemical composition of the STMW with high accuracy and precision using carbon- and oxygen-isotope composition of semi-fossil *B. lucida* shells collected off the Ryukyu Islands. Then, we apply the way to fossil *B. lucida* shells dated to the Last Glacial Maximum (LGM). Finally, we will present the *B. lucida*-based seawater temperature/salinity and dissolved inorganic carbon concentration of the STMW at the LGM.

Keywords: North Pacific Subtropical Mode Water, Last Glacial Maximum, carbon-isotope composition, oxygen-isotope composition, brachiopod

©2021. Japan Geoscience Union. All Right Reserved.

Evaluation of proxy system models for stable water isotopes and introduction of their application to paleoclimate studies

*Okazaki Atsushi[1], Kei Yoshimura[2]

1. The Pennsylvania State University, 2. The University of Tokyo

Proxy system models (PSMs) are an important bridge between climate simulations and climate records prior to the period where instrumental observations are available. PSMs help to interpret what proxies show and how they record climate. Although previous studies have evaluated PSMs for individual sites, their systematic evaluation on a global scale has not been conducted. This study evaluated the performance of PSMs for stable water isotopes in ice cores, corals, and tree-ring cellulose for the period 1950–2007. We used an isotope enabled atmospheric GCM named MIROC5-iso to provide input data for the PSMs. MIROC5-iso was nudged toward NCEP/NCAR Reanalysis to synchronize the model with nature. The evaluation result shows that the mean state and the variability were generally well simulated for all proxy types. However, the reproducibility of interannual variability in ice cores was markedly lower. Although the reproducibility was limited by the atmospheric forcing used to drive the model, the results suggest that the PSM may be missing post-depositional processes, such as sublimation for ice cores on the interannual time scale.
In the presentation, recent studies on paleoclimate data assimilation as an application of PSMs will be also introduced.

Keywords: proxy system models, stable water isotopes, data assimilation, paleoclimate reconstruction

©2021. Japan Geoscience Union. All Right Reserved.

[J] Oral | M (Multidisciplinary and Interdisciplinary) : M-IS Intersection

Fri. Jun 4, 2021 10:45 AM - 12:15 PM JST | Fri. Jun 4, 2021 1:45 AM - 3:15 AM UTC | Ch.19 Zoom Room 19

[M-IS18] Drilling Earth Science

convener:Junichiro Kuroda(Department of Ocean Floor Geoscience, Atmosphere and Ocean Research Institute, the University of Tokyo), Katsuyoshi Michibayashi(Department of Earth and Planetary Sciences, Nagoya University), Osamu Fujiwara(Geological Survey of Japan, National Institute of Advanced Industrial Science and Technology), Kohtaro Ujiie(Faculty of Life and Environmental Sciences, University of Tsukuba), Chairperson:Junichiro Kuroda(Department of Ocean Floor Geoscience, Atmosphere and Ocean Research Institute, the University of Tokyo), Kazutaka Yasukawa(Frontier Research Center for Energy and Resources, School of Engineering, The University of Tokyo)

This session, Drilling Earth Science, encourages the presentations of every scientific research done with samples and data obtained through ocean and land-based drilling projects such as the International Ocean Discovery Program (IODP) and the International Continental Drilling Program (ICDP). This session provides a place to exchange the latest information on the scientific drilling programs including the future science plan/framework of the programs. We also welcome the presentation on the summary of recently implemented expeditions/projects, introduction of new proposal ideas, and report on the new methods and technology developments related to scientific drilling.

10:45 AM - 11:00 AM JST | 1:45 AM - 2:00 AM UTC

[MIS18-01] Age determination of pelagic clay using Monte Carlo simulation constrained by ichthyolith biostratigraphy and bulk cobalt concentrations

*Kazuhide Mimura[1], Kentaro Nakamura[1], Kazutaka Yasukawa[1,2], Junichiro Ohta[1,2], Koichiro Fujinaga[2,1], Yoichi Usui[3], Yasuhiro Kato[1,2] (1.Department of Systems Innovation, School of Engineering, the University of Tokyo, 2.Ocean Resources Research Center for Next Generation, Chiba Institute of Technology, 3.Japan Agency for Marine-Earth Science and Technology)

11:00 AM - 11:15 AM JST | 2:00 AM - 2:15 AM UTC

[MIS18-02] Preliminary report of IODP Expedition 378: South Pacific Paleogene Climate

*Kazutaka Yasukawa[1,2], Erika Tanaka[1], Deborah J Thomas[3], Ursula Röhl[4], Laurel Childress[3], IODP Expedition 378 Science Party[5] (1.School of Engineering, The University of Tokyo, 2.ORCeNG, Chiba Institute of Technology, 3.Texas A&M University, 4.MARUM, University of Bremen, 5.List of scientific participants (http://iodp.tamu.edu/scienceops/precruise/southpacific/participants.html))

11:15 AM - 11:30 AM JST | 2:15 AM - 2:30 AM UTC

[MIS18-03] IODP proposal for re-drilling in the East China Sea to understand the millennial-scale variability of the Asian monsoon during the Quaternary

★Invited Papers

*Yoshimi Kubota[1], Ken Ikehara[2], Kenji Matsuzaki[3], Saki Ishino[2], Ayanori Misawa[2], Makoto Otsubo[2], Masataka Kinoshita[4], Katsura Kameo[3], Chiori Tamura[3], Ryuta Arai[5], Tomohiro Toki[6], Yuki Mitsutome[6], Zhirong Cai[7], Keiko Takehara[8], Kato Koudai[8], Daisuke Kuwano[9], Koshiro Matsuo[10], Keita Suzuki[11], Misaki Horiuchi[11], Yohei Katayama[12], Satoshi Okumura[13], Ryuji Tada[14], Tomohisa Irino[15], Kohsaku Arai[2], Takahiko Inoue[2], Takuya Sagawa[16], Minoru Ikehara[8], Yusuke Okazaki[10], Keiji Horikawa[17] (1.National Museum of Nature and Science, 2.National Institute of Advanced Industrial Science and Technology, 3.Atmosphere and Ocean Research Institute, The university of Tokyo, 4.Earthquake Research Institute, University of Tokyo, 5.Japan Agency for Marine-Earth Science and Technology, 6.University of the Ryukyus, 7.Kyoto University, 8.Kochi University, 9.China University, 10.Kyusyu University, 11.Nippon Marine Enterprises, Ltd., 12.Marine Works Japan, Ltd., 13.MOL Marine Co., Ltd., 14.Hokkaido University, 15.Graduate School of Science, The Univeristy of Tokyo, 16.Kanazawa University, 17.Toyama University)

11:30 AM - 11:45 AM JST | 2:30 AM - 2:45 AM UTC

[MIS18-04] **SCORE proposal off Shikoku, SW Japan: Reconstruction of the Kuroshio state for super interglacials during the Brunhes chron**

*Minoru Ikehara[1], Hiroshi Nishi[2], Tabito Matsu'ura, Kyoko Hagino[1], Takuya Itaki[3], Kyung Eun Lee[4], Yuan-Pin Chang[5], Jianjun Zou[6] (1.Center for Advanced Marine Core Research, Kochi University, 2.Fukui Prefectural University, 3.AIST, 4.Korea Maritime and Ocean University, 5.National Sun Yat-sen University, 6.First Institute of Oceanography)

11:45 AM - 12:00 PM JST | 2:45 AM - 3:00 AM UTC

[MIS18-05] **Organic geochemical characteristic and its significance of Jurassic-Cretaceous terrestrial sediments recovered by IODP deep sea drilling**

*Shutaro Fukushima[1], Takashi Hasegawa[1] (1.Kanazawa University)

12:00 PM - 12:15 PM JST | 3:00 AM - 3:15 AM UTC

[MIS18-06] Carbon isotope stratigraphy of C40-alkenone and its significance: Cretaceous OAE2 horizon, IODP Site U1516

*Takashi Hasegawa[1], Akiko S. Goto[1,2] (1.Faculty of Geoscience and Engineering, Institute of Science and Engineering, Kanazawa University, 2.Center of Ecological Research, Kyoto University)

Age determination of pelagic clay using Monte Carlo simulation constrained by ichthyolith biostratigraphy and bulk cobalt concentrations

*Kazuhide Mimura[1], Kentaro Nakamura[1], Kazutaka Yasukawa[1,2], Junichiro Ohta[1,2], Koichiro Fujinaga[2,1], Yoichi Usui[3], Yasuhiro Kato[1,2]

1. Department of Systems Innovation, School of Engineering, the University of Tokyo, 2. Ocean Resources Research Center for Next Generation, Chiba Institute of Technology, 3. Japan Agency for Marine-Earth Science and Technology

Pelagic clay is one of the most widely-distributed types of seafloor sediment in the global ocean [1]. It has been, therefore, regarded as an important medium recording global and long-term environmental changes in Earth’ s history, such as changes in atmospheric/oceanic circulations and surface ocean productivity [2]. Recent studies show that bulk chemical compositions of pelagic clay are highly variable, reflecting changes in depositional position and environment [3, 4]. However, paleoenvironmental reconstructions from pelagic clay are still challenging due to difficulties in determination of depositional ages resulting from scarcity in age-diagnostic calcareous/siliceous microfossils and an ambiguity in paleomagnetic reversals.

Some previous studies constrained depositional ages of pelagic clay using biostratigraphy of fish teeth and denticles, called ichthyoliths, which are only the microfossils that commonly occur in pelagic clay of deep-sea basins [5]. However, in contrast to the well-developed biostratigraphy of siliceous/calcareous microfossils, depositional ages constrained by ichthyoliths still have large uncertainties. In addition to the ichthyolith biostratigraphy, some previous studies estimated the depositional ages of pelagic clay by assuming that cobalt precipitates to seafloor at a constant flux [2, 6], whereas the assumption that the cobalt precipitates at a constant rate throughout the geologic time is questioned [6].

Here, we develop a new practical method to constrain depositional ages of pelagic clay by combining ichthyolith biostratigraphy and a cobalt-based age model. We first assume that a depositional flux of cobalt from seawater to seafloor can vary in accordance with a probability distribution. Then, a Monte Carlo simulation is performed to calculate a reasonable range of sedimentation rates under constraints of depositional ages inferred from the ichthyolith biostratigraphy. We have applied this method to pelagic clay cores recovered from the Pacific Ocean, and obtained the reasonable depositional ages with uncertainties significantly smaller than that constrained only by ichthyolith biostratigraphy. This new method is applicable to a variety of sediments having some constraints in depositional ages and sedimentation rates.

References : [1] Dutkiewicz et a l. (2015). *Geology*, **43**, 795-798. [2] Kyte et al. (1993) *Geochim. Cosmochim. Acta*, **57**, 1719-1740. [3] Yasukawa et al. (2016) *Sci. Rep.* **6**, 1-12. [4] Mimura et al. (2019) *J. Asian Earth Sci.*, **186**, 104059. [5] Doyle and Riedel (1985) *Init. Repts. DSDP* **86**, 349-366. [6] Dunlea et al. (2015) *Geochem. Geophys. Geosyst.*, **16**, 2694-2710.

Keywords: deep-sea sediment, pelagic clay, depositional age determination, microfossils, bulk geochemistry, Monte Carlo simulations

©2021. Japan Geoscience Union. All Right Reserved.

Preliminary report of IODP Expedition 378: South Pacific Paleogene Climate

*Kazutaka Yasukawa[1,2], Erika Tanaka[1], Deborah J Thomas[3], Ursula Röhl[4], Laurel Childress[3], IODP Expedition 378 Science Party[5]

1. School of Engineering, The University of Tokyo, 2. ORCeNG, Chiba Institute of Technology, 3. Texas A&M University, 4. MARUM, University of Bremen, 5. List of scientific participants (http://iodp.tamu.edu/scienceops/precruise/southpacific/participants.html)

International Ocean Discovery Program Expedition 378 “South Pacific Paleogene Climate” was conducted from January to February 2020. The major objective of this expedition was to recover a continuous sedimentary sequence to reconstruct the paleoceanographic and paleoclimatologic records during the Paleogene in the high latitude of the South Pacific Ocean, with particular emphasis on the key events including the Eocene-Oligocene Transition, Middle Eocene Climatic Optimum, Early Eocene Climatic Optimum, Eocene hyperthermal events, and the Paleocene-Eocene Thermal Maximum. We drilled five Holes at Site U1553, located at 1,221 meters of water depth on the southern Campbell Plateau, south of New Zealand [1]. Site U1553 builds on the legacy of Deep Sea Drilling Project Site 277, a single, partially spot cored hole, providing a unique opportunity to refine and augment existing reconstructions of the Paleogene climate history [1]. In the presentation, we will introduce an overview of the expedition as well as the preliminary report of Site U1553, mainly focusing on the lithostratigraphy.

[1] Thomas, D.J., Röhl, U., Childress, L.B., and the Expedition 378 Scientists, 2020. *Expedition 378 Preliminary Report: South Pacific Paleogene Climate.* International Ocean Discovery Program. https://doi.org/10.14379/iodp.pr.378.2020

Keywords: Paleogene, IODP, paleoceanography, paleoclimate, Campbell Plateau

©2021. Japan Geoscience Union. All Right Reserved.

IODP proposal for re-drilling in the East China Sea to understand the millennial-scale variability of the Asian monsoon during the Quaternary

*Yoshimi Kubota[1], Ken Ikehara[2], Kenji Matsuzaki[3], Saki Ishino[2], Ayanori Misawa[2], Makoto Otsubo[2], Masataka Kinoshita[4], Katsura Kameo[3], Chiori Tamura[3], Ryuta Arai[5], Tomohiro Toki[6], Yuki Mitsutome[6], Zhirong Cai[7], Keiko Takehara[8], Kato Koudai[8], Daisuke Kuwano[9], Koshiro Matsuo[10], Keita Suzuki[11], Misaki Horiuchi[11], Yohei Katayama[12], Satoshi Okumura[13], Ryuji Tada[14], Tomohisa Irino[15], Kohsaku Arai[2], Takahiko Inoue[2], Takuya Sagawa[16], Minoru Ikehara[8], Yusuke Okazaki[10], Keiji Horikawa[17]

1. National Museum of Nature and Science, 2. National Institute of Advanced Industrial Science and Technology, 3. Atmosphere and Ocean Research Institute, The university of Tokyo, 4. Earthquake Research Institute, University of Tokyo, 5. Japan Agency for Marine-Earth Science and Technology, 6. University of the Ryukyus, 7. Kyoto University, 8. Kochi University, 9. China University, 10. Kyusyu University, 11. Nippon Marine Enterprises, Ltd., 12. Marine Works Japan, Ltd., 13. MOL Marine Co., Ltd., 14. Hokkaido University, 15. Graduate School of Science, The Univeristy of Tokyo, 16. Kanazawa University, 17. Toyama University

Understanding and predicting how monsoons respond to global climate change is a critical scientific and societal issue since monsoonal rainfall provides the water supply for more than half of the world's population and sometimes leads to natural catastrophes such as floods and droughts. The East China Sea (ECS) is a marginal basin located on the rim of the western North Pacific, receiving massive runoff from the Yangtze (Changjiang) River; the discharge accounts for ~90% of the total river discharge to the ECS, making surface salinity well-correlated with basin-wide summer precipitation in southern China. IODP Expedition 346 was held in 2013 to understand the long-term millennial-scale variability of the East Asian monsoon during the Quaternary. During IODP Expedition 346, we drilled the proposed sites to ~200 mbsf at Site U1429 in the northern ECS. Site U1429 recovered a continuous record of hemipelagic sediments for the last 400 ky with a high sedimentation rate of 30–70 cm/ky. The advantage of using the marine core is the oxygen isotope ($\delta^{18}O$) of calcite from planktic foraminifers preserved in nearshore marine sediments can be quantitatively partitioned into sea surface temperature and $\delta^{18}O$ of seawater ($\delta^{18}O_w$), a function of sea surface salinity (a proxy of the monsoonal rainfall), using well-established methods of paired Mg/Ca and $\delta^{18}O$. Results from Site U1429 show that the $\delta^{18}O_w$ marks the detectable millennial-scale variability, which correlates to the Chinese speleothem $\delta^{18}O$ for the last 400 ky. The remarkable correlation between the ECS and the Chinese speleothem demonstrates that the ECS is a great candidate of a benchmark for the Asian monsoon record, especially for the early part of the Quaternary.
Here we propose to extend this excellent sediment archive through the last 1.5 Ma to reveal the underlying mechanism of the millennial-scale monsoon variability. In this presentation, we also report our recent progress on the site survey (KH-21-3) for re-drilling in the northern ECS.

Keywords: Asian monsoon, IODP, East China Sea, Quaternary, Millennial-scale, Speleothem

©2021. Japan Geoscience Union. All Right Reserved.

SCORE proposal off Shikoku, SW Japan: Reconstruction of the Kuroshio state for super interglacials during the Brunhes chron

*Minoru Ikehara[1], Hiroshi Nishi[2], Tabito Matsu'ura, Kyoko Hagino[1], Takuya Itaki[3], Kyung Eun Lee[4], Yuan-Pin Chang[5], Jianjun Zou[6]

1. Center for Advanced Marine Core Research, Kochi University, 2. Fukui Prefectural University, 3. AIST, 4. Korea Maritime and Ocean University, 5. National Sun Yat-sen University, 6. First Institute of Oceanography

We propose to drill at site SKK-02 (32°26.48’ N, 133°13.67’ E, 2,877m) off Shikoku in the Northwest Pacific to reconstruct high-resolution variability of the Kuroshio Current (KC) for the past super interglacials. The KC is a strong western boundary current and supplies heat and water vapor to the subarctic from the tropical Pacific, influencing climate conditions over the East Asia including the Japanese Islands. The past “super interglacials” are thought to be important analogues for the future global warming climate. However, there are no reliable information on the heat transport and temperature of the KC during the super interglacials due to a lack of the suitable sediment cores from the Northwest Pacific. The Mid-Brunhes Event (MBE) is a climate shift in the Brunhes chron and correspond to the transition between MIS 12 and MIS 11. It is characterized by a clear increase in atmospheric CO_2 and polar ice volume. It is also important to understand the state of the KC for the MBE. In this proposal, we show the following scientific objective.

Main Objective: How does the Kuroshio respond to “super interglacials” compared to today and to Mid-Brunhes Event with different atmospheric CO_2 level?

In addition, we would like to investigate the detailed tephrostratigraphy from caldera volcano in Kyushu Island since the obtained sediment cores should have many volcanic ashes.

Keywords: Kuroshio, SCORE, super interglacial, tephrostratigraphy

©2021. Japan Geoscience Union. All Right Reserved.

Organic geochemical characteristic and its significance of Jurassic-Cretaceous terrestrial sediments recovered by IODP deep sea drilling

*Shutaro Fukushima[1], Takashi Hasegawa[1]

1. Kanazawa University

International Ocean Discovery Program (IODP) is an international deep-sea scientific drilling program to investigate the history and dynamics of the Earth by collecting data recorded in sediments and rocks on the seafloor and monitoring the environment of the seafloor. In IODP Expedition 369, sediment samples with the following four conditions were drilled : ① sediments from the southern margin of the Tethys Sea, ② ages are Jurassic to Early-Cretaceous, ③ terrestrial sediments, ④ immature in terms of organic geochemistry with less metamorphism after burial (Huber et al, 2019). There are no examples of organic geochemical studies on such samples, and it is highly expected that organic geochemical studies on the sediment samples from Site U1515 will provide new insights into organic geochemistry. As a preliminary step to progress such a study, fundamental investigation of biomarkers of Site U1515 sediment samples was conducted in this study. Specifically, the purpose of research is to describe biomarkers, such as whether the sample contains the necessary amount of biomarkers for analysis, what specific biomarkers are included, how diverse they are, and whether the preservation (thermal maturity) of these biomarkers is suitable for research. Biomarker analysis of such unknown samples, which have not been studied, is as important as conducting field surveys in unknown areas and describing fossils there, and lays the foundation for future research.
Gas chromatography (GC) and gas chromatography-mass spectrometry (GC/MS) were performed on eight samples from the Jurassic to Early Cretaceous age sedimentary range of U1515A, and all eight samples were found to contain enough biomarkers to be useful for research. The biomarkers included were roughly divided into eight categories: n-alkanes, aliphatic hopanoids, aliphatic steroids, aromatic hydrocarbons, phenolic diterpenoids, hopanones and steroidketones, and the distribution of n-alkanes, aliphatic hopanoids, aliphatic steroids and steroidketones suggested that all eight samples were immature terrestrial sediments. The distribution of phenolic diterpenoids and n-alkane suggests paleovegetation, and terrestrial higher plants were dominant in organic matter input to the sediments in all eight samples. Among them, the plant groups that were the dominant organic matter input sources differed in each sample. As for phenolic diterpenoids, based on further comparison with previous studies (Marynowski et al., 2006), it is clear for the first time that conifers of these origins were once distributed throughout the northern and southern hemispheres during the Jurassic to at least the Early Cretaceous.

Keywords: biomarker, IODP Expedition 369

©2021. Japan Geoscience Union. All Right Reserved.

Carbon isotope stratigraphy of C40-alkenone and its significance: Cretaceous OAE2 horizon, IODP Site U1516

*Takashi Hasegawa[1], Akiko S. Goto[1,2]

1. Faculty of Geoscience and Engineering, Institute of Science and Engineering, Kanazawa University, 2. Center of Ecological Research, Kyoto University

Alkenone (strait chain alkyl ketone) molecules from marine sediments are known to be products of haptophyte algae and are often employed for paleothermometry for Quaternary and Neogene. Di- and Tri-unsaturated alkenones with 37 carbon atoms (C37 alkenones) are the target molecules for this purpose. On the other hand, only di-unsaturated one has been reported from Paleocene or Cretaceous. Thus alkenone paleothermometry cannot be applied as same way for these greenhouse periods although di-unsaturated alkenone molecules with 37-41 carbon atoms have been reported.

This study detected alkenones with 37-40 carbon atoms in the late Cretaceous sediments from southern margin of proto-Indian Ocean (IODP Exp. 369 Site U1516). Di-unsaturated C40 alkenone ($C_{40:2}$Et) was the most dominant species among the alkenones. In addition to $C_{40:2}$Et, tri-unsaturated C40 alkenone ($C_{40:3}$ Et) was observed by this study for the first time.

Stratigraphic fluctuation of $C_{40:2}$Et content showed conspicuous high value at the top of black clay layer (BCL: sediment associated with OAE2). It is relatively low through the interval below BCL. It decreased above BCL and reach to substantially zero at 30 cm above top of BCL, then no detection above. This is concordant with the fluctuation of TOC.

Carbon isotope values of $C_{40:2}$Et were obtained from 12 horizons. Upper nine samples are from the interval without $d^{13}C$ curve because of low carbonate content. Our $d^{13}C$ data of $C_{40:2}$Et filled the part of the gap and give clue to the international correlation of OAE2 interval based on $d^{13}C$ stratigraphy. The $d^{13}C$ value showed gradual increase through the lower part with minor fluctuation, then dramatic increase through the BCL, and recorded its maximum value (~-29‰) near the top of BCL. Modest drop to -30‰ was observable within the interval 20 cm above the BCL whereas $d^{13}C$ value could not be obtained through the interval above as the abundance of $C_{40:2}$Et was too low. Total magnitude of the excursion at the top of BCL reached as large as 4‰. It could be correlated to a peak that comprises well known carbon isotope excursion of OAE2. If this interpretation is correct, then accumulation of organic matter was limited in the early stage of OAE2 and was interpreted to be as multiple short-lived events. Further collaborative researches are required with chronostratigraphers for age calibration.

Keywords: carbon isotope, alkenones, Cretaceous

©2021. Japan Geoscience Union. All Right Reserved.

[J] Oral | M (Multidisciplinary and Interdisciplinary)：M-IS Intersection

Fri. Jun 4, 2021 1:45 PM - 3:15 PM JST | Fri. Jun 4, 2021 4:45 AM - 6:15 AM UTC | Ch.19 Zoom Room 19

[M-IS18] Drilling Earth Science

convener:Junichiro Kuroda(Department of Ocean Floor Geoscience, Atmosphere and Ocean Research Institute, the University of Tokyo), Katsuyoshi Michibayashi(Department of Earth and Planetary Sciences, Nagoya University), Osamu Fujiwara(Geological Survey of Japan, National Institute of Advanced Industrial Science and Technology), Kohtaro Ujiie(Faculty of Life and Environmental Sciences, University of Tsukuba), Chairperson:Yuki Morono(Kochi Institute for Core Sample Research, Japan Agency for Marine-Earth Science and Technology), Junichiro Kuroda(Department of Ocean Floor Geoscience, Atmosphere and Ocean Research Institute, the University of Tokyo)

This session, Drilling Earth Science, encourages the presentations of every scientific research done with samples and data obtained through ocean and land-based drilling projects such as the International Ocean Discovery Program (IODP) and the International Continental Drilling Program (ICDP). This session provides a place to exchange the latest information on the scientific drilling programs including the future science plan/framework of the programs. We also welcome the presentation on the summary of recently implemented expeditions/projects, introduction of new proposal ideas, and report on the new methods and technology developments related to scientific drilling.

1:45 PM - 2:00 PM JST | 4:45 AM - 5:00 AM UTC

[MIS18-07] Chronostratigraphic big data assimilation to characterize the Late Cenozoic warming episodes

*Masao IWAI[1], Yuji YAMAMOTO[1], Hiroshi ASAHI[1], Yurika Ujiie[1], Minoru Ikehara[1], Eiichi TOKUYAMA[1] (1.Center for Advanced Marine Core Research, Kochi University)

2:00 PM - 2:15 PM JST | 5:00 AM - 5:15 AM UTC

[MIS18-08] Magnetostratigraphy of IODP Site U1524A from the Ross Sea, Antarctica

*Xiangyu Zhao[1], Saiko Sugisaki[2], Tim van Peer[3], Yusuke Suganuma[1,4], Laura De Santis[5], Robert McKay[6], Denise Kulhanek[7] (1.National Institute of Polar Research, 2.National Institute of Advanced Industrial Science and Technology, Japan, 3.National Oceanography Centre Southampton, University of Southampton, UK, 4.Department of Polar Science, SOKENDAI (The Graduate University for Advanced Studies), Japan , 5.Instituto Nazionale di Oceanografia e di Geofisica Sperimentale, Italy, 6.Antarctic Research Centre, Victoria University of Wellington, Wellington, New Zealand, 7.International Ocean Discovery Program, Texas A&M University, College Station, TX, USA)

2:15 PM - 2:30 PM JST | 5:15 AM - 5:30 AM UTC

[MIS18-09] Discovery of living microbes from the ancient subseafloor sediment up to 101.5 million years old: How is it possible for microbes to survive for such a geological timescale?

★Invited Papers

*Yuki Morono[1] (1.Kochi Institute for Core Sample Research, Japan Agency for Marine-Earth Science and Technology)

2:30 PM - 2:45 PM JST | 5:30 AM - 5:45 AM UTC

[MIS18-10] A signature of heat along a micro-fault in Hikurangi margin, New Zealand: IODP Expedition 375, Site U1518

*Yoshitaka Hashimoto[1], Tomoki Masaoka[1], Hirohito Fujiwara[1] (1.Kochi University)

2:45 PM - 3:00 PM JST | 5:45 AM - 6:00 AM UTC

[MIS18-11] Drilling and monitoring in Hyuga-Nada: Unveiling effects of ridge subduction on slow earthquakes

★Invited Papers

*Rie Nakata[1], Masataka Kinoshita[1], Yoshitaka Hashimoto[2], Yohei Hamada[3] (1.Earthquake Research Institute, University of Tokyo, 2.Kochi University, 3.JAMSTEC)

3:00 PM - 3:15 PM JST | 6:00 AM - 6:15 AM UTC

[MIS18-12] ICDP DSeis project: an overview of the 2020 research activity

★Invited Papers

*Hiroshi Ogasawara[1], Team ICDP DSeis (1.Faculty of Science and Engineering, Ritsumeikan University)

Chronostratigraphic big data assimilation to characterize the Late Cenozoic warming episodes

*Masao IWAI[1], Yuji YAMAMOTO[1], Hiroshi ASAHI[1], Yurika Ujiie[1], Minoru Ikehara[1], Eiichi TOKUYAMA[1]

1. Center for Advanced Marine Core Research, Kochi University

Various paleoceanographic big data from deep sea cores, including the core logging data, age models and multi proxy data, are now accessible basically through the online databases at the IODP websites and others. However, data quality and resolutions of data set from different sites are different each other and taxonomic concept used to establish onboard age model are changing and changing, and also the Geologic Time Scale has been revised several times for the last half Century. So, it is important to assimilate chronostratigraphic data with precise and accurate stratigraphic correlation, and it is essential for better understanding of geologic Earth history including such as the past warming episodes during Late Cenozoic Ice Age, which will be important as an analogue of the upcoming global warming during the 21st Century ad will provide us insight to survive warming world.
Our research project on the chronostratigraphic data assimilation is one of three subprojects of the Joint Usage/Research Project on the Super Warm Earth: Understanding Global Warming Processes from Paleoceanographic Big Data (a.k.a. “Big Data Project”) . Objectives of the projects are to reevaluate and reassess the Cenozoic magnetobiochronology by using legacy cores at Kochi Core Center (KCC) and cores from on-going IODP expeditions, to establish high quality and high-resolution paleoceanographic data sets in order to reveal tempo and mode of the global warming under the >400ppm CO2 emission, and to understand biotic response to those environmental changes from cored materials.
The Workshop on Paleoceanographic Big Data: Chronostratigraphic data assimilation held on 20th February, a total of 33 professionals in various research fields from 5 countries (NZ, UK, France, Germany, Japan) had been meet together at KCC/CMCR, Kochi University, in order to share our experiences on chronostratigraphic, taxonomic and genetic big data, and to discuss on those data assimilation and future collaboration to integrate those big data sets and pass it to the next generation. In addition, we also discussed on the following issues to establish an open science platform for researches related to those scientific drillings; 1) Sample and data traceability, 2) Utilizing legacy cores for research and education, and 3) AI-IoT opportunity for the IODP core repositories.

Keywords: DSDP, ODP, IODP Legacy core, Cenozoic, magnetobiostratigraphy, chronostratigraphy, KCC

©2021. Japan Geoscience Union. All Right Reserved.

Magnetostratigraphy of IODP Site U1524A from the Ross Sea, Antarctica

*Xiangyu Zhao[1], Saiko Sugisaki[2], Tim van Peer[3], Yusuke Suganuma[1,4], Laura De Santis[5], Robert McKay[6], Denise Kulhanek[7]

1. National Institute of Polar Research, 2. National Institute of Advanced Industrial Science and Technology, Japan, 3. National Oceanography Centre Southampton, University of Southampton, UK, 4. Department of Polar Science, SOKENDAI (The Graduate University for Advanced Studies), Japan , 5. Instituto Nazionale di Oceanografia e di Geofisica Sperimentale, Italy, 6. Antarctic Research Centre, Victoria University of Wellington, Wellington, New Zealand, 7. International Ocean Discovery Program, Texas A&M University, College Station, TX, USA

International Ocean Discovery Program (IODP) Expedition 374 aims at resolving the Ross Sea ice sheet history since the Miocene. Site U1524 is located ~120 km north of the Ross Sea continental shelf edge. Hole U1524A is the longest among all three holes at this site. To reconstruct the magnetostratigraphy, natural remanent magnetization (NRM) and its demagnetization data derived from shipboard measurements of archive-half sections, u-channel samples taken from the top 8 cores and discrete cube samples taken from the other cores are jointly analyzed. Results of u-channel and discrete samples demonstrate that undesired secondary magnetization can usually be removed at 20 mT peak alternating field (AF). The combined dataset provides a reliable and continuous reconstruction of geomagnetic polarity, which dates the bottom of U1524A being deposited before 3.3 Ma ago. Frequency analysis based on this age model reveals that the magnetic susceptibility of U1524A bears 405-kyr and 41-kyr cycles. The 405-kyr component has a close in-phase correlation with the theoretical long eccentricity cycles, while the 41-kyr component has a more complicated relationship with the theoretical obliquity cycles. It indicates that the astronomical influence plays an important role in the sedimentary process at Site U1524.

Keywords: IODP Exp. 374, paleomagnetism, magnetostratigraphy, Antarctica, Ross Sea

©2021. Japan Geoscience Union. All Right Reserved.

Discovery of living microbes from the ancient subseafloor sediment up to 101.5 million years old: How is it possible for microbes to survive for such a geological timescale?

*Yuki Morono[1]

1. Kochi Institute for Core Sample Research, Japan Agency for Marine-Earth Science and Technology

Marine subseafloor harbors a remarkable microbial population that comprises 12-45% of total microbial biomass or ~0.6-2% of total living biomass on Earth (1-3). Recent findings also demonstrated the large diversity of the subseafloor microbial population that matches marine or soil microbiome (4). However, the rate at which they use energy is reported to be extremely low, at energy fluxes lower than previously shown to support life (5).
In 2009, we obtained subseafloor sediment samples at an ultraoligotrophic oceanic region of South Pacific Gyre (SPG) during the Integrated Ocean Drilling Program (IODP) Expedition 329. Incubation experiments conducted using old (4.3-101.5 Ma) sediments showed that diverse aerobic members of communities in SPG sediments could readily incorporate carbon and nitrogen substrates and dividing(6). In contrast, anaerobic microbes were only minimally revived from this oxic sediment. These results suggested that microbial communities distributed in organic-poor abyssal sediment consist mainly of aerobes that retain their metabolic potential under extremely low-energy conditions for up to 101.5 Ma. Still, the mechanism that enabled microbes to survive is uncertain. The constraints in nutrient, energy, and spatial structure will be discussed in the context of microbial survival in the subseafloor sedimentary environment.

1. Bar-On et al. 2018. The biomass distribution on Earth. Proc Natl Acad Sci USA 115:6506-6511.
2. Magnabosco et al. 2018. The biomass and biodiversity of the continental subsurface. Nature Geoscience 11:707-717.
3. Kallmeyer et al. 2012. Global distribution of microbial abundance and biomass in subseafloor sediment. Proc Natl Acad Sci USA 109:16213-16216.
4. Hoshino et al. 2020. Global diversity of microbial communities in marine sediment. Proceedings of the National Academy of Sciences 117:27587-27597.
5. Bradley et al. 2020. Widespread energy limitation to life in global subseafloor sediments. Science Advances 6:eaba0697.
6. Morono et al. 2020. Aerobic microbial life persists in oxic marine sediment as old as 101.5 million years. Nature Communications 11:3626.

Keywords: Subseafloor biosphere, South Pacific Gyre, Extreme nutrient limitation

©2021. Japan Geoscience Union. All Right Reserved.

A signature of heat along a micro-fault in Hikurangi margin, New Zealand: IODP Expedition 375, Site U1518

*Yoshitaka Hashimoto[1], Tomoki Masaoka[1], Hirohito Fujiwara[1]

1. Kochi University

In Hikurangi margin, New Zealand, slow slips have been observed every 1-2 years repeatedly, and the slip could reach around the shallow portion at the trench axis. In this study, we measured reflectance of carbonaceous material (R) along a micro-fault within a core sample obtained from IODP Expedition 375 to examine a signature of heating event around the micro-fault.
The sample is taken from the depth of 290 m below seafloor (mbsf) in Site U1518 which is located at the frontal thrust. A thrust fault zone with fault breccia is located around 300 mbsf close to the sample location. Therefore, the micro-fault at the bottom of the sample can be expected to be related to the fault zone. The surface of harf-cut sample was polished and scanned by a fluorescence microscope. Grains with black in the scanned image by a fluorescence microscope and with reflective in the reflection microscope can be identified as carbonaceous materials. Reflectance of the grains were measured with the positions in the samples. Additionally, R for background value was measured on carbonaceous grains separated from the bulk samples.
The number of measured grains is 950. The R ranges about 0.1-15 %. The measured grains include both primarily matured one in situ and previously matured detrital one. To pick the primarily matured one, a statistic examination was conducted. The histogram for all R shows the peak at 0.6 %. While the distribution of R below 0.6 % with a function of the distance from the fault at the bottom of the sample indicates decrease trend in R with distance, such trend was obscured in the distribution of R for all data, which suggests that the grains with R above 0.6 % are randomly distributed due to the detrital origin. In addition, the minimum baseline of the distribution of R below 0.6 % consistent with the background value of 0.1-0.2 %, whereas the minimum baseline of the distribution of R for all data indicates significantly higher value than the background value. Therefore, the R below 0.6 % was taken as the value for the primarily matured grains in situ.
The decrease trend from the micro-fault suggests that a heating event was recorded in the sample by frictional heating or hot fluid migration. The distance of the decrease trend is about 10 mm. If the frictional heating makes the trend, the slip duration is estimated as 6.25-25.0 s, which is consistent with the VLFEs.

Keywords: Heating along a micro-fault, Hikurangi margin, New Zealand, IODP Expedition 375, reflectance of carbonaceous material

©2021. Japan Geoscience Union. All Right Reserved.

Drilling and monitoring in Hyuga-Nada: Unveiling effects of ridge subduction on slow earthquakes

*Rie Nakata[1], Masataka Kinoshita[1], Yoshitaka Hashimoto[2], Yohei Hamada[3]

1. Earthquake Research Institute, University of Tokyo, 2. Kochi University, 3. JAMSTEC

Shallow slow earthquakes, which last minutes to years, are important indicators of subduction megathrust slip behavior and future seismic and tsunami potential. Subducting plate roughness and seamounts have been proposed to promote slow earthquakes by inducing local geomechanical and hydrogeological anomalies. The Hyuga-Nada region offshore Kyushu, Japan is an outstanding locale for drilling and observatory experiments to investigate these effects. In this region, slow earthquakes are repeatedly observed on and near the subducting Kyushu-Palau-Ridge, KPR, chain of seamounts thus providing excellent opportunities to explore the effects of seamounts on geomechanical/hydrological/thermal properties, and ultimately seismic coupling. Long-term monitoring enabled by a planned permanent network (N-net) will allow subsurface processes during frequent (~1 year) periodical slow earthquakes and ~M7 earthquakes (~20-30 year interval) to be captured with high fidelity. Drilling, logging, and coring will provide key constraints on stress state, hydrological processes, and sediment physical properties in the region above the ridge. We have originally proposed the drilling and monitoring plan to IODP in 2019 (Nakata et al. 2019). In this presentation, we report the updated proposal plan along with initial processing results of new site survey data acquired with JAMSTEC (Miura et al., 2021, Arai et al., 2021, Ma et al., 2021).

We propose to drill and install observatories at three primary locations in Hyuga-Nada to address two hypotheses: 1) Seamount subduction modulates stress and pore pressure, creates fracture networks and influences the thermal and hydrological state of the margin. 2) The spatiotemporal distribution of slow earthquakes is strongly influenced by seamount subduction through the processes outlined in Hypothesis 1. We will drill three primary distinct sites relative to the seamount, to (1) measure physical properties, and (2) describe deformation by LWD, APCT-3, and core analysis to characterize in-situ stress state, fracture density, heat flow, and pore fluid flow. Spatial variations in the upper plate disruption caused by seamount subduction will be revealed by comparing results from sites in the leading and lateral edges, and top of the currently subducting seamount; and these will constrain geomechanical, hydrological, and thermal models. At two of the sites, we will install a “Fiber-CORK” observatory equipped with conventional pressure and temperature sensors and cutting-edge fiber-optic sensors. One site will be connected to the N-net node for real-time data streaming. The combination will fill a gap in slip durations currently observable in this region with seismic and geodetic instrumentation. Fully characterizing slow earthquakes will reveal the degree to which they accommodate plate motion, and whether strain is accumulated for future earthquakes.

Keywords: Drilling, Monitoring, Hyuga-nada, Slow earthquakes , Nankai

©2021. Japan Geoscience Union. All Right Reserved.

ICDP DSeis project: an overview of the 2020 research activity

*Hiroshi Ogasawara[1], Team ICDP DSeis

1. Faculty of Science and Engineering, Ritsumeikan University

The ICDP DSeis project (Ogasawara et al. 2017 AfriRock) has accomplished drilling and down-ole logging at the seismogenic zones in deep gold mines in South Africa. In this presentation, we will review the research activity of the FY2020.

On a mining horizon, Naoi et al. (2013 Pageoph, 2015 JGR, Tectonophysics, etc.) successfully elucidated that the microfracturings evolve planarly ahead of mining faces. The host rock, fractured materials and fracture structures of a tens of meter sized fracture zone were very well recovered with a BQ triple tube 1.5 meter long. With the recovered materials and host rocks, friction experiments at the Kyoto University Tsutsumi Laboratory was conducted. Comparison of frictional properties between gouge and rock-to-rock was published in Mngadi et al. (2021 Int. J. Rock Mech. Min. Sci.).

Below another mine, we have accomplished the core recovery with a total length of 1.6 km in NQ size from the upper fringe of the seismogenic zone of the 2014 M5.5 Orkney sinistral earthquake, (Ogasawara et al. 2019 Deep Mining; ICDP 2019 The Thrill to Drill). In FY2020, we conducted compilation of borehole logging, core logging at Kochi Core Center, and recovered core information (Yoshida 2021 Ritsumeikan MSc thesis; Ogasawara et al. 2021 JpGU), integrated analysis of core stress measurement stress (Higashi 2021 Ritsumeikan MSc thesis), aftershock DD relocation (Tadokoro 2021 Ritsumeikan MSc thesis), and analysis of 3D seismic reflection data (Suzuki et al. SSJ 2020 and AGU 2020). It is now becoming clear that the host rock of the seismogenic zone, which has density and velocity comparable to those of the upper crust, is greatly influenced by the altered mafic intrusive rock (density and velocity comparable to those of the lower crust), and that it also defines the streak distribution of aftershocks.

At the intersection of the Dolerite Sill and another mafic dyke, teams of microbiologists from the U.S., Germany, and other countries have also found brine fissures and gases (similar to those near hydrothermal vents at oceanic ridges?) that are non-meteoric and rich in dissolved organic hydrocarbons of non-biogenic origin (Wiersberg et al. 2019 EGU; Rusley et al. 2018 AGU; Nisson et al. 2019 AGU). Warr et al. (2020 AGU) made progress in isotope analysis.

The ICDP team consists of researchers from Japan, South Africa, USA, Germany, Switzerland, India, Israel, Australia, and practitioners from the mining industry in South Africa. The core members include Y. Yabe and T. Ito (Tohoku Univ.), J. Mori (Kyoto Univ.), T. Hirono (Osaka Univ.), Y. Yamamoto (Kochi Univ.), B. Liebenberg (Moab Khotsong mine), T.C. Onsott (Princeton Univ.), T.L. Kieft (New Mexico Tech), T. Wiersberg and M. Zimmer (GFZ), R.J. Durrheim (Wits Univ.). Durrheim (Wits Univ.), J. Castillo (Free State Univ.), M. Ziegler (ETH, Zurich), and their students.

This drilling program was built on the projects supported by JST-JICA SATREPS and JSPS Kakenhi. It is currently supported by AngloGold Ashanti, Harmony, Sibanye Stillwater, ICDP, JSPS Core-to-Core Program, JSPS-SA NRF bilateral Program, Ritsumeikan University, Kochi Core Center, Collaborative Research Program for Seismic Volcanic Observations to Mitigate Hazards, US NSF, German DFG, South African NRF, CSIR and CGS.

©2021. Japan Geoscience Union. All Right Reserved.

Keywords: Seismogenic zone , ICDP scientific drilling, Deep goold mines in South Africa, Altered intrusives as dense as lower crustal material

©2021. Japan Geoscience Union. All Right Reserved.

[J] Oral | M (Multidisciplinary and Interdisciplinary)：M-IS Intersection

Fri. Jun 4, 2021 3:30 PM - 5:00 PM JST | Fri. Jun 4, 2021 6:30 AM - 8:00 AM UTC | Ch.19 Zoom Room 19

[M-IS18] Drilling Earth Science

convener:Junichiro Kuroda(Department of Ocean Floor Geoscience, Atmosphere and Ocean Research Institute, the University of Tokyo), Katsuyoshi Michibayashi(Department of Earth and Planetary Sciences, Nagoya University), Osamu Fujiwara(Geological Survey of Japan, National Institute of Advanced Industrial Science and Technology), Kohtaro Ujiie(Faculty of Life and Environmental Sciences, University of Tsukuba), Chairperson:Osamu Fujiwara(Geological Survey of Japan, National Institute of Advanced Industrial Science and Technology), Tomoaki Morishita(School of Geoscience and Civil Engineering, College of Science and Technology, Kanazawa University), Kohtaro Ujiie(Faculty of Life and Environmental Sciences, University of Tsukuba)

This session, Drilling Earth Science, encourages the presentations of every scientific research done with samples and data obtained through ocean and land-based drilling projects such as the International Ocean Discovery Program (IODP) and the International Continental Drilling Program (ICDP). This session provides a place to exchange the latest information on the scientific drilling programs including the future science plan/framework of the programs. We also welcome the presentation on the summary of recently implemented expeditions/projects, introduction of new proposal ideas, and report on the new methods and technology developments related to scientific drilling.

3:30 PM - 3:45 PM JST | 6:30 AM - 6:45 AM UTC

[MIS18-13] Drilling of Kikai caldera volcano for elucidation of magma plumbing system and flow-deposition processes of large ignimbrite

★Invited Papers

*Katsuya Kaneko[1], Takeshi Hanyu[1], Reina NAKAOKA[3], Koji Kiyosugi[3], Nobukazu Seama[1], Tetsuo Matsuno[3], Yojiro Yamamoto[2], Tomoko Hanyu[3] (1.Department of Planetology, Graduate School of Science, Kobe University, 2.Japan Agency for Marine-Earth Science and Technology, 3.Kobe Ocean-Bottom Exploration Center, Kobe University)

3:45 PM - 4:00 PM JST | 6:45 AM - 7:00 AM UTC

[MIS18-14] Mado Megamullion: a potential new target for IODP drilling to understand backarc basin lithosphere

*Yasuhiko Ohara[1,2,3], Masakazu Fujii[4], Norikatsu Akizawa[5], Valentin Basch[6], Yumiko Harigane[7], Ken-ichi Hirauchi[8], Osamu Ishizuka[7], Shiki Machida[9], Katsuyoshi Michibayashi[3], Kyoko Okino[5], Alessio Sanfilippo[6], Camilla Sani[6], Sen Atlanta[10], Jonathan E Snow[11], Kenichiro Tani[12], Hiroyuki Yamashita[13] (1.Hydrographic and Oceanographic Department of Japan, 2.Japan Agency for Marine-Earth Science and Technology , 3.Nagoya University, 4.National Insitute of Polar Reseach, 5.Atmosphere and Ocean Research Institute, University of Tokyo, 6.University of Pavia, 7.Geological Survey of Japan, AIST, 8.Shizuoka University, 9.Chiba Institute of Technology, 10.University of Houston, 11.Louisiana State University, 12.National Science Museum, 13.Kanagawa Prefectural Museum of Natural Histroy)

4:00 PM - 4:15 PM JST | 7:00 AM - 7:15 AM UTC

[MIS18-15] Understanding of Oceanic Plate Hydration by drillings into plate bending-induced normal fault in incoming plate at off-Tohoku and the Horoman Peridotite complex

★Invited Papers

*Tomoaki Morishita[1] (1.School of Geoscience and Civil Engineering, College of Science and Technology, Kanazawa University)

4:15 PM - 4:30 PM JST | 7:15 AM - 7:30 AM UTC

[MIS18-16] Introduction to ‘New Caledonia Ophiolite Land-to-Sea Drilling Project’

Marguerite Godard[1], Julien Collot[2], Juerg Matter[3], Rupert Sutherland[4], Christian Betzler[5], Vasileios Chatzaras[6], Gaël Erauso[7], François Fournier[7], Frieder Klein[8], Othmar Müntener[9], Martin Patriat[10], Roy

Price[11], Shino Suzuki[12], *Yasuhiro Yamada[13] (1.Université de Montpellier, CNRS, France, 2.Geological Survey of New Caledonia, France, 3.University of Southampton, UK, 4.Victoria University of Wellington, NZ, 5.University Hamburg, Germany, 6.The University of Sydney, Australia, 7.Aix-Marseille Université, France, 8.Woods Hole Oceanographic Insitution, USA, 9.University of Lausanne, Switzerland, 10.Ifremer, France, 11.Stony Brook University, USA, 12.Japan Aerospace Exploration Agency, Japan, 13.Japan Agency for Marine-Earth Science and Technology)

4:30 PM - 4:45 PM JST | 7:30 AM - 7:45 AM UTC

[MIS18-17] In-situ stress at the basement under Osaka plain -estimation of stress values by DCDA method in deep seismic obsevation wells-

*Kentaro Omura[1], Akio Funato[2], Takatoshi Ito[3] (1.National Research Institute for Earth Science and Disaster Resilience, 2.Fukada Geological Institute, 3.Institute of Fluid Science, Tohoku University)

4:45 PM - 5:00 PM JST | 7:45 AM - 8:00 AM UTC

[MIS18-18] **Tidally-modulated temperature observed at a drillsite in the Noho hydrothermal field in the mid-Okinawa Trough**

*Masataka Kinoshita[1], Kazuya Kitada[2], Tatsuo Nozaki[2], Yuka Masaki[3], Lena Maeda[2], Hidenori Kumagai[2] (1.Earthquake Research Institute, University of Tokyo, 2.Japan Agency for Marine-Earth Science and Technology, 3.Cosmos Shoji Co., Ltd.)

Drilling of Kikai caldera volcano for elucidation of magma plumbing system and flow-deposition processes of large ignimbrite

*Katsuya Kaneko[1], Takeshi Hanyu[1], Reina NAKAOKA[3], Koji Kiyosugi[3], Nobukazu Seama[1], Tetsuo Matsuno[3], Yojiro Yamamoto[2], Tomoko Hanyu[3]

1. Department of Planetology, Graduate School of Science, Kobe University, 2. Japan Agency for Marine-Earth Science and Technology, 3. Kobe Ocean-Bottom Exploration Center, Kobe University

Caldera volcanoes universally exist in volcanic regions with continental crust and their activities are characterized by catastrophic caldera-forming eruptions (CCFEs) that discharge more than 40 km^3 of silicic magma as pyroclastics. The CCFEs are rare but extremely hazardous events. Mechanisms of magma generation and eruption in the caldera volcanoes are important to understand igneous processes in continental crust and mitigate volcanic hazard.

Kikai caldera volcano in the southwest Japan arc caused three CCFEs in the past, has a caldera of 19×22 km formed by the latest 7.3-ka CCFE, and is active at the present. So far, we have reported a giant lava dome inside the caldera that was formed at the post caldera stage and accurate volume estimation of the latest CCFE. We have been comprehensively researching it to know all about it with surveys of geology, bathymetry, seismic reflection, geomagnetic field, and resistivity structure and analyses of volcanic products in the Kikai caldera region. Our purposes are to clarify the current situation of magma beneath the volcano, mechanisms and evolution of the magma plumbing system, and transportation and deposition processes of submarine pyroclastics.

In our project on Kikai caldera volcano, drilling, coring, and dredge are conducted for the last two purposes. Some volcanics samples by coring and dredge in Kikai sea area were obtained in 2019 and 2020. These samples with the previously obtained samples clearly show temporal change of petrological features of the Kikai magmas in whole-rock composition. The cored samples were obtained down to the second CCFE deposit (95 ka) and show different occurrence of the submarine pyroclastic deposits from the subaerial ones. In order to advance understanding of evolution of the Kikai magmas and sedimentological processes of the submarine pyroclastics, further drilling at a proximal subaerial area of Kikai caldera volcano is needed, because Kikai caldera volcano which is a submarine volcano gives us only limited exposure of its ejecta and is not fully understood in terms of its detailed history and occurrence of pyroclastic ejecta. Collecting volcanics samples throughout the activity of Kikai caldera volcano allow us to elucidate magmatic evolution in petrological and geochemical characteristics. Comparison between the submarine and subaerial pyroclastic deposits in the same eruption clearly shows key processes of pyroclastic transportation and deposition in submarine condition; volcanic fields that have both the submarine and subaerial deposits from the same eruption source are rare and precious.

We propose new drilling of 300 m depth at two sites in Takeshima island which is a subaerial area of Kikai caldera volcano to proceed with the investigations mentioned above, and submitted the preliminary proposal to the ICDP. The two sites are near the outcrops of the first and second CCFEs (140 ka and 95 ka, respectively). We plan to clarify eruption sequences of the older two CCFEs which are much less understood and activity of the volcano at the early stage, and analyze petrographical and geochemical characterization of the samples with many analyses such as major/trace elements composition, isotope composition, volatile content for whole-rock, volcanic glass, and phenocryst. On the basis of these results,

©2021. Japan Geoscience Union. All Right Reserved.

we attack to reveal mechanisms of magma processes for caldera volcanoes. We plan to analyze sedimentary structure, grain size, and component for the submarine and subaerial pyroclastic deposits, compare the sedimentological characteristics between them, and reconstruct traveling and sedimentation of pyroclastic clasts produced by submarine eruptions.

Keywords: Kikai caldera volcano, magma plumbing system, Submarine pyroclastic flow

©2021. Japan Geoscience Union. All Right Reserved.

Mado Megamullion: a potential new target for IODP drilling to understand backarc basin lithosphere

*Yasuhiko Ohara[1,2,3], Masakazu Fujii[4], Norikatsu Akizawa[5], Valentin Basch[6], Yumiko Harigane[7], Ken-ichi Hirauchi[8], Osamu Ishizuka[7], Shiki Machida[9], Katsuyoshi Michibayashi[3], Kyoko Okino[5], Alessio Sanfilippo[6], Camilla Sani[6], Sen Atlanta[10], Jonathan E Snow[11], Kenichiro Tani[12], Hiroyuki Yamashita[13]

1. Hydrographic and Oceanographic Department of Japan, 2. Japan Agency for Marine-Earth Science and Technology , 3. Nagoya University, 4. National Insitute of Polar Reseach, 5. Atmosphere and Ocean Research Institute, University of Tokyo, 6. University of Pavia, 7. Geological Survey of Japan, AIST, 8. Shizuoka University, 9. Chiba Institute of Technology, 10. University of Houston, 11. Louisiana State University, 12. National Science Museum, 13. Kanagawa Prefectural Museum of Natural Histroy

Oceanic core complexes (OCCs) or megamullions are domal bathymetric highs with axis-normal corrugations, and with exposure of serpentinized peridotite and gabbroic rocks, interpreted as exhumed footwalls of low-angle detachment faults. OCCs are the only places at which the petrological crust/mantle boundary can be reached by ocean drilling with current technology.

A significant fraction of the ocean floor is created in backarc basins where water plays a major role in magmatic processes, leading to an accretionary style potentially contrasting to that of normal mid-ocean ridges. A better understanding the architecture and composition of backarc basins is therefore important to understand the oceanic crustal accretion process globally. However, there has been no single core of lower oceanic crust or uppermost mantle located at backarc basin to characterize this important tectonic setting. On this rationale, we have been proposing an IODP proposal to drill Godzilla Megamullion, the largest known OCC on Earth, located in an extinct backarc basin, the Parece Vela Basin, in the Philippine Sea.

Here, we introduce our intention to drill another OCC located in a backarc setting, Mado Megamullion, in the Shikoku Basin, located ~1100 km north of Godzilla Megamullion. Mado Megamullion is the OCC that is most easily accessible OCC from major city; it is located only ~1200 km from Tokyo. Importantly, it has a ~20 km square corrugated surface, comparable in areal size to typical OCCs in the Mid-Atlantic Ridge, such as Atlantis Massif and Kane Megamullion. It thus represents an ideal case to make a comparative study with well-known OCCs exposed at the slow-spreading Mid-Atlantic Ridge. This will provide useful information to understand the fundamental differences of the lithospheric characteristics between the two major oceanic settings.

We believe that IODP drilling of Godzilla Megamullion will provide important datasets to understand the long-term evolution of this unique OCC. On the other hand, IODP drilling of Mado Megamullion will provide complimentary data, necessary to understand the difference of the lithospheric characteristics between the two major oceanic settings. In this contribution, we will summarize the dataset available to a preliminary IODP drilling proposal, and discuss its scientific framework.

Keywords: Mado Megamullion, IODP, oceanic core complex, backarc basin

©2021. Japan Geoscience Union. All Right Reserved.

Understanding of Oceanic Plate Hydration by drillings into plate bending-induced normal fault in incoming plate at off-Tohoku and the Horoman Peridotite complex

*Tomoaki Morishita[1]

1. School of Geoscience and Civil Engineering, College of Science and Technology, Kanazawa University

The oceanic plate has played an essential role in Earth’ s water circulation. In the last two decades, it has generally accepted that hydration due to plate bending-induced normal faults (bend-faults) occurs in the region between trench and outer-rise region. The northwest Pacific (NW Pacific) region is one of the world oldest, thus coldest, and most studied oceanic plates, and is therefore a high priority region to study bend-fault hydration. Water circulation (deep penetration and deep upwelling) and hydration through bend-faults in the NW Pacific region is supported by results from extensive recent geophysical surveys. In order to deepen our understanding of bend-fault hydration processes and their effects on changing in physical properties in incoming oceanic plate in many subduction zones, such as the young-hot middle America and the old-cold northwest Pacific region. An International Oceanic Drilling proposal named Bending fault hydrology of the Old Incoming Plate (H-ODIN) for the northwest Pacific region is developed. Hydration of oceanic plate prior to subduction is also key to describing and quantifying water flux into the deep Earth. Mantle drilling project is aimed at obtaining the pristine material of the oceanic plate and can provide a reference for the less-altered oceanic plate. It should be emphasized that little is known about the onset of hydration of the uppermost mantle. In order to address this fundamental question, we are also developing a new on-land drilling project into a fresh peridotite body, the Horoman peridotite body, Hokkaido, Japan. In the presentation, we will introduce the main scientific objectives and drilling strategies of these drilling projects.

Keywords: Hydration of Oceanic Plate, Drilling project into plate bending-induced fault at outerrise region, The first touch of water with the uppermost mantle in incoming plate

©2021. Japan Geoscience Union. All Right Reserved.

Introduction to ‘New Caledonia Ophiolite Land-to-Sea Drilling Project’

Marguerite Godard[1], Julien Collot[2], Juerg Matter[3], Rupert Sutherland[4], Christian Betzler[5], Vasileios Chatzaras[6], Gaël Erauso[7], François Fournier[7], Frieder Klein[8], Othmar Müntener[9], Martin Patriat[10], Roy Price[11], Shino Suzuki[12], *Yasuhiro Yamada[13]

1. Université de Montpellier, CNRS, France, 2. Geological Survey of New Caledonia, France, 3. University of Southampton, UK, 4. Victoria University of Wellington, NZ, 5. University Hamburg, Germany, 6. The University of Sydney, Australia, 7. Aix-Marseille Université, France, 8. Woods Hole Oceanographic Insitution, USA, 9. University of Lausanne, Switzerland, 10. Ifremer, France, 11. Stony Brook University, USA, 12. Japan Aerospace Exploration Agency, Japan, 13. Japan Agency for Marine-Earth Science and Technology

The New Caledonia Ophiolite and its offshore extension to the south (ca. 900km) is one of the world’s largest peridotite massifs, which formed during Eocene subduction initiation. It is an ideal place to study heat and mass exchanges between the solid Earth and its external envelopes, the formation mechanisms of metal and energy resources, the deep biosphere of ultramafic rocks, and impacts on the biological and climate system of both subduction initiation and resultant geochemical fluxes with ultramafic rocks.

We have submitted a preproposal of the New Caledonia Ophiolite Land-to-Sea Drilling Project (NCDP), with proposed drill sites on-land (9 ICDP sites) and off-shore (7 IODP sites). This presentation outlines the proposed scientific objectives and drilling strategy.

©2021. Japan Geoscience Union. All Right Reserved.

In-situ stress at the basement under Osaka plain -estimation of stress values by DCDA method in deep seismic obsevation wells-

*Kentaro Omura[1], Akio Funato[2], Takatoshi Ito[3]

1. National Research Institute for Earth Science and Disaster Resilience, 2. Fukada Geological Institute, 3. Institute of Fluid Science, Tohoku University

In-situ crustal stress is an important factor to understand earthquake mechanism and tectonic activities. However, the reliable in-situ stress data seems to still be poor, because complicated procedures are necessary for measurement in a borehole. We tried in-situ crustal stress measurements at deep seismic observation wells of NIED in Osaka plain, western Japan. Borehole-televiewer (BHTV) loggings revealed borehole breakout (shear fractures due to stress concentration on the circular borehole wall), and stress orientations are already reported (Omura, 2020, SSJ Fall Meeting). In present study, we applied DCDA (Diametrical Core Deformation Analysis) method to recovered rock core samples to estimate stress values. DCDA method measures the circumferential diameter variation due to stress relief after the core recovery, and use elastic constants of the rock core. Previous studies suggest that the DCDA method can be applied to rock cores from deep boreholes.
We used rock cores from NIED Konohana (34:39:45.92N, 135:23:22.53E, 2038m depth) and Tajiri (34:23:52.14N, 135:17:01.24E, 1535m depth) deep observation wells in Osaka plain. The core depth is 2035.5m from Konohana and 1202.4m and 1494.8m from Tajiri. The circumferential core diameter variation was measured by an apparatus at NIED designed by Funato and Ito, 2017, IJRMMS. We got sine curves of circumferential diameter variation associated with stress relief, suggesting the DCDA method is applicable to these core samples. We used elastic constants of the rock cores, Young's modulus and Poisson's ratio, deduced from rock mass P and S wave velocities by means of P-S logging at the drilling sites assuming the value of densities, 2.5 g/cm3. Then, values of differential stresses are around 60 MPa. We will apply laboratory rock tests to measure the elastic constants of rock cores themselves.
Those results suggest a pair of DCDA method by recovered rock core and borehole breakout observation by BHTV logging is recommended to measure both of value and orientation of in-situ crustal stress in the case of borehole breakout is produced.

Keywords: DCDA method, in-situ crustal stress, rock core, Osaka plain, borehole televiewer, breakout

©2021. Japan Geoscience Union. All Right Reserved.

Tidally-modulated temperature observed at a drillsite in the Noho hydrothermal field in the mid-Okinawa Trough

*Masataka Kinoshita[1], Kazuya Kitada[2], Tatsuo Nozaki[2], Yuka Masaki[3], Lena Maeda[2], Hidenori Kumagai[2]

1. Earthquake Research Institute, University of Tokyo, 2. Japan Agency for Marine-Earth Science and Technology, 3. Cosmos Shoji Co., Ltd.

In the Okinawa Trough, various active hydrothermal vents have been found and explored. One of them is the Noho hydrothermal field located on the south side of the Iheya Minor Ridge, mid-Okinawa Trough. From March to December 2016, a black-ore cultitivation system was installed at the top of the drilled Hole C9017B under the Cross-ministerial Strategic Innovation Promotion Program (SIP) funded by CSTI of the Cabinet Office of Japan. Two pairs of temperature and pressure gauges, as well as flowmeter, loca cell and their loggees, were installed within the system, and continuous data were obtained.
Hole C9017B was drilled up to 50 m, after which the screened casing was installed down to ~20 m. The black-ore system directly attached to the hole consists of a 2” inner diameter pipe extending from the hole and a cultivation tank (called Cell) attached to the top of the pipe. T/P gauges were installed inside of the pipe and the Cell, and data were obtained at 2-minute intervals. Here we describe their fluctuations and discuss possible causes.
We found that the temperature and pressure of the pipes and cells fluctuated in accordance with the tidal (M2) period. In the beginning, the average temperature was 75-76 degC, and the half-amplitude of tidal modulation was about 0.3 degC. Since their modulation started immediately after the installation to Hole C9017B, it is probably attributed to the tidal modulation at the hydrothermal reservoir beneath the hole, rather than to the variation in the ambient water column. Although the resolution was insufficient, the pressure data also recorded the tidal modulation that is in good agreement, both amplitude and phase, with the theoretical tide, predicted by the ‘NAOTIDE' tide prediction program (Matsumoto et al., 2000). It indicates that the pressure in the cultivation system corresponds to the ocean tide.
The phase of the temperature fluctuation of both the pipe and Cell is delayed by about 150 deg from the pressure estimate by NAOTIDE. The possible mechanisms of such fluctuation may be the variation of ambient seawater (periodic movement in response to the tide), or the change in flow velocity in the cultivation system leading to the variation in dynamic pressure change and the conductive cooling efficiency. However, we assess that neither can sufficiently explain the observed temperature fluctuation. Therefore, we propose that the temperature and pressure of venting fluid are actually modulated by the oceanic tide. Jupp & Schultz (2004) proposed a one-dimensional poroelastic and heat conduction model, by which the temperature, pressure, and velocity of the venting fluid are affected by tides. Based on this, we assess that the phase delay of temperature by 150 deg requires a high permeability in the formation, a deeper tidal penetration depth, and the larger Darcy velocity.
Another possibility is that cracks fluctuate with changes in tidal stress, causing the change in permeability. Since the compressibility of water is larger than that of solids, tides will open and close underground cracks. We propose the most probable model by further analyses.
As an aperiodic change, the measured temperatures gradually decreased (to 30-40 ˚C) in August, accompanied by the amplitude increase in tidal modulation. It is probably caused by the clogging of pipes in the cultivation system due to the hydrothermal precipitation.

Keywords: Okinawa Trough hydrothermal activity, Tidal modulation, Kuroko cultivation system

©2021. Japan Geoscience Union. All Right Reserved.

©2021. Japan Geoscience Union. All Right Reserved.

[J] Oral | M (Multidisciplinary and Interdisciplinary)：M-IS Intersection

Fri. Jun 4, 2021 9:00 AM - 10:30 AM JST | Fri. Jun 4, 2021 12:00 AM - 1:30 AM UTC | Ch.13 Zoom Room 13

[M-IS23] Mountain Science

convener:Keisuke Suzuki(Research Center for Mountain Environment, Shinshu University), Yoshihiko Kariya(Department of Environmental Geography, Senshu University), Akihiko SASAKI(Department of Geography and Environmental Studies, Kokushikan University), Chiyuki Narama(Niigata University, Program of Field Research in the Environmental Sciences), Chairperson:Kenshiro Arie(Niigata University)

Mountainous areas provide water resources to the populated downstream areas, protecting the diversity of ecosystem and providing tourism attraction. To access the mountain environment changes and mitigate the impacts of global warming influences, a cross-cutting session is proposed to share the scientific knowledge among various fields; such as climatology, hydrology, geomorphology, glaciology, water/carbon/material cycle, eco-diversity, etc.

9:00 AM - 9:15 AM JST | 12:00 AM - 12:15 AM UTC

[MIS23-01] Stratigraphy and ages of cores recovered from three linear depressions on the landslide bodies of deep-seated gravitational deformation slopes in the Kamikochi Valley, northern Japanese Alps

*Yoshihiko Kariya[1], Sadao Takaoka[1] (1.Department of Environmental Geography, Senshu University)

9:15 AM - 9:30 AM JST | 12:15 AM - 12:30 AM UTC

[MIS23-02] Comparison between Himalayan river sands and deep-sea Benga Fan sands using heavy mineral assemblage

*Kohki Yoshida[1], Subhadeep Kumar[2], Tomoyuki Hakiai[1], Asako Masuda[1], Lalit Kumar Rai[3] (1.Department of Geology, Faculty of Science, Shinshu University, 2.Department of Geology, Presidency University, 3.Interdisciplinary Graduate School of Science and Technology, Shinshu University)

9:30 AM - 9:45 AM JST | 12:30 AM - 12:45 AM UTC

[MIS23-03] The Characteristic Water Level Changes Mechanism of Kinugasanoike Pond on the Northern Japanese Alps

*Akihiko SASAKI[1], Motoshi Nishimura[2], Keisuke Suzuki[3,4] (1.Department of Geography and Environmental Studies, Kokushikan University, 2.National Institute of Polar Research, 3.Shinshu University, 4.Omachi Alpine Museum)

9:45 AM - 10:00 AM JST | 12:45 AM - 1:00 AM UTC

[MIS23-04] Large-scale flood in North India on 7 February 2021.

*Chiyuki Narama[1], Naho Yamada[2] (1.Niigata University, Program of Field Research in the Environmental Sciences, 2.Graduate School of Science and Technology, Niigata University)

10:00 AM - 10:15 AM JST | 1:00 AM - 1:15 AM UTC

[MIS23-05] Rapid drainage of Lago Greve, a large proglacial lake in Patagonia, observed by satellite in 2020

*Shuntaro Hata[1,2], Shin Sugiyama[2], Kosuke Heki[3] (1.Division of Earth System Science, Graduate School of Environmental Science, Hokkaido University, 2.Institute of Low Temperature Science, Hokkaido University, 3.Department of Earth and Planetary Sciences, Hokkaido University)

10:15 AM - 10:30 AM JST | 1:15 AM - 1:30 AM UTC

[MIS23-06] Mass balance characteristics of three recognized glaciers in the Northern Japanese Alps

★Invited Papers

*Takanobu Sawagaki[1], Satoru Yamaguchi[2], Kotaro FUKUI[3] (1.Faculty of Social Sciences, Hosei University, 2.Snow and ice Research center,, National Research Institute for Earth Science and Disaster prevention, 3.Tateyama Caldera Sabo Museum)

Stratigraphy and ages of cores recovered from three linear depressions on the landslide bodies of deep-seated gravitational deformation slopes in the Kamikochi Valley, northern Japanese Alps

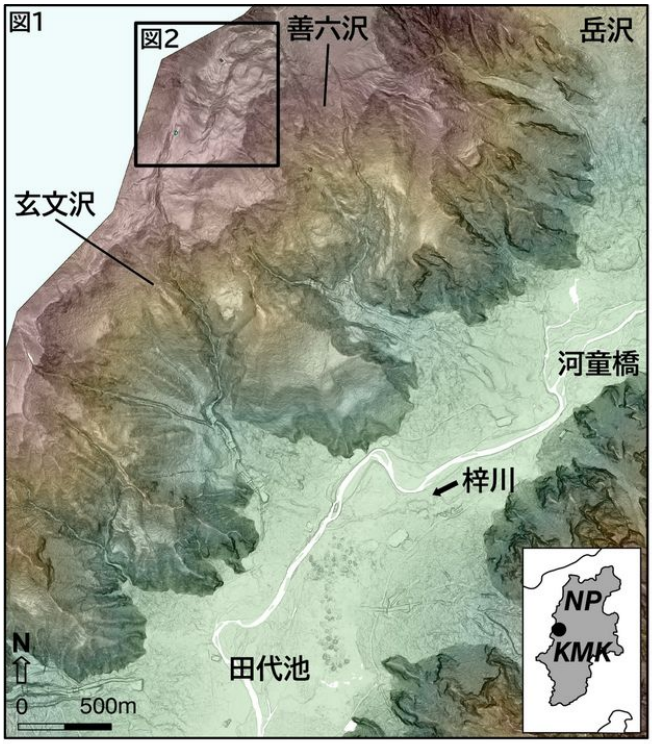
*Yoshihiko Kariya[1], Sadao Takaoka[1]

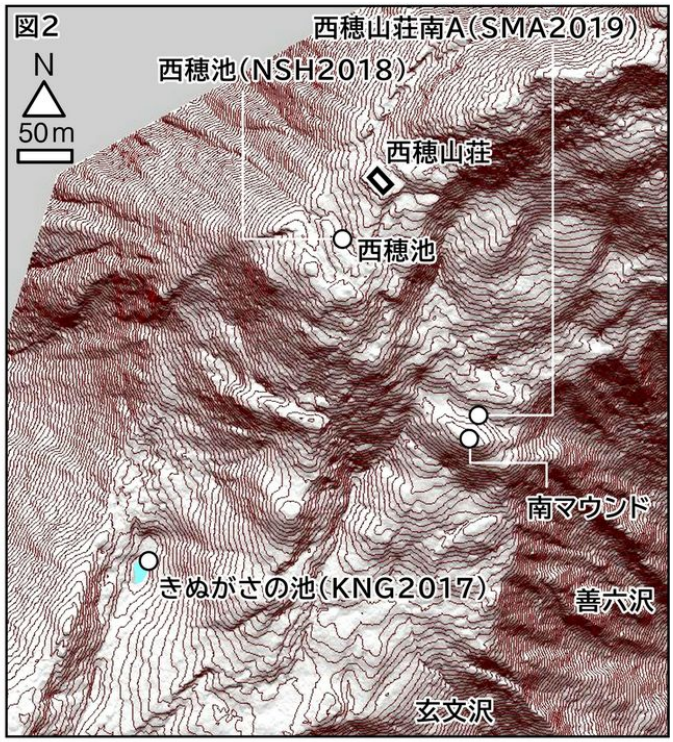
1. Department of Environmental Geography, Senshu University

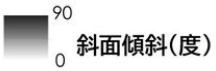
In the Kamikochi Area of the northern Japanese Alps, deep-seated gravitational slope deformation (DSGSD) is common on mountain slopes and ridges of various types of bedrocks. On the slopes around Mount Nishihodaka-dake (2909 m ASL), Quaternary granodiorite is wide-spread, and slopes are well-deformed by DSGSD with characteristic features such as depressions, antiscarps, and bulges. We conducted drilling surveys using a hand-corer at two ponds and a bog on DSGSD-derived depressions and was successful to recover cores: 1) Kinugasano-ike pond (KNG2017 core), 2) Nishiho-ike pond (NSH2018 core), and 3) Nishihosanso Minami A bog (SMA2019 core). Three cores gave geological and chronological information beneficial for reconstructing environmental changes and natural history during the Holocene epoch.
All the depressions were formed in the period from the latest Pleistocene (~ 20 cal ka for KNG2017) to early Holocene (~ 8 ka for NSH2018 and SMA2019) during which global climate had drastically changed. In the study slopes, full-scale DSGSD would begin by this period and caused depression features. Subsequently, accumulation of humic silt and peat had started in the depressions with or without an aqueous body, suggesting onset of vegetation cover around each coring site. Timing of early accumulation of humic silt and peat were around 8 cal ka (KNG2017), 4.2 cal ka (NSH2018), and 6.3 cal ka (SMA2019). Differences in onset time of soils between three sites are thought to be affected by global to local climate and micro-scale topographic situations. The study slopes also received thin volcanic ash layers supplied from nearby Yakedake Volcano around 4 cal ka and 2.3 cal ka, respectively, useful for key beds. In this presentation, we show columnar sections of cores, calendar-calibrated ^{14}C ages, and time-depth diagrams for all sites.

Keywords: deep-seated gravitational slope deformation, landslide, Holocene epoch, peat, Yakedake Volcano

©2021. Japan Geoscience Union. All Right Reserved.









NP 長野県
KMK 上高地

©2021. Japan Geoscience Union. All Right Reserved.

Comparison between Himalayan river sands and deep-sea Benga Fan sands using heavy mineral assemblage

*Kohki Yoshida[1], Subhadeep Kumar[2], Tomoyuki Hakiai[1], Asako Masuda[1], Lalit Kumar Rai[3]

1. Department of Geology, Faculty of Science, Shinshu University, 2. Department of Geology, Presidency University, 3. Interdisciplinary Graduate School of Science and Technology, Shinshu University

The Asian and Indian continental collision resulted in the Bengal Fan due to the formation of the Himalayan and Tibet regions during the Cenozoic era[1]. Numerous studies have elucidated Bengal Fan deposits to obtain accurate data on the detrital mineral assemblage, chemical composition, and detrital zircon U-Pb age[2]. However, the reference datasets of the composition, mineral assemblage, and specific mineral chemistry in each catchment basin of the Himalayan and Tibet areas are inadequate to reconstruct the erosional history of the Himalayas. Therefore, this study examined the heavy mineral assemblage and chemical composition of detrital garnets found in the sediments of Himalayan rivers, and compared them with those of the Bengal Fan deposits. The sands and heavy minerals in modern river sediments were sourced from the Kari Gandaki River in central Nepal as well as the Siang, Lohit, Diban, and Noa Dihing rivers in the upper tributaries of the Brahmaputra River in eastern India, and subsequently compared with the Bengal Fan deposits.
The assemblage of heavy minerals in the Kari Gandaki River, Nepal and Sian River, India, clearly shows the bed rock assemblage distributed in the catchment area. In particular, the detritus supplied from the catchment area, in which the High Himalayan Crystalline Sequence (HHCS) is distributed, show a predominance of high-temperature metamorphic minerals, such as amphibole, kyanite, and sillimanite. However, mafic minerals (chromian spinels, olivine and orthopyroxene) are found in the eastern tributaries of the Brahmaputra River, including the Lohit, Diban, and Noa Dhing rivers; they are sourced from the catchment area occupied by the Trans-Himalayan rocks along with the Yarlung-Zangbo suture zone that comprises mylonite and ophiolitic rocks.

Detrital garnet compositions are also dependent on the geological units distributed in the catchment area; the area occupied by the HHSC mainly comprises almandine (Mg>20 mol %) garnets, whereas the Lesser Himalayan rocks and low-grade parts of the HHCS produce Mg-poor (Mg<20 mol %) almandine garnets. Detrital ilmenite is common in the catchment of the Tethys Himalayan and Lesser Himalayan rocks, whereas it is rare in the HHCS area.

A comparison with the Bengal Fan deposits indicated that detrital amphiboles increased since the Middle Miocene (13 Ma), suggesting that the initial major supply from the HHCS started during this period. However, Mg-rich garnets became a major component since the Late Miocene (9 Ma). The chroman spinels were observed since the Early Miocene (17-16Ma) and sporadically found in the Late Miocene sediments, indicating a supply from the eastern tributaries of the Brahmaputra River.

Reference
[1] Yin, A. & Harrison, M.T. (2000). Geologic Evolution of the Himalayan-Tibetan Orogen. Annual Review of Earth and Planetary Sciences, 28, 211-218.
[2] France-Lanord, C., Michard, A., Bouquillon, A. & Tiercelin, J. J. (1990). Isotopic chemistry and sedimentology of the Bengal fan sediments: The denudation of the Himalaya. Chemical Geology, 84, 368–370.

©2021. Japan Geoscience Union. All Right Reserved.

Keywords: Himalaya, weathering, Bengal Fan

©2021. Japan Geoscience Union. All Right Reserved.

The Characteristic Water Level Changes Mechanism of Kinugasanoike Pond on the Northern Japanese Alps

*Akihiko SASAKI[1], Motoshi Nishimura[2], Keisuke Suzuki[3,4]

1. Department of Geography and Environmental Studies, Kokushikan University, 2. National Institute of Polar Research, 3. Shinshu University, 4. Omachi Alpine Museum

Kinugasanoike (36.262˚N, 137.615˚E, 2215 m *a.s.l.*) is a small pond in a linear depression on the main ridge of the Northern Japanese Alps, caused by gravitational deformation of the mountain’ s bedrock. The Kinugasanoike is thought to form in relation to evolution of the linear depression on the main ridge, however the recharge mechanism of the pond is not clear. The authors aim to clarify the characteristic water level changes mechanism of the Kinugasanoike due to observation of hydrostatic water level, water temperature, chemical characteristics of water (EC, pH, main ion concentration), and precipitation, in addition, analysis of the picture images of interval camera.
Kinugasanoike is completely iced and covered with 4m of snowpack in winter. The pond surface appears in mid-June every year when the snow melt is completed. The area of the catchment of the Kinugasanoike is 26724 m^2, of which the area of the lake surface at steady water level is 258 m^2. The snow-melting water is supplied from the surroundings to the Kinugasanoike, but snow-malting water accumulates on the ice because surface of the pond is still iced when early snow-melt season. On rainfall events, the pond level is sensitive to rainfall exceeding 2 mm per hour. This suggests that hourly precipitation exceeding 2 mm will cause surface runoff and raise the lake level even if there is no preceding rainfall. The Baiu and typhoon season brings a large amount of precipitation. The hourly rainfall of 20mm continues for 3 hours causes the water level of the pond rapidly rise more than 1m, but it take rapidly decreese return to the steady water level after the rainfall.

Keywords: Kinugasanoike, alpine ponds, water level, water balance, Northern Japanese Alps

©2021. Japan Geoscience Union. All Right Reserved.

Large-scale flood in North India on 7 February 2021.

*Chiyuki Narama[1], Naho Yamada[2]

1. Niigata University, Program of Field Research in the Environmental Sciences, 2. Graduate School of Science and Technology, Niigata University

A large-scale flood occurred in Uttarakhand, North India, around 10:30 local time on February 7, 2021. About 170 or more missing workers and 38 people were confirmed dead at the Tapovan Vishnugad Hydro Power Plant, and structures such as houses, dams, hydroelectric power plants, and bridges were damaged. The flood occurred upstream of the Rishiganga River, then merged with the Dhauliganga River and passed through the Raini Village (2000 m asl) in the Chamoli District and the Topoban Vishnugad Hydro Power Plant (1800 m asl) located downstream. As the causes of the flood, we confirmed the collapse of rock slope and small hanging glacier, based on the satellite images before and after the flood.

Keywords: ice avalanche, rock slope failure, flood, Indian Himalaya

©2021. Japan Geoscience Union. All Right Reserved.

Rapid drainage of Lago Greve, a large proglacial lake in Patagonia, observed by satellite in 2020

*Shuntaro Hata[1,2], Shin Sugiyama[2], Kosuke Heki[3]

1. Division of Earth System Science, Graduate School of Environmental Science, Hokkaido University, 2. Institute of Low Temperature Science, Hokkaido University, 3. Department of Earth and Planetary Sciences, Hokkaido University

As a consequence of recent warming climate, the number, area, and volume of glacial lakes are increasing all over the world. While storage in the glacial lakes prevent immediate contribution of glacial meltwater to sea level rise, they threaten societies in mountain regions by posing a risk of glacial lake outburst flood (GLOF). Along the margins of the Patagonia Icefields, glacial lakes are expanding under the influence of glacier retreats. However, due to the remoteness of the lake locations, observations of GLOF are sparse and flood mechanisms are poorly understood. In May 2020, satellite imagery showed a sudden drop in the water level of Lago Greve, the largest proglacial lake in the western side of the Southern Patagonia Icefield. In this presentation, we report the rapid water drainage by analyzing several types of satellite based remote sensing data.

Before the drainage event, the lake area increased by 3.1±2.6 km^2 from September 2016 to April 2020 and the lake level was stable (0.19±0.15 m) from November 2018 to February 2020. Thereafter, the lake area decreased by 15.0±2.6 km^2 during April–November 2020 and the lake level dropped by 18.7±0.2 m during February–July 2020. Satellite image indicates that a gorge at the northern lake margin collapsed and drained lake water through a deepened water channel.

The amount of discharge during April–November 2020 was estimated as 3.7±0.6 km^3 (3.6±0.6 Gt) from the changes in the water level and lake area. Satellite gravimetry in May–August showed a negative gravity change centered on the lake compared to the March 2020. The magnitude of this gravity change was consistent with the amount of drained water. The loss of water from the lake is equivalent to 25–32% of annual ice mass loss from the Southern Patagonia Icefield.

Keywords: Glacial lake, Satellite remote sensing, Patagonia

©2021. Japan Geoscience Union. All Right Reserved.

Mass balance characteristics of three recognized glaciers in the Northern Japanese Alps

*Takanobu Sawagaki[1], Satoru Yamaguchi[2], Kotaro FUKUI[3]

1. Faculty of Social Sciences, Hosei University, 2. Snow and ice Research center,, National Research Institute for Earth Science and Disaster prevention, 3. Tateyama Caldera Sabo Museum

English

Keywords: glacier, Northern Japanese Alps, mass balance

©2021. Japan Geoscience Union. All Right Reserved.

[J] Oral | M (Multidisciplinary and Interdisciplinary)：M-IS Intersection

Fri. Jun 4, 2021 10:45 AM - 12:15 PM JST | Fri. Jun 4, 2021 1:45 AM - 3:15 AM UTC | Ch.13 Zoom Room 13

[M-IS23] Mountain Science

convener:Keisuke Suzuki(Research Center for Mountain Environment, Shinshu University), Yoshihiko Kariya(Department of Environmental Geography, Senshu University), Akihiko SASAKI(Department of Geography and Environmental Studies, Kokushikan University), Chiyuki Narama(Niigata University, Program of Field Research in the Environmental Sciences), Chairperson:Motoshi NISHIMURA(Arctic Environmental Research Center, National Institute of Polar Research)

Mountainous areas provide water resources to the populated downstream areas, protecting the diversity of ecosystem and providing tourism attraction. To access the mountain environment changes and mitigate the impacts of global warming influences, a cross-cutting session is proposed to share the scientific knowledge among various fields; such as climatology, hydrology, geomorphology, glaciology, water/carbon/material cycle, eco-diversity, etc.

10:45 AM - 11:00 AM JST | 1:45 AM - 2:00 AM UTC

[MIS23-07] Snow depth distribution in the Kamikochi-Azusa River basin in the Northern Japan Alps

*Keisuke Suzuki[1], Akihiko Sasaki[2] (1.Research Center for Mountain Environment, Shinshu University, 2.Kokushikan University)

11:00 AM - 11:15 AM JST | 2:00 AM - 2:15 AM UTC

[MIS23-08] Snow depth distribution of Mt. Norikura in the Northern Japan Alps

Rui Tanaka[1], Motoshi Nishimura[2], Akihiko Sasaki[3], *Keisuke Suzuki[4] (1.Shinshu University, 2.National Institute of Polar Research, 3.Kokushikan University, 4.Research Center for Mountain Environment, Shinshu University)

11:15 AM - 11:30 AM JST | 2:15 AM - 2:30 AM UTC

[MIS23-09] Cold air pool formed in Kamikochi, Northern Japan Alps

Sari Koyama[1], Motoshi Nishimura[2], Akihiko Sasaki[3], *Keisuke Suzuki[4] (1.Shinshu University, 2.National Institute of Polar Research, 3.Kokushikan University, 4.Research Center for Mountain Environment, Shinshu University)

11:30 AM - 11:50 AM JST | 2:30 AM - 2:50 AM UTC

[MIS23-10] Long-term Measurements of Atmospheric Aerosol, Cloud and Snow at Mt. Tateyama

★Invited Papers

*Kazuma Aoki[1] (1.University of Toyama)

11:50 AM - 12:10 PM JST | 2:50 AM - 3:10 AM UTC

[MIS23-11] Future projections in snow cover over high mountainous areas in central Japan simulated by non-hydrostatic regional climate model

★Invited Papers

*Hiroaki Kawase[1], Takeshi Yamazaki[2], Shiori Sugimoto[3], Akihiko Murata[1], Masaya Nosaka[1], Hidetaka Sasaki[1] (1.Meteorological Research Institute, Japan Meteorological Agency, 2.Tohoku University, 3.Japan Agency for Marine-Earth Science and Technology)

12:10 PM - 12:15 PM JST | 3:10 AM - 3:15 AM UTC

[MIS23-12] Discussion

Snow depth distribution in the Kamikochi-Azusa River basin in the Northern Japan Alps

*Keisuke Suzuki[1], Akihiko Sasaki[2]

1. Research Center for Mountain Environment, Shinshu University, 2. Kokushikan University

In the Northern Japan Alps region, large amounts of precipitation in the form of snow constitute a more important water resource than rain. During the winter, precipitation that is deposited as snowfall accumulates in the river basins, and it forms natural dams known as “white dams.” A quantitative understanding of snow depth distribution in these mountainous areas is important not only for evaluating water resource volume, but also for understanding the effects of snow in terms of its impact on landforms and its effect on the distribution of vegetation. We report the distribution of snow depth in the Kamikochi-Azusa River basin in the Northern Japan Alps.

Keywords: water resource

©2021. Japan Geoscience Union. All Right Reserved.

Snow depth distribution of Mt. Norikura in the Northern Japan Alps

Rui Tanaka[1], Motoshi Nishimura[2], Akihiko Sasaki[3], *Keisuke Suzuki[4]

1. Shinshu University, 2. National Institute of Polar Research, 3. Kokushikan University, 4. Research Center for Mountain Environment, Shinshu University

It is considered that the snow depth is larger on the leeward slope than on the windward slope. This is due to the effect of the snow being blown off from the windward side and the snowdrift on the leeward side. In this study, we discuss the difference in snow depth between the western and eastern slopes of Mt. Norikura in the Northern Japan Alps.

Keywords: winter type pressure distribution, leeward slope, south coast cyclone

©2021. Japan Geoscience Union. All Right Reserved.

Cold air pool formed in Kamikochi, Northern Japan Alps

Sari Koyama[1], Motoshi Nishimura[2], Akihiko Sasaki[3], *Keisuke Suzuki[4]

1. Shinshu University, 2. National Institute of Polar Research, 3. Kokushikan University, 4. Research Center for Mountain Environment, Shinshu University

At night when it is quiet and cloudless, radiative cooling forms a temperature inversion layer near the ground surface. The temperature inversion layer in the terrain such as basins and deep valleys is called a cold air pool. There are still many unexplained issues between the formation process of cold air pool and meteorological conditions. In this study, we discuss the meteorological conditions under which the patterns of each cold air pool are formed for the cold ait pool that are frequently formed in Kamikochi, Northern Japan Alps, which has deep valley topography.

Keywords: radiative cooling, travelling anticyclone, temperature inversion layer

©2021. Japan Geoscience Union. All Right Reserved.

Long-term Measurements of Atmospheric Aerosol, Cloud and Snow at Mt. Tateyama

*Kazuma Aoki[1]

1. University of Toyama

The aerosol, cloud and snow play an important role in the earth environment at high mountain region (Aoki and Watanabe, 2009). Especially, it is important in the free troposphere, that the aerosol particles are very low. However, our mountain observation sites has shown that large quantities of anthropogenic aerosols, Asian dust, and Siberia forest fire from the Asian continent are transported through the source region to the Mt.Tateyama region. We were studied at the Mt.Tateyama areas, Tateyama Research Laboratory (University of Toyama Mountain observatory) located on top of the Mt.Jodo, Toyama, Japan (36.57˚N, 137.61˚E, 2839 m asl.) and at the Murododaira, Toyama, Japan (36.58˚N, 137.60˚E, 2450 m asl.). Mt. Tateyama, the Northern Japan Alps, is located in southeastern Toyama Prefecture, near the Toyama bay on the coast of Sea of Japan. Horizontal distance is about 30 km from Mountain to Sea. We conducted the measurements of weather, remote sensing of aerosol and cloud, the analysis of snow layer sampled and so on. Furthermore, we measured weather and the aerosol optical properties by using sky radiometer in the city of Toyama (Aoki et al., 2013), our University on the top of roof (36.70˚N, 137.19˚E, 30 m asl.). We started the long-term monitoring of snow layer from Murododaira since 1970’s every mid of April (This season is the maximum snow depth, about six or seven meter every year). The plied snow layers exhibit the chronology of transport and deposition of atmosphere during autumn to spring. It was found that the physical and chemical properties of snow (e.g. Aoki and Watanabe, 2009, Mochizuki et al., 2016, Hayakawa et al., 2019), bio-aerosols (e.g. Maki et al., 2018) and simulation of snow amounts (Kawase et al., 2018). Furthermore, we measured the aerosol optical properties by using sky radiometer at Mt.Jodo and University of Toyama (vertical distance is about 3000 m.). The aerosol optical properties have a significant vertical characteristic. We provide the information, in the presentation, on the mountain science with respect to their temporal and spatial variability of aerosol, cloud and snow on the Mt.Tateyama areas.

Keywords: High mountain atmospheric research, Tateyama, Aerosol, Cloud, Snow, Earth environment

©2021. Japan Geoscience Union. All Right Reserved.

Future projections in snow cover over high mountainous areas in central Japan simulated by non-hydrostatic regional climate model

*Hiroaki Kawase[1], Takeshi Yamazaki[2], Shiori Sugimoto[3], Akihiko Murata[1], Masaya Nosaka[1], Hidetaka Sasaki[1]

1. Meteorological Research Institute, Japan Meteorological Agency, 2. Tohoku University, 3. Japan Agency for Marine-Earth Science and Technology

We investigate the future changes in snow cover and snowfall in Japan using a high-resolution non-hydrostatic regional climate model (NHRCM) with 5 km and 1 km grid spacings. Boundary conditions of NHRCM are derived from future climate projections conducted by the Meteorological Research Institute Atmospheric General Circulation Model (MRI-AGCM60) and the database for Policy Decision making for Future climate change (d4PDF). Experiments with 1 km grid spacing are performed focusing on heavy and light snow-cover years over the mountainous areas in central Japan under present and future climates.
Total snowfall will decrease due to global warming in most parts of Japan, while the mid-winter snowfall will increase in Hokkaido, the northern part of Japan. In the mountainous areas in central Japan, monthly maximum daily snowfall will increase due to global warming. In the years with heavy snow cover under the 4 K warming climate, the mid-winter snowfall is enhanced over 2,000 m above sea level (mASL) in the Japan’ s Northern Alps. On the other hand, at low elevations below 500 mASL, snowfall decreases. In contract, remarkable reductions in snow cover and snowfall are projected in years with light snow cover even over 2,000 mASL in the Japan’ s Northern Alps. Our results indicate that global warming can increase and decrease the mid-winter snowfall in extremely heavy and light snow-cover years, respectively, at high elevations of Japan’ s Northern Alps.

Keywords: Chubu Mountains, Snowfall and snow cover, global warming, regional climate change, high-resolution regional climate model

©2021. Japan Geoscience Union. All Right Reserved.

[J] Oral | M (Multidisciplinary and Interdisciplinary) | M-IS Intersection

[M-IS23] Mountain Science

convener:Keisuke Suzuki(Research Center for Mountain Environment, Shinshu University), Yoshihiko Kariya(Department of Environmental Geography, Senshu University), Akihiko SASAKI(Department of Geography and Environmental Studies, Kokushikan University), Chiyuki Narama(Niigata University, Program of Field Research in the Environmental Sciences), Chairperson:Motoshi NISHIMURA(Arctic Environmental Research Center, National Institute of Polar Research)
Fri. Jun 4, 2021 10:45 AM - 12:15 PM Ch.13 (Zoom Room 13)
Mountainous areas provide water resources to the populated downstream areas, protecting the diversity of ecosystem and providing tourism attraction. To access the mountain environment changes and mitigate the impacts of global warming influences, a cross-cutting session is proposed to share the scientific knowledge among various fields; such as climatology, hydrology, geomorphology, glaciology, water/carbon/material cycle, eco-diversity, etc.

12:10 PM - 12:15 PM

[MIS23-12]Discussion

©Japan Geoscience Union

[J] Oral | M (Multidisciplinary and Interdisciplinary)：M-IS Intersection

Fri. Jun 4, 2021 1:45 PM - 3:15 PM JST | Fri. Jun 4, 2021 4:45 AM - 6:15 AM UTC | Ch.13 Zoom Room 13

[M-IS23] Mountain Science

convener:Keisuke Suzuki(Research Center for Mountain Environment, Shinshu University), Yoshihiko Kariya(Department of Environmental Geography, Senshu University), Akihiko SASAKI(Department of Geography and Environmental Studies, Kokushikan University), Chiyuki Narama(Niigata University, Program of Field Research in the Environmental Sciences), Chairperson:Asaka Konno(Tokoha University)

Mountainous areas provide water resources to the populated downstream areas, protecting the diversity of ecosystem and providing tourism attraction. To access the mountain environment changes and mitigate the impacts of global warming influences, a cross-cutting session is proposed to share the scientific knowledge among various fields; such as climatology, hydrology, geomorphology, glaciology, water/carbon/material cycle, eco-diversity, etc.

1:45 PM - 2:00 PM JST | 4:45 AM - 5:00 AM UTC

[MIS23-13] An automated method for drawing land cover maps from time-lapse photographs of alpine landscapes

*Ryotaro Okamoto[1], Hiroyuki Oguma[2], Reiko Ide[2] (1.University of Tsukuba, 2.National Institute for Environmental Studies)

2:00 PM - 2:20 PM JST | 5:00 AM - 5:20 AM UTC

[MIS23-14] The role of mountains in the creation of biodiversity

★Invited Papers

*Tomoya Suzuki[1], Koji Tojo[1,2] (1.Faculty of Science, Shinshu University, 2.Institute of Mountain Science, Shinshu University)

2:20 PM - 2:35 PM JST | 5:20 AM - 5:35 AM UTC

[MIS23-15] Comparison of hypotheses about formation of the pseudo-alpine zone in accordance with topo-climatological survey

*Shiho Maniwa[1], Atsushi Ikeda[1] (1.University of Tsukuba)

2:35 PM - 2:55 PM JST | 5:35 AM - 5:55 AM UTC

[MIS23-16] Expanding process of *Abies mariesii* woodland from pollen records since the early Holocene at the Komatsubara peat bogs, Mt. Naeba, central Japan

★Invited Papers

*Akihiro Yoshida[1], Arata Momohara[2], Yuichiro Kudo[3], Yasuhiro Taniguchi[4] (1.Kagoshima Univ., 2.Chiba Univ., 3.Gakushuin Women's College, 4.Kokugakuin Univ.)

2:55 PM - 3:15 PM JST | 5:55 AM - 6:15 AM UTC

[MIS23-17] The formation of mountain landscape in the headwaters area of the Yodo river : A case study of Large Old-growth Japanese Horse-chestnut Forest

★Invited Papers

*Koki Teshirogi[1] (1.Setsunan University)

An automated method for drawing land cover maps from time-lapse photographs of alpine landscapes

*Ryotaro Okamoto[1], Hiroyuki Oguma[2], Reiko Ide[2]

1. University of Tsukuba, 2. National Institute for Environmental Studies

Alpine ecosystems are one of the most vulnerable ecosystems to the recent climate changes. Some studies have already reported on-going changes in physiological (e.g., Glaciers, Snow-melting) and biological (e.g., Species distributions, Phenology) environments. Over-time monitoring of alpine ecosystems is required to detect their changes against climate change to define the conservation plans. We have conducted 10-years long monitoring of Japanese alpine ecosystems using automated time-lapse cameras. This study aims to clarify the space-time distributions of such as vegetation and snow cover by developing a set of open-source software. It has two steps, 1. semantic segmentation of time-lapse photographs with semi-supervised deep learning, 2. georectification of segmentation results. The developed software will be published as open-source tools to expand alpine ecosystems' monitoring network using time-lapse cameras. In the session, we will explain the overview and future applications of it.

Keywords: Remote-sensing, Deep Leaning, Alpine Area

©2021. Japan Geoscience Union. All Right Reserved.

The role of mountains in the creation of biodiversity

*Tomoya Suzuki[1], Koji Tojo[1,2]

1. Faculty of Science, Shinshu University, 2. Institute of Mountain Science, Shinshu University

Elucidation of the creation process of biodiversity is one of the most important tasks in biology. The mountain region is one of the suitable fields for elucidating the factors contributing to the creation of biodiversity. Because many organisms which are adapted to severe mountain environments (e.g., low temperature, strong winds, and strong ultraviolet rays), are distributed in mountainous regions. In particular, organisms which are exclusively adapted to alpine zones are not capable of migration via low elevation areas. Because of such a situation, there are some cases in which similar adaptation within alpine zone environments occurs in seperate mountainous areas independently. We have studied such a case using the scorpionfly *Panorpodes paradoxa* (Mecoptera, Panorpodidae), which are distributed from the mountain zone to the alpine zone. In this species, it is reported that the short-winged type female (i.e., alpine type) is observable in the alpine to the subalpine zone, and the long-winged type (i.e., general type) is observable in the elevational region blow the alpine type's distribution range. In addition, it has been suggested that these two types constitute distinct species. From the above situation, we conducted molecular phylogenetic analyses using mtDNA and nDNA data sets from the Japanese *Panorpodes* species in order to estimate their evolutionary history. The molecular phylogenetic analyses' results suggested that the parallel evolution of the alpine type from the general type occurred at least two times independently in different mountain regions. Therefore, our results indicate that the alpine type is an "ecomorph", which adapted to the high elevation region environment. As mentioned above, mountains are an important environment in that they promote the adaptive radiation of organisms. In addition, mountains have one more important function in the creation of biodiversity, their function as geographic barriers. There are some cases in which a population of organisms which are distributed in low elevation regions, become divided by the formation of high elevation mountains. Thereby, the gene flow between the resulting divided populations is restricted, thereby promoting genetic differentiation between the populations. From this viewpoint, we focused on two East Asian giant water bugs, *Appasus japonicus* and *Appasus major* (Heteroptera, Belostomatidae), and conducted their molecular phylogenetic analyses. They are distributed in lowland lentic habitats, and it is considered that mountains act as a geographic barrier between them. As a result, *A. japonicus*and *A. major* were divided into two and three genetic lineages in the Japanese Archipelago respectively. And the boundary regions between their separated genetic lineages are the Chugoku Mountains for *A. japonicus*, and the Ou Mountains and the Central Mountainous Area of Japan for *A. major*. Furthermore, we conducted fine-scale molecular phylogenetic analyses in the boundary regions of each genetic lineage. Thereby we found a secondary contact zone between the primary differentiated genetic lineages in the Sanyo region (Hiroshima and Yamaguchi Prefectures) for *A. japonicus*, and also their secondary contact zones in Aomori, Niigata and Fukushima Prefectures for *A. major*. It is considered that these instances of secondary contact of previously differentiated genetic lineages are very important events for the creation and preservation of the genetic diversity of organisms. Our results of the molecular phylogenetic analyses of these two East Asian giant water bugs suggested that mountains have had a very important function in the creation and preservation of intra-specific genetic diversity. In conclusion, our study indicated that mountain areas are critical environments being deeply related to the creation of various levels of biodiversity.

Keywords: Phylogeography, Biodiversity, Genetic diversity

©2021. Japan Geoscience Union. All Right Reserved.

©2021. Japan Geoscience Union. All Right Reserved.

Comparison of hypotheses about formation of the pseudo-alpine zone in accordance with topo-climatological survey

*Shiho Maniwa[1], Atsushi Ikeda[1]

1. University of Tsukuba

On some mountains from central to northeastern Japan, the subalpine area is mostly covered with grass, dwarf bamboo or shrubs instead of conifers. This area called a pseudo-alpine zone was firstly thought to develop because large snow pressure prevents coniferous trees growing in the mountains with heavy snowfall (snow hypothesis). Historical perspectives later added two popular hypotheses. Warmer climate in the early Holocene may have shifted the lower limit of the subalpine zone above the summits (kick-out hypothesis). Scarcity of *Abies mariesii* habitats under former climate has been possibly succeeded by the present pseudo-alpine zone (limited *Abies mariesii* hypothesis). This study tests these three hypotheses using digital geographic data which were recently provided.
Some topo-climatological conditions under the subalpine climate on 34 mountains in the Tohoku to Chubu regions were studied to know habitat segregation. On a GIS software, habitats including *Abies mariesii* were extracted from digital vegetation maps provided by the Ministry of Environments in Japan and the occupancy of these habitats were determined for each mountain. Then, altitudinal ranges, slope angles and the annual maximums of snow thickness were compared respectively to discuss differences between mountains having the pseudo-alpine zone and the other mountains.
In 3 mountains without thick snow cover, *Abies veitchii - Abies mariesii* community accounts for more than 30% of the total area. On the other hand, *Abies mariesii* community accounts for more than 30% of the total area in 9 mountains. Some of the latter mountains are covered with thick snow, whereas some mountains lack coniferous forests despite less snowfall. These cases are inconsistent with the snow hypothesis. The absence of *Abies mariesii* on some high mountains cannot be explained from the kick-out hypothesis. The mountains dominated by *Abies mariesii* community are considerably gentler than the other mountains, which corresponds to the limited *Abies mariesii* hypothesis. According to the hypothesis, the poorly drained gentle slopes provide the niche of *Abies mariesii* until the early Holocene before *Abies mariesii* becoming dominant.

Keywords: pseudo-alpine zone, mountains with heavy snowfall, Abies mariesii, GIS, historical botany

©2021. Japan Geoscience Union. All Right Reserved.

Expanding process of *Abies mariesii* woodland from pollen records since the early Holocene at the Komatsubara peat bogs, Mt. Naeba, central Japan

*Akihiro Yoshida[1], Arata Momohara[2], Yuichiro Kudo[3], Yasuhiro Taniguchi[4]

1. Kagoshima Univ., 2. Chiba Univ., 3. Gakushuin Women's College, 4. Kokugakuin Univ.

Our reconstruction of vegetation changes from the well-dated pollen records since the early Holocene at Komatsubara peat bogs, Mt. Naeba, advanced our understanding vegetation history on the sub-alpine zone. The pollen records from the Shimo-no-shiro (1,330m a. s. l.) and Kami-no-shiro (1,570m a. s. l.) peat bogs indicate that *Abies* pollen appeared continuously from ca. 5,000-4,500 cal BP, at least. Additionally, our spatio-temporal comparison of pollen records from different altitude sites on Mt. Naeba shows that the distribution of *Abies mariesii* moved gradually to a higher altitude from the middle Holocene to the present. It is highly possible that the geomorphological environment and soil development on the alpine area influenced the colonization of *Abies mariesii*.

Keywords: Pollen analysis, Abies pollen, Subalpine conifer woodland, Mt. Naeba, Central Japan , Holocene

©2021. Japan Geoscience Union. All Right Reserved.

The formation of mountain landscape in the headwaters area of the Yodo river : A case study of Large Old-growth Japanese Horse-chestnut Forest

*Koki Teshirogi[1]

1. Setsunan University

There are many large old-growth Japanese horse-chestnut (*Aesculus turbinata*) growing in the Kutsuki region, Shiga Prefecture, central Japan whose diameter at breast height (DBH) is ≧1 m. Large old-growth trees are ecologically important as keystone structures in forests as they provide valuable habitat for many animal and plant species. In recent years, however, large old-growth trees have rapidly declined in many places around the world. In this study, we examine the characteristics of the growth environments of large old-growth Japanese horse-chestnut, and analyse the natural and social factors related to the establishment of these trees in a catchment area in the Kutsuki region. In our field survey, 230 Japanese horse-chestnut individuals including young trees were identified in the riparian zone, and 47 individuals (20%) were large old-growth trees. These old-growth trees were mostly located in the upper parts of the catchment area, and partly on the knick line of the side slope and upper part of the head hollow zone compared with the location of the small- and middle-class individuals of <1 m DBH. Additionally, we found that most of them were distributed along belts of 15–20 m height above the riverbed and that the smaller individuals tended to grow in the lower zone. These results show that the large old-growth trees probably established under more stable geomorphological conditions with fewer topographical disturbances. Additionally, intensive use of deciduous broad-leaved forest in the Kutsuki region has taken place throughout history, such as periodic gathering of wood for firewood and charcoal production, and branches for fertiliser for rice cultivation. However, the Japanese horse-chestnut trees were unsuitable for these purposes. It was also strictly prohibited to cut them under the customary law of the local government during the Edo Period. Also, local inhabitants collected the nuts for consumption to mix into rice cake. Considering the social aspects, the large old-growth Japanese horse-chestnut trees have been maintained in the region under satoyama conditions, and by the selective conservation policies of the local government and local inhabitants. We conclude that the large old-growth Japanese horse-chestnut forest established under a combination of relatively stable geomorphological conditions in the catchment area, selective conservation, and periodical disturbances of other tree species by local inhabitants.

Keywords: Aesculus turbinata, Mountainous riparian forest, Forest use

©2021. Japan Geoscience Union. All Right Reserved.

[J] Oral | M (Multidisciplinary and Interdisciplinary)：M-GI General Geosciences, Information Geosciences & Simulations

Fri. Jun 4, 2021 9:00 AM - 10:30 AM JST | Fri. Jun 4, 2021 12:00 AM - 1:30 AM UTC | Ch.03 Zoom Room 03

[M-GI35] Computational sciences on the universe, galaxies, stars, planets, and their environments

convener:Yoshi-Yuki Hayashi(Department of Planetology/CPS, Graduate School of Science, Kobe University), Junichiro Makino(Kobe University), Kanya Kusano(Institute for Space-Earth Environmental Research, Nagoya University), Shigeru Ida(Earth-Life Science Institute, Tokyo Institute of Technology), Chairperson:Junichiro Makino(Kobe University), Yoshi-Yuki Hayashi(Department of Planetology/CPS, Graduate School of Science, Kobe University), Kanya Kusano(Institute for Space-Earth Environmental Research, Nagoya University), Eiichiro Kokubo(Division of Science, National Astronomical Observatory of Japan), Takayuki Saitoh(Kobe university)

Computer simulations have been recognized as one of the fundamental tools in understanding not only planetary formation, evolution and diversity of surface environment, but also the structure formation of the universe and its possible evolutions. However, it may be notified that the continuous development of computational abilities in recent years does not seem to be well utilized in improving numerical simulations in those fields; computational efficiency has been improved by 6 orders of magnitude compared from the early 90's, many of our simulations do not seem to catch up qualitatively and quantitatively such improvement. We propose here in this session, with the support of the MEXT program for promoting researches on the supercomputer Fugaku, to ask those who are interested in computational sciences of various fields not only of planetary formation and evolution but of earth, planetary and astrophysical sciences in general to join. The aim is to discuss various scientific and technical aspects of our numerical simulations to improve our skills to fully utilize those development of computational resources that has been exemplified by "Fugaku".

9:00 AM - 9:15 AM JST | 12:00 AM - 12:15 AM UTC

[MGI35-01] Development of a non-hydrostatic global model of the Venus atmosphere: A simplified Venus simulation

*Hiroki Kashimura[1], Hisashi Yashiro[2], Seiya Nishizawa[3], Hirofumi Tomita[3], Masahiro Takagi[4], Norihiko Sugimoto[5], Kazunori Ogohara[4], Takeshi Kuroda[6], Kensuke Nakajima[7], Masaki Ishiwatari[8], Yoshiyuki O. Takahashi[1], Yoshi-Yuki Hayashi[1] (1.Department of Planetology, Graduate School of Science, Kobe University, 2.Center for Global Environmental Research, National Institute for Environmental Studies, 3.RIKEN Center for Computational Science, 4.Faculty of Science, Kyoto Sangyo University, 5.Department of Physics, Keio University, 6.Department of Geophysics Tohoku University, 7.Department of Earth and Planetary Sciences, Flculty of Sciences, Kyushu University, 8.Department of Cosmosciences, Graduate school of Science, Hokkaido University)

9:15 AM - 9:30 AM JST | 12:15 AM - 12:30 AM UTC

[MGI35-02] MHD simulations of solar flares associated with sunspot formation and evolution

*Takafumi Kaneko[1], Hideyuki Hotta[2], Kanya Kusano[1] (1.Institute for Space-Earth Environmental Research, Nagoya University, 2.Chiba University)

9:30 AM - 9:45 AM JST | 12:30 AM - 12:45 AM UTC

[MGI35-03] A large-eddy simulation of atmospheric boundary layer turbulence using the discontinuous Galerkin method

*Yuta Kawai[1], Hirofumi Tomita[1] (1.RIKEN Center for Computational Science)

9:45 AM - 10:00 AM JST | 12:45 AM - 1:00 AM UTC

[MGI35-04] Semi-analytic modeling of galaxies and AGN in the Fugaku era

*Taira Oogi[1], Hikari Shirakata[2], Masahiro Nagashima[3], Takahiro Nishimichi[4], Toshihiro Kawaguchi[5], Takashi Okamoto[6], Tomoaki Ishiyama[1], Motohiro Enoki[7] (1.Chiba University, 2.Tadano Ltd., 3.Bunkyo

University, 4.Yukawa Institute for Theoretical Physics, Kyoto University, 5.Onomichi City University, 6.Hokkaido University, 7.Tokyo Keizai University)

10:00 AM - 10:15 AM JST | 1:00 AM - 1:15 AM UTC

[MGI35-05] Numerical study of the origin of merging binary black holes

*Ataru Tanikawa[1], Michiko S. Fujii[1], Jun Kumamoto[1], Long Wang[1], Alessandro Alberto Trani[1] (1.The University of Tokyo)

10:15 AM - 10:30 AM JST | 1:15 AM - 1:30 AM UTC

[MGI35-06] Discussion

Development of a non-hydrostatic global model of the Venus atmosphere: A simplified Venus simulation

*Hiroki Kashimura[1], Hisashi Yashiro[2], Seiya Nishizawa[3], Hirofumi Tomita[3], Masahiro Takagi[4], Norihiko Sugimoto[5], Kazunori Ogohara[4], Takeshi Kuroda[6], Kensuke Nakajima[7], Masaki Ishiwatari[8], Yoshiyuki O. Takahashi[1], Yoshi-Yuki Hayashi[1]

1. Department of Planetology, Graduate School of Science, Kobe University, 2. Center for Global Environmental Research, National Institute for Environmental Studies, 3. RIKEN Center for Computational Science, 4. Faculty of Science, Kyoto Sangyo University, 5. Department of Physics, Keio University, 6. Department of Geophysics Tohoku University, 7. Department of Earth and Planetary Sciences, Flculty of Sciences, Kyushu University, 8. Department of Cosmosciences, Graduate school of Science, Hokkaido University

Venus is fully covered by thick clouds of sulfuric acid, and its atmospheric circulation and inherent phenomena are not well understood. However, recent observations by the Venus Climate Orbiter/Akatsuki have revealed a variety of atmospheric phenomena from the planetary-scale bow-shaped structure (Fukuhara et al., 2017) and streak-structure (Kashimura et al., 2019) to a front-like structure to small-scale vortices and waves of several hundred kilometers (Limaye et al., 2018). There have also been active attempts to reproduce these phenomena using Venusian atmospheric general circulation models and to understand the mechanisms involved. In particular, AFES-Venus (Sugimoto et al., 2014), which was developed based on AFES (Ohfuchi et al., 2004; Enomoto et al., 2008), the atmospheric general circulation model highly optimized for the Earth Simulator, has realized high-resolution simulations of the Venus atmosphere, and the planetary-scale streak-structure, thermal tides, gravity waves, meridional circulations, and other structures have been analyzed (e.g., Kashimura et al., 2019; Takagi et al., 2018; Sugimoto et al., in revision; Takagi et al., in prep.). However, AFES is a hydrostatic model, which is not suitable for phenomena whose horizontal scales are less than several tens of kilometers and cannot explicitly express convections in the cloud layer. The convections in the cloud layer are not only interesting in themselves but are also very important in the Venusian atmosphere because the neutral or low-stability layer resulting from convections is closely related to the formation of the planetary-scale bow-shaped structure and the streak structure. Though non-hydrostatic regional models have been used to study convective activities in the cloud layer and the resulting gravity waves (e.g., Baker et al., 1998; Imamura et al., 2014; Yamamoto 2014, Lefèvre et al., 2017), due to the limitation of the domain size, effects of the convective activities on large-scale phenomena have not been investigated.

Then, we have started developing a non-hydrostatic Venusian atmospheric general circulation model to realize a global simulation of the Venusian atmosphere that explicitly represents convective activities in the cloud layer. We utilize SCALE-GM (http://r-ccs-climate.riken.jp/scale/) for the dynamical core, which determines the coordinate system and calculates atmospheric motions. As a first step in the development, the various planetary and atmospheric constants are changed to Venusian values, and the solar heating and Newtonian cooling functions used in AFES-Venus (Tomasko et al., 1980; Crisp et al., 1986; Sugimoto et al., 2014) are imported to SCALE-GM. We then tried a simplified Venus simulation similar to AFES-Venus in various resolutions to explore the necessary numerical properties such as time-step intervals and strength of the numerical diffusion and the sponge layer. The planetary-scale streak-structure are represented in the same way as in AFES-Venus, in case of the resolution of a horizontal grid spacing of dx ~ 52 km and 120 layers (dz = 1 km) in vertical with a second-order Laplacian for the horizontal diffusion whose e-folding time for the minimum scale is 100 s. However, in SCALE-GM, a strong sponge layer that dumps not only the eddies but also the mean flow is necessary for computational

©2021. Japan Geoscience Union. All Right Reserved.

stability. Therefore, the superrotation strength and the angular momentum budget of the atmosphere are influenced by the artificial sponge layer, and we need to seek better ways to keep computational stability. We are attempting to calculate in higher horizontal resolution with 240 vertical layers (dz = 500 m), and we will also present these results.

Keywords: Venus atmosphere, Non-hydrostatic global model, high-resolution simulation

©2021. Japan Geoscience Union. All Right Reserved.

MHD simulations of solar flares associated with sunspot formation and evolution

*Takafumi Kaneko[1], Hideyuki Hotta[2], Kanya Kusano[1]

1. Institute for Space-Earth Environmental Research, Nagoya University, 2. Chiba University

Solar flares and coronal mass ejections (CMEs) are caused by a release of magnetic energy in the solar atmosphere. Large flares and CMEs have a potential impact on modern society depending on technologies. Superflares and CMEs have also been found in the other Sun-like stars, suggesting an impact on the habitability of exoplanets. It is important for space weather and stellar physics to reveal how large energy can be released by a single flare or CME. The sun is the only star that we can observe the photospheric magnetic fields and various kinds of magnetic activities in detail.
To estimate the possible energy release, we need to comprehend the evolution of magnetic fields from the solar interior (convection zone) to the upper plasma atmosphere (corona). In the observations, large flares are likely to occur in delta spots (one type of sunspots). Recent radiative MHD simulations revealed that the delta spots can be formed when the magnetic fluxes are transported from much deeper convection zone to the photosphere. The remained issue is to reveal the reason why the delta spots tend to cause large flares in the corona.
In this study, we investigated the evolution of coronal magnetic fields using zero-beta MHD simulations. We introduced the numerical data of the delta spot simulation into bottom boundary of the corona simulation. As a result, a large flare corresponding to M-class in the observations was reproduced. We also performed parameter survey on the ratio between toroidal and poloidal components of the initial flux ropes in the convection zone and spatial resolution as well. We found that, in the case of high spatial resolution, the released energy was larger. The onset of flare seemed to be random: we were not able to find out clear relationship between the tested parameters and the onset of flares. This result might be due to randomness of the turbulent flows in the photosphere. We need to perform further parameter surveys covering a sufficiently broad range of parameters to take ensemble.

Keywords: sunspots, flares, magnetohydrodynamic simulation

©2021. Japan Geoscience Union. All Right Reserved.

A large-eddy simulation of atmospheric boundary layer turbulence using the discontinuous Galerkin method

*Yuta Kawai[1], Hirofumi Tomita[1]

1. RIKEN Center for Computational Science

1. Introduction

Recently, spatial resolution of global atmospheric models has been approaching the spatial scales targeted in large-eddy simulations (LES). One of the challenges toward global LES is the numerical accuracy of the dynamical process. Focusing on the atmospheric boundary layer, Kawai and Tomita (2020) discussed the order of accuracy required for discretization errors of the advection terms not to dominate the eddy viscosity term by the turbulence model in the framework of the finite difference method (FDM). The derived criteria suggest that at least seventh- or eighth-order accuracy is required. The next issues are to verify the effect of increasing numerical accuracy of all terms, and to attempt the dynamics-physics coupling considered the effective resolution of the dynamics. In addition, we need to explore numerical schemes providing the accurate representation of the physical field and highly computational efficiency when considering large-scale parallel computers. The discontinuous Galerkin method (DGM) may be useful for these issues. The strategy of high-order discretization is straightforward and compact. In terms of the dynamics-physics coupling, many degrees of freedom within the element may give us some knowledges for utilizing accurate dynamical fields to calculate the physical processes. In this study, to investigate the applicability of DGM to global LES, we constructed a limited-area atmospheric LES model using DGM, and conducted numerical experiments. Here, we present the preliminary results.

2. LES of atmospheric boundary layer turbulence using DGM

2.1 Numerical method

The governing equations of dynamics is the fully compressible equations, and the turbulent process is represented by a Smagorinsky-Lilly type model (e.g., Brown et al., 1994). The spatial discretization is based on the nodal DGM (e.g., Hesthaven & Warburton, 2008). To archive the eight-th order accuracy in terms of truncation errors, we use the hexahedral finite element with 8^3 nodes. As the numerical flux, we adopt the Rusanov flux for inviscid terms and the central flux for eddy viscous terms. As the spatial filter in LES, we use the16th-order elementwise modal filter with the exponential form. This filter rapidly removes the fluid structure whose wavelength is near two-grids. For this case, although the definition of spatial filter length seems to be not obvious, here we consider the filter length is essentially located between two- and four-grids.

2.2 Experimental setup

We conduct numerical experiments of idealized atmospheric boundary layer turbulence based on Nishizawa et al. (2015). The domain size is 9.6x9.6x3 km^3. Initially, the horizontal wind is 5m/s, and the perturbation of potential temperature is added into stably stratified atmosphere. The constant heat flux with 200 W/m^2 is injected at the surface. We perform the integration over four hours. The size of finite element is set to 200 m, which means the corresponding grid size in FDM (Δx) is approximately 30 m. To obtain the knowledge of the dynamic-physics coupling in DGM, we investigate how sensitive is the intensity of the modal filter (represented by the decay time for maximum wavenumber, T_{nd}) and the spatial filter length for turbulent model (Δ_{sgs}) to the energy spectra. We set these parameters such that $T_{nd}/\Delta t \sim 0.1, 10, 100$ (where Δt is the time step), and $\Delta_{sgs}/\Delta x = 1, 2, 4$. Here, we regard the case of $T_{nd}/\Delta t \sim 10$

©2021. Japan Geoscience Union. All Right Reserved.

and $\Delta_{sgs}/\Delta x=2$ as the control experiment.

2.3 Results

We show the energy spectra of three-dimensional winds in the figure. For comparison, the results of SCALE-RM using the conservative FDM are also shown by gray lines. The slope for the control experiment becomes steeper than that of the -5/3 power law at wavelengths shorter than 200 m. Over the wavelength between 500 m and 200 m, the spectra for the control experiment and the stronger modal filter case has a little shallower slope than that of the -5/3 power law. This indicates the accumulation of energy. The sensitivity of the spatial filter length is higher than that of the modal filter’ s intensity. In terms of the dynamics-physics coupling considering the effective resolution of dynamics, we expected that $\Delta_{sgs}/\Delta x=4$ would be appropriate in this experiment, however the actual spectra for $\Delta_{sgs}/\Delta x=4$ show too strong dissipation and deviate significantly from the -5/3 power law. To consider the reasons for the above results, we will revisit the formulation of LES in DGM. We will also conduct additional experiments with the higher resolution to make precise discussion, because the resolved inertial subrange is slightly narrow.

Keywords: atmospheric boundary layer, large eddy simulation, high-order numerical scheme

©2021. Japan Geoscience Union. All Right Reserved.

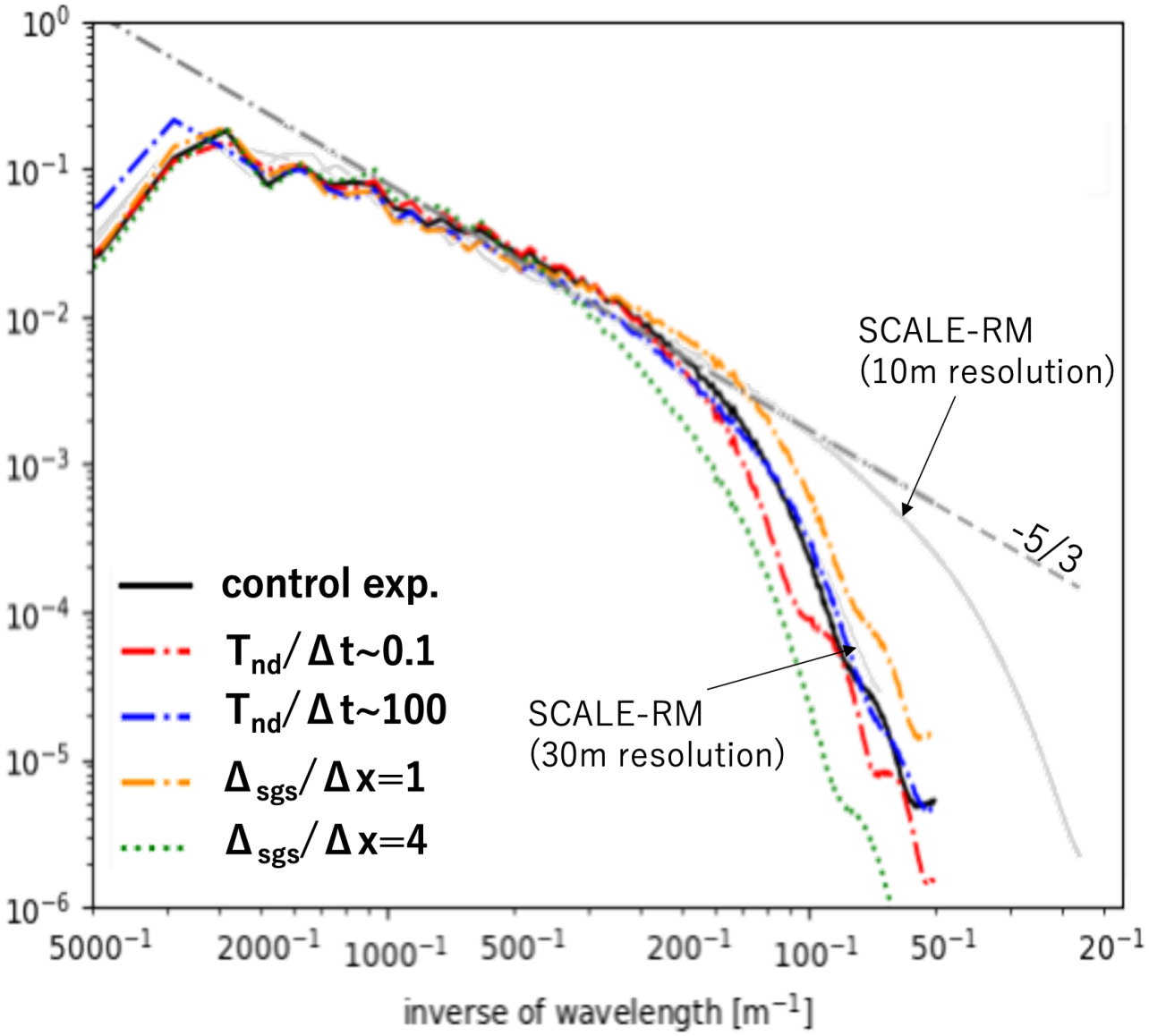


Figure: Energy spectra of three-dimensional winds (at z=500 m) obtained from LES of atmospheric boundary layer turbulence using DGM.

©2021. Japan Geoscience Union. All Right Reserved.

Semi-analytic modeling of galaxies and AGN in the Fugaku era

*Taira Oogi[1], Hikari Shirakata[2], Masahiro Nagashima[3], Takahiro Nishimichi[4], Toshihiro Kawaguchi[5], Takashi Okamoto[6], Tomoaki Ishiyama[1], Motohiro Enoki[7]

1. Chiba University, 2. Tadano Ltd., 3. Bunkyo University, 4. Yukawa Institute for Theoretical Physics, Kyoto University, 5. Onomichi City University, 6. Hokkaido University, 7. Tokyo Keizai University

We present an updated version of our semi-analytic galaxy and AGN formation model, the New Numerical Galaxy Catalog, nu^{2}GC.
The major update of the model is the merger trees of dark matter halos.
We construct the halo merger trees using an ultralarge cosmological N-body simulation, named Uchuu, which consists of 262 billion particles in a box of 2 Gpc/h.
The unprecedentedly large and high-resolution simulation allows us accurate determination of measurements of rare objects, such as autocorrelation functions of AGNs.
We show the basic statistical properties of galaxies and AGNs in our model, focusing on the spacial clustering of them.
The model prediction indicates that the time-scale of gas accretion on to the supermassive black holes plays a significant role in allowing massive halos to host relatively faint population of AGNs.
We find that the shape of the predicted AGN correlation function shows remarkable agreement with those from observations.

Keywords: Galaxies, Active Galactic Nuclei, Large Scale Structure of the Universe, Cosmological N-body simulation

©2021. Japan Geoscience Union. All Right Reserved.

Numerical study of the origin of merging binary black holes

*Ataru Tanikawa[1], Michiko S. Fujii[1], Jun Kumamoto[1], Long Wang[1], Alessandro Alberto Trani[1]

1. The University of Tokyo

Gravitational wave (GW) observatories have discovered many mergers of black holes (BHs) for these several years. Their origins have been highly uncertain, and many formation scenarios have been suggested: isolated binary evolution from population I, II and III stars, dynamical capture in open clusters, globular clusters, and nuclear star clusters, and so on. In order to elucidate their origins, we need to compare properties of observed binary BHs with those of theoretically predicted binary BHs. Such properties can be merger rate, primary mass distribution, mass ratio distribution, spin magnitude distribution, spin-orbit misalignment distribution, eccentricity distribution, redshift distribution, and so on. Numerical simulations are powerful tools to investigate properties of binary BHs theoretically. We have investigated binary BHs formed through isolated binary evolution and dynamical capture.

Binary population synthesis (BPS) calculations are commonly used to predict properties of binary BHs. In BPS calculations, we prepare initial conditions of binary stars: binary component masses, semi-major axes, and eccentricities. Each star evolves from zero-age main-sequence stars to stellar remnants like BHs. When either of stars fill their Roche lobes, mass transfer or stellar merger set in. We have made stellar evolution tracks of population II and III stars for the BPS calculations (Tanikawa et al. 2020, MNRAS, 495, 4170). Using the stellar evolution tracks, we have revealed properties of binary BHs formed from population III stars. We have found that their merger rate is 100 times smaller than the observed rate (Tanikawa et al. 2020, arXiv:2008.01890). However, we have made clear that GW190521 can be formed from population III stars (Tanikawa et al. 2020, arXiv:2010.0716), where GW190521 is thought to be difficult to be formed in isolated binaries.

Binary BHs in star clusters are usually studied with gravitational N-body simulations coupled with BPS calculations. Here, N-body simulations solve stellar dynamics, and BPS calculations follow single and binary star evolutions. Using such simulations and detail three-body simulations, we have predicted merger rate, mass distribution, mass ratio distribution, spin magnitude distribution, and spin-orbit misalignment distribution of binary BHs formed in open clusters. Their merger rate indicates that binary BHs formed in open clusters can be one of major components of observed binary BHs (Kumamoto et al. 2019, MNRAS, 486, 3942). Their mass and spin

©2021. Japan Geoscience Union. All Right Reserved.

distributions are also consistent with observed ones' (Kumamoto et al. 2020, MNRAS, 495, 4268; Trani et al. 2021, submitted).

We are now studying binary BHs formed in globular clusters, massive star clusters. Gravitational N-body simulations of globular clusters were impossible, since their calculation costs are extremely high. Recently, a N-body simulation code ``PeTar'' have been developed. The PeTar code calculates gravitational forces between all pairs of stars, reducing their calculation costs with the Barnes-Hut tree algorithm. Moreover, the PeTar code works well on massively parallel computing environment. The PeTar code enables us to perform gravitational N-body simulations of realistically massive and dense globular clusters. Using the PeTar code, we have shown that a top-heavy initial mass function does not always increase a merger rate of binary BHs formed in globular clusters (Wang et al. 2021, arXiv:2101.09283).

Keywords: Black hole, Binary star, Star cluster, Binary population synthesis, Gravitational N-body simulation

©2021. Japan Geoscience Union. All Right Reserved.

[J] Oral | M (Multidisciplinary and Interdisciplinary) | M-GI General Geosciences, Information Geosciences & Simulations

[M-GI35] Computational sciences on the universe, galaxies, stars, planets, and their environments

convener:Yoshi-Yuki Hayashi(Department of Planetology/CPS, Graduate School of Science, Kobe University), Junichiro Makino(Kobe University), Kanya Kusano(Institute for Space-Earth Environmental Research, Nagoya University), Shigeru Ida(Earth-Life Science Institute, Tokyo Institute of Technology), Chairperson:Junichiro Makino(Kobe University), Yoshi-Yuki Hayashi(Department of Planetology/CPS, Graduate School of Science, Kobe University), Kanya Kusano(Institute for Space-Earth Environmental Research, Nagoya University), Eiichiro Kokubo(Division of Science, National Astronomical Observatory of Japan), Takayuki Saitoh(Kobe university)

Fri. Jun 4, 2021 9:00 AM - 10:30 AM Ch.03 (Zoom Room 03)

Computer simulations have been recognized as one of the fundamental tools in understanding not only planetary formation, evolution and diversity of surface environment, but also the structure formation of the universe and its possible evolutions. However, it may be notified that the continuous development of computational abilities in recent years does not seem to be well utilized in improving numerical simulations in those fields; computational efficiency has been improved by 6 orders of magnitude compared from the early 90's, many of our simulations do not seem to catch up qualitatively and quantitatively such improvement. We propose here in this session, with the support of the MEXT program for promoting researches on the supercomputer Fugaku, to ask those who are interested in computational sciences of various fields not only of planetary formation and evolution but of earth, planetary and astrophysical sciences in general to join. The aim is to discuss various scientific and technical aspects of our numerical simulations to improve our skills to fully utilize those development of computational resources that has been exemplified by "Fugaku".

10:15 AM - 10:30 AM

[MGI35-06]Discussion

©Japan Geoscience Union

[J] Oral | M (Multidisciplinary and Interdisciplinary)：M-GI General Geosciences, Information Geosciences & Simulations

Fri. Jun 4, 2021 10:45 AM - 12:15 PM JST | Fri. Jun 4, 2021 1:45 AM - 3:15 AM UTC | Ch.18 Zoom Room 18

[M-GI35] Computational sciences on the universe, galaxies, stars, planets, and their environments

convener:Yoshi-Yuki Hayashi(Department of Planetology/CPS, Graduate School of Science, Kobe University), Junichiro Makino(Kobe University), Kanya Kusano(Institute for Space-Earth Environmental Research, Nagoya University), Shigeru Ida(Earth-Life Science Institute, Tokyo Institute of Technology), Chairperson:Yoshi-Yuki Hayashi(Department of Planetology/CPS, Graduate School of Science, Kobe University), Kanya Kusano(Institute for Space-Earth Environmental Research, Nagoya University), Junichiro Makino(Kobe University), Eiichiro Kokubo(Division of Science, National Astronomical Observatory of Japan), Takayuki Saitoh(Kobe university)

Computer simulations have been recognized as one of the fundamental tools in understanding not only planetary formation, evolution and diversity of surface environment, but also the structure formation of the universe and its possible evolutions. However, it may be notified that the continuous development of computational abilities in recent years does not seem to be well utilized in improving numerical simulations in those fields; computational efficiency has been improved by 6 orders of magnitude compared from the early 90's, many of our simulations do not seem to catch up qualitatively and quantitatively such improvement. We propose here in this session, with the support of the MEXT program for promoting researches on the supercomputer Fugaku, to ask those who are interested in computational sciences of various fields not only of planetary formation and evolution but of earth, planetary and astrophysical sciences in general to join. The aim is to discuss various scientific and technical aspects of our numerical simulations to improve our skills to fully utilize those development of computational resources that has been exemplified by "Fugaku".

10:45 AM - 11:00 AM JST | 1:45 AM - 2:00 AM UTC

[MGI35-07] Acceleration program for Fugaku output generation: Unified view from cosmology to planets

*Junichiro Makino[1] (1.Kobe University)

11:00 AM - 11:15 AM JST | 2:00 AM - 2:15 AM UTC

[MGI35-08] Discussion

11:15 AM - 11:30 AM JST | 2:15 AM - 2:30 AM UTC

[MGI35-09] High-resolution magnetohydrodynamic simulations of two-temperature jet propagation using code CANS+

*Takumi Ohmura[1], Mami Machida[2], Yosuke Matsumoto[3], Ken Ohsuga[4], Ryoji Matsumoto[3] (1.Kyushu University, 2.National Astronomical Observatory of Japan, 3.Chiba University, 4.University of Tsukuba)

11:30 AM - 11:45 AM JST | 2:30 AM - 2:45 AM UTC

[MGI35-10] Core-Collpase Supernova Simulations by Boltzmann-Hydro Code

*Wakana Iwakami[1], Hirotada Okawa[1], Hiroki Nagakura[2], Akira Harada[3], Ryuichiro Akaho[1], Shun Furusawa[6], Hideo Matsufuru[5], Kosuke Sumiyoshi[4], Shoichi Yamada[1] (1.Waseda University, 2.Princeton University, 3.University of Tokyo, 4.Numazu College of Technology, 5.High Energy Accelerator Research Organization, 6.Tokyo University of Science)

11:45 AM - 12:00 PM JST | 2:45 AM - 3:00 AM UTC

[MGI35-11] Development of N-body Simulation Code for Planetary System Formation: GPLUM

*Yota Ishigaki[1,2], Eiichiro Kokubo[3], Junichiro Makino[4], Masaki Fujimoto[2] (1.University of Tokyo, 2.Institute of Space and Astronautical Science, Japan Aerospace Exploration Agency, 3.National Astronomical Observatory of Japan, 4.Kobe University)

12:00 PM - 12:15 PM JST | 3:00 AM - 3:15 AM UTC

[MGI35-12] Rocky Planetesimal Accretion under a Realistic Accretion Condition

*Takashi Shibata[1], Eiichiro Kokubo[1,2], Junichiro Makino[3], Yota Ishigaki[2] (1.National Astronomical Observatory of Japan, 2.The University of Tokyo, 3.Kobe University)

Acceleration program for Fugaku output generation: Unified view from cosmology to planets

*Junichiro Makino[1]

1. Kobe University

Supercomputer Fugaku was completed in FY2020 and realized the theoretical peak performance of 537 PF in double precision. It is about a factor of 50 times faster than K computer. To make best use of Fugaku, "Acceleration program for Fugaku output generation" has been started. It is a successor for the previous "Social and scientific priority issues to be tackled by using the Post-K computer" and "Exploratory challenge" programs. In the filed of planetary science, one project, "Unified view from cosmology to planets" has been selected and started. In this talk, I'll overview the goal, structure and early results of this project.

Keywords: Computational Science, Supercomputer Fugaku, HPC

©2021. Japan Geoscience Union. All Right Reserved.

[J] Oral | M (Multidisciplinary and Interdisciplinary) | M-GI General Geosciences, Information Geosciences & Simulations

[M-GI35] Computational sciences on the universe, galaxies, stars, planets, and their environments

convener:Yoshi-Yuki Hayashi(Department of Planetology/CPS, Graduate School of Science, Kobe University), Junichiro Makino(Kobe University), Kanya Kusano(Institute for Space-Earth Environmental Research, Nagoya University), Shigeru Ida(Earth-Life Science Institute, Tokyo Institute of Technology), Chairperson:Yoshi-Yuki Hayashi(Department of Planetology/CPS, Graduate School of Science, Kobe University), Kanya Kusano(Institute for Space-Earth Environmental Research, Nagoya University), Junichiro Makino(Kobe University), Eiichiro Kokubo(Division of Science, National Astronomical Observatory of Japan), Takayuki Saitoh(Kobe university)

Fri. Jun 4, 2021 10:45 AM - 12:15 PM Ch.18 (Zoom Room 18)

Computer simulations have been recognized as one of the fundamental tools in understanding not only planetary formation, evolution and diversity of surface environment, but also the structure formation of the universe and its possible evolutions. However, it may be notified that the continuous development of computational abilities in recent years does not seem to be well utilized in improving numerical simulations in those fields; computational efficiency has been improved by 6 orders of magnitude compared from the early 90's, many of our simulations do not seem to catch up qualitatively and quantitatively such improvement. We propose here in this session, with the support of the MEXT program for promoting researches on the supercomputer Fugaku, to ask those who are interested in computational sciences of various fields not only of planetary formation and evolution but of earth, planetary and astrophysical sciences in general to join. The aim is to discuss various scientific and technical aspects of our numerical simulations to improve our skills to fully utilize those development of computational resources that has been exemplified by "Fugaku".

11:00 AM - 11:15 AM

[MGI35-08]Discussion

©Japan Geoscience Union

High-resolution magnetohydrodynamic simulations of two-temperature jet propagation using code CANS+

*Takumi Ohmura[1], Mami Machida[2], Yosuke Matsumoto[3], Ken Ohsuga[4], Ryoji Matsumoto[3]

1. Kyushu University, 2. National Astronomical Observatory of Japan, 3. Chiba University, 4. University of Tsukuba

Jet launched from an active galactic nucleus provides a large amount of energy to the surroundings through shocks and turbulence. As a result, jet-driven turbulence inhibits the growth of the host galaxy by suppressing the mass accretion onto it. Therefore, the jet plays a major role in galactic evolution and the history of the structure formation of the universe. However, the physics of the interaction between the jet and the surrounding environment is still poorly understood.

In this study, we focus on the jet stability. The jet is a magnetized supersonic flow, which is a magnetohydrodynamic (MHD) unstable system because of the velocity shear with the surroundings. In particular, it has been pointed out that the development of the Kelvin-Helmholtz (KH) instability, Rayleigh-Taylor (RT) instability, and current-driven kink instability influence jet dynamics. The nonlinear growth of these instabilities depends not only on the internal structure of the jet itself but also on the surrounding environment. However, since the surrounding environment is determined by the cocoon which is a by-product of a propagating jet, it is finally necessary to solve the jet propagation problem.

On the other hand, the two-temperature nature of the plasma is an important physics in the system of jets and surroundings. In the high-density and low-temperature gas, the electron and proton temperatures become equal instantly by Coulomb collisions. Thus, the large-scale plasma dynamics can be treated as a single-temperature fluid. In contrary to this, when the plasma temperature is reached electron relativistic temperature, this picture changes. The Coulomb coupling becomes inefficient, and the electrons and protons can have a different temperature, i.e. plasma has "two-temperature". Thus, we should solve the thermodynamics equations for both electrons and protons to deal with two-temperature plasma.

Numerous numerical simulations have been performed to study the basic structure and stability of the propagating jet. However, due to the limitation of the numerical resources, the simulation box size only reaches 100 times the initial jet radius. Also, the two-temperature nature of the plasma has been ignored in the previous studies. Therefore, by using high-order MHD code CANS+ and the supercomputer "Fugaku", we aim at the high-resolution and two-temperature MHD simulation which follows the long-term jet propagation to 1000 times of the initial jet radius. As a result, we can connect the multilayer structure from sub-kpc to hundred kpc scale in one calculation. At present, we have been conducted test simulations that the jet propagates at the spatial scale of 300 times the initial jet radius by using "Fugaku".

We first report our previous results of two-temperature simulations with the different jet magnetic energy to investigate the effect of jet dynamics and electron heating. strongly magnetized jet suffered from current-driven kink mode. Meanwhile, weakly magnetized jets were decelerated by the high-mixing ratio between the jet beam and cocoon gas, which were induced by KH and RT instability. Also, jet magnetization affected the distribution of magnetic fields. The turbulent scale of the weakly magnetized jet was shorter than that of the strongly magnetized jets since the magnetic tension suppressed the turbulence motion. Through the three-dimensional studies, we found that there are two steps for the thermodynamics of electron and proton in the evolution of jet: First, most of the bulk kinetic energy of the jet is converted into thermal energy of proton through shocks, which are formed in the jet beam. Second,

©2021. Japan Geoscience Union. All Right Reserved.

while magnetic fields are relatively strong, shocked-electrons stored in the cocoon evolve toward energy equipartition with magnetic energy through turbulent dissipation. In this presentation, in the addition to these results, we report the progress results by using "Fugaku".

©2021. Japan Geoscience Union. All Right Reserved.

Core-Collpase Supernova Simulations by Boltzmann-Hydro Code

*Wakana Iwakami[1], Hirotada Okawa[1], Hiroki Nagakura[2], Akira Harada[3], Ryuichiro Akaho[1], Shun Furusawa[6], Hideo Matsufuru[5], Kosuke Sumiyoshi[4], Shoichi Yamada[1]

1. Waseda University, 2. Princeton University, 3. University of Tokyo, 4. Numazu College of Technology, 5. High Energy Accelerator Research Organization, 6. Tokyo University of Science

A core-collapse supernova is considered as an explosion of a massive star at the end of life. Its explosion mechanism has not been fully understood yet. An iron core is formed in a massive star whose mass is 10 times larger than the mass of the sun. At the core the photodisintegration reaction of iron nuclei or the electron capture reaction occur by increasing temperature and density due to the gravitational contraction. These endthermal reactions take away heat from the matter, and lead to the sudden decrease of the central pressure which prevent the fall of the matter toward the central region. Then the gravitational collapse starts, and the shock wave is launched after the core-bounce which occur when the central density reaches the nuclear density. The explosion succeeds if the shock wave reach the surface of the star, and is observed as a supernova on the earth.

Currently, the most promising explosion mechanism is the neutrino heating mechanism. Neutrinos, enclosed into the central part during gravitational collapse, diffuse out from the proto-neutron star formed at the central part after the core-bounce. The diffusing neutrinos can heat the matter in the gain region below the shock wave. However, explosions have not occurred in one-dimensional spherically symmetric simulations, except for the very low mass star. On the other hand, the hydrodynamical instabilities and turbulence grow in the gain region in the multi-dimensional simulations. This multi-dimensional effect plays an important rule for explosion, since it increases the dwell time of the falling matter in the gain region. The hydrodynamical instabilities grown in the gain region are mainly divided into the neutrino-driven convection and the standing accretion shock instability (SASI). The former is driven by the neutrino heating, and the various scale of the vorticies are developed. The latter is the aspherical deformation of the shock wave, and the large scale of the matter motion is induced. Depending on the neutrino luminosity and the mass accretion rate, one of them is dominant or both of them coexist. Therefore, we might obtain the information about the explosion mechanism or progenitor star if we can detect the signal of convection and SASI by the gravitational wave or neutrino observation.

In order to predict the signals of gravitational waves and neutrinos, the accurate neutrino transport is important for the gravitational core-collapse simulations. The basic equation of the neutrino transport is the Boltzmann equation. Since it is computationally expensive to solve the Boltzmann equation directly, the approximate methods are used for the neutrino transport of the core-collapse simulations. Such methods are constructed using the characteristics of the optically thin and thick limits. Hence, the accuracy of these methods should be validated in the transition region between two limits. Furthermore, the understanding of the neutrino transport in the transition region is important for clarifying the explosion mechanism, because the neutrino heating region corresponds to the transition regions. Recently, we have developed the Boltzmann-Hydro code for solving both Boltzmann equation for neutrino transport and Euler equations for hydrodynamics. This code can calculate correctly the neutrino heating rate and the radiation pressure if the resolution is high enough. In this poster, we introduce the results obtained from the Boltzmann-Hydro code in K and Fugaku computer systems. The neutrino transport is investigated in the situations of growing hydrodynamical instabilities.

©2021. Japan Geoscience Union. All Right Reserved.

Keywords: Core-collapse supernovae, Neutrino Radiation Transfer, Hydrodynamical Instability

©2021. Japan Geoscience Union. All Right Reserved.

Development of N-body Simulation Code for Planetary System Formation: GPLUM

*Yota Ishigaki[1,2], Eiichiro Kokubo[3], Junichiro Makino[4], Masaki Fujimoto[2]

1. University of Tokyo, 2. Institute of Space and Astronautical Science, Japan Aerospace Exploration Agency, 3. National Astronomical Observatory of Japan, 4. Kobe University

In general, the planetary system is thought to be formed from protoplanetary disks surrounding the central star. In particular, it is accepted that terrestrial planets and the cores of gas giant planets are formed by accretion of km size objects (planetesimals) in the protoplanetary disk. The accretion process of the planets has been mainly discussed using the gravitational multi-body simulations (N-body simulations) of planetesimal systems.

We have developed a new N-body simulation code with particle-particle particle-tree (P^3T) scheme for planetary system formation, GPLUM. The code GPLUM uses a fourth-order Hermite scheme to calculate gravitational interactions between particles within a cut-off radius and a Barnes-Hut tree scheme for gravitational interactions from particles beyond. The conventional simulation codes with P^3T scheme has the bottleneck that the calculation speed decreases when the mass ratio among the particles becomes large. We have solved it by implementing an algorithm which determines the cut-off radius based on mass and velocity dispersion of particles individually for each particle. The performance of GPLUM is significantly improved for the simulations of particle systems with mass distribution. We have tested the calculation performance of GPLUM for large-scale calculation using the supercomputer Fugaku.

By improving the performance of the N-body simulation code, we made it possible to carry out numerous global simulation with various parameters. By using GPLUM, we will perform N-body simulations with wide range and high resolution and investigate various parameters by perform parameter studies with N-body simulations.
We will report results of the performance evaluation of GPLUM in Fugaku and the large-scale sumulations of planetary accumulation.

Keywords: planet formation, N-body simulation

©2021. Japan Geoscience Union. All Right Reserved.

Rocky Planetesimal Accretion under a Realistic Accretion Condition

*Takashi Shibata[1], Eiichiro Kokubo[1,2], Junichiro Makino[3], Yota Ishigaki[2]

1. National Astronomical Observatory of Japan, 2. The University of Tokyo, 3. Kobe University

Terrestrial planets, ice giants, and the cores of gas giants are thought to be formed by the accretion of planetesimals. The limited numbers of planetesimals around the proto-sun grow rapidly because of their self-gravity. The growing mode is named runaway growth. The scattering planetesimals by runaway growing planetesimals heat up the planetesimal system and the numbers of the planetesimal collisions on the runaway growing ones decrease. This phase is named oligarchic growth of planetesimals. To know these accretion processes are necessary to know the whole view of planet formation. There is no research on the planetesimal accretion process correctly considering the realistic merging criteria to distinguish merging and hit-and-run at the time of the planetesimal collision. The hit-and-run is going to affect the accretion process significantly. Although there are several previous studies to know the accretion process of planetesimals using *N*-body simulation, they used not realistic merging criteria such as that for protoplanets. Thus, we need to know the realistic merging criteria. And we have already studied the criteria in the previous paper. Now we study the accretion process under the realistic accretion condition by using *N*-body simulation. We use the *N*-body simulation code that is named GPLUM (Global PLanetary system simulation code with Mass-dependent cut-off method). The method is useful to know the evolution of mass, velocity, and spatial distribution of planetesimals during the accretion process since the method calculates the orbit of planetesimals directly. We apply to GPLUM the merging criteria necessary to distinguish merging and hit-and-run of planetesimals. We set two hundred thousand rocky 100km-sized planetesimals as a narrow ring around the sun and calculate the orbits of the planetesimals. We compare the results of the imperfect merging case that considers hit-and-run and perfect merging case where all colliding planetesimals merge. Planetesimals grow similarly in each case but the time for sweeping surrounding planetesimals elongates in the imperfect merging case. The mass distribution is polarized since the growth of planetesimals is prevented by the hit-and-run. Then, runaway growth and oligarchic growth becomes more prominent than the perfect merging case. We will show the result of accretion of spin angular momentum on the planetesimals and additionally discuss the spin properties of protoplanets in this speech.

Keywords: Formation of Planets, Planetesimal Accretion, Merging Criteria of Planetesimals

©2021. Japan Geoscience Union. All Right Reserved.

[J] Oral | M (Multidisciplinary and Interdisciplinary)：M-SD Space Development & Earth Observation from Space

Fri. Jun 4, 2021 9:00 AM - 10:30 AM JST | Fri. Jun 4, 2021 12:00 AM - 1:30 AM UTC | Ch.08 Zoom Room 08

[M-SD40] Future Missions of Satellite Earth Observation

convener:Yoshiaki HONDA(Center for Environmental Remote Sensing, Chiba University), Yukari Takayabu(Atmosphere and Ocean Research Institute, the University of Tokyo), Shinichi Sobue(Japan Aerospace Exploration Agency), Kosuke Yamamoto(Japan Aerospace Exploration Agency), Chairperson:Yoshiaki HONDA(Center for Environmental Remote Sensing, Chiba University), Nobuhiro Takahashi(Institute for Space-Earth Environmental Research, Nagoya University), Kosuke Yamamoto(Japan Aerospace Exploration Agency)

Satellite observation can be an effective tool in earth science and making human society apply to the rapid global environmental change. Monitoring for a long term, advancing new ideas and developing technologies to support them are needed. The Task Force on Future Space R&D System of the Subcommittee on Remote Sensing (TF) supported by 26 academic societies and affiliated organizations has formulated the ''Grand Design of Earth Observation'' from FY2017. From the academic point of view, it suggests earth observation missions that Japan should conduct within a decade. The TF calls for proposals of earth observation missions as a trial that aims to discover new ideas from the scientific and practical domains and refine those ideas through multidisciplinary discussion. The adopted proposals will be mentioned in the revised Grand Design, and the TF will work with the government on using it as a reference in updating the Implementation Plan of the Committee on National Space Policy. This session consists of oral presentations of the proposals that passed the preliminary examination of documents and active discussions to expand and deepen the study. We welcome attendees from various backgrounds who are interested in earth observation.

9:00 AM - 9:15 AM JST | 12:00 AM - 12:15 AM UTC

[MSD40-01] Introduction

9:15 AM - 9:30 AM JST | 12:15 AM - 12:30 AM UTC

[MSD40-02] Consideration status of the sensors of Himawari follow-on satellite

*Kotaro BESSHO[1], Hiromi OWADA[1], Takuya Sakashita[1], Mikito Yamamoto[1] (1.Japan Meteorological Agency)

9:30 AM - 9:45 AM JST | 12:30 AM - 12:45 AM UTC

[MSD40-03] Lightning Observation from Geo-Stationary Orbit

*Tomoo Ushio[1], LightningGroup MInt (1.Osaka University)

9:45 AM - 10:00 AM JST | 12:45 AM - 1:00 AM UTC

[MSD40-04] Experimental platform for design and advance evaluation of frequent satellite observations to innovate weather, ocean and land surface predictions

*Takemasa Miyoshi[1], Koji Terasaki[1], Shunji Kotsuki[2,1], Shigenori Otsuka[1], Takumi Honda[1], Kohei Takatama[1], Atsushi Okazaki[3,1] (1.RIKEN, 2.Chiba University, 3.Pennsylvania State University)

10:00 AM - 10:15 AM JST | 1:00 AM - 1:15 AM UTC

[MSD40-05] Geostationary Optical Earth Observation Satellite (3)

*Kazuo Oki[1,2], Toshiyoshi Kimura[3], Tadahito Mizutani[3], Masuo Takahashi[3], Takeo Tadono[3] (1.The Univ. of Tokyo, 2.KUAS, 3.JAXA)

10:15 AM - 10:30 AM JST | 1:15 AM - 1:30 AM UTC

[MSD40-06] Geostationary Satellite Ocean Color Mission

*Joji Ishizaka[1], Mitsuhiro Toratani[2], Toru Hirawake[3], Takafumi Hirata[4], Hiroshi Kobayashi[5], Yuji Sakuno[6], Hiroshi Higa[7] (1.Institute for Space-Earth Environmental Research, Nagoya University, 2.Faculty of Engineering, Tokai University, 3.Fisheries Sciences, Hokkaido University, 4.Arctic Research Center,

Hokkaido University, 5.Graduate Faculty of Interdisciplinary Research, University of Yamanashi, 6.Graduate School of Engineering, Hiroshima University, 7.Graduate School of Urban Innovation, Yokohama National University)

[J] Oral | M (Multidisciplinary and Interdisciplinary) | M-SD Space Development & Earth Observation from Space

[M-SD40] Future Missions of Satellite Earth Observation

convener:Yoshiaki HONDA(Center for Environmental Remote Sensing, Chiba University), Yukari Takayabu(Atmosphere and Ocean Research Institute, the University of Tokyo), Shinichi Sobue(Japan Aerospace Exploration Agency), Kosuke Yamamoto(Japan Aerospace Exploration Agency), Chairperson:Yoshiaki HONDA(Center for Environmental Remote Sensing, Chiba University), Nobuhiro Takahashi(Institute for Space-Earth Environmental Research, Nagoya University), Kosuke Yamamoto(Japan Aerospace Exploration Agency)

Fri. Jun 4, 2021 9:00 AM - 10:30 AM Ch.08 (Zoom Room 08)

Satellite observation can be an effective tool in earth science and making human society apply to the rapid global environmental change. Monitoring for a long term, advancing new ideas and developing technologies to support them are needed. The Task Force on Future Space R&D System of the Subcommittee on Remote Sensing (TF) supported by 26 academic societies and affiliated organizations has formulated the "Grand Design of Earth Observation" from FY2017. From the academic point of view, it suggests earth observation missions that Japan should conduct within a decade. The TF calls for proposals of earth observation missions as a trial that aims to discover new ideas from the scientific and practical domains and refine those ideas through multidisciplinary discussion. The adopted proposals will be mentioned in the revised Grand Design, and the TF will work with the government on using it as a reference in updating the Implementation Plan of the Committee on National Space Policy. This session consists of oral presentations of the proposals that passed the preliminary examination of documents and active discussions to expand and deepen the study. We welcome attendees from various backgrounds who are interested in earth observation.

9:00 AM - 9:15 AM

[MSD40-01]Introduction

©Japan Geoscience Union

Consideration status of the sensors of Himawari follow-on satellite

*Kotaro BESSHO[1], Hiromi OWADA[1], Takuya Sakashita[1], Mikito Yamamoto[1]

1. Japan Meteorological Agency

In this presentation, consideration status of the sensors of Himawari follow-on satellite will be shown from Japan Meteorological Agency.

Keywords: geostationary meteorological satellite, Himawari, follow-on satellite program, visible/infrared imager, hyperspectral infrared sounder, lightning imager

©2021. Japan Geoscience Union. All Right Reserved.

Lightning Observation from Geo-Stationary Orbit

*Tomoo Ushio[1], LightningGroup MInt

1. Osaka University

Recently, Geostationary Lightning Mapper (GLM) was launched into geostationary orbit from the US. Even though only four years have passed since its launch, the GLM is shown to be establishing a legacy of applications likely to become ubiquitous accross a wide variety of meteorological domains. For example, the GLM has been shown to be useful in the following application areas: 1) Improving Lightning Safety, 2) Improving Sever Thunderstorm and Tornado Warning, 3) Improving Safety and Effectiveness of Wildfire Response, 4) Improving Short-term Model Forecast (Data Assimilation), 5) Improving Precipitation Estimation, 6) Improving Tropical Cyclone Diagnosis and Warning, 7) Improving Climate Applications, 8) Value of Filling Data Gaps, 9) Value of Mitigation Aviation Hazards (Rudlosky et al. 2020). In this presetnation, based on the assessment report published from NOAA, we will report the major application areas of the geostationary lightning sensor.

©2021. Japan Geoscience Union. All Right Reserved.

Experimental platform for design and advance evaluation of frequent satellite observations to innovate weather, ocean and land surface predictions

*Takemasa Miyoshi[1], Koji Terasaki[1], Shunji Kotsuki[2,1], Shigenori Otsuka[1], Takumi Honda[1], Kohei Takatama[1], Atsushi Okazaki[3,1]

1. RIKEN, 2. Chiba University, 3. Pennsylvania State University

We propose to develop a unique platform with an advanced data assimilation technology, realizing numerical simulation experiments for advance evaluation of future satellite missions in their design phase. This will provide a scientific, objective approach to an effective design of future satellite missions to maximize the benefit to practical applications such as hydrometeorological prediction and resource control of fisheries. The authors have been leading data assimilation research to explore the best mix of computer model simulations and real-world data for weather forecasting, taking advantage of new-generation technologies such as the K computer and Himawari-8 satellite. The authors' previous research revealed that every-10-minute Himawari-8 observations could lead to a large improvement of typhoon and heavy rainfall predictions, though every-30-minute observation was insufficient. We would expect that frequent observations would also be beneficial for ocean and land surface prediction. Therefore, we aim to develop a platform for numerical experimentation to evaluate potential future satellite missions such as quasi-zenith orbiters and small cube-sat constellations for frequent observation over Japan and its surrounding area. This platform will be useful for designing future satellite missions with high cost-benefit performance.

Keywords: Numerical Weather Prediction, Data Assimilation, OSSE, Platform, Satellite Observation

©2021. Japan Geoscience Union. All Right Reserved.

Geostationary Optical Earth Observation Satellite (3)

*Kazuo Oki[1,2], Toshiyoshi Kimura[3], Tadahito Mizutani[3], Masuo Takahashi[3], Takeo Tadono[3]

1. The Univ. of Tokyo, 2. KUAS, 3. JAXA

Geostationary satellite is the most practical Earth Observation for its instantaneous observation and ability to choose target area on demand. However, the observation requirements have not been satisfied, especially in fields such as disaster observation that requires immediate observation and agriculture that required daily observation, from the viewpoint of spatial or temporal resolution or immediate observations even existing observation satellite systems including meteorological satellites require observation. Here, we present on the research on new observation results that can be expected for on-demand constant observation on a ground surface resolution scale of about 10m, which has never been observed before, and the status of key technical research to realize this system. According to the Japan Meteorological Agency's report on the Great East Japan Earthquake, it is necessary to complete the process from the observation request to the distribution of the observation data within 30 minutes. Although the acquired observation data is not of high resolution, it is sufficiently suitable for the purpose of identifying the scale and extent of damage, and is indispensable information for determining more detailed investigation /observation plans and emergency evacuation orders. Regarding normal operation other than disasters, some products are currently under consideration with researchers in the fields of disaster prevention, forestry, agriculture, and oceans, considering the characteristics of geostationary optical observation satellites. For example, in agriculture, where it is important to determine the harvest time, the unobservable situation due to clouds, which is a problem with conventional satellites, is greatly improved to the situation where images with few clouds can be obtained by geostationary satellite observation. From this, it is expected that unprecedented results will be obtained even in normal times, especially for events that change rapidly over time. Regarding the technical research status, regarding the large telescope, which is the key technology in this system, the satellite manufacturer and JAXA are working on confirming the basic principle of the light wave synthesis aperture by the divided lightweight ceramic mirror and prototyping a movable mirror related to Active / Adaptive Optics. By the end of 2020, we plan to make a development outlook for these key technologies and summarize observation plans during disasters and normal times.

Keywords: Geostationary Optical Earth Observation Satellite , Disasters observation, Normal observation

©2021. Japan Geoscience Union. All Right Reserved.

Geostationary Satellite Ocean Color Mission

*Joji Ishizaka[1], Mitsuhiro Toratani[2], Toru Hirawake[3], Takafumi Hirata[4], Hiroshi Kobayashi[5], Yuji Sakuno[6], Hiroshi Higa[7]

1. Institute for Space-Earth Environmental Research, Nagoya University, 2. Faculty of Engineering, Tokai University, 3. Fisheries Sciences, Hokkaido University, 4. Arctic Research Center, Hokkaido University, 5. Graduate Faculty of Interdisciplinary Research, University of Yamanashi, 6. Graduate School of Engineering, Hiroshima University, 7. Graduate School of Urban Innovation, Yokohama National University

It is expected that the coastal marine ecosystem, which was originally greatly affected by humans, is further changing under the significant changes of seawater temperature and freshwater inflow due to climate change. Observation of ocean colors is making it possible to continuously monitor the status of coastal ecosystems, such as phytoplankton and suspended matter. However, because visible observations are disturbed by clouds, sufficient data is difficult to be obtained, specifically in coastal areas where short term variations is large, such as influence of river water and tides. It was clarified that the high-frequency observation of "Himawari" on an hourly basis makes it possible to observe short-term fluctuations under moving clouds. On the other hand, the wavelength and radiance resolution are insufficient to obtain sufficient ocean color information. Therefore, we propose here the observation of high frequency, high resolution, and high radiance resolution by the geostationary satellite ocean color sensor with additional bands. This makes it possible to monitor phenomena that affect coastal fisheries and aquaculture, such as red tides and river water, and to make observations related to coastal material cycles. Moreover, it is possible to contribute to understand the environment not only in Japan, but also in the coastal areas of southeastern Asia, which are greatly affected by human activities and climate change and by relatively many clouds. Furthermore, it is considered to be effective not only for observation of the ocean but also for observation of the atmosphere (aerosol particles) and land (vegetation).

Keywords: Geostationary Satellite, Ocean Color

©2021. Japan Geoscience Union. All Right Reserved.

[J] Oral | M (Multidisciplinary and Interdisciplinary)：M-SD Space Development & Earth Observation from Space

Fri. Jun 4, 2021 10:45 AM - 12:15 PM JST | Fri. Jun 4, 2021 1:45 AM - 3:15 AM UTC | Ch.08 Zoom Room 08

[M-SD40] Future Missions of Satellite Earth Observation

convener:Yoshiaki HONDA(Center for Environmental Remote Sensing, Chiba University), Yukari Takayabu(Atmosphere and Ocean Research Institute, the University of Tokyo), Shinichi Sobue(Japan Aerospace Exploration Agency), Kosuke Yamamoto(Japan Aerospace Exploration Agency), Chairperson:Yoshiaki HONDA(Center for Environmental Remote Sensing, Chiba University), Nobuhiro Takahashi(Institute for Space-Earth Environmental Research, Nagoya University), Kosuke Yamamoto(Japan Aerospace Exploration Agency)

Satellite observation can be an effective tool in earth science and making human society apply to the rapid global environmental change. Monitoring for a long term, advancing new ideas and developing technologies to support them are needed. The Task Force on Future Space R&D System of the Subcommittee on Remote Sensing (TF) supported by 26 academic societies and affiliated organizations has formulated the ''Grand Design of Earth Observation'' from FY2017. From the academic point of view, it suggests earth observation missions that Japan should conduct within a decade. The TF calls for proposals of earth observation missions as a trial that aims to discover new ideas from the scientific and practical domains and refine those ideas through multidisciplinary discussion. The adopted proposals will be mentioned in the revised Grand Design, and the TF will work with the government on using it as a reference in updating the Implementation Plan of the Committee on National Space Policy. This session consists of oral presentations of the proposals that passed the preliminary examination of documents and active discussions to expand and deepen the study. We welcome attendees from various backgrounds who are interested in earth observation.

10:45 AM - 11:00 AM JST | 1:45 AM - 2:00 AM UTC

[MSD40-07] Role of Japan on polarization observations from space

*Makiko Nakata[1], Itaru Sano[1], Sonoyo Mukai[2] (1.Kindai University, 2.The Kyoto College of Graduate Studies for Informatics)

11:00 AM - 11:15 AM JST | 2:00 AM - 2:15 AM UTC

[MSD40-08] Comprehensive atmospheric composition measurements and emissions estimations from geostationary orbit over Asia: Rationalizing decarbonization and air pollution mitigation strategies

*Yugo Kanaya[1], YASUKO KASAI[2], Hiroshi Tanimoto[3], Naoko Saitoh[4], Nawo Eguchi[5], Tomohiro Sato[2], Tamaki Fujinawa[3], Prabir Patra[1], Takashi Sekiya[1], Masayuki Takigawa[1], Satellite committee JpSAC (1.JAMSTEC, 2.NICT, 3.NIES, 4.Chiba Univ., 5.Kyushu Univ.)

11:15 AM - 11:30 AM JST | 2:15 AM - 2:30 AM UTC

[MSD40-09] **Multi-footprint Observation Lidar and Imager (MOLI) mission for performing highly precise estimation of elevation, forest height & biomass, and also for providing results of clouds & aerosols measurement**

*Kazuhiro Asai[1], Yasumasa - Hirata[2], Gen - Takao[2], Yoshiaki - Honda[3], Koji - Kajiwara[3], Yoshio - Awaya[4], Junichi - Susaki[5], Takahiro - Endo[6], Nobuo - Sugimoto[7], Tomoaki - Nishizawa[7], Kohei - Mizutani[10], Shoken - Ishii[8], Toshiyoshi - Kimura[9], Tadashi - Imai[9], Yoshito - Sawada[9], Masato - Hayashi[9], Daisuke - Sakaizawa[9], Rei - Mitsuhashi[9], Trung Tat Nguyen[9] (1.Tohoku Institute of Technology, 2.Forestry and Forest Products Research Institute, 3.Chiba University, 4.Gifu University, 5.Kyoto University, 6.The Remote Sensing Technology Center of Japan, 7.National Institute for Environmental Research, 8.Tokyo Metropolitan University, 9.Japan Aerospace Exploration Agency, 10.National Institute of Information and Communications Technology)

11:30 AM - 11:45 AM JST | 2:30 AM - 2:45 AM UTC

[MSD40-10] Cloud-Precipitation observation mission by active sensors (2)

*Nobuhiro Takahashi[1], Kinji Furukawa[2], Yukari Takayabu[3] (1.Institute for Space-Earth Environmental Research, Nagoya University, 2.JAXA, 3.The Atmosphere and Ocean Research Institute (AORI) , the University of Tokyo)

11:45 AM - 12:00 PM JST | 2:45 AM - 3:00 AM UTC

[MSD40-11] Discussion

*Kosuke Yamamoto[1] (1.Japan Aerospace Exploration Agency)

12:00 PM - 12:15 PM JST | 3:00 AM - 3:15 AM UTC

[MSD40-12] Discussion

Role of Japan on polarization observations from space

*Makiko Nakata[1], Itaru Sano[1], Sonoyo Mukai[2]

1. Kindai University, 2. The Kyoto College of Graduate Studies for Informatics

The color composite images from Himawari-8/AHI (Advanced Himawari Imager) and SGLI (Second-Generation GLobal imager) are presented in Fig.1a and 1b, respectively. The images by Himawari have become an integral part of our daily lives. The image by SGLI visualizes the heavy smoke over large scale forest fires in the western Canada on Aug. 14, 2018. It is well known that large-scale wild fires have occurred worldwide since 2018 owing to global warming and climate change.
The so-called imagers currently on board the Japanese satellite are AHI, SGLI and CAI-2. The AHI mounts on the geostationary meteorological satellite Himawari-8 launched on October 7, 2014. The functions and specifications of AHI are notably improved. AHI is a 16 channel multispectral imager to capture visible light and infrared images of the Asia-Pacific region, then AHI contributes to not only weather prediction but also environmental monitoring. The SGLI on board GCOM-C launched on December 23, 2017 contains 19 channels from near-UV (380 nm) to infrared. The CAI (Cloud and Aerosol Imager)-2 on the GOSAT-2 launched on October 29, 2018 is a push-broom radiometer with 10 channels in the spectral ranges from ultra violet to short wavelength infrared for the observation of aerosols and clouds optical properties and for monitoring of air pollution. These imagers not only have the capability of high resolution at multiple wavelengths, but also each has its own unique capability and makes a great contribution to the global environment by utilizing the excellent features of AHI's high temporal resolution, SGLI's polarization information, and CAI-2's two-way observation. It is clear that these sensors are not just for capturing the satellite images that the word "imager" implies, but it is also clear that the information that satellite images directly appeal to intuitively is large and strong.
The usefulness and important role of imagers in atmospheric environment analysis will be partly introduced, focusing on the SGLI that our group has been involved in. The SGLI encompasses two polarization channels PL1 (674 nm) and PL2 (869 nm) with 1 km instantaneous field-of-view (IFOV). Note that this polarization measurement is the smallest resolution obtained to date. As shown in Figure 2, the sensitivities of the non-PL band (674) (b) and PL band (674) (c) are different. This is likely because the radiance channel considers the observations of darker targets, such as vegetation and land cover. Thus, the black area exists in color composite image (a). The dark yellow color spreading in the upper central region of the image (a) denotes the smoke caused by the wild fire events owing to the near-UV band (380). Further, the swaths of both images (b) and (c) are different because of differences in observation angles, wherein the radiance observation telescope observes downward, and the polarization telescope observes at 45˚ oblique. In other words, two-directional observation is available, and geometrical information is obtained.
This is just one example, but it shows the effectiveness of the complementarity between the polarization information and the non-polarized radiance measurements from the SGLI for biomass burning aerosol retrieval. In this way, the SGLI observables have various possibilities. The technology and experience of multi-wavelength polarization sensors cultivated by SGLI should be inherited. Even if the revolutionary aerosol and cloud sensor 3MI; muti-viewing, -channel, -polarization imager: will fly to space on the MetOp-SGA satellite in 2022, the successor of SGLI is still very valuable. There's no substitute for sustainability.

©2021. Japan Geoscience Union. All Right Reserved.



Fig.1 Color composite images from Himawari-8/AHI over Japan on Jan. 12,2020 (a), and GCOM-C/SGLI over the large forest fire in western Canada on Aug. 14, 2018 (b).

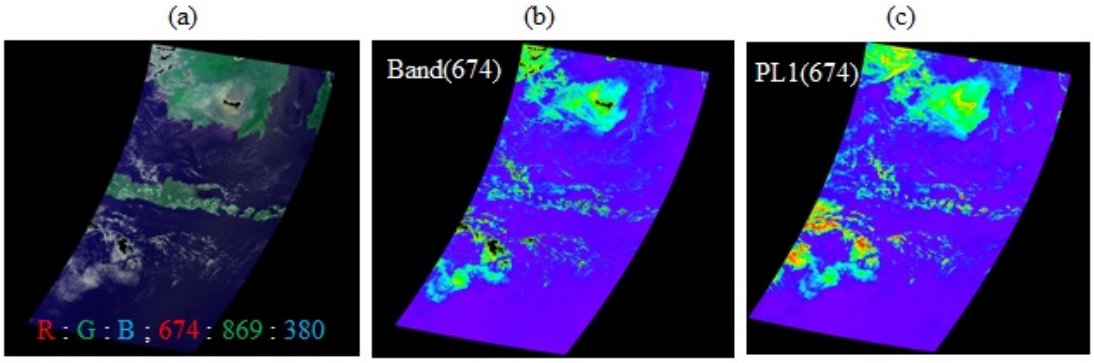


Fig. 2. Color composite image (a), radiance (b) and polarization (c) measurements by SGLI over Kalimantan, Indonesia on September 15, 2020.

©2021. Japan Geoscience Union. All Right Reserved.

Comprehensive atmospheric composition measurements and emissions estimations from geostationary orbit over Asia: Rationalizing decarbonization and air pollution mitigation strategies

*Yugo Kanaya[1], YASUKO KASAI[2], Hiroshi Tanimoto[3], Naoko Saitoh[4], Nawo Eguchi[5], Tomohiro Sato[2], Tamaki Fujinawa[3], Prabir Patra[1], Takashi Sekiya[1], Masayuki Takigawa[1], Satellite committee JpSAC

1. JAMSTEC, 2. NICT, 3. NIES, 4. Chiba Univ., 5. Kyushu Univ.

Climate change and global air pollution are urgent social issues in the 21st century. We aim strategic monitoring of atmospheric long-lived greenhouse gases (GHGs including CO2) and short-lived climate forcers (SLCFs, including NO2, methane), simultaneously, to develop and optimize mitigation strategies on the basis of real-world/real-time information. In order to ensure our steps toward stringent decarbonization, with 1.5-degree target in mind, we immediately estimate "emissions" from the satellite observations regarding huge point sources and important regions and thereby enable iterative optimization of mitigation policy, consisting of observations, emissions estimation, and evaluation of effectiveness of current policy - we shall provide such scientific knowledge as social commons. Similar mitigation approach is undertaken for the air pollution issue, regarding Asia as a hotspot, aiming efficient reduction of global premature death rate, estimated to be up to 4.2million per year. As demonstrated recently during the COVID-19 affecting period, satellite NO2 observations are powerful in diagnosing economy/emission reductions relevant to GHGs –such air quality/GHG synergies will also be explored. We thereby contribute to the Paris Agreement, global stocktake, national SLCF inventory as a new task to be introduced by IPCC TFI, and SDGs. Health tourism would also be an interesting area of data application. Observations from geostationary satellites shall be targeted, in order to fully quantify atmospheric abundances of relevant chemical substances, spreading from individual sources to Asian regions, with spatial continuity and a high temporal resolution. The highest spatial resolution of ca. 1 km as ever achieved from hyperspectral sensors should also be targeted. Diurnal cycles of human activities, photochemical reactions, and of photosynthesis would become discernible. The main sensors will be UV/vis/NIR imaging spectrometers, while potentials of IR sounders should also be examined for retrievals of vertical profiles and new species (ammonia as well as O3 and CO).

Keywords: Asian air pollution, global warming, atmospheric composition, rationalization of mitigation policy, green innovation

©2021. Japan Geoscience Union. All Right Reserved.

Multi-footprint Observation Lidar and Imager (MOLI) mission for performing highly precise estimation of elevation, forest height & biomass, and also for providing results of clouds & aerosols measurement

*Kazuhiro Asai[1], Yasumasa - Hirata[2], Gen - Takao[2], Yoshiaki - Honda[3], Koji - Kajiwara[3], Yoshio - Awaya[4], Junichi - Susaki[5], Takahiro - Endo[6], Nobuo - Sugimoto[7], Tomoaki - Nishizawa[7], Kohei - Mizutani[10], Shoken - Ishii[8], Toshiyoshi - Kimura[9], Tadashi - Imai[9], Yoshito - Sawada[9], Masato - Hayashi[9], Daisuke - Sakaizawa[9], Rei - Mitsuhashi[9], Trung Tat Nguyen[9]

1. Tohoku Institute of Technology, 2. Forestry and Forest Products Research Institute, 3. Chiba University, 4. Gifu University, 5. Kyoto University, 6. The Remote Sensing Technology Center of Japan, 7. National Institute for Environmental Research, 8. Tokyo Metropolitan University, 9. Japan Aerospace Exploration Agency, 10. National Institute of Information and Communications Technology

Forests have a strong impact on our survival and are highly relevant to climate change and extreme weather events associated with recent global warming. They, as is well known, are the second largest carbon reservoir on Earth after the oceans because they convert atmospheric CO_2 absorbed through photosynthesis into organic biomass for fixation. Most of the forest carbon is contained in living biomass (aboveground biomass (AGB) + aboveground biomass (BGB), 44%) and soil organic matter (45%), with the remainder in dead trees and litter. The total carbon stock is estimated to be 662 Gt in 2020 (FAO). The explosive population growth in the 20th and 21st centuries has resulted in deforestation and forest degradation due to rapid changes in land use associated with increased food production and the need to develop infrastructure such as residential and industrial areas. The amount converted into CO_2 by land use change including illegal logging and wildfires is, surprisingly, equivalent to 13% of anthropogenic CO_2 emissions. Therefore, there is a strong need for 24-hour global monitoring of our precious forests from space.

L-band SAR (PALSAR/ALOS, PALSAR-2/ALOS-2, etc.) has provided valuable data on forest biomass around the world. However, it is said that the backscatter signal is saturated in dense tropical rainforests where the biomass exceeds 150 Mg/ha. In addition, in closed mature forests, wetland forests and mangrove forests in Japan, there are some problems such as overestimation of biomass estimates due to double reflection by water surface. In this regard, a space lidar based on pulsed laser altimetry can essentially evaluate the height of the forest canopy (DCHM) by calculating the time difference between the scattered signal from the top of the forest canopy (DSM) and the scattered signal from the ground surface (DTM). The AGB in the footprint can also be estimated using full waveform data and multiple regression analysis.

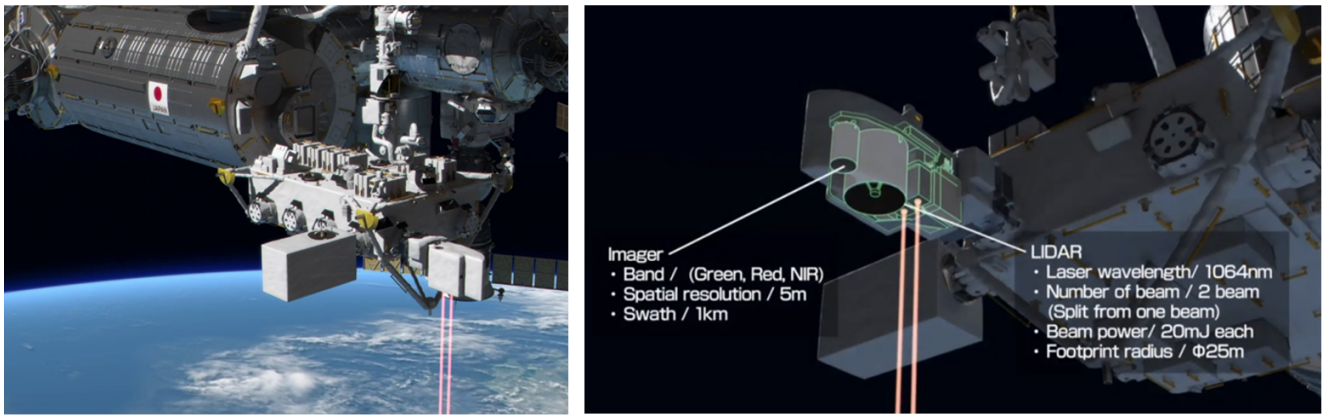
The objectives of MOLI (Multi-footprint Observation Lidar and Imager) mission proposed in this paper is to demonstrate Japan's first space-based lidar and to perform highly precise estimation of elevation, forest canopy height, and three-dimensional structure information necessary for AGB evaluation, but also to provide optical atmospheric parameters. Furthermore, we aim to establish a fusion analysis algorithm with MOLI data, L-band SAR data, and passive spectral data from GCOM-C/SGLI etc., which will contribute to remarkable improvement of global forest biomass monitoring. We are currently working on the development of the laser transmitters for the lidar and algorithms for Level-1 and Level-2 products as follows.
I. Regarding the lidar, the space qualified prototype laser (EM level) maintained output power of 40mJ,

©2021. Japan Geoscience Union. All Right Reserved.

repetition rate of 150Hz, and pulse width of 7nsec. A thermal shock test in a thermostatic bath, a thermal vacuum test, and a vibration test showed good results.
II. Development of a method for estimating elevation and slope using MOLI data: In this study, we developed a method for estimating slope and aspect of footprints using AW3D, the global DSM data set. i) The time gap problem was cleared, ii) the developed method can estimate the slope and aspect even in the missing conditions from 1DEM to 3DEM.
III. Development of Level-2 Product Algorithm: The AGB estimation model was validated using point cloud data of 34,000 ha acquired by airborne LiDAR, and it was confirmed that the model could estimate with an accuracy of 47 Mg ha^{-1}, ii) We will improve the accuracy and the model.
IV. Algorithm development to detect cloud layers and retrieve optical properties of atmospheric particles: We focused on i) simulating lidar signals for cloud, aerosol, and clear-sky layer detection, ii) cloud detection using the threshold method, and iii) extinction/backscatter retrieval of aerosols and clouds.

Figure shows a conceptual diagram of MOLI onboard the ISS-JEM-EF.

Keywords: Lidar, Canopy height, Forest biomass, L-band SAR, Imager, Clouds & Aerosols



©2021. Japan Geoscience Union. All Right Reserved.

Cloud-Precipitation observation mission by active sensors (2)

*Nobuhiro Takahashi[1], Kinji Furukawa[2], Yukari Takayabu[3]

1. Institute for Space-Earth Environmental Research, Nagoya University, 2. JAXA, 3. The Atmosphere and Ocean Research Institute (AORI) , the University of Tokyo

In the JpGU2020, dual-frequency (Ku/Ka) scanning radar is proposed as the Cloud-Precipitation observation mission by active sensors and the Task Force (TF) team for future remote sensing from space recommended the Cloud-Precipitation observation mission by active sensors as one the highest priority mission. In this presentation, we report on recent activities for the mission achieved. In the US, an architecture study to realize the aerosol, cloud, convection and precipitation (ACCP) mission according to the decadal survey report issued by the National Academy of Science, Engineering and Medicine. In the decadal survey, active sensors including lidar, W/Ka/Ku band Doppler radar are recommended. In addition, international collaboration is strongly recommended. In the original plan of the Cloud-Precipitation observation mission proposed to TF equips Ku and Ka band radar without Doppler measurement capability and the cloud observation is owed by the international partners. Since the ACCP is good opportunity to realize our purpose, JAXA with Japanese community proposed a radar to the ACCP. The major changes from the original proposal is single frequency (Ku-band only) Doppler radar (nadir only). Because of the Doppler observation, antenna size of the radar became 2 x 4 m aperture (original is 2 x 2 m). An intensive study on the Doppler measurement was implemented by the JAXA and scientists of Japanese community.

Keywords: Cloud and Precipitation, Spaceborne Doppler radar

©2021. Japan Geoscience Union. All Right Reserved.

Discussion

*Kosuke Yamamoto[1]

1. Japan Aerospace Exploration Agency

This session will be used for question & answer and discussion.

©2021. Japan Geoscience Union. All Right Reserved.

[J] Oral | M (Multidisciplinary and Interdisciplinary) | M-SD Space Development & Earth Observation from Space

[M-SD40] Future Missions of Satellite Earth Observation

convener:Yoshiaki HONDA(Center for Environmental Remote Sensing, Chiba University), Yukari Takayabu(Atmosphere and Ocean Research Institute, the University of Tokyo), Shinichi Sobue(Japan Aerospace Exploration Agency), Kosuke Yamamoto(Japan Aerospace Exploration Agency), Chairperson:Yoshiaki HONDA(Center for Environmental Remote Sensing, Chiba University), Nobuhiro Takahashi(Institute for Space-Earth Environmental Research, Nagoya University), Kosuke Yamamoto(Japan Aerospace Exploration Agency)

Fri. Jun 4, 2021 10:45 AM - 12:15 PM Ch.08 (Zoom Room 08)

Satellite observation can be an effective tool in earth science and making human society apply to the rapid global environmental change. Monitoring for a long term, advancing new ideas and developing technologies to support them are needed. The Task Force on Future Space R&D System of the Subcommittee on Remote Sensing (TF) supported by 26 academic societies and affiliated organizations has formulated the "Grand Design of Earth Observation" from FY2017. From the academic point of view, it suggests earth observation missions that Japan should conduct within a decade. The TF calls for proposals of earth observation missions as a trial that aims to discover new ideas from the scientific and practical domains and refine those ideas through multidisciplinary discussion. The adopted proposals will be mentioned in the revised Grand Design, and the TF will work with the government on using it as a reference in updating the Implementation Plan of the Committee on National Space Policy. This session consists of oral presentations of the proposals that passed the preliminary examination of documents and active discussions to expand and deepen the study. We welcome attendees from various backgrounds who are interested in earth observation.

12:00 PM - 12:15 PM

[MSD40-12]Discussion

©Japan Geoscience Union

[J] Oral | M (Multidisciplinary and Interdisciplinary)：M-ZZ Others

Fri. Jun 4, 2021 3:30 PM - 5:00 PM JST | Fri. Jun 4, 2021 6:30 AM - 8:00 AM UTC | Ch.13 Zoom Room 13

[M-ZZ47] Renewable energy and earth science

convener:Hideaki Ohtake(National Institute of Advanced Industrial Science and Technology), Daisuke Nohara(Central Research Institute of Electric Power Industry), Teruhisa Shimada(Graduate School of Science and Technology, Hirosaki University), Fumichika Uno(Nihon University, College of Humanities and Sciences), Chairperson:Teruhisa Shimada(Graduate School of Science and Technology, Hirosaki University)

Renewable energy penetration is increasing dramatically in the world. Renewable energy power generations have become a strong presence in grid operations. However, it is a challenge for renewable energy to be stable power sources due in part to natural variability of renewable energy and its uneven distribution. For effective use of renewable energy, a combinational of various power resources and energy storage technologies (e.g., pumped-storage power generation, storage battery system, electric vehicles) should be desired. Therefore, we need to understand the amount of renewable resources, causes of variation, and the predictability of power output. Then, observation and forecast information from earth science fields should be analyzed and applied to power energy fields to achieve easy use of earth science databases.
Recently, observation databases from remote sensing technology and/or forecasts from numerical models have become essential for both renewable energy and electric power system. Impacts of both earth science data and optimization are essential to economic evaluation of grid operations.
This proposed session needs your presentation from the whole of renewable energy fields (wind power, solar power, geothermal power, tidal power, wave power and biomass power generations). Our goal of this session is to exchange views with various researchers between renewable energy fields and earth science fields (e.g., usage-trends of earth science datasets for renewable energy fields, earth science datasets availability, integrated studies, renewable energy resources in future climate system, and a request from renewable energy fields to earth science fields).
The proposed session features contribution of general interest within earth sciences community.

3:30 PM - 3:32 PM JST | 6:30 AM - 6:32 AM UTC

[MZZ47-01] Introduction

3:32 PM - 3:47 PM JST | 6:32 AM - 6:47 AM UTC

[MZZ47-02] Assessment of small hydropower generation potential in Shiribeshi subprefecture, Hokkaido

Mikiya Kato[2], *Masahiko Fujii[1,2] (1.Faculty of Environmental Earth Science, 2.Graduate School of Environmental Science, Hokkaido University)

3:47 PM - 4:02 PM JST | 6:47 AM - 7:02 AM UTC

[MZZ47-03] Assessment of snow and ice cryogenic energy potential in Hokkaido: a case study in Niseko Town

*Hehuan DUAN[1], Masahiko FUJII[1,2] (1.Graduate School of Environmental Science, Hokkaido University, 2.Faculty of Environmental Earth Science, Hokkaido University)

4:02 PM - 4:17 PM JST | 7:02 AM - 7:17 AM UTC

[MZZ47-04] Examination of the statistical forecast method of sunshine duration in Hokkaido

*Takao Sunamura[1], Hisashi Kato[1], Fumichika Uno[1] (1.Nihon University, College of Humanities and Sciences)

4:17 PM - 4:32 PM JST | 7:17 AM - 7:32 AM UTC

[MZZ47-05] Probabilistic Photovoltaic Power Prediction Based on Ensemble Weather Forecasting

*Daisuke Nohara[1], Yuki Kanno[1] (1.Central Research Institute of Electric Power Industry)

4:32 PM - 4:47 PM JST | 7:32 AM - 7:47 AM UTC

[MZZ47-06] Consideration of the use of the meso-ensemble prediction system under high penetration of renewable energy in future

*Hideaki Ohtake[1,3], Takashi Oozeki[1], Takahiro Takamatsu[1], Yuya Takane[1], Yusuke Mori[4], Shinji Wakao[4], Fumichika Uno[5], Masahiro Kazumori[2], Toshiyuki Nakaegawa[3] (1.National Institute of Advanced Industrial Science and Technology, 2.Japan Meteorological Agency, 3.Meteorological Research Institute, 4.Waseda University, 5.Nihon University)

4:47 PM - 5:00 PM JST | 7:47 AM - 8:00 AM UTC

[MZZ47-07] Discussion

[J] Oral | M (Multidisciplinary and Interdisciplinary) | M-ZZ Others

[M-ZZ47] Renewable energy and earth science

convener:Hideaki Ohtake(National Institute of Advanced Industrial Science and Technology), Daisuke Nohara(Central Research Institute of Electric Power Industry), Teruhisa Shimada(Graduate School of Science and Technology, Hirosaki University), Fumichika Uno(Nihon University, College of Humanities and Sciences), Chairperson:Teruhisa Shimada(Graduate School of Science and Technology, Hirosaki University)

Fri. Jun 4, 2021 3:30 PM - 5:00 PM Ch.13 (Zoom Room 13)

Renewable energy penetration is increasing dramatically in the world. Renewable energy power generations have become a strong presence in grid operations. However, it is a challenge for renewable energy to be stable power sources due in part to natural variability of renewable energy and its uneven distribution. For effective use of renewable energy, a combinational of various power resources and energy storage technologies (e.g., pumped-storage power generation, storage battery system, electric vehicles) should be desired. Therefore, we need to understand the amount of renewable resources, causes of variation, and the predictability of power output. Then, observation and forecast information from earth science fields should be analyzed and applied to power energy fields to achieve easy use of earth science databases.

Recently, observation databases from remote sensing technology and/or forecasts from numerical models have become essential for both renewable energy and electric power system. Impacts of both earth science data and optimization are essential to economic evaluation of grid operations.

This proposed session needs your presentation from the whole of renewable energy fields (wind power, solar power, geothermal power, tidal power, wave power and biomass power generations). Our goal of this session is to exchange views with various researchers between renewable energy fields and earth science fields (e.g., usage-trends of earth science datasets for renewable energy fields, earth science datasets availability, integrated studies, renewable energy resources in future climate system, and a request from renewable energy fields to earth science fields).

The proposed session features contribution of general interest within earth sciences community.

3:30 PM - 3:32 PM

[MZZ47-01]Introduction

©Japan Geoscience Union

Assessment of small hydropower generation potential in Shiribeshi subprefecture, Hokkaido

Mikiya Kato[2], *Masahiko Fujii[1,2]

1. Faculty of Environmental Earth Science, 2. Graduate School of Environmental Science, Hokkaido University

In Japan, Prime Minister Yoshihide Suga declared in his policy speech in October 2020 that the government would aim to cut greenhouse gases to zero by 2050 and become a carbon-neutral society. Under the condition, the demand for developing renewable energy has been risen recently, especially for small-scale, distributed, base-loaded renewable energy sources. Small hydro power (SHP) is one of the renewable energy sources that meet these requirements (Sawadate, 2017), and can create employment in the region for development, construction, and maintenance, which may lead directly to regional revitalization (Fujii and Sawadate, 2018). On the other hand, there is a risk that development of SHP will cause environmental destruction such as riverine ecosystems, even though it is not as large-scale hydro power. Therefore, overall assessment of the suitability of SHP generation from various aspects before installation locally.

In this study, the suitability of SHP generation was assessed from both environmental, economic and social aspects. As a case study, the assessment was applied to Shiribeshi subprefecture, Hokkaido, Japan, where a relatively large amount of SHP generation was expected by Hokkaido (2014). The assessment method was primarily based on previous studies (Tanabe, 2015; Rospriandana, 2016; Sawadate, 2017), i.e. the amount of SHP generation was estimated by using the geographic information system (GIS) software (ESRI ArcGIS 10.7.1) and digital elevation model (DEM), data of land use pattern and precipitation. Then, suitable sites were selected based on conditions such as consideration for riverine ecosystem, the presence or absence of electric power facilities and disaster risk zones in the surrounding area.

First, the assessment was applied to Niseko town in the subprefecture, which was assigned as a “SDGs Future City”. In the town, population decline is expected to be relatively small in the future with a large number of inbound tourists. Therefore, it is considered that the town could maintain SHP facilities for next decades once they are installed. This study shows that Niseko town is expected to have 6,598 MWh of SHP capacity, equivalent to the electricity demand for 2,200 households, which is three-fourths of the total number of households in the town. There are also hotels and villa areas in the surrounding area, suggesting the possibility of local production and consumption of SHP in the local community.

Then, the assessment was expanded to the entire subprefecture. It was found that Akaigawa village also has a large potential of SHP generation. On the other hand, since Otaru city and Kutchan town have relatively large population, the self-sufficiency rate of SHP alone was not high. In the towns and villages with snow resorts such as Niseko and Kiroro, it is expected that local promotion of SHP generation encourages the revitalization of the local community, suggesting that it may become a model for "strong

©2021. Japan Geoscience Union. All Right Reserved.

urban development".

Keywords: small hydro power, revitalization of local communities, riverine ecosystem, population, climate change, distributed energy

©2021. Japan Geoscience Union. All Right Reserved.

Assessment of snow and ice cryogenic energy potential in Hokkaido: a case study in Niseko Town

*Hehuan DUAN[1], Masahiko FUJII[1,2]

1. Graduate School of Environmental Science, Hokkaido University, 2. Faculty of Environmental Earth Science, Hokkaido University

With the frequent occurrence of extreme weather events and disasters on a global scale due to global warming, there is a need to reduce greenhouse gas (GHG) and achieve a decarbonized society. In September 2018, the people of Hokkaido, Japan experienced a power outage throughout Hokkaido due to the Hokkaido Eastern Iburi Earthquake. Therefore, in an emergency, the centralized power supply system is considered to be vulnerable, and it is recognized that research and development for the utilization of locally produced and locally consumed energy distributed in each region and the promotion of energy mix are important. The purpose of this study is to evaluate the effective utilization of snow and ice cryogenic energy, which is characteristic regional energy of Hokkaido. As a case study, we focused on Niseko Town, which is selected as "Environmental Future City" and "SDGs Future City".

In this study, the electric storage facilities operated mainly by fossil fuel sources and the snow storage facilities using snow and ice cryogenic energy were compared in terms of both environmental and economic aspects. GHG emissions were regarded as an environmental index, and life cycle assessment (LCA) was applied to assess the environmental aspect. The Japanese version of the damage calculation type impact assessment method (LIME2), which is one of the life cycle impact assessment (LCIA) methods, was used for quantitative evaluation of the environmental impacts. Moreover, the total cost (economic / environmental cost) was regarded as an economic index, and the full cost accounting (FCA) was used as the evaluation method. The internal and external cost was calculated using the life cycle cost (LCC) and LCIA, and these were added up to evaluate the total cost. The LCA calculation software MiLCA 2.2.1.0 (2019) and the LCI database IDEA v2 (2019) were used for the calculation.

The total GHG emissions associated with the construction, use and disposal of snow storage facilities were estimated to be 130t-CO_2eq per year. Assuming that the environmental cost associated with CO_2 emissions is 2.33 (yen / kg-CO_2), the cost of damage to the environment is estimated to be 303,000 yen / year. As a result of the interview survey, the construction cost and operation cost of the snow storage facility were calculated to be 180 million yen and 3.25 million yen, respectively. In addition, the cost of disposing the facility was estimated to be 60 million yen based on the market price of the demolition cost of steel-framed reinforced concrete buildings in Hokkaido (about 21,000 yen per m^2). These values were divided by the useful life span of the snow storage facility (21 years) to calculate each cost per year. The construction cost of snow storage facility accounts for 60% of the total costs, and therefore, the economic efficiency is considered to be highly dependent upon the amount of initial investment.

This study suggests that there is an advantage in utilizing snow and ice cryogenic energy in the heavy snowfall areas, because the amount of GHG emissions and the transportation costs in the process of collection and delivery can be suppressed substantially. On the other hand, considering that half of the total GHG emissions and total costs of using the snow storage facility are caused by the construction process of the facility , it is suggested that further innovation in constructing the snow storage facility is necessary to sufficient reduction of both CO_2 emission and costs.

©2021. Japan Geoscience Union. All Right Reserved.

Keywords: snow and ice cryogenic energy, endowment, import snow, carbon dioxide, full cost

©2021. Japan Geoscience Union. All Right Reserved.

Examination of the statistical forecast method of sunshine duration in Hokkaido

*Takao Sunamura[1], Hisashi Kato[1], Fumichika Uno[1]

1. Nihon University, College of Humanities and Sciences

Photovoltaics (PV) is the one of the useful energy productions for mitigating global warming. This energy is depending on solar radiation and sunshine duration, so these electric productions have large variations. Therefore, PV is called as the unstable power generation. Electric power companies have to keep electric power balance between supply and demand. The large forecasting error makes energy power shortage or surplus. Therefore, high accuracy forecasting method is needed for stable energy supply by renewable energy. Hokkaido is attention PV penetration area in recent years. However, this area is considered PV unsuitable power plant because of heavy snowfall area. Although PV in Hokkaido enough electric power can be expected, due to do not reache baiu/meiyu front. But There aren't almost studies to forecast solar radiation or sunshine duration in Hokkaido. Therefore, in this study, we used only surface observation data in Hokkaido and examined the statistical forecast method for sunshine duration.

This study used hourly data of see level pressure (SLP) in station of Japan meteorological Agency (JMA) at all 22 stations in Hokkaido. We accumulated the sunshine duration data between 9 to 13 hour at 6 stations (Wakkanai, Rumoi, Abasiri, Obihiro, Nemuro, Suttu). The forecast method is used principal component analysis (PCA) of SLP in Hokkaido. Result of PCA, first principal component (Z1) indicated East-West SLP pattern, second principal component (Z2) indicated North-South SLP pattern and cumulative contribution rate is 90.0%. We forecasted accumulated sunshine duration using the statisical relationship between the principal scores (Z scores) of SLP at 9:00 and accumulated sunshine duration.

As the results, the Mean Bias Errors (MBE) of accumulated sunshine duration were -0.1 to 0.1 hour, the Root Mean Square Errors (RMSE) on almost stations were about 1.7 hour. The largest value of RMSE was shown at Nemuro (1.8 hour). It is considered that the advection fog caused the forecast error in Nemuro. This fog come from Pacific Ocean and occurs almost every day in summer. This events were difficult to prediction using only SLP patterns. In order to find out the main factor of forecast error in Nemuro, we forecasted accumulated sunshine duration using calculated Z score in each season. The MBEs in summer were overestimated only in Nemuro, and the RMSE shown highest in Nemuro. Of cause, the other factors (eg., sea ice, topography) also considered to affect forecast accuracy. The drift sea ice are changed surface wind fields, topography are blocked low level cloud, and so on. It is difficult to consider the effect of several factors with only SLP patterns.

©2021. Japan Geoscience Union. All Right Reserved.

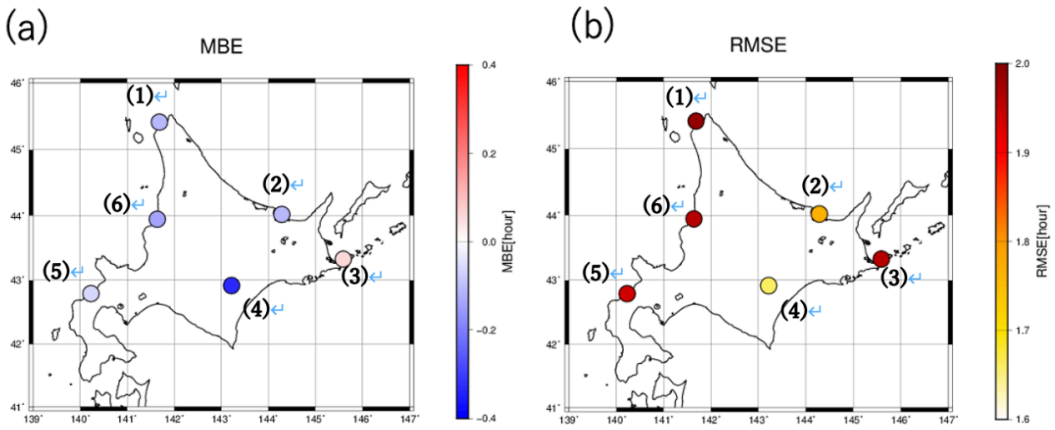


Fig.1, Forecast accuracy each station in summer season.

These plots indicate MBE(a) and RMSE(b). The forecast stations are (1) Wakkanai, (2) Abasiri, (3) Nemuro, (4) Obihiro, (5) Suttu, and (6) Rumoi.

©2021. Japan Geoscience Union. All Right Reserved.

Probabilistic Photovoltaic Power Prediction Based on Ensemble Weather Forecasting

*Daisuke Nohara[1], Yuki Kanno[1]

1. Central Research Institute of Electric Power Industry

Renewable energy such as photovoltaic generation becomes widespread in the world. Since the renewable energy has character of volatility due in part to time evolution of weather system, prediction of the power generations is one of the most cost-effective and easily implemented tools. Despite the recent increase in the accuracy of numerical weather prediction models, there is a limitation to reduce the prediction error. The limitation can be addressed through the use of probabilistic prediction. Herein, we present a probabilistic photovoltaic prediction method based on a numerical weather prediction model, using a power conversion table empirically estimated from the relationship between area-averaged solar radiation and area-integrated photovoltaic generation to project photovoltaic power while accounting for the inherent uncertainty associated with the conversion table. The established probabilistic prediction method exhibits high statistical consistency and reliably captures the confidence interval of photovoltaic power variability.

Keywords: photovoltaic, ensemble forecast, probabilistic forecast

©2021. Japan Geoscience Union. All Right Reserved.

Consideration of the use of the meso-ensemble prediction system under high penetration of renewable energy in future

*Hideaki Ohtake[1,3], Takashi Oozeki[1], Takahiro Takamatsu[1], Yuya Takane[1], Yusuke Mori[4], Shinji Wakao[4], Fumichika Uno[5], Masahiro Kazumori[2], Toshiyuki Nakaegawa[3]

1. National Institute of Advanced Industrial Science and Technology, 2. Japan Meteorological Agency, 3. Meteorological Research Institute, 4. Waseda University, 5. Nihon University

Recently, a large amount of photovoltaic (PV) power systems has been installed in Japan. The value of PV power generation forecast based on a numerical weather prediction (NWP) model has become higher in order to maintain the balance between the power generation and electric power demand. On the other hand, the importance of the uncertainty of day-ahead PV power forecast based on the NWP has increased because of large prediction errors of PV power generation. In our research institute, AIST, we collaborate with the Japan Meteorological Agency (JMA) and the meteorological research institute of the JMA and Nihon University to perform the research project of “The study of renewable energy power forecast using the meso-ensemble prediction system (MEPS)”. We start to study intra day-ahead and day-ahead forecasts using the MEPS for energy management with renewable energy. In this talk, we are going to introduce the treatment of the research project.

Keywords: renewable energy, solar power, electric power demand, power supply and demand, energy management

©2021. Japan Geoscience Union. All Right Reserved.

[J] Oral | M (Multidisciplinary and Interdisciplinary) | M-ZZ Others

[M-ZZ47] Renewable energy and earth science

convener:Hideaki Ohtake(National Institute of Advanced Industrial Science and Technology), Daisuke Nohara(Central Research Institute of Electric Power Industry), Teruhisa Shimada(Graduate School of Science and Technology, Hirosaki University), Fumichika Uno(Nihon University, College of Humanities and Sciences), Chairperson:Teruhisa Shimada(Graduate School of Science and Technology, Hirosaki University)

Fri. Jun 4, 2021 3:30 PM - 5:00 PM Ch.13 (Zoom Room 13)

Renewable energy penetration is increasing dramatically in the world. Renewable energy power generations have become a strong presence in grid operations. However, it is a challenge for renewable energy to be stable power sources due in part to natural variability of renewable energy and its uneven distribution. For effective use of renewable energy, a combinational of various power resources and energy storage technologies (e.g., pumped-storage power generation, storage battery system, electric vehicles) should be desired. Therefore, we need to understand the amount of renewable resources, causes of variation, and the predictability of power output. Then, observation and forecast information from earth science fields should be analyzed and applied to power energy fields to achieve easy use of earth science databases.

Recently, observation databases from remote sensing technology and/or forecasts from numerical models have become essential for both renewable energy and electric power system. Impacts of both earth science data and optimization are essential to economic evaluation of grid operations.

This proposed session needs your presentation from the whole of renewable energy fields (wind power, solar power, geothermal power, tidal power, wave power and biomass power generations). Our goal of this session is to exchange views with various researchers between renewable energy fields and earth science fields (e.g., usage-trends of earth science datasets for renewable energy fields, earth science datasets availability, integrated studies, renewable energy resources in future climate system, and a request from renewable energy fields to earth science fields).

The proposed session features contribution of general interest within earth sciences community.

4:47 PM - 5:00 PM

[MZZ47-07]Discussion

©Japan Geoscience Union

[J] Oral | EVENT：EVENT

Fri. Jun 4, 2021 12:20 PM - 1:40 PM JST | Fri. Jun 4, 2021 3:20 AM - 4:40 AM UTC | Ch.01 Zoom Room 01

[EV-16] Lunchtime Special Lecture

12:20 PM - 1:00 PM JST | 3:20 AM - 4:00 AM UTC

[E-11-19] Progress and Prospects of Global Flood Risk Research

---

1:00 PM - 1:40 PM JST | 4:00 AM - 4:40 AM UTC

[E-11-20] For whom do we do GLOF research in the Himalaya?

[J] Oral | EVENT | EVENT

[EV-16] Lunchtime Special Lecture

Fri. Jun 4, 2021 12:20 PM - 1:40 PM Ch.01 (Zoom Room 01)

12:20 PM - 1:00 PM

[E-11-19]Progress and Prospects of Global Flood Risk Research

With the advancement of earth observation data and computer science, the accuracy of global river models has dramatically improved over the past two decades. In this presentation, I will introduce the progress of flood risk research using such models, and consider what kind of information needs to be generated to promote adaptation and mitigation measures against climate change

©Japan Geoscience Union

[J] Oral | EVENT | EVENT

[EV-16] Lunchtime Special Lecture

Fri. Jun 4, 2021 12:20 PM - 1:40 PM Ch.01 (Zoom Room 01)

1:00 PM - 1:40 PM

[E-11-20]For whom do we do GLOF research in the Himalaya?

Glacial lakes in the Himalaya have rapidly expanded since the 1950s due to melting glaciers. This attracted world' s researchers to glacial lake outburst flood (GLOF) studies in the region. Local residents have been threatened to see the field research teams. This happens because they have no feedback from the researchers. Through such observations in the field, I will discuss how researchers and the locals can/should address environmental issues in developing countries.

©Japan Geoscience Union

[J] Oral | EVENT：EVENT

Fri. Jun 4, 2021 11:30 AM - 12:15 PM JST | Fri. Jun 4, 2021 2:30 AM - 3:15 AM UTC | Ch.17 Zoom Room 17

[EV-18] Exhibitors' Seminar

昨年と同じく、出展者様にセミナーを開催していただきます。
地球惑星科学関連の、有用な情報を発信してくださいますので是非ご参加ください。

11:30 AM - 12:15 PM JST | 2:30 AM - 3:15 AM UTC

[E-11-18] Quantitative EDS Explained - How to achieve great results

[J] Oral | EVENT | EVENT

[EV-18] Exhibitors' Seminar

Fri. Jun 4, 2021 11:30 AM - 12:15 PM Ch.17 (Zoom Room 17)

昨年と同じく、出展者様にセミナーを開催していただきます。
地球惑星科学関連の、有用な情報を発信してくださいますので是非ご参加ください。

11:30 AM - 12:15 PM

[E-11-18]Quantitative EDS Explained - How to achieve great results

Quantitative EDS Explained - How to achieve great results

©Japan Geoscience Union

[J] Oral | EVENT：EVENT

Fri. Jun 4, 2021 1:45 PM - 3:15 PM JST | Fri. Jun 4, 2021 4:45 AM - 6:15 AM UTC | Ch.17 Zoom Room 17

[EV-19] Exhibitors' Pop-Up

New for 2021 Meeting !
Exhibitors will introduce the highlights of their organizations and exhibits in about one minute in real time. Exhibitors will be given one minute to introduce their organization and exhibit highlights in real time.
This is a great chance to meet unexpected exhibitors and find information you never knew
There will be an exchange with the moderator, and you may be able to hear things you can't hear anywhere else.

1:45 PM - 3:15 PM JST | 4:45 AM - 6:15 AM UTC

[E-11-21] Exhibitors' Pop-Up

[J] Oral | EVENT | EVENT

[EV-19] Exhibitors' Pop-Up

Fri. Jun 4, 2021 1:45 PM - 3:15 PM Ch.17 (Zoom Room 17)

New for 2021 Meeting !

Exhibitors will introduce the highlights of their organizations and exhibits in about one minute in real time. Exhibitors will be given one minute to introduce their organization and exhibit highlights in real time.

This is a great chance to meet unexpected exhibitors and find information you never knew

There will be an exchange with the moderator, and you may be able to hear things you can't hear anywhere else.

1:45 PM - 3:15 PM

[E-11-21]Exhibitors' Pop-Up

Exhibitors' Pop-Up

©Japan Geoscience Union

[J] Oral | EVENT：EVENT

Fri. Jun 4, 2021 9:45 AM - 10:30 AM JST | Fri. Jun 4, 2021 12:45 AM - 1:30 AM UTC | Ch.19 Zoom Room 19

[EV-20] Exhibitors' Seminar

昨年と同じく、出展者様にセミナーを開催していただきます。
地球惑星科学関連の、有用な情報を発信してくださいますので是非ご参加ください。

9:45 AM - 10:30 AM JST | 12:45 AM - 1:30 AM UTC

[E-11-17] Graduate School Programs on Earth Science and Geophysics at Tohoku University

[J] Oral | EVENT | EVENT

[EV-20] Exhibitors' Seminar

Fri. Jun 4, 2021 9:45 AM - 10:30 AM Ch.19 (Zoom Room 19)

昨年と同じく、出展者様にセミナーを開催していただきます。
地球惑星科学関連の、有用な情報を発信してくださいますので是非ご参加ください。

9:45 AM - 10:30 AM

[E-11-17]Graduate School Programs on Earth Science and Geophysics at Tohoku University

Graduate School Programs on Earth Science and Geophysics at Tohoku University

©Japan Geoscience Union

[J] Oral | EVENT：EVENT

Fri. Jun 4, 2021 9:00 AM - 9:45 AM JST | Fri. Jun 4, 2021 12:00 AM - 12:45 AM UTC | Ch.24 Zoom Room 24

[EV-21] Exhibitors' Seminar

昨年と同じく、出展者様にセミナーを開催していただきます。
地球惑星科学関連の、有用な情報を発信してくださいますので是非ご参加ください。

9:00 AM - 9:45 AM JST | 12:00 AM - 12:45 AM UTC

[E-11-16] The Challenges of Scientific Drilling Sample Return: (1) IODP Exp. 386 - The Challenging Piston Coring from the Deepest Water Depth Ever / (2) The Science of Mantle Drilling Revisited

[J] Oral | EVENT | EVENT

[EV-21] Exhibitors' Seminar

Fri. Jun 4, 2021 9:00 AM - 9:45 AM Ch.24 (Zoom Room 24)

昨年と同じく、出展者様にセミナーを開催していただきます。
地球惑星科学関連の、有用な情報を発信してくださいますので是非ご参加ください。

9:00 AM - 9:45 AM

[E-11-16]The Challenges of Scientific Drilling Sample Return: (1) IODP Exp. 386 - The Challenging Piston Coring from the Deepest Water Depth Ever / (2) The Science of Mantle Drilling Revisited

The Challenges of Scientific Drilling Sample Return: (1) IODP Exp. 386 - The Challenging Piston Coring from the Deepest Water Depth Ever / (2) The Science of Mantle Drilling Revisited

©Japan Geoscience Union